ARCHIVES OF MECHANICS

Aims and Scope

ARCHIVES OF MECHANICS provides a forum for original research on mechanics of solids, fluids and discrete systems, including the development of mathematical methods for solving mechanical problems. The journal encompasses all aspects of the field, with the emphasis placed on:

- mechanics of materials: elasticity, plasticity, time-dependent phenomena, phase transformation, damage, fracture; physical and experimental foundations, micromechanics, thermodynamics, instabilities
- methods and problems in continuum mechanics: general theory and novel applications, thermomechanics, structural analysis, porous media, contact problems
- dynamics of material systems
- fluid flows and interactions with solids

Address of the Editorial Office:
Institute of Fundamental Technological Research
Świętokrzyska 21
PL 00-049 Warsaw, Poland

Tel.: (48-22) 826 60 22, Fax: (48-22) 826 98 15
E-mail: publikac@ippt.gov.pl

Polish Academy of Sciences
Institute of Fundamental Technological Research

Archives of Mechanics

Archiwum Mechaniki Stosowanej

SPECIAL ISSUE

volume 51 issue 3-4

Agencja Reklamowo-Wydawnicza A. Grzegorczyk
Warszawa 1999

SUBSCRIPTIONS

Address of the Editorial Office: Archives of Mechanics
Institute of Fundamental Technological Research, Świętokrzyska 21
PL 00-049 Warsaw, Poland
Tel.: (48-22) 826 60 22, Fax: (48-22) 826 98 15, E-mail: publikac@ippt.gov.pl

Subscription orders for all journals edited by IFTR may be sent directly to the Editorial Office of the Institute of Fundamental Technological Research

Subscription rates

Annual subscription rate (1999) including postage is US $ 174.
Please transfer the subscription fee to our bank account: Payee: IPPT PAN,
Bank: PKO SA. IV O/Warszawa,
Account no. 12401053-40054492-3000-401112-001.

All journals edited by IFTR are available also through:

- Foreign Trade Enterprise ARS POLONA Krakowskie Przedmieście 7, 00-068 Warszawa, Poland fax: (48-22) 826 86 73
- RUCH S.A. ul. Towarowa 28, 00-958 Warszawa, Poland fax:(48-22) 620 17 62
- Agencja Reklamowo-Wydawnicza A. Grzegorczyk, Bitwy Warszawskiej 1920r. 3, 00-973 Warszawa, Poland tel./fax: (48-22) 822 49 36

Warunki prenumeraty

Redakcja przyjmuje prenumeratę na wszystkie czasopisma wydawane przez IPPT PAN. Bieżące numery można nabyć a także zaprenumerować roczne wydanie Archiwum Mechaniki Stosowanej bezpośrednio w Dziale Wydawnictw IPPT PAN, Świętokrzyska 21, 00-049 Warszawa, Tel.: (48-22) 826 60 22; Fax: (48-22) 826 98 15.
Cena rocznej prenumeraty z bonifikatą (na rok 1999) dla krajowego odbiorcy wynosi 80 zł

Również można je nabyć, a także zamówić (przesyłka za zaliczeniem pocztowym) we Wzorcowni Ośrodka Rozpowszechniania Wydawnictw Naukowych PAN,
00-818 Warszawa, ul. Twarda 51/55, tel. (48-22) 697 88 35.

Wpłaty na prenumeratę przyjmują także jednostki kolportażowe RUCH S.A. Oddział Krajowej Dystrybucji Prasy, 00-958 Warszawa, ul. Towarowa 28. Konto: PBK.S.A. XIII Oddział Warszawa nr 11101053-16551-2700-1-67. Dostawa odbywa się pocztą zwykłą w ramach opłaconej prenumeraty z wyjątkiem zlecenia dostawy pocztą lotniczą, której koszt w pełni pokrywa zleceniodawca. Tel.: (48-22) 620 10 39, fax: (48-22) 620 17 62

Arkuszy wydawniczych 23,27. Arkuszy drukarskich 25,25/A5.
Papier offset. kl III 70 g. B1.
Oddano do składania w lipcu 1999 r. Druk ukończono we wrześniu 1999 r.
Skład i łamanie: G. Wasilewska. Druk i oprawa: Drukarnia OMIKRON, Stare Babice ul. Kutrzeby 15.

Arch. Mech., **51**, 3–4, pp. 227–228, Warszawa 1999

Preface

The 32nd Solid Mechanics Conference, SolMec'98, followed a long tradition of the Polish Solid Mechanics Conferences organized by the Institute of Fundamental Technological Research of the Polish Academy of Sciences in co-operation with the Committee of Mechanics of the Academy.

Starting with the first conference in 1953 at Karpacz, these conferences were initially of summer school type, concentrating on problems of elasticity and plasticity with application to structural mechanics. Later they became international conferences with considerable participation of both Polish and foreign researchers and with much wider scope covering most important aspects of solid mechanics. These conferences have maintained for 45 years high scientific standard and served as a forum for exchange of ideas and research information. Numerous participants both foreign and Polish delivered here lectures many times and certainly remember the period when they first came as young beginning researchers, now presenting general or key-note lectures as eminent scientists. It was a pleasure for us to see old friends with whom we shared our ideas and enthusiasm for mechanics. It was also a pleasure to meet young generation of researchers working in new fields and contributing new important results.

The 32nd Solid Mechanics Conference, SolMec'98, held in Zakopane, September 1-5, 1998, was organized by the Centre of Mechanics of the Institute of Fundamental Technological Research. The scientific program included more than 200 papers including 16 invited general and sectional lectures delivered by 140 Polish and 80 foreign researchers. These contributions have roughly been classified into the following main areas

Plasticity and Damage	46 papers
Biomechanics	16 papers
Composite Mechanics	15 papers
Dynamics of Structures and Materials	24 papers
Optimization and Sensitivity Analysis	16 papers
Smart Structures	5 papers
Structural Mechanics	16 papers
Elasticity	20 papers
Geomechanics	14 papers
Numerical Methods	12 papers
Homogenization	12 papers

Porous Media	6 papers
Identification	6 papers

The Conference was accompanied by a Polish-Japanese Workshop on *Testing and Modelling the Behaviour of Shape Memory Alloys* chaired by Professor B. Raniecki.

Though no conference proceedings volume was planned, all participants were encouraged to submit their contributions as full-length papers for publication in special issues of *Archives of Mechanics* or *Engineering Transactions*. The present issue of *Archives of Mechanics* contains the submitted and reviewed contributions of a more basic orientation. The contributions with a more engineering character will soon appear in a special issue of *Engineering Transaction*.

Warszawa, August 1999

Zenon Mróz
Conference Chairman

Arch. Mech., **51**, 3–4, pp. 229–241, Warszawa 1999

On rate and gradient-dependence of solids as dynamical systems

P. B. BÉDA

Research Group of the Dynamics of Machines and Vehicles,
Technical University of Budapest
P.O. Box 91. H-1502 Budapest, Hungary

THIS PAPER AIMS at presenting a mathematical background of material instability problems such like strain localization or flutter, as an application of the theory of dynamical systems. The basic field equations of the solid continuum are the kinematic equations, the Cauchy equations of motion and the constitutive equations. This system of equations is completed with initial and boundary value conditions and can define a dynamical system. Then, a condition of material stability can be obtained using Lapunov's indirect method. Also the basic material instability modes can be classified as static (divergence type) or dynamic (Hopf) bifurcations of dynamical systems. Such formulation gives a mathematical interpretation of rate and gradient-dependence in the constitutive equations and mesh dependence in numerical studies, pointing out their close relationship to the structure of the critical eigenspace of an operator defined by the dynamical system.

1. Introduction

IN THE RECENT YEARS several new results of the theory of dynamical systems [1, 18] have already been successfully used in various fields of mechanics [5, 16]. The main aim of this paper is to analyze the effect of rate and gradient-dependence in material instability and postlocalization by considering solid continua as dynamical systems [4, 6]. This kind of investigation is closely related to the perturbation analysis [9, 19] as it will be explained in Section 3.

In the theory of dynamical systems, the linear concept of the loss of stability of a state of the system means that the real part of certain eigenvalues of the linear operator describing its behavior changes sign. The eigenvectors connected with them are used in applications to the critical eigenmodes [16]. In a nonlinear case, the postbifurcation can be studied and described analytically using these critical eigenmodes.

Unfortunately, for the classical setting [13] there is no possibility to obtain specific critical eigenmodes at the onset of material instability. On the other

hand, in the finite element calculation of material instability problems, the classical formulation of the basic equations of solid continua results in a definite mesh dependence [7, 14, 15]. These are very similar phenomena. In those papers the mesh dependence was eliminated by the inclusion of rate-dependence or nonlocality (gradient effects) into the constitutive equations.

In this paper we study how and when the inclusion of rate and gradient dependent terms into the constitutive equations changes the structure of critical eigenmodes, and we show how the postlocalization can be studied for a nonlinear constitutive equation.

The second section presents the basic equations for the solid body. We neglect geometrical nonlinearities, but include the nonlinearity in the constitutive equation. The equations will be transformed into the velocity field, because such form is convenient for our investigation. The third section starts with a survey of the basic notions of the theory of dynamical systems and formulates a linear stability condition for a state of the body based on the Lapunov stability definition. These conditions are formulated as linear boundary value problems. By solving them, the eigenfunctions can be considered as critical eigenmodes. In case of a unique critical eigenmode, a static bifurcation investigation is performed for the nonlinear equation.

In section four the effect of rate and gradient-dependence is studied in uniaxial cases. These are mostly linear problems, but at the end we show how the critical eigenmode can be used for the analysis of a static post-localization in presence of a material nonlinearity.

2. Basic equations

In case of small strains the kinematic equation [11] is

$$\epsilon = \frac{1}{2}\left(\mathbf{u} \circ \nabla + \nabla \circ \mathbf{u}\right), \tag{2.1}$$

where ϵ is the strain tensor, $\mathbf{u}$ is the displacement vector and $\circ$ denotes a diadic product. The equation of motion [11] without body forces is

$$\rho \ddot{\mathbf{u}} = \sigma \nabla, \tag{2.2}$$

where ρ is the mass density and σ denotes the symmetric stress tensor.

Let the constitutive equation have the form

$$F\left(\dot{\sigma}, \epsilon, \dot{\epsilon}, \nabla^2 \epsilon, \nabla \epsilon, \sigma\right) = 0 \tag{2.3}$$

representing both the rate-dependent and gradient effects. Equation (2.3) is a combination of the rate-dependent second gradient theory [17] and of the first

gradient constitutive equation suggested in [2], which is developed on the basis of the wave dynamics [3] and of several experimental results [2].

By studying the stability of a state S^0 described by $\sigma^0, \epsilon^0 \ldots$ the constitutive equation can be linearized at S^0. Let the new variables $\bar{\sigma} = \sigma - \sigma^0$, $\bar{\epsilon} = \epsilon - \epsilon^0 \ldots$ be introduced for arbitrarily small perturbations. Because at state S^0 the variables satisfy (2.3), we may assume that the linearized constitutive equation is

$$\dot{\bar{\sigma}} = \mathbf{C^1}\bar{\epsilon} + \mathbf{C^2}\dot{\bar{\epsilon}} + \mathbf{C^3}\nabla^2\bar{\epsilon} + \mathbf{C^4}\nabla\bar{\epsilon} + \mathbf{C^5}\bar{\sigma}. \tag{2.4}$$

Now equations (2.1), (2.2) and (2.4) form the basic equations for the stability investigation of state S^0. These equations should be transformed into the velocity field $\mathbf{v}$. For the sake of simplicity the bars are omitted in the following derivations but all equations concern the small perturbations of state S^0, thus all the calculations are performed in a sufficiently small neighbourhood of S^0.

From (2.2) and by using the rate form of (2.1) and (2.4), the basic equation is

$$\begin{aligned} 2\rho\,\ddot{\mathbf{v}} = {} & \mathbf{C^1}\left(\mathbf{v}\circ\nabla + \nabla\circ\mathbf{v}\right)\nabla + \mathbf{C^2}\left(\dot{\mathbf{v}}\circ\nabla + \nabla\circ\dot{\mathbf{v}}\right)\nabla \\ & + \mathbf{C^3}\nabla^2\left(\mathbf{v}\circ\nabla + \nabla\circ\mathbf{v}\right)\nabla + \mathbf{C^4}\nabla\left(\mathbf{v}\circ\nabla + \nabla\circ\mathbf{v}\right)\nabla + \mathbf{C^5}\rho\ddot{\mathbf{v}}. \end{aligned} \tag{2.5}$$

The initial and boundary conditions assumed by the mechanical problem under consideration are also needed. In the following considerations, the stability investigation of state S^0 will be based on (2.5).

3. Dynamical systems and bifurcations

In operator form Eq. (2.5) reads

$$\ddot{v} = F^1 v + F^2\dot{v} + F^3\ddot{v}. \tag{3.1}$$

Here $v = (v_1, v_2, v_3)$ is a vector of the coordinates of the velocity field satisfying the boundary conditions and F^1, F^2 and F^3 are linear differential operators defined by the right-hand side of (2.5). Equation (3.1) can be considered as an infinite-dimensional dynamical system.

The stability of state S^0 of the continuum is defined by the Lapunov stability of a solution $v^0(t)$ of (3.1). That is, a state represented by $v^0(t)$ is stable, when the perturbed velocity field $v^0(t) + \bar{v}(t)$ remains sufficiently close to the unperturbed one. Such definitions are also used in solid mechanics [11, 12]. The stability investigation of $v^0(t)$ starts with a transformation into a local form at that solution by substituting

$$v(t) = v^0(t) + \bar{v}(t)$$

into (3.1):

$$\ddot{v}^0 + \ddot{\bar{v}} = F^1\left(v^0 + \bar{v}\right) + F^2\left(\dot{v}^0 + \dot{\bar{v}}\right) + F^3\left(\ddot{v}^0 + \ddot{\bar{v}}\right). \tag{3.2}$$

While v^0 is a solution of (3.1) and F^1, F^2 and F^3 are linear operators, the first terms of all parts in (3.2) are equal, thus the equation of motion (3.2) for the perturbation $\bar{v}(t)$ has the same form as (3.1). Then (3.2) can be transformed into a system of first order equations by introducing new variables and vectors

$$y_1 = \bar{v}_1, \quad \ldots, \quad y_3 = \bar{v}_3, \quad y_4 = \dot{\bar{v}}_1, \quad \ldots, \quad y_6 = \dot{\bar{v}}_3, \quad y_7 = \ddot{\bar{v}}_1, \quad \ldots, \quad y_9 = \ddot{\bar{v}}_3$$

$$y_\alpha, \quad (\alpha = 1, \ldots, 3), \quad y_\beta, \quad (\beta = 4, \ldots, 6), \quad y_\psi, \quad (\psi = 7, \ldots, 9).$$

The transformed equations are

$$\dot{y}_\alpha = y_\beta, \tag{3.3}$$

$$\dot{y}_\beta = y_\psi, \tag{3.4}$$

$$\dot{y}_\psi = F^1 y_\alpha + F^2 y_\beta + F^3 y_\psi. \tag{3.5}$$

The stability properties are determined by the eigenvalues of linear operator $\hat{F}$ defined by the right-hand sides of (3.3), (3.4) and (3.5),

$$\hat{F}(y_\alpha, y_\beta, y_\psi) = (y_\beta, y_\psi, F^1 y_\alpha + F^2 y_\beta + F^3 y_\psi).$$

Using Lapunov's indirect method [8] v^0 is asymptotically stable, when the real parts of all eigenvalues of $\hat{F}$ are negative. In case of zero real parts, the system is on the stability boundary. The characteristic equation of $\hat{F}$ reads

$$\begin{aligned} \lambda y_\alpha &= y_\beta, \\ \lambda y_\beta &= y_\psi, \\ \lambda y_\psi &= F^1 y_\alpha + F^2 y_\beta + F^3 y_\psi. \end{aligned} \tag{3.6}$$

By substituting the first two equations of (3.6) into the third one, equation

$$\lambda^3 y_\alpha - \lambda^2 F^3 y_\alpha - \lambda F^2 y_\alpha - F^1 y_\alpha = 0 \tag{3.7}$$

is obtained. The condition of asymptotic stability is $\mathrm{Re}\lambda_i < 0, \quad i = 1 \ldots$ for all λ_i satisfying (3.7).

The typical ways of loosing stability are the following cases: when (SB) a real λ_c or (DB) the real part of a pair of complex conjugate λ_{c1} and $\lambda_{c2}(= \bar{\lambda}_{c1})$ changes sign, while all the others satisfy $\mathrm{Re}\lambda_i < 0, \quad i \neq c$ and $i \neq c1, c2$, respectively. Thus the loss of stability can either be a generic static (SB) or dynamic (DB) bifurcation [6]. In case of a (SB), Eq. (3.7) has a zero eigenvalue $\lambda_c = 0$. From (3.7) the condition of (SB) is

$$F^1 y_\alpha = 0. \tag{3.8}$$

This phenomenon is also called the divergence instability or the onset of strain localization [13], because also the uniqueness of the solution v^0 is lost and other, localized nontrivial solutions appear.

At (DB) the eigenvalues are imaginary values, thus the necessary condition is

$$\left(\left(F^3\right)^{-1} F^1 + F^2\right) y_\alpha = 0. \tag{3.9}$$

The main difference between instabilities (SB) and (DB) is that at (DB) the uniqueness of v^0remains valid, but Lapunov stability is lost.

While (2.5) and (3.1) show that F^1 depends on the so-called hardening parameter and F^2 on the rate-sensitivity, this classification is similar to that in [19], where (SB) is called the strain-hardening type and (DB) is the rate sensitivity type.

Notice that all functions y_α should also satisfy the boundary conditions, thus expressions (3.8), (3.9) are partial differential equations with those boundary conditions. To obtain the critical eigenfunctions (eigenmodes), these linear boundary value problems should be solved. Unfortunately, in a general case this step cannot be done analytically. Instead of solving it we could use two kinds of simplifications.

Firstly, we could restrict ourselves to one-dimensional problems. Then an analytical solution can easily be calculated (see the example in the following).

Secondly, in the three-axial case special solutions could be studied using the method called the perturbation technique. It is widely used (see for instance [9, 19]) to omit the boundary value problem. Then the treatment is restricted to the study of the functions

$$q_k(t) \exp(i n_p^k x_p),$$

substituted into the equation of motion. Then conditions (3.8), (3.9) turn out to be systems of algebraic equations. A detailed study of the linear case is given in [6].

At the end of this section the nonlinear post-localization will be studied in case of an (SB) of a stationary (or steady state) solution. A solution of (3.3) and (3.5) is called stationary, when

$$\dot{y}_\alpha = \dot{y}_\beta = \dot{y}_\psi = 0.$$

Let us study what happens with such solutions at a static bifurcation. In the investigation also the nonlinear terms $\hat{N}(y_\alpha, y_\psi)$ are necessary. When also nonlinear terms are added to Eqs. (3.3) and (3.5), for the stationary solutions

$$0 = F^1 y_\alpha + N(y_\alpha) \tag{3.10}$$

is obtained, where $N(y_\alpha) = \hat{N}(y_\alpha, 0)$. Assume that F^1 depends on a (for example loading) parameter μ, and at $\mu = 0$ condition (3.8) of the static bifurcation is satisfied by the eigenmode y_α^0,

$$F^1\Big|_{\mu=0} y_\alpha^0 = 0. \tag{3.11}$$

Defining $\bar{F}^1(\mu) = F^1 - F^1|_{\mu=0}$, Eq. (3.10) assumes the form

$$0 = \left(\bar{F}^1(\mu) + F^1|_{\mu=0}\right) y_\alpha + N(y_\alpha). \tag{3.12}$$

In static bifurcation theory [5] in a small neighbourhood of v^0 (or state S^0), the nontrivial solution can be searched for in the form

$$y_\alpha = q y_\alpha^0,$$

where q is a small real number. By substituting this form into (3.12), relation

$$0 = q\bar{F}^1(\mu) y_\alpha^0 + N\left(q y_\alpha^0\right) \tag{3.13}$$

is obtained because of (3.11). Introducing a scalar product $< .,. >$, from (3.13) an approximation of the bifurcation equation [16]

$$0 = q\left\langle y_\alpha^0, \bar{F}^1(\mu) y_\alpha^0\right\rangle + \left\langle y_\alpha^0, N\left(q y_\alpha^0\right)\right\rangle \tag{3.14}$$

is obtained, which is a nonlinear algebraic equation for q. By performing power series expansions and considering only the first few terms, it can be solved for $q = q(\mu)$. Then for a sufficiently small μ, the nontrivial solution is

$$y_\alpha = q(\mu) y_\alpha^0.$$

4. Rate and gradient dependence

In the following parts the static and dynamic bifurcations of solid bodies will be studied in a one-dimensional example. We will also analyse the static post-bifurcation (post-localization) of a second gradient dependent nonlinear material. Let a rod of length L be considered. Several kinds of rate-dependence of the constitutive equations will also be investigated. These are second gradient-dependent and gradient-independent materials. We also study two types of instability problems of rate and first gradient dependent materials.

4.1. A linear second gradient-dependent material

In case of a second gradient-dependent material, the constitutive equation in rate form [17]

$$\dot{\sigma} = \bar{c}_1 \dot{\epsilon} + \bar{c}_2 \ddot{\epsilon} - \bar{c}_3 \frac{\partial^2 \dot{\epsilon}}{\partial x^2} \tag{4.1}$$

is a widely used one, based on the second gradient theory and succesfully used in static post-localization. Equations (3.4) and (3.5) in this case are

$$\dot{y}_1 = y_2, \tag{4.2}$$

$$\dot{y}_2 = \left(c_1 \frac{\partial^2}{\partial x^2} - c_3 \frac{\partial^4}{\partial x^4} \right) y_1 + c_2 \frac{\partial^2}{\partial x^2} y_2, \tag{4.3}$$

where $c_i = \frac{\bar{c}_i}{\rho}$, $i = 1, 2, 3$. Now, the characteristic Eq. (3.7) is a second order one

$$\lambda^2 y_1 - \lambda c_2 \frac{\partial^2}{\partial x^2} y_1 - \left(c_1 \frac{\partial^2}{\partial x^2} - c_3 \frac{\partial^4}{\partial x^4} \right) y_1 = 0. \tag{4.4}$$

In case of homogeneous boundary conditions, the eigenfunctions are

$$y_1 = e^{i\alpha_k x}, \quad \text{where} \quad \alpha_k = \frac{k\pi}{L} \quad (k = 1, ...) \tag{4.5}$$

and the eigenvalues are

$$\lambda_{1,2,k} = \frac{-c_2\alpha_k^2 \pm \sqrt{c_2^2\alpha_k^4 - 4\alpha_k^2 \left(c_3\alpha_k^2 + c_1\right)}}{2}. \tag{4.6}$$

When c_1 and c_2 are positive, the real parts of all the eigenvalues are negative. Thus the state is stable, if $c_2 > 0$ and

$$\left(c_3\alpha_k^2 + c_1\right) > 0. \tag{4.7}$$

The (SB) loss of stability happens, when

$$\left(c_3\alpha_k^2 + c_1\right) = 0. \tag{4.8}$$

Then

$$\alpha_k = \alpha_{k*} = \sqrt{-\frac{c_1}{c_3}}. \tag{4.9}$$

In this case the only function of form (4.5) satisfying (4.9) is

$$v = e^{i\sqrt{-\frac{c_1}{c_3}}x}. \tag{4.10}$$

Obviously, when for some k

$$\alpha_k < \alpha_{k*}, \tag{4.11}$$

one of the eigenvalues $\lambda_{1,2,k}$ has a positive real part. For that k this implies instability.

Since c_1 is the tangent of the stress-strain diagram at state S^0 and during a quasistatic loading process it gets increasingly negative values on the softening side, the first critical α_k is at $k = 1$. In case of the so-called adiabatic localization [13] L tends to infinity. Then the instability condition (4.8) can be satisfied by

any arbitrary small real α, thus the state loses stability, when c_1 assumes negative values. Thus the stability boundary for the adiabatic case is $c_1 = 0$.

When the loss of stability is of type (DB), the condition is

$$c_2 = 0.$$

Before the loss of stability $\mathrm{Re}(\lambda_{1,2,k}) < 0$, thus (4.7) should be satisfied. Assume that it remains true during the dynamic loss of stability. Then at $c_2 = 0$ all eigenvalues are imaginary numbers

$$\lambda_{1,2,k} = \pm i\alpha_k \sqrt{(c_3\alpha_k^2 + c_1)} \tag{4.12}$$

and each of them can be attached to a critical eigenmode. Unfortunately, at $\alpha_k = \alpha_{k*}$ expression (4.12) yields a zero eigenvalue, thus a coexistent (SB) and (DB) instability happens.

From (4.6) we can see that rate-independence for such a material is equivalent with the (DB) condition. Thus such material is always on the stability boundary (of course it may be Lyapunov stable but not asymptotically stable [18]). The "real" loss of stability happens as an additional (SB), if $c_1 = 0$. Then we obtain again coexistent (SB) and (DB) instabilities. (For details see [6].)

4.2. The gradient-independent case

Expression (4.6) shows the differences between the gradient-dependent and independent cases. When the material is gradient-independent, $c_3 = 0$. Then from (4.6)

$$\lambda_{1,2,k} = \frac{-c_2\alpha_k^2 \pm \sqrt{c_2^2\alpha_k^4 - 4\alpha_k^2 c_1}}{2}. \tag{4.13}$$

The condition of (SB) is $c_1 = 0$, because then (4.13) implies

$$\lambda_{1,2,k} = \frac{-c_2\alpha_k^2 \pm |c_2|\alpha_k^2}{2}, \tag{4.14}$$

that is,

$$\lambda_{1,k} = \frac{-c_2 + |c_2|}{2}\alpha_k^2, \quad k = 1, 2, \ldots \tag{4.15}$$

$$\lambda_{2,k} = \frac{-c_2 - |c_2|}{2}\alpha_k^2, \quad k = 1, 2, \ldots \tag{4.16}$$

By comparing (4.8) and (4.14) we see, that the main difference is that (4.8) defines a critical $k = k*$ (see (4.9)) and consequently, a critical eigenmode $e^{i\alpha_{k*}x}$ for the perturbation. In (4.14) all values k, $k = 1, 2...$ and all perturbations

$e^{i\alpha_k x}$ are critical when $c_1 = 0$. In other words, for gradient-independent constitutive equation all wavelengths are critical. At the postbifurcation investigation, the nontrivial solutions were searched for as linear combination of the critical eigenmodes. Such study cannot be performed for rate-independent constitutive equation because of the infinite number of critical eigenmodes. Moreover, while $c_2 > 0$ suffices to ensure stability for eigenvalues (4.16), the other group (4.13) results in a zero eigenvalue with infinite multiplicity.

In case of (DB) instability, the necessary condition is $c_2 = 0$ and for the eigenvalues

$$\lambda_{1,2,k} = \pm i\sqrt{c_1}\alpha_k.$$

Contrary to the previous case, now (SB) and (DB) instabilities are distinct phenomena.

When rate-dependence is omitted we again have the permanent (DB) as in part 4.1.

4.3. The effect of material nonlinearity

In this subsection a nonlinear constitutive equation proposed in [20] is used. This one contains both second gradient-dependent and rate-dependent terms

$$\dot{\sigma} = c_1\dot{\epsilon} + c_2\ddot{\epsilon} - c_3\frac{\partial^2\dot{\epsilon}}{\partial x^2} + c_4\left(\frac{\partial\dot{\epsilon}}{\partial x}\right)^2 \tag{4.17}$$

for the adiabatic postlocalization investigation in the one-dimensional case. Assume that the loss of stability of state S^0 happens at c_{10}. A small bifurcation parameter $0 < \mu \ll 1$ is introduced,

$$c_1 = c_{10} - \mu. \tag{4.18}$$

Using (4.17), (4.18) and the one-dimensional form of (2.1) and (2.2), the equation of motion for the velocity field is

$$\rho\ddot{v} = \left(c_{10}\frac{\partial^2}{\partial x^2} - c_3\frac{\partial^4}{\partial x^4}\right)v - \mu\frac{\partial^2}{\partial x^2}v + c_2\frac{\partial^2}{\partial x^2}\dot{v} + c_4\left(\frac{\partial^3 v}{\partial x^3}\right)^2. \tag{4.19}$$

While the localization is a static bifurcation [6], the postbifurcation investigation can be restricted to the steady state solutions $\ddot{v} = \dot{v} = 0$ of (4.19). Then instead of (4.19), equation

$$\left(c_{10}\frac{\partial^2}{\partial x^2} - c_3\frac{\partial^4}{\partial x^4}\right)v - \mu\frac{\partial^2}{\partial x^2}v + c_4\left(\frac{\partial^3 v}{\partial x^3}\right)^2 = 0 \tag{4.20}$$

is used.

In the linear study of the previous subsection at the loss of stability, the velocity function in form (4.10) was obtained. Thus, as the first critical eigenmode, function $\sin(\alpha x)$ can be identified. Similarly to the general treatment, the bifurcated nontrivial solution of (4.20) can be searched for as a linear combination of the critical eigenmodes. Now there is a unique critical eigenmode, thus

$$v^c = q\sin(\alpha x),$$

where $|q| \ll 1$ and α satisfies (4.9). Function v^c can be substituted into (4.20) and then the scalar product (the right-hand side of (3.14)

$$g(q,\mu) = \int_0^L \left(\left(\left(c_{10}\frac{\partial^2}{\partial x^2} - c_3\frac{\partial^4}{\partial x^4} - \mu\frac{\partial^2}{\partial x^2} \right) q\sin(\alpha x) \right) \sin(\alpha x) \right.$$

$$\left. + c_4 \left(\frac{\partial^3 q\sin(\alpha x)}{\partial x^3} \right)^2 \right) \sin(\alpha x) dx$$

defines function $g(q,\mu)$ for the approximate bifurcation equation

$$g(q,\mu) = 0. \tag{4.21}$$

Solving (4.21), we obtain

$$q = -\frac{3\mu}{4\pi c_4 \alpha^4} \tag{4.22}$$

and thus a transcritical bifurcation is obtained and the nontrivial solution is

$$v^c = -\frac{3}{4\pi c_4 \alpha^4}\mu\sin(\alpha x),$$

or, using (4.9),

$$v^c = -\frac{3c_3^2}{4\pi c_4 c_{10}^2}\mu\sin\left(x\sqrt{-\frac{c_{10}}{c_3}}\right). \tag{4.23}$$

4.4. First gradient effects

Let us study now the first gradient effects. Then the constitutive equation has the generalized form

$$\dot{\sigma} = \bar{d}_1\dot{\epsilon} + \bar{d}_2\frac{\partial\epsilon}{\partial x} + \bar{d}_3\epsilon + d_4\sigma, \tag{4.24}$$

which was studied in connection with acceleration waves, both theoretically and experimentally in [3], and contains a first gradient term.

Firstly, let us set $d_4 = 0$, which is an experimental result for copper [2]. Then the characteristic equation (3.7) is

$$\lambda^3 y_1 - \lambda d_1 \frac{\partial^2}{\partial x^2} y_1 - d_3 \frac{\partial^2}{\partial x^2} y_1 - d_2 \frac{\partial^3}{\partial x^3} y_1 = 0, \tag{4.25}$$

where $d_i = \dfrac{\bar{d}_i}{\rho}$, $i = 1, 2, 3$. For homogeneous boundary conditions, as before Eq. (4.5) can be substituted into (4.25) and then a complex equation

$$\lambda^3 + \lambda d_1 \alpha_k^2 + d_3 \alpha_k^2 + i d_2 \alpha_k^3 = 0 \tag{4.26}$$

is obtained.

The necessary condition of (SB) instability is

$$d_2 = d_3 = 0.$$

Then

$$\lambda_{1,k} = 0$$

and from (4.26)

$$\lambda_{2,3,k} = \pm \alpha_k \sqrt{d_1}.$$

While $d_1 > 0$ (see [3]) these are all real values and a half of them has positive signs, that is, this case is not a stability boundary.

For (DB) instability the necessary condition is

$$d_3 = 0.$$

Assume that $\lambda = \nu + i\omega$. Then at $\nu = 0$ for the imaginary parts from (4.26)

$$-\omega^3 + \omega d_1 \alpha_k^2 + d_2 \alpha_k^3 = 0. \tag{4.27}$$

Equation (4.27) should always have at least one real solution $\omega = \omega(\alpha_k)$. For this kind of material, the dynamic type of instability (DB) is the only possible way of stability loss because the conditions of (SB) can only be satisfied in the instability region.

Now let us study the case when in (4.24) instead of ϵ the stress σ is present ($d_3 = 0$, $d_4 \neq 0$). Now the characteristic equation (3.7) with homogeneous boundary conditions is

$$\lambda^3 - d_4 \lambda^2 + \lambda d_1 \alpha_k^2 + i d_2 \alpha_k^2 = 0. \tag{4.28}$$

The necessary condition of (SB) instability from (4.28) is

$$d_2 = 0$$

and for the other (nonzero) eigenvalues

$$\lambda^2 - d_4\lambda + d_1\alpha_k^2 = 0. \tag{4.29}$$

The solutions of (4.29) are

$$\lambda_{2,3,k} = \frac{d_4 \pm \sqrt{d_4^2 - 4\alpha_k^2 d_1}}{2}. \tag{4.30}$$

In (4.30) the sign of d_4 has a great importance. When it is negative, there is a static bifurcation, but in case of $d_4 > 0$ it does not exist.

For (DB) instability the bifurcation condition is

$$d_4 = 0$$

and then we have Eq. (4.27) and the same results as before for the eigenvalues.

5. Concluding remarks

The results show that by considering the system of the basic equations of a solid continuum as a dynamical system, the material stability conditions can be formulated by using the linear Lapunov stability conditions. The loss of stability can be classified into the classes of static and dynamic bifurcations. In one-dimensional mechanical problems the selection of the constitutive equation has the most important effect on the type of instability. We studied rate and gradient-dependent and independent constitutive equations as well. We found that rate-dependence in most of the cases separates the (SB) and (DB) types of instability, while the inclusion of gradient-dependence has a more complex effect. The one which was detected here is the role in determining the dimension of the critical eigenspace at the loss of stability. In case of the so-called second gradient-dependent material we have a very simple eigenspace at (SB), thus we could also perform a nonlinear static bifurcation investigation. For the other material models, the study ended up in infinite-dimensional critical nullspaces. Therefore an exciting theoretical question has arisen: does such behavior belong to the essence of the real physical phenomenon or it is caused only by the use of improper material models.

Acknowledgements

This work was supported by the National Scientific Research Foundation Hungary (under contract: OTKA F017331). This support is gratefully acknowledged.

References

1. V.I. ARNOLD, *Geometrical methods in the theory of ordinary differential equations*. Springer, New York 1983.
2. Gy. BÉDA, *Methode zur Bestimmung der Materialgleichung*, Publ. of the Tech. Univ. for Heavy Ind. Miskolc, **12**, 271–286, 1962.
3. Gy. BÉDA, *Possible constitutive equations of the moving plastic body*, Advances in Mech., **10**, 65–87, 1987.
4. P.B. BÉDA, *Localization as instability of dynamical systems*, Material Instabilities, R.C. Batra, H. Zbib [Ed.], ASME Press, New York 1994, pp. 279–284.
5. P.B. BÉDA, *Bifurcation and postbifurcation of rods*, J. of Theoretical and Applied Mech. **34**, 91–100, 1996.
6. P.B. BÉDA, *Material instability in dynamical systems*, European Journal of Mechanics, A/Solids, **16**, 501–513, 1997.
7. R. DE BORST, L.J. SLUYS, H-B. MÜHLHAUS and J. PAMIN, *Fundamental issues in finite element analyses of localization of deformation*, Engineering Computations, **10**, 99–121, 1993.
8. N.G. CHETAYEV, *The stability of motion*, Pergamon Press, New York 1961.
9. I. DOBOVSEK, *Adiabatic material instabilities in rate-dependent solids*, Arch. Mech., **46**, 893–936, 1994.
10. R. HILL, *Accelerations waves in solids*, J. Mech. and Phys. of Solids, **10**, 1–16, 1962.
11. C. ERINGEN, *Continuum physics*, Vol. II, Academic Press, New York 1975.
12. Q.S. NGUYEN, *Bifurcation and stability of dissipative systems*, Springer, New York 1992.
13. J.R. RICE, *The localization of plastic deformation* [in:], Theoretical and applied mechanics [Ed.] W.T. Koiter, North-Holland Publ. Amsterdam, 1976, pp. 207–220.
14. L.J. SLUYS, *Wave propagation, localization and dispersion in softening solids*, Dissertation, Delft University of Technology, Delft 1992.
15. L.J. SLUYS and R. DE BORST, *Wave propagation and localization in a rate-dependent cracked medium – model formulation and one-dimensional examples*, Int. J. Solids Structures, **29**, 2945–2958, 1992.
16. H. TROGER and A. STEINDL, *Nonlinear stability and bifurcation theory, An Introduction for Scientists and Engineers*, Springer, Wien, New York 1990.
17. I. VARDOULAKIS, *Potentials and limitations of softening models in geomechanics*, European Journal of Mechanics, A/Solids, **13**, 195–226, 1994.
18. S. WIGGINS, *Introduction to applied nonlinear dynamical systems and chaos*, Springer, New York 1990.
19. H.M. ZBIB and E.C. AIFANTIS, *On the localization and postlocalization behavior of plastic deformation*, I. Res Mechanica, **23**, 261–277, 1988.
20. H.M. ZBIB and E.C. AIFANTIS, *On the structure and width of shear bands in finite elastoplastic deformations* [in:] Anisotropy and Localization of Plastic Deformations, J-P. Boehler, A.S. Khan [Eds.] Elsevier, New York 1991, pp. 99–103.

Received November 25, 1998.

Arch. Mech., **51**, 3–4, pp. 243–274, Warszawa 1999

Macroscopic equations for nonstationary flow of Stokesian fluid through porous elastic medium

W. BIELSKI[1], J.J. TELEGA[2] and R. WOJNAR[2]

[1] *Institute of Geophysics, Warsaw, Poland*
[2] *Institute of Fundamental Technological Research, Warsaw, Poland*
e-mail: wbielski@igf.edu.pl, jtelega@ippt.gov.pl, rwojnar@ippt.gov.pl

THE AIM OF THIS CONTRIBUTION is to apply homogenization methods in order to describe the nonstationary flow of a viscous fluid through a microperiodic porous elastic medium. By using the method of two-scale asymptotic expansions, the macroscopic phenomenological equations describing such a two-phase structure are derived and the formulae for the effective mechanical coefficients are given. The asymptotic approach is justified by the two-scale convergence. It is shown that Darcy's law is nonlocal in time.

1. Introduction

ONE CAN DISTINGUISH two approaches to modelling the mechanical behaviour of porous media. The first approach, more traditional, dates back to the papers by BIOT [16 – 19], and may be called a phenomenological one. The nice book by COUSSY [26] develops such an approach within the framework of modern continuum mechanics and applies it to elastic, thermoelastic and inelastic porous media, cf. also the paper by CIESZKO and KUBIK [23, 24] and the references cited therein. The second approach exploits the microstructure of the medium. The micro-macro passage is performed by using averaging techniques, the mixture theory or various homogenization methods. ALLAIRE [6] and MIKELIĆ [40] studied flows of Stokesian fluids through undeformed microperiodic porous media by using the homogenization theory. The first of these authors assumed the scaling of the viscosity while the second author scaled the liquid density. After homogenization they arrived at different Darcy's laws. More precisely, Darcy's law derived by Allaire is nonlocal in time while that obtained by MIKELIĆ [40] coincides with the well known Darcy's law derived by many authors for stationary flow. The aim of the present contribution is to investigate nonstationary flows of Stokesian fluids through linear elastic porous medium, and in particular, to derive macroscopic equations of the Biot type. The scaling of viscosity is assumed. Thus our results extend those due to ALLAIRE [6].

Our considerations differ from those performed in the papers [9 – 12, 22, 24, 25, 27, 37, 38]. In contrast to [10, 11, 12], we do not exploit the time transformation method. The approach employed by us is straightforward and exploits the two-scale asymptotic method which is justified by the two-scale convergence method developed by NGUETSENG [44] and ALLAIRE [7]. The comprehensive papers [2, 15] and the books [14, 20, 33, 46, 47] provide many applications of homogenization methods to modelling the flows through porous media. Stationary flow of electrolytes through such media was studied in [30, 49, 51, 52].

The plan of the paper is as follows. In Secs. 2 and 3 the microperiodic medium is introduced. Asymptotic homogenization is performed in Sec. 4. In Sec. 5 the formal results obtained in the previous section are justified by the two-scale convergence method. The passage to the stationary case is studied in Sec. 6. In Sec. 7 important earlier contributions are discussed. Two appendices complete the paper.

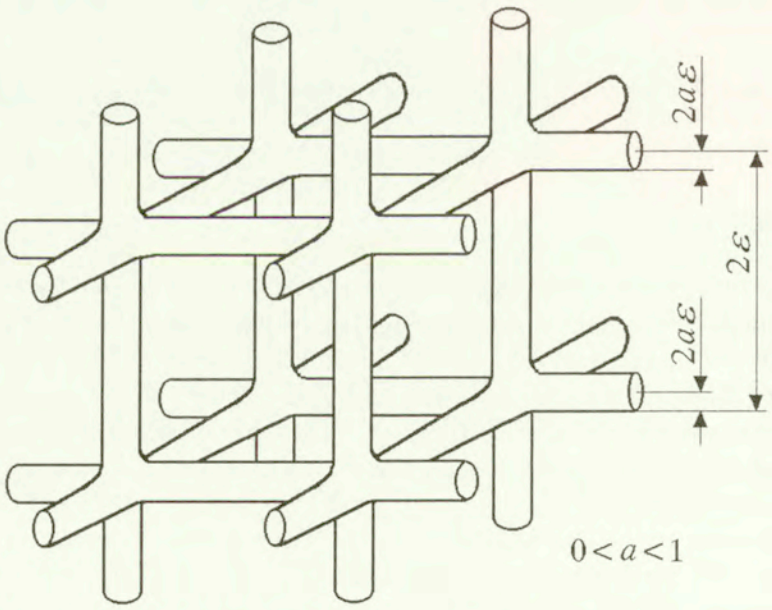

FIG. 1. Example of a skeleton, after ALLAIRE [4].

2. Notations and basic relations

Let $Y = (-1,1)^N \subset \mathbb{R}^N$ $(N \geqslant 2)$ be the basic cell and Y_S – a closed subset of $\overline{Y}$ (the bar denotes the closure of the set), cf. [4, 5]. Further, we set $Y_L = Y \backslash Y_S$; Y_L denotes that part of Y which is occupied by the fluid. Obviously, Y_S stands for the part of Y occupied by the solid. The closed set Y_S is repeated by Y-periodicity

and fills the entire space $\mathbb{R}^N$, in order to obtain a closed set of $\mathbb{R}^N$, denoted E_S; further $E_L = \mathbb{R}^N \backslash E_S$ and $E_S = \{(x_1, x_2, \ldots, x_N) \in \mathbb{R}^N \mid \exists (k_1, \ldots, k_N) \in \mathbb{Z}^N$ such that $(x_1 - 2k_1, \ldots, x_N - 2k_N) \in Y_S\}$. Here $\mathbb{Z}$ denotes the set of integers.

HYPOTHESES, cf. [4]

(i) Y_L and Y_S have strictly positive measures in $\overline{Y}$.

(ii) E_L and the interior of E_S are open sets with boundary of class C^1, and are locally situated on one side of their boundary. Moreover, E_L is connected.

(iii) Y_L is an open connected set with a locally Lipschitz boundary.

REMARK 2.1. The hypothesis (i) implies that the elementary cell Y contains fluid and solid together. Next, (ii) says that Y_L is Y-periodic (E_L has a boundary of class C^1) and $\overline{Y}$ has an intersection with each of its faces which has a strictly positive surface measure, cf. Figs. 2, 3.

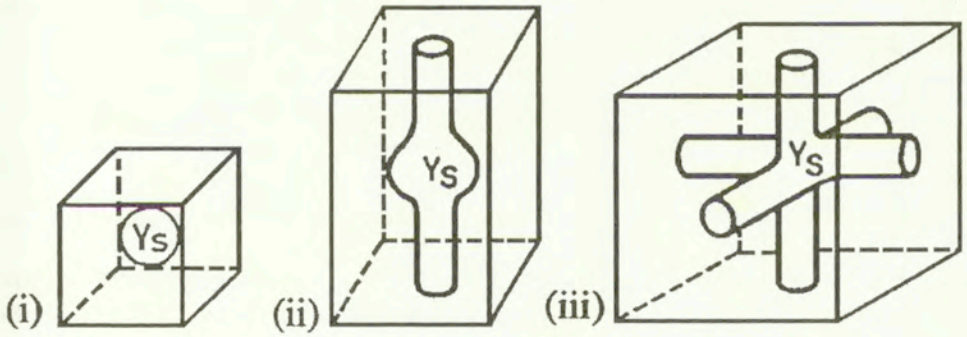

FIG. 2. Three typical situations, which agree with hypotheses (i)-(iii), after ALLAIRE [4].

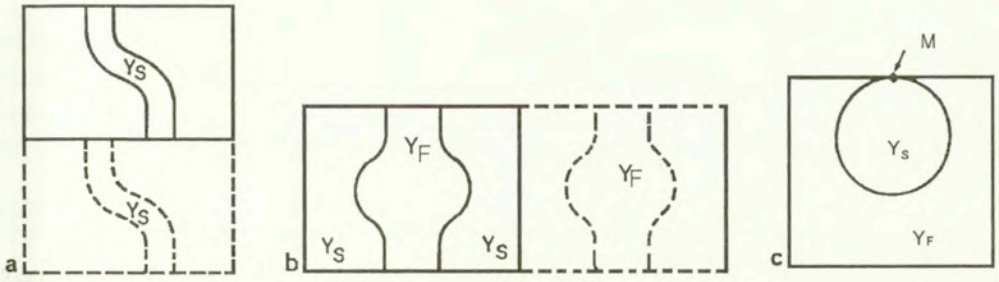

FIG. 3. Forbidden situations. (a) The boundary of E_S is not of class C^1 because Y_S is not Y-periodic. (b) No contact between the fluid parts of two adjacent cells implies that E_L is not connected. (c) Although E_L has a smooth boundary, ∂Y_L is not locally Lipschitz at point M, after ALLAIRE (1989).

Let Ω be an open bounded and connected set of $\mathbb{R}^N$ with the boundary $\partial\Omega$ of class C^1. In fact, it is sufficient to assume that $\partial\Omega$ and ∂E_L are locally Lipschitz. The domain Ω is assumed to have an εY-periodic structure, $\varepsilon = l/\mathsf{L}$, where l, L, are typical length scales associated with pores and the region and Ω, respectively. Next, we set

$$\Omega_L^\varepsilon = \Omega \setminus \bigcup_{i=1}^{N(\varepsilon)} Y_{S_i}^\varepsilon, \qquad \Omega_S^\varepsilon = \Omega \setminus \Omega_L^\varepsilon. \tag{2.1}$$

The set Ω is covered with a regular mesh of size ε, each cell being a cube Y_i^ε, $1 \leqslant i \leqslant N(\varepsilon)$, and

$$N(\varepsilon) = \frac{|\Omega|}{(2\varepsilon)^N}[1 + o(1)]. \tag{2.2}$$

The interface solid-liquid is denoted by Γ^ε; $\partial\Omega_S^\varepsilon$ ($\partial\Omega_L^\varepsilon$) is the boundary of Ω_S^ε (Ω_L^ε). For more details related to the description of the porous body the reader is referred to [4].
We set

$$\langle(\cdot)\rangle = \frac{1}{|Y|}\int_Y (\cdot)\,dy, \qquad \langle(\cdot)\rangle_\alpha = \frac{1}{|Y|}\int_{Y_\alpha} (\cdot)\,dy, \qquad \alpha = S, L \tag{2.3}$$

and $\partial Y_S = \Gamma_Y \cup P_S$, $\partial Y_L = \Gamma_Y \cup P_L$; Γ_Y is the local solid-liquid contact surface; and P_S and P_L are the parts of the surfaces of the solid and liquid, respectively, coinciding with the boundary of Y. The porosity f is defined as the volume fraction of the liquid in the considered solid-liquid composite medium

$$f = \frac{|Y_L|}{|Y|}, \qquad 1 - f = \frac{|Y_S|}{|Y|}. \tag{2.4}$$

By $\mathbf{n} = \mathbf{n}^L$ we denote the exterior unit vector normal to $\partial\Omega_L^\varepsilon$.

3. Equations of microperiodic porous media

For a fixed $\varepsilon > 0$ all the relevant quantities are denoted by the superscript ε. Let us denote by $\mathbf{u}^\varepsilon$ and $\mathbf{v}^\varepsilon$ the fields of displacements in the elastic skeleton and the velocity field in Ω_L^ε, respectively. By p^ε we denote the pressure in the liquid phase. These fields satisfy the following equations:

$$
(3.1)\qquad \left|\begin{array}{l}
\varrho^S \ddot{u}_i^\varepsilon(t,x) = \dfrac{\partial}{\partial x_j}\Big(a_{ijmn} e_{mn}(\boldsymbol{u}^\varepsilon(t,x))\Big) + F_i^S(t,x) \quad \text{in} \quad (0,T)\times\Omega_S^\varepsilon,\\
\varrho^L \dot{v}_i(t,x) = \dfrac{\partial}{\partial x_j}\Big(-p^\varepsilon(t,x)\delta_{ij} + \varepsilon^2 \eta_{ijmn} e_{mn}\left(\mathbf{v}^\varepsilon(t,x)\right)\Big) + F_i^L(t,x)\\
\qquad\qquad\qquad\qquad\qquad\qquad\qquad\qquad\qquad\qquad \text{in} \quad (0,T)\times\Omega_L^\varepsilon,\\
\operatorname{div}\mathbf{v}^\varepsilon(t,x) = 0 \qquad \text{in} \qquad (0,T)\times\Omega_L^\varepsilon.
\end{array}\right.
$$

The conditions imposed on the solid-liquid interface Γ^ε read

$$
(3.2)\qquad [\![\sigma_{ij}^\varepsilon]\!] n_j = 0 \quad \text{on} \quad (0,T)\times\Gamma^\varepsilon,
$$

$$
(3.3)\qquad \mathbf{v}^\varepsilon(t,x) = \dot{\mathbf{u}}^\varepsilon(t,x) \quad \text{on} \quad (0,T)\times\Gamma^\varepsilon.
$$

The stress tensor $\boldsymbol{\sigma}^\varepsilon$ is specified by

$$
(3.4)\qquad \sigma_{ij}^\varepsilon = \begin{cases} a_{ijmn} e_{mn}(\mathbf{u}^\varepsilon) & \text{in} \quad (0,T)\times\Omega_S^\varepsilon,\\ -p^\varepsilon\delta_{ij} + \varepsilon^2\eta_{ijmn} e_{mn}(\mathbf{v}^\varepsilon) & \text{in} \quad (0,T)\times\Omega_L^\varepsilon. \end{cases}
$$

Here $e_{ij}(\boldsymbol{z}) = z_{(i,j)} = \dfrac{1}{2}\left(\dfrac{\partial z_i}{\partial x_j} + \dfrac{\partial z_j}{\partial x_i}\right)$, $\mathbf{F}^S$ and $\mathbf{F}^L$ stand for the body forces. The jump $[\![\sigma_{ij}^\varepsilon]\!]$ on Γ^ε is given by

$$
[\![\sigma_{ij}^\varepsilon]\!] n_j = \sigma_{ij}^{L\varepsilon} n_j - \sigma_{ij}^{S\varepsilon} n_j.
$$

For an isotropic liquid the tensor $\boldsymbol{\eta} = (\eta_{ijkl})$ takes the following form:

$$
\eta_{ijmn} = \eta(\delta_{im}\delta_{jn} + \delta_{jm}\delta_{in} - \frac{2}{3}\delta_{ij}\delta_{mn}),
$$

where η denotes the viscosity. For the sake of simplicity, the nonlinear convective term in the equations of the fluid motion has been neglected. The moduli a_{ijkl} and η_{ijkl} satisfy the standard symmetry and coercivity conditions. Note that in Eq. $(3.1)_2$ and $(3.4)_2$ the following rescaling is introduced, cf. [4, 6, 22]

$$
(3.5)\qquad \eta_{ijmn} \rightsquigarrow \varepsilon^2 \eta_{ijmn}.
$$

According to the method of two-scale asymptotic expansions we make the following *Ansatz*, cf. [47]:

$$
(3.6)\qquad \begin{aligned} p^\varepsilon(t,x) &= p^{(0)}(t,x,y) + \varepsilon p^{(1)}(t,x,y) + \varepsilon^2 p^{(2)}(t,x,y) + \ldots, \qquad y = x/\varepsilon,\\ \mathbf{u}^\varepsilon(t,x) &= \mathbf{u}^{(0)}(t,x,y) + \varepsilon \mathbf{u}^{(1)}(t,x,y) + \varepsilon^2 \mathbf{u}^{(2)}(t,x,y) + \ldots, \qquad y = x/\varepsilon, \end{aligned}
$$

and similarly for $\mathbf{v}^\varepsilon(t,x)$. The functions $p^{(0)}(t,x,y)$, $p^{(1)}(t,x,y)$, etc., and $\mathbf{u}^{(0)}(t,x,y)$, $\mathbf{u}^{(1)}(t,x,y)$ etc., are Y-periodic in y.

The parabolic-hyperbolic system of Eqs. (3.1) – (3.4) is to be supplemented by the initial conditions, here assumed to be homogeneous

$$\mathbf{v}^\varepsilon(0,x) = \mathbf{0} \qquad \text{in} \qquad \Omega_L^\varepsilon,$$

$$\mathbf{u}^\varepsilon(0,x) = \mathbf{0}; \qquad \dot{\mathbf{u}}^\varepsilon(0,x) = \mathbf{0} \quad \text{in} \qquad \Omega_S^\varepsilon.$$

Next, taking into account the formula for the total derivative

$$\frac{d}{dx_i} f(x,y) = \left(\frac{\partial}{\partial x_i} + \frac{1}{\varepsilon}\frac{\partial}{\partial y_i}\right) f(x,y), \qquad y = \frac{x}{\varepsilon},$$

and comparing terms with the same power of ε, we arrive at the homogenized set of equations.

We observe that the quasi-stationary flow of a viscous fluid through a linear elastic microperiodic media was examined in [9].

4. Homogenization

The interface condition (3.2) can be rewritten as follows:

$$a_{ijmn} e_{mn}(\mathbf{u}^\varepsilon) n_j = \left(-p^\varepsilon \delta_{ij} + \varepsilon^2 \eta_{ijmn} \frac{\partial v_m^\varepsilon}{\partial x_n}\right) n_j. \tag{4.1}$$

After substitution of expansions (3.6) we get

$$\left[a_{ijmn}\left(\frac{\partial}{\partial x_n} + \frac{1}{\varepsilon}\frac{\partial}{\partial y_n}\right)\left(u_m^{(0)} + \varepsilon u_m^{(1)} + \varepsilon^2 u_m^{(2)} + \ldots\right)\right] n_j = -(p^{(0)} + \varepsilon p^{(1)} \tag{4.2}$$

$$+\varepsilon^2 p^{(2)} + \ldots)\delta_{ij} n_j + \varepsilon^2 \eta_{ijmn}\left(\frac{\partial}{\partial x_n} + \frac{1}{\varepsilon}\frac{\partial}{\partial y_n}\right)(v_m^{(0)} + \varepsilon v_m^{(1)} + \ldots) n_j$$

$$\text{on} \quad (0,T) \times \Gamma^\varepsilon.$$

Comparing the terms associated with ε^{-1} we obtain

$$a_{ijmn} e_{mn}^y(\mathbf{u}^{(0)}) N_j = 0 \qquad \text{on} \quad (0,T) \times \Omega \times \Gamma_Y, \tag{4.3}$$

where $e_{ij}^y(\boldsymbol{\xi}) = \left(\frac{\partial \xi_i}{\partial y_j} + \frac{\partial \xi_j}{\partial y_i}\right)/2$ and $\mathbf{N}$ stands for the exterior unit vector normal to ∂Y_L. Further, the terms linked with ε^0 in Eq. (4.2) yield

$$\left[a_{ijmn}\left(\frac{\partial u_m^{(0)}}{\partial x_n} + \frac{\partial u_m^{(1)}}{\partial y_n}\right)\right] N_j = -p^{(0)} N_i. \tag{4.4}$$

It can be shown that, cf. (A.3),

$$\mathbf{u}^{(0)} = \mathbf{u}^{(0)}(t,x). \tag{4.5}$$

Equations (A.4) and (4.4) are satisfied provided that

$$u_m^{(1)}(t,x,y) = A_m^{(pq)}(t,x,y)\,\frac{\partial}{\partial x_q}u_p^{(0)}(t,x) + P^{(m)}(t,x,y)\,p^{(0)}(t,x), \tag{4.6}$$

and the functions $\mathbf{A}^{(pq)}$ and $P^{(m)}$ are Y-periodic solutions to the following local equations on $(0,T)\times Y_S$:

$$\begin{aligned} \frac{\partial}{\partial y_j}\Big(a_{ijpq} + a_{ijmn}e_{mn}^y(\mathbf{A}^{(pq)})\Big) &= 0, \\ \frac{\partial}{\partial y_j}\Big(a_{ijmn}\frac{\partial}{\partial y_n}P^{(m)} + \delta_{ij}\Big) &= 0. \end{aligned} \tag{4.7}$$

Hence we get

$$\begin{aligned} \Big(a_{ijpq} + a_{ijmn}e_{mn}^y(\mathbf{A}^{(pq)})\Big)N_j = 0, \quad &\text{on} \qquad (0,T)\times\Gamma_Y, \\ \Big(a_{ijmn}\frac{\partial}{\partial y_n}P^{(m)} + \delta_{ij}\Big)N_j = 0, \quad &\text{on} \qquad (0,T)\times\Gamma_Y. \end{aligned} \tag{4.8}$$

In (4.7) and (4.8) the macroscopic variable x is treated as a parameter.

The interface condition (3.3) assumes the form

$$\begin{aligned} \dot{\mathbf{u}}^{(0)}(t,x) + \varepsilon\dot{\mathbf{u}}^{(1)}(t,x,y) + \varepsilon^2\dot{\mathbf{u}}^{(2)}(t,x,y) + \ldots \\ = \mathbf{v}^{(0)}(t,x,y) + \varepsilon\mathbf{v}^{(1)}(t,x,y) + \varepsilon^2\mathbf{v}^{(2)}(t,x,y) + \ldots \end{aligned} \tag{4.9}$$

Hence we obtain

$$\dot{\mathbf{u}}^{(\ell)} = \mathbf{v}^{(\ell)}, \qquad \ell = 0,1,2,\ldots \tag{4.10}$$

Applying asymptotic expansions to the constitutive relation (3.4) and comparing the terms linked with ε^0 we get

$$\sigma_{ij}^{(0)} = \begin{cases} a_{ijmn}\Big(e_{mn}(\mathbf{u}^{(0)}) + e_{mn}^y(\mathbf{u}^{(1)})\Big) & \text{in} \quad (0,T)\times\Omega\times Y_S, \\ -p^{(0)}\delta_{ij} & \text{in} \quad (0,T)\times\Omega\times Y_L. \end{cases} \tag{4.11}$$

We observe that

$$\langle\sigma_{ij}^{(0)}\rangle = \langle\sigma_{ij}^{(0)}\rangle_S + \langle\sigma_{ij}^{(0)}\rangle_L. \tag{4.12}$$

Using Eqs. (4.6), (4.11) and (4.12) we get

$$\langle \sigma_{ij}^{(0)} \rangle = a_{ijpq}^{h} e_{pq}(\mathbf{u}^{(0)}) + \Big(\langle a_{ijmn} \frac{\partial}{\partial y_n} P^{(m)} \rangle_S - f\delta_{ij} \Big) p^{(0)}, \tag{4.13}$$

where

$$a_{ijpq}^{h} = \langle a_{ijpq} + a_{ijmn} e_{mn}(\mathbf{A}^{(pq)}) \rangle_S. \tag{4.14}$$

The coefficients $\mathbf{A}^{(pq)}$ and $P^{(m)}$ are to be determined from the local equations (4.7) jointly with Eq. (4.8).

From Eqs. $(3.1)_1$ and $(3.1)_2$, by comparing the terms linked with ε^0 we get

$$\varrho^S \ddot{u}_i^{(0)} = F_i^S + \frac{\partial}{\partial x_j} \Big[a_{ijmn} \Big(e_{mn}(\mathbf{u}^{(0)}) + e_{mn}^y(\mathbf{u}^{(1)}) \Big) \Big] + \frac{\partial}{\partial y_j} \Big[a_{ijmn} \Big(e_{mn}(\mathbf{u}^{(1)}) + e_{mn}^y(\mathbf{u}^{(2)}) \Big) \Big] \quad \text{in} \quad (0,T) \times \Omega \times Y_S, \tag{4.15}$$

$$\varrho^L \dot{v}_i^{(0)} = F_i^L - \frac{\partial}{\partial x_i} p^{(0)} - \frac{\partial}{\partial y_i} p^{(1)} + \frac{\partial}{\partial y_j} \Big(\eta_{ijmn} e_{mn}^y(\boldsymbol{v}^{(0)}) \Big) \quad \text{in} \quad (0,T) \times \Omega \times Y_L. \tag{4.16}$$

On the other hand, the terms linked with ε in the interface condition (4.2) lead to the relation

$$\Big[a_{ijmn} \Big(e_{mn}(\mathbf{u}^{(1)}) + e_{mn}^y(\mathbf{u}^{(2)}) \Big) \Big] N_j = \Big(-p^{(1)} \delta_{ij} - \eta_{ijmn} e_{mn}(\mathbf{v}^{(0)}) \Big) N_j \quad \text{on} \quad (0,T) \times \Omega \times \Gamma_Y. \tag{4.17}$$

Integration of Eq. (4.15) over Y_S and (4.16) over Y_L yields

$$\begin{aligned} (1-f)\varrho^S \ddot{u}_i^{(0)} &= (1-f) F_i^S + \frac{\partial}{\partial x_j} \langle a_{ijmn} \Big(e_{mn}(\mathbf{u}^{(0)}) + e_{mn}^y(\mathbf{u}^{(1)}) \Big) \rangle_S \\ &\quad - \frac{1}{|Y|} \int\limits_{\partial Y_S} \Big[a_{ijmn} \Big(e_{mn}(\mathbf{u}^{(1)}) + e_{mn}^y(\mathbf{u}^{(2)}) \Big) \Big] N_j \, dA \quad \text{in} \quad (0,T) \times \Omega, \end{aligned} \tag{4.18}$$

$$\langle \varrho^L \dot{v}_i^{(0)} \rangle_L = f F_i^L - f \frac{\partial}{\partial x_i} p^{(0)} + \frac{1}{|Y|} \int\limits_{\partial Y_L} \Big[-p^{(1)} \delta_{ij} + \eta_{ijmn} e_{mn}^y(\mathbf{v}^{(0)}) \Big] N_j \, dA, \quad \text{in} \quad (0,T) \times \Omega.$$

Adding Eqs. (4.18), using the interface relation (4.17) and taking into account (4.11) and (4.12), we arrive at

$$(4.19)\qquad (1-f)\varrho^S \ddot{u}_i^{(0)} + \varrho^L \langle \dot{v}_i^{(0)} \rangle_L = \frac{\partial}{\partial x_j}\langle \sigma_{ij}^{(0)} \rangle + (1-f)F_i^S + fF_i^L \quad \text{in} \quad (0,T)\times\Omega.$$

This is the macroscopic equation of motion of the porous medium filled with liquid.

Since $\mathbf{u}^{(0)} = \mathbf{u}^{(0)}(t,x)$, therefore (4.16) furnishes

$$(4.20)\qquad \varrho^L \dot{\overline{v}}_i^{(0)} = F_i^L - \varrho^L \ddot{u}_i^{(0)} - \frac{\partial}{\partial x_i}p^{(0)} - \frac{\partial}{\partial y_i}p^{(1)} + \frac{\partial}{\partial y_j}\Big(\eta_{ijmn} e^y_{mn}(\overline{\mathbf{v}}^{(0)})\Big),$$

where

$$(4.21)\qquad \overline{v}_m^{(0)}(t,x,y) = v_m^{(0)}(t,x,y) - \dot{u}_m^{(0)}(t,x) \qquad \text{on} \quad (0,T)\times\Omega\times\Gamma_Y.$$

In virtue of (4.10), for $\ell = 0$ we get

$$(4.22)\qquad \overline{\mathbf{v}}^{(0)}(t,x,y) = \mathbf{0} \qquad \text{on} \quad (0,T)\times\Omega\times\Gamma_Y.$$

Since the problem considered is linear, therefore $p^{(1)}$ is of the form

$$(4.23)\qquad p^{(1)}(t,x,y) = \gamma^{(m)}(t,y)\Big(F_m^L(t,x) - \varrho^L \ddot{u}_m^{(0)}(t,x) - \frac{\partial}{\partial x_m}p^{(0)}(t,x)\Big),$$

where $\gamma^{(m)}$ is Y-periodic in y. Then Eq. (4.20) is written as follows:

$$(4.24)\qquad \varrho^L \dot{\overline{v}}_i^{(0)} = \left(F_m^L - \varrho^L \ddot{u}_m^{(0)} - \frac{\partial}{\partial x_m}p^{(0)}\right)\left(\delta_{im} - \frac{\partial}{\partial y_i}\gamma^{(m)}\right) + \frac{\partial}{\partial y_j}\left(\eta_{ijmn}\frac{\partial}{\partial y_n}\overline{v}_m^{(0)}\right).$$

The last equation is satisfied provided that $\overline{\mathbf{v}}^{(0)}$ is given in the form of time-convolution

$$(4.25)\qquad \overline{v}_m^{(0)}(t,x,y) = \frac{1}{\varrho^L}\int_0^t \Big(F_s^L(\tau,x) - \varrho^L \ddot{u}_s^{(0)}(\tau,x) - \frac{\partial}{\partial x_s}p^{(0)}(\tau,x)\Big)\,\chi_m^{(s)}(t-\tau,y)\,d\tau \qquad \text{in } (0,T)\times\Omega\times Y_L.$$

The functions $\gamma^{(m)}(t,y)$ and $\chi_m^{(s)}(t,y)$ are Y-periodic solutions to the following local problem:

$$(4.26)\qquad \frac{\partial}{\partial y_j}\Big(\eta_{ijmn} e^y_{mn}(\chi^{(k)}(t,y))\Big) = \left[\varrho^L \frac{\partial \chi_m^{(k)}}{\partial t}(t,y) - \left(\delta_{km} - \frac{\partial}{\partial y_m}\gamma^{(k)}(t,y)\right)\delta(t)\right]\delta_{im} \qquad \text{in} \quad (0,T)\times Y_L,$$

$$\text{(4.27)} \qquad \operatorname{div}_y \chi^{(i)} = \frac{\partial \chi_k^{(i)}}{\partial y_k} = 0,$$

$$\chi^{(k)}(t,y) = \mathbf{0} \qquad \text{on} \quad (0,T) \times \Gamma_Y, \qquad \chi^{(k)}(0,y) = \mathbf{0} \qquad \text{in } Y_L,$$

where $\delta(t)$ stands for the Dirac delta. The relation (4.26) is a consequence of (A.9), and relation (4.27) is a consequence of Eqs. (4.21), (4.5) and the local incompressibility condition $\operatorname{div}_y \mathbf{v}^{(0)} = 0$, cf. (A.7).

After averaging of (4.25) we get

$$\text{(4.28)} \qquad \langle \overline{v}_m^{(0)} \rangle_L = \frac{1}{\varrho^L} \int_0^t \langle \chi_m^{(s)}(t-\tau, y) \rangle_L \left(F_s^L(\tau, x) - \varrho^L \ddot{u}_s^{(0)}(\tau, x) \right.$$

$$\left. - \frac{\partial}{\partial x_s} p^{(0)}(\tau, x) \right) d\tau.$$

The last relation is the *nonstationary Darcy's law*.

From Eq. $(3.1)_3$, comparing the terms associated with ε^0 we conclude

$$\text{(4.29)} \qquad \operatorname{div}_x \mathbf{v}^{(0)}(t,x,y) + \operatorname{div}_y \mathbf{v}^{(1)}(t,x,y) = 0 \qquad \text{in} \quad (0,T) \times \Omega \times Y_L.$$

Hence, after averaging we get

$$\operatorname{div}_x \langle \mathbf{v}^{(0)} \rangle_L = -\langle \operatorname{div}_y \mathbf{v}^{(1)} \rangle_L, \qquad \text{in} \quad (0,T) \times \Omega,$$

or

$$\text{(4.30)} \qquad \operatorname{div}_x \langle \mathbf{v}^{(0)}(t,x,y) \rangle_L = -\frac{1}{|Y|} \int_{\partial Y_L} v_i^{(1)}(t,x,y) N_i \, dA.$$

Moreover, in virtue of (4.21), (4.22), (4.6) and periodicity of $\dot{\mathbf{u}}^{(1)}$, $\mathbf{v}^{(1)}$ with respect to y, we also have

$$\text{(4.31)} \qquad \operatorname{div}_x \langle \mathbf{v}^{(0)}(t,x,y) \rangle_L = \frac{1}{|Y|} \int_{\partial Y_S} \dot{u}_i^{(1)}(t,x,y) N_i \, dA$$

$$= \frac{1}{|Y|} \int_{\partial Y_S} \frac{\partial}{\partial t} \left[A_m^{(pq)}(t,x,y) \frac{\partial}{\partial x_q} u_p^{(0)}(t,x) + P^{(m)}(t,x) p^{(0)}(t,x) \right] N_m \, dA,$$

or

$$\text{(4.32)} \qquad \operatorname{div}_x \langle \mathbf{v}^{(0)} \rangle_L = \frac{\partial}{\partial t} \left[\langle e_{mnm}^y(\mathbf{A}^{(pq)}(t,x,y)) \rangle_S \, e_{pq}(\mathbf{u}^{(0)}(t,x)) \right.$$

$$\left. + \langle \frac{\partial}{\partial y_m} P^{(m)}(t,x) \rangle_S \, p^{(0)}(t,x) \right].$$

Equations (4.28) and (4.32) are Biot's type equations modelling the nonstationary flow of viscous fluid through the microperiodic porous media. Jointly with

Eq. (4.19) they constitute a system of 7 equations for the determination of 7 macroscopic fields: $\mathbf{u}^{(0)}, \langle \mathbf{v}^{(0)} \rangle_L$ and $p^{(0)}$.

REMARK 4.1. Let us set $\chi^{(k)} = \dot{\mathbf{w}}^{(k)}$ and $\gamma^{(k)} = \dot{q}^{(k)}$ in (4.26) and (4.27), and perform integration over the interval $(0,t)$. Then we obtain:

$$\varrho^L \dot{\mathbf{w}}^{(k)}(t,y) = \operatorname{div}_y (\eta \mathbf{e}^y(\mathbf{w}^{(k)}(t,y))) - \nabla_y q^{(k)}(t,y) + \mathbf{e}_k, \quad \text{in} \quad (0,T) \times Y_L,$$

$$\operatorname{div}_y \mathbf{w}^{(k)}(t,y) = 0, \quad \text{in} \quad (0,T) \times Y_L, \tag{4.33}$$

$$\mathbf{w}^{(k)}(t,y) = 0 \quad \text{in} \quad (0,T) \times \Gamma_Y, \qquad \mathbf{w}^{(k)}(0,y) = 0 \quad \text{on} \quad Y_L,$$

where $\mathbf{e}_k$ $(k = 1, \dots N)$ are the unit base vectors in $\mathbb{R}^N$. The local problem (4.33) coincides with the corresponding local problem derived by ALLAIRE [6] for the flow through rigid skeleton. The Darcy law (4.28), however, involves the motion of the elastic skeleton. The permeability matrix $\mathbf{A}(t)$ is given by

$$A_{ij}(t) = \frac{1}{\varrho^L |Y|} \int_{Y_L} \frac{\partial \mathbf{w}^{(i)}(t,y)}{\partial t} \cdot \mathbf{e}_j \, dy = \frac{1}{|Y|} \int_{Y_L} \dot{\mathbf{w}}^{(i)} \cdot \dot{\mathbf{w}}^{(j)} \, dy + \frac{1}{\varrho^L |Y|} \int_{Y_L} \eta_{mnpq} e^y_{pq}(\mathbf{w}^{(i)}) e^y_{mn}(\dot{\mathbf{w}}^{(j)}) \, dy. \tag{4.34}$$

The last formula is obtained from $(4.33)_1$ by multiplying it by $\dot{\mathbf{w}}^{(j)}$ and dividing by ϱ^L. Performing then averaging over Y, integrating by parts and exploiting the periodicity conditions, we arrive at (4.34).

REMARK 4.2. The system (4.19), (4.28) and (4.32) involves the macroscopic displacement field $\mathbf{u}^{(0)}$, macroscopic velocity $\langle \mathbf{v}^{(0)} \rangle_L$ and macroscopic pressure $p^{(0)}$. Various boundary conditions can be imposed to solve the initial-boundary value problem for such system, cf. [9, 35]. For instance, let $\partial\Omega = \overline{\Gamma}_0 \cup \overline{\Gamma}_1$. On Γ_0 one can assume the homogeneous Dirichlet conditions whilst on the complementary part Γ_1 the homogeneous Neumann conditions are plausible.

REMARK 4.3. It would be interesting to weaken the assumption of periodicity and exploit the ideas proposed in [3, 21].

5. Justification of the asymptotic analysis by the two-scale convergence

The aim of this section is to justify rigorously the results obtained by the formal method of two-scale asymptotic expansions. To this end, we exploit the notion of the two-scale convergence, cf. [7] and Appendix B.

For the sake of simplicity we assume that the liquid is isotropic with the viscosity $\eta = 1$.

Consequently, the following system of equations is investigated:

$$\varrho^S \ddot{\mathbf{u}}^\varepsilon(t,x) = \operatorname{div}[\mathbf{a}\,\mathbf{e}(\mathbf{u}^\varepsilon(t,x))] + \mathbf{F}^S(t,x) \quad \text{in} \quad (0,T)\times\Omega_S^\varepsilon, \tag{5.1}$$

$$\varrho^L \dot{\mathbf{v}}^\varepsilon(t,x) = \varepsilon^2 \Delta \mathbf{v}^\varepsilon(t,x) - \nabla p^\varepsilon(t,x) + \mathbf{F}^L(t,x) \quad \text{in} \quad (0,T)\times\Omega_L^\varepsilon, \tag{5.2}$$

$$\operatorname{div}\mathbf{v}^\varepsilon(t,x) = 0 \quad \text{in} \quad (0,T)\times\Omega_L^\varepsilon, \tag{5.3}$$

$$(\mathbf{a}\,\mathbf{e}(\mathbf{u}^\varepsilon))\,\mathbf{n} = (-p^\varepsilon \mathbf{I} + \varepsilon^2 \mathbf{e}(\mathbf{v}^\varepsilon))\,\mathbf{n} \quad \text{on} \quad (0,T)\times\Gamma^\varepsilon, \tag{5.4}$$

$$\mathbf{v}^\varepsilon(t,x) = \dot{\mathbf{u}}(t,x) \quad \text{on} \quad (0,T)\times\Gamma^\varepsilon, \tag{5.5}$$

$$\mathbf{u}^\varepsilon(0,x) = \dot{\mathbf{u}}(0,x) = 0 \quad \text{in} \quad \Omega_S^\varepsilon, \qquad \dot{\mathbf{v}}^\varepsilon(0,x) = 0 \quad \text{in} \quad \Omega_L^\varepsilon. \tag{5.6}$$

For definitions of Lebesgue and Sobolev spaces the reader is referred to the book by ADAMS [1]. The main result of this section is formulated as

THEOREM 5.1. *The sequence* $\{\mathbf{u}^\varepsilon, \mathbf{v}^\varepsilon, \mathbf{p}^\varepsilon\}_{\varepsilon>0}$ *of solutions of the system (5.1) – (5.6) two-scale converges to the solution* $(\mathbf{u}^{(0)}(t,x), \mathbf{v}^{(0)}(t,x,y), p^{(0)}(t,x))$ *of the two-scale homogenized problem:*

$$(1-f)\varrho^S \ddot{\mathbf{u}}^\varepsilon(t,x) + \varrho^L \langle \dot{\mathbf{v}}^{(0)} \rangle_{Y_L} = \operatorname{div}_x \int_{Y_S} [\mathbf{a} : (\nabla_x \mathbf{u}^{(0)} + \nabla_y \mathbf{u}^{(1)})]\, dy \tag{5.7}$$

$$- \int_{Y_L} \nabla_y p^{(1)}(t,x,y)\, dy - f\nabla_x p^{(0)}(t,x) + (1-f)\mathbf{F}^S(t,x) + f\mathbf{F}^L(t,x)$$

$$\text{in} \quad (0,T)\times\Omega,$$

$$\operatorname{div}_y[\mathbf{a} : (\nabla_x \mathbf{u}^{(0)}(t,x) + \nabla_y \mathbf{u}^{(1)}(t,x,y))] = 0 \quad \text{in} \quad (0,T)\times\Omega\times Y_S, \tag{5.8}$$

$$\varrho^L \dot{\mathbf{v}}^{(0)}(t,x,y) = \Delta_y \mathbf{v}^{(0)}(t,x,y) - \nabla_x p^{(0)}(t,x) - \nabla_y p^{(1)}(t,x,y) \tag{5.9}$$

$$+ \mathbf{F}^L(t,x) \quad \text{in} \quad (0,T)\times\Omega\times Y_L,$$

$$\text{(5.10)} \qquad \operatorname{div}_y \mathbf{v}^{(0)}(t,x,y) = 0 \qquad \text{in} \quad (0,T)\times\Omega\times Y_L,$$

$$\text{(5.11)} \qquad \operatorname{div}_x \int_{Y_L} \mathbf{v}^{(0)}(t,x,y)dy = \frac{1}{|Y|}\int_{\Gamma_Y} \dot{\mathbf{u}}^{(1)}(t,x,y)\cdot\mathbf{N}\,ds \qquad \text{in} \quad (0,T)\times\Omega,$$

$$\text{(5.12)} \qquad \mathbf{a} : (\nabla_x \mathbf{u}^{(0)}(t,x) + \nabla_y \mathbf{u}^{(1)}(t,x,y))\mathbf{N} = -p^{(0)}(t,x)\mathbf{N}$$
$$\text{in} \qquad (0,T)\times\Omega\times\Gamma_Y,$$

$$\text{(5.13)} \qquad \mathbf{u}^{(0)}(0,x) = \dot{\mathbf{u}}^{(0)}(0,x) = \mathbf{0} \qquad \text{in} \quad \Omega,$$

$$\text{(5.14)} \qquad \mathbf{v}^{(0)}(0,x,y) = \mathbf{0} \qquad \text{in} \quad \Omega\times Y_F.$$

P r o o f. It is not difficult to show that there exists a constant $c > 0$ independent of ε such that

$$\|\mathbf{u}^\varepsilon\|_{H^1(\Omega)^3} \leqslant c,\ \|\mathbf{v}^\varepsilon\|_{L^2(\Omega)^3} \leqslant c,\ \varepsilon\|\nabla\mathbf{v}^\varepsilon\|_{L^2(\Omega,\mathbb{E}^N)} \leqslant c,$$

where $\mathbb{E}^N$ stands for the space of $N\times N$ matrices. The two-scale limits of these sequences satisfy the following properties, cf. Appendix B:

$$\operatorname{div}_y \mathbf{v}^{(0)}(t,x,y) = 0 \qquad \text{in} \qquad (0,T)\times\Omega\times Y_L,$$

$$\operatorname{div}_x \mathbf{v}^{(0)}(t,x,y) + \operatorname{div}_y \mathbf{v}^{(1)}(t,x,y) = 0 \qquad \text{in} \qquad (0,T)\times\Omega\times Y_L,$$

$$\nabla_y \mathbf{u}^{(0)}(t,x,y) = 0, \qquad \text{or} \qquad \mathbf{u}^{(0)} = \mathbf{u}^{(0)}(t,x),\ t\in(0,T),\ x\in\Omega.$$

Moreover from (5.2) one can conclude that, cf. [6],

$$\nabla_y p^{(0)}(t,x,y) = 0,\ \text{or}\ p^{(0)} = p^{(0)}(t,x)\ t\in(0,T),\ x\in\Omega.$$

Let $\chi_S^\varepsilon(x)$ and $1-\chi_S^\varepsilon(x) = \chi_L^\varepsilon(x)$ be the characteristic functions of the domains Ω_S^ε and Ω_L^ε, respectively. Let $\phi = \phi(t)\in C^\infty(0,T)$ be such that $\phi(0) = \phi(T) = 0$. Let $\mathbf{\Phi}^\varepsilon(x)$ be a test function such that

$$\mathbf{\Phi}^\varepsilon(x) = \boldsymbol{\eta}(x) + \varepsilon\boldsymbol{\psi}\left(x, \frac{x}{\varepsilon}\right),$$

where $\boldsymbol{\eta}\in\mathcal{D}(\Omega)^3$ and $\boldsymbol{\psi}(x,y)\in\mathcal{D}[\Omega; C^\infty_{per}(Y)]^3$. Multiplying (5.1) by χ_S^ε and (5.2) by χ_L^ε and by the test functions $\phi(t)\mathbf{\Phi}^\varepsilon(x)$ and next integrating over the $[0,T]\times\Omega$ and finally, integrating by parts with respect to time t, we obtain

$$
\begin{aligned}
(5.15)\qquad & \int_0^T\!\!\int_\Omega \chi_S^\varepsilon(x)\varrho^S(x)\mathbf{u}^\varepsilon(t,x)\cdot\left[\boldsymbol{\eta}(x)+\varepsilon\boldsymbol{\psi}\left(x,\frac{x}{\varepsilon}\right)\right]\ddot{\phi}(t)\,dx\,dt \\
& \quad -\int_0^T\!\!\int_\Omega \chi_L^\varepsilon(x)\varrho^L\mathbf{v}^\varepsilon(t,x)\cdot\left[\boldsymbol{\eta}(x)+\varepsilon\boldsymbol{\psi}\left(x,\frac{x}{\varepsilon}\right)\right]\dot{\phi}(t)\,dx\,dt \\
& = \int_0^T\!\!\int_\Omega \chi_S^\varepsilon(x)\,\mathrm{div}[\mathbf{a}\nabla_x\mathbf{u}^\varepsilon(t,x)]\cdot\left[\boldsymbol{\eta}(x)+\varepsilon\boldsymbol{\psi}\left(x,\frac{x}{\varepsilon}\right)\right]\phi(t)\,dx\,dt \\
& \quad +\int_0^T\!\!\int_\Omega \chi_L^\varepsilon(x)\varepsilon^2\Delta\mathbf{v}^\varepsilon(t,x)\cdot\left[\boldsymbol{\eta}(x)+\varepsilon\boldsymbol{\psi}\left(x,\frac{x}{\varepsilon}\right)\right]\phi(t)\,dx\,dt \\
& \quad +\int_0^T\!\!\int_\Omega \chi_L^\varepsilon(x)[-\nabla p^\varepsilon(t,x)]\cdot\left[\boldsymbol{\eta}(x)+\varepsilon\boldsymbol{\psi}\left(x,\frac{x}{\varepsilon}\right)\right]\phi(t)\,dx\,dt \\
& \quad +\int_0^T\!\!\int_\Omega \chi_S^\varepsilon(x)\mathbf{F}^S(t,x)\cdot\left[\boldsymbol{\eta}(x)+\varepsilon\boldsymbol{\psi}\left(x,\frac{x}{\varepsilon}\right)\right]\phi(t)\,dx\,dt \\
& \quad +\int_0^T\!\!\int_\Omega \chi_L^\varepsilon(x)\mathbf{F}^L(t,x)\cdot\left[\boldsymbol{\eta}(x)+\varepsilon\boldsymbol{\psi}\left(x,\frac{x}{\varepsilon}\right)\right]\phi(t)\,dx\,dt.
\end{aligned}
$$

Passing to the two-scale limit when $\varepsilon\to 0$ and applying the Theorems B.2, B.3 for the vector case and eventually making integration by parts with respect to time t, we get

$$
\begin{aligned}
(5.16)\qquad & \int_0^T\!\!\int_\Omega\!\!\int_Y \chi_S(y)\varrho^S\ddot{\mathbf{u}}^{(0)}(t,x)\cdot[\phi(t)\boldsymbol{\eta}(x)]\,dx\,dy\,dt \\
& \quad +\int_0^T\!\!\int_\Omega\!\!\int_Y \chi_L(y)\varrho^L\dot{\mathbf{v}}^{(0)}(t,x,y)\cdot[\phi(t)\boldsymbol{\eta}(x)]\,dx\,dy\,dt \\
& = -\int_0^T\!\!\int_\Omega\!\!\int_Y \chi_S(y)\mathbf{a}\left[\nabla_x\mathbf{u}^{(0)}(t,x)+\nabla_y\mathbf{u}^{(1)}(t,x,y)\right]:[\nabla_x\boldsymbol{\eta}(x) \\
& \quad +\nabla_y\boldsymbol{\psi}(x,y)]\phi(t)\,dx\,dy\,dt+0 \\
& \quad +\int_0^T\!\!\int_\Omega\!\!\int_Y \chi_L(y)p^{(0)}(t,x)[\mathrm{div}_x\boldsymbol{\eta}(x)+\mathrm{div}_y\boldsymbol{\psi}(x,y)]\phi(t)\,dx\,dy\,dt \\
& \quad +\int_0^T\!\!\int_\Omega\!\!\int_Y \left[\chi_S(y)\mathbf{F}^S(t,x)+\chi_L(y)\mathbf{F}_L(t,x)\right]\cdot\boldsymbol{\eta}(x)\phi(t)\,dx\,dy\,dt.
\end{aligned}
$$

We recall that

$$\chi_S^\varepsilon \overset{*}{\rightharpoonup} \frac{1}{|Y|}\int\limits_{Y_S} dy = \frac{|Y_S|}{|Y|} = \frac{1}{|Y|}\int\limits_{Y} \chi_S(y)\,dy \qquad \text{in} \quad L^\infty(Y) \text{ weak}-*,$$

and similarly for χ_L^ε. Let $\boldsymbol{\eta} \equiv \mathbf{0}$ in Eq. (5.16). Then we get

$$\int\limits_0^T \int\limits_\Omega \int\limits_{Y_S} \operatorname{div}_y \left[\mathbf{a}(\nabla_x \mathbf{u}^{(0)} + \nabla_y \mathbf{u}^{(1)})\right] \cdot \boldsymbol{\psi}(x,y)\phi(t)\,dx\,dy\,dt \tag{5.17}$$

$$- \int\limits_0^T \int\limits_\Omega \int\limits_{Y_F} p^{(0)}(t,x) \operatorname{div}_y \boldsymbol{\psi}(x,y)\phi(t)\,dx\,dy\,dt = 0.$$

After some calculations we arrive at

$$\int\limits_0^T \int\limits_\Omega \int\limits_{Y_S} \operatorname{div}_y \left(\mathbf{a}(\nabla_x \mathbf{u}^{(0)} + \nabla_y \mathbf{u}^{(1)}\right) \boldsymbol{\psi}(x,y))\phi(t)\,dx\,dy\,dt \tag{5.18}$$

$$- \int\limits_0^T \int\limits_\Omega \int_{Y_S} \operatorname{div}_y \left[\mathbf{a}\left(\nabla_x \mathbf{u}^{(0)} + \nabla_y \mathbf{u}^{(1)}\right)\right] \cdot \boldsymbol{\psi}(x,y)\phi(t)\,dx\,dy\,dt$$

$$- \int\limits_0^T \int\limits_\Omega \int\limits_{Y_L} \operatorname{div}_y \left[p^{(0)}(t,x)\boldsymbol{\psi}(x,y)\right] \phi(t)\,dx\,dy\,dt = 0.$$

Hence we conclude that

$$\operatorname{div}_y \left[\mathbf{a}\left(\nabla_x \mathbf{u}^{(0)} + \nabla_y \mathbf{u}^{(1)}\right)\right] = 0 \qquad \text{in} \quad (0,T) \times \Omega \times Y_S,$$

and

$$\left[\mathbf{a}\left(\nabla_x \mathbf{u}^{(0)} + \nabla_y \mathbf{u}^{(1)}\right)\right] \mathbf{N} - p^{(0)}\mathbf{N} = 0 \qquad \text{on} \quad (0,T) \times \Omega \times \Gamma_Y.$$

Taking now in (5.16) $\boldsymbol{\psi} \equiv 0$ we obtain

$$(1-f)\varrho^S \ddot{\mathbf{u}}^{(0)}(t,x) + \frac{1}{|Y|}\int\limits_{Y_L} \varrho^L \dot{\mathbf{v}}^{(0)}(t,x,y)\,dy$$

$$= \frac{1}{|Y|}\operatorname{div}_x \int\limits_{Y_S} \mathbf{a}(\nabla_x \mathbf{u}^{(0)} + \nabla \mathbf{u}^{(1)})\,dy$$

$$-f\nabla_x p^{(0)}(t,x) + (1-f)\mathbf{F}^S(t,x) + f\mathbf{F}^L(t,x) \qquad \text{in} \quad (0,T) \times \Omega.$$

Multiplying Eq. (5.2) by a test function $\psi\left(x, \frac{x}{\varepsilon}\right)$ with support in Ω_L^ε and next integrating over Ω, we arrive at

$$\int_\Omega \varrho^L \mathbf{v}^\varepsilon(t,x)\cdot\psi\left(x,\frac{x}{\varepsilon}\right)dx = \int_\Omega \varepsilon^2 \Delta\mathbf{v}^\varepsilon(t,x)\cdot\psi\left(x,\frac{x}{\varepsilon}\right)dx \tag{5.19}$$

$$-\int_\Omega \nabla p^\varepsilon(t,x)\cdot\psi\left(x,\frac{x}{\varepsilon}\right)dx + \int_\Omega \mathbf{F}_L(t,x)\cdot\psi\left(x,\frac{x}{\varepsilon}\right)dx.$$

In the last relation $\mathbf{v}^\varepsilon$ is to be viewed as any extension to Ω such that $\mathbf{v}^\varepsilon = \dot{\mathbf{u}}^\varepsilon$ on Γ^ε, cf. [45]. We have

$$\int_\Omega \varepsilon^2 \Delta\mathbf{v}^\varepsilon\cdot\psi\left(x,\frac{x}{\varepsilon}\right)dx = \int_\Omega \varepsilon^2 \mathrm{div}\left(\nabla\mathbf{v}^\varepsilon\,\psi\left(x,\frac{x}{\varepsilon}\right)\right)dx \tag{5.20}$$

$$-\int_\Omega \varepsilon^2 \nabla\mathbf{v}^\varepsilon : \left[\nabla_x\psi\left(x,\frac{x}{\varepsilon}\right) + \frac{1}{\varepsilon}\nabla_y\psi\left(x,\frac{x}{\varepsilon}\right)\right]dx.$$

Taking into account (5.20) in (5.19) we find the following two-scale limit as $\varepsilon \to 0$:

$$\int_\Omega\int_{Y_L} \varrho^L \dot{\mathbf{v}}^{(0)}(t,x,y)\cdot\psi(x,y)\,dx\,dy \tag{5.21}$$

$$= -\int_\Omega\int_{Y_L} \nabla_y\mathbf{v}^{(0)}(t,x,y) : \nabla_y\psi(x,y)\,dx\,dy - \int_\Omega\int_{Y_L} (\nabla_x p^{(0)}(t,x)$$

$$+\nabla_y p^{(1)}(t,x,y))\cdot\psi(x,y)\,dx\,dy + \int_\Omega\int_{Y_L} \mathbf{F}_L(t,x)\cdot\psi(x,y)\,dx\,dy.$$

From (5.21) we get, cf. Eq. (5.9),

$$\varrho^L\dot{\mathbf{v}}^{(0)}(t,x,y) = \Delta_y\mathbf{v}^{(0)}(t,x,y) - \nabla_x p^{(0)}(t,x) - \nabla_y p^{(1)}(t,x,y)$$

$$+\mathbf{F}^L(t,x) \quad \text{in } (0,T)\times\Omega\times Y_S.$$

This completes the proof. □

6. Passage to the stationary case

ALLAIRE [8] suggested us how to pass to the stationary flow. Assume now that $\eta = 1$, cf. Sec. 5. We observe that the stationary case is not obtained by

simply putting $\dfrac{\partial \mathbf{w}^{(i)}}{\partial t} = 0$, cf. (4.33). In fact we have to pass with time to infinity. We find, cf. (4.34)

$$\int_0^t A_{ij}(t-s)\,ds = \frac{1}{\varrho^L|Y|}\int_{Y_L}\left(\int_0^t \frac{\partial \mathbf{w}^{(i)}(t-\sigma,y)}{\partial\sigma}\,d\sigma\right)\cdot \mathbf{e}_j\,dy$$

$$= \frac{1}{\varrho^L|Y|}\int_{Y_L}\mathbf{w}^{(i)}(t,y)\cdot\mathbf{e}_j\,dy.$$

The forcing $\left(F_i^L - \varrho^L \ddot{u}_i^{(0)} - \dfrac{\partial p^{(0)}}{\partial x_i}\right)$ is now time-independent. Hence

$$\langle \bar{\mathbf{v}}_i^{(0)}\rangle_L = \left(\int_0^t A_{ij}(t-s)\,ds\right)\left[F_j^L(x) - \frac{\partial p^{(0)}(x)}{\partial x_j}\right], \tag{6.1}$$

because $\ddot{\mathbf{u}}^{(0)} = 0$. From (6.1) and (6.2), taking into account (4.28) we get

$$\langle \bar{\mathbf{v}}_i^{(0)}\rangle_L = \frac{1}{\varrho^L|Y|}\left(\int_{Y_L}\mathbf{w}^{(i)}(t,y)\cdot\mathbf{e}_j\,dy\right)\left[F_j^L(x) - \frac{\partial p^{(0)}(x)}{\partial x_j}\right]. \tag{6.2}$$

Letting t tend to infinity we find

$$\langle \bar{\mathbf{v}}_i^{(0)}\rangle_L = \frac{1}{\varrho^L|Y|}\left(\int_{Y_L}\mathbf{w}_\infty^{(i)}(y)\cdot\mathbf{e}_j\,dy\right)\left[F_j^L(x) - \frac{\partial p^{(0)}(x)}{\partial x_j}\right] \tag{6.3}$$

$$= K_{ij}\left[F_j^L(x) - \frac{\partial p^{(0)}(x)}{\partial x_j}\right],$$

where $\langle \bar{\mathbf{w}}^{(0)}\rangle_L = \langle \mathbf{v}^{(0)}\rangle_L$ and $\mathbf{K} = (K_{ij})$ coincides with the well-known permeability matrix for the stationary flow, cf. [4, 15, 47]. Indeed, the local equation (4.33) yields

$$\varrho^L \lim_{t\to\infty}\frac{1}{t}\int_0^t \frac{\partial \mathbf{w}^{(i)}(s,y)}{\partial s}\,ds + \lim_{t\to\infty}\frac{1}{t}\int_0^t \nabla_y q^{(i)}(s,y)\,ds \tag{6.4}$$

$$- \lim_{t\to\infty}\frac{1}{t}\Delta_y \mathbf{w}^{(i)}(s,y)\,ds = \lim_{t\to\infty}\frac{1}{t}\int_0^t \mathbf{e}_i\,ds = \mathbf{e}_i.$$

We have

$$\lim_{t\to\infty}\frac{1}{t}\int_0^t \frac{\partial \mathbf{w}^{(i)}}{\partial s}(s,y)\,ds = \lim_{t\to\infty}\frac{1}{t}\mathbf{w}^{(i)}(t,y) = 0, \tag{6.5}$$

$$\lim_{t\to\infty}\frac{1}{t}\int_0^t \nabla_y q^{(i)}(s,y)\,ds = \nabla_y \lim_{t\to\infty}\frac{1}{t}\int_0^t q^{(i)}(s,y)\,ds = \nabla_y q_\infty^{(i)}(y). \tag{6.6}$$

Thus

$$\begin{aligned} \nabla_y q_\infty^{(i)}(y) - \Delta_y \mathbf{w}_\infty^{(i)}(y) &= \mathbf{e}_i \qquad \text{in} \quad Y_L, \\ \operatorname{div}_y \mathbf{w}_\infty^{(i)} &= 0 \qquad \text{in} \quad Y_L. \end{aligned} \tag{6.7}$$

The components of the permeability matrix $\mathbf{K}$ are eventually given by

$$K_{ij} = \frac{1}{\varrho^L |Y|}\int_{Y_L} \left(\nabla_y \mathbf{w}_\infty^{(i)}\right) : \nabla_y \mathbf{w}_\infty^{(j)}\,dy. \tag{6.8}$$

We recall that it was assumed that $\eta = 1$. In the general case we have

$$K_{ij} = \frac{1}{\varrho^L |Y|}\int_{Y_L} \eta\left(\nabla_y \mathbf{w}_\infty^{(i)}\right) : \nabla_y \mathbf{w}_\infty^{(j)}\,dy. \tag{6.9}$$

7. Comments on related papers

7.1. The works by BIOT [16 – 19] are now classical. In [16] an elastic skeleton with a statistical distribution of interconnected pores is considered. The porosity is denoted by

$$f = \frac{V_p}{V_b}, \tag{7.1}$$

where V_p is the volume of pores contained in a sample of bulk volume V_b, cf. the definition $(2.4)_1$. It is assumed, however, that f represents also a ratio of areas

$$f = \frac{S_p}{S_b}, \tag{7.2}$$

i.e. the fraction S_p occupied by the pores in any cross-sectional area S_b. This assumption is not needed in our approach. In the next two papers BIOT [17, 18] proposed to consider frequency-dependent characteristics of materials of skeleton and liquid and derived a time convolution-type law for nonstationary flow through a porous medium.

The resulting stress tensor S_{ij}^Z in porous material is assumed in the form

$$S_{ij}^Z = s_{ij} + \sigma\delta_{ij}, \qquad \sigma = -fp \tag{7.3}$$

where p denotes the hydrostatic pressure of the liquid. If a cube of unit size of the bulk material is considered, σ represents the total normal tension applied

to the liquid part of the faces of the cube, while s_{ij} represent the forces applied to the portion of the cube faces occupied by the solid. This assumption clearly corresponds to (4.12); nevertheless, the assumption (7.2) was not needed in our consideration.

This liquid-solid system is regarded as an elastic system. The liquid may be compressible. The average displacement of the solid is denoted by $\mathbf{u}$ and that of the liquid by $\mathbf{U}$, whilst $e = \operatorname{div}\mathbf{U}$ stands for the dilatation of the liquid. At this point there is a difference with our theory. In our case the liquid is incompressible, cf. $(3.1)_3$; however the divergence of the average velocity does not vanish, cf. (4.30), and $e \neq 0$ also in our theory.

The potential energy W per unit volume of aggregate is given by

$$W = \frac{1}{2}\left(s_{ij}\, e_{ij} + \sigma\, e\right). \tag{7.4}$$

The stress-strain relations are expressed by

$$s_{ij} = \frac{\partial W}{\partial e_{ij}}, \qquad \sigma = \frac{\partial W}{\partial e}, \tag{7.5}$$

and reduce to the form

$$s_{ij} = c_{ijmn} e_{mn} + Q_{ij} e, \qquad \sigma = Q_{ij} e_{ij} + Re. \tag{7.6}$$

The coefficients c_{ijmn} are elastic moduli, whilst R is a measure of the pressure required to force a certain volume of the liquid into the aggregate provided that the total volume remains constant. The coefficients Q_{ij} describe the coupling effect. The equation (7.6) is of the type (4.13) thus confirming Biot's idea. Biot assumed the equation of motion in the form

$$\varrho_{11}\ddot{u}_i + \varrho_{12}\ddot{U}_i + b_{ij}\left(\dot{u}_j - \dot{U}_j\right) = s_{ij,j} + \check{F}_i^S, \tag{7.7}$$

$$\varrho_{12}\ddot{u}_i + \varrho_{22}\ddot{U}_i - b_{ij}\left(\dot{u}_j - \dot{U}_j\right) = \sigma_{,i} + \check{F}_i^L. \tag{7.8}$$

The coefficients ϱ_{11}, ϱ_{12}, ϱ_{22} are mass-like coefficients which take into account the fact that the relative liquid flow through pores is not uniform. The meaning of ϱ_{12} is rather obscure. One shows that

$$\varrho_{11} + 2\varrho_{12} + \varrho_{22} = \varrho, \tag{7.9}$$

represents the total mass of the solid-liquid aggregate per unit volume, and $b_{ij} K_{ij} = f$.

For frequency-dependent permeability matrix $\mathbf{K}$, AURIAULT *et al.* [11] propose to treat the mass-like coefficients: ϱ_{11}, ϱ_{12}, ϱ_{22} as tensors

$$
\begin{aligned}
&(\varrho_{11})_{ij} = \langle \varrho^S \rangle \delta_{ij} - (\varrho_{12})_{ij},\\
&(\varrho_{22})_{ij} = \frac{f^2}{\omega} H^{\mathcal{I}}_{ij},\\
&(\varrho_{12})_{ij} = (\varrho_{21})_{ij} = f\varrho^L \delta_{ij} - (\varrho_{22})_{ij},\\
&\varrho = (1-f)\varrho^S + f\varrho^L,
\end{aligned}
\tag{7.10}
$$

where $< \varrho^S >= (1-f)\varrho^S$ and

$$\mathbf{H} = \mathbf{H}^{\mathcal{R}} + i\mathbf{H}^{\mathcal{I}} = \mathbf{K}^{-1}.$$

Hence, in the isotropic case one has $\varrho_{11} \geqslant \varrho, \quad \varrho_{12} = \varrho_{21} \leqslant 0, \quad \varrho_{22} \geqslant f\varrho.$

In Biot's theory, Darcy's law is given by

$$(\dot{U}_i - \dot{u}_i) = K_{ij}\Big(\frac{\partial \sigma}{\partial x_j} + F^L_j\Big). \tag{7.11}$$

However, we observe the discrepancy between the Darcy law (7.11) and the equation of motion (7.8). Only for stationary flows both equations coincide. Adding Eqs. (7.7) and (7.8) we obtain

$$(\varrho_{11} + \varrho_{12})\ddot{u}_i + (\varrho_{12} + \varrho_{22})\ddot{U}_i = \frac{\partial}{\partial x_j}(s_{ij} + \sigma\delta_{ij}) + \check{F}^S_i + \check{F}^L_i. \tag{7.12}$$

After comparison with (4.19) we conclude that

$$\check{F}^S_i = (1-f)Fi^S \qquad \check{F}^L_i = fF^L_i$$

$$\varrho_{11} + \varrho_{12} = (1-f)\varrho^S, \tag{7.13}$$

and

$$(\varrho_{12} + \varrho_{22})\ddot{U}_i = \varrho^L \langle \dot{v}^{(0)}_i \rangle_L, \tag{7.14}$$

or

$$(\varrho_{12} + \varrho_{22})\ddot{U}_i = \varrho^L f \frac{1}{|Y_L|} \int\limits_{Y_L} \dot{v}^{(0)}_i \, dy. \tag{7.15}$$

Hence

$$\varrho_{12} + \varrho_{22} = f\varrho^L, \tag{7.16}$$

and

$$\varrho_{11} + 2\varrho_{12} + \varrho_{22} = (1-f)\varrho^S + f\varrho^L = \varrho, \tag{7.17}$$

where ϱ is the same as in (7.9). Consider now the nonstationary Darcy's law (4.28). We have

$$\langle v_i^{(0)} \rangle_L - \dot{u}_i^{(0)} = K_{ij}(t) * \Big(F_j^L - \varrho^L \ddot{u}_j^{(0)} - \frac{\partial}{\partial x_j} p^{(0)} \Big)(t,x), \tag{7.18}$$

where

$$K_{ij} = K_{ij}(t) = \frac{1}{\varrho^L} \langle \chi_i^{(j)}(t,y) \rangle_L, \tag{7.19}$$

and $*$ denotes the convolution with respect to time t. After taking the Laplace transformation of (7.18) defined as

$$\tilde{f} = \int_0^\infty f(t)\, \mathrm{e}^{izt}\, dt, \quad z = \omega + i\zeta, \quad \omega = \Re z, \quad \zeta = \Im z > 0,$$

we get

$$\langle \tilde{v}_i^{(0)} \rangle_L - \tilde{\dot{u}}_i^{(0)} = \tilde{K}_{ij}(z) \Big(F_j^L - \varrho^L \ddot{u}_j^{(0)} - \frac{\partial}{\partial x_j} p^{(0)} \Big)\tilde{}\,(z,x). \tag{7.20}$$

Thus, after the inversion

$$\Big(F_i^L - \varrho^L \ddot{u}_i^{(0)} - \frac{\partial}{\partial x_i} p^{(0)} \Big)\tilde{} = \tilde{H}_{ij} \Big(\langle \tilde{v}_i^{(0)} \rangle_L - \tilde{\dot{u}}_i^{(0)} \Big), \tag{7.21}$$

where

$$\tilde{\mathbf{H}} = \tilde{\mathbf{K}}^{-1}.$$

The inverse transformation yields

$$F_i^L - \varrho^L \ddot{u}_i^{(0)} - \frac{\partial}{\partial x_i} p^{(0)} = H_{ij}(t) * \Big(\langle v_j^{(0)} \rangle_L - \dot{u}_j^{(0)} \Big)(t,x). \tag{7.22}$$

Therefore

$$F_i^L - \frac{\partial}{\partial x_i} p^{(0)} = H_{ij}(t) * \Big(\langle v_j^{(0)} \rangle_L - \dot{u}_j^{(0)} \Big) + \varrho^L \ddot{u}_i^{(0)}. \tag{7.23}$$

The matrix $\tilde{\mathbf{H}}$ can be written as follows:

$$\tilde{H}_{ij} = \tilde{H}_{ij}^{\Re} + i \tilde{H}_{ij}^{\Im}. \tag{7.24}$$

Then (7.21) becomes

$$\Big(F_j^L - \frac{\partial}{\partial x_j} p^{(0)} \Big)\tilde{} = \tilde{H}_{ij}^{\Re} \Big(\langle \tilde{v}_i^{(0)} \rangle_L - \tilde{\dot{u}}_i^{(0)} \Big) + \Big(\varrho^L \delta_{ij} + \frac{1}{z} \tilde{H}_{ij}^{\Im} \Big) \tilde{\ddot{u}}_j^{(0)} \tag{7.25}$$

$$- \frac{1}{z} \tilde{H}_{ij}^{\Im} \langle \tilde{\dot{v}}_i^{(0)} \rangle_L$$

and we find

$$(\tilde{\varrho}_{12})_{ij} = \varrho^L \delta_{ij} + \frac{1}{z}\tilde{H}^{\Im}_{ij} \qquad \text{and} \qquad (\tilde{\varrho}_{22})_{ij} = -\frac{1}{z}\tilde{H}^{\Im}_{ij}, \tag{7.26}$$

cf. also the paper by AURIAULT et al. [11].

7.2. BURRIDGE and KELLER [22] employed the homogenization theory, though not quite rigorously. Performing Fourier transformation in time, the basic system of equations is given by, cf. (2.3) – (2.8),

$$\begin{aligned}
-\omega^2 \varrho^S \tilde{u}_i &= \tilde{S}_{ij,j} + F^S_i && \text{in } Y_S,\\
\tilde{S}_{ij} &= a_{ijmn}\tilde{e}_{mn} && \text{in } Y_S,\\
i\omega\varrho^L \tilde{v}_i &= \left(-\tilde{p}\delta_{ij} + \eta_{ijmn}\tilde{v}_{m,n}\right)_{,j} + F^L_i && \text{in } Y_L,\\
i\omega\tilde{p} &= -\kappa \operatorname{div}\tilde{\mathbf{v}} && \text{in } Y_L,\\
\tilde{S}_{ij}n_j &= \left(-\tilde{p}\delta_{ij} + \eta_{ijmn}e_{mn}(\tilde{\mathbf{v}})\right)n_j && \text{on } \partial Y_S \cap \partial Y_L,\\
i\omega\tilde{u}_i &= \tilde{v}_i && \text{on } \partial Y_S \cap \partial Y_L.
\end{aligned} \tag{7.27}$$

Here ω denotes the frequency. Now the incompressibility condition $(3.1)_3$ is replaced by compressibility equation $(7.27)_4$.

The two-scale asymptotic method was applied to the system (7.27). The macroscopic equations describe a liquid-filled porous elastic medium with isotropic stochastic distribution of pores. A comparison with Biot's result for an isotropic stochastic medium was performed. The averaging used is typical for stochastic media.

The use of time-Fourier transforms is also characteristic for other papers on the subject, cf. LÉVY [38], AURIAULT *et al.* [11]. Such an approach corresponds to steady vibration of the porous medium.

7.3. The question of the form of the nonlinear effects has been raised by FORCHHEIMER already in 1901, cf. [29], and was studied by LINDQUIST [39]. MUSKAT [43] distinguishes 3 zones of Reynolds number $\mathcal{R}$, namely: (i) Darcy zone where $\mathcal{R}$ is low, (ii) transition zone, and (iii) linear deviation zone for high values of $\mathcal{R}$.

WODIE and LÉVY [51] considered the influence of the convective term $\mathbf{v}\nabla\mathbf{v}$ on Darcy's law in the case of a stationary flow. If the nonlinear term is of the same order as the viscosity term, then

$$\eta \rightsquigarrow \epsilon^{3/2}\eta$$

instead of (3.5). We note the difference with the linear case where the scaling parameter is ϵ^2. These authors show that up to the second order approximation, Darcy's law is given by

$$(7.28) \qquad < v_i >= \frac{1}{\eta} K_{ij} \left(F_j - \frac{\partial p^{(0)}}{\partial x_j} \right) + \frac{\varrho}{\eta} T_{ijk} \left(F_j - \frac{\partial p^{(0)}}{\partial x_j} \right) \left(F_k - \frac{\partial p^{(0)}}{\partial x_k} \right),$$

where the tensor $\mathbf{T}$ satisfies the following relation:

$$T_{ijk} + T_{kij} + T_{jki} = 0.$$

In the case of macroscopic isotropy and one-dimensional flow, the correction term vanishes. However, one can calculate the third correction being the first nonvanishing nonlinear contribution in Darcy's law which can be written in the form

$$(7.29) \qquad \mathbf{F} - \nabla p^{(0)} = \frac{\eta}{K^\epsilon} < \mathbf{v} > + \frac{\varrho^2 c^\epsilon}{\eta (K^\epsilon)^4} | < \mathbf{v} > |^2 < \mathbf{v} >,$$

where K^ϵ and c^ϵ are positive constants of order ϵ^8 completely determined by the microstructure. Such law is not in agreement with the generally used empirical law of FORCHHEIMER [29] but agrees with the numerical calculation of BARRÈRE (1990).

The results of Wodie and Lévy on vanishing of the first nonlinear correction were confirmed by FIRDAOUSS *et al.* [28].

8. Concluding remarks

ALLAIRE'S [6] results were extended to the flow of a viscous fluid through a microperiodic, linear elastic anisotropic porous medium. To justify rigorously the formal asymptotic approach, the two-scale convergence method developed by ALLAIRE [7] and NGUETSENG [44] was successfully used. In contrast to several previous papers on similar flow problem [10, 22, 27, 45], our approach is straightforward and avoids using time-transformation. Also, the local problem was explicitly formulated and the formula for the permeability matrix was derived.

TORZILLI and MOW [50] employed the mixture theory to describe the interaction of the fluid and solid phases of articular cartilage. The equations of motion for each phase and the total mixture were derived from the extended Hamilton's principle, where the Rayleigh dissipative resistance is considered as a generalized body-force field. This procedure yields, as special cases, the classical Darcy's law for the liquid transport due to direct pressure gradients, as well as Biot's consolidation equation for the liquid transport due to dilatation of the solid phase. For further results on modelling of articular cartilage the reader is referred to [31, 32,

34, 36, 41, 42, 48]. We are convinced that, since the cartilage exhibits a hierarchical microstructure, the homogenization methods can be used to macroscopic modelling of its behaviour.

Appendix A

Analysis of terms of ε^{-2} order

Equation $(3.1)_1$ yields

$$\frac{\partial}{\partial y_j}\left[a_{ijmn}\frac{\partial}{\partial y_n}u_m^{(0)}\right]=0 \qquad \text{in} \quad Y_S. \tag{A.1}$$

Multiplying (A.1) by $u_i^{(0)}$ and integrating by parts we get

$$\int\limits_{\partial Y_S} a_{ijmn}e_{mn}^y(\boldsymbol{u}^{(0)})u_i^{(0)}N_j\,dA-\int\limits_{Y_S} a_{ijmn}e_{ij}^y(\boldsymbol{u}^{(0)})e_{mn}^y(\boldsymbol{u}^{(0)})\,dy=0. \tag{A.2}$$

By virtue of the interface condition (4.3), the surface integral in the last equation vanishes and consequently we get

$$\mathbf{u}^{(0)}=\mathbf{u}^{(0)}(t,x). \tag{A.3}$$

Analysis of terms of ε^{-1} order

Equation $(3.1)_1$ now yields

$$\frac{\partial}{\partial y_j}\left[a_{ijmn}\left(\frac{\partial}{\partial x_n}u_m^{(0)}+\frac{\partial}{\partial y_n}u_m^{(1)}\right)\right]=0, \qquad x\in\Omega, \quad y\in Y_S. \tag{A.4}$$

Similarly, Eq. $(3.1)_2$ gives

$$\nabla_y p^{(0)}=0, \quad x\in\Omega \qquad y\in Y_L. \tag{A.5}$$

Hence

$$p^{(0)}=p^{(0)}(t,x). \tag{A.6}$$

The incompressibility Eq. $(3.1)_3$ yields

$$\operatorname{div}_y\mathbf{v}^{(0)}=0. \tag{A.7}$$

Local function for the flow problem

By (4.25) we have

$$\dot{v}_m^{(0)}(t,x,y) = \frac{1}{\varrho^L}\left(F_s^L - \varrho^L \ddot{u}_s^{(0)} - \frac{\partial}{\partial x_s}p^{(0)}\right)(t,x)\chi_m^{(s)}(0,y)$$

$$+\frac{1}{\varrho^L}\int_0^t \left(F_s^L - \varrho^L \ddot{u}_s^{(0)} - \frac{\partial}{\partial x_s}p^{(0)}\right)(\tau,x)\frac{d\chi_m^{(s)}(t-\tau,y)}{dt}\,d\tau.$$

Since $\chi_m^{(s)}(0,y) = 0$, we write

$$\dot{v}_m^{(0)}(t,x,y) = \frac{1}{\varrho^L}\int_0^t \left(F_s^L - \varrho^L \ddot{u}_s^{(0)} - \frac{\partial}{\partial x_s}p^{(0)}\right)(\tau,x)\frac{d\chi_m^{(s)}(t-\tau,y)}{dt}\,d\tau. \tag{A.8}$$

Therefore, substitution of (4.25) into (4.24) yields

$$\int_0^t \left(F_s^L(\tau,x) - \varrho^L \ddot{u}_s^{(0)}(\tau,x) - \frac{\partial}{\partial x_s}p^{(0)}(\tau,x)\right) \times \left[\varrho^L \frac{\partial \chi_i^{(s)}(t-\tau,y)}{\partial t}\right.$$

$$\left. -\left(\delta_{si} - \frac{\partial}{\partial y_i}\gamma_s(\tau,y)\right)\delta(t-\tau) - \frac{\partial}{\partial y_j}\left(\eta_{ijmn}\frac{\partial \chi_m^{(s)}(t-\tau,y)}{\partial y_n}\right)\right] d\tau = 0. \tag{A.9}$$

This equation implies the relation (4.26).

Appendix B. Two-scale convergence

The aim of this Appendix is to gather basic facts about two-scale convergence. For details the reader is referred to [7, 44]. We observe that this notion was introduced to justify the formal method of two-scale asymptotic expansions. We also note that the Γ-convergence method is confined to sequences of functionals.

Let Ω be an open set in $\mathbb{R}^N$ ($N \geqslant 1$) and Y – a closed cube. As usual, $L^2(\Omega)$ is the Lebesgue space of real-valued functions that are measurable and square integrable in Ω, cf. [1]. Let $C^\infty_{\mathrm{per}}(Y)$ be the space of infinitely differentiable functions in $\mathbb{R}^N$ that are Y-periodic. Then $L^2_{per}(Y), (H^1_{\mathrm{per}}(Y))$ is the completion for the norm of $L^2(Y)(H^1(Y))$ of $C^\infty_{\mathrm{per}}(Y)$. We note that $L^2_{\mathrm{per}}(Y)$ coincides with the space of functions in $L^2(Y)$ extended by Y-periodicity to the whole of $\mathbb{R}^N$. Consider a sequence of functions $\{u^\varepsilon\}_{\varepsilon>0}$ in $L^2(\Omega)$ ($\varepsilon > 0$ and $\varepsilon \to 0$).

DEFINITION B.1. *A sequence of functions $\{u^\varepsilon\}_{\varepsilon>0}$ in $L^2(\Omega)$ is said to two-scale converge to a limit $u^{(0)}(x,y) \in L^2(\Omega \times Y)$ if, for any function $\psi(x,y)$ in $\mathcal{D}[\Omega; C^\infty_{\mathrm{per}}(Y)]$, we have*

$$\lim_{\varepsilon\to 0}\int_{\Omega} u^{\varepsilon}(x)\psi(x,x/\varepsilon)\,dx = \frac{1}{|Y|}\int_{\Omega}\int_{Y} u^{(0)}(x,y)\psi(x,y)\,dx\,dy. \tag{B.1}$$

REMARK B.1. For evolution problems when $u^{\varepsilon} = u^{\varepsilon}(t,x)$, the variable t is treated as a parameter and instead of (B.1) we have [7]

$$\lim_{\varepsilon\to 0}\int_{0}^{T}\int_{\Omega} u^{\varepsilon}(x)\psi(x,x/\varepsilon)\phi(t)\,dx\,dt$$

$$= \frac{1}{|Y|}\int_{0}^{T}\int_{\Omega}\int_{Y} u^{(0)}(x,y)\psi(x,y)\phi(t)\,dx\,dy\,dt,$$

where ϕ is a smooth test function.

The following compactness theorem establishes that the notion of two-scale convergence makes sense.

THEOREM B.1. *From each bounded sequence $\{u^{\varepsilon}\}_{\varepsilon>0}$ in $L^2(\Omega)$ we can extract a subsequence and there exists a limit $u^{(0)}(x,y) \in L^2(\Omega\times Y)$ such that this subsequence two-scale converges to $u^{(0)}$.* □

It is interesting to note that the two-scale limit furnishes more information than the weak limit in L^2. The relationship between the two-scale and weak L^2-convergence is established by

PROPOSITION B.1. Let $\{u^{\varepsilon}\}_{\varepsilon>0}$ be a sequence of functions in $L^2(\Omega)$, which two-scale converges to a limit $u^{(0)} \in L^2(\Omega\times Y)$. Then u^{ε} converges also to $u(x) = \dfrac{1}{|Y|}\displaystyle\int_{Y} u^{(0)}(x,y)\,dy$ in L^2-weakly. Furthermore, we have

$$\lim_{\varepsilon\to 0}\|u^{\varepsilon}\|_{L^2(\Omega)} \geqslant \|u^{(0)}\|_{L^2(\Omega\times Y)} \geqslant \|u\|_{L^2(\Omega)}. \tag{B.2}$$

□

The next proposition gives two-scale limit of the product of two sequences.

PROPOSITION B.2. Let $\{u^{\varepsilon}\}_{\varepsilon>0}$ be a sequence of functions in $L^2(\Omega)$, which two-scale converges to $u^{(0)}(x,y) \in L^2(\Omega\times Y)$. Assume that

$$\lim_{\varepsilon\to 0}\|u^{\varepsilon}\|_{L^2(\Omega)} = \|u^{(0)}\|_{L^2(\Omega\times Y)}. \tag{B.3}$$

Then for any sequence $\{v^{\varepsilon}\}_{\varepsilon>0}$ two-scale convergent to $v^{(0)} \in L^2(\Omega\times Y)$ one has

$$u^{\varepsilon}(x)\,v^{\varepsilon}(x) \rightharpoonup \frac{1}{|Y|}\int_{Y} u^{(0)}(x,y)\,v^{(0)}(x,y)\,dy \qquad \text{in} \quad \mathcal{D}'(\Omega). \tag{B.4}$$

Moreover, if $u^{(0)} \in L^2(\Omega; C_{\text{per}}(Y))$ then

$$\lim_{\varepsilon \to 0} \left\| u^\varepsilon(x) - u^{(0)}\left(x, \frac{x}{\varepsilon}\right) \right\|_{L^2(\Omega)} = 0. \tag{B.5}$$

□

Of practical importance is the two-scale convergence of sequences with bounds on derivatives. The relevant results are summarized as follows.

THEOREM B.2. *Let $\{u^\varepsilon\}_{\varepsilon>0}$ be a bounded sequence in $H^1(\Omega)$ that converges weakly to a limit u in $H^1(\Omega)$. Then u^ε two-scale converges to u and there exists a function $u^{(1)}(x,y)$ in $L^2[\Omega; H^1_{\text{per}}(Y)/\mathbb{R}]$ such that, up to a subsequence, ∇u^ε two-scale converges to $\nabla_x u(x) + \nabla_y u^{(1)}(x,y)$.* □

THEOREM B.3. *Let $\{u^\varepsilon\}_{\varepsilon>0}$ and $\{\varepsilon \nabla u^\varepsilon\}_{\varepsilon>0}$ be two bounded sequences in $L^2(\Omega)$. Then there exists a function $u^{(0)}$ in $L^2(\Omega; H^1_{per}(Y))$ such that, up to a subsequence, u^ε and $\varepsilon \nabla u^\varepsilon$ two-scale converge to $u^{(0)}(x,y)$ and $\nabla_y u^{(0)}(x,y)$, respectively.* □

THEOREM B.4. *Let $\{u^\varepsilon\}_{\varepsilon>0}$ be a free-divergence bounded sequence in $L^2(\Omega)^N$, which two-scale converges to $u^{(0)}(x,y)$ in $[L^2(\Omega \times Y)]^N$. Then, the two-scale limit satisfies*

$$\operatorname{div}_y u^{(0)}(x,y) = 0 \tag{B.6}$$

and

$$\int_Y \operatorname{div}_x u^{(0)}(x,y)\, dy = 0. \tag{B.7}$$

□

EXAMPLE B.1. To illustrate the two-scale convergence method let us consider the problem of homogenization of linear second-order elliptic equations, cf. ALLAIRE [7].

Let Ω be a bounded open set of $\mathbb{R}^N$. Let f be a given function in $L^2(\Omega)$. Consider the following equation:

$$-\operatorname{div}\left(A\left(x, \frac{x}{\varepsilon}\right) \nabla u^\varepsilon\right) = f \quad \text{in} \quad \Omega, \tag{B.8}$$

$$u^\varepsilon = 0 \quad \text{on} \quad \partial\Omega, \tag{B.9}$$

where $\mathbf{A}\left(x, \dfrac{x}{\varepsilon}\right)$ is a matrix defined on $\Omega \times Y$, Y-periodic in y, such that there exist two positive constants $0 < \alpha \leqslant \beta$ satisfying

$$\alpha|\xi|^2 \leqslant \sum_{i,j=1}^{N} A_{ij}(x,y)\xi_i\xi_j \leqslant \beta|\xi|^2 \quad \text{for any} \quad \xi \in \mathbb{R}^N. \tag{B.10}$$

Additionally we assume that $A_{ij}(x, x/\varepsilon)$ satisfies

$$\lim_{\varepsilon \to 0} \int_{\Omega} \left[A_{ij}\left(x, \frac{x}{\varepsilon}\right)\right]^2 dx = \int_{\Omega} \int_{Y} [A_{ij}(x,y)]^2 \, dx \, dy. \tag{B.11}$$

Under the assumptions (B.10) and (B.11), the system of Eqs. (B.8) – (B.9) admits a unique solution u^ε in $H_0^1(\Omega)$, which satisfies the a priori estimate

$$\|u^\varepsilon\|_{H_0^1(\Omega)} \leqslant C\|f\|_{L^2(\Omega)}, \tag{B.12}$$

where C is a positive constant that depends only on Ω and α, and not on ε. The homogenized problem is given by

$$-\operatorname{div}\left[\mathbf{A}^h(x)\nabla u(x)\right] = f \qquad \text{in} \quad \Omega, \tag{B.13}$$

$$u = 0 \qquad \text{on} \quad \partial\Omega, \tag{B.14}$$

where the matrix $\mathbf{A}^h$ has the following form

$$A_{ij}^h(x) = \frac{1}{|Y|} \int_{Y} \mathbf{A}(x,y)\left[\nabla_y w^{(i)}(x,y) + \mathbf{e}_i\right] \cdot \left[\nabla_y w^{(j)}(x,y) + \mathbf{e}_j\right] dy \tag{B.15}$$

and, for $1 \leqslant i \leqslant N$, $w^{(i)}$ is the solution of the so-called cell problem

$$-\operatorname{div}_y\left[\mathbf{A}(x,y)(\nabla_y w^{(i)}(x,y) + \mathbf{e}_i)\right] = 0 \qquad \text{in} \quad Y. \tag{B.16}$$

Here $w^{(i)}(x,y)$ is Y-periodic with respect to y. The result of two-scale convergence are summarized is the following form:

THEOREM B. 5. *The sequence $\{u^\varepsilon\}$ of solutions of the problem (B.8) converges weakly to $u(x)$ in $H_0^1(\Omega)$, and the sequence ∇u^ε two-scale converges to $\nabla u(x) + \nabla_y u^{(1)}(x,y)$, where $(u, u^{(1)})$ is the unique solution in $H_0^1(\Omega) \times L^2[\Omega; H^1_{\mathrm{per}}(Y)/\mathbb{R}]$ of the following two-scale homogenized system:*

$$-\operatorname{div}_y\left(\mathbf{A}(x,y)\left[\nabla u(x) + \nabla_y u^{(1)}(x,y)\right]\right) = 0 \qquad \text{in} \quad \Omega \times Y, \tag{B.17}$$

$$-\mathrm{div}_x \left(\int_Y \mathbf{A}(x,y) \left[\nabla u(x) + \nabla_y u^{(1)}(x,y) \right] dy \right) = f \qquad \text{in} \quad \Omega, \tag{B.18}$$

$$u(x) = 0 \qquad \text{on} \quad \partial\Omega. \tag{B.19}$$

Furthermore the system is equivalent to the usual homogenized and cell equations through the relation

$$u^{(1)}(x,y) = \sum_{i=1}^{N} \frac{\partial u}{\partial x_i}(x) w^{(i)}(x,y). \tag{B.20}$$

P r o o f. Due to the a priori estimates (B.12), there exists a limit u such that, up to a subsequence, u^ε converges weakly to u in $H_0^1(\Omega)$. We multiply now the Eq. (B.8) by a test function $\eta(x) + \varepsilon\psi(x, x/\varepsilon)$ with $\eta(x) \in \mathcal{D}(\Omega)$ and $\psi(x,y) \in \mathcal{D}[\Omega; C^\infty_{\mathrm{per}}(Y)]$. This yields

$$\int_\Omega \mathbf{A}\left(x, \frac{x}{\varepsilon}\right) \nabla u^\varepsilon \left[\nabla\eta(x) + \nabla_y \psi\left(x, \frac{x}{\varepsilon}\right) + \varepsilon \nabla_x \psi\left(x, \frac{x}{\varepsilon}\right) \right] dx \tag{B.21}$$

$$= \int_\Omega f(x) \left[\eta(x) + \varepsilon\psi\left(x, \frac{x}{\varepsilon}\right) \right] dx.$$

By Theorem B.1 and B.2 we can pass to the two-scale limit in (B.21):

$$\int_\Omega \int_Y \mathbf{A}(x,y) \left[\nabla u(x) + \nabla_y u^{(1)}(x,y) \right] \cdot \left[\nabla\eta(x) + \nabla_y \psi(x,y) \right] dx\, dy \tag{B.22}$$

$$= \int_\Omega f(x)\eta(x)\, dx.$$

By density, (B.22) holds true for any (η, ψ) in $H_0^1(\Omega) \times L^2[\Omega; H^1_{\mathrm{per}}(Y)/\mathbb{R}]$. The integration by parts show that (B.22) is a variational formulation associated to (B.13) – (B.15). To prove that (B.17) – (B.19) is equivalent to (B.13) – (B.16), it is sufficient to use (B.20). □

Acknowledgment

This work was supported by the State Committee for Scientific Research (KBN – Poland) through the grant No. 6 P04D 039 15. The second author was also supported through the grant No. 8 T11F 018 12.

References

1. R.A. ADAMS, Sobolev Spaces, Academic Press, New York 1975.
2. P.M. ADLER and J.-F. THOVERT, *Real porous media: local geometry and macroscopic properties*, Appl. Mech. Rev., **51**, 537–585, 1998.
3. R. ALEXANDRE, *Homogenisation and $\theta - 2$ convergence*, Proc. Roy. Soc. Edinburgh, **127A**, 441–455, 1997.
4. G. ALLAIRE, *Homogenization of the Stokes flow in a connected porous medium*, Asymptotic Analysis, **2**, 203–222, 1989.
5. G. ALLAIRE, *Continuity of the Darcy's law in the low-volume fraction limit*, Annali della Scuola Norm. Sup. di Pisa, Sci. Fis. e Mat., Ser. IV, 475–499, 1991.
6. G. ALLAIRE, *Homogenization of the unsteady Stokes equations in porous media* [in:] Progress in partial differential equations: calculus of variations, applications, [Ed.:] C. BANDLE, J. BEMELMANS, M. CHIPOT and J SAINT JEAN PAULIN, 109–123, Longman 1991.
7. G. ALLAIRE, *Homogenization and two-scale convergence*, SIAM J. Math. Anal., **23**, 1482–1518, 1992.
8. G. ALLAIRE, *Private communication*, 1998.
9. J.-L. ARIAULT and E. SANCHEZ-PALENCIA, *Étude du comportement macroscopique d'un milieu poreux saturé déformable*, J. de Mécanique **16**, 575–603, 1977.
10. J.-L. AURIAULT, *Dynamic behaviour of a porous medium saturated by a Newtonian fluid*, Int. J. Engng Sci., **18**, 775–785, 1980.
11. J.-L. AURIAULT, L. BORNE and R. CHAMBON, *Dynamics of porous saturated media, checking of the generalized law of Darcy*, J. Acoust. Soc. Am., **77**, 1641–1650, 1985.
12. J.-L. AURIAULT, C. BOUTIN and J. LEWANDOWSKA, Mécanique des milieux hétérogènes, [in:] Some Selected Topics on Advanced Mechanics in Porous Materials, [Ed.:] J.-L. AURIAULT, F. DAVRE, E. DEMBICKI, Z. SIKORA, 1–199, Technical University of Gdańsk, Misiura, Gdańsk 1997.
13. J. BARRÈRE, Thèse, Université Bordeaux I, spécialité Mécanique, 1990.
14. J. BEAR and Y. BACHMAT, *Introduction to modeling of transport phenomena in porous media*, Kluwer AP, 1991.
15. W. BIELSKI and J. J. TELEGA, *Effective properties of geomaterials: rocks and porous media*, Publications of the Institute of Geophysics, Polish Academy of Sciences, **A – 26(285)**, Warszawa 1997.
16. M.A. BIOT, *Theory of elasticity and consolidation for a porous anisotropic solid*, J. Appl. Phys., **26**, 182–185, 1955.
17. M. A. BIOT, *Theory of propagation of elastic waves in a fluid-saturated porous solid.* I. *Low-frequency range*, J. Acoust. Soc. of Amer., **28**, 168–178, 1956.
18. M. A. BIOT, *Theory of propagation of elastic waves in a fluid-saturated porous solid.* II. *Higher-frequency range*, J. Acoust. Soc. of Amer., **28**, 179–191, 1956.
19. M.A. BIOT, *Mechanics of deformation and acoustic propagation in porous media*, J. Appl. Phys., **33**, 1482–1498, 1962.
20. A.P. BOURGEAT, C. CARASSO, S. LUCKHAUS and A. MIKELIĆ [Eds.:], *Mathematical modelling of flow through porous media*, World Scientific, Singapore-New Jersey-London-Hong Kong 1995.

21. M. BRIANE, *Homogenization of a non-periodic material*, J. Math. Pures Appl., **73**, 47–66, 1994.

22. R. BURRIDGE and J.B. KELLER, *Poroelasticity derived equations derived from microstructure*, J. Acoust. Soc. Am., **70**, 1140–1146, 1981.

23. M. CIESZKO, J. KUBIK, *Constitutive relations and internal equilibrium condition for fluid-saturated porous solids. Nonlinear description*, Arch. Mech., **48**, 893–910, 1996.

24. M. CIESZKO, J. KUBIK, *Constitutive relations and internal equilibrium condition for fluid-saturated porous solids. Linear description*, Arch. Mech., **48**, 911–925, 1996.

25. D. CIORANESCU and J. SAINT JEANT PAULIN, *Particules déformables en suspension dans un fluide visqueux*, C. R. Acad. Sci. Paris, I, **300**, 335–338, 1985.

26. O. COUSSY, *Mécanique des milieux poreux*, Edition Technique, Paris 1991.

27. S. DASSER, *Méthode de pénalisation pour l'homogénésation d'un problème de couplage fluide-structure*, C. R. Acad. Sci. Paris, I, **320**, 759–764, 1995.

28. M. FIRDAOUSS, J.-L. GUERMOND and P. Le QUÉRÉ, *Nonlinear corrections to Darcy's law at low Reynolds numbers*, J. Fluid Mech., **343**, 331–350, 1997.

29. P. FORCHHEIMER, *Wasserbewegung durch Boden*, Z. Vereines deutscher Ingenieure, **45, 49, 50**, 1901.

30. A. GAŁKA, J.J. TELEGA and R. WOJNAR, *Equations of electrokinetics and flow of electrolytes in porous media*, J. Techn. Physics, **35**, 49–59, 1994.

31. W.Y. GU, W.M. LAI and V.C. MOW, *Transport of fluid and ions through a porous-permeable charged-hydrated tissue, and streaming potential data on normal bovine articular cartilage*, J. Biomechanical Engng, **26**, 709–723, 1993.

32. W.Y. GU, W.M. LAI and V.C. MOW, *A mixture theory for charged-hydrated soft tissues containing multi-electrolytes: passive transport and swelling behaviors*, J. Biomechanical Engng., **120**, 169–180, 1998.

33. U. HORNUNG, [Ed.], *Homogenization and Porous Media*, Springer, Berlin 1997.

34. J.M. HUYGHE and J.D. JANSSEN, *Thermo-chemo-electro-mechanical formulation of saturated charged porous solids*, Transport in Porous Media, 1998.

35. W. JÄGER and A. MIKELIĆ, *On the boundary conditions at the contact interface between a porous medium and a free fluid*, preprint, 1996.

36. V.M. LAI, V.C. MOW, W. ZHU, *Constitutive modeling of articular cartilage and biomacromolecular solutions*, J. Biomech. Eng., **115**, 474–480, 1993.

37. C.K. LEE and C.C. MEI, *Re-examination of the equations of poroelasticity*, Int. J. Engng Sci., **35**, 329–352, 1997.

38. T. LÉVY, *Propagation of waves in a fluid-saturated porous elastic solid*, Int. J. Engng Sci., **17**, 1005–1014, 1979.

39. E. LINDQUIST, [in:] Proc. Premier Congrés des Grands Barrages, Stockholm 1930.

40. A. MIKELIĆ, *Homogenization of nonstationary Navier Stokes equations in a domain with a grained boundary*, Ann. Mat. Pura ed Appl., **158**, 167–179, 1991.

41. V.C. MOW, M.C. HOLMES, W.M. LAI, *Fluid transport and mechanical properties of articular cartilage: a review*, J. Biomech., **17**, 377–394, 1984.

42. V.C. MOW, S.C. KUEI, W.M. LAI, C.G. ARMSTRONG, *Biphasic creep and stress relaxation of articular cartilage in compression: theory and experiments*, J. Biomech. Eng., **102**, 73–84, 1980.

43. M. MUSKAT, *The Flow of Homogeneous fluids through porous media*, J. W. Edwards, Ann Arbor, Michigan, The Mapple Press Co, York PA 1946.

44. G. NGUETSENG, *A general convergence result for a functional related to the theory of homogenization*, SIAM J. Math. Anal., **20**, 608–623, 1989.

45. G. NGUETSENG, *Asymptotic analysis for a stiff variational problem arising in mechanics*, SIAM J. Math. Anal., **21**, 1394–1414, 1990.

46. M. SAHIMI, *Flow and transport in porous media and fractured rock: from classical methods to modern approaches*, VCH, Weinheim – New York 1995.

47. E. SANCHEZ-PALENCIA, *Non-homogeneous media and vibration theory*, Springer, Berlin 1980.

48. J.-K. SUH, S. BAI, *Finite element formulation of biphasic poroviscoelastic model for articular cartilage*, J. Biomech. Eng., **120**, 195–201, 1998.

49. J.J. TELEGA and R. WOJNAR, *Flow of conductive fluids through poroelastic media with piezoelectric properties*, J. Theor. Appl. Mech., **36**, 775–794, 1998.

50. P.A. TORZILLI, V.C. MOW, *On the fundamental fluid transport mechanisms through normal and pathological articular cartilage during function – I. The formulation*, J. Biomech., **9**, 541–552, 1976; *II. The analysis, solution and conclusions*, ibid., **9**, 587–606, 1976.

51. J.-CH WODIE, and TH. LEVY, *Correction nonlinéaire de la loi de Darcy*, C. R. Acad. Sci. Paris, II, **312**, 157–169, 1991.

52. R. WOJNAR and J.J. TELEGA, *Electrokinetics in dielectric porous media* [In:] Problems of Environmental and Damage Mechanics, [Ed.] W. KOSIŃSKI, R. de BOER, D. GROSS, Wydawnictwa IPPT PAN, Warszawa, 97–136, 1997.

Received January 14, 1999; revised version March 12, 1999.

Arch. Mech., **51**, 3–4, pp. 275–291, Warszawa 1999

Sensitivity analysis of 2D elastic structures in presence of stress singularities

M. BOCHNIAK and A.-M. SÄNDIG

Universität Stuttgart, Mathematisches Institut A

THE OBJECT OF THIS PAPER is the investigation of the influence of stress singularities on the sensitivity of two-dimensional linearized elastic fields and the corresponding functionals under a variation of the domain. This requires a detailed study of the local behaviour of the material and of the shape derivatives of the displacement field in the vicinity of boundary corner points. Using these regularity results, we apply the method of adjoint problems to express the shape derivatives of the functionals as boundary integrals and give precise conditions under which this approach can be justified. It turns out that in case of elastic structures with cracks, the sensitivity of the functionals depends also on the stress intensity factors of the solution of the adjoint problem.

Notations

$\langle \cdot, \cdot \rangle$	inner product in $\mathbb{R}^2$,
$\mathbf{s} : \mathbf{t}$	inner product of tensors $\mathbf{s}, \mathbf{t}$,
δ_{ij}	Kronecker's delta,
$\mathbf{D}v$	Jacobian of a vector function v,
$\mathbf{n}_\varepsilon$	perturbed unit normal vector,
u_ε	perturbed displacement field,
$e(u_\varepsilon)$	perturbed linearized strain tensor,
$\mathbf{C}$	$= \{c_{ijkl} : i, j, k, l = 1, 2\}$ Hooke's tensor,
$\sigma(u_\varepsilon)$	$= C : e(u_\varepsilon)$ perturbed linearized stress field,
$\dot{u}$	material derivative of u_ε,
u'	shape derivative of u_ε.

1. Introduction

THE INFLUENCE OF THE SHAPE of the domain on the elastic behaviour has been studied by many authors (see the monographs [6, 18] and the references therein). The corresponding sensitivity analysis is well developed for problems in smooth domains. In particular, the method of adjoint systems [2, 3] allows to express the

shape derivatives of the functionals as boundary integrals if the underlying elastic fields are smooth enough. In practical situations the regularity of elastic fields is low because of stress singularities which appear at geometrical peculiarities like corners, cracks and notches and at points where the boundary conditions change. In this case the sensitivity analysis is much less developed and only few mathematically rigorous results are available. For example, in [13] the existence and the $H^1(\Omega)$–regularity of the material derivative is proved for the mixed boundary value problem for the Laplace equation in a smooth domain, using the implicit function theorem. Moreover, there exist a lot of papers on particular problems of fracture mechanics, where the sensitivity of the potential energy with respect to a variation of the crack tip is analyzed (see the classical paper by RICE [15] and the subsequent mathematical works [11, 4, 10, 12]).

In this paper we study the influence of stress singularities on the sensitivity of linearized elastic fields in general two–dimensional domains with corners, and of a class of corresponding functionals with respect to shape perturbation. To this end we apply the material derivative approach [5, 17, 6, 18], i.e. we introduce a fixed reference configuration and consider a class of small perturbations of the reference domain. The state equations as well as all fields which are defined over the actual configuration are transformed to the fixed reference configuration. Thus the investigation of the shape sensitivity can be reduced to the investigation of a regular perturbed boundary value problem for the transformed elastic fields. We expand the transformed quantities asymptotically with respect to the perturbation parameter ε and justify the asymptotics with the help of a–priori estimates in weighted Sobolev spaces. In this way we obtain the existence and precise regularity results for the material and the shape derivatives of the displacement fields. We apply the method of adjoint problems in order to express the derivatives of the functionals as boundary integrals and give conditions under which this approach can be justified. Then we show that in case of cracked structures, the sensitivity of functionals depends also on the stress intensity factors of the adjoint field, and the original version of the method of adjoint problems [2, 3] has to be modified. Finally, we apply these results to the sensitivity of several basic functionals.

2. Formulation of the problem

Let $\Omega \subset \mathbb{R}^2$ be a bounded domain, whose boundary $\partial\Omega$ consists of two smooth open manifolds Γ^D, Γ^N and a set S of isolated points where stress singularities can occur, i.e. corner points and points where the boundary conditions change (see e.g. Fig. 1). We assume that $\Gamma^D \neq \emptyset$ and that the domain Ω is locally diffeomorphic in a neighbourhood of each singular point $P_i \in S$ to a wedge.

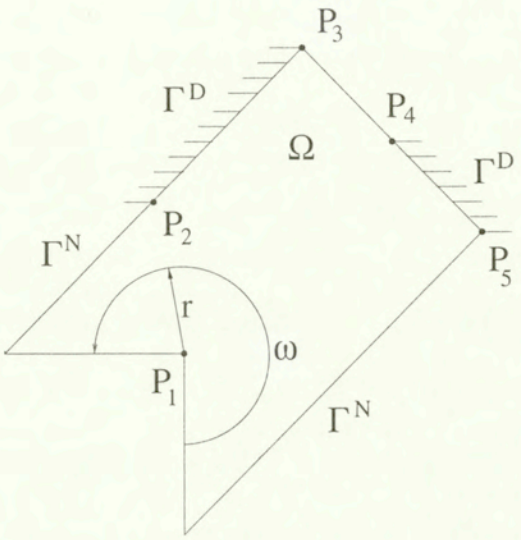

FIG. 1. A plate with singular points $P_1, \ldots, P_5$.

We introduce a family of mappings

$$\{\Phi_\varepsilon \in [C^3(\overline{\Omega})]^2;\ \varepsilon \in [0, \varepsilon_0]\} \tag{2.1}$$

which admit Taylor expansions

$$\Phi_\varepsilon(x) = x + \varepsilon\Phi(x) + \varepsilon^2\Phi_R(\varepsilon, x) \tag{2.2}$$

with $\Phi, \Phi_R \in [C^3(\overline{\Omega})]^2$. The function $\Phi_R(\varepsilon, x)$ is bounded with respect to ε for every $x \in \Omega$. The perturbations $(\Omega_\varepsilon, \Gamma_\varepsilon^D, \Gamma_\varepsilon^N)$ of the reference configuration $(\Omega, \Gamma^D, \Gamma^N)$ are defined by

$$\Omega_\varepsilon = \Phi_\varepsilon(\Omega), \quad \Gamma_\varepsilon^D = \Phi_\varepsilon(\Gamma^D), \quad \Gamma_\varepsilon^N = \Phi_\varepsilon(\Gamma^N). \tag{2.3}$$

Since $\Phi_\varepsilon \in [C^3(\overline{\Omega})]^2$, the number of singular points in Ω_ε is constant for every ε.

We consider the following mixed boundary value problem for the displacement field u_ε in an anisotropic linear elastic body occupying the perturbed configuration

$$\begin{aligned} Lu_\varepsilon(x_\varepsilon) := -\mathrm{div}\sigma(u_\varepsilon)(x_\varepsilon) &= f_\varepsilon(x_\varepsilon) \qquad \text{in} \quad \Omega_\varepsilon, \\ u_\varepsilon(x_\varepsilon) &= 0 \qquad\quad \text{on} \quad \Gamma_\varepsilon^D, \\ \sigma(u_\varepsilon)\mathbf{n}_\varepsilon(x_\varepsilon) &= h_\varepsilon(x_\varepsilon) \qquad \text{on} \quad \Gamma_\varepsilon^N, \end{aligned} \tag{2.4}$$

where $\sigma(u_\varepsilon) = C : e(u_\varepsilon)$ is the linearized stress tensor with the components $\sigma_{ij} = c_{ijkl}e_{ij}$, $e_{ij} = (\partial_i u_j + \partial_j u_i)/2$ is the linearized strain tensor,

$\mathbf{C} = \{c_{ijkl}, i,j,k,l = 1,2\}$ is the Hooke's tensor and $\mathbf{n}_\varepsilon$ is the outer unit normal vector on $\partial\Omega_\varepsilon$. Moreover, we consider functionals associated with the elastic fields u_ε and $\sigma(u_\varepsilon)$

$$J(\Omega_\varepsilon) = \int_{\Omega_\varepsilon} F(u_\varepsilon, \sigma(u_\varepsilon))dx_\varepsilon. \tag{2.5}$$

The function F satisfies for a positive constant c the growth conditions

$$F(p,q) \leqslant a(p)(c + |q|^2),\ \partial_q F(p,q) \leqslant a(p)(c + |q|) \tag{2.6}$$

for some $a \in C(\mathbb{R}^2)$ and all $p \in \mathbb{R}^2$, $q \in \mathbb{R}^4$. This guarantees that the functional (2.5) is well defined for all displacements $u_\varepsilon \in [W^1_{2+\delta}(\Omega_\varepsilon)]^2$ and all stresses $\sigma(u_\varepsilon) \in [L_{2+\delta}(\Omega_\varepsilon)]^4$ with a small $\delta > 0$ [1, Lemma 9.5]. Examples of such functionals will be given in Sec. 7.

Our goal is to derive formulae for the sensitivity of the functional J with respect to the perturbation mapping Φ_ε, i.e. we want to calculate the shape derivative

$$dJ(\Omega, \Phi_\varepsilon) = \lim_{\varepsilon \to 0} \frac{J(\Phi_\varepsilon(\Omega)) - J(\Omega)}{\varepsilon} \tag{2.7}$$

and to express $dJ(\Omega, \Phi_\varepsilon)$ as an integral over $\partial\Omega$.

3. Regularity of elastic fields in 2D non-smooth domains

In this section we omit the index ε.

The behaviour of solutions of elliptic boundary value problems like (2.4) in the neighbourhood of singular points $P_i \in S$ was mathematically analyzed by KONDRAT'EV [8] (see also the monograph [9], whose general theory was applied to problems of the theory of isotropic linearized elasticity in [16]. Stress singularities were investigated earlier by many engineers using formal methods (see e.g. [7]). According to Kondrat'ev's results, the weak solution $\theta u - u_\varepsilon$ of the boundary value problem (2.4) admits a decomposition into a linear combination of singular functions S_j which have (in polar coordinates (r, ω) centred on P_i) the form

$$S_j = r^{\alpha_j}\varphi_j(\log r, \omega), \tag{3.1}$$

and a more regular remainder $\tilde{u}$

$$u = \sum_j c_j S_j + \tilde{u} \tag{3.2}$$

provided that the given forces satisfy appropriate regularity assumptions. The singular functions S_j are solutions of the problem (2.4) with vanishing body and

boundary forces in the infinite wedge $W(P_i)$ which coincides with Ω in some neighbourhood of P_i. The exponents α_j and the functions φ_j can be interpreted as eigenvalues and (generalized) eigenfunctions of a certain operator pencil $\mathcal{A}(P_i)$ (see [8, 9] for details). The exponents α_j in (3.1) are complex roots of special transcendent equations [7, 16] and have to be calculated numerically. For the functions φ_j of S_j many explicit formulae are available (see [7, 16] for isotropic elasticity). In this paper we are interested mainly in the eigenvalue with the smallest positive real part which determines the regularity of the weak solution. To this end we define $a_0 = \min\{\mathrm{Re}\alpha_j\}$, where the minimum is taken over all eigenvalues α_j of $\mathcal{A}(P_i)$ with a positive real part $\mathrm{Re}\alpha_j$ for every singular point $P_i \in S$. Note that $a_0 \geqslant 1/2$ in case of a pure Dirichlet or a pure Neumann problem, whereas for mixed boundary value problems we have only $a_0 \geqslant 1/4$ [16]. In case of a pure Dirichlet or a pure Neumann problem in a domain with reentrant corners we have $a_0 < 1$, i.e. the stresses are unbounded. At points where the boundary conditions change, stress singularities can occur even if the boundary is smooth.

For the formulation of the regularity results we use weighted Sobolev spaces which describe not only the regularity of functions in the interior of Ω but also their behaviour near singular points.

DEFINITION 3.1. [8, 9] *For $d = 0, 1, 2, \ldots$ we define the weighted Sobolev space $V_\beta^d(\Omega)$ as the closure of $C_0^\infty(\overline{\Omega} \setminus S)$ with respect to the norm*

$$\|u\|_{V_\beta^d(\Omega)} := \left(\sum_{|\gamma| \leqslant d} \|\tilde{r}^{\beta - d + |\gamma|} D_x^\gamma u\|_{L_2(\Omega)}^2 \right)^{1/2}, \tag{3.3}$$

where $\tilde{r} = \mathrm{dist}(x, S)$. The trace spaces $V_\beta^{d+1/2}(\partial\Omega)$, $V_\beta^{d+1/2}(\Gamma^D)$, $V_\beta^{d+1/2}(\Gamma^N)$ are defined in the usual way.

Roughly speaking, a function u belongs to $V_\beta^d(\Omega)$ if it belongs to $H^d(\tilde{\Omega})$ for every open subset $\tilde{\Omega} \subset \Omega$ and $u(x) \leqslant c|x - P_i|^{d-\beta-1}$ in the neighbourhood of every singular point $P_i \in S$ with some positive constant c.

THEOREM 3.2. [8, 16, 9] *Let $d = 0, 1, 2, \ldots$, $\beta := d + 1 - a_0 + \delta$ with a small positive δ and $f \in [V_\beta^d(\Omega)]^2$, $h \in [V_\beta^{d+1/2}(\Gamma^N)]^2$. Then the unique weak solution $u \in [H^1(\Omega)]^2$ of (2.4) belongs to $[V_\beta^{d+2}(\Omega)]^2$ and the following a priori estimate is valid:*

$$\|u\|_{[V_\beta^{d+2}(\Omega)]^2} \leqslant c \left\{ \|f\|_{[V_\beta^d(\Omega)]^2} + \|h\|_{[V_\beta^{d+1/2}(\Gamma^N)]^2} \right\} \tag{3.4}$$

with a positive real constant c.

4. Existence and regularity of the material and the shape derivative

Let us investigate the existence and the regularity of the material derivative

$$\dot{u} := \left.\frac{d(u_\varepsilon \circ \Phi_\varepsilon)}{d\varepsilon}\right|_{\varepsilon=0} \tag{4.1}$$

and the shape derivative

$$u' := \left.\frac{du_\varepsilon}{d\varepsilon}\right|_{\varepsilon=0} \tag{4.2}$$

of the perturbed displacement field u_ε. To this end we transform the problem (2.4) onto the reference configuration by means of a change of variables $x_\varepsilon = \Phi_\varepsilon(x)$ and obtain in this way a boundary value problem for the transformed field $u_\varepsilon \circ \Phi_\varepsilon$

$$\begin{aligned} L^\varepsilon(u_\varepsilon \circ \Phi_\varepsilon)(x) &= f_\varepsilon \circ \Phi_\varepsilon(x) && \text{in} \quad \Omega, \\ u_\varepsilon \circ \Phi_\varepsilon(x) &= 0 && \text{on} \quad \Gamma^D, \\ \sigma^\varepsilon(u_\varepsilon \circ \Phi_\varepsilon)(\mathbf{n}_\varepsilon \circ \Phi_\varepsilon)(x) &= h_\varepsilon \circ \Phi_\varepsilon(x) && \text{on} \quad \Gamma^N. \end{aligned} \tag{4.3}$$

Here, L^ε and σ^ε are differential operators whose coefficients depend smoothly on ε and admit expansions in Taylor series

$$L^\varepsilon := L + \varepsilon L_1 + \varepsilon^2 L_R(\varepsilon), \tag{4.4}$$

$$\sigma^\varepsilon := \sigma + \varepsilon\sigma_1 + \varepsilon^2\sigma_R(\varepsilon), \tag{4.5}$$

where $L = -\mathrm{div}\sigma$ and the coefficients of L_R and σ_R are bounded with respect to $\varepsilon \in [0, \varepsilon_0]$. Note that the Theorem 3.2 can be applied also to boundary value problems with the operators $L^\varepsilon, \sigma^\varepsilon$ instead of L, σ provided that ε is small enough.

Let us assume that the transformed forces $f_\varepsilon \circ \Phi_\varepsilon$ and $h_\varepsilon \circ \Phi_\varepsilon$ also depend smoothly on ε

$$f_\varepsilon \circ \Phi_\varepsilon = f_0 + \varepsilon f_1 + \varepsilon^2 f_R(\varepsilon), \tag{4.6}$$

$$h_\varepsilon \circ \Phi_\varepsilon = h_0 + \varepsilon h_1 + \varepsilon^2 h_R(\varepsilon). \tag{4.7}$$

Inserting these expansions together with

$$\mathbf{n}_\varepsilon \circ \Phi_\varepsilon = \mathbf{n}_0 + \varepsilon\dot{\mathbf{n}} + \varepsilon^2\mathbf{n}_R(\varepsilon) \tag{4.8}$$

and the formal ansatz

$$(u_\varepsilon \circ \Phi_\varepsilon)(x) = u_0(x) + \varepsilon\dot{u}(x) + O(\varepsilon^2) \tag{4.9}$$

into (4.3) and comparing the terms of the order $O(\varepsilon)$ we obtain a boundary value problem for the material derivative $\dot{u}$

$$
\begin{aligned}
-\mathrm{div}\sigma(\dot{u}) &= f_1 - L_1 u_0 && \text{in} \quad \Omega, \\
\dot{u} &= 0 && \text{on} \quad \Gamma^D, \\
\sigma(\dot{u})\mathbf{n}_0 &= h_1 - \sigma_1(u_0)\mathbf{n}_0 - \sigma(u_0)\dot{\mathbf{n}} && \text{on} \quad \Gamma^N.
\end{aligned} \tag{4.10}
$$

The ansatz (4.9) has to be justified, i.e. we have to show that the function $\dot{u}$ in (4.9) coincides with the material derivative $\dot{u}$ defined by (4.1). The correctness of (4.9) can be easily proved with the help of the *a priori* estimate (3.4). Indeed, the following Theorem holds:

THEOREM 4.1. *Suppose that the Taylor expansions* ((4.6), (4.7)) *are valid with* $f_\varepsilon \circ \Phi_\varepsilon, f_0, f_1, f_R \in [V^1_\beta(\Omega)]^2$, $h_\varepsilon \circ \Phi_\varepsilon, h_0, h_1, h_R \in [V^{3/2}_\beta(\Gamma^N)]^2$ *and* $\beta := 2 - a_0 + \delta$ *with a small positive* δ. *Then the following estimate is valid*

$$
\|u_\varepsilon \circ \Phi_\varepsilon - u_0 - \varepsilon \dot{u}\|_{[V^3_\beta(\Omega)]^2} \leqslant c\varepsilon^2 \tag{4.11}
$$

with a positive real constant c.

P r o o f: From the formal ansatz (4.9) and the Taylor expansions (4.4) – (4.8) follows that the function $v := u_\varepsilon \circ \Phi_\varepsilon - u_0 - \varepsilon \dot{u}$ satisfies the following elliptic boundary value problem:

$$
\begin{aligned}
L^\varepsilon(v) &= \varepsilon^2(f_R - L_R u_0) + O(\varepsilon^3) && \text{in} \quad \Omega, \\
v &= 0 && \text{on} \quad \Gamma^D, \\
\sigma^\varepsilon(v)(\mathbf{n}_\varepsilon \circ \Phi_\varepsilon) &= \varepsilon^2(h_R - \sigma(u_0)\mathbf{n}_R - \sigma(\dot{u})\dot{\mathbf{n}} - \sigma_R(u_0)\dot{\mathbf{n}} \\
&\quad -\sigma_R(\dot{u})\mathbf{n}_0 - \sigma_R(u_0)\mathbf{n}_0) + O(\varepsilon^3) && \text{on} \quad \Gamma^N.
\end{aligned} \tag{4.12}
$$

From Theorem 3.2 applied to (4.10) it follows that $\dot{u} \in [V^3_\beta(\Omega)]^2$. Since $f_R \in [V^1_\beta(\Omega)]^2$, $h_R \in [V^{3/2}_\beta(\Gamma^N)]^2$, the right-hand sides of (4.12) satisfy the assumptions of Theorem 3.2. Applying the *a priori* estimate (3.4) to (4.12) we obtain the assertion. □.

The above theorem states that the material derivative $\dot{u}$ exists and belongs to the space $[V^3_{2-a_0+\delta}(\Omega)]^2$. It means, both u_0 and $\dot{u}$ behave at least as $O(r^{a_0})$ in the vicinity of singular points. Furthermore, we obtain immediately the existence and the regularity of the shape derivative u'. Indeed, from the identity

$$
u' = \dot{u} - \mathbf{D}u_0 \cdot \Phi \tag{4.13}
$$

follows that u' belongs to $[V^2_{2-a_0+\delta}(\Omega)]^2$ and it behaves at least as $O(r^{a_0-1})$ near the singular points. If $a_0 < 1$ and the perturbation mapping Φ does not vanish near the singular points, then u' is a displacement field of infinite potential energy, $u' \notin [H^1(\Omega)]^2$. From now on, we will assume that the given body and surface forces do not depend on the parameter ε, i.e. there exist functions f, L defined on R^2 such that $f_\varepsilon = f|_{\Omega_\varepsilon}$, $h_\varepsilon = h|_{\Gamma^N_\varepsilon}$.

Inserting (4.13) into (4.10) we find out that the shape derivative u' satisfies the following boundary value problem (see e.g. [18, Chapter 3.1.5]):

$$
\begin{aligned}
-\mathrm{div}\sigma(u') &= 0 && \text{in } \Omega,\\
u' &= -\langle \Phi, \mathbf{n}_0\rangle \partial_{\mathbf{n}} u_0 && \text{on } \Gamma^D,\\
\sigma(u')\mathbf{n}_0 &= \langle \Phi, \mathbf{n}_0\rangle (f + \kappa h) - \mathrm{div}_\Gamma(\langle \Phi, \mathbf{n}_0\rangle \sigma_T(u_0)) && \text{on } \Gamma^N.
\end{aligned} \tag{4.14}
$$

Here we denote by $\partial_n u_0$ the normal derivative of u_0 on $\partial\Omega$, $\sigma_T(u_0)$ is the tangential component of the stress tensor on $\partial\Omega$, κ is the curvature of $\partial\Omega$ and the tangential divergence operator div_Γ is defined by

$$
\mathrm{div}_\Gamma v = \mathrm{div} v - \langle \mathbf{D}v \cdot \mathbf{n}_0, \mathbf{n}_0\rangle. \tag{4.15}
$$

REMARK 4.1. The boundary value problem (4.14) is in general not suitable for the numerical computation of u' because $u' \notin [H^1(\Omega)]^2$ is not a variational solution of (4.14). The right-hand sides of (4.14) depend on the derivatives of $u_0 \in [H^{1+a_0}(\Omega)]^2$ and are also singular if $a_0 < 1$. However, in the following we use only the information on the dependence of the boundary values of u' on the boundary values of $\partial_{\mathbf{n}} u_0, \sigma_T(u_0)$ and $\langle \Phi, \mathbf{n}_0\rangle$.

5. Sensitivity of functionals by the method of adjoint problems

In this and in the following sections we write shortly σ_0 for $\sigma(u_0)$ and denote by $\dot{\sigma}, \sigma'$ the material and the shape derivative of $\sigma(u_\varepsilon)$, respectively.

5.1. Sensitivity via the material derivative

Let us assume that the scalar function F in (2.5) is continuously differentiable with respect to all its arguments and satisfies the growth conditions (2.6). Standard formulae for the sensitivity of integrals over varying domains yield [17, 14]

$$
\begin{aligned}
dJ(\Omega, \Phi_\varepsilon) = \int_\Omega \{ &\langle \partial_u F(u_0, \sigma_0), \dot{u}\rangle + \partial_\sigma F(u_0, \sigma_0) : \dot{\sigma}\\
&+ F(u_0, \sigma_0)\mathrm{div}\,\Phi\}\, dx.
\end{aligned} \tag{5.1}
$$

This formula is valid without any restrictions on the strength of the stress singularities. However, the expression (5.1) depends on the values of Φ inside Ω.

5.2. Sensitivity via shape derivative

Let us assume that the constant a_0 which determines the regularity of the displacement field u_0 and of the derivatives $\dot{u}, u'$ is not less than $1/2$. Otherwise we have to require that the mapping Φ vanishes in the neighbourhood of singular points where the stress singularities are stronger. Replacing the material derivatives $\dot{u}, \dot{\sigma}$ in (5.1) by the corresponding shape derivatives u', σ' using the identity (4.13), we obtain an expression for $dJ(\Omega, \Phi_\varepsilon)$ which depends only on the boundary values of the perturbation mapping Φ [17, 14]

$$dJ(\Omega,\Phi_\varepsilon) = \int_\Omega \left\{ \langle \partial_u F(u_0,\sigma_0), u' \rangle + \partial_\sigma F(u_0,\sigma_0) : \sigma' \right\} dx + \int_{\partial\Omega} F(u_0,\sigma_0)\langle \Phi, \mathbf{n}_0 \rangle ds_x. \tag{5.2}$$

The assumption $a_0 \geqslant 1/2$ and the growth conditions (2.6) ensure that all integrals in (5.2) exist.

5.3. Boundary expression for the sensitivity

The expression (5.2) still contains a domain integral. It can be transformed to a boundary integral using the method of adjoint problems [2, 3]. Here we assume that $a_0 > 1/2$. The interesting case of elastic bodies with cracks, where $a_0 = 1/2$, requires a more careful investigation and will be treated in the next section. Furthermore, we assume that the function F is twice continuously differentiable. Following the ideas from [3] we replace $\partial_\sigma F(u_0,\sigma_0) : \sigma'$ in (5.2) by $\partial_\sigma F(u_0,\sigma_0) : (\mathbf{C} : e(u'))$ and use Green's first formula (9.1) applied to a field v with $\sigma(v) = \mathbf{C} : \partial_\sigma F(u_0,\sigma_0)$ and to the field u'

$$\int_\Omega (\mathbf{C} : \partial_\sigma F(u_0,\sigma_0)) : e(u')dx = \int_{\partial\Omega} \langle u', (\mathbf{C} : \partial_\sigma F(u_0,\sigma_0))\mathbf{n}_0 \rangle ds_x - \int_\Omega \langle u', \operatorname{div}(\mathbf{C} : \partial_\sigma F(u_0,\sigma_0)) \rangle dx. \tag{5.3}$$

In this way we obtain

$$dJ(\Omega,\Phi_\varepsilon) = \int_\Omega \langle \partial_u F(u_0,\sigma_0) - \operatorname{div}(\mathbf{C} : \partial_\sigma F(u_0,\sigma_0)), u' \rangle dx + \int_{\partial\Omega} \left\{ F(u_0,\sigma_0)\langle \Phi, \mathbf{n}_0 \rangle + \langle (\mathbf{C} : \partial_\sigma F(u_0,\sigma_0))\mathbf{n}_0, u' \rangle \right\} ds_x. \tag{5.4}$$

We introduce an adjoint displacement field w as the solution of the boundary value problem

$$
\begin{aligned}
-\mathrm{div}\sigma(w) &= \partial_u F(u_0,\sigma_0) - \mathrm{div}(\mathbf{C} : \partial_\sigma F(u_0,\sigma_0)) && \text{in} \quad \Omega,\\
w &= 0 && \text{on} \quad \Gamma^D,\\
\sigma(w)\mathbf{n}_0 &= (\mathbf{C} : \partial_\sigma F(u_0,\sigma_0))\mathbf{n}_0 && \text{on} \quad \Gamma^N.
\end{aligned} \tag{5.5}
$$

LEMMA 5.1. *Let the assumptions of Theorem 4.1 be satisfied. Then the boundary value problem* (5.5) *has a unique weak solution w which belongs to* $[V^3_{2-a_0+\delta}(\Omega)]^2$.

P r o o f: Under the assumptions of Theorem 4.1 we have $u_0 \in [V^3_{2-a_0+\delta}(\Omega)]^2$, $\sigma_0 \in [V^2_{2-a_0+\delta}(\Omega)]^2$. Therefore $\partial_u F(u_0,\sigma_0), \mathrm{div}(\mathbf{C} : \partial_\sigma F(u_0,\sigma_0)) \in [V^1_{2-a_0+\delta}(\Omega)]^2$ and $(\mathbf{C} : \partial_\sigma F(u_0,\sigma_0))\mathbf{n}_0 \in [V^{3/2}_{2-a_0+\delta}(\Gamma^N)]^2$ because of the growth conditions (2.6). Thus we can apply Theorem 3.2 and obtain the assertion. □

The domain integral in (5.4) can now be transformed to a boundary integral by using second Green's formula (9.2) applied to the displacement fields u' and w. Note that in case of cracked bodies, where $a_0 = 1/2$, all integrals in (9.2) exist but the formula (9.2) is not valid any more.

Since $\mathrm{div}\sigma(u') = 0$, we obtain finally

$$
\begin{aligned}
dJ(\Omega,\Phi_\varepsilon) = &\int_{\partial\Omega} F(u_0,\sigma_0)\langle\Phi,\mathbf{n}_0\rangle ds_x + \int_{\Gamma^N} \langle w, \sigma(u')\mathbf{n}_0\rangle ds_x\\
&+ \int_{\Gamma^D} \langle (\mathbf{C} : \partial_\sigma F(u_0,\sigma_0))\mathbf{n}_0 - \sigma(w)\mathbf{n}_0, u'\rangle ds_x.
\end{aligned} \tag{5.6}
$$

Inserting the boundary values of u' from (4.14) into (5.6) we get:

THEOREM 5.2. *Under previous assumptions we have*

$$
\begin{aligned}
dJ(\Omega,\Phi_\varepsilon) = &\int_{\partial\Omega} F(u_0,\sigma_0)\langle\Phi,\mathbf{n}_0\rangle ds_x + \int_{\Gamma^N} \langle w, \langle\Phi,\mathbf{n}_0\rangle(f+\kappa h)\\
&-\mathrm{div}_\Gamma(\langle\Phi,\mathbf{n}_0\rangle\sigma_T(u_0))\rangle ds_x - \int_{\Gamma^D} \langle\Phi,\mathbf{n}_0\rangle\langle(\mathbf{C} : \partial_\sigma F(u_0,\sigma_0))\mathbf{n}_0\\
&- \sigma(w)\mathbf{n}_0, \partial_{\mathbf{n}} u_0\rangle ds_x.
\end{aligned} \tag{5.7}
$$

6. Method of adjoint problems for 2D crack problems

Let us consider an elastic body with a smooth crack (see e.g. Fig. 2). On the outer parts of the boundary, mixed boundary conditions are given, whereas the crack lips are stress-free. For the sake of simplicity we suppose that the material is isotropic, i.e. only two independent material constants λ, μ appear and

$$c_{ijkl} = \lambda \delta_{ij}\delta_{kl} + \mu\left(\delta_{ik}\delta_{jl} + \delta_{il}\delta_{jk}\right). \tag{6.1}$$

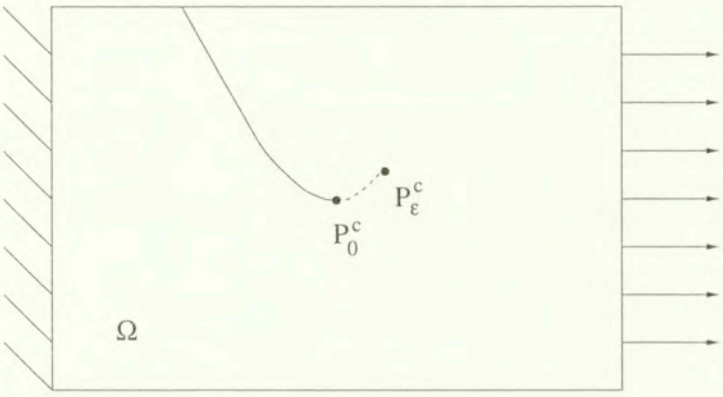

FIG. 2. A plate with a crack.

For every singular point P_i lying on the outer boundary we assume that there exists no eigenvalue α_j of $\mathcal{A}(P_i)$ with $0 < \mathrm{Re}\alpha_j \leqslant 1/2$, i.e. there is no stress singularity near P_i stronger than the singularity at the crack tip. Otherwise we must assume that the singular point P_i is not perturbed by Φ_ε. In this way we ensure that the crack tip singularity is dominating and we have $a_0 = 1/2$. Furthermore we suppose that the perturbed crack tip P_ε^c moves along a smooth curve and $\langle \Phi(x), \mathbf{n}_0(x)\rangle = O(|x - P_0^c|^{2\delta})$ with a small positive δ near the unperturbed crack tip P_0^c. Moreover, we can assume without loss of generality that the vector tangent to the crack curve at the unperturbed crack tip P_0^c coincides with the vector $(1,0)^\top$. In this case the perturbation mapping has locally in the vicinity of P_0^c the form

$$\Phi_\varepsilon\begin{pmatrix} x \\ y \end{pmatrix} = \begin{pmatrix} x \\ y \end{pmatrix} + \varepsilon\begin{pmatrix} 1 \\ 0 \end{pmatrix} + O(\varepsilon^2). \tag{6.2}$$

Let us describe precisely the behaviour of the displacement fields u_ε and u'. Under the previous assumptions on the regularity of given forces, the displacement field u_ε belongs to $[V^3_{3/2+\delta}(\Omega_\varepsilon)]^2$ and admits in the neighbourhood of the perturbed crack tip P_ε^c the asymptotics (see e.g. [9, 10])

$$u_\varepsilon(r_\varepsilon,\omega_\varepsilon)=\sum_{j=1}^{2}K_j(u_\varepsilon)r_\varepsilon^{1/2}\varphi_j(\omega_\varepsilon)+O(r_\varepsilon) \tag{6.3}$$

with

$$\varphi_1(\omega)=\frac{1}{4\mu\sqrt{2\pi}}\begin{pmatrix}-\cos(3\omega/2)+(2\tau-1)\cos(\omega/2)\\ \sin(3\omega/2)-(2\tau+1)\sin(\omega/2)\end{pmatrix}, \tag{6.4}$$

$$\varphi_2(\omega)=\frac{1}{4\mu\sqrt{2\pi}}\begin{pmatrix}3\sin(3\omega/2)-(2\tau-1)\sin(\omega/2)\\ 3\cos(3\omega/2)-(2\tau+1)\cos(\omega/2)\end{pmatrix}, \tag{6.5}$$

where $\tau=(\lambda+3\mu)(\lambda+\mu)^{-1}$. Here, $(r_\varepsilon,\omega_\varepsilon)$ are polar coordinates with origin in P_ε^c and the angular variable ω_ε is oriented in such a way that the crack lips correspond to the angles $\pi,-\pi$. Furthermore we have written the singular functions $\varphi_j, j=1,2$, in polar components $\varphi_j=(\varphi_j^r,\varphi_j^\omega)^\top$. The coefficients $K_1(u_\varepsilon)$ and $K_2(u_\varepsilon)$ are called stress intensity factors of Mode I and Mode II, respectively, and are given by

$$K_j(u_\varepsilon)=\int\limits_{\Omega_\varepsilon}f_\varepsilon\cdot\zeta_{j,\varepsilon}dx_\varepsilon+\int\limits_{\Gamma_\varepsilon^N}h_\varepsilon\cdot\zeta_{j,\varepsilon}ds_{x_\varepsilon}, \tag{6.6}$$

where the weight functions $\zeta_{j,\varepsilon}\in[V^2_{3/2+\delta}(\Omega_\varepsilon)]^2$, $j=1,2$, satisfy the problem (2.4) in Ω_ε with vanishing body and boundary forces and admit the asymptotics

$$\zeta_{j,\varepsilon}(r_\varepsilon,\omega_\varepsilon)=r_\varepsilon^{-1/2}\psi_j(\omega_\varepsilon)+O(r_\varepsilon^{1/2}). \tag{6.7}$$

with

$$\psi_1(\omega)=\frac{1}{(1+\tau)\sqrt{8\pi}}\begin{pmatrix}-3\cos(\omega/2)+(2\tau+1)\cos(3\omega/2)\\ 3\sin(\omega/2)-(2\tau-1)\sin(3\omega/2)\end{pmatrix}, \tag{6.8}$$

$$\psi_2(\omega)=\frac{1}{(1+\tau)\sqrt{8\pi}}\begin{pmatrix}\sin(\omega/2)-(2\tau+1)\sin(3\omega/2)\\ \cos(\omega/2)-(2\tau-1)\cos(3\omega/2)\end{pmatrix}. \tag{6.9}$$

The following theorem plays the key role in the application of the adjoint method to problems with cracks.

THEOREM 6.1. *Let $\gamma=(1+\tau)/(4\mu)$ and $\langle\Phi(x),\mathbf{n}_0(x)\rangle=O(|x-P_0^c|^{2\delta})$ near the crack tip P_0^c. Then the shape derivative $u'\in[V^2_{3/2+\delta}(\Omega)]^2$ has the following decomposition:*

$$u'=\gamma\sum_{i=1}^{2}K_i(u_0)\zeta_{i,0}+\tilde{u}' \tag{6.10}$$

with $\tilde{u}'\in[V^2_{3/2-\delta}(\Omega)]^2$.

P r o o f. Since $-1/2$ is the only eigenvalues of $\mathcal{A}(P_0^c)$ in the interval $(-\frac{1}{2}-\delta, -\frac{1}{2}+\delta)$, we can apply the general theory of elliptic systems in domains with corners [8, 9] to the problem (4.14). The condition $\langle \Phi(x), \mathbf{n}_0(x)\rangle = O(|x-P_0^c|^{2\delta})$ implies that the right-hand sides of (4.14) belong to $[V^{3/2}_{3/2-\delta}(\Gamma^D)]^2 \times [V^{1/2}_{3/2-\delta}(\Gamma^N)]^2$ and we obtain the decomposition

$$u' = \sum_{i=1}^{2} c_i \zeta_{i,0} + \tilde{u}' \tag{6.11}$$

with $\tilde{u}' \in [V^2_{3/2-\delta}(\Omega)]^2$ and real coefficients c_1, c_2 to be determined.

Let us calculate these coefficients. To this end we calculate the singular terms in the asymptotics of u' near the crack tip using the identity (4.13). Since $\dot{u} \in [V^3_{3/2+\delta}(\Omega)]^2$, the main parts of the asymptotics of the functions u' and $-\mathbf{D}u_0 \cdot \Phi$ coincide. Furthermore $\mathbf{D}u_0 \cdot \Phi = \partial_{x_1} u_0$ near the crack tip P_0^c because of the special form (6.2) of the perturbation mapping Φ_ε. Using the identity (see e.g. [9, 10])

$$\partial_{x_1}(r_0^{1/2}\varphi_j(\omega_0)) = -\gamma r_0^{-1/2}\psi_j(\omega_0), \quad j = 1, 2, \tag{6.12}$$

we obtain from (6.3) with $\varepsilon = 0$

$$\partial_{x_1} u_0(r_0, \omega_0) = -\gamma \sum_{j=1}^{2} K_j(u_0) r_0^{-1/2} \psi_j(\omega) + O(r_0^{1/2}) \tag{6.13}$$

and the assertion follows. □

THEOREM 6.2. *Under the assumptions of the previous theorem we have*

$$\begin{aligned} dJ(\Omega, \Phi_\varepsilon) = \gamma \sum_{i=1}^{2} K_i(u_0) K_i(w) + \int_{\partial\Omega} F(u_0, \sigma_0)\langle \Phi, \mathbf{n}_0\rangle ds_x \\ + \int_{\Gamma^N} \langle w, \langle \Phi, \mathbf{n}_0\rangle (f + \kappa h) - \operatorname{div}_\Gamma(\langle \Phi, \mathbf{n}_0\rangle \sigma_T(u_0))\rangle ds_x \\ - \int_{\Gamma^D} \langle \Phi, \mathbf{n}_0\rangle \langle (\mathbf{C} : \partial_\sigma F(u_0, \sigma_0))\mathbf{n}_0 - \sigma(w)\mathbf{n}_0, \partial_n u_0\rangle ds_x. \end{aligned} \tag{6.14}$$

P r o o f. We insert the decomposition (6.10) into (5.3). The integrals with the weight functions $\zeta_{i,0}$ can be interpreted as $\gamma \sum_{i=1}^{2} K_i(u_0) K_i(w)$ due to formula (6.6). The remaining integrals with $\tilde{u}'$ are reduced to the boundary as described

in Section 5.3 because $\tilde{u}' \in [V^2_{3/2-\delta}(\Omega)]^2$ is regular enough in order to apply the method of adjoint problems. Thus (6.14) follows. □

7. Examples

Let us apply the results of the last section to calculate the sensitivity of some special functionals. The resulting formulae have a particularly simple form if we assume that the crack tip moves along a straight line and the remaining boundary is fixed. In this case we have $\langle \Phi, \mathbf{n}_0 \rangle = 0$ on the whole boundary and formula (6.14) simplifies to

$$dJ(\Omega, \Phi_\varepsilon) = \gamma \sum_{i=1}^{2} K_i(u_0) K_i(w). \tag{7.1}$$

A formula similar to (7.1) was obtained in [13] for the mixed boundary value problem for the Laplace equation in a smooth domain with collision points (i.e. points where the boundary conditions change) moving along the boundary.

EXAMPLE 1. Let $\tilde{u} \in L_2(\tilde{\Omega})$ where $\Omega_\varepsilon \subset \tilde{\Omega}$ $\forall \varepsilon \in [0, \varepsilon_0]$ and let the functional J be defined by

$$J(\Omega_\varepsilon) = \frac{1}{2} \int_{\Omega_\varepsilon} (u_\varepsilon - \tilde{u})^2 dx_\varepsilon. \tag{7.2}$$

Here we obtain formula (7.1) with the adjoint field w satisfying the following boundary value problem:

$$\begin{aligned} -\mathrm{div}\sigma(w) &= u_0 - \tilde{u} \quad \text{in} \quad \Omega, \\ w &= 0 \qquad\quad \text{on} \quad \Gamma^D, \\ \sigma(w)\mathbf{n}_0 &= 0 \qquad\quad \text{on} \quad \Gamma^N. \end{aligned} \tag{7.3}$$

EXAMPLE 2. In case of the energy functional

$$J(\Omega_\varepsilon) = \frac{1}{2} \int_{\Omega_\varepsilon} \sigma(u_\varepsilon) : e(u_\varepsilon) dx_\varepsilon, \tag{7.4}$$

the adjoint field w coincides with the displacement field u_0. In this way we obtain the well known Irwin formula [15, 11, 4, 10]

$$dJ(\Omega, \Phi_\varepsilon) = \gamma \sum_{i=1}^{2} K_i(u_0)^2. \tag{7.5}$$

8. Conclusions

The occurence of stress singularities in elastic bodies demands in the sensitivity analysis the consideration of the regularity of underlying elastic fields. Since singular stresses belong only to $L_2(\Omega)$, it is necessary to impose restrictions on the class of admissible functionals. Integral functionals over singular stresses are well defined only if the integrands satisfy quadratic growth conditions with respect to the components of the stress tensor.

The sensitivity of integral functionals can be easily expressed with the help of the material derivatives of the elastic fields. In this case we do not need any restrictions on the strength of stress singularites but the resulting expression depends on the perturbation of the interior of the domain. If all stress singularities in a body are weaker than the singularities at a crack tip (all singular exponents greater than $1/2$), then the sensitivity of the functionals can be expressed as boundary integrals using the method of adjoint problems. This method is based on the application of Green's formulae to the original displacement field and to the solution of an appropriately defined adjoint problem. In the limiting case of bodies with cracks, the sensitivity depends also on the stress intensity factors of the original and of the adjoint field. In case of stronger singularities, the method of adjoint problems can not be applied because the Green formulae are not valid.

The same approach can be also applied to three–dimensional elastic structures and to interface problems. The difficulty in the mathematical justification of the adjoint method in these cases stems from the necessity to define the weighted Sobolev spaces which take all possible stress singularities into accout (singularities at conical points, at smooth edges, intersections of edges etc.).

The problem how to reduce the sensitivity of the functionals to a boundary expression is still unsolved for problems where boundary points with very strong singularities (singular exponents smaller than $1/2$) are perturbed. One should note that singular exponents smaller than $1/2$ occur often in applications (change of boundary conditions at reentrant corners, interior interface corners etc.).

9. Appendix

In the literature, the Green integral formulae are usually formulated under assumptions on the regularity of underlying integrands which are too restrictive for the application in this paper. Therefore we give here precise assumptions which can be best formulated in weighted Sobolev spaces.

THEOREM 9.1. *a) Let* $v \in [V_\alpha^{d+2}(\Omega)]^2$, $w \in [V_\beta^{d+1}(\Omega)]^2$, $d = 0, 1, 2, \ldots$ *and* $\alpha, \beta \in \mathbb{R}$ *with* $\alpha + \beta < 2d + 1$. *Then Green's first formula holds*

$$\int_{\Omega} \sigma(v) : \epsilon(w) dx = \int_{\partial\Omega} \langle w, \sigma(v)\mathbf{n}_0 \rangle ds_x - \int_{\Omega} \langle w, \mathrm{div}\sigma(v) \rangle dx \tag{9.1}$$

b) Let $v \in [V_\alpha^{d+2}(\Omega)]^2$, $w \in [V_\beta^{d+2}(\Omega)]^2$, $d = 0, 1, 2, \ldots$ and $\alpha, \beta \in \mathbb{R}$ with $\alpha + \beta < 2d + 2$. Then Green's second formula holds

$$\int_{\Omega} \{\langle \mathrm{div}\sigma(v), w \rangle - \langle v, \mathrm{div}\sigma(w) \rangle\} \, dx = \int_{\partial\Omega} \{\langle \sigma(v)\mathbf{n}_0, w \rangle - \langle v, \sigma(w)\mathbf{n}_0 \rangle\} \, ds_x. \tag{9.2}$$

References

1. J. APPELL and P.P. ZABREJKO, *Nonlinear superposition operators,* Cambridge University Press, Cambridge 1990.
2. K. DEMS and Z. MRÓZ, *Variational approach by means of adjoint systems to structural optimization and sensitivity analysis II. Structure shape variation,* Int. J. Solids Struct., **20**, 527–552, 1984.
3. K. DEMS and Z. MRÓZ, *Shape sensitivity in mixed Dirichlet–Neumann boundary–value problems and associated class of path–independent integrals,* Eur. J. Mech. A/Solids, **14**, 169–203, 1995.
4. P. DESTUYNDER and M. DJAOUA, *Sur une interprétation mathématique de l'integrale de Rice en théorie de la rupture fragile,* Math. Meth. Appl. Sci., **3**, 70–87, 1981.
5. P.R. GARABEDIAN and M. SCHIFFER, *Convexity of domain functionals,* J. d'Anal. Math., **2**, 281–368, 1952/53.
6. E.J. HAUG, K.K. CHOI and V. KOMKOV, *Design sensitivity analysis of structural systems,* Academic Press Inc., Orlando 1986.
7. S.N. KARP and F.C. KARAL, *The elastic–field behaviour in the neighbourhood of a crack of arbitrary angle,* Comm. Pure Appl. Math., **15**, 413–421, 1962.
8. V.A. KONDRAT'EV, *Boundary problems for elliptic equations in domains with conical or angular points,* Trans. Moscow Math. Soc., **16**, 209–292, 1967.
9. S.A. NAZAROV and B.A. POLYAKOVA, *Elliptic problems in domains with piecewise smooth boundaries,* Walter de Gruyter, Berlin 1994.
10. S.A. NAZAROV and O.R. POLYAKOVA, *Rupture criteria, asymptotic conditions at crack tips, and selfadjoint extensions of the Lamé operator,* Trans. Moscow Math. Soc., **57**, 13–66, 1996.
11. K. OHTSUKA, *Generalized J–integral and three-dimensional fracture mechanics I,* Hiroshima Math. J., **11**, 21–52, 1981.
12. K. OHTSUKA and M, BOCHNIAK, *Shape sensitivity analysis of stress intensity factors by generalized J–integrals,* Math. Meth. Appl. Sci., **21**, 1343–1363, 1998.
13. B. PALMERIO and A. DERVIEUX, *Hadamard's variational formula for a mixed problem and an application to a problem related to a Signorini–like variational inequality,* Numer. Funct. Anal. Optimiz., **1**, 113–144, 1979.

14. H. PETRYK and Z. MRÓZ, *Time derivatives of integrals and functionals defined on varying volume and surface domains*, Arch. Mech., **38**, 697–724, 1986.

15. J.R. RICE, *A path independent integral and the approximate analysis of strain concentration by notches and cracks*, J. Appl. Mech., **35**, 379–386, 1968.

16. A.-M. SÄNDIG, U. RICHTER and R. SÄNDIG, *The regularity of boundary value problems for the Lamé equations in a polygonal domain*, Rostocker Math. Kolloqium, **36**, 21–50, 1989.

17. J. SIMON, *Differentiation with respect to the domain in boundary value problems*, Numer. Funct. Anal. Optimiz., **2**, 649–687, 1980.

18. J. SOKOŁOWSKI and J.P. ZOLESIO, *Introduction to shape optimization*, Springer Verlag, Berlin 1992.

Received December 7, 1998; new version March 28, 1999.

Arch. Mech., **51**, 3–4, pp. 293–310, Warszawa 1999

Laminated pressurized elastic tube and its homogenization

H. BUFLER

Institute of Mechanics (Civil Engineering)
Stuttgart University
Pfaffenwaldring 7, D-70550 Stuttgart, Germany

In this paper the state of stress and deformation of a pressurized tube consisting of various elastic isotropic or transversely isotropic layers is evaluated. Especially a periodically laminated tube made of many thin layers is analysed by means of a homogenization process, and closed-form solutions are obtained. The results are illustrated by means of a numerical example.

Key words: Theory of elasticity, layered tube, heterogeneous media, homogenization.

1. Introduction

Laminates consisting of a great number of different layers are characterized by a considerable amount of parameters, and an exact analysis seems therefore to be more or less hopeless. However, as shown by the author [1], the method of transfer matrices (possibly in connection with integral transforms) turns out to be a clear and effective procedure for the construction of solutions without simplifying assumptions. The transfer matrix method usually applied to problems which are governed by differential equations with constant coefficients, see Pestel and Leckie [2], has been used for isotropic layered tubes (governed by differential equations with variable coefficients) already by Saumweber [3], however without taking into account the homogenization. The homogenization is studied additionally in the present paper. It applies to a periodically laminated tube made of many thin isotropic or transversely isotropic layers, and consists in the transformation of an original discrete problem (governed by a matrix difference equation for the "state vector" at the boundaries of a finite layer group) into a continuous one (governed by a matrix differential equation) by means of a limiting process. The resulting differential equation is of the same type as that for a homogeneous transversely isotropic tube, and its exact solution is given in closed form. The procedure is similar to that proposed by the author [4] in a recent paper which deals with laminated hollow spheres.

As a numerical example, a pressurized tube consisting of only five double layers is considered. The results for the radial displacement, the radial and the circumferential stresses are evaluated according the the exact (inhomogeneous) model and the approximate (homogenized) one, respectively, and compared to each other. It turns out that the homogenization procedure leads to a sufficiently accurate solution, even for the considered low number of double layers.

2. Basic equations and transfer matrix for a transversely isotropic and homogeneous thick tube

Using cylindrical coordinates r, φ, z, and assuming an axisymmetric state of stress and deformation (without torsion), the remaining equilibrium equation and strain-displacement relations are

$$r\frac{d\sigma_r}{dr} + \sigma_r - \sigma_\varphi = 0; \qquad \varepsilon_r = \frac{du}{dr}; \qquad \varepsilon_\varphi = \frac{u}{r} \tag{2.1}$$

(σ_r radial stress, σ_φ tangential stress, ε_r and ε_φ corresponding strains, and u radial displacement). Since no shear is involved with respect to the cylindrical coordinates, in the case of a transversely isotropic tube we have only the following equations of the generalized Hooke's law:

$$\begin{bmatrix} \varepsilon_r \\ \varepsilon_\varphi \\ \varepsilon_z \end{bmatrix} = \begin{bmatrix} 1/E' & -\nu'/E' & -\nu'/E' \\ -\nu'/E' & 1/E & -\nu/E \\ -\nu'/E' & -\nu/E & 1/E \end{bmatrix} \begin{bmatrix} \sigma_r \\ \sigma_\varphi \\ \sigma_z \end{bmatrix},$$

where E, E', ν and ν' are material parameters such that the strain energy is positive definite. In the case of *plane strain* ($\varepsilon_z = 0$) one obtains

$$\begin{aligned} \varepsilon_r &= \frac{1}{E'}\left(1 - \nu'^2\frac{E}{E'}\right)\sigma_r - \frac{\nu'}{E'}(1+\nu)\sigma_\varphi; \\ \varepsilon_\varphi &= \frac{1}{E}(1-\nu^2)\sigma_\varphi - \frac{\nu'}{E'}(1+\nu)\sigma_r; \\ \sigma_r &= \frac{(1-\nu)E'}{1-\nu-2\nu'^2E/E'}\left(\varepsilon_r + \frac{\nu'}{1-\nu}\frac{E}{E'}\varepsilon_\varphi\right); \\ \sigma_\varphi &= \frac{1-\nu'^2E/E'}{1-\nu-2\nu'^2E/E'}\frac{E}{1+\nu}\left(\varepsilon_\varphi + \frac{(1+\nu)\nu'}{1-\nu'^2E/E'}\varepsilon_r\right). \end{aligned} \tag{2.2}$$

In the case of *plane stress* ($\sigma_z = 0$) there is

$$\varepsilon_r = \frac{1}{E'}\sigma_r - \frac{\nu'}{E'}\sigma_\varphi; \tag{2.2$'$}$$

(2.2)′ [cont.]

$$\varepsilon_\varphi = \frac{1}{E}\sigma_\varphi - \frac{\nu'}{E'}\sigma_r;$$

$$\sigma_r = \frac{E'}{1-\nu'^2 E/E'}(\varepsilon_r + \nu'\frac{E}{E'}\varepsilon_\varphi);$$

$$\sigma_\varphi = \frac{E}{1-\nu'^2 E/E'}(\varepsilon_\varphi + \nu'\varepsilon_r).$$

Eliminating the strains, the basic equations (2.1) and (2.2) for the state of plane strain and (2.1) and (2.2)′ for the state of plane stress can be put into the following common form:

$$\sigma_\varphi(r) = [N \quad L/r]\begin{bmatrix}\sigma_r(r)\\ u^*(r)\end{bmatrix}; \qquad u^* = \frac{E^*}{h^*}u; \tag{2.3}$$

(h^* reference thickness, E^* reference modulus of elasticity), and

$$\frac{d\mathbf{a}(r)}{dr} = \mathbf{A}(r)\mathbf{a}(r) \tag{2.4}$$

with

$$\mathbf{A}(r) = \begin{bmatrix}-K/r & L/r^2\\ M & -N/r\end{bmatrix}; \qquad \mathbf{a}(r) = \begin{bmatrix}\sigma_r(r)\\ u^*(r)\end{bmatrix}. \tag{2.5}$$

In (2.4) and (2.5) $\mathbf{a}$(r) is called *state vector* and $\mathbf{A}$(r) – *fundamental matrix.*

The quantities K, L, M and N contain the material parameters and are defined as follows:

(a) For *plane strain and transversely isotropic material*

$$K = 1 - \frac{\nu'}{1-\nu}\frac{E}{E'}; \qquad L = \frac{1}{1-\nu^2}\frac{E}{E^*}h^*;$$
$$M = \left(1 - \frac{2\nu'^2}{1-\nu}\frac{E}{E'}\right)\frac{E^*}{E'}\frac{1}{h^*}; \qquad N = \frac{\nu'}{1-\nu}\frac{E}{E'}. \tag{2.6}$$

(b) For *plane strain and isotropic material* ($\nu' = \nu$ and $E' = E$)

$$K = 1 - \frac{\nu}{1-\nu}; \qquad L = \frac{1}{1-\nu^2}\frac{E}{E^*}h^*;$$
$$M = \frac{(1+\nu)(1-2\nu)}{1-\nu}\frac{E^*}{E}\frac{1}{h^*}; \qquad N = \frac{\nu}{1-\nu}. \tag{2.7}$$

(c) For *plane stress and transversely isotropic material*

$$K = 1 - \nu'\frac{E}{E'}; \qquad L = \frac{E}{E^*}h^*;$$
$$M = \left(1 - \nu'^2\frac{E}{E'}\right)\frac{E^*}{E'}\frac{1}{h^*}; \qquad N = \nu'\frac{E}{E'}. \tag{2.6}′$$

(d) For *plane stress and isotropic material*

$$(2.7)' \qquad \begin{aligned} K &= 1-\nu; & L &= \frac{E}{E^*}h^*; \\ M &= (1-\nu^2)\frac{E^*}{E}\frac{1}{h^*}; & N &= \nu. \end{aligned}$$

It can be easily seen that the quantities K, L, M and N are not independent of each other. There exist the following compatibility equations:
For *transversely isotropic material* (cases (a) and (c))

$$K + N = 1, \tag{2.8}$$

and for *isotropic material* (cases (b) and (d))

$$K + N = 1 \quad \text{and} \quad ML + N^2 = 1. \tag{2.9}$$

In order to integrate (2.4), a matrix differential equation with variable coefficients, we eliminate there σ_r and get

$$\frac{d^2u^*}{dr^2} + \frac{1}{r}\frac{du^*}{dr} - \frac{c}{r^2}u^* = 0, \tag{2.10}$$

with

$$c = ML + N^2. \tag{2.11}$$

Taking into account (2.6), (2.7), (2.6)′ and (2.7)′ there follows

$$(2.12) \qquad c = \begin{cases} \dfrac{1}{1-\nu^2}\dfrac{E}{E'}\left(1-\nu'^2\dfrac{E}{E'}\right) > 0 & \text{for case (a)}, \\ \dfrac{E}{E'} > 0 & \text{for case (c)}, \\ 1 & \text{for cases (b) and (d)}, \end{cases}$$

where the positiveness of the strain energy density has been used. The change of variable r according to $r = e^t$ yields finally

$$\frac{d^2u^*}{dt^2} - cu^* = 0,$$

with the solution – again in terms of r –

$$u^* = C_1 r^{\lambda_1} + C_2 r^{\lambda_2}, \tag{2.13}$$

where C_1 and C_2 mean integration constants, and $\lambda_{1,2}$ – the roots of the characteristic equation:

$$\lambda_{1,2} = \pm\lambda; \qquad \lambda = \sqrt{c}. \tag{2.14}$$

Due to relations (2.12), these roots are real.

With (2.3) and (2.1), there follows from (2.2) (plane strain) and (2.2)′ (plane stress) the radial stress component

$$\sigma_r = \frac{1}{M}\left(\frac{du^*}{dr} + \frac{N}{r}u^*\right), \tag{2.15}$$

where M and N are given in (2.6), (2.7) and (2.6)′, (2.7)′, respectively. Taking further into account (2.13), we obtain the solution of (2.4)

$$\begin{bmatrix} \sigma_r(r) \\ u^*(r) \end{bmatrix} = \begin{bmatrix} \dfrac{N+\lambda}{M} r^{\lambda-1} & \dfrac{N-\lambda}{M} r^{-\lambda-1} \\ r^{\lambda} & r^{\lambda} \end{bmatrix} \begin{bmatrix} C_1 \\ C_2 \end{bmatrix}. \tag{2.16}$$

Inverting this equation for $r = r_0$, one obtains for the integration constants C_1 and C_2

$$\begin{bmatrix} C_1 \\ C_2 \end{bmatrix} = \frac{1}{2\lambda} \begin{bmatrix} M r_0^{1-\lambda} & -(N-\lambda) r_0^{-\lambda} \\ -M r_0^{1+\lambda} & (N+\lambda) r_0^{\lambda} \end{bmatrix} \begin{bmatrix} \sigma_{r_0} \\ u_0^* \end{bmatrix}. \tag{2.17}$$

Their elimination in (2.16) leads finally to

$$\mathbf{a}(r) = \mathbf{T}(r)\mathbf{a}(r_0), \tag{2.18}$$

where the *field-transfer-matrix* $\mathbf{T}(r)$ (from radius r_0 to radius r) is

$$\mathbf{T}(r) = \frac{1}{2\lambda} \begin{bmatrix} (N+\lambda)\left(\dfrac{r}{r_0}\right)^{\lambda-1} - (N-\lambda)\left(\dfrac{r}{r_0}\right)^{-\lambda-1} & \\ Mr_0\left[\left(\dfrac{r}{r_0}\right)^{\lambda} - \left(\dfrac{r}{r_0}\right)^{-\lambda}\right] & \\ \dfrac{(N+\lambda)(N-\lambda)}{Mr_0}\left[-\left(\dfrac{r}{r_0}\right)^{\lambda-1} + \left(\dfrac{r}{r_0}\right)^{-\lambda-1}\right] & \\ -(N-\lambda)\left(\dfrac{r}{r_0}\right)^{\lambda} + (N+\lambda)\left(\dfrac{r}{r_0}\right)^{-\lambda} & \end{bmatrix}. \tag{2.19}$$

For case (d) – plane stress and isotropic material – this formula corresponds to that given by SAUMWEBER [3].

REMARK 1. The fundamental matrix $\mathbf{A}(r)$ in (2.5) and the field-transfer-matrix $\mathbf{T}(r)$ are related to each other according to

$$\mathbf{A}(r_0) = \frac{d\mathbf{T}(r)}{dr}\Big|_{r=r_0}. \tag{2.20}$$

■

Let us consider, as an example, a thick-walled tube with radii r_0 and r_1 under internal pressure p. From the boundary conditions $\sigma_r(r_0) = -p$ and $\sigma_r(r_1) = 0$, one obtains from (2.12) and (2.13) at first

$$u_0^* = \frac{-(N+\lambda)\left(\frac{r_1}{r_0}\right)^{\lambda-1} + (N-\lambda)\left(\frac{r_1}{r_0}\right)^{-\lambda-1}}{(N+\lambda)(N-\lambda)\left[\left(\frac{r_1}{r_0}\right)^{\lambda-1} - \left(\frac{r_1}{r_0}\right)^{-\lambda-1}\right]} M r_0 p, \tag{2.21}$$

and then

$$u = \frac{pb}{\left(\frac{a}{b}\right)^{\lambda-1} - \left(\frac{a}{b}\right)^{-\lambda-1}} \frac{h^*}{E^*} M \left[\frac{\left(\frac{r}{b}\right)^{-\lambda}}{N-\lambda} - \frac{\left(\frac{r}{b}\right)^{\lambda}}{N+\lambda}\right],$$

$$\sigma_r = -\frac{p}{\left(\frac{a}{b}\right)^{\lambda-1} - \left(\frac{a}{b}\right)^{-\lambda-1}} \left[\left(\frac{r}{b}\right)^{\lambda-1} - \left(\frac{r}{b}\right)^{-\lambda-1}\right], \tag{2.22}$$

$$\sigma_\varphi = -\frac{p\lambda}{\left(\frac{a}{b}\right)^{\lambda-1} - \left(\frac{a}{b}\right)^{-\lambda-1}} \left[\left(\frac{r}{b}\right)^{\lambda-1} + \left(\frac{r}{b}\right)^{-\lambda-1}\right],$$

where $a = r_0$ and $b = r_1$. The last formula had been derived from (2.3). For an *isotropic material* – cases (b) and (d) – the well-known result is (see e.g. TIMOSHENKO and GOODYEAR [5]):

$$u = \frac{pb}{1 - \left(\frac{a}{b}\right)^{-2}} \frac{h^*}{E^*} M \left[\frac{\left(\frac{r}{b}\right)^{-1}}{N-1} - \frac{\frac{r}{b}}{N+1}\right],$$

$$\sigma_r = -\frac{p}{1 - \left(\frac{a}{b}\right)^{-2}} \left[1 - \left(\frac{r}{b}\right)^{-2}\right], \tag{2.23}$$

$$\sigma_\varphi = -\frac{p}{1 - \left(\frac{a}{b}\right)^{-2}} \left[1 + \left(\frac{r}{b}\right)^{-2}\right],$$

with M and N given by (2.7) and (2.7)′, respectively. Note that the state of stress for transversely isotropic material – cases (a) and (c) – depends on the material via λ, while it is independent of the material in the case of isotropy.

3. Arbitrarily layered thick tube

In Fig. 1 is sketched an n-layer system consisting of different transversely isotropic or isotropic layers which are considered to be either in a state of plane strain or in a state of plane stress. Layer (k) is characterized by the corresponding material parameters (marked by index k) and the radii r_{k-1} and r_k, or radius r_{k-1} and thickness h_k. The coordinate z and the dimensionless coordinate ρ for layer (k) are defined as follows:

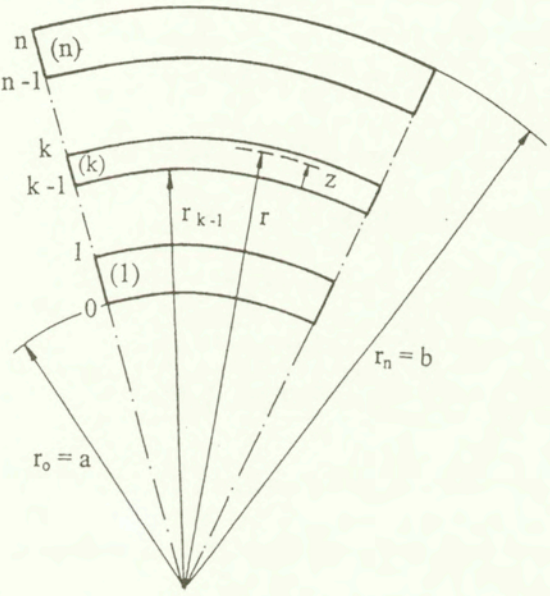

FIG. 1. Arbitrarily laminated thick tube consisting of n finite layers.

$$z = r - r_{k-1}; \qquad \rho = \frac{z}{r_{k-1}};$$

(3.1)

$$\rho_k = \frac{h_k}{r_{k-1}}; \qquad \frac{r}{r_{k-1}} = 1 + \rho;$$

$$0 \leqslant z \leqslant h_k, \qquad r_{k-1} \leqslant r \leqslant r_k, \qquad 0 \leqslant \rho \leqslant \rho_k.$$

Then with $r_0 = r_{k-1}$ in (2.19), the transfer Eq. (2.18) reads

$$\mathbf{a}^{(k)}(\rho) = \mathbf{T}^{(k)}(\rho)\mathbf{a}^{(k)}(0), \tag{3.2}$$

where

$$\mathbf{T}^{(k)}(\rho) = \begin{bmatrix} t_k^{11}(\rho) & t_k^{12}(\rho) \\ t_k^{21}(\rho) & t_k^{22}(\rho) \end{bmatrix}, \tag{3.3}$$

with

$$2\lambda_k t_k^{11}(\rho) = (N_k+\lambda_k)(1+\rho)^{\lambda_k-1} - (N_k-\lambda_k)(1+\rho)^{-\lambda_k-1},$$

$$2\lambda_k t_k^{12}(\rho) = \frac{(N_k+\lambda_k)(N_k-\lambda_k)}{M_k r_{k-1}}\left[-(1+\rho)^{\lambda_k-1} + (1+\rho)^{-\lambda_k-1}\right],$$

$$2\lambda_k t_k^{21}(\rho) = M_k r_{k-1}\left[(1+\rho)^{\lambda_k} - (1+\rho)^{-\lambda_k}\right],$$

$$2\lambda_k t_k^{22}(\rho) = -(N_k-\lambda_k)(1+\rho)^{\lambda_k} + (N_k+\lambda_k)(1+\rho)^{-\lambda_k},$$

is the *field-transfer matrix* of the layer k. Further there holds

$$\mathbf{a}^{(k)}(\rho_k) = \mathbf{T}^{(k)}(\rho_k)\mathbf{a}^{(k)}(0), \tag{3.4}$$

and the interface continuity condition is

$$\mathbf{a}^{(k)}(0) = \mathbf{a}^{(k-1)}(\rho_{k-1}) \equiv \mathbf{a}_{k-1} \qquad (k = 2, 3 \ldots, n). \tag{3.5}$$

Consequently, (3.4) can be written in the form

$$\mathbf{a}_k = \mathbf{T}_k \mathbf{a}_{k-1}, \tag{3.6}$$

with

$$\mathbf{T}_k = \mathbf{T}^{(k)}(\rho_k), \tag{3.7}$$

representing the *layer-transfer-matrix*. Applying (3.6) from $k = 1$ to $k = n$, one obtains

$$\mathbf{a}_n = \mathbf{S}\mathbf{a}_0; \qquad \mathbf{S} = \mathbf{T}_n \mathbf{T}_{n-1} \ldots \mathbf{T}_1, \tag{3.8}$$

where $\mathbf{S}$ is called *system-transfer-matrix*.

Due to the boundary conditions, one component of $\mathbf{a}_0$ and one component of $\mathbf{a}_n$ are prescribed, and the remaining ones can be calculated from(3.8). Further, (3.6) yields all *initial state vectors* of the individual layers $\mathbf{a}_1 \ldots \mathbf{a}_{n-1}$, and the exact state of radial stress and displacement follows from (3.2) with (3.3). Finally, the circumferential stress can be evaluated from (2.3). Concerning the transfer matrix method, the reader is referred to PESTEL and LECKIE [2].

REMARK 2. The layer-transfer-matrix (3.7) has the following properties:

(1) For two succesive layers (k) and $(k+1)$ with identical materials ($\lambda_k = \lambda$, $M_k = M$, $N_k = N$) we may write $\mathbf{T}^{(k)}(\rho_k) = \mathbf{T}(\rho_k)$ and $\mathbf{T}^{(k+1)}(\rho_{k+1}) = \mathbf{T}(\rho_{k+1})$, respectively in (3.3), and there holds

$$\mathbf{T}\left(\frac{h_{k+1}}{r_k}\right)\mathbf{T}\left(\frac{h_k}{r_{k-1}}\right) = \mathbf{T}\left(\frac{h_k + h_{k+1}}{r_{k-1}}\right). \tag{3.9}$$

(2) The inverse layer-transfer-matrix $\mathbf{T}^{-1}$ is obtained from the original one $\mathbf{T}(\rho_k) = \mathbf{T}\left(\frac{r_k}{r_{k-1}} - 1\right)$ by replacing r_k/r_{k-1} with its reciprocal r_{k-1}/r_k:

$$\left[\mathbf{T}\left(\frac{r_k}{r_{k-1}} - 1\right)\right]^{-1} = \mathbf{T}\left(\frac{r_{k-1}}{r_k} - 1\right). \tag{3.10}$$

These statements are plausible physically and can be proved directly using (3.3). Note that, for simplicity, $T(\cdot)$ is used in Sec. 2 (Eqs. (2.18) – (2.20)) and Sec. 3 (Eqs. (3.9) – (3.10)) simultaneously as a symbol for the transfer matrix and a symbol for a function. Of course, $\mathbf{T}(r)$ and $\mathbf{T}(\rho)$ mean the same transfer matrix, but different functions, since the corresponding arguments are different.

■

4. Periodically layered thick tube and its homogenization

In what follows we consider a tube which consists of many thin *layer groups* with equal thickness h. A layer group (Fig. 2) is composed of m (generally different) transversely isotropic or purely isotropic *basic layers* which are characterized (in addition to their radii) by their material parameters $E_k, E'_k, \nu_k, \nu'_k (k = 1, 2 \ldots m)$, and their thickness h_k. Denoting by κ_k the thickness ratio of basic layer (k), there holds

$$h_k = \kappa_k h; \qquad h = \sum_{k=1}^{m} h_k; \qquad \sum_{k=1}^{m} \kappa_k = 1 \tag{4.1}$$

$$(0 < \kappa_k < 1;\ k = 1, 2, \ldots m).$$

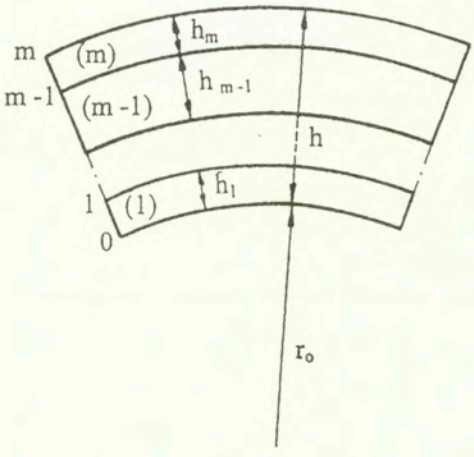

FIG. 2. Layer group consisting of m thin layers.

Let the layer group be bounded by the inner radius r_0 and the outer radius r_m, and let us assume $h \ll r_0$. Then after (3.1) there is

$$\rho_1 = \frac{h_1}{r_0} = \kappa_1 \frac{h}{r_0}; \qquad \rho_k = \frac{h_k}{r_{k-1}} = \frac{\kappa_k h}{r_0 + h \sum_{i=1}^{k-1} \kappa_i} \tag{4.2}$$

$$= \frac{\kappa_k h}{r_0} + O((h/r_0)^2) \qquad (k = 2,3,\dots m),$$

and a series expansion of (3.3) in (3.7) with respect to h/r_0 results in the *thin-layer transfer-matrix* of basic layer (k)

$$\overset{\circ}{\mathbf{T}}_k = \begin{bmatrix} 1 - \kappa_k K_k h/r_0 & \kappa_k L_k h/r_0^2 \\ \kappa_k M_k h & 1 - \kappa_k N_k h/r_0 \end{bmatrix} + \mathbf{O}((h/r_0)^2). \tag{4.3}$$

Consequently for the thin layer group, according to (3.8), there follows

$$\mathbf{a}_m = \overset{\circ}{\mathbf{S}}\, \mathbf{a}_0; \qquad \overset{\circ}{\mathbf{S}} = \overset{\circ}{\mathbf{T}}_m \overset{\circ}{\mathbf{T}}_{m-1} \cdots \overset{\circ}{\mathbf{T}}_1, \tag{4.4}$$

particularly

$$\overset{\circ}{\mathbf{S}} = \begin{bmatrix} 1 - \bar{K}h/r_0 & \bar{L}h/r_0^2 \\ \bar{M}h & 1 - \bar{N}h/r_0 \end{bmatrix} + \mathbf{O}((h/r_0)^2), \tag{4.5}$$

with

$$\bar{K} = \sum \kappa_k K_k; \qquad \bar{L} = \sum \kappa_k L_k;$$

$$\bar{M} = \sum \kappa_k M_k; \qquad \bar{N} = \sum \kappa_k N_k; \tag{4.6}$$

$$\text{(The sum extends from } k = 1 \text{ to } k = \mathrm{m}\,; \quad \sum \kappa_k = 1)\,.$$

The quantities K_k, L_k, M_k and N_k have to be taken from (2.6) or (2.7) or (2.6)′ or (2.7)′, after attaching index k at E, E', ν, ν', K, L, M and N. As can be easily verified , the following compatibility equation exists:

$$\bar{K} + \bar{N} = 1. \tag{4.7}$$

The *homogenization* is performed by replacing the finite relation (4.4), written in the form

$$\frac{\mathbf{a}_m - \mathbf{a}_0}{h} = \frac{\overset{\circ}{\mathbf{S}} - \mathbf{I}}{h} \mathbf{a}_0,$$

and to be interpreted as a difference equation, by the differential equation

$$\frac{d\mathbf{a}}{dr} = \lim_{h\to 0} \frac{\mathbf{a}_m - \mathbf{a}_0}{h} = \lim_{h\to 0} \frac{\overset{\circ}{\mathbf{S}} - \mathbf{I}}{h} \mathbf{a}_0 = \bar{\mathbf{A}}(r_0)\mathbf{a}_0,$$

or, taking $r_0 = r$ and $\mathbf{a}_0 = \mathbf{a}$, by

$$\frac{d\mathbf{a}}{dr} = \bar{\mathbf{A}}(r)\mathbf{a}, \tag{4.8}$$

with the *fundamental matrix of the periodical layering*

$$\bar{\mathbf{A}}(r) = \begin{bmatrix} -\bar{K}/r & \bar{L}/r^2 \\ \bar{M} & -\bar{N}/r \end{bmatrix}. \tag{4.9}$$

Since the fundamental matrix of the *basic layer* k is

$$\mathbf{A}_k(r) = \begin{bmatrix} -K_k/r & L_k/r^2 \\ M_k & -N_k/r \end{bmatrix},$$

taking into account (4.6), one obtains the relation

$$\bar{\mathbf{A}}(r) = \sum_{k=1}^{m} \kappa_k \mathbf{A}_k. \tag{4.10}$$

REMARK 3. We have derived the thin-layer transfer-matrix $\overset{\circ}{\mathbf{T}}_k$ in (4.3) via the layer-transfer-matrix $\mathbf{T}_k$ (given in (3.7) with (3.3)). Alternatively one can obtain this directly by integrating (2.4) in the neighbourhood of $r = r_0$, i.e. for a constant fundamental matrix $\mathbf{A}_k(r_0)$:

$$\mathbf{a}_k = e^{\mathbf{A}_k(r_0)h_k}\mathbf{a}_{k-1} = \left[\mathbf{I} + \mathbf{A}_k(r_0)\kappa_k h + \mathbf{O}(h^2)\right]\mathbf{a}_{k-1} = \overset{\circ}{\mathbf{T}}_k\,\mathbf{a}_{k-1}.$$

Consequently there is

$$\overset{\circ}{\mathbf{T}}_k = \mathbf{I} + \kappa_k \mathbf{A}_k(r_0)h + \mathbf{O}((h/r_0)^2) \tag{4.11}$$

in agreement with (4.3). ■

Since the governing differential equation of the homogenized periodically layered tube, (4.8) with (4.9), has the same structure as that for the homogeneous transversely isotropic tube, (2.4) with (2.5), the corresponding solutions of Sec. 3 can be taken over. One has only to substitute K, L, M, N by $\bar{K}, \bar{L}, \bar{M}, \bar{N}$ and as a consequence, c by $\bar{c}$ and λ by $\bar{\lambda}$, where

$$\bar{c} = \bar{M}\bar{L} + \bar{N}^2; \qquad \bar{\lambda} = \sqrt{\bar{c}}. \tag{4.12}$$

In this way one obtains from (2.22), for a thick tube with outer radius b and inner radius a and loaded by internal pressure p,

$$u = \frac{pb}{\left(\frac{a}{b}\right)^{\bar{\lambda}-1} - \left(\frac{a}{b}\right)^{-\bar{\lambda}-1}} \frac{h^*}{E^*} \bar{M} \left[\frac{\left(\frac{r}{b}\right)^{-\bar{\lambda}}}{\bar{N}-\bar{\lambda}} - \frac{\left(\frac{r}{b}\right)^{\bar{\lambda}}}{\bar{N}+\bar{\lambda}} \right];$$

$$\sigma_r = -\frac{p}{\left(\frac{a}{b}\right)^{\bar{\lambda}-1} - \left(\frac{a}{b}\right)^{-\bar{\lambda}-1}} \left[\left(\frac{r}{b}\right)^{\bar{\lambda}-1} - \left(\frac{r}{b}\right)^{-\bar{\lambda}-1} \right]; \tag{4.13}$$

$$\sigma_\varphi = -\frac{p\bar{\lambda}}{\left(\frac{a}{b}\right)^{\bar{\lambda}-1} - \left(\frac{a}{b}\right)^{-\bar{\lambda}-1}} \left[\left(\frac{r}{b}\right)^{\bar{\lambda}-1} + \left(\frac{r}{b}\right)^{-\bar{\lambda}-1} \right].$$

Here σ_φ is to be considered as an average value; it follows from (2.3) with $\bar{N}$ and $\bar{L}$ instead of N and L, or equivalently from the equilibrium equation in (2.1) using σ_r from (4.13). Note, however, that for a finite layering, $u(r)$ and $\sigma_r(r)$ are continuous while $\sigma_\varphi(r)$ is discontinuous at the interfaces. Therefore the knowledge of σ_φ in the individual layers of a thin, but finite layer group is of interest. Assuming that for this case u and σ_r from (4.13) are a sufficient approximation, one obtains with (2.3) for layer (k) of a layer group at first

$$\sigma_{\varphi k}(r) = N_k \sigma_r(r) + \frac{L_k}{r} u^*(r) \qquad (k = 1, 2 \ldots m), \tag{4.14}$$

and finally

$$\sigma_{\varphi k} = -\frac{p}{\left(\frac{a}{b}\right)^{\bar{\lambda}-1} - \left(\frac{a}{b}\right)^{-\bar{\lambda}-1}} \left[\left(\frac{\bar{M} L_k}{\bar{N}+\bar{\lambda}} + N_k \right) \left(\frac{r}{b}\right)^{\bar{\lambda}-1} - \left(\frac{\bar{M} L_k}{\bar{N}-\bar{\lambda}} + N_k \right) \left(\frac{r}{b}\right)^{-\bar{\lambda}-1} \right]. \tag{4.15}$$

It is further interesting to note that the individual circumferential stresses $\sigma_{\varphi k}$ (4.15) and the smeared stress σ_φ in (4.13) are related to each other according to

$$\sigma_\varphi = \sum_{k=1}^{m} \kappa_k \sigma_{\varphi k}. \tag{4.16}$$

For the proof, the relations (4.15), (4.6) and (4.12) are needed. It can easily be checked that in the case of identical materials of all basic layers, the difference between formulae (4.13) and formulae (2.22) disappears.

According to (4.9) (periodical layering) and (2.5) (homogeneous tube under plane stress or plane strain, respectively), both problems are formally equivalent. Especially a periodically layered tube consisting of isotropic basic layers can be substituted uniquely by a homogeneous, transversely isotropic tube in the case of plane stress. Indeed, equating (2.6)′ and (4.6), one obtains, taking into account (2.8), three independent equations for the three material parameters being involved, namely E, E' and ν'. The result is

$$E = \frac{E^*}{h^*}\bar{L} = \frac{E^*}{h^*}\sum \kappa_k L_k = \sum \kappa_k E_k;$$

$$\frac{1}{E'} = \frac{h^*}{E^*}\left(\bar{M} + \frac{\bar{N}^2}{\bar{L}}\right) = \frac{h^*}{E^*}\left(\sum \kappa_k M_k + \frac{(\sum \kappa_k N_k)^2}{\sum \kappa_k L_k}\right)$$

$$= \sum \kappa_k \frac{1-\nu_k^2}{E_k} + \frac{(\sum \kappa_k \nu_k)^2}{\sum \kappa_k E_k};$$

$$\frac{\nu'}{E'} = \frac{h^*}{E^*}\frac{\bar{N}}{\bar{L}} = \frac{h^*}{E^*}\frac{\sum \kappa_k N_k}{\sum \kappa_k L_k} = \frac{\sum \kappa_k \nu_k}{\sum \kappa_k E_k},$$

and with (4.1)

$$(4.17) \qquad Eh = \sum E_k h_k; \qquad \frac{h}{E'} = \sum (1-\nu_k^2)\frac{h_k}{E_k} + \frac{(\sum \nu_k h_k)^2}{\sum E_k h_k};$$

$$\frac{\nu'}{E'} = \frac{\sum \nu_k h_k}{\sum E_k h_k},$$

(all sums from k =1 to k = m).

As it can be seen from (4.18), the resulting stiffness of the layered tube in tangential direction is the sum of the stiffnesses of the individual layers. In radial direction the statement, that the resulting compliance of the layered tube equals the sum of the compliances of the individual layers holds exactly only if $\nu_k = 0$, otherwise approximatively.

5. Numerical Example

The numerical example concerns a tube under internal pressure consisting of five double layers, see Fig. 3. This periodically layered tube is analysed first by means of the exact (inhomogeneous) model. All basic layers have the same

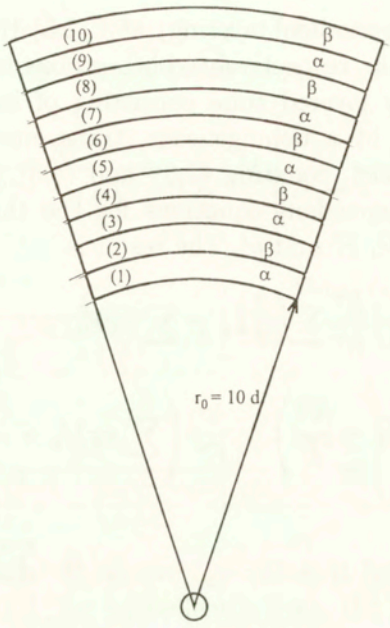

FIG. 3. Periodically layered tube consisting of 5 double layers.

thickness d and are assumed to be isotropic and under plane strain. For the layers of type α and the layers of type β (Fig. 3), we take

$$h_k = d \quad (k = 1, 2, \dots 10); \qquad \nu_\alpha = \nu_\beta = \frac{1}{3}; \quad E_\alpha = E; \quad E_\beta = 3E$$

and we choose $h^* = d$ and $E^* = E$. Then from (2.7), (2.12) and (2.14) there follows

$$K_\alpha = \frac{1}{2}; \qquad L_\alpha = \frac{9}{8}d; \qquad M_\alpha = \frac{2}{3}\frac{1}{d}; \qquad N_\alpha = \frac{1}{2}; \qquad \lambda_\alpha = 1;$$

$$K_\beta = \frac{1}{2}; \qquad L_\beta = \frac{27}{8}d; \qquad M_\beta = \frac{2}{9}\frac{1}{d}; \qquad N_\beta = \frac{1}{2}; \qquad \lambda_\beta = 1;$$

and after (3.1) $\rho_k = \dfrac{1}{9+k}$. Next the elements of the *layer transfer-matrices* $\mathbf{T}_k$ can be evaluated from (3.7) and (3.3). For instance, one obtains

$$t_k^{12}(\rho_k) = \left\{ \begin{array}{c} 1 \\ 3 \end{array} \right\} \frac{9}{16}\rho_k \left[1 - (1+\rho_k)^{-2}\right] \quad \text{for} \quad k = \left\{ \begin{array}{c} 1,3,5,7,9 \\ 2,4,6,8,10 \end{array} \right. .$$

Further from (3.8) and from the boundary conditions $\sigma_{r_0} = -p$ and $\sigma_{r_{10}} = 0$ one gets $u_0^* = (s_{11}/s_{12})p$ and hence the *initial state vector* $\mathbf{a}_0$ and subsequently – from (3.6) – $\mathbf{a}_1, \mathbf{a}_2, \dots \mathbf{a}_{10}$ i.e. the *radial stresses* σ_{rk} and the *radial displacements* u_k.

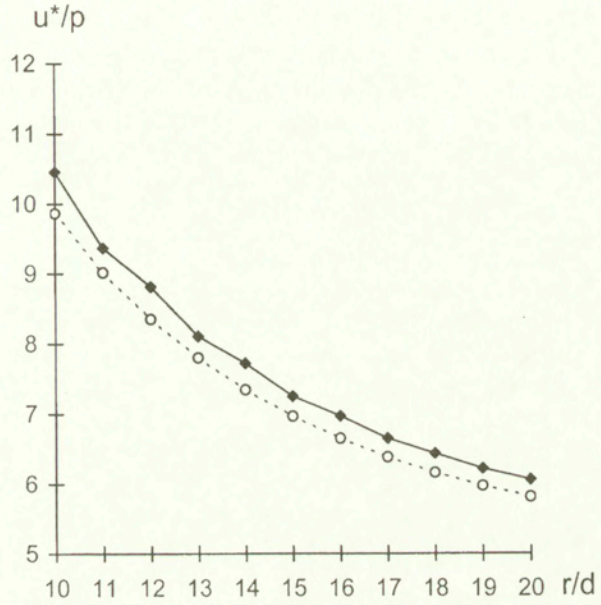

FIG. 4. Radial displacement distribution for the tube in Fig. 3, —— inhomogeneous model, - - - - homogenized model.

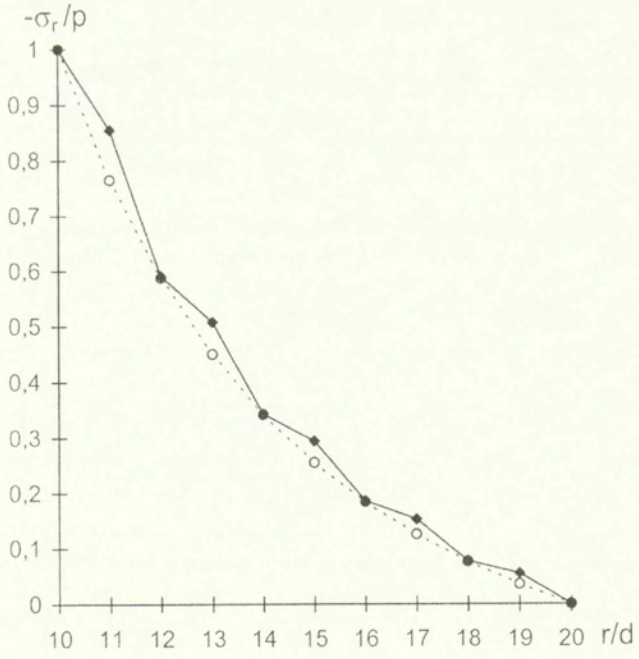

FIG. 5. Radial stress distribution for the tube in Fig. 3, —— inhomogeneous model, - - - - homogenized model.

These ones are sketched as solid lines in Figs. 4 and 5, respectively, where $u^* = (E/d)u$. The solid line in Fig. 6 represents the circumferential stress distribution which is discontinous due to the discontinuity of the stiffness parameters. They have been calculated from (2.3) for $r = r_k = (10 + k)d$ and $k = 0, 1, \ldots 10$

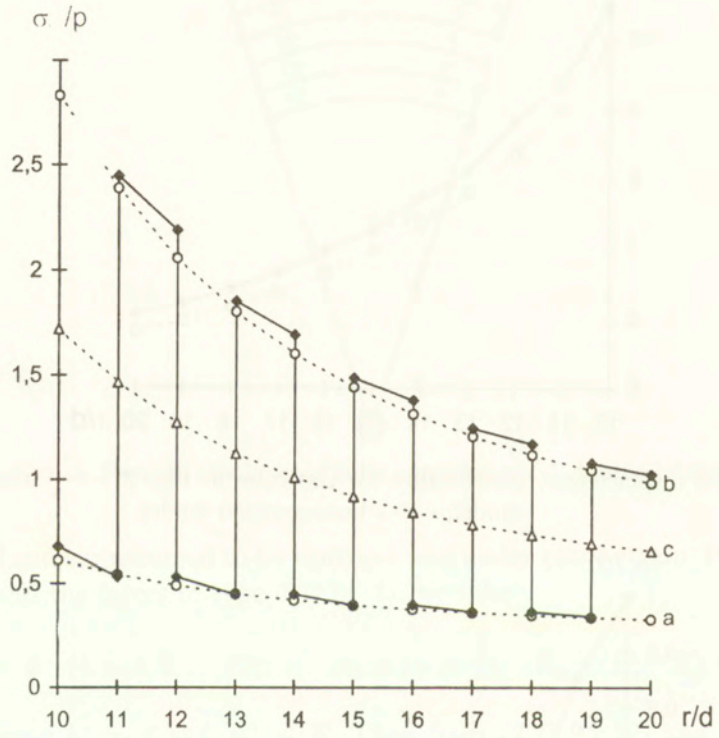

FIG. 6. Circumferential stress distribution for the tube in Fig. 3, —— inhomogeneous model, - - - - homogenized model, (a) for layers of type α, (b) for layers of type β; (c) mean values).

$$\left.\begin{matrix}\sigma_{k|\alpha}\\ \sigma_{k|\beta}\end{matrix}\right\} = \frac{1}{2}\sigma_{rk} + \left\{\begin{matrix}1\\ 3\end{matrix}\right\} \frac{9}{8(10+k)} \frac{E}{d} u \quad \text{for layers} \left\{\begin{matrix}\alpha\\ \beta\end{matrix}\right. .$$

The corresponding *homogenized model* (being exact only in the case of infinitely many double layers with vanishing thickness) yields an approximate solution for the layered tube in Fig. 3. For this one there is

$$h = 2d; \quad a = 10d; \quad b = 20d; \quad \kappa_1 = \kappa_2 = \frac{1}{2};$$

$$K_1 = K_\alpha; \quad L_1 = L_\alpha; \quad M_1 = M_\alpha; \quad N_1 = N_\alpha;$$

$$K_2 = K_\beta; \quad L_2 = L_\beta; \quad M_2 = M_\beta; \quad N_2 = N_\beta$$

and according to (4.6) and (4.12)

$$\bar{K} = \frac{1}{2}; \quad \bar{L} = \frac{9}{4}d; \quad \bar{M} = \frac{4}{9}\frac{1}{d}; \quad \bar{N} = \frac{1}{2}; \quad \bar{c} = \frac{5}{4}; \quad \bar{\lambda} = \frac{\sqrt{5}}{2}.$$

The closed-form solution is given in (4.13). For instance, the radial displacements as a function of the radial coordinate r reads

$$u = \frac{d}{E}p\frac{160}{9}\frac{1}{2^{(\sqrt{5}+2)/2} - 2^{-(\sqrt{5}-2)/2}}\left[\frac{1}{\sqrt{5}+1}\left(\frac{r}{20d}\right)^{\sqrt{5}/2} + \frac{1}{\sqrt{5}-1}\left(\frac{r}{20d}\right)^{-\sqrt{5}/2}\right].$$

The corresponding graphs for u, σ_r and σ_φ are given in Fig. 4, 5 and 6 (dotted lines). The circumferential stress σ_φ $(4.13)_3$ is the mean value $(\sigma_{\varphi\alpha} + \sigma_{\varphi\beta})/2$, while the formulae (4.15), namely

$$\left.\begin{matrix}\sigma_{\varphi\alpha}\\ \sigma_{\varphi\beta}\end{matrix}\right\} = p\frac{1}{2^{(\sqrt{5}+2)/2} - 2^{-(\sqrt{5}-2)/2}}\left[\left(\left\{\begin{matrix}1\\3\end{matrix}\right\}\frac{1}{\sqrt{5}+1} + \frac{1}{2}\right)\left(\frac{r}{20d}\right)^{(\sqrt{5}-2)/2} + \left(\left\{\begin{matrix}1\\3\end{matrix}\right\}\frac{1}{\sqrt{5}-1} - \frac{1}{2}\right)\left(\frac{r}{20d}\right)^{-(\sqrt{5}+2)/2}\right] \quad \text{for layers} \quad \left\{\begin{matrix}\alpha\\ \beta\end{matrix}\right.$$

represent the values which are valid piecewise for the layers of type α (lower curve) and type β (upper curve), respectively.

The comparison of the results for the exact (inhomogeneous), but expensive and the approximate (homogenized) model shows that, even for a relatively low number of layer groups (double layers), one gets a rather good agreement.

Acknowledgement

This paper was written during the author's stay in summer semester 1998 at the Institute of Applied Mathematics and Mechanics of the University of Warsaw and at the Institute of Fluid-Flow Machinery of the Polish Academy of Sciences in Gdańsk. This author thanks these institutions, and especially Prof. Dr. Z. Olesiak and Docent Dr. A. Zmitrowicz, for the hospitality and support, and the Foundation for Polish Science for awarding him the Alexander von Humboldt Honorary Research fellowship. Some financial support was provided by KBN grant No. 7T07A00913.

References

1. H. BUFLER, *Theory of elasticity of multilayered medium*, J.Elasticity, **1**, 125–143, 1971.
2. E.C. PESTEL and F.A. LECKIE, *Matrix methods in elastomechanics*. Mc Graw Hill, New York, San Francisco, Toronto, London 1963.
3. E. SAUMWEBER, *Der Spannungs- und Verschiebungszustand in homogen- und inhomogen-elastischen Ringen*, ZAMM, 46, 49–64, 1966.
4. H. BUFLER, *The arbitrarily and the periodically laminated elastic hollow sphere: Exact solutions and homogenization*, Arch. Appl. Mech., **68**, 579–588, 1998.
5. S. TIMOSHENKO and J.N. GOODYEAR, *Theory of elasticity*. Mc Graw Hill, New York, Toronto, London 1951.

Received September 8, 1998; new version December 30, 1998.

Arch. Mech., **51**, 3–4, pp. 311–334, Warszawa 1999

Localisation effect during wave pulse propagation in randomly stratified elastic medium

K. DOLIŃSKI and Z. KOTULSKI

Polish Academy of Sciences
Institute of Fundamental Technological Research
Świętokrzyska 21, 00-049 Warszawa, Poland

IN THIS PAPER the propagation of the planar wave pulses in a two-dimensional randomly stratified elastic medium is considered. The waves propagate in the plane (x_1, x_2) and are independent of the third variable z. The problem is described by means of the transition matrix method. The transition matrix and the wave equation for a homogeneous layer is presented. The equations for the wave fields reflected from and transmitted through the randomly stratified elastic slab are derived. The theoretical results are illustrated by graphically presented numerical calculations. A possibility of application of the wave analysis to modelling of the fatigue crack propagation initiated at the interfaces and continued due to sequences of the reflected and transmitted stress waves is discussed.

1. Introduction

IN THE PAPER we consider wave pulses in two-dimensional elastic stratified medium. The results represent a certain generalisation of those given in [3], where the wave pulses in a one-dimensional elastic medium were considered. On the other hand, the paper extends the model presented in [4] for two-dimensional harmonic waves to the non-stationary phenomenon of wave pulses. The main mathematical tool used for the analysis of the problem is the so-called *transition matrix method*. This method is very effective in solving wave problems in stratified media – both deterministic and stochastic. The historical development of the transition matrix approach was presented in [5] and our other papers on wave problems in the stochastic stratified media [3, 4]. The advantage of the method is the fact that one can perform large part of solving the equation procedure analytically and only the last inversion of the Fourier transformation of the wave amplitudes must be numerical.

The schedule of the paper is the following. First we introduce the notation used throughout the paper and present the derivation of the Fourier transformed wave equation for wave pulses in a homogeneous layer. Then we derive the

equation for the planar elastic wave pulse and give the expressions for its solution. In Sec. 3 we consider waves in the medium built of homogeneous parallel layers. We introduce such a system of independent variables that interfaces of the layers (where the material parameters change their values) are perpendicular to the x-axis. Inside of each layer the wave field satisfies the wave equations derived in Sec. 2 and at the discontinuity planes the displacements and traction vector are continuous. Finally we derive the equation for the (Fourier transformed) wave field in all the layered medium and solve it, obtaining the analytical expressions for the amplitudes of the reflected and transmitted wave pulses. In Sec. 4 we present the results of an example calculating numerically the inverse Fourier transforms and observing the evolution in time of the pulses. Section 5 gives a discussion of the possible effect of the observed phenomena on the fatigue crack propagation initiated at the interfaces and continued due to sequences of the reflected and transmitted stress waves.

2. The wave equation for a single layer

We consider a linear elastic wave propagating in the homogeneous isotropic medium. The wave propagation is governed by the following system of partial differential equations [7]:

$$\rho \frac{\partial^2}{\partial t^2} u_i = \sigma_{ij,j}, \qquad i = 1, 2, 3, \tag{2.1}$$

where σ_{ij} is the stress tensor defined as

$$\sigma_{ij} = \mu(u_{i,j} + u_{j,i}) + \lambda u_{k,k}\delta_{ij} \tag{2.2}$$

(double indexes denote the summation from 1 to 3; the subscript "1" corresponds to the independent variable x, "2" to y and "3" to z). In the above equation λ and μ are the elastic Lamé constants and ρ is density of the medium.

We consider waves propagating in the plane (x, y) and independent of the third spatial variable z. In our co-ordinate system the wave field has got the following form:

$$\mathbf{u}(x, y, z, t) = (u_1(x, y, t), u_2(x, y, t), 0)^T. \tag{2.3}$$

Condition (2.3) makes some elements of the stress tensor equal to zero and slightly simplifies the governing equations. Since in further considerations we deal with the problem of wave propagation in a layered medium, where the interfaces of homogeneous layers are perpendicular to the x-axis, we can equivalently describe the wave problem (2.1) – (2.2) by the following matrix differential equation

$$\frac{d}{dx}\hat{\mathbf{u}} = \mathbf{M}\hat{\mathbf{u}}, \tag{2.4}$$

with the solution $\hat{\mathbf{u}}$ searched for and the system matrix $\mathbf{M}$ defined as:

$$\mathbf{M} = \begin{bmatrix} 0 & -ik\alpha & \kappa & 0 \\ -ik & 0 & 0 & \eta \\ -\omega^2\rho & 0 & 0 & -ik \\ 0 & k^2\beta - \omega^2\rho & -ik\alpha & 0 \end{bmatrix}, \qquad \hat{\mathbf{u}} = \begin{bmatrix} \hat{u}_1 \\ \hat{u}_2 \\ \hat{\tau}_1 \\ \hat{\tau}_2 \end{bmatrix}, \tag{2.5}$$

where $\hat{u}_1$, $\hat{u}_2$, $\hat{\tau}_1$ and $\hat{\tau}_2$ are the Fourier transform of the non-zero displacement co-ordinates, u_1, u_2, and the non-zero co-ordinates of the traction vector, τ_1 and τ_2; the parameters in the matrix are (see [5]):

$$\alpha = \frac{\lambda}{(\lambda + 2\mu)}, \qquad \beta = \frac{4\mu(\lambda + \mu)}{(\lambda + 2\mu)}, \qquad \kappa = \frac{1}{(\lambda + 2\mu)}, \qquad \eta = \frac{1}{\mu}.$$

In solving the wave problem described by equation (2.4) for a single layer, a boundary condition:

$$\hat{\mathbf{u}}(0, k, \omega) = \hat{\mathbf{u}}_0(k, \omega) = \begin{bmatrix} \hat{u}_1(0, k, \omega) \\ \hat{u}_2(0, k, \omega) \\ \hat{\tau}_1(0, k, \omega) \\ \hat{\tau}_2(0, k, \omega) \end{bmatrix}, \tag{2.6}$$

representing jointly the incident wave pulse reaching the plane $x = 0$ and the pulse reflected from it, has to be introduced. Then the value at the opposite side of the layer, at $x = L$, say, can be represented as:

$$\hat{\mathbf{u}}(L, k, \omega) = \mathbf{T}(L)\hat{\mathbf{u}}_0(k, \omega), \tag{2.7}$$

where $\mathbf{T}(L)$ is the transition matrix for the two-dimensional waves propagating through the layer of thickness L. This matrix can be represented by the following Sylvester formula [11, 5]:

$$\mathbf{T}(L) = \exp\{\mathbf{M}L\} = \sum_{i=1}^{4} \left(\mathbf{\Pi} \frac{(\mathbf{M} - p_k \mathbf{Id})}{p_i - p_k} \right) \exp\{p_i, L\} \tag{2.8}$$

where $p_i, i = 1, 2, 3, 4$ are the eigenvalues of the system matrix $\mathbf{M}$:

$$p_{1,2} = \pm \frac{\sqrt{k^2\mu - \omega^2\rho}}{\sqrt{\mu}}, \qquad p_{3,4} = \pm \frac{\sqrt{k^2(\lambda + 2\mu) - \omega^2\rho}}{\sqrt{\lambda + 2\mu}}. \tag{2.9}$$

The elements of the transition matrix have got a rather complicated form. They are presented explicitly in [5].

The transition matrix $\mathbf{T}(.)$ makes it possible to express the wave field $\hat{\mathbf{u}}$,

$$\hat{\mathbf{u}}(x,k,\omega) = \begin{bmatrix} \hat{u}_1(x,k,\omega) \\ \hat{u}_2(x,k,\omega) \\ \hat{\tau}_1(x,k,\omega) \\ \hat{\tau}_2(x,k,\omega) \end{bmatrix}, \tag{2.10}$$

at any point $x \in [0, L] \subset R^+$ in a homogeneous medium (inside a layer), provided the boundary condition $\hat{\mathbf{u}}_0 = \hat{\mathbf{u}}(0,k,\omega)$ at $x = 0$ is known. This wave field has got the form (2.7) with $\mathbf{T}(x)$ as the transition matrix.

3. Elastic waves in the layered medium

The approach developed in Sec. 2 allows us also to describe the transition of the two-dimensional elastic wave through a multi-layered medium. In such a case, knowing the transition matrices through any individual layers, we can obtain the transition matrix through all the stratified medium as a product of them.

Let us consider the multi-layered medium (slab) built of N layers of elastic materials, with thickness $\Delta_j, j = 1, 2, , \ldots, N$. Assume that the stratified medium is surrounded by the homogeneous elastic environment, at $x < 0$ and $x > L = \sum_{j=1}^{N} \Delta_j$. Since the wave field $\hat{\mathbf{u}}$ must be continuous at the layer interfaces, the wave on the back surface, at $x = L$, can be expressed in the following form:

$$\hat{\mathbf{u}}(L) = \mathbf{T}_N(\Delta_N)\mathbf{T}_{N-1}(\Delta_{N-1})...\mathbf{T}_2(\Delta_2)\mathbf{T}_1(\Delta_1)\hat{\mathbf{u}}_0, \tag{3.1}$$

where $\hat{\mathbf{u}}_0$ is the boundary condition at $x = 0$, $\hat{\mathbf{u}}(L)$ is the vector of the transmitted wave and $\mathbf{T}_j(.)$, for $j = 1, 2, ..., N$, is the transition matrix for the j-th layer, depending on the material parameters (possibly random).

In Equation (3.1) all the material properties of the multi-layered medium are completely described by a 4×4 matrix $\mathbf{T}$, being the product of the transition matrices through the individual layers and interpreted as a transition matrix through the slab built of N layers of homogeneous elastic materials:

$$\mathbf{T} = \prod_{j=1}^{N} \mathbf{T}_j(\Delta_j) = \begin{bmatrix} T_{11} & T_{12} & T_{13} & T_{14} \\ T_{21} & T_{22} & T_{23} & T_{24} \\ T_{31} & T_{32} & T_{33} & T_{34} \\ T_{41} & T_{42} & T_{43} & T_{44} \end{bmatrix}. \tag{3.2}$$

Let us notice that the vector $\hat{\mathbf{u}}_0$ describes jointly the (Fourier transforms of) incident wave pulse (going to the right) and all the reflected pulses leaving the slab (going to the left), generated by all the reflections at the interfaces of the layers, measured at the plane $x \equiv 0$. Analogously, $\hat{\mathbf{u}}(L)$ represents the transmitted pulses measured at the plane $x \equiv L$ and generated by all reflections at the internal interfaces of the layers and transmitted through the layers. To make the obtained formulae effective we must separate the incident and reflected waves from $\hat{\mathbf{u}}_0$. The waves in every region of environment surrounding the layered slab can be described in the following way. In the left-hand environment (for $x_1 < 0$) there is the incident (right-going) wave, represented as:

$$\begin{bmatrix} \hat{u}_1^{\mathrm{inc}}(x) \\ \hat{u}_2^{\mathrm{inc}}(x) \\ \hat{\tau}_1^{\mathrm{inc}}(x) \\ \hat{\tau}_2^{\mathrm{inc}}(x) \end{bmatrix} = \begin{bmatrix} A_1 \\ A_2 \\ A_3 \\ A_4 \end{bmatrix} \exp\{-ip_1 x\} + \begin{bmatrix} B_1 \\ B_2 \\ B_3 \\ B_4 \end{bmatrix} \exp\{-ip_3 x\}, \tag{3.3}$$

and the reflected (left-going) wave:

$$\begin{bmatrix} \hat{u}_1^{\mathrm{ref}}(x) \\ \hat{u}_2^{\mathrm{ref}}(x) \\ \hat{\tau}_1^{\mathrm{ref}}(x) \\ \hat{\tau}_2^{\mathrm{ref}}(x) \end{bmatrix} = \begin{bmatrix} C_1 \\ C_2 \\ C_3 \\ C_4 \end{bmatrix} \exp\{ip_1 x\} + \begin{bmatrix} D_1 \\ D_2 \\ D_3 \\ D_4 \end{bmatrix} \exp\{ip_3 x\}. \tag{3.4}$$

In the right-hand environment (for $x > L$) there is only the transmitted (right-going) wave, having the following form:

$$\begin{bmatrix} \hat{u}_1^{\mathrm{tr}}(x) \\ \hat{u}_2^{\mathrm{tr}}(x) \\ \hat{\tau}_1^{\mathrm{tr}}(x) \\ \hat{\tau}_2^{\mathrm{tr}}(x) \end{bmatrix} = \begin{bmatrix} E_1 \\ E_2 \\ E_3 \\ E_4 \end{bmatrix} \exp\{-ip_1 x\} + \begin{bmatrix} F_1 \\ F_2 \\ F_3 \\ F_4 \end{bmatrix} \exp\{-ip_3 x\}. \tag{3.5}$$

Since the displacements and tractions are related quantities, the number of independent amplitude constants, $A_1 - F_4$, can be reduced. Calculating the Fourier transforms of the respective Eqs. (2.2) we obtain:

$$\hat{\tau}_1 = (\lambda + 2\mu)\frac{d\hat{u}_1}{dx} + ik\hat{u}_2 \tag{3.6}$$

and

$$\hat{\tau}_2 = i\mu k\hat{u}_1 + \mu\frac{d\hat{u}_2}{dx}, \tag{3.7}$$

what applied in (3.3) – (3.5), results in the following expressions for the incident, reflected and transmitted wave:

$$
(3.8)\qquad \begin{bmatrix} \hat{u}_1^{\mathrm{inc}}(x) \\ \hat{u}_2^{\mathrm{inc}}(x) \\ \hat{\tau}_1^{\mathrm{inc}}(x) \\ \hat{\tau}_2^{\mathrm{inc}}(x) \end{bmatrix} = \begin{bmatrix} A_1 \\ A_2 \\ i[-(\lambda+2\mu)p_1A_1 + kA_2] \\ i\mu(kA_1 - p_1A_2) \end{bmatrix} \exp\{-ip_1x\}
$$

$$
+ \begin{bmatrix} B_1 \\ B_2 \\ i[-(\lambda+2\mu)p_3B_1 + kB_2] \\ i\mu(kB_1 - p_3B_2) \end{bmatrix} \exp\{-ip_3x\},
$$

$$
(3.9)\qquad \begin{bmatrix} \hat{u}_1^{\mathrm{ref}}(x) \\ \hat{u}_2^{\mathrm{ref}}(x) \\ \hat{\tau}_1^{\mathrm{ref}}(x) \\ \hat{\tau}_2^{\mathrm{ref}}(x) \end{bmatrix} = \begin{bmatrix} C_1 \\ C_2 \\ i[(\lambda+2\mu)p_1C_1 + kC_2] \\ i\mu(kC_1 + p_1C_2) \end{bmatrix} \exp\{ip_1x\}
$$

$$
+ \begin{bmatrix} D_1 \\ D_2 \\ i[(\lambda+2\mu)p_3D_1 + kD_2] \\ i\mu(kD_1 + p_3D_2) \end{bmatrix} \exp\{ip_3x\}.
$$

$$
(3.10)\qquad \begin{bmatrix} \hat{u}_1^{\mathrm{tr}}(x) \\ \hat{u}_2^{\mathrm{tr}}(x) \\ \hat{\tau}_1^{\mathrm{tr}}(x) \\ \hat{\tau}_2^{\mathrm{tr}}(x) \end{bmatrix} = \begin{bmatrix} E_1 \\ E_2 \\ i[-(\lambda+2\mu)p_1E_1 + kE_2] \\ i\mu(kE_1 - p_1E_2) \end{bmatrix} \exp\{-ip_1x\}
$$

$$
+ \begin{bmatrix} F_1 \\ F_2 \\ i[-(\lambda+2\mu)p_3F_1 + kF_2] \\ i\mu(kF_1 - p_3F_2) \end{bmatrix} \exp\{-ip_3x\}.
$$

In these equations the parameters of the incident wave, A_1, A_2, B_1, B_2, are calculated from the postulated incident wave pulse. The remaining parameters are included into the wave Eq. (3.2) where we substitute $x = 0$ and $x = L$ into the left and right-hand waves, respectively. Then we have got the system of 4

algebraic equations for 8 unknown parameters, C_1, C_2, D_1, D_2, E_1, E_2, F_1, F_2. To solve them uniquely we need 4 additional conditions on the wave amplitudes. The conditions are concerned with the directions of motion of the wave pulses (reflected and transmitted) governed by the direction of the incident pulse. The relations are analogous to the Snelius law known in optics or in the theory of harmonic elastic wave propagation.

As usually, the derivation of the reflection law is based on the assumption that the component of the wave vector parallel to the reflection (transmission) surface must be continuous. Let us denote the wave vector by $\mathbf{p}$. Then the law can be written as

$$\mathbf{p}_{\parallel}^{\mathrm{inc}} = \mathbf{p}_{\parallel}^{\mathrm{ref}} = \mathbf{p}_{\parallel}^{\mathrm{tr}}, \tag{3.11}$$

or equivalently:

$$\mathbf{p}^{\mathrm{inc}} \sin\varphi^{\mathrm{inc}} = \mathbf{p}^{\mathrm{ref}} \sin\varphi^{\mathrm{ref}} = \mathbf{p}^{\mathrm{tr}} \sin\varphi^{\mathrm{tr}}, \tag{3.12}$$

where φ^{inc}, φ^{ref} and φ^{tr} are, respectively, the angles of incidence, reflection and transmission of waves of certain type (longitudinal and transversal).

From the formulae (3.8) – (3.10) we see that the Fourier-transformed waves propagate only in the direction perpendicular to the interface surface. We also know the co-ordinate of the wave vectors perpendicular to the interface surface; it is $\mathbf{p}_{\perp} = p_3$ for the longitudinal wave and $\mathbf{p}_{\perp} = p_1$ for the transversal one. Knowing the incidence angle we can reduce the number of unknown constants in (3.8) – (3.10), using the Snelius-like relations (3.12).

Assume that the incident wave pulse is only longitudinal one and it reaches the interface surface at the angle of incidence $\varphi^{\mathrm{inc}} = \alpha$ (Fig. 1). This means that the amplitudes can be represented as

$$A_1 = A_2 = 0, \qquad B_1 = B\cos\alpha, \qquad B_2 = B\sin\alpha. \tag{3.13}$$

Hence the incident wave takes the following form:

$$\begin{bmatrix} \hat{u}_1^{\mathrm{inc}}(x) \\ \hat{u}_2^{\mathrm{inc}}(x) \\ \hat{\tau}_1^{\mathrm{inc}}(x) \\ \hat{\tau}_2^{\mathrm{inc}}(x) \end{bmatrix} = \begin{bmatrix} B_1 \\ B_2 \\ i[-(\lambda+2\mu)p_3 B_1 + kB_2] \\ i\mu(kB_1 - p_3 B_2) \end{bmatrix} \exp\{-ip_3 x\} \tag{3.14}$$

$$= \begin{bmatrix} B\cos\alpha \\ B\sin\alpha \\ iB[-(\lambda+2\mu)p_3\cos\alpha + k\sin\alpha] \\ i\mu B(k\cos\alpha - p_3\sin\alpha) \end{bmatrix} \exp\{-ip_3 x\}.$$

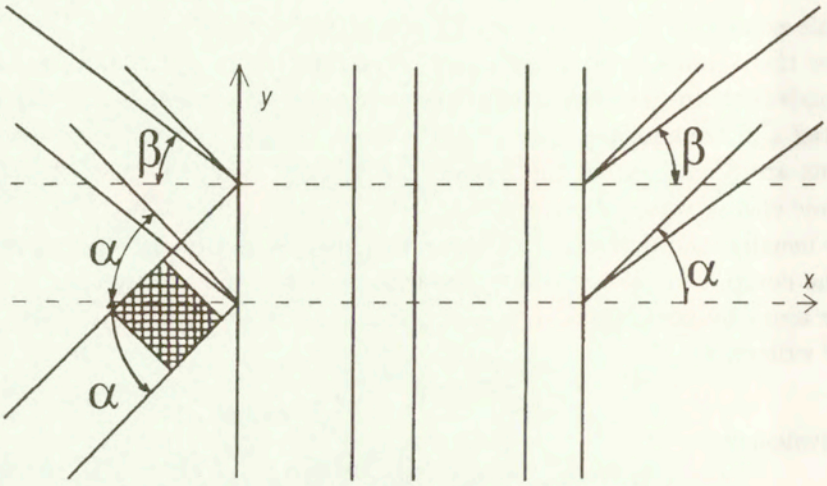

FIG. 1. The model of layered medium ($n = 2$ pairs of layers).

To obtain the relations restricting the number of amplitude constants, we transform the formula (3.12) into the more convenient form

$$\mathbf{p}_{\parallel}^{\mathrm{inc}} = \mathbf{p}_{\perp}^{\mathrm{inc}} \tan \varphi^{\mathrm{inc}} = \mathbf{p}_{\parallel}^{\mathrm{ref}} = \mathbf{p}_{\perp}^{\mathrm{ref}} \tan \varphi^{\mathrm{ref}} = \mathbf{p}_{\parallel}^{\mathrm{tr}} = \mathbf{p}_{\perp}^{\mathrm{tr}} \tan \varphi^{\mathrm{tr}}. \tag{3.15}$$

The solution of amplitude problem requires the calculation of the following angles:

$\varphi_{\mathrm{lon}}^{\mathrm{ref}}$ – the angle for reflected longitudinal wave;

$\varphi_{\mathrm{tr}}^{\mathrm{ref}}$ – the angle for reflected transversal wave;

$\varphi_{\mathrm{lon}}^{\mathrm{tr}}$ – the angle for transmitted longitudinal wave;

$\varphi_{\mathrm{tr}}^{\mathrm{tr}}$ – the angle for transmitted transversal wave.

Similarly to the case of harmonic waves [3], the above defined angles satisfy the following conditions:

$$\varphi_{\mathrm{lon}}^{\mathrm{ref}} = \varphi_{\mathrm{lon}}^{\mathrm{tr}} = \varphi_{\mathrm{lon}}^{\mathrm{inc}} = \alpha \tag{3.16}$$

and

$$\varphi_{\mathrm{tr}}^{\mathrm{ref}} = \varphi_{\mathrm{tr}}^{\mathrm{tr}} = \beta \tag{3.17}$$

Using formula (3.15) we find

$$p_3 \tan \varphi_{\mathrm{lon}}^{\mathrm{inc}} = p_1 \tan \varphi_{\mathrm{tr}}^{\mathrm{ref}} \tag{3.18}$$

or eventually

$$\beta = \arctan\left(\frac{p_3}{p_1} \tan \alpha\right) \tag{3.19}$$

Knowing the angles, we can write the direction vectors of every wave in the form:

$\mathbf{n} = (\cos\alpha, \sin\alpha)$ – the direction vector for incident longitudinal wave (the same as for transmitted longitudinal wave);

$\mathbf{m} = (-\cos\alpha, \sin\alpha)$ – the direction vector for reflected longitudinal wave;

$\mathbf{g} = (\cos\beta, \sin\beta)$ – the direction vector for transmitted transversal wave;

$\mathbf{h} = (-\cos\beta, \sin\beta)$ – the direction vector for reflected transversal wave.

Since the displacements of the medium for transversal waves are perpendicular to the direction vector, the displacement vectors are ($\mathbf{a}$ is the unit vector perpendicular to the reference plane):

$\mathbf{a} \times \mathbf{g} = (-\sin\beta, \cos\beta)$ – the displacement vector for transmitted transversal wave;

$\mathbf{a} \times \mathbf{h} = (-\sin\beta, -\cos\beta)$ – the displacement vector for reflected transversal wave.

The displacement vectors for the longitudinal waves are the same as those for the direction vectors.

Now, using the vectors defined above and the relations analogous to (3.13), we transform the waves (3.9) and (3.10) to the following form:

$$\begin{bmatrix} \hat{u}_1^{\mathrm{ref}}(x) \\ \hat{u}_2^{\mathrm{ref}}(x) \\ \hat{\tau}_1^{\mathrm{ref}}(x) \\ \hat{\tau}_2^{\mathrm{ref}}(x) \end{bmatrix} = -C \begin{bmatrix} \sin\beta \\ \cos\beta \\ i[(\lambda+2\mu)p_1 \sin\beta + k\cos\beta] \\ i\mu(k\sin\beta + p_1\cos\beta) \end{bmatrix} \exp\{ip_1 x\} + D \begin{bmatrix} -\cos\alpha \\ \sin\alpha \\ i[-(\lambda+2\mu)p_3\cos\alpha + k\sin\alpha] \\ i\mu(-k\cos\alpha + p_3\sin\alpha) \end{bmatrix} \exp\{ip_3 x\}. \tag{3.20}$$

$$\begin{bmatrix} \hat{u}_1^{\mathrm{tr}}(x) \\ \hat{u}_2^{\mathrm{tr}}(x) \\ \hat{\tau}_1^{\mathrm{tr}}(x) \\ \hat{\tau}_2^{\mathrm{tr}}(x) \end{bmatrix} = E \begin{bmatrix} -\sin\beta \\ \cos\beta \\ i[(\lambda+2\mu)p_1 \sin\beta + k\cos\beta] \\ i\mu(-k\sin\beta - p_1\cos\beta) \end{bmatrix} \exp\{-ip_1 x\} + F \begin{bmatrix} \cos\alpha \\ \sin\alpha \\ i[-(\lambda+2\mu)p_3\cos\alpha + k\sin\alpha] \\ i\mu(k\cos\alpha - p_3\sin\alpha) \end{bmatrix} \exp\{-ip_3 x\}. \tag{3.21}$$

To complete the wave Eq. (3.1) we conclude that

$$(3.22)\qquad \hat{\mathbf{u}}_0 = \begin{bmatrix} \hat{u}_1^{\mathrm{inc}}(0) \\ \hat{u}_2^{\mathrm{inc}}(0) \\ \hat{\tau}_1^{\mathrm{inc}}(0) \\ \hat{\tau}_2^{\mathrm{inc}}(0) \end{bmatrix} + \begin{bmatrix} \hat{u}_1^{\mathrm{ref}}(0) \\ \hat{u}_2^{\mathrm{ref}}(0) \\ \hat{\tau}_1^{\mathrm{ref}}(0) \\ \hat{\tau}_2^{\mathrm{ref}}(0) \end{bmatrix} = B \begin{bmatrix} \cos\alpha \\ \sin\alpha \\ i[-(\lambda+2\mu)p_3\cos\alpha + k\sin\alpha] \\ i\mu(k\cos\alpha - p_3\sin\alpha) \end{bmatrix}$$

$$-C \begin{bmatrix} \sin\beta \\ \cos\beta \\ i[(\lambda+2\mu)p_1\sin\beta + k\cos\beta] \\ i\mu(k\sin\beta + p_1\cos\beta) \end{bmatrix} + D \begin{bmatrix} -\cos\alpha \\ sin\alpha \\ i[-(\lambda+2\mu)p_3\cos\alpha + k\sin\alpha] \\ i\mu(-k\cos\alpha + p_3\sin\alpha) \end{bmatrix}$$

and

$$(3.23)\qquad \hat{\mathbf{u}}(L) = \begin{bmatrix} \hat{u}_1^{\mathrm{tr}}(L) \\ \hat{u}_2^{\mathrm{tr}}(L) \\ \hat{\tau}_1^{\mathrm{tr}}(L) \\ \hat{\tau}_2^{\mathrm{tr}}(L) \end{bmatrix} = E \begin{bmatrix} -\sin\beta \\ \cos\beta \\ i[(\lambda+2\mu)p_1\sin\beta + k\cos\beta] \\ i\mu(-k\sin\beta - p_1\cos\beta) \end{bmatrix} \exp\{-ip_1L\}$$

$$+F \begin{bmatrix} \cos\alpha \\ \sin\alpha \\ i[-(\lambda+2\mu)p_3\cos\alpha + k\sin\alpha] \\ i\mu(k\cos\alpha - p_3\sin\alpha) \end{bmatrix} \exp\{-ip_3L\}.$$

The aim of calculations is to obtain the parameters C, D, E and F from the Eq. (3.1) if the amplitude B of the incident wave is known.

In the particular case, if the incidence angle $\alpha = 0$, we have got:

$$(3.24)\qquad \hat{\mathbf{u}}_0 = B \begin{bmatrix} 1 \\ 0 \\ -i(\lambda+2\mu)p_3 \\ i\mu k \end{bmatrix} - C \begin{bmatrix} 0 \\ 1 \\ ik \\ i\mu p_1 \end{bmatrix} - D \begin{bmatrix} 1 \\ 0 \\ i(\lambda+2\mu)p_3 \\ i\mu k \end{bmatrix}$$

and

$$\hat{\mathbf{u}}(L) = E \begin{bmatrix} 0 \\ 1 \\ ik \\ -i\mu p_1 \end{bmatrix} \exp\{-ip_1 L\} \tag{3.25}$$

$$+F \begin{bmatrix} 1 \\ 0 \\ -i(\lambda+2\mu)p_3 \\ i\mu k \end{bmatrix} \exp\{-ip_3 L\}.$$

To proceed with calculations tending to the solution of the algebraic wave Eqs. (3.1) – (3.2), we substitute (3.24) – (3.25) and obtain:

$$\begin{bmatrix} F\exp\{-ip_3 L\} \\ E\exp\{-ip_1 L\} \\ ikE\exp\{-ip_1 L\} - i(\lambda+2\mu)p_3 F\exp\{-ip_3 L\} \\ -i\mu p_1 E\exp\{-ip_1 L\} + i\mu k F\exp\{-ip_3 L\} \end{bmatrix} \tag{3.26}$$

$$+ \begin{bmatrix} T_{11} & T_{12} & T_{13} & T_{14} \\ T_{21} & T_{22} & T_{23} & T_{24} \\ T_{31} & T_{32} & T_{33} & T_{34} \\ T_{41} & T_{42} & T_{43} & T_{44} \end{bmatrix} \begin{bmatrix} D \\ C \\ ikC + i(\lambda+2\mu)p_3 D \\ i\mu p_1 C + i\mu k D \end{bmatrix}$$

$$= \begin{bmatrix} T_{11} & T_{12} & T_{13} & T_{14} \\ T_{21} & T_{22} & T_{23} & T_{24} \\ T_{31} & T_{32} & T_{33} & T_{34} \\ T_{41} & T_{42} & T_{43} & T_{44} \end{bmatrix} \begin{bmatrix} B \\ 0 \\ -i(\lambda+2\mu)p_3 B \\ i\mu k B \end{bmatrix}.$$

Ordering the terms in (3.26) we write the system of equations in the following form:

$$
(3.27)\quad
\begin{bmatrix}
T_{12}+ikT_{13}+i\mu p_1 T_{14} & T_{11}+i(\lambda+2\mu)p_3T_{13}+i\mu kT_{14} \\
T_{22}+ikT_{23}+i\mu p_1 T_{24} & T_{21}+i(\lambda+2\mu)p_3T_{23}+i\mu kT_{24} \\
T_{32}+ikT_{33}+i\mu p_1 T_{34} & T_{31}+i(\lambda+2\mu)p_3T_{33}+i\mu kT_{34} \\
T_{42}+ikT_{43}+i\mu p_1 T_{44} & T_{41}+i(\lambda+2\mu)p_3T_{43}+i\mu kT_{44}
\end{bmatrix}
\begin{bmatrix}
0 & \exp\{-ip_3L\} \\
\exp\{-ip_1L\} & 0 \\
ik\exp\{-ip_1L\} & -i(\lambda+2\mu)p_3\exp\{-ip_3L\} \\
i\mu p_1\exp\{-ip_1L\} & i\mu k\{-ip_3L\}
\end{bmatrix}
\begin{bmatrix} C \\ D \\ E \\ F \end{bmatrix}
$$

$$
= \begin{bmatrix}
T_{11}-i(\lambda+2\mu)p_3T_{13}+i\mu kT_{14} \\
T_{21}-i(\lambda+2\mu)p_3T_{23}+i\mu kT_{24} \\
T_{31}-i(\lambda+2\mu)p_3T_{33}+i\mu kT_{34} \\
T_{41}-i(\lambda+2\mu)p_3T_{43}+i\mu kT_{44}
\end{bmatrix} B.
$$

4. Numerical results

In Sec. 3 we presented the analytical formulae solving the two-dimensional dynamical wave problem in layered medium. However, to make the proposed method fully effective, we have to proceed with computer calculations. The computational procedure leads from the initial wave pulse that travels through the homogeneous half-space and reaches the front interface of the stratified layer, to the pulses that are generated by the multiple reflections within the stratified slab. There result two pulses (with a very complicated structure): the reflected one that goes back in the homogeneous half-space and the transmitted one that propagates further beyond the back surface of the stratified medium.

The equations applied for calculations, that is Eq. (3.1) and the following ones, are written for the quantities (matrices and vectors) depending on two parameters k and ω (the variables of Fourier transformation with respect to the spatial variable and the time). Solving Eq. (3.1) we do this for a fixed pair of variables k and ω. A complete solution of the problem requires the Eq. (3.1) to be solved in the whole domain of the variables. Thereafter, the inverse Fourier transformation allows us to determine the evolution of the pulses in the actual time.

The scheme of calculations for some incident wave pulse can be given as follows. Let us assume, for simplicity, that the incident wave pulse is longitudinal

and reaches the front surface of the stratified layer at the angle of incidence $\alpha = 0$. In this case the Fourier transformation of the excitation, c.f. Eq. (3.14), takes the following form:

$$\begin{bmatrix} \hat{u}_1^{\mathrm{inc}}(x,k,\omega) \\ \hat{u}_2^{\mathrm{inc}}(x,k,\omega) \\ \hat{\tau}_1^{\mathrm{inc}}(x,k,\omega) \\ \hat{\tau}_2^{\mathrm{inc}}(x,k,\omega) \end{bmatrix} = B \begin{bmatrix} 1 \\ 0 \\ -i(\lambda+2\mu)p_3 \\ i\mu k \end{bmatrix} \exp\{-ip_3 x\}. \tag{4.1}$$

We have to remember that the eigenvalues p_1 and p_3 defined in (2.9) are functions of variables k and ω, as the coefficient B must have the form:

$$B = B(k,\omega), \qquad k,\omega \in (-\infty,\infty). \tag{4.2}$$

Moreover, the elements of the transition matrix $\mathbf{T}$ defined in (3.2) depend also on the variables k and ω, i.e.:

$$\mathbf{T} = \mathbf{T}(k,\omega). \tag{4.3}$$

To solve the problem, we substitute the calculated coefficient B in equation (3.27) and solve it with respect to the coefficients C, D, E and F. All of them are some functions of k and ω. We substitute the calculated values of the coefficients in the expressions (3.20) and (3.21) defining the reflected and transmitted wave pulses (or, more precisely, their Fourier transformations). Those expressions for $\alpha = 0$ take the following form:

$$\begin{bmatrix} \hat{u}_1^{\mathrm{ref}}(0,k,\omega) \\ \hat{u}_2^{\mathrm{ref}}(0,k,\omega) \\ \hat{\tau}_1^{\mathrm{ref}}(0,k,\omega) \\ \hat{\tau}_2^{\mathrm{ref}}(0,k,\omega) \end{bmatrix} = -C \begin{bmatrix} 0 \\ 1 \\ ik \\ i\mu p_1 \end{bmatrix} - D \begin{bmatrix} 1 \\ 0 \\ i(\lambda+2\mu)p_3 \\ i\mu k \end{bmatrix}, \tag{4.4}$$

$$\begin{bmatrix} \hat{u}_1^{\mathrm{tr}}(L,k,\omega) \\ \hat{u}_2^{\mathrm{tr}}(L,k,\omega) \\ \hat{\tau}_1^{\mathrm{tr}}(L,k,\omega) \\ \hat{\tau}_2^{\mathrm{tr}}(L,k,\omega) \end{bmatrix} = E \begin{bmatrix} 0 \\ 1 \\ ik \\ -i\mu p_1 \end{bmatrix} \exp\{-ip_1 L\} \tag{4.5}$$

$$+ F \begin{bmatrix} 1 \\ 0 \\ -i(\lambda+2\mu)p_3 \\ i\mu k \end{bmatrix} \exp\{-ip_3 L\}.$$

Two-dimensional inverse Fourier transformation of the vectors (4.4) and (4.5) give us eventually the pulses as the functions of time, t, and the second space variable, y, i.e.:

$$(4.6) \qquad \begin{bmatrix} u_1^{\mathrm{ref}} \\ u_2^{\mathrm{ref}} \\ \tau_1^{\mathrm{ref}} \\ \tau_2^{\mathrm{ref}} \end{bmatrix} = \begin{bmatrix} u_1^{\mathrm{ref}}(0,y,t) \\ u_2^{\mathrm{ref}}(0,y,t) \\ \tau_1^{\mathrm{ref}}(0,y,t) \\ \tau_2^{\mathrm{ref}}(0,y,t) \end{bmatrix} \quad \text{and} \quad \begin{bmatrix} u_1^{\mathrm{tr}} \\ u_2^{\mathrm{tr}} \\ \tau_1^{\mathrm{tr}} \\ \tau_2^{\mathrm{tr}} \end{bmatrix} = \begin{bmatrix} u_1^{\mathrm{tr}}(L,y,t) \\ u_2^{\mathrm{tr}}(L,y,t) \\ \tau_1^{\mathrm{tr}}(L,y,t) \\ \tau_2^{\mathrm{tr}}(L,y,t) \end{bmatrix}.$$

It should be noticed that practical calculations must be performed in several steps. First we must choose a grid in the region of changes of the variables k and ω, and then express the coefficient $B(k,\omega)$ over this grid. Next we solve the Eq. (3.27) for all points of this grid to obtain the values of coefficients C, D, E and F in all grid points. Finally, we have got the expressions (4.4) and (4.5) in the grid points and we can calculate the inverse Fourier transformation that is the solution of the problem.

As an example, in numerical calculation we have considered a slab built of two metals: steel and titanium surrounded by an aluminium environment. Material constants for aluminium, steel and titanium are, respectively, cf. [12]:

$$\lambda^0 = 5.44 \times 10^{10}\ \mathrm{kg \cdot m^{-1} \cdot sec^{-2}}, \quad \mu^0 = 2.75 \times 10^{10}\ \mathrm{kg \cdot m^{-1} \cdot sec^{-2}},$$

$$\lambda^1 = 10.71 \times 10^{10}\ \mathrm{kg \cdot m^{-1} \cdot sec^{-2}}, \quad \mu^1 = 8.14 \times 10^{10}\ \mathrm{kg \cdot m^{-1} \cdot sec^{-2}},$$

$$\lambda^2 = 7.08 \times 10^{10}\ \mathrm{kg \cdot m^{-1} \cdot sec^{-2}}, \quad \mu^2 = 4.31 \times 10^{10}\ \mathrm{kg \cdot m^{-1} \cdot sec^{-2}},$$

$$\rho^0 = 2750\ \mathrm{kg \cdot m^{-3}},$$

$$\rho^1 = 8670\ \mathrm{kg \cdot m^{-3}},$$

$$\rho^2 = 4300\ \mathrm{kg \cdot m^{-3}}.$$

Such a material configuration was chosen because the values of corresponding parameters differ from each other and enable us to observe the strong effect of stratification on the wave. We consider the incident longitudinal wave pulse of a constant unit amplitude and a finite duration of reaching the stratified slab of the fixed thickness at some finite instant (see Fig. 2). In our calculations the time axis is scaled in seconds while the spatial variable is represented by numbers of points of the grid used in calculations (we used 128 points of the spatial grid and 4096 points of the grid over time).

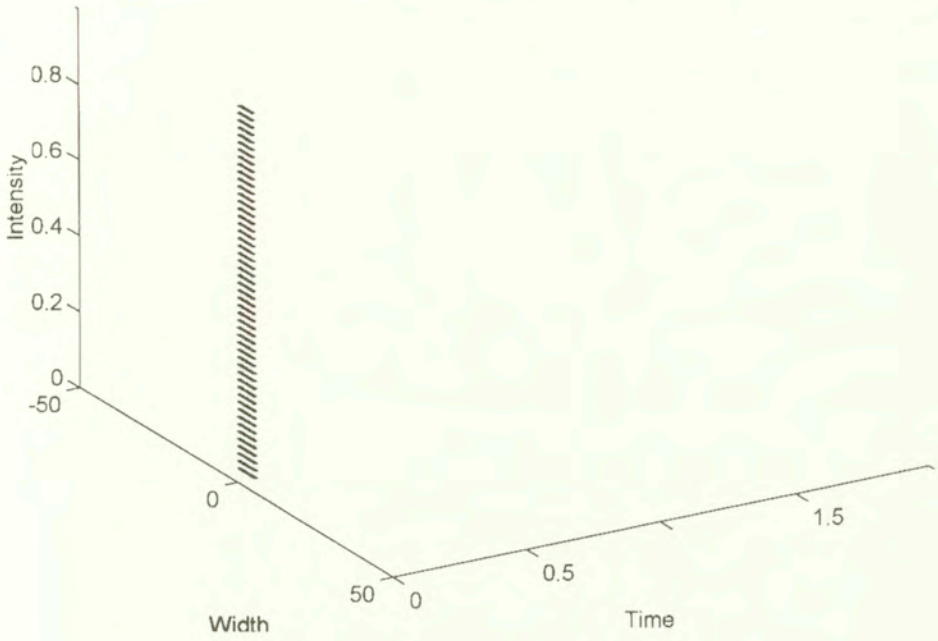

FIG. 2. Incident longitudinal wave pulse.

In our numerical studies we assumed that the material of the slab is located in pairs of the same thickness: one layer of steel and one layer of titanium. At Figure 3 we presented the evolution of the wave pulse longitudinal displacement (measured at the back surface of the slab) transmitted through the slab built of only one pair of layers steel-titanium, each of thickness $L/2$. We observe that the first wave pulse reaches the back surface after some time (we call it the travel time through the slab) and then it is followed by a number of pulses generated by the left and right-going pulses due to multiple reflections and transmissions at all the interfaces (internal interfaces of the layers within the slab and the interfaces of the slab and the surrounding environment). We see that the maximal peaks (except for the first peak generated directly by the transmitted incident pulse) correspond to the pulses reflected from the internal interfaces of the layers (the distance between peaks is the doubled travel time through a single layer). If the number of pairs of layers in the slab grows, we can observe an interesting effect of homogenisation. Figure 4 shows that for $n = 20$ pairs of layers (each layer of thickness $L/40$), the distances between maximal peaks are equal (approximately) to the double travel time through all the slab. Figure 5 shows the maps of peaks for the growing number of pairs of layers in the slab (from $n = 1$ to $n = 20$). We can see how this effect of homogenisation increases together with stronger mixing of the material in the slab.

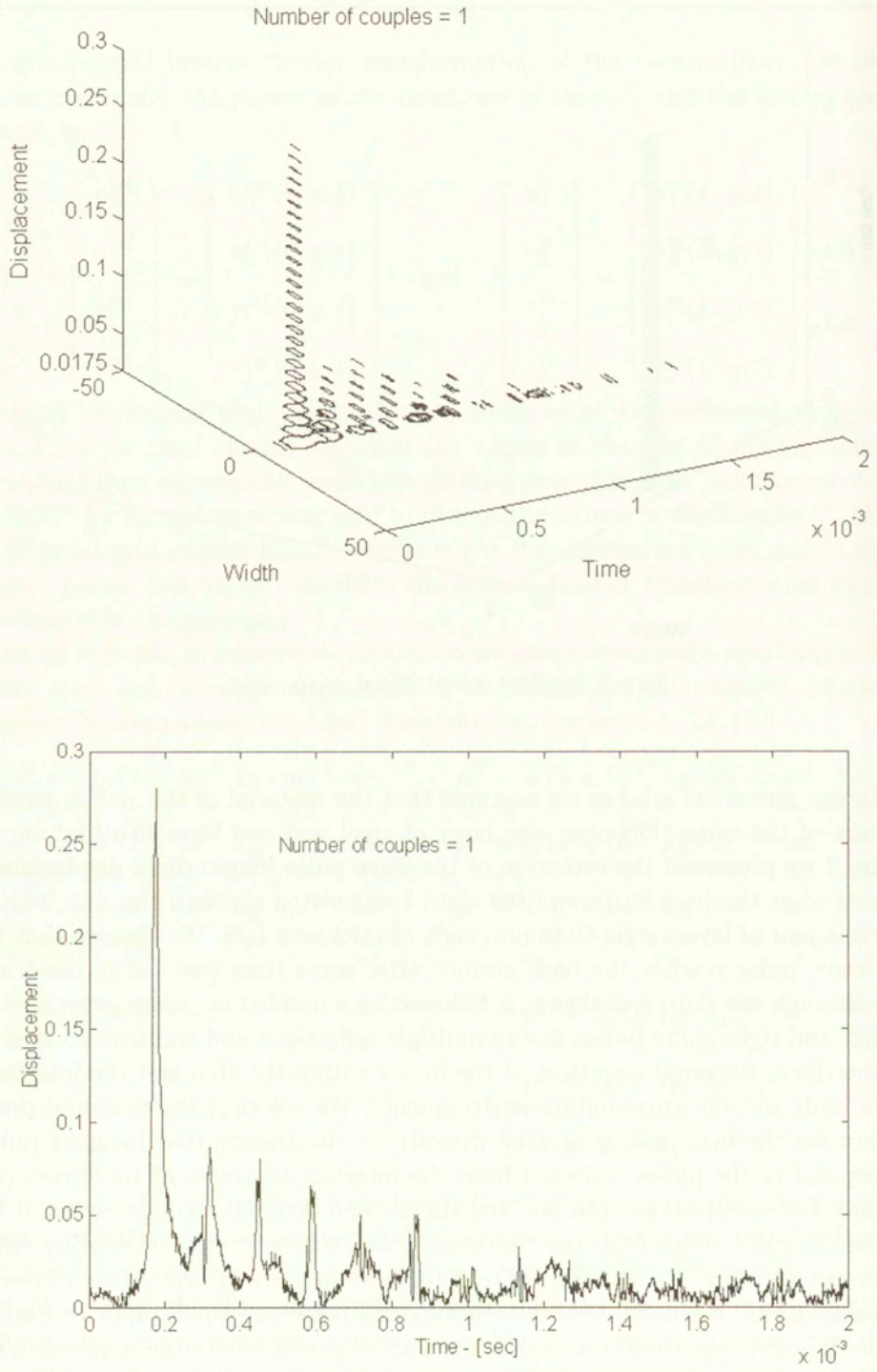

FIG. 3. Transmitted longitudinal wave pulse (n=1 pair of layers). Two-dimensional picture One-dimensional cross-section at the middle of pulse.

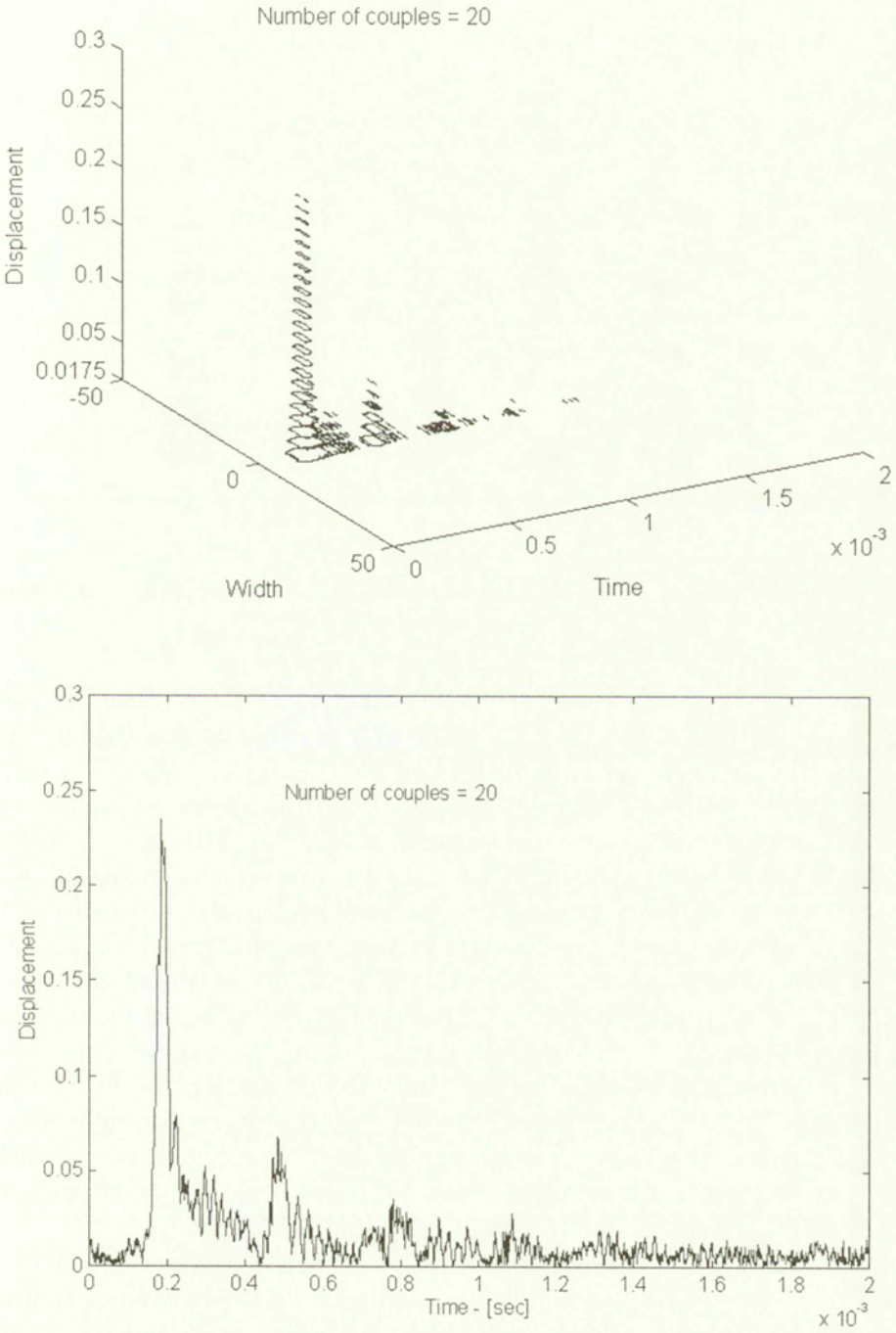

FIG. 4. Transmitted longitudinal wave pulse (n=20 pairs of layers). a) Two-dimensional picture; b) One-dimensional cross-section at the middle of pulse.

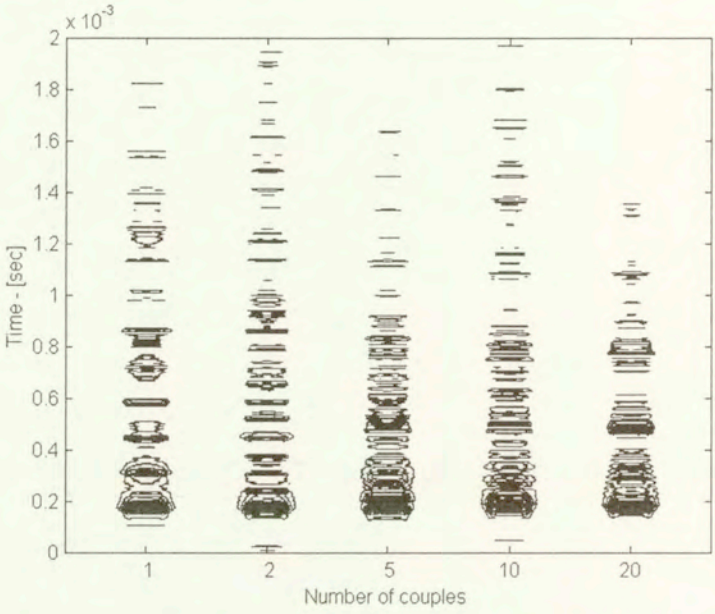

FIG. 5. Map of the transmitted longitudinal wave pulses for $n = 1, 2, 5, 10$ and 20 pairs of layers.

Our calculations and, what follows, the accuracy of the obtained picture is strongly restricted by the number the grid points possible for calculations within a realistic time (this is the time restriction for the applied algorithm of two-dimensional Fast Fourier Transformation – [8]). For this reason we cannot study the transmission of pulses for a greater number of layers (too few points of grid at every layer). However, calculations for the one-dimensional model [4], where only one-dimensional Fourier transformations are needed, show two effects. One is the convergence of the shape of the transmitted wave pulse to the shape of the incident pulse if the number of layers inside the slab grows (in our example the transmitted pulse is of the constant amplitude). The localisation of the wave pulse is another effect generated by a multi-layered medium. We can see that the wave pulse goes through the homogenised slab (the slab with many pairs of very narrow layers) longer than the sum of travel times through the material components. On the other hand, we can observe the concentration of displacements (and, what it follows, stresses) due to summation of several pulses, reflected and transmitted inside the slab, what can be called the localisation of stresses.

As it is known, the incident longitudinal wave pulse generates, except for the reflected and transmitted longitudinal wave pulses, also the transversal (reflected and transmitted) pulses. Figures 6a, 6b show the transmitted transversal pulses measured at the back surface of the layered slab for $n = 1$ and $n = 20$ pairs of layers, respectively, and for two instants of time. It is seen that the transverse

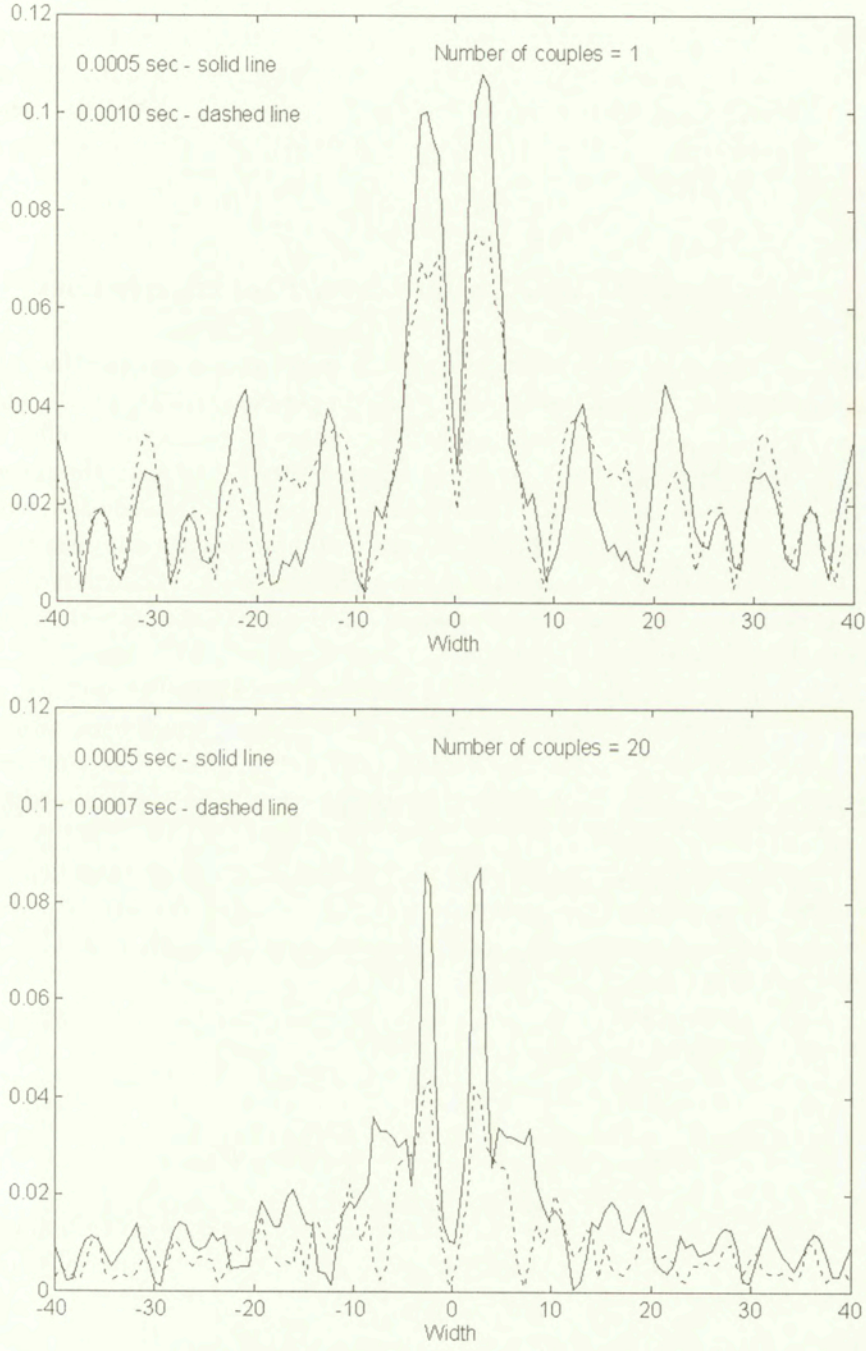

FIG. 6. Transmitted transversal wave pulse. a) $n = 1$ pair of layers. The cross-sections at time $t = 0.0005$ sec (solid line) and $t = 0.001$ sec (dashed line); b) $n = 20$ pairs of layers. The cross-sections at time $t = 0.0003$ sec (solid line) and $t = 0.0007$ sec (dashed line).

displacements are generated on the edges of the longitudinal wave. Unfortunately, in our calculations (to rare grid) we obtain a very high level of numerical noise, so too it is hard to conclude about evolution of this wave in time. We can only say that transverse pulses are proportional to the longitudinal ones, so they have peaks at the same time.

5. Wave pulses effect on fatigue fracture at interface imperfections

Two-dimensional analysis of the wave pulse propagation in stratified elastic medium provides the normal and shear stress components within a slab. Though the layers are assumed to be perfectly bonded, there is still a probability of an inclusion to be present at the interface. Assuming the inclusion in the form of a crack, the questions arise what a single impulse can be applied to the slab without initiating the fracture of the bond or how many and how intense impulses the slab can sustain without failing due to the fatigue damage. Both problems require the fracture mechanics theory for an interface in an idealised infinite plane between two linear elastic materials to be used.

For two perfectly bonded materials of different mechanical properties, shear modules, G_j, and Poisson's ratios, ν_j, $j = 1, 2$, say, both the tensile and shear stresses exist always at the crack tip affecting the fracture mode. There are several papers devoted to the interface crack growth initiation in dissimilar media, e.g. [9, 10, 13] and many others. It is commonly recognised that the crack branches initially from an interface in the softer of the two materials, at an angle depending on the stress components and material properties. As the branch extends, the crack tends to return to a path parallel to the interface with a driving force similar to that of an unbranched crack, cf. [6].

In order to prevent the propagation of an interface crack, the following criterion, cf. [13], can be adopted:

$$K_{\theta_{\max}} = B(\theta_0, \varepsilon, \gamma) \cdot \frac{\sqrt{K_1^2 + K_2^2}}{2 \cdot \cosh(\pi\varepsilon)} < K_{\mathrm{IC}} \tag{5.1}$$

where K_1 and K_2 are the real and imaginary parts of the complex stress intensity factor, $K = K_1 + iK_2$, for an interface crack, and ε is the bimaterial constant defined by

$$\varepsilon = \frac{1}{2\pi} \cdot \ln\left(\frac{\kappa_1/G_1 + 1/G_2}{\kappa_2/G_2 + 1/G_1}\right) \tag{5.2}$$

with $\kappa_j = 3 - 4\nu_j$ for plane strain or $\kappa_j j = (3 - \nu_j)/(1 + \nu_j)$ for plain stress problem, $j = 1, 2$. The parameter $\gamma = \tan^{-1}(K_2/K_1)$ and K_{IC} denotes the fracture

toughness. The criterion (5.1) is derived for $|\varepsilon| < 0.1$ under an assumption that the direction for which the circumferencial stress component, σ_θ, of the stress field in the polar co-ordinate system originated in the crack tip reaches its maximum, coincides with the initial crack growth direction, θ_0, i.e.

$$\frac{\partial \sigma_\theta}{\partial \theta} = 0. \tag{5.3}$$

The branching direction, θ_0, can be eventually calculated from the following equation:

$$\begin{aligned} \varepsilon \cdot e^{\varepsilon(\theta-\pi)} \cdot \left[2\cos\left(\frac{\theta}{2}+\gamma\right) - (\cos\theta + 2\varepsilon\sin\theta)\cdot\cos\left(\frac{\theta}{2}-\gamma\right)\right] \\ -e^{\varepsilon(\theta-\pi)}\cdot\left[\sin\left(\frac{\theta}{2}+\gamma\right) - (\sin\theta - 2\varepsilon\cos\theta)\cdot\cos\left(\frac{\theta}{2}-\gamma\right)\right. \\ \left. -\frac{1}{2}(\cos\theta - 2\varepsilon\sin\theta)\cdot\sin\left(\frac{\theta}{2}-\gamma\right)\right] \\ -e^{-\varepsilon(\theta-\pi)}\cdot\left[\varepsilon\cos\left(\frac{3\theta}{2}+\gamma\right) + \frac{3}{2}\sin\left(\frac{3\theta}{2}+\gamma\right)\right] = 0. \end{aligned} \tag{5.4}$$

The function term $B(\theta, \varepsilon, \gamma)$ occurring in (5.1) results from the formula for σ_θ and has got the following form:

$$\begin{aligned} B(\theta,\varepsilon,\gamma) = e^{\varepsilon(\theta-\pi)}\cdot\left[2\cos\left(\frac{\theta}{2}+\gamma\right) - (\cos\theta + 2\varepsilon\sin\theta)\cdot\cos\left(\frac{\theta}{2}-\gamma\right)\right] \\ + e^{-\varepsilon(\theta-\pi)}\cdot\cos\left(\frac{3\theta}{2}+\gamma\right). \end{aligned} \tag{5.5}$$

The components, K_1 and K_2, of the complex stress intensity factor are determined numerically, cf. [13], or analytically using the following formulae based on those derived in [9], say,

$$\begin{aligned} K_1 = \sigma\left[\cos(\varepsilon\log 2a) + 2\varepsilon\sin(\varepsilon\log 2a)\right] \\ + \tau\left[\sin(\varepsilon\log 2a) - 2\varepsilon\cos(\varepsilon\log 2a)\right]\cdot\sqrt{\pi\cdot a}, \end{aligned} \tag{5.5}_1$$

$$\begin{aligned} K_2 = \tau\left[\cos(\varepsilon\log 2a) + 2\varepsilon\sin(\varepsilon\log 2a)\right] \\ - \sigma\left[\sin(\varepsilon\log 2a) - 2\varepsilon\cos(\varepsilon\log 2a)\right]\cdot\sqrt{\pi\cdot a}. \end{aligned} \tag{5.5}_2$$

Substituting the latter into (5.1), the fracture criterion takes the simple form as follows

$$K_{\theta_{\max}} = B(\theta_0, \varepsilon, \gamma) \cdot \frac{\sqrt{(\sigma^2 + \tau^2) \cdot (1 + 4\varepsilon^2)}}{2 \cdot \cosh(\pi\varepsilon)} \cdot \sqrt{\pi \cdot a} < K_{\mathrm{IC}}. \tag{5.6}$$

In analogy to the fatigue crack growth modelling in homogenous materials the amplitude of the equivalent one-dimensional stress intensity factor, $\Delta K_{\theta_{\max}}$, cf. (5.6), related to the amplitudes of the stress components, $\Delta\sigma$ and $\Delta\tau$, can be likely used in a fatigue crack evolution equation in the form $da/dn = f(\Delta K_{\theta_{\max}})$ or more specifically, recalling the Paris-Erdogan equation, $da/dn = C \cdot \Delta K^m_{\theta_{\max}}$ with C and m as some constants. The further the crack penetrates into the material, the weaker becomes the effect of the interface on the crack propagation, in particular on its direction. It seems to be rational to assume the fatigue plastic zone size, r_p, as a characteristic distance between the crack tip and the interface when $\varepsilon = 0$ should be admitted in calculation of a new crack path direction, θ_0, cf. (5.4), and of the stress intensity factor amplitude, $\Delta_{\theta_{\max}}(\theta_0, 0, \gamma)$, cf. (5.6). Since the problem of plastic zone size calculation for the interface crack is rather obscure, cf. [10], the approximate equation

$$r_p \approx \frac{\pi}{2} \cdot (1 + 4\varepsilon^2) \cdot \frac{\Delta\sigma^2 + \Delta\tau^2}{\sigma_0^2} \cdot a \tag{5.7}$$

where σ_0 denotes the yield stress, can be adopted to indicate the moment when the interface effect might be neglected.

6. Conclusions

In the paper we considered the model of the stratified medium – the slab built of some number of isotropic, homogeneous elastic layers. Such a medium, globally, is both anisotropic and nonhomogeneous. It is known that if we assume the global thickness of the slab of layers to be constant but increase infinitely the number of layers inside the slab, we perform a homogenisation procedure so that after this process, the slab becomes homogeneous but remains anisotropic (locally and globally transversally isotopic). The homogenisation effect, observed during the numerical experiment, can be confirmed analytically, both for periodic and random layered media [5]. To prove this fact we can calculate the limit transition matrix (using the law of large numbers for products of matrices in the random case, cf. [1]). The elastic properties of the obtained effective medium are described by a tensor whose 5 elements are independent [3, 5]. However, as we have seen from the considerations of Section 2, for the description of the elastic waves in the case of the plane state of displacement we need only four elastic constants. Two constants are needed in the anti-plane state of displacement (one of them being different than that in the plane state). This statement remains valid both

in the dynamic nonstationary case, studied in this paper, and in the stationary one [3].

In this paper we have presented an analytical method of solution of the dynamic wave problem in a layered medium. However, to express the resulting waves (reflected and transmitted) generated by some incident pulse in an explicit way some numerical calculations are necessary. The two-dimensional inverse Fourier transform using the Fast Fourier Transform algorithm [8] appears to be the most effective numerical tool to perform the calculations.

Because of the multiple reflections and possible localisation of the stress pulses in the stratified media, the fatigue fracture effects must not be neglected in reliability assessment of structures made of such composites. Therefore some remarks on the interface crack propagation were given to point out the problem and suggest a possible approach to deal with it. Some numerical calculation and, what is of the greatest importance, experimental verification are now going on and will be reported elsewhere in the future.

Acknowledgement

The paper has been prepared with the financial support of the Committee of Scientific Research (KBN) under grant no. 7T07A03312.

References

1. M.A. BERGER, *Central limit theorem for products of random matrices*, Trans. A.M.S., **285**, 777–803, 1984.
2. S. KALISKI, [Ed.:], *Vibrations and waves in solids*, Polish Scientific Publishers, Warsaw 1966.
3. Z. KOTULSKI, *Elastic waves in randomly stratified medium, Part 1: Analytical results*, Acta Mechanica, **83**, 61–75, 1990, *Part 2: Numerical results*, Acta Mechanica, **85**, 143–163, 1992.
4. Z. KOTULSKI, *On the effective reflection properties of the randomly segmented elastic bar*, European Journal of Mechanics, A/Solids, **13**, 5, 677–696, 1994.
5. Z. KOTULSKI, *Wave pulses in two-dimensional randomly stratified elastic media*, Arch. Mech., **47**, 1, 125–139, 1995.
6. D.J. MUKAI, R. BALLARINI and G.R. MILLER, *Analysis of branched interface cracks*, J. Applied Mech., **57**, 887–893, 1990.
7. W. NOWACKI, *Theory of elasticity*, Polish Scientific Publishers, Warsaw 1970.
8. W.H. PRESS, B.F. FLANNERY, S.A. TEUKOLSKY and W.T. VETTERLING, *Numerical Recipes. The art of scientific computing*, Cambridge University Press, London 1986.
9. J.R. RICE and G.C. SIH, *Plane problems of cracks in dissimilar media*, J Applied Mech., Trans. ASME, **32**, 418–423, 1965.

10. J.R. RICE, *Elastic fracture mechanics concepts for interfacial cracks*, J Applied Mech., Trans. ASME, **55**, 98–103, 1988.

11. V.I. SMIRNOV, *Course of Higher Mathematics*, vol. **3**, part 2, State Editors of Physical and Mathematical Literature, Moscow 1961.

12. J.J. TUMA, *Handbook of physical calculations*, McGraw-Hill 1976.

13. R. YUUKI and J.-Q. XU, *Stress based criterion for an interface crack kinking out of the interface in dissimilar materials*, Engng Fract. Mech., **41**, 5, 635–644, 1992.

Received December 2, 1998; revised version 23 April 1999.

Arch. Mech., **51**, 3–4, pp. 335–355, Warszawa 1999

Application of homogenization to evaluation of effective moduli of linear elastic trabecular bone with plate-like structure

A. GAŁKA, J.J. TELEGA and S. TOKARZEWSKI

Polish Academy of Sciences
Institute of Fundamental Technological Research
Świętokrzyska 00–049 Warszawa, Poland
e-mail: jtelega@ippt.gov.pl

CANCELLOUS BONE with plate-like architecture is modelled as an elastic cellular solid with regular microstructure. General formulae for the effective moduli are derived. Specific examples concern plate-like cancellous bone with isotropic trabeculae.

1. Introduction

BONES OCCUR IN TWO FORMS: as a dense solid *(compact bone)* and as a porous network of interconnected rods and plates *(cancellous or trabecular bone)*. The most obvious difference between these two types of bones appears in their relative densities measured by volume fractions of solids, cf. Fig 1.

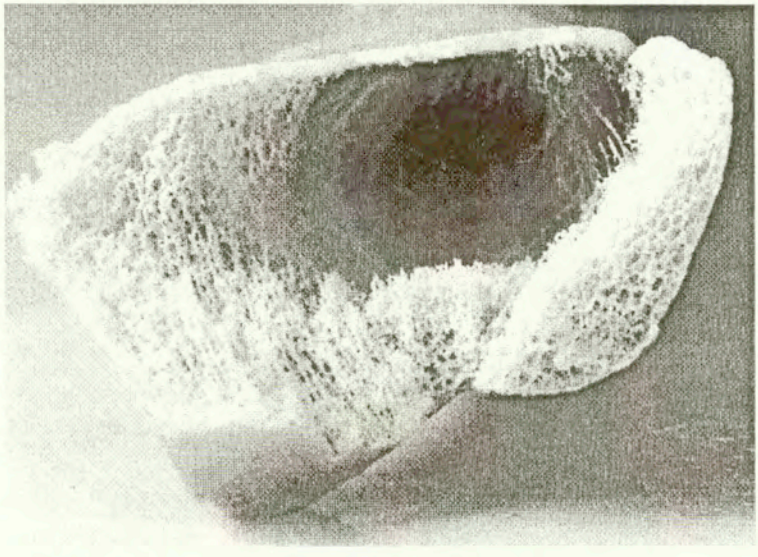

FIG. 1. Photograph of proximal part of the human femur.

Bone with a volume fraction of less than 70% is classified as cancellous while that over 70% is compact, cf. [13]. Most bones in the body are of both types, the dense compact bone forming an outer shell surrounding a core of spongy cancellous bone. This paper investigates cancellous bones of volume fractions of solid less than 70%. Typical examples of trabecular bones are shown in Figs. 2–4.

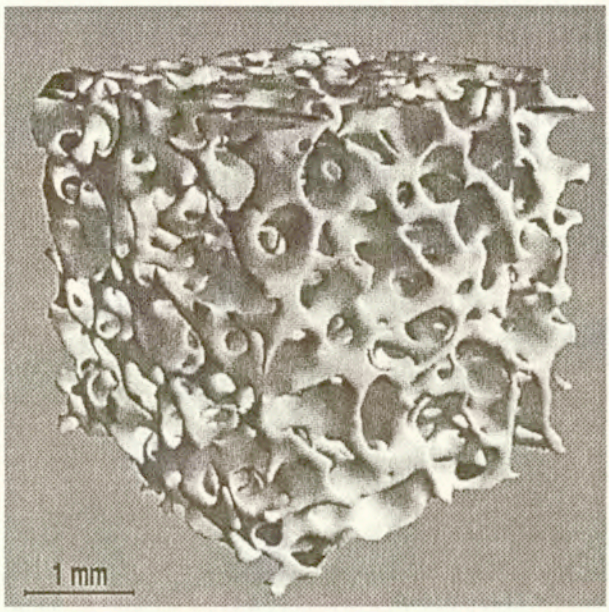

FIG. 2. Micro-CT image of a trabecular bone specimen with rod-like architecture and a bone volume fraction of 26%, after [33].

These figures provide interesting visualization of human trabecular bone architecture obtained by micro-computed tomography [24, 33]. According to MÜLLER and RÜEGSEGGER [24], specimens with diameters of a few millimeters to a maximum of 18 mm can be measured. Microstructure analyses of trabecular bone have followed the general approach used in the cellular plastics fields. MCELHANEY *et al.* [22] developed a porous block model of trabecular bone based on integration of spring stiffness loaded in parallel or in series. Using this model, they found good agreement between the prediction of apparent stiffness and the experimentally measured stiffness values in some internal layer of human skull. PUGH *et al.* [27] modelled the subchondral trabecular bone as a collection of structural plates and concluded that bending and buckling were major modes of deformation of the trabecular bone. WILLIAMS and LEWIS [34] modelled the exact structure of a two-dimensional section of trabecular bone with plane strain finite elements to predict the apparent transversely isotropic elastic constants. GIBSON [12] developed the models of trabecular bone structure using analytical

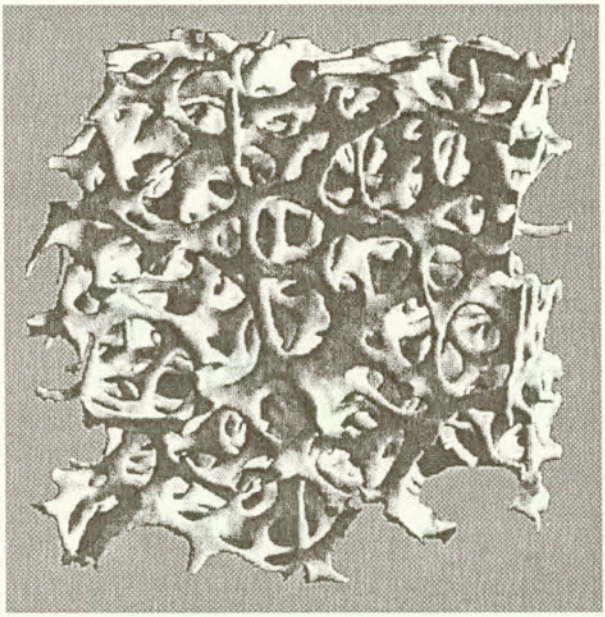

FIG. 3. Trabecular bone with distinct rod-like columnar structure, after [24].

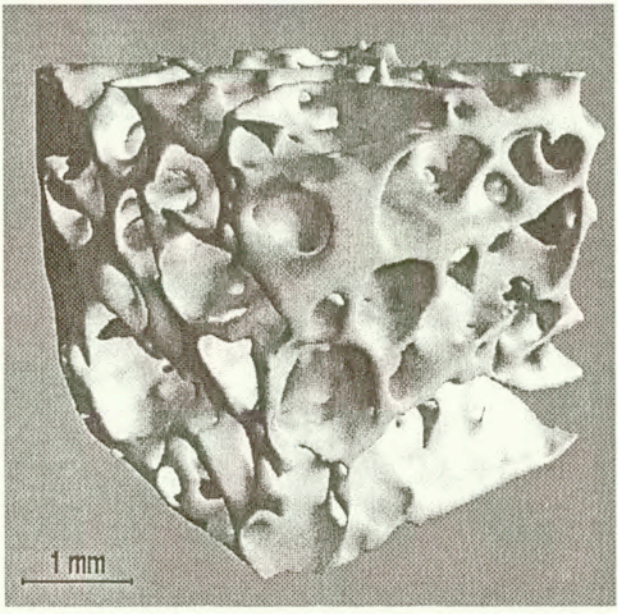

FIG. 4. Micro-CT image of a trabecular bone specimen with plate-like architecture and a bone volume fraction of 26%, after [33].

techniques for porous solids. He predicted the dependence of apparent stiffness on apparent density for different structural types of trabecular bones. BEAUPRÉ and HAYES [3] developed a three-dimensional spherical void model of trabecular bone and used finite element analyses to predict apparent stiffness and strength, as well the stress distribution within the trabecular bone. HOLLISTER *et al.* [14, 15] applied the homogenization theory [6, 19, 28, 29] for an investigation of mechanical behaviour of rod-like structures modelling the trabecular bones. By using the finite element method they evaluated the apparent, orthogonal Young's moduli and compared them with the experimental data obtained for proximal humerus, proximal tibia and distal femur. Bone may be viewed as a structurally hierarchical porous material. It is then possible to use the iterative homogenization [6] to derive the formulae for the macroscopic elastic moduli, cf. [1, 2, 10, 11]. Optimal design of structures often involves the homogenization and relaxation methods [4, 5, 18, 19, 21, 30]. Such an approach may be used to model bone microstructure via adaptive elasticity. PAYTEN *et al.* [26] presented an optimisation process that has, as its basis, an algorithm originally developed for predicting anatomical density distributions in natural human bones.

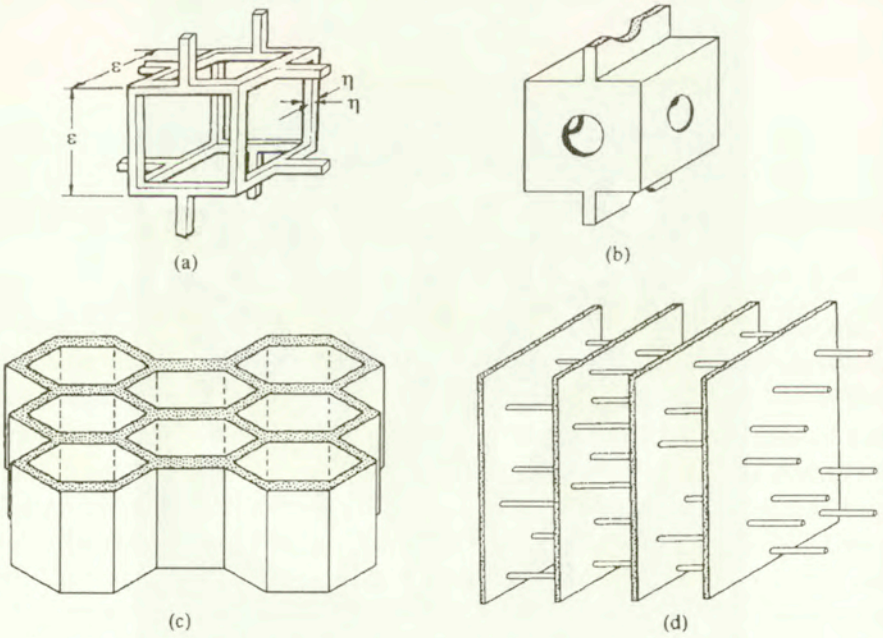

FIG. 5. Models for the structure of cancellous bone: (a) the low-density equiaxed structure, (b) the higher-density equiaxial structure, (c) the stress-oriented prismatic structure and (d) the stress-oriented parallel plate structure, after [13].

The microstructure of bone is such that at the macroscopic level its behaviour is anisotropic. To model bone anisotropy one can use Cowin's fabric tensor,

see [9, 16, 20] and the references cited therein. JEMIOŁO and TELEGA [16] prove that compact bone is close to transverse isotropy whilst trabecular bone is approximately orthotropic, cf. also [35]. The approach employed in [16] exploits Cowin's fabric tensor. In [35] the authors claim to use the homogenization method for finding the orthotropic elastic constants, yet no precise formulation was unfortunately given.

A challenging problem in the estimation of bone elastic moduli is the influence of marrow. No satisfactory modelling of this problem seems to have been proposed so far. KASRA and GRYNPAS [17] proposed an idealized three-dimensional finite element model of a rod-like trabecular bone structure to study its static and dynamic response under compressive loading. Static analysis of the model predicted hydraulic stiffening of trabecular bone due to the presence of bone narrow. The predicted power equation relating the trabecular bone apparent elastic modulus to its apparent density was in good agreement with those of the reported experimental data.

The aim of this paper is to develop a macroscopic model of cancellous bone by using the homogenization methods. In contrast to numerical considerations adopted in [14, 15] for the study of strut-like trabecular bone, our approach applies to plate-like architecture of cancellous bone and was inspired by the papers [7, 8]. General considerations are performed in Secs. 2 and 3 and extend those obtained in [7], where only the scalar case was investigated. In fact, the homogenization problem considered involved two small positive parameters: ε and η. The first parameter is standard in the homogenization whilst the second one characterizes the thickness of the trabecular plates. To derive the formula for the elastic macroscopic moduli, we first pass with ε to zero and next we let η tend to zero. It means that a two-parameter homogenization has been performed. Section 4 deals with a specific case of trabecular bone with plate-like structure, where the trabecular plates are isotropic. By properly choosing the geometry of the basic cell one can model anisotropic (orthotropic or transversely isotropic) behaviour of the cancellous bone at the macroscopic level. If $\alpha = \beta = 1$, at the macroscopic level the bone reveals the cubic symmetry, cf. formula (4.1).

2. Formulation of the problem

Let Ω denote a bounded open subset of $\mathbb{R}^3$. As usual by Y we denote the basic cell, cf. [6, 19, 28, 29]. The part of Y occupied by the material is denoted by Y^*. It is assumed that the hole T in Y does not intersect the boundary ∂Y, cf. [7, 19], though this assumption may be weakened. By Ω_ε^* we denote the part of Ω occupied by the material. Here $\varepsilon > 0$ is a small parameter. We asume that the holes do not meet the boundary $\partial\Omega$.

Let us consider the following boundary value problem of linear elasticity:

$$\frac{\partial}{\partial x_j}\left(C_{ijkl}\left(\frac{\mathbf{x}}{\varepsilon}\right)\frac{\partial u_k^\varepsilon}{\partial x_l}\right)+f_i=0 \quad \text{in } \Omega_\varepsilon^*,$$

$$u_k^\varepsilon = 0 \quad \text{on } \partial\Omega, \tag{2.1}$$

$$C_{ijkl}\left(\frac{\mathbf{x}}{\varepsilon}\right)\frac{\partial u_k^\varepsilon}{\partial x_l}n_j = 0 \quad \text{on } \partial\Omega_\varepsilon^*\backslash\partial\Omega,$$

where $\mathbf{n}=(n_j)$ is outer the unit vector normal to $\partial\Omega_\varepsilon^*\backslash\partial\Omega$.

We make the following assumptions:

(i) $f\in L^2(\Omega)$.

(ii) $C_{ijkl}\in L^\infty(Y^*)$, $C_{ijkl}=C_{klij}=C_{jikl}$, $i,j,k,l=1,2,3$.

(iii) There exist a positive constant c_0 such that for almost every $\mathbf{y}\in Y$:

$$C_{ijkl}(\mathbf{y})e_{ij}e_{kl}\geqslant C_0 e_{ij}e_{ij} \quad \text{for any} \quad \mathbf{e}=(e_{ij}),\ e_{ij}=e_{ji}.$$

(iv) The material coefficients $C_{ijkl}(\mathbf{y})$ are Y-periodic.

The passage with ε to zero is now standard. Let us recall the related basic results which will next be exploited in Sec. 3, where we will let η tend to zero. Under these assumptions, there exists an extension $P_\varepsilon\mathbf{u}^\varepsilon\in\left[H_0^1(\Omega)\right]^3$ of $\mathbf{u}^\varepsilon$ such that, cf. [7, 19],

$$P_\varepsilon\mathbf{u}^\varepsilon \rightharpoonup \mathbf{u} \quad \text{in } \left[H_0^1(\Omega)\right]^3 \text{ weakly},$$

with $\mathbf{u}=(u_k)$ being the solution of the equation

$$C_{ijkl}^h\frac{\partial^2 u_k}{\partial x_j\partial x_l}+\frac{|Y^*|}{|Y|}f_i=0 \quad \text{in } \Omega, \tag{2.2}$$

$$\mathbf{u}=\mathbf{0}, \quad \text{on } \partial\Omega.$$

Here $|Y|=vol\ Y$.

The homogenized coefficient C_{ijkl}^h are given by

$$C_{ijmn}^h = < C_{ijmn} > + < C_{ijpq}\frac{\partial\chi_p^{(mn)}}{\partial y_q} >, \tag{2.3}$$

where

$$< \cdot >= \frac{1}{|Y|}\int_{Y^*}(\cdot)d\mathbf{y}. \tag{2.4}$$

The Y-periodic functions $\chi_p^{(mn)}$ are solutions to the local problem

$$\frac{\partial}{\partial y_i}\left(C_{ijmn}\frac{\partial}{\partial y_n}\left(\chi_m^{(pq)}+\delta_m^p y^q\right)\right)=0 \quad \text{in } Y^*, \tag{2.5}$$

$$C_{ijmn}\frac{\partial}{\partial y_n}\left(\chi_m^{(pq)}+\delta_m^p y^q\right)N_i=0 \quad \text{on } \partial T. \tag{2.6}$$

Here $\mathbf{N}$ stands for the inner unit vector normal to ∂T. Written in the weak form, this problem is expressed by

$$\int\limits_{Y^*} C_{ijmn}\frac{\partial\chi_m^{(pq)}}{\partial y_n}\frac{\partial\Psi_j}{\partial y_i}\,d\mathbf{y}=-\int\limits_{Y^*} C_{ijpq}\frac{\partial\Psi_j}{\partial y_i}\,d\mathbf{y}, \qquad \forall\,\Psi_j\in H_{\mathrm{per}}(Y^*), \tag{2.7}$$

where

$$H_{\mathrm{per}}(Y^*)=\left\{v\in H^1(Y^*)\mid v \text{ is } Y-\text{periodic}\right\}.$$

For $\Psi_j=\chi_j^{(mn)}$ we get

$$\int\limits_{Y^*} C_{ijmn}\frac{\partial\chi_m^{(pq)}}{\partial y_n}\frac{\partial\chi_j^{(mn)}}{\partial y_i}\,d\mathbf{y}=-\int\limits_{Y^*} C_{ijpq}\frac{\partial\chi_j^{(mn)}}{\partial y_i}\,d\mathbf{y}. \tag{2.8}$$

3. Plate-like structure

In this section we shall derive the macroscopic moduli for a cellular solid with plate-like architecture. The plates are characterized by a small parameter $\eta>0$. The second step of homogenization consists in passing with η to zero. Let now the basic cell Y be given by

$$Y=\left[-\frac{1}{2},\frac{1}{2}\right)\times\left[-\frac{1}{2},\frac{1}{2}\right)\times\left[-\frac{1}{2},\frac{1}{2}\right). \tag{3.1}$$

Due to periodicity, the homogenized coefficients do not depend on the basic cell and consequently, one may take a translated cell of the basic one. Consequently we take the translated cell represented in Fig. 6.

We observe that the thicknesses of three orthogonal plates are not necessarily equal, thus allowing for a macroscopically orthotropic response of the trabecular bone. Let us introduce the following notation:

$$\begin{aligned}
Y_1&=\left\{\mathbf{y}\in Y, |y_1|\leqslant\frac{\eta}{2}\right\},\\
Y_2&=\left\{\mathbf{y}\in Y, |y_2|\leqslant\alpha\frac{\eta}{2}\right\},\\
Y_3&=\left\{\mathbf{y}\in Y, |y_3|\leqslant\beta\frac{\eta}{2}\right\},\\
Y_{12}&=\left\{\mathbf{y}\in Y, |y_1|\leqslant\frac{\eta}{2} \text{ and } |y_2|\leqslant\alpha\frac{\eta}{2}\right\},
\end{aligned} \tag{3.2}$$

(3.2) [cont.]

$$Y_{23} = \left\{ \mathbf{y} \in Y, |y_2| \leqslant \alpha \frac{\eta}{2} \text{ and } |y_3| \leqslant \beta \frac{\eta}{2} \right\},$$

$$Y_{13} = \left\{ \mathbf{y} \in Y, |y_1| \leqslant \frac{\eta}{2} \text{ and } |y_3| \leqslant \beta \frac{\eta}{2} \right\},$$

$$Y_{123} = \left\{ \mathbf{y} \in Y, |y_1| \leqslant \frac{\eta}{2} \text{ and } |y_2| \leqslant \alpha \frac{\eta}{2} \text{ and } |y_3| \leqslant \beta \frac{\eta}{2} \right\},$$

$$Y_\eta^* = \left\{ \mathbf{y} \in Y, |y_1| \leqslant \frac{\eta}{2} \text{ or } |y_2| \leqslant \alpha \frac{\eta}{2} \text{ or } |y_3| \leqslant \beta \frac{\eta}{2} \right\}.$$

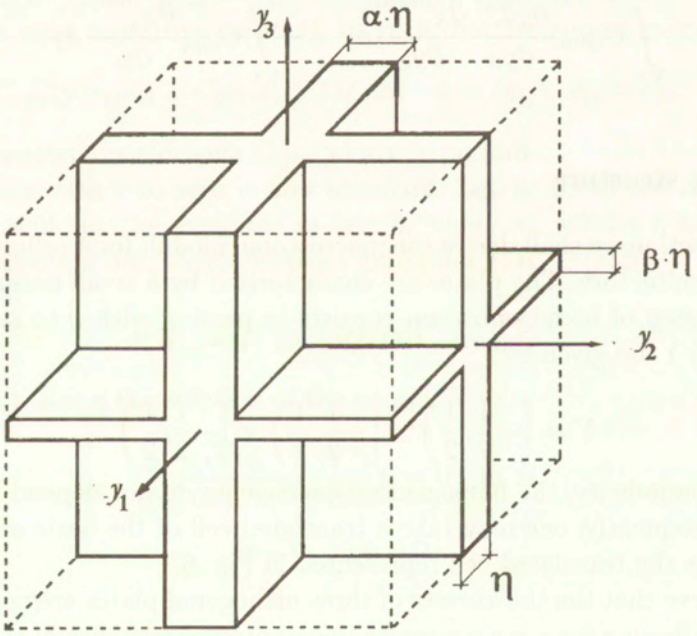

FIG. 6.

We follow the paper [7], where only two-dimensional scalar case was examined. Since $|Y_\eta^*| = (1+\alpha+\beta)\,\eta - (\alpha+\beta+\alpha\,\beta)\,\eta^2 + \alpha\,\beta\,\eta^3$, we get the following estimate:

$$||\mathrm{e}^y(\chi^{(pq)})||_{L^2(Y_\eta^*)} \leqslant c\,\eta^{1/2}. \tag{3.3}$$

Obviously $\chi^{(pq)}$ depend on α, β and η. The constant c is independent of η and

$$e^y(\mathbf{w}) = \frac{1}{2}\left(\frac{\partial w_i}{\partial y_j} + \frac{\partial w_j}{\partial y_i} \right).$$

Using this estimate in (2.3) we conclude that

$$\eta^{-1} C^h_{ijmn} \to C^*_{ijmn}$$

(after extraction of a subsequence, if necessary) We can pass to the limit as $\eta \to 0$ in the homogenized equation (2.2), whose solution is denoted by $\mathbf{u}^\eta$. We have

$$u^\eta_k \rightharpoonup u^*_k \quad \text{in} \quad H^1_0(\Omega) \text{ weakly},$$

where $\mathbf{u}^*$ is the solution to the equation:

$$C^*_{ijkn} \frac{\partial^2 u^*_k}{\partial x_j \partial x_n} + (1 + \alpha + \beta) f_i = 0 \quad \text{in} \quad \Omega, \tag{3.4}$$

$$\mathbf{u}^* = 0 \quad \text{on} \quad \partial\Omega.$$

We observe that now $|Y| = 1$.

Let us pass to finding the limit coefficients C^*_{ijkn}.
Using Eq. (2.3) and the decomposition of Y^* given by (3.2), we obtain:

$$\begin{aligned} \eta^{-1} C^h_{ijmn} = \eta^{-1} |Y^*| C_{ijmn} - \eta^{-1} \int\limits_{Y_1} C_{ijpq} \frac{\partial \chi^{(mn)}_p}{\partial y_q} \, d\mathbf{y} \\ - \eta^{-1} \int\limits_{Y_2} C_{ijpq} \frac{\partial \chi^{(mn)}_p}{\partial y_q} \, d\mathbf{y} - \eta^{-1} \int\limits_{Y_3} C_{ijpq} \frac{\partial \chi^{(mn)}_p}{\partial y_q} \, d\mathbf{y} \\ + \eta^{-1} \int\limits_{Y_{12}} C_{ijpq} \frac{\partial \chi^{(mn)}_p}{\partial y_q} \, d\mathbf{y} + \eta^{-1} \int\limits_{Y_{23}} C_{ijpq} \frac{\partial \chi^{(mn)}_p}{\partial y_q} \, d\mathbf{y} \\ + \eta^{-1} \int\limits_{Y_{13}} C_{ijpq} \frac{\partial \chi^{(mn)}_p}{\partial y_q} \, d\mathbf{y} - \eta^{-1} \int\limits_{Y_{123}} C_{ijpq} \frac{\partial \chi^{(mn)}_p}{\partial y_q} \, d\mathbf{y}. \end{aligned} \tag{3.5}$$

We have to pass to the limit with $\eta \to 0$ in (3.5), where the integral terms are taken over domains depending on η. To avoid this difficulty we transform Y_1, Y_2, Y_3, Y_{12}, Y_{23}, Y_{13} and Y_{123} in $\overline{Y}$.

For instance, using the a priori estimate (3.3) we have

$$\int\limits_{Y_1} \left| \mathbf{e}^y \left(\boldsymbol{\chi}^{(pq)} \right) \right| \, d\mathbf{y} \leqslant c\eta.$$

Hence, after transformation

$$z_1 = \eta^{-1} y_1, \; z_2 = y_2, \; z_3 = y_3,$$

and using Korn's inequality we get

$$\int\limits_Y \left[\left(\eta^{-1} \frac{\partial \chi_{p1}^{(mn)}}{\partial z_1} \right)^2 + \left(\frac{\partial \chi_{p1}^{(mn)}}{\partial z_2} \right)^2 + \left(\frac{\partial \chi_{p1}^{(mn)}}{\partial z_3} \right)^2 \right] d\mathbf{z} \leqslant c_1,$$

where $\chi_{p1}^{(mn)} = \chi_{p1}^{(mn)}(z_1, z_2, z_3) = \chi_p^{(mn)}(\eta z_1, z_2, z_3)$ and c_1 does not depend on η.

Thus

$$\eta^{-1} \frac{\partial \chi_{p1}^{(mn)}}{\partial z_1} \rightharpoonup h_{p1,1}^{(mn)}, \quad \frac{\partial \chi_{p1}^{(mn)}}{\partial z_2} \rightharpoonup h_{p1,2}^{(mn)}, \quad \frac{\partial \chi_{p1}^{(mn)}}{\partial z_3} \rightharpoonup h_{p1,3}^{(mn)}, \tag{3.6}$$

in $L^2(Y)$ weakly

and similarly

$$\frac{\partial \chi_{p2}^{(mn)}}{\partial z_1} \rightharpoonup h_{p2,1}^{(mn)}, \quad \eta^{-1} \frac{\partial \chi_{p2}^{(mn)}}{\partial z_2} \rightharpoonup h_{p2,2}^{(mn)}, \quad \frac{\partial \chi_{p2}^{(mn)}}{\partial z_3} \rightharpoonup h_{p2,3}^{(mn)},$$

in $L^2(Y)$ weakly,

$$\frac{\partial \chi_{p3}^{(mn)}}{\partial z_1} \rightharpoonup h_{p3,1}^{(mn)}, \quad \frac{\partial \chi_{p3}^{(mn)}}{\partial z_2} \rightharpoonup h_{p1,3}^{(mn)}, \quad \eta^{-1} \frac{\partial \chi_{p3}^{(mn)}}{\partial z_3} \rightharpoonup h_{p3,3}^{(mn)},$$

in $L^2(Y)$ weakly,

$$\eta^{-1/2} \frac{\partial \chi_{p12}^{(mn)}}{\partial z_1} \rightharpoonup h_{p12,1}^{(mn)}, \quad \eta^{-1/2} \frac{\partial \chi_{p12}^{(mn)}}{\partial z_2} \rightharpoonup h_{p12,2}^{(mn)}, \quad \frac{\partial \chi_{p12}^{(mn)}}{\partial z_3} \rightharpoonup h_{p12,3}^{(mn)},$$

in $L^2(Y)$ weakly,

(3.7)

$$\frac{\partial \chi_{p23}^{(mn)}}{\partial z_1} \rightharpoonup h_{p23,1}^{(mn)}, \quad \eta^{-1/2} \frac{\partial \chi_{p23}^{(mn)}}{\partial z_2} \rightharpoonup h_{p23,2}^{(mn)}, \quad \eta^{-1/2} \frac{\partial \chi_{p23}^{(mn)}}{\partial z_3} \rightharpoonup h_{p23,3}^{(mn)},$$

in $L^2(Y)$ weakly,

$$\eta^{-1/2} \frac{\partial \chi_{p13}^{(mn)}}{\partial z_1} \rightharpoonup h_{p13,1}^{(mn)}, \quad \frac{\partial \chi_{p13}^{(mn)}}{\partial z_2} \rightharpoonup h_{p13,2}^{(mn)}, \quad \eta^{-1/2} \frac{\partial \chi_{p13}^{(mn)}}{\partial z_3} \rightharpoonup h_{p13,3}^{(mn)},$$

in $L^2(Y)$ weakly,

$$\frac{\partial \chi_{p123}^{(mn)}}{\partial z_1} \rightharpoonup h_{p123,1}^{(mn)}, \quad \frac{\partial \chi_{p123}^{(mn)}}{\partial z_2} \rightharpoonup h_{p123,2}^{(mn)}, \quad \frac{\partial \chi_{p123}^{(mn)}}{\partial z_3} \rightharpoonup h_{p123,3}^{(mn)},$$

in $L^2(Y)$ weakly.

Here

$$\chi_{p2}^{(mn)} = \chi_{p2}^{(mn)}(z_1, z_2, z_3) = \chi_p^{(mn)}(z_1, \alpha\eta z_2, z_3),$$

$$\chi_{p3}^{(mn)} = \chi_{p3}^{(mn)}(z_1, z_2, z_3) = \chi_p^{(mn)}(z_1, z_2, \beta\eta z_3),$$

$$\chi_{p12}^{(mn)} = \chi_{p12}^{(mn)}(z_1, z_2, z_3) = \chi_p^{(mn)}(\eta z_1, \alpha\eta z_2, z_3),$$

$$\chi_{p23}^{(mn)} = \chi_{p23}^{(mn)}(z_1, z_2, z_3) = \chi_p^{(mn)}(z_1, \alpha\eta z_2, \beta\eta z_3),$$

$$\chi_{p13}^{(mn)} = \chi_{p13}^{(mn)}(z_1, z_2, z_3) = \chi_p^{(mn)}(\eta z_1, z_2, \beta\eta z_3),$$

$$\chi_{p123}^{(mn)} = \chi_{p123}^{(mn)}(z_1, z_2, z_3) = \chi_p^{(mn)}(\eta z_1, \alpha\eta z_2, \beta\eta z_3).$$

We observe that due to the periodicity of $\chi_p^{(mn)}$ one has:

$$\int_Y h_{p1,2}^{(mn)}\, d\mathbf{z} = 0, \quad \int_Y h_{p1,3}^{(mn)}\, d\mathbf{z} = 0, \quad \int_Y h_{p2,1}^{(mn)}\, d\mathbf{z} = 0,$$

$$\int_Y h_{p2,3}^{(mn)}\, d\mathbf{z} = 0, \quad \int_Y h_{p3,1}^{(mn)}\, d\mathbf{z} = 0, \quad \int_Y h_{p3,2}^{(mn)}\, d\mathbf{z} = 0, \tag{3.8}$$

$$\int_Y h_{p12,3}^{(mn)}\, d\mathbf{z} = 0, \quad \int_Y h_{p23,1}^{(mn)}\, d\mathbf{z} = 0, \quad \int_Y h_{p13,2}^{(mn)}\, d\mathbf{z} = 0.$$

By using (3.3) one finds

$$\left|\eta^{-1} \int_{Y_{12}} C_{ijpq} \frac{\partial \chi_p^{(mn)}}{\partial y_q}\, d\mathbf{y}\right| \leqslant c_1 \eta^{1/2}, \quad \left|\eta^{-1} \int_{Y_{23}} C_{ijpq} \frac{\partial \chi_p^{(mn)}}{\partial y_q}\, d\mathbf{y}\right| \leqslant c_1 \eta^{1/2},$$

$$\left|\eta^{-1} \int_{Y_{13}} C_{ijpq} \frac{\partial \chi_p^{(mn)}}{\partial y_q}\, d\mathbf{y}\right| \leqslant c_1 \eta^{1/2}, \quad \left|\eta^{-1} \int_{Y_{123}} C_{ijpq} \frac{\partial \chi_p^{(mn)}}{\partial y_q}\, d\mathbf{y}\right| \leqslant c_1 \eta.$$

We now pass to the limit in (3.5). Taking into account (3.6) – (3.8), one obtains:

$$C_{ijmn}^* = (1 + \alpha + \beta)\, C_{ijmn} + C_{ijp1} \int_Y h_{p1,1}^{(mn)}\, d\mathbf{z} + \alpha\, C_{ijp2} \int_Y h_{p2,2}^{(mn)}\, d\mathbf{z} + \beta\, C_{ijp3} \int_Y h_{p3,3}^{(mn)}\, d\mathbf{z}. \tag{3.9}$$

The last step is to calculate explicitly the integral terms of this formula. Let Ψ_j in (2.7) be a smooth function, Y-periodic and dependent only on y_1. We find

$$\eta^{-1}\int\limits_{Y_1} C_{1jmn}\frac{\partial\chi_m^{(pq)}}{\partial y_n}\frac{\partial\Psi_j}{\partial y_1}d\mathbf{y}$$

$$= \eta^{-1}C_{1jm1}\int\limits_{-\eta/2}^{\eta/2}\frac{\partial\Psi_j}{\partial y_1}\left(\int\limits_{-1/2}^{1/2}\int\limits_{-1/2}^{1/2}\frac{\partial\chi_m^{(pq)}}{\partial y_1}\,dy_2\,dy_3\right)dy_1$$

$$\to C_{1jm1}\frac{\partial\Psi_j}{\partial y_1}(0)\int\limits_Y h_{m1,1}^{(pq)}\,d\mathbf{y},$$

$$\eta^{-1}\int\limits_{Y_2} C_{1jmn}\frac{\partial\chi_m^{(pq)}}{\partial y_n}\frac{\partial\Psi_j}{\partial y_1}d\mathbf{y} \to C_{1jm1}\int\limits_Y h_{m2,1}^{(pq)}\frac{\partial\Psi_j}{\partial y_1}\,d\mathbf{y},$$

$$\eta^{-1}\int\limits_{Y_3} C_{1jmn}\frac{\partial\chi_m^{(pq)}}{\partial y_n}\frac{\partial\Psi_j}{\partial y_1}d\mathbf{y} \to C_{1jm1}\int\limits_Y h_{m3,1}^{(pq)}\frac{\partial\Psi_j}{\partial y_1}\,d\mathbf{y},$$

$$\eta^{-1}\int\limits_{Y^*} C_{1jpq}\frac{\partial\Psi_j}{\partial y_1}d\mathbf{y} \to C_{1jpq}\frac{\partial\Psi_j}{\partial y_1}(0).$$

Multiplying (2.7) by η^{-1} and passing to the limit $(\eta\to 0)$, we obtain

$$C_{1jm1}\int\limits_Y\left(h_{m2,1}^{(pq)}+h_{m3,1}^{(pq)}\right)\frac{\partial\Psi_j}{\partial y_1}\,d\mathbf{z} \tag{3.10}$$

$$+\frac{\partial\Psi_j}{\partial y_1}(0)\left(C_{1jm1}\int\limits_Y h_{m1,1}^{(pq)}\,d\mathbf{z}+C_{1jpq}\right)=0.$$

To proceed further we need the following result, cf. [7].

LEMMA 3.1 Let w be a periodic function in $L^2(-1/2,-1/2)$, and let a be a real constant. If the following, relation holds true:

$$a\,\Psi(0)+\int\limits_{-1/2}^{1/2} w(x)\Psi(x)\,dx=0,$$

for any smooth and periodic function Ψ defined on $(-1/2, 1/2)$ and such that $\int_{-1/2}^{1/2} \Psi(x)\,dx = 0$, then

$$a = 0 \quad \text{and} \quad w = \text{ const.} \qquad \square$$

Applying this lemma to (3.10) we obtain

$$\int_Y h^{(pq)}_{m1,1} = -\left(\mathbf{C}_1^{-1}\right)_{mj} C_{1jpq},$$

where $\left(\mathbf{C}_1^{-1}\right)_{mj}$ are the components of the matrix inverse to (C_{1mj1}). Similar computation with Ψ_j depending only on y_2 leads to

$$\int_Y h^{(pq)}_{m2,2} = -\left(\mathbf{C}_2^{-1}\right)_{mj} C_{2jpq}.$$

Next, if Ψ_j depends only on y_3, then

$$\int_Y h^{(pq)}_{m3,3} = -\left(\mathbf{C}_3^{-1}\right)_{mj} C_{3jpq}.$$

Here $\left(\mathbf{C}_2^{-1}\right)_{mj}$ and $\left(\mathbf{C}_3^{-1}\right)_{mj}$ are the components of the matrices inverse to (C_{2mj2}) and (C_{3mj3}) respectively. From (3.9) we eventually obtain

$$C^*_{ijmn} = (1+\alpha+\beta)\,C_{ijmn} - C_{ijp1}\left(\mathbf{C}_1^{-1}\right)_{pq} C_{1qmn} - \alpha\, C_{ijp2}\left(\mathbf{C}_2^{-1}\right)_{pq} C_{2qmn} - \beta\, C_{ijp3}\left(\mathbf{C}_3^{-1}\right)_{pq} C_{3qmn}. \tag{3.11}$$

If we take a more general basic cell:

$$Y = \left[-\frac{1}{2}, \frac{1}{2}\right) \times \left[-\frac{A}{2}, \frac{A}{2}\right) \times \left[-\frac{B}{2}, \frac{B}{2}\right)$$

then we obtain the following formula:

$$C^*_{ijmn} = \left(1 + \frac{\alpha}{A} + \frac{\beta}{B}\right) C_{ijmn} - C_{ijp1}\left(\mathbf{C}_1^{-1}\right)_{pq} C_{1qmn} - \frac{\alpha}{A}\, C_{ijp2}\left(\mathbf{C}_2^{-1}\right)_{pq} C_{2qmn} - \frac{\beta}{B}\, C_{ijp3}\left(\mathbf{C}_3^{-1}\right)_{pq} C_{3qmn}. \tag{3.12}$$

4. Specific case: trabecular plates made of a homogeneous and isotropic material

Let the plate trabeculae be isotropic and homogeneous; then

$$C_{ijmn} = \mu\left(\delta_{mj}\delta_{ni} + \delta_{mi}\delta_{nj}\right) + \lambda\delta_{ij}\delta_{mn}.$$

From (3.11) we obtain the following form of the elasticity matrix:

(4.1)

$$\mathbf{C}^* = \begin{bmatrix} \frac{4\mu(\alpha+\beta)(\lambda+\mu)}{2\mu+\lambda} & \frac{2\alpha\lambda\mu}{2\mu+\lambda} & \frac{2\alpha\lambda\mu}{2\mu+\lambda} & 0 & 0 & 0 \\ \frac{2\beta\lambda\mu}{2\mu+\lambda} & \frac{4\mu(1+\beta)(\lambda+\mu)}{2\mu+\lambda} & \frac{2\lambda\mu}{2\mu+\lambda} & 0 & 0 & 0 \\ \frac{2\alpha\lambda\mu}{2\mu+\lambda} & \frac{2\lambda\mu}{2\mu+\lambda} & \frac{4\mu(1+\alpha)(\lambda+\mu)}{2\mu+\lambda} & 0 & 0 & 0 \\ 0 & 0 & 0 & 2\mu & 0 & 0 \\ 0 & 0 & 0 & 0 & 2\alpha\mu & 0 \\ 0 & 0 & 0 & 0 & 0 & 2\beta\mu \end{bmatrix}$$

Obviously, here Voigt's notation has been used, cf. [25].

Having in mind Fig. 6, the *physical* effective elasticity tensor, now denoted by $\mathbf{C}^{\text{eff}}$, is given by

(4.2) $$\mathbf{C}^{\text{eff}} = \frac{v}{1+\alpha+\beta}\,\mathbf{C}^*,$$

where v is the volume fraction.

In the case of $\mathbf{C}^*$ given by Eq. (3.12) we have

$$\mathbf{C}^{\text{eff}} = \frac{vAB}{AB+B\alpha+A\beta}\,\mathbf{C}^*.$$

By $\mathbf{A}$ we denote the matrix inverse to $(\mathbf{C}^{\text{eff}})$, i.e. $\mathbf{A} = \left(\mathbf{C}^{\text{eff}}\right)^{-1}$. The technical elasticity constants are, cf. [16, 25]

(4.3) $$E_1 = \frac{1}{A_{11}}, \qquad E_2 = \frac{1}{A_{22}}, \qquad E_3 = \frac{1}{A_{33}},$$

(4.4) $$G_{12} = \frac{1}{2\,A_{66}}, \qquad G_{13} = \frac{1}{2\,A_{55}}, \qquad G_{23} = \frac{1}{2\,A_{44}},$$

(4.5) $$\nu_{12} = -\frac{A_{12}}{A_{22}}, \qquad \nu_{21} = -\frac{A_{12}}{A_{11}}, \qquad \nu_{13} = -\frac{A_{13}}{A_{33}},$$

$$\nu_{31} = -\frac{A_{12}}{A_{11}}, \qquad \nu_{23} = -\frac{A_{23}}{A_{33}}, \qquad \nu_{32} = -\frac{A_{23}}{A_{22}}.$$

Let us pass now to the presentation of specific cases, which show the usefulness of the formulae (4.2) for the determination of macroscopic elastic moduli of a trabecular bone with a plate-like architecture. These particular cases are presented in the form of Tables 1, 2 and 3 and Figs. 7–9 below.

The third column of Table 1 provides technical constants calculated by using formulae (4.3) – (4.5). The following data, corresponding to the hydroxyapatite, cf. [9, 11], are assumed:

$$E = 114\,[\mathrm{GPa}], \qquad \nu = 0.27.$$

Then the Lamé coefficients are given by $\lambda = 52.69\,[\mathrm{GPa}]$, $\mu = 44.88\,[\mathrm{GPa}]$. The calculations have been performed for

$$\alpha = \frac{3}{4}, \quad \beta = \frac{1}{4}, \quad v = \frac{1}{5}.$$

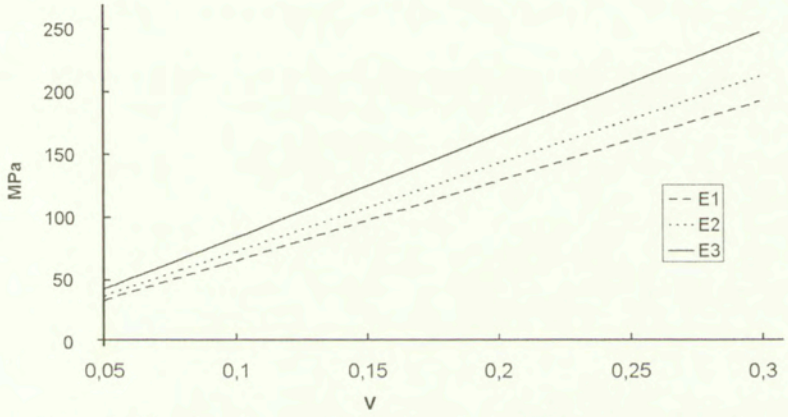

FIG. 7. Young's moduli in the three orthotropic principal directions versus bone volume fractions; $\alpha = 56/67$, $\beta = 73/134$; isotropic trabeculae with $E = 1$ [GPa], $\nu = 0.35$.

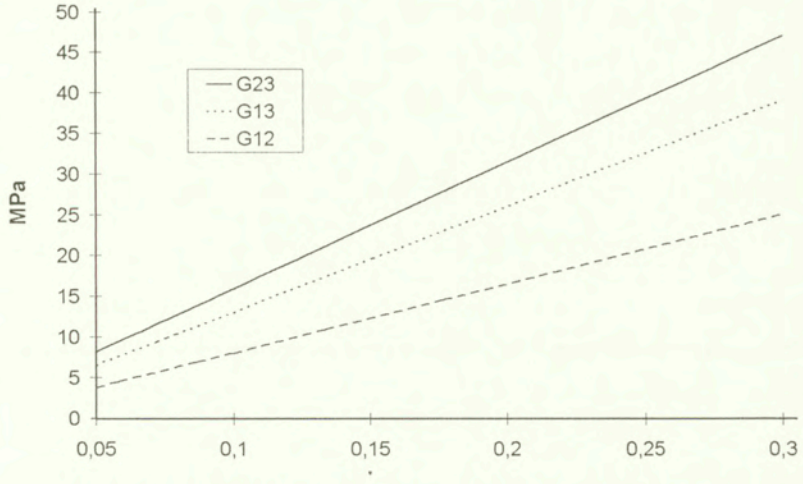

FIG. 8. Shear moduli in the three orthotropic principal directions versus bone volume fractions; $\alpha = 56/67$, $\beta = 73/134$; isotropic trabeculae with $E = 1$ [GPa], $\nu = 0.35$.

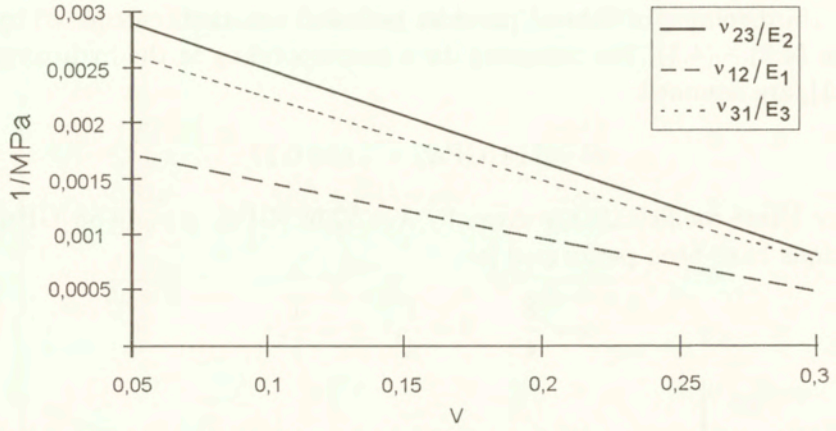

FIG. 9. Poisson's ratio divided by Young's moduli in the three orthotropic principal directions versus bone volume fraction; $\alpha = 56/67$, $\beta = 73/134$; isotropic trabeculae with $E = 1$ [GPa], $\nu = 0.35$.

The second column in Table 1 is taken from [16, Table 1].

Table 1. Technical constants

Technical constants (average)	human cortical bone	from (4.3) – (4.5) $E = 114$ [GPa], $\nu = 0.27$
E_1	11.7 (1.6) [GPa]	11.7 [GPa]
E_2	13.2 (1.8) [GPa]	14.4 [GPa]
E_3	19.8 (2.4) [GPa]	19.8 [GPa]
G_{12}	4.53 (0.37) [GPa]	1.1 [GPa]
G_{13}	5.61 (0.4) [GPa]	3.27 [GPa]
G_{23}	6.23 (0.48) [GPa]	4.36 [GPa]
ν_{12}	0.375 (0.095)	0.04
ν_{21}	0.416 (0.118)	0.03
ν_{23}	0.237 (0.083)	0.21
ν_{32}	0.346 (0.096)	0.15
ν_{13}	0.374 (0.108)	0.19
ν_{31}	0.234 (0.088)	0.11

Two further specific cases are summarized in the third and fourth column of Table 2. To calculate the moduli given in the third column of this table it was assumed that

$$\lambda = 52.69 \text{ [GPa]}, \qquad \mu = 44.88 \text{ [GPa]}, \qquad \alpha = \frac{56}{67},$$

$$\beta = \frac{73}{134}, \qquad v = 0.007.$$

Similarly, the moduli contained in the fourth column were calculated for the following data:

$$\lambda = 17.28 \text{ [GPa]}, \qquad \mu = 7.41 \text{ [GPa]}, \qquad \alpha = \frac{56}{67},$$

$$\beta = \frac{73}{134}, \qquad v = 0.043.$$

The second column of Table 2 is taken from [16, Table 1]. According to COWIN [9, Table 9], $E = 20$ [GPa] estimates the value of the elastic modulus of the wet human trabecula.

Table 2. Technical constants

Technical constants (average)	human cancellous bone (proximal tibia)	from (4.3) – (4.5) $E = 114$ [GPa], $\nu = 0.27$	from (4.3) – (4.5) $E = 20$ [GPa], $\nu = 0.35$
E_1	237 (63) [MPa]	496 [MPa]	545 [MPa]
E_2	309 (93) [MPa]	552 [MPa]	604 [Mpa]
E_3	823 (337) [MPa]	649 [MPa]	706 [MPa]
G_{12}	73 (0.37) [MPa]	73 [MPa]	73 [MPa]
G_{13}	112 (0.4) [MPa]	112 [MPa]	112 [MPa]
G_{23}	134 (0.48) [MPa]	134 [MPa]	134 [MPa]
ν_{12}	0.169 (0.304)	0.08	0.1
ν_{21}	0.209 (0.209)	0.07	0.09
ν_{23}	0.063 (0.217)	0.15	0.18
ν_{32}	0.245 (0.626)	0.11	0.14
ν_{13}	0.423 (0.356)	0.16	0.2
ν_{31}	0.145 (0.123)	0.14	0.17

We observe that the second column of Table 1 in [16], or the second column in our Table 1, present technical constants for specimens of human femoral cortical bone, where the 1-direction is radial, the 2-direction is circumferential and the 3-direction is longitudinal. The second column of Table 2 presents average technical constants for 9 specimens of human cancellous bone from the proximal tibia, where the 1-direction is anterior-posterior, the 2-direction is medial and 3-direction is logitudinal. In Tables 1 and 2 the numbers in parantheses stand for the standard deviations. The second column of Table 2 implies a possibility of appearance of negative values of Poisson's ratios. The plate-like architecture studied in the present paper precludes such possibility. Examples of cellular solids with negative Poisson's ratio are given in [23, 31]. Thus a natural question arises: can a trabecular bone, at a certain stage of human or animal life, behave like a cellular solid with negative Poisson's ratio? From the theoretical point of view, such possibility is obviously possible. The decisive answer, however, is to be expected from experimentalists.

We observe that according to Table 9 in [9], the value of E equal to 1.17 [GPa] characterises individual bovine trabeculae. This result was obtained by CHRISTENSEN (cf. [9]) using statistical data analysis. In Table 9 in [9] one also finds the following values of E [GPa] for individual trabeculae:

$E = 10.90 \pm 1.6$ (wet bovine femur, ultrasonic test method),

$E = 12.70 \pm 2$ (wet human femur, ultrasonic test method),

$E = 8.69 \pm 3.17$ (dry human distal femur, buckling test method),

$E = 5.3 \pm 2.6$ (dried human femur, experimental test method with finite element method).

According to Table 9 in [9], the estimates for the elastic modulus of the trabeculae of human cancellous bone vary from 1 to 20 [GPa]. Future research should be directed towards resolving this problem of great scatter of Young's moduli.

Table 3. Technical constants from (4.1) – (4.3)

Technical constants	$E = 1$ [GPa] $\nu = 0.35$ $\alpha = 0.836$ $\beta = 0.545$ $v = 0.1$	$E = 1$ [GPa] $\nu = 0.35$ $\alpha = 0.836$ $\beta = 0.545$ $v = 0.3$	$E = 5$ [GPa] $\nu = 0.3$ $\alpha = 0.9$ $\beta = 0.2$ $v = 0.2$	$E = 10$ [GPa] $\nu = 0.35$ $\alpha = 0.9$ $\beta = 0.2$ $v = 0,2$
E_1	0.0633 [GPa]	0.19 [GPa]	0.545 [GPa]	1.14 [GPa]
E_2	0.701 [GPa]	0.21 [GPa]	0.603 [GPa]	1.23 [GPa]
E_3	0.819 [GPa]	0.246 [GPa]	0.924 [GPa]	1.87 [GPa]
G_{23}	0.0156 [GPa]	0.0467 [GPa]	0.183 [GPa]	0.353 [GPa]
G_{13}	0.013 [GPa]	0.039 [GPa]	0.165 [GPa]	0.317 [GPa]
G_{12}	0.008 [GPa]	0.0254 [GPa]	0.0366 [GPa]	0.0705 [GPa]
ν_{23}	0.204	0.204	0.238	0.276
ν_{32}	0.175	0.175	0.156	0.182
ν_{12}	0.101	0.101	0.0164	0.0114
ν_{21}	0.0913	0.0913	0.0151	0.105
ν_{13}	0.184	0.184	0.232	0.269
ν_{31}	0.142	0.142	0.14	0.164

Figures 7–9 correspond to the data listed in the second and third column of Table 3.

Concluding remarks

The effective elastic moduli for a plate-like cellular solids were derived by using a mathematically rigorous homogenization approach. The solid considered is characterized by two small parameters: ϵ and η. The parameter η is related

to plates (trabeculae) thickness, cf. Fig. 6. The effective elasticity tensor is, in general, anisotropic. For $\alpha = \beta$ the macroscopic anisotropy is due to anisotropy of trabeculae. For $\alpha = \beta = 1$ and isotropic trabeculae the macroscopic elasticity tensor reveals the cubic symmetry (three material constants). If α is different from β and the trabeculae are isotropic, the macroscopic elasicity tensor is orthotropic. In Sec. 3 the basic cell was assumed to be given by (3.1). Unequal dimensions of this cell allong the three axes also influence the effective moduli.

In a separate paper we shall study the macroscopic behaviour of rod-like, trabecular bone. The first attempt was accomplished by us in [32].

Acknowledgement

The authors were supported by the State Committee for Scientific Research (Poland) through the grant No 8 T11F 018 12.

References

1. B. AOUBIZA, *Homogénéisation d'un composite multi-échelle: application à une modélisation numérique de l'os haversien compact*, Thèse, Université de Franche-Comté, 1991.
2. B. AOUBIZA and J.M. CROLET, A. MEUNIER, *On the mechanical characterization of compact bone structure using the homogenization theory*, J. Biomechanics, **29**, 1539–1547, 1996.
3. G.S. BEAUPRÉ and W.C. HAYES, *Finite element analysis of a three-dimensional opened-celled model for trabecular bone*, J. Biomech. Engng., **107**, 249–256, 1985.
4. M.P. BENDSØE, *Optimization of structural topology, shape, and material*, Springer-Verlag, Berlin 1995.
5. M.P. BENDSØE and N. KIKUCHI, *Generating optimal topologies in structural design using a homogenization method*, Comp. Mech. Appl. Mech. Enging. **71**, 192–224, 1988.
6. A. BENSOUSSAN, J.L. LIONS and G. PAPANICOULAOU, *Asymptotic analysis for periodic structures*, North-Holland, Amsterdam 1978.
7. D. CIORANESCU and J. SAINT JEAN PAULIN, *Reinforced and honey-comb structures*, J. Math. Pures Appl., **65**, 403–422, 1986.
8. D. CIORANESCU and J. SAINT JEANT PAULIN, *Asymptotic analysis of elastic wireworks*, Laboratoire d'analyse numérique, R89008, 1989.
9. S.C. COWIN, *The mechanical properties of cancellous bone* [in:] Bone mechanics, ed. by S.C. Cowin, pp. 129–157, CRC Press, Inc. Boca Raton, Florida 1989.
10. J.M. CROLET, *Homogenization: mathematical method applied to haversian cortical bone structure*, Proc. 1st World Congress of Biomechanics, 156–172, 1990.
11. J.M. CROLET, B. AOUBIZA and A. MEUNIER, *Compact bone: numerical simulation of mechanical characteristics*, J. Biomechanics, **26**, 677–687, 1993.
12. L.J. GIBSON, *The mechanical behaviour of cancellous bone*, J. Biomechanics, **18**, 317–328, 1985.
13. L.J. GIBSON and M.F. ASHBY, *Cellular solids: structure and properties*, Pergamon Press, New York 1988.

14. S.J. HOLLISTER, J.M. BRENNAN and N. KIKUCHI, *A homogenization sampling procedure for calculating trabecular bone effective stiffness and tissue level stress*, J. Biomechanics, **27**, 433–444, 1994.

15. S.J. HOLLISTER, D.P. FYHIRE, K.J. JEPSEN and S.A. GOLDSTEIN, *Application of homogenization theory to the study of trabecular bone mechanics*, J. Biomechanics, **24**, 825–839, 1991.

16. S. JEMIOŁO and J.J. TELEGA, *Fabric tensors in bone mechanics*, Engng. Trans., **46**, 3–26, 1998.

17. M. KASRA and M.D. GRYNPAS, *Static and dynamic finite element analyses of an idealized structural model of vertebral trabecular bone*, J. Biomech. Eng., **120**, 267–272, 1998.

18. R.V. KOHN and G. STRANG, *Optimal design and relaxation of variational problems*, I, II, III, Comm. Pure Appl. Math., **39**, 113–137, 139–182, 353–377, 1986.

19. T. LEWIŃSKI and J.J. TELEGA, Plates, Laminates and Shells: Asymptotic Analysis and Homogenization, World Scientific, in press.

20. G. LOWET, P. RÜEGSEGGER, H. WEINANS and A. MEUNIER [Eds], Bone Research in Biomechanics, IOS Press, Amsterdam 1997.

21. K.A. LURIE, A.V. FEDOROV and A.V. CHERKAEV, *Regularization of optimal design problems for bars and plates*, I and II, J. Opt. Theory Appl., **37**, 499–522, 523–543, 1982.

22. J. MCELHANEY, N. ALEM and V. ROBERTS, *A porous block model for cancellous bones*, ASME Publication No 70-WA/BHF-2, 1–9, 1970.

23. G.W. MILTON, *Composite materials with Poisson's ratio close to -1*, J. Mech. Phys. Solids, **40**, 1105–1137, 1992.

24. R. MÜLLER and P. RÜGSEGGER, *Micro-tomographic imaging for the nondestructive evaluation of trabecular bone architecture* [in:] Bone Research in Biomechanics, ed. by G. Lowet, P. Rüegsegger, H. Weinans and A. Meunier, pp. 61–79, IOS Press, Amsterdam 1997.

25. W. NOWACKI, *Elasticity theory* [in Polish], Państwowe Wydawnictwo Naukowe, Warszawa 1970.

26. W.M. PAYTEN, B. BEN-NISSAN and D.J. MERCER, *Optimal topology design using global self-organisational approach*, Int. J. Solids Structures, **35**, 219–237, 1998.

27. J.W. PUGH, R.M. ROSE and E.L. RADIN, *A structural model for the mechanical behavior of trabecular bone*, J. Biomechanics, **6**, 657–670, 1973.

28. E. SANCHEZ-PALENCIA, *Non- homogeneous media and vibration theory*, Springer-Verlag, Berlin 1980.

29. P.M. SUQUET, *Elements of homogenization theory for inelastic solid mechanics* [in:] Homogenization techniques for composite media, [Ed.] by E. Sanchez-Palencia and A. Zaoui, pp. 194–278, Springer-Verlag, Berlin 1985.

30. J.J. TELEGA and T. LEWIŃSKI, *A note on a saddle-point theorem in optimal compliance design*, [submitted.]

31. P.S. THEOCARIS, G.E. STAVROULAKISA and P.D. PANAGIOTOPOULOS, *Negative Poisson's ratio in composites with star-shaped inclusions: a numerical homogenization approach*, Arch. Appl. Mech., **67**, 274–286, 1997.

32. S. TOKARZEWSKI, A. GAŁKA and J.J. TELEGA, *Cancellous bone as a cellular solid: the determination of effective material properties* [Polish] [in:] Proc. of the Conf. on Biomechanics: Modelling, Computational Methods, Experiments and Biomedical Applications, [Ed.] by J. AWRAJCEWICZ, M. CIACH and M. KLEIBER, pp. 191–196, Technical University of Łódź 1998.

33. D. ULRICH, T. HILDEBRAND, B. van RIETBERGEN, R. MÜLLER and P. RÜEGSEGGER, *The quality of trabecular bone evaluated with micro-computed tomography, FEA and mechanical testing*, [in:] Bone research in biomechanics, [Ed.] by G. LOVET, P. RÜEGSEGGER, H. WEINANS and A. MEUNIER, pp. 97–112, IOS Press, Amsterdam 1997.

34. J.L. WILLIAMS and J.L. LEWIS, *Properties and anisotropic model of cancellous bone from the proximal tibia epiphysis*, J. Biomech. Engng., **104**, 50–56, 1982.

35. P.K. ZYSSET, R.W. GOULET and S.J. HOLLISTER, *A global relationship between trabecular bone morphology and homogenized elasic properties*, J. Biomech. Eng., **120**, 640–646, 1998.

Received January 14, 1999; revised version March 26, 1999.

Arch. Mech., **51**, 3–4, pp. 357–390, Warszawa 1999

Ratcheting and constitutive patterns of rate-form defined in Preferred Reference Frames

Dedicated to the legacy of W. Ślebodziński as a token of scientific gratitude

P. GUELIN [1], W.K. NOWACKI [2], D. QUEREYRON [1] and A. TOURABI [1]

[1] *Laboratoire Sols, Solides, Structures, Grenoble*
e-mail: Ali.Tourabi@hmg.fr

[2] *Institute of Fundamental Technological Research, Warsaw*
e-mail: wnowacki@ippt.gov.pl

A PATTERN of Rate Form allowing the modelling of the thermomechanical features of the cyclic plasticity has proved to be effective in order to take into account various isotropic behaviours, ranging from those of granular media exhibiting isotropic-deviatoric coupling effects, to those distinguished by shape memory effects or ferrohysteresis ([1] to [8]). Under its basic form, of pure hysteresis type, this discrete memory pattern is able, by definition of a formalism brought into play in the fixed frame and in the A.A. Iliushin space of stress, to describe the behaviour involving perfectly closed cycles. Owing to this fact, it is also unable, in its basic form, to take into account second order effects such as those of multiaxial effects of ratchet type. In order to introduce a well founded and straightforward approach to the continuum thermomechanics of the isotropic solid-like inelastic behaviours, *including* rate-independent and hardening-independent *second order* tensorial coupling effects of *ratchet* type, a new approach is introduced. It is founded on the following assumptions: firstly, the formalism of the initial pattern is not modified, maintaining its role in the A.A. Iliushin spaces of stress and strain (of power and geometry); secondly, the unaltered initial formalism is no longer brought into play in the fixed frame and works now in the Preferred Reference Frame (PRF); thirdly, the definition of this PRF is basically thermomechanical and may be dependent on a mesoscale of Nél-Krumhansl type. The formalism of the general multiaxial isotropic case is introduced and the approach is shown to be straightforward even when the pattern is (easily) generalized to the viscoelastoplastic case. It is shown that the usual multiaxial effect of ratchet type obtained through cyclic torsion is not necessarily hardening-dependent and is existing under zero axial load, in accordance with experimental evidence.

Notations

$(\mathbf{0}, \mathbf{e}_i)$	orthonormal fixed reference frame ($i = 1, 2, 3$),
t	absolute time,
$\bullet$ or $\partial/\partial t$	partial time derivative, the only time derivative which is implemented,
$M(x^k)$	material point of invariant convected co-ordinates x^k, (following the old-fashioned classical terminology of J.A. Schouten type, the x^k are the dragged along co-ordinates),
$(M, \mathbf{H}_i)$	initial ($t = 0$) field of orthonormal Preferred Reference Frame (PRF),
$(M, \mathbf{h}_i)$	current ($t > 0$) field of PRF,
$(M, \mathbf{G}_i)$	initial ($t = 0$) field of Convected Reference Frame (DARF),
$(M, \mathbf{g}_i)$	current ($t > 0$) field of DARF,
$\mathbf{OP}(M, 0)$	initial position vector of $M(x^k)$ in $(O, \mathbf{e}_i)$,
$\mathbf{Op}(M, t)$	current position vector of $M(x^k)$ in $(O, \mathbf{e}_i)$,
$Z_i(M)$	components of $\mathbf{OP}$ in $(O, \mathbf{e}_i)$,
$z_i(M, t)$	components of $\mathbf{Op}$ in $(O, \mathbf{e}_i)$,
$x_i(M)$	invariant co-ordinates of M in the convected co-ordinate system defined at $t = 0$,
$\mathbf{G}, g_{ii}, g$	current metric tensor and associated covariant components and determinant,
$\rho(M, t)$	current specific mass ($\rho\sqrt{g} =$ constant masse at M),
$\mathbf{V}(M, t)$	current velocity vector defined in $(O, \mathbf{e}_i)$ ($\mathbf{e}_i V_i = \mathbf{e}_i \partial z_i/\partial t = \partial\, \mathbf{Op}/\partial t$),
$\nu^i, \nu_i(M, t)$	current components of $\mathbf{V}$ expressed in the DARF at M,
Lv	generic symbol of the four Lie derivatives: L .. , L ·· , L · · , L · · ,
$\nu, \mathbf{N}$	relative and absolute normal vector ($Lv\nu = 0$; N $\mathbf{N} \cdot \mathbf{N} = 1$),
$\mathbf{D}(M, t)$	current strain rate tensor of $M(2D_{ij} = \partial g_{ij}/\partial t = Lv..g_{ij} = \nabla_j \nu_i + \nabla_i \nu_j)$,
$T(M, t)$	current absolute temperature of the material point $M(x^k)$,
$\mathbf{D}_T(M, t)$	strain rate associated with the usual (isotropic) thermal dilatation $\mathbf{D}_T = \alpha(T)\dot{T}\mathbf{G}$,
$K_n(M, t)$	current stretches along $\mathbf{e}_n$ for the material point $M(x^k)$,
$J_n(t)$	$1 + K_n(M, t)$,
$\gamma_1, \gamma_2, \gamma_3$	current shears in the directions of $\mathbf{e}_3, \mathbf{e}_1, \mathbf{e}_2$ for the material point $M(x^k)$,
$\mathbf{d}_n(M, t)$	current unit vectors of the principal directions (PPD) of $\mathbf{D}$, resulting in an orthonormal frame $(M, \mathbf{d}_n(M, t))$,
$\mathbf{I}_\phi(M, t)$	current inertia-like tensor of the material point $M(x^k)$,
$\mathbf{i}_n(M, t)$	current unit vectors of the PPD of $\mathbf{I}_\phi$,, resulting in the frame $(M, \mathbf{i}_n(M, t))$,
$\psi_\delta, \theta_\delta, \phi_\delta$	current Euler's angles (precession, nutation and proper rotation) of $(M, \mathbf{d}_n(M, t))$,
$\psi_\phi, \theta_\phi, \phi_\phi$	current Euler's angles (precession, nutation and proper rotation) of $(M, \mathbf{i}_n(M, t))$,
$\Omega_\delta, \Omega_\phi$	current angular velocity pseudo-vectors in $(0, \mathbf{e}_i)$ of $(M, \mathbf{d}_n(M, t))$ and $(M, \mathbf{i}_n(M, t))$,
$\Omega(M, t)$	current angular velocity pseudo-vector in $(0, \mathbf{e}_i)$ of the PRF,
$\dot{\alpha}_\delta(M, t)$	scalar used instead of Ω_δ in the special simple kinematics with only one shear γ_3,

$\dot{\theta}_\phi(M,t)$ scalar used instead of Ω_ϕ in the special simple kinematics with only one shear γ_3,

$\dot{\alpha}(M,t)$ scalar used instead of Ω in the special simple kinematics with only one shear γ_3,

${}^t_R\mathbf{G}$ current Cauchy strain tensor convected from $t_R < t$ to the current state at t,

$\Delta^t_R\varepsilon$ current Almansi strain tensor defined as the $\mathbf{G}$ variation $\Delta^t_R\varepsilon = (\mathbf{G} - {}^t_R\mathbf{G})/2$ on $]t_R, t]$,

$\mathbf{S}, \sigma(M,t)$ current Cauchy stress tensor ($\sigma = \mathbf{S}\sqrt{g}$),

${}^t_R\mathbf{S}, {}^t_R\sigma$ current Cauchy stress tensor convected from $t_R < t$ to the current state at t,

$\Delta^t_R\mathbf{S}$ current "variation" stress tensor defined as the $\mathbf{S}$ variation $\mathbf{S} - {}^t_R\mathbf{S}$ on $[t_R, t]$,

$\overline{\mathbf{S}}, \mathrm{I_s}, \overline{\mathrm{II}}_\mathrm{s}, \overline{\mathrm{III}}_\mathrm{s}$ deviator of $\mathbf{S}$, trace of $\mathbf{S}$, trace of $(\mathrm{tr}\overline{\mathbf{S}}^2)/2$, trace of $(\mathrm{tr}\overline{\mathbf{S}}^3)/3$, respectively,

$\hat{P}_i, P_i, p_i$ current internal power received by M per unit extent of x^k, of volume, of mass, respectively ($\hat{P}_i = P_i\sqrt{g} = p_i\rho\sqrt{g}$; $P_i(M,t) = \rho(M,t)p_i(M,t)$),

$\hat{\Pi}_i, \Pi, \pi$ current reversible power received by M,

$\hat{\Phi}, \Phi, \phi$ current intrinsic dissipation received by M ($\Phi = -P_i - \Pi$; etc.),

$\hat{E}, E, e$ current internal energy received by M,

$\hat{Q}_i, Q_b, q_i$ current internal intrinsic heat supply received by M,

$\hat{Q}_e, Q_e, q_e$ current reversible heat supply received by M (Q_{ek} for Kelvin effect),

$\hat{K}, K, k$ current kinetic energy received by M,

S_0 limit stress of the Huber-von Mises criterion $\overline{II}_s = S_0^2$ (associated cylinder of radius $Q_0 = \sqrt{2}S_0$),

λ, μ Lamé parameters or similar parameters,

θ_ν relaxation time parameter of the Oldroyd pattern,

η_1, η_2 viscosity parameters of the Oldroyd pattern,

$\overset{\mathrm{def}}{=}$ equality giving a definition,

$\overset{\mathrm{ident}}{=}$ identity,

δ_{ij} Kronecker delta,

ε_{ijk} relative alternator ($e_{ijk} = \sqrt{g}\varepsilon_{ijk}$),

1. Introduction

THE MAIN RESTRICTIVE assumptions of the study are as follows:

1. The behaviour of the material is supposed to be *isotropic*.

2. *Fatigue* effects as well as ageing effects are neglected.

3. Rate-independent hardening effects are neglected for the sake of simplicity, in spite of the fact that they can be taken into account, to a great extent, through an effective modelling defined previously [4].

4. Rate-dependent hardening effects are taken into account through a thermomechanical modelling which have proved to be effective in the case of a solid polymer [14].

5. The temperature is supposed to be constant for the sake of simplicity, but it is worth noting that the temperature-dependent case can be taken into account through effective modelling, including the cases of shape memory effects and of thermomechanical coupling effects [4, 14].

6. The limit plastic behaviour of the material is supposed to be of Huber – von Mises type for the sake of simplicity, but the Coulomb-like case has been previously taken into account through effective modelling able to describe the isotropic-deviatoric coupling effects exhibited by granular materials [5].

7. The cyclic loading paths which are actually considered in this preliminary paper are "rather simple", namely *not* of demagnetization type [7]. Owing to the above restrictive assumptions, the study is devoted mainly to a simultaneous modelling of the first and second order effects which are specific of the (elastoplastic) *pure hysteresis* solid behaviour [1, 3] in the isothermal, isotropic and without hardening case (cf. Fig. 1a). Moreover, the definition of a rate-dependent thermomechanical modelling is up to now introduced (cf. Fig. 1b, d) in order to compare the theory with thermomechanical experimental results obtained through the study of a solid polymer [14].

It is possibly useful to give some hints concerning some of the features of the presentation. First, the study is mainly confined to the case of shear-type kinematics, a feature which may suggest that one neglects the use of the classical way, going from a general framework to a special case, or conversely. This feature of the presentation is connected with the fact that the case of *rotational* kinematics is, in essence, the only one which is of fundamental *theoretical* interest in the framework of the proposed approach. On the contrary, in the framework of this approach, the case of irrotational kinematics, of course being of a fundamental *technological* interest, may be investigated (in the isotropic case) through a much simpler study than that of the rotational case.

Second, the (idealized) homogeneous kinematics is the only one introduced in the study, giving *only* the opportunity to define some extremely special initial-value problems. Moreover, with regard to the matter of the Lagrangian-Eulerian dilemma, the approach is old-fashioned for it follows the line of LODGE [15]. Consequently, a feeling of doubt may arise concerning the effectiveness of such an approach with respect to the matter of boundary-value problem. It is worth noting that a comprehensive study of implicit numerical strategies has been given elsewhere, concerning the step-by-step advancement of quasi-static elastic-plastic solutions of large size problems discretized through finite elements such as, for example, notched bar problems, plate with hole problems, necking problems with shear-band localization and shell problems [16 to 21].

Third, this preliminary paper does not provide any hints concerning a *comparison* between our proposal and the set of current approaches to cyclic plasticity and ratchetting effects. On the one hand, it is well known that many papers

on cyclic plasticity appear every year. On the other hand, it is worth noting that one of the most impressive efforts ever achieved in the field of fundamental technological research based on continuum mechanics, has been indeed applied to the matter of (quasi-isothermal) second order effects of ratchetting type (see Fig. 7 of [22] and [23 to 25]). Consequently, it should be useful to give, in a concise form, a clue allowing to imagine the sketch of the comparison mentioned above. In order to be concise, it is convenient to avoid the introduction of various theoretical elements concerning the notions of reference frame $(0, \mathbf{e}_i)$ [26], of motion $z^i(M(x^k), t)$, of current metric tensor $\mathbf{G}(M(x^k), t)$, of current strain tensor $\Delta^t_R\boldsymbol{\varepsilon}(M(x^k), t)$, of current strain rate tensor $\mathbf{D}(M(x^k), t)$ and of discrete memory of a previously selected metric tensor (Cauchy tensor ${}^t_R\mathbf{G}$), and of a previously selected stress tensor (owing to [27] let us say the "Ślebodzinski-Cauchy" tensor ${}^t_R\mathbf{S}$). Secondly, it is also convenient to make use of the fact that the various approaches of Armstrong-Frederick-Ohno-Wang type are well known. Hence the introduction of the following elements allowing a comparison between the proposed pattern and the usual set of theories:

(1) The *strain rate* tensor $\mathbf{D}$ involved in the constitutive pattern of irreversible behaviour is implemented without the aid of some splitting up (of $\mathbf{D}^e + \mathbf{D}^p$ type).

(2) From (1) it follows that the hardening notion is not involved *before* the definition of a hardening-independent and rate-independent basic behaviour (pure hysteresis [1 to 3]) which is *always* irreversible, independly of how small are the cycle amplitudes of the loading-unloading cyclic path. With the aid of this basic theory, the effects of transient rate-independent hardening and of rate-dependent hardening are more easily distinguished and classified.

(3) Following Gibbs (plasticity cannot be described in the framework of the thermostatics), one drops the idea of some "T.I.P.- like" generalization of classical thermodynamics.

(4) Following the old-fashioned sketch of Prager allowing continuous transition between quasi-elasticity to quasi-perfect plasticity, the basic classical notions involved in the pure hysteresis pattern are *only* those of infinitesimal Hookean behaviour and of *single* limit surface of plasticity. Moreover, owing to the fact that manufacturing processes often involve large strains and large temperature variations on which depends the future material behaviour, the theory must be, from the outset, defined in the finite strain form.

(5) From (3) and (4), the current Cauchy stress tensor $\mathbf{S}(M(x^k), t)$ of the material point M is the only stress tensor involved in the constitutive definition and, owing to the *perfectly closed cycle* problem, one admits the use of

$$ {}^t_R\mathbf{S} = \mathbf{S}(t_R) \qquad t_R < t; \qquad \text{rate of } {}^t_R\mathbf{S} = 0, $$

an assumption involving the use of $\Delta^t_R\mathbf{S} = \mathbf{S} - {}^t_R\mathbf{S}$ and of rate of $\Delta^t_R\mathbf{S}$ equal to the rate of $\mathbf{S}$ along a branch of cycle. Consequently, the use of the *discrete*

memory notion is accepted, as well as the implementation of differential-difference equations in which the delay ${}^{t}_{R}\mathbf{S}$ is a piecewise constant (tensorial) functional of the loading history.

(6) From (1) to (5), the pattern cannot be based mainly on differential-difference equations specific to a given material. It must be founded, to a great extent, on general rules involving explicitly both several ordered discrete sets of pure scalars and the *intrinsic dissipation functional Φ of discrete memory form.* Thereby a process is allowed of *comparison* between elements of ordered discrete sets of energy levels or, still better, between elements of ordered discrete sets of intensities of rates of Φ.

(7) From (5) and (6), the pattern is rate-form and the *stress rate* definition is a basic issue. Hence the role of Preferred Reference Frames.

(8) The generalization to second order effects must make invariant the basic ingredients of the first order pattern.

(9) The implementation of Preferred Reference Frames is accepted as relevant [3].

Fourth, a comment may be useful regarding the "rather simple loading path" restrictive assumption. It means that the features of the ratchet effect during demagnetization-like cyclic loading processes is not studied in this paper. This is the main theoretical gap of the study, because the proposed approach already covers, in the three-dimensional case, the first order effects of plastic hysteresis and of ferrohysteresis including application to electromechanical coupling effects [28 – 30]. Owing to this gap, it should be useful to find some clues in the field of the current ferrohysteretic modelling.

However, the *three-dimensional first order* effects of ferrohysteresis, including the intricate case of demagnetization processes, remain difficult to describe through the usual non-mechanical approaches [31 to 35]. Hence the difficulty to find from now on, concerning *second order effects involved in three-dimensional* situations, some useful clues in order to guide the study to come.

1.1. From a constitutive pattern of the first order effects to taking into account the second order effects

Up to now, only simple hints have been given about the Preferred Reference Frame definition (cf. [6], Sec. 3.3, 3.5.4. and Fig. 16, for example). This definition seems to provide an effective and rather general theory in order to deal with the problem of a *simultaneous* treatment of the first order behaviour and of the second order effects. Consequently, it is useful to give immediately a short reminder concerning the treatment of the first order effects (such as those involved in the field of multiaxial cyclic plasticity and viscoelastoplasticity). Then, it will be easy to state how it is possible, with the aid of the relevant PRF, to take into

account the second order ratchet effects. At first, the two-fold foundation of the initial constitutive modelling is suggested (Sec.1.2). Next, some simple intuitive hints (Sec. 1.3) are given regarding the modelling of the second order effects.

1.2. From stress splitting approach and preponderant role of the pure hysteresis stress contribution to the associated viscoelastoplastic theory

1.2.1. A clue of special interest is as follows: *owing to the status of the strain rate notion and to experimental evidences (at microscopic and at macroscopic scale), it is not reasonable to introduce a splitting process of this tensor (cf. [6], Sec. 2.1); consequently, the first assumption which must be introduced in order to respect the thermodynamical distinction between reversibility and irreversibility, is that of a splitting up of the* **stress**. Let us suppose that (cf. Figs. 1, 2):

$$\mathbf{S} \overset{\text{def}}{=} \mathbf{S}_a + \mathbf{S}_\nu + \mathbf{S}_r; \qquad P \overset{\text{def}}{=} P_a + P_\nu + P_r, \tag{1.1}$$

so that the internal powers associated with an *always irreversible* process, with a viscous-viscoelastic process and with the *reversible* (elastic) process, are respectively:

$$P_a \overset{\text{ident}}{=} \hat{P}_a/\sqrt{g} \overset{\text{def}}{=} -\operatorname{tr}(\mathbf{S}_a\mathbf{D});$$

$$P_\nu \overset{\text{ident}}{=} \hat{P}_\nu/\sqrt{g} \overset{\text{def}}{=} -\operatorname{tr}(\mathbf{S}_\nu\mathbf{D});$$

$$P_r \overset{\text{ident}}{=} \hat{P}_r/\sqrt{g} \overset{\text{def}}{=} -\operatorname{tr}(\mathbf{S}_r\mathbf{D}).$$

Then we postulate the following associated splitting:

$$\dot{E} = \left[-P_a + \dot{Q}_{ia}\right] + \left[-P_\nu + \dot{Q}_{i\nu}\right] + \left[-P_r + \dot{Q}_{ek}\right],$$

$$\dot{E} = (\Pi_a - P_r) + \cancel{I_a} + \cancel{I_\nu} + \cancel{Q_{ek}}),$$

of the first principle and of the fundamental equation of Gibbs. Note that the internal intrinsic rate of heat supply has a non-viscous part $\dot{Q}_{ia}$ which is completely non-classical [1]. This splitting allows to preserve the role of the fundamental equation of Gibbs, namely the role of a hinge between the first principle and its "entropic" form. Such a formalism results indeed in the following equations of rate form:

$$\Phi \overset{\text{def}}{=} \Phi_a + \Phi_\nu = (\dot{I}_a + \dot{I}_\nu) + (-\dot{Q}_{ia} - \dot{Q}_{i\nu})$$

$$= -P - (\Pi_a - P_r) = (-P_a - \Pi_a) - P_\nu.$$

The main implicit equations of the rate form of the stress splitting approach (1.1) are:

$$\dot{E}_a = -P_a + \dot{Q}_{ia}, \qquad \dot{E}_a = \Pi_a + \dot{I}_a,$$

$$\dot{E}_\nu = -P_\nu + \dot{Q}_{i\nu}, \qquad \dot{E}_\nu = 0 + \dot{I}_\nu, \tag{1.2}$$

$$\dot{E}_r = -P_r + \dot{Q}_{ek}, \qquad \dot{E}_r = -P_r + 0 + \dot{Q}_{ek},$$

and

$$\dot{\mathbf{S}} = \dot{\mathbf{S}}_v + \dot{\mathbf{S}}_r + \dot{S}_a; \qquad \dot{\mathbf{S}}_c(M,t) = \mathbf{f}_c(\mathbf{D}(M,t), ...); \tag{1.3}$$

$$\mathbf{S}_c(M,0) = 0; \qquad c = v, r, a.$$

Let us suppose that the explicit forms of the reversible stress rate $\dot{S}_r$ and of the pure hysteresis stress rate $\dot{S}_a$ are well defined. Then, the above stress splitting approach becomes obviously a strongly constraining approach. The only remaining "degree of freedom" of the modelling is that concerning the viscous stress contribution. Consequently, the whole theory is not flexible and has two fundamental epistemological advantages: firstly, it may be easily invalidated through some experimental evidence; secondly, the definitions of the explicit forms of viscous type are almost necessarily simple and straightforward as regards the physical readings of the formalism.

Let us consider that a promising modelling may be founded on the most effective viscoelastic modelling currently available, namely that of Oldroyd. One obtains immediately the one-dimensional purely mechanical pattern of the form:

$$S_\nu \overset{\text{def}}{=} S_1 + S_2; \qquad S_2 \overset{\text{def}}{=} \eta_2 D; \qquad S_1/(\theta_\nu \mu_1) + \dot{S}_1/\mu_1 \overset{\text{def}}{=} D$$

and an associated global mechanical rate form:

$$\theta_\nu \dot{S}_\nu + S_\nu = (\eta_1 + \eta_2) D + \theta_\nu \eta_2 \dot{D}, \tag{1.4}$$

which is easily generalized to the tensorial case (Sec. 3.1). It is then obvious that the associated itemized thermodynamical forms are:

$$\dot{E}_2 = 0; \qquad -\dot{Q}_2 = S_2 D = \eta_2 D^2,$$

$$\dot{E}_1 = S_1(\dot{S}_1/\mu_1) = (\theta_\nu/\eta_1)(S_\nu - S_2)(\dot{S}_\nu - \dot{S}_2);$$

$$-\dot{Q}_1 = S_1(S_1/\mu_1) = (1/\eta_1)(S_\nu - S_2)^2,$$

resulting in the global forms:

$$m\dot{E}_\nu = (\theta_\nu/\eta_1)(S_\nu - \eta_2 D)(\dot{S}_\nu - \eta_2 \dot{D}); \tag{1.5}$$

$$-\dot{Q}_\nu = (1/\eta_1)(S_\nu - \eta_2 D)^2 + \eta_2 D^2.$$

Consequently, the set of basic forms defining the viscoelastoplastic theory involves, regarding the viscous features, a tensorial generalized split into its isotropic and deviatoric parts:

$$\dot{E}_\nu = \dot{E}_{\nu 0} + \dot{E}_{\nu d}, \qquad \dot{Q}_\nu = \dot{Q}_{\nu 0} + \dot{Q}_{\nu d},$$

with

$$\begin{aligned} \dot{E}_{\nu d} &= (\theta_\nu / 2\eta_{\delta 1})\mathrm{tr}(\overline{S}_\nu - 2\eta_{\delta 2}\overline{D})(\dot{\overline{S}}_\nu - 2\eta_{\delta 2}\dot{\overline{D}}) \\ -\dot{Q}_{\nu d} &= (1/2\eta_{\delta 1})\mathrm{tr}(\overline{S}_\nu - 2\eta_{\delta s}\overline{D})^2 + 2\eta_{\delta 2}\mathrm{tr}\overline{D}^2, \end{aligned} \tag{1.6}$$

and

$$\begin{aligned} \dot{E}_{\nu 0} = (\theta_\nu/3)[1/(3\eta_{01} + 2\eta_{\delta 1})][I_\nu - (3\eta_{02} + 2\eta_{\delta 2})][\dot{I}_\nu \\ -(3\eta_{02} + 2\eta_{\delta 2})\dot{I}_D, \end{aligned}$$

$$\begin{aligned} -\dot{Q}_{\nu 0} = (1/3)[1/(3\eta_{01} + 2\eta_{\delta 1})][I_\nu - (3\eta_{02} + 2\eta_{\delta 2})I_D]^2 \\ +(1/3)(3\eta_{02} + 2\eta_{\delta 2})I_D^2. \end{aligned} \tag{1.7}$$

Regarding the pure hysteresis contribution one has always the thermomechanical equations:

$$\begin{aligned} \omega\dot{E}_a &= -\omega P_{ia} - \Phi_a + C_a; \qquad -\omega\dot{Q}_a = \Phi + C_a; \qquad \omega = 1 \text{ or } 2; \\ -P_{ia} &= S_a D; \qquad C_a \approx \dot{S}_a \Delta_R^t G, \qquad {}^t_R\dot{S}_a = 0; \\ \Delta_R^t \dot{S}_a &= \dot{S}_a = \mu_r D + \beta\Phi_a \Delta_R^t S_a; \\ \beta &\approx -2\mu/(\omega Q_0)^2; \qquad \Phi_a = \Delta_R^t S_a D, \end{aligned}$$

but the tensorial generalizations of Φ_a, of C_a and of the mechanical rate form giving $\dot{S}_a$, already suggested elsewhere (cf. [6], Sec. 3.5.1, for example), cannot be easily recalled in a comprehensive form in the present short section (cf. Sec. 3.2).

A heuristic illustration may be obtained through the one-dimensional numerical simulation of a viscoelastoplastic cyclic behaviour. This illustration is inspired by the famous experimental study of MADELUNG [9]. More exactly, the qualitative modelling regards the results obtained by Madelung at relatively moderate rates and exhibiting therefore moderate viscous effects. The parameters of the pure hysteresis stress contribution (Fig. 1a) are: $\mu = 150$ GPa and $S_o = 200$ MPa. Those concerning the viscous effects (Fig. 1b) are: $\eta_1 = \eta_2 = 100$ GPa s, $\theta_\nu = 100$ s. The reversible pattern (Fig. 1c) is of power type (cf. Sec. 3.1) in order to obtain the qualitative features of ferrohysteresis (Fig. 1d). The rates $\dot{E}_a, \dot{E}_\nu, -\dot{Q}_a, -\dot{Q}_\nu$ are shown in Fig. 2 (parts a, b, c, d, respectively).

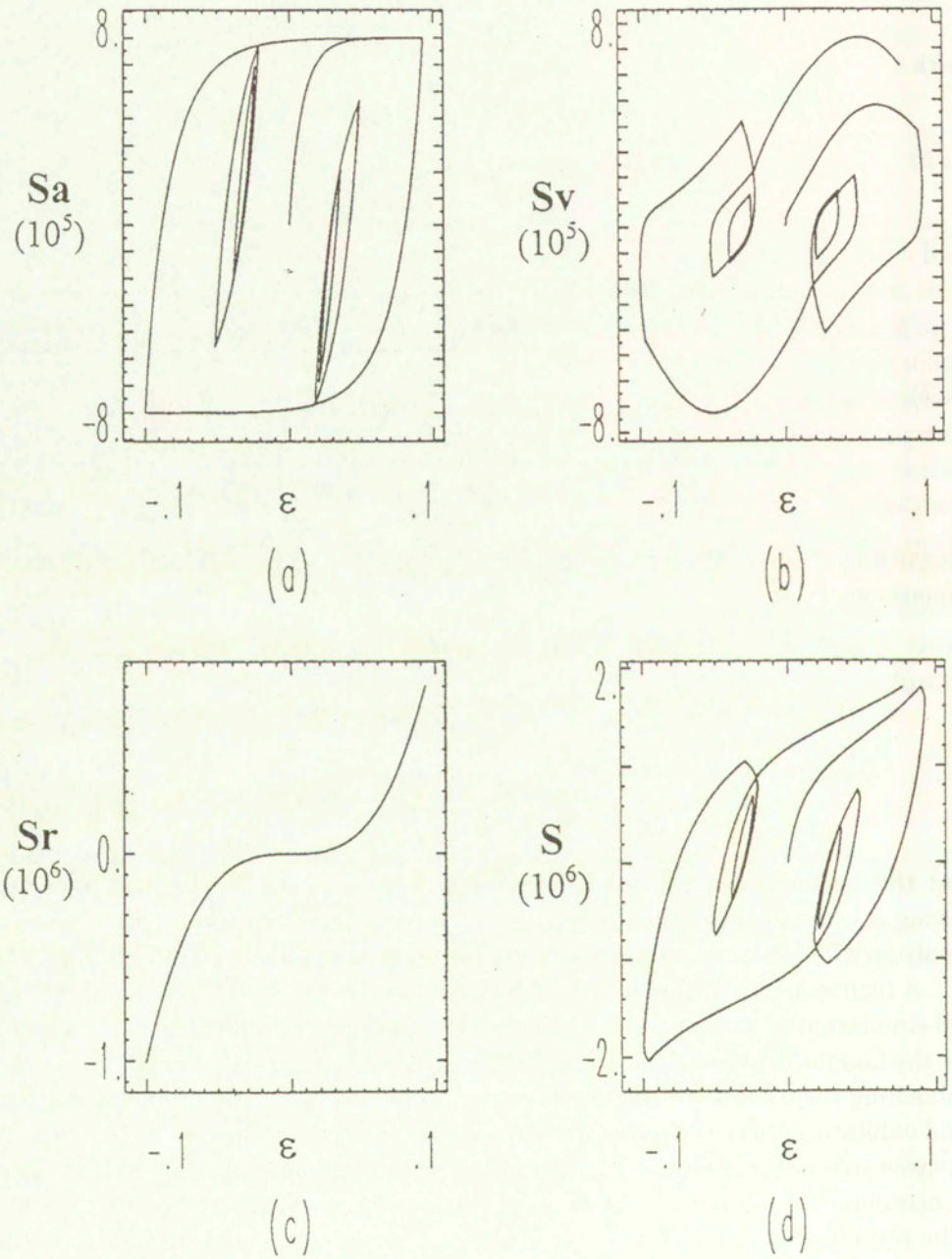

FIG. 1. The stress splitting approach: mechanical sketch.

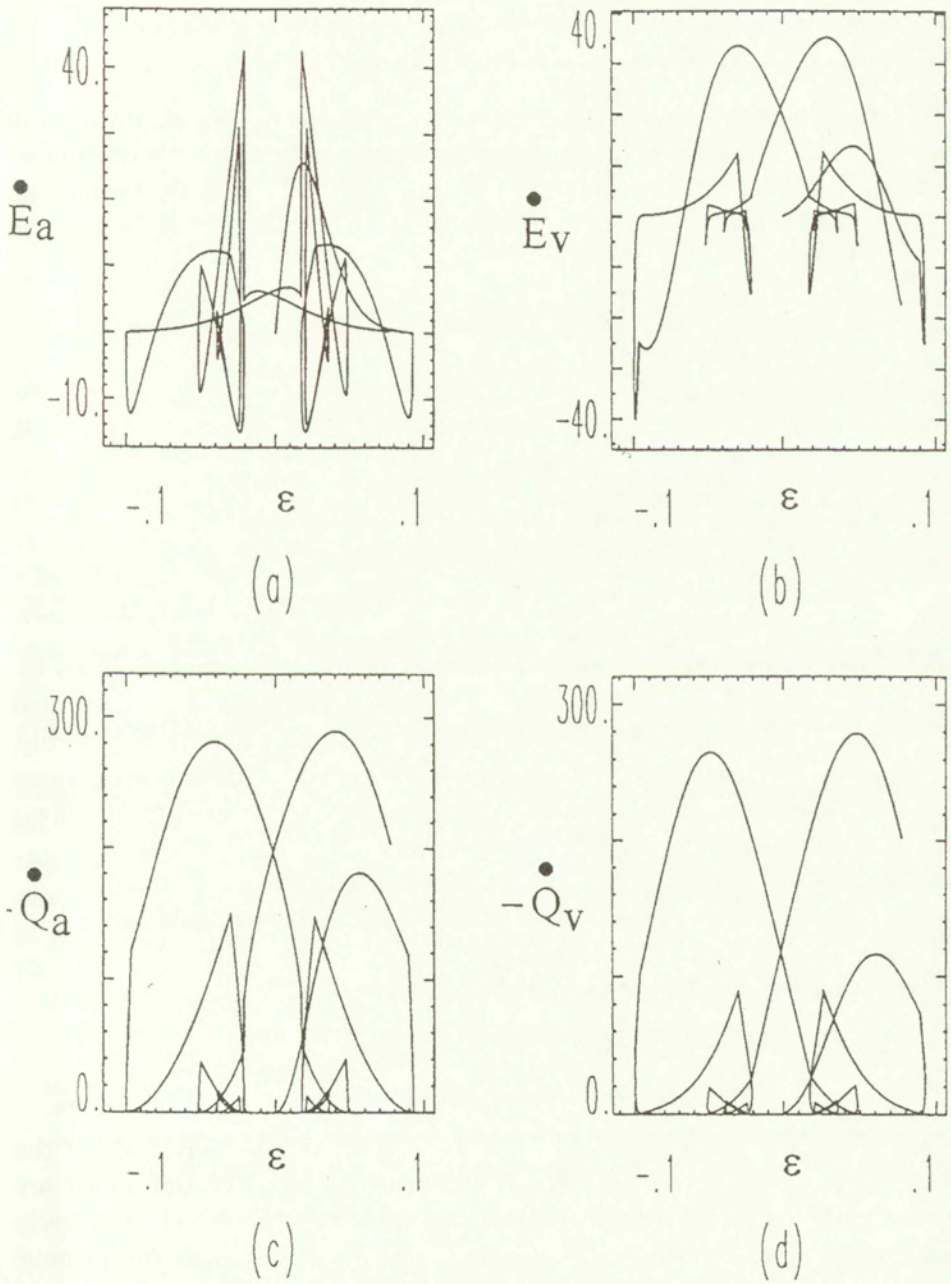

FIG. 2. The stress splitting approach: thermomechanical sketch.

1.2.2. *The preponderant role of the pure hysteresis stress contribution* $\mathbf{S}_a$ has been suggested previously (cf. [1] to [8], particularly in [6] and [7]). It is made conspicuous through the above illustration.

1.3. Short reminder intending to suggest the modelling through the heuristic case of the rotational triaxial kinematics with only one shear

1.3.1. Let us consider one of the three stress contributions $\mathbf{S}_r$, $\mathbf{S}_\nu$, $\mathbf{S}_a$ involved in the splitting of the actual stress $\mathbf{S}$. For the sake of formal simplicity it is convenient and not restrictive to choose the reversible contribution $\mathbf{S}_r$ in a Hookean form. The obvious generalization of the thermomechanical definition of $\mathbf{S}_r$ is done "in the PRF", namely

$$[\partial S_r^{ij}/\partial t]\mathbf{hr}_i \otimes \mathbf{hr}_j \stackrel{\text{def}}{=} Br^{ij}\mathbf{hr}_i \otimes \mathbf{hr}_j = \mathbf{Br};$$

$$Br^{ij} = \lambda_r I_d \delta^{ij} + 2\mu_r D^{ij}; \qquad \dot{Q}_r \stackrel{\text{def}}{=} 0,$$

$$\dot{E}_r \stackrel{\text{def}}{=} \operatorname{tr}(\mathbf{SD}) = (1/3)I_{sr}I_d + \overline{S}_r^{ij}\overline{D}^{ij}$$

$$= (1/3)[1/(3\lambda_r + 2\mu_r)]I_{sr}\dot{I}_{sr} + (1/2\mu_r)\overline{S}_r^{ij}\dot{\overline{S}}_r.$$

It is formally similar to the infinitesimal Hookean form, except that it implies firstly, a time derivative in the PRF, secondly, an appropriate definition – presented below – of the base vectors $\mathbf{hr}_n(x^k, t)$ at the material point $M(x^k)$ and thirdly, no energetical drawbacks (cf. [10], for example). One of the obvious consequences of the new constitutive definition is that its expression in the fixed frame $(0, \mathbf{e}_i)$ involves a complementary term $[\Sigma_r]$. Starting from

$$\partial S_r/\partial t \stackrel{\text{ident}}{=} \partial\left[\Sigma_r^{kl}\mathbf{e}_k \otimes \mathbf{e}_l\right]/\partial t \stackrel{\text{ident}}{=} \partial\left[S_r^{kl}\mathbf{hr}_i \otimes \mathbf{hr}_j\right]/\partial t$$

and substituting the above stress rate definition, one obtains:

$$\dot{\Sigma}_r^{kl}\mathbf{e}_k \otimes \mathbf{e}_l = B_r^{ij}\mathbf{hr}_i \otimes \mathbf{hr}_j + [\mathbf{\Sigma}_r] = B_r^{kl}\mathbf{e}_k \otimes \mathbf{e}_l + [\mathbf{\Sigma}_r],$$

$$[\mathbf{\Sigma}_r] = S_r^{ij}(\Sigma_r^{kl})(\dot{\mathbf{hr}}_i \otimes \mathbf{hr}_j + \mathbf{hr}_i \otimes \dot{\mathbf{hr}}_j); \qquad Br_e^{kl} = \lambda_r I_d \delta^{kl} + 2\mu_r D_e^{kl}.$$

1.3.2. From the hints given above, one may conclude that the derivation of the additional tensors $[\mathbf{\Sigma}]$ results in forms which are not working and which are similar to that of Jaumann regarding the role of the stress, but which are utterly *different* regarding the role of the *kinematics*. These points are made conspicuous below (Sec. 1.3.4 and 1.3.5) in a special case and are studied further in the main part of the paper (Sec. 2.5).

1.3.3. However, a special comment is required concerning the third additional term generally involved by the stress splitting up approach, namely concerning the tensor $[\Sigma_a]$. Let us consider the deviatoric part of the contribution of pure hysteresis type defined as follows:

$$\left[{}^{t}_{R}\dot{\overline{S}}^{ij}_{a}\right]\mathbf{ha}_i \otimes \mathbf{ha}_j = 0;$$

$$\left[\overline{\Delta}^{t}_{R}\dot{\overline{S}}^{ij}_{a}\right]\mathbf{ha}_i \otimes \mathbf{ha}_j = \left[\dot{\overline{S}}^{ij}\right]\mathbf{ha}_i \otimes \mathbf{ha}_j$$

$$= \left[2\mu_r \overline{D}^{ij} + \overline{\beta}\,\overline{\Phi}_a\,\overline{\Delta}^{t}_{R}\,\overline{S}^{ij}\right]\mathbf{ha}_i \otimes \mathbf{ha}_j.$$

It is necessary to know if such a definition results in the relation

$$\partial\overline{\Sigma}^{kl}_{a}/\partial t = \overline{B}^{kl}_{a} + [\overline{\Sigma}_a]^{kl}; \qquad [\overline{\Sigma}_a] = \overline{S}^{ij}_{a}(\overline{\Sigma}^{kl}_{a})(\dot{\mathbf{h}}\mathbf{a} \otimes \mathbf{ha}_j + \mathbf{ha}_i \otimes \dot{\mathbf{h}}\mathbf{a}_j)$$

or

$$\partial\Delta^{t}_{R}\overline{\Sigma}^{kl}_{a}/\partial t = \overline{B}^{kl}_{a} + [\Delta^{t}_{R}\overline{\Sigma}_a]^{kl}; \qquad [\Delta^{t}_{R}\overline{\Sigma}_a]$$

$$= \Delta^{t}_{R}\overline{S}^{ij}_{a}(\overline{\Delta}^{t}_{R}\overline{\Sigma}^{kl}_{a})(\dot{\mathbf{h}}\mathbf{a}_i \otimes \mathbf{ha}_j + \mathbf{ha}_i \otimes \dot{\mathbf{h}}\mathbf{a}_j).$$

A short derivation shows that it results in the former expression involving $[\overline{\Sigma}_a]$. Consequently, there is no amalgamation of the *intrinsic* notions of discrete memory $({}^{t}_{R}\overline{S}^{ij}_{a})$ and of stress variation $(\Delta^{t}_{R}S^{ij}_{a})$ with a spin effect which cannot be entirely intrinsic, due to its partial dependence upon the loading process (a feature suggested below in Sec. 1.3.5), and studied further in the main part of the paper.

1.3.4. Before dealing with the definition of the base vectors $\mathbf{hr}_i$, $\mathbf{ha}_i$ and $\mathbf{hv}_i$, let us consider once again the case where $\mathbf{S}$ may be represented by only one of the three possible types of stress contribution (for example: $\mathbf{S} = \mathbf{S}_r; \mathbf{h} = \mathbf{h}_r$, like above, Sec. 1.3.1). The formal consequences of the approach are easily introduced in a simple kinematical case, namely that of a simple or pure shear defined in $(0, \mathbf{e}_k)$ through the following forms:

$$0 = -z^1 + J_1 Z^1 = -z^2 + J_2 Z^2 + 2\gamma_3(t)Z^3 = -z^3 + J_3 Z^3,$$

$$(J_n = 1 + K_n, \qquad n = 1, 2, 3),$$

$$\mathbf{D} = \sum_{1}^{3} D_n \mathbf{e}_n \otimes \mathbf{e}_n + D_4(\mathbf{e}_2 \otimes \mathbf{e}_3 + \mathbf{e}_3 \otimes \mathbf{e}_2), \qquad D_n = \dot{K}_n/J_n,$$

$$J_3 D_4 = \dot{\gamma} + \gamma D_2,$$

$$\mathbf{S} = \sum_{l}^{3} \Sigma_n \mathbf{e}_n \otimes \mathbf{e}_n + \Sigma_4\,(\mathbf{e}_2 \otimes \mathbf{e}_3 + \mathbf{e}_3 \otimes \mathbf{e}_2)\,,$$

$$0 = -\mathbf{h}_1 + \mathbf{e}_1 = -\mathbf{h}_2 + \mathbf{e}_2 \cos\alpha + \mathbf{e}_3 \sin\alpha = -\mathbf{h}_3 - \mathbf{e}_2 \sin\alpha + \mathbf{e}_3 \cos\alpha,$$

$$\alpha(0) = \gamma_3(0) = 0; \qquad \alpha(\gamma_3(t)) \ll \pi/2,$$

where the subscript r is omitted. One obtains:

$$\begin{aligned}
\dot{\Sigma}_1 &= (\lambda + 2\mu)D_1 + \lambda D_2 + \lambda D_3, \\
\dot{\Sigma}_2 + 2\Sigma_4\dot{\alpha}(\gamma_3, \dot{\gamma}_3) &= \lambda D_1 + (\lambda + 2\mu)D_2 + \lambda D_3, \\
\dot{\Sigma}_3 - 2\Sigma_4\dot{\alpha}(\gamma_3, \dot{\gamma}_3) &= \lambda D_1 + \lambda D_2 + (\lambda + 2\mu)D_3, \\
\dot{\Sigma}_4 - (\Sigma_2 - \Sigma_3)\dot{\alpha}(\gamma_3, \dot{\gamma}_3) &= (\mu\gamma_3/J_3)D_2 + (2\mu/J_3)\dot{\gamma}_3.
\end{aligned}$$

The complementary tensor is deviatoric and does no work ($\dot{E} = 2(\Sigma_2 - \Sigma_3)\Sigma_4\dot{\alpha} - 2\Sigma_4(\Sigma_2 - \Sigma_3)\dot{\alpha} = 0$). The right-hand sides of these equations are 0, 0, 0 and $2\mu\dot{\gamma}$ respectively, in the simple shear case ($D_n = 0$, $n = 1, 2, 3$). Consequently, one may imagine firstly, that the second order effects are exhibited through such a system of differential equations (giving the relationships between $\dot{S}_1 \ldots \dot{S}_4$ and $\dot{K}_1, \dot{K}_2, \dot{K}_3, \dot{\gamma}_3$) and that, secondly, ratchet effects are involved in the pure hysteresis case, namely in the case where the system of equations is of differential-difference type.

1.3.5. It remains to suggest the definition of the base vectors $\mathbf{h}_i$, *both* in the case of a unique contribution *and* in the case where several contributions are simultaneously involved, in order to define a relevant pattern of the actual behaviour. It is convenient to consider at first the more interesting contribution, namely that of pure hysteresis, making the assumption: $\mathbf{S} = \mathbf{S}_a$.

Let us suppose that the problem of the initial position of the PRF is solved. The definition of the current motion of the base vectors $\mathbf{ha}_i$ is then given by the following set of rules:

1) The motion of the PRF is *continuous* and defined by the angular velocity which is generally the sum of two terms, kinematical and thermomechanical, respectively.

2) The kinematical angular velocity $\dot{\alpha}_\delta$ of the PRF is given by that of the principal directions of the strain rate tensor $\mathbf{D}$. Consequently, $\dot{\alpha}_\delta$ is obtained through the time derivative of

$$\operatorname{tg} 2\alpha_\delta = 2(J_2\dot{\gamma} - \gamma J_2)/(J_3\dot{J}_2 - J_2\dot{J}_3), \tag{1.8}$$

so that the second derivatives of the stretches are involved in the $\dot{\alpha}\delta$ form:

$$\begin{aligned}
\dot{\alpha}_\delta = \Big[&(\dot{J}_3\gamma - J_3\dot{\gamma})\ddot{J}_2 - (\dot{J}_2\gamma - J_2\dot{\gamma})\ddot{J}_3 \\
&+ \Big((J_3\dot{J}_2 - J_2\dot{J}_3)\ddot{\gamma}\Big]\Big[J_2\cos 2\alpha\delta/(J_3\dot{J}_2 - J_2\dot{J}_3)\Big).
\end{aligned} \tag{1.9}$$

It is worth noting that, for the isotropic continua, pure shear kinematics $K_2 = K_3 = 0$ result in $\dot{\alpha}_\delta = 0$, like in the case of triaxial kinematics with fixed principal directions of stress and strain.

3) The (complementary) thermomechanical angular velocity of the PRF, $\dot{\alpha}_{\phi a}$, is defined by three-fold approach.

a) In the first step one considers the angular velocity $\dot{\theta}_\varphi$ of the principal directions of the "Φ_a-inertia" of the deformable material point endowed with a homogeneous field of intrinsic dissipation Φ_a. The role of Φ_a is prominent because it allows the cases of homogeneous mesostructures to be distinguished from those of heterogeneous types.

b) Secondly, the explicit relationships between $\dot{\theta}_\varphi$and the kinematics is obtained (in the homogeneous case), by means of the time derivative of

$$\operatorname{tg} 2\theta_\varphi = 4\gamma_3 J_3/[(J_2)^2 - (J_3)^2 + (2\gamma_3)^2], \tag{1.10}$$

(cf. Fig. 8), so that $\dot{\theta}_\varphi$ is a linear form:

$$\begin{aligned} \dot{\theta}_\varphi &= A_1\dot{K}_1 + A_2\dot{K}_2 + A_3\dot{K}_3 + A_4\dot{\gamma}; \qquad A_1 = 0; \\ A_2 &= -4\gamma J_2 J_3 A^{-1}; \\ A_3 &= 2\gamma(4\gamma^2 + J_2^2 + J_3^3)A^{-1}, \\ A_4 &= 2J_3(J_2^2 - J_3^2 - 4\gamma^2)A^{-1}; \qquad A = 16\gamma^2 J_3^2 + (4\gamma^2 + J_2^2 - J_3^2)^2, \end{aligned} \tag{1.11}$$

with respect to the rate of stretches, the coefficients A being however non-linear functions.

c) In the third step, the thermomechanical angular velocity is defined as a "small" and constitutive part of the spin $\dot{\theta}_\varphi$, defined by the general condition

$$\dot{\alpha}_{\phi a}\dot{\theta}_\phi < 0, \tag{1.12}$$

and by a constitutive definition of pure hysteresis type:

$$\begin{aligned} {}^t_R\dot{\alpha}_{\phi a} &= {}^t_R\dot{\theta}_\phi = 0, \\ \dot{\alpha}_{\phi a} &= \Delta^t_R\alpha_{\phi a} = F'((\Delta^t_R\theta_\phi)/\omega)\dot{\theta}_\phi, \\ \Delta^t_R\alpha_{\phi a} &= \omega F((\Delta^t_R\theta_\phi)/\omega), \end{aligned} \tag{1.13}$$

suggested in Fig. 3 (where the $\alpha_{\phi a} - \theta_\varphi$ and $\alpha_{\phi r} - \theta_\varphi$ diagrams are able to make conspicuous the relationship between $\dot{\alpha}_\phi$ and $\dot{\theta}_\varphi$ as soon as the reading is done under the assumption: $\dot{\theta}_\varphi = 1$). This definition may be obtained through the time derivative of a form such as:

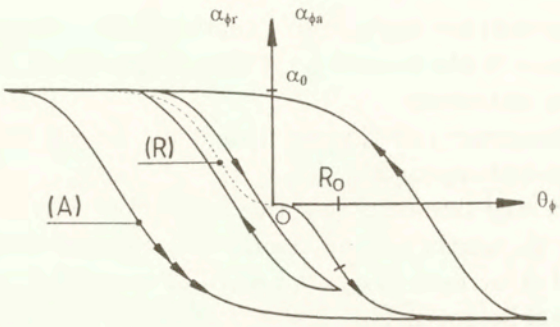

FIG. 3. A sketch suggesting the definition of the thermomechanical angular velocity involved in the definition of the PRF.

$$F(\theta) = -\alpha_0(1 - \exp -(-\theta^2/R_0^2))\mathrm{th}(\theta/R_0); \tag{1.14}$$

$$0 < \alpha_0 \ll 1; \qquad 0 < R_0 \ll 1,$$

where the constitutive parameters are α_0 (intensity parameter, $\sim S_0/\mu$) and R_0 (location parameter, $\sim S_0/\mu$).

4) Finally, following the splitting rule 1:

$$\dot{\alpha}_a = \dot{\alpha}_\delta + \dot{\alpha}_{\phi a}; \qquad \dot{\mathbf{h}}_{a2} = (-\sin\alpha_a \mathbf{e}_2 + \cos\alpha_a \mathbf{e}_3)\dot{\alpha}_a; \tag{1.15}_1$$

$$\dot{\mathbf{h}}_{a3} = (\cos\alpha_a \mathbf{e}_2 - \sin\alpha_a \mathbf{e}_3)\dot{\alpha}_a$$

and, if a reversible contribution is involved ($\mathbf{S} = \mathbf{S}_a + \mathbf{S}_r$), one has also (cf. Fig. 3):

$$\dot{\alpha}_r = \dot{\alpha}_\delta + \dot{\alpha}_{\varphi r}; \qquad \dot{\alpha}_{\varphi r} = F'_{\theta\varphi}(\theta_\varphi)\dot{\theta}\varphi; \qquad \alpha_{\phi r} = F(\theta_\varphi) \tag{1.15}_2$$

in order to define the base vectors $\mathbf{h}_{rn}$. Consequently, it is not necessary to make use of a specific set of constitutive parameters α_{or} and R_{or}.

5) It is worth noting that it is not effective to modify the definitions of $\dot{\alpha}_a$ and $\dot{\alpha}_r$ making use of a very simple form of $\mathrm{tg}\,2\theta_\varphi$, such as $2\gamma_3/J_3$, resulting in

$$\dot{\theta}_\varphi = (2\dot{\gamma}_3 J_3 - 2\gamma_3 \dot{K}_3)/(J_3^2 + 4\gamma_3^2). \tag{1.16}$$

1.3.6. An example of illustration is given in Fig. 4 a,b where the "axial stress-shear strain" diagram is obtained by a numerical simulation of the above pattern under the following conditions: $\mathbf{S} = \mathbf{S}_a$; $\gamma_3 > 0$, $K_n = 0$, $n = 1, 2, 3$, resulting in fixed principal directions ($\dot{\alpha}_\delta = 0$) of the strain rate tensor $\mathbf{D}$. The constitutive parameters are: $\lambda = 2\mu = 150$ GPa; $S_0 = 200$ MPa; $\alpha_0 = (1/2)\ S_0/\mu$; $R_0 = 4\ (S_0/\mu)$. Note that the ratchet effects are also obtained using the intuitive

definition (1.16) of the spin $\dot{\theta}_\varphi$ but that these effects are not physically relevant (Fig. 4 c, d). The intuitive approach is no more satisfying in the case of "not symmetrical" sets of cycles of different constant amplitudes (cf. Fig. 5 a, b for the thermomechanical approach and Fig. 5 c, d for the intuitive approach, both obtained under a small initial compression $-S_0/1000$).

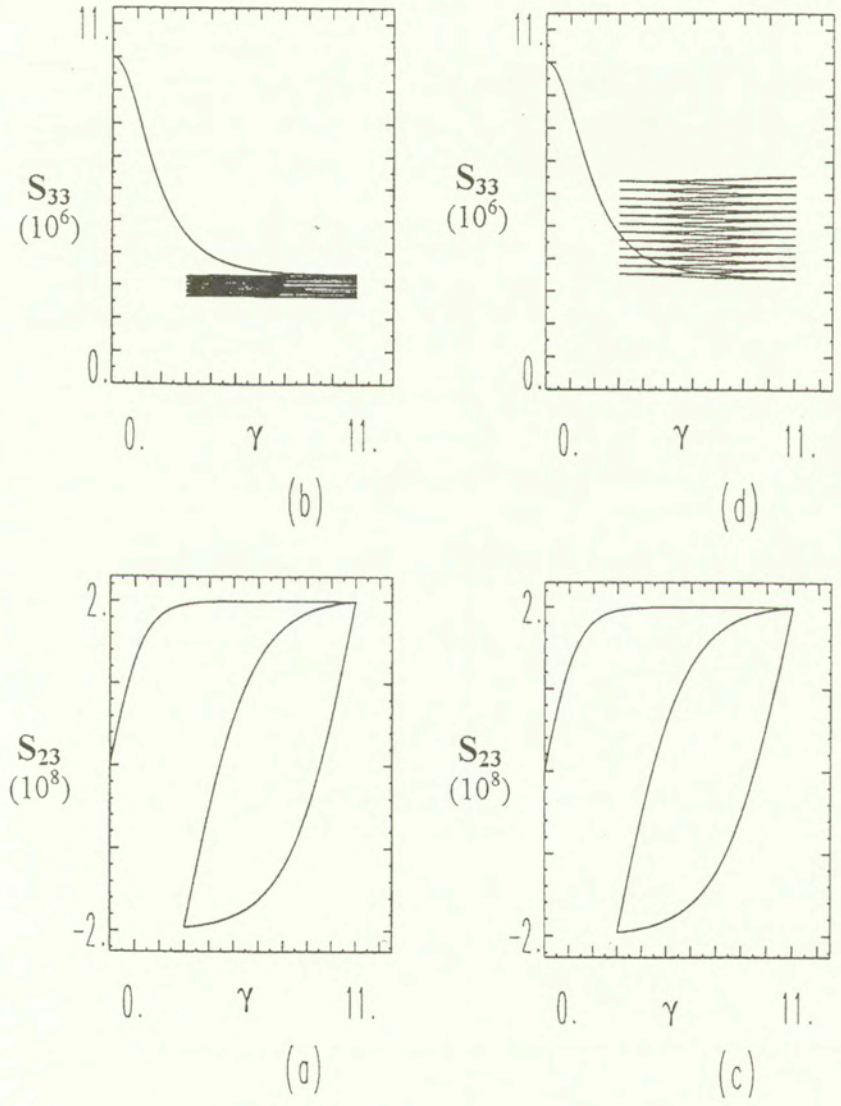

FIG. 4. Ratchet effect (b) exhibited after a small traction through the cumulative increase of the axial stress compression S_{33} during the cyclic simple shear (a).

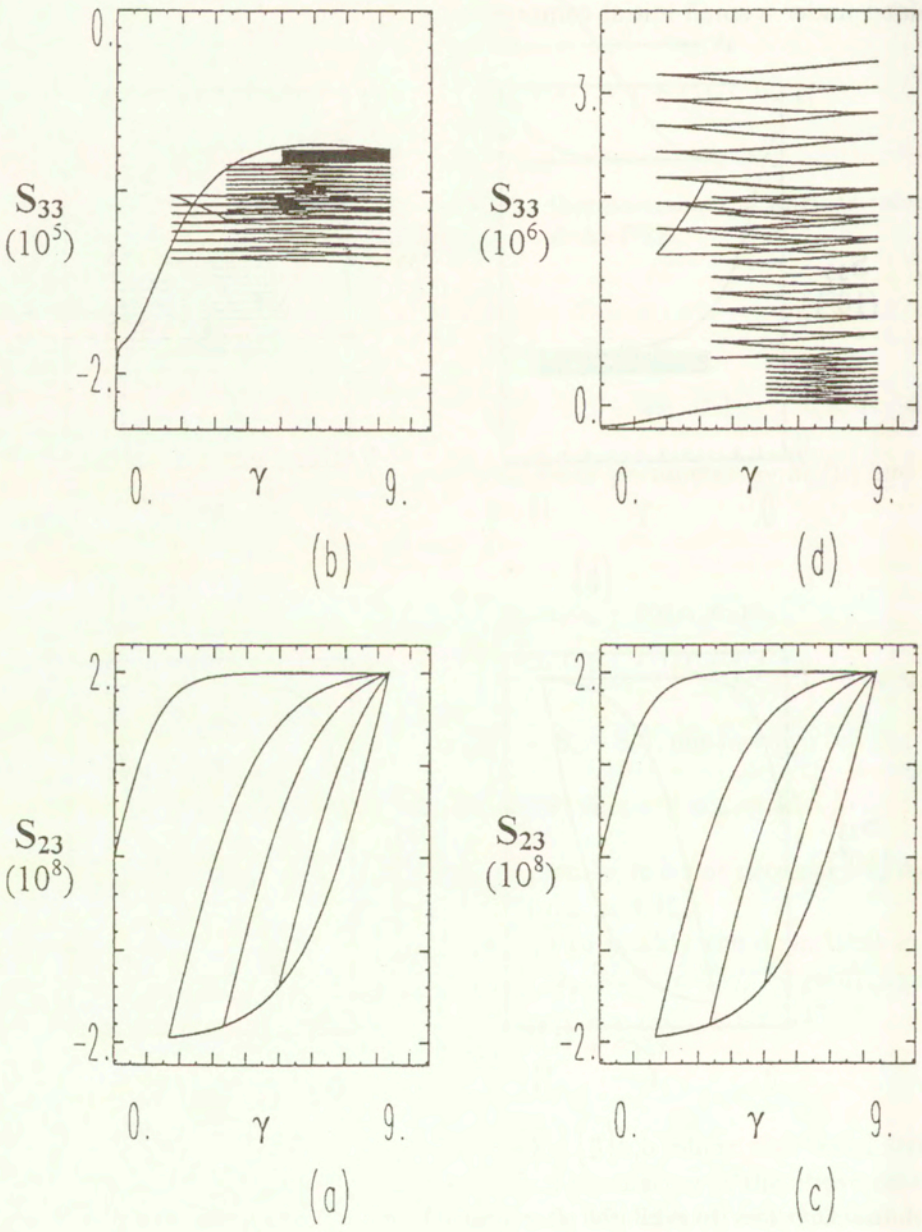

FIG. 5. Ratchet effect (b) in the case of several sets of cycles (a). The intuitive approach based on (1.16) results in (d) for a first order behaviour (c) identical to (a).

1.4. Towards a rather general pattern of rate form defined in the PRF

The first part of the paper is devoted to the *definition* of the PRF (Sec. 2). Some remarks are added concerning the three basic *stress contributions* of the viscoelastoplastic pattern (Sec. 3). In order to supplement briefly the illustration given by Figures 4 and 5, comments are added concerning the results available from now on through various numerical *simulations* (Sec. 4).

2. Definition of the Preferred References Frames

In this section the clue of the presentation is that suggested above (Sec. 1.3.5), namely a series of relationships, firstly between frames and spins, secondly between spins and spins, finally between spins and frames. In the first part of the paragraph (a generalization of point 2, Sec. 1.3.5), one starts from the frame $(M, \mathbf{d}_n)$ of $\mathbf{D}$ to derive the "kinematical" spin $\boldsymbol{\Omega}_\delta$. The cumbersome formalism is two-fold: a) that of giving, through $\dot{\mathbf{d}}_n$, the notions of the principal directions; b) that associated with the basic "direct" form $\Sigma_3^1 \mathbf{d} \wedge \dot{\mathbf{d}}$. The second part (a generalization of points 3 a,b, Sec. 1.3.5) is devoted only to the definition of the "inertia-like" tensor $\mathbf{I}$ (the derivation of the relationships between the frame $(M, \mathbf{i}_n)$ and the spin $\boldsymbol{\Omega}_\phi$ is omitted because it is similar to that concerning $(M, \mathbf{d}_n)$ and $\boldsymbol{\Omega}_\delta$). The third part of the paragraph (a generalization of point 3c, Sec. 1.3.5) is the only one which may be interesting from the constitutive point of view. One defines a constitutive relationship between the spin $\boldsymbol{\Omega}_\phi$ and the thermomechanical spin $\boldsymbol{\Omega}_\mu$, in order to obtain the spin of the PRF through the spin splitting, similar to (1.15):

$$\boldsymbol{\Omega} = \boldsymbol{\Omega}_\delta + \boldsymbol{\Omega}_\mu(\boldsymbol{\Omega}_\phi); \qquad \boldsymbol{\Omega}_\mu = f\boldsymbol{\Omega}_\phi.$$

Note that the proposed relationship between $\boldsymbol{\Omega}_\mu$ and $\boldsymbol{\Omega}_\phi$ is isotropic, and that the definition of the involved scalar factor f is a basic issue. The fourth paragraph (a generalization of point 4, Sec. 1.3.5) deal with the relationship between the spin $\boldsymbol{\Omega}$ and the PRF. The cumbersome formalism is that expressing the rates of the base vectors in terms of the basic "inverse" form $\boldsymbol{\Omega} \wedge \mathbf{d}$.

2.1. The "kinematical" term involved in the splitting of the angular velocity of the PRF

2.1.1. In spite of the fact that, in the isotropic case, simple kinematics is sufficient to study the constitutive functional relationships between the space of strain and the space of stress, the anisotropic generalization must be kept in view. Therefore, it is not suitable to consider an oversimplified form of the strain rate tensor. In $(0, \mathbf{e}_a)$, an interesting expression of

$$\mathbf{D} = \Sigma_3^1 D_n \mathbf{e}_n \otimes \mathbf{e}_n + D_4(\mathbf{e}_2 \otimes \mathbf{e}_3 + \mathbf{e}_3 \otimes \mathbf{e}_2) + D_5(\mathbf{e}_3 \otimes \mathbf{e}_1 + \mathbf{e}_1 \otimes \mathbf{e}_3) + D_6(\mathbf{e}_1 \otimes \mathbf{e}_2 + \mathbf{e}_2 \otimes \mathbf{e}_1)$$

may be, for example, that obtained in the case of a six-parameter deformation in the reference planes of the fixed frame $(0, \mathbf{e}_a)$:

$$0 = z^1 + J_1 Z^1 + 2\gamma_2 Z^2, \qquad x^1 = Z^1 \quad \text{for example,}$$

$$0 = -z^2 + J_2 Z^2 + 2\gamma_3 Z^3, \quad x^2 = Z^2 \quad \text{for example,}$$

$$0 = -z^3 + J_3 Z^3 + 2\gamma_1 Z^1, \quad x^3 = Z^3 \quad \text{for example.}$$

One obtains immediately:

$$\mathbf{D} = (1/2)\partial \mathbf{G}/\partial t = [\mathbf{g}^1 \otimes \mathbf{g}^1][J_1 \dot{J}_1 + 4\gamma_1 \dot{\gamma}_1] + \dots$$

$$+ [\mathbf{g}^2 \otimes \mathbf{g}^3 + \mathbf{g}^3 \otimes \mathbf{g}^2][\dot{J}_2 \gamma_3 + J_2 \dot{\gamma}_3] + \dots$$

$$= [\mathbf{e}_1 \otimes \mathbf{e}_1][(\dot{J}_1/J_1 + 8\gamma_1 \dot{\gamma}_2 \gamma_3 / J_1 J_2 J_3)(1+K)^{-1}] + \dots$$

$$+[\mathbf{e}_2 \otimes \mathbf{e}_3 + \mathbf{e}_3 \otimes \mathbf{e}_2][(\dot{\gamma}_3/J_3 - 2\gamma_2 \dot{\gamma}_1 / J_2 J_1 - \dot{J}_2 \gamma_3 / J_2 J_3$$

$$+2\gamma_2 \gamma_1 \dot{J}_3 / J_1 J_2 J_3)(1+K)^{-1}] + \dots$$

$$= [\mathbf{e}_1 \otimes \mathbf{e}_1][\dot{J}_1/J_1 + 8\gamma_1 \dot{\gamma}_2 \gamma_3 / J_1 J_2 J_3](1+K)^{-1} + \dots$$

$$[\mathbf{e}_2 \otimes \mathbf{e}_3 + \mathbf{e}_3 \otimes \mathbf{e}_2][\dot{C}_3/J_3 - (2\gamma_2/J_2)(\dot{C}_1/J_1)]$$

$$\dot{C}_n = \dot{\gamma}_n - (\dot{J}_m/J_m)\gamma_n; \qquad m(n) = 3, 1, 2; \qquad n = 1, 2, 3;$$

$$K = 8\gamma_1 \gamma_2 \gamma_3 / J_1 J_2 J_3.$$

This form make conspicuous the difference between 3-shear and 1 or 2-shears. In the current study T is supposed to be constant and $\mathbf{D}$ is not modified by $\mathbf{D}_T$. However, it is worth noting that the stress splitting approach may be generalized to the variable temperature case [4].

2.1.2. In order to introduce an explicit overview of the algorithm giving the kinematical spin $\mathbf{\Omega}_\delta$ for a given $\mathbf{D}$ (and giving also $\mathbf{\Omega}_\phi$ for a given $\mathbf{I}$), it is useful to set the notations needed for the derivation of the components in $(0, \mathbf{e}_a)$ of the unit vectors $\mathbf{d}_n$. The notation of the determinant equation and of its associated roots (supposed to be unequal) are:

$$\det[D_{rs} - d\delta_{rs}] = e^{ijk}[D_{1i} - d\delta_{1i}][D_{2j} - d\delta_{2j}][D_{3k} - d\delta_{3k}] = 0,$$

$$d^3 - I_D d^2 + \Pi_D d - \det D = d^3 + pd^2 + qd + r = 0;$$

$$I_D = -p = D_1 + D_2 + D_3,$$

$$\Pi_D = (1/2)(I_D^2 - D_{ij}D_{ij}) = q = D_2D_3 + D_3D_1 + D_1D_2$$
$$-D_4^2 - D_5^2 - D_6^2; \qquad III_D = \det\mathbf{D} = -r,$$

$$d_m = 2\sqrt{-a/3}\cos[y/3 + (m-1)2\pi/3)], \qquad m = 1,2,3,$$

$$\cos y = (-b/2)/(a^3/27)^{1/2}, \qquad 3a = 3q - p^2, \qquad 27b = 2p^3 - 9pq + 27r.$$

The notations concerning the principal directions are:

$$(D_{rs} - d_m\delta_{rs})d_m^s = 0; \qquad \mathbf{d}_m = d_m^s\mathbf{e}_s$$

giving, in $(0, \mathbf{e}_a)$, the three unit vectors $\mathbf{d}_m$ (associated with the above roots d_m and giving the principal directions of $\mathbf{D}$); it is also possible to derive the explicit forms giving the components d_m^s of $\mathbf{d}_m$ in $(0, \mathbf{e}_a)$. The derivation is obtained through the implementation of a relevant set of minors:

$$M_n^{ir} = (1/2)e^{ijk}e^{rst}(D_{js} - d_n\delta_{js})(D_{kt} - d_n\delta_{kt}) \quad \text{of} \quad (\mathbf{D} - d_n\delta).$$

Explicitly:

$$M_n^{11} = (D_2 - d_n)(D_3 - d_n) - (D_4)^2; \qquad M_n^{12} = D_4D_5 - (D_3 - d_n)D_6;$$
$$M_n^{13} = D_6D_4 - (D_2 - d_n)D_5;$$

$$M_n^{22} = (D_3 - d_n)(D_1 - d_n) - (D_5)^2; \qquad M_n^{23} = D_5D_6 - (D_1 - d_n)D_4;$$

$$M_n^{33} = (D_1 - d_n)(D_2 - d_n) - (D_6)^2$$

$$\mathbf{d}_n = (M_n^{11}\mathbf{e}_1 + M_n^{12}\mathbf{e}_2 + M_n^{13}\mathbf{e}_3)/[(M_n^{11})^2 + (M_n^{12})^2 + (M_n^{13})^2]^{1/2};$$
$$n, i = 1,2,3,$$

$$\mathbf{d}_n = (A_n\mathbf{e}_1 + B_n\mathbf{e}_2 + C_n\mathbf{e}_3)/E_n; \qquad E_n^2 = A_n^2 + B_n^2 + C_n^2;$$
$$A_n = M_n^{n1}; \qquad B_n = M_n^{n2}; \qquad C_n = M_n^{n3},$$

associated with the convention $i = n$, namely with the implementation of the set of minors $[M^{n1}, M^{n2}, M^{n3}]$ with the root d_n, for the derivation of the vector $\mathbf{d}_n$.

2.1.3. It remains necessary to obtain the explicit form of the components Ω_δ^n of the angular velocity pseudo-vector:

$$\boldsymbol{\Omega}_\delta = \Omega_\delta^a\mathbf{e}_a = (1/2)\Sigma_1^3\mathbf{d}_n \wedge \dot{\mathbf{d}}_n; \qquad \mathbf{d}_n = d_n^m\mathbf{e}_m \tag{2.1}$$

The rate $\dot{d}_n^m$ involves the rates $\dot{A}_n, \ldots, \dot{E}_n$, namely the rates of the products $D_a D_b$ and $D_a d_n$. Hence, the second order time derivative $\ddot{K}$ and $\ddot{\gamma}$ are involved. One has indeed:

$$\dot{A}_1 = \partial[(D_2 - d_1)(D_3 - d_1) - (D_4)^2]/\partial t;$$

$$E_3\dot{E}_3 = A_3\dot{A}_3 + B_3\dot{B}_3 + C_3\dot{C}_3, \ldots$$

$$(1+K)\dot{D}_n = \ddot{J}_1/J_1 - (\dot{J}_1/J_1)^2 + [2\ddot{\gamma}_1/J_1 - 2\dot{\gamma}_1\dot{J}_1/J_1^2][4\gamma_2\gamma_3/J_2J_3]$$

$$+(\dot{\gamma}_1/J_1)[[\partial(\gamma_2/J_2)/\partial t](\gamma_3/J_3) + [\partial(\gamma_3/J_3)/\partial t]]$$

$$(\gamma_2/J_2)] - D_n\partial K/\partial t; \ldots$$

$$\dot{d}_n = \partial[2(-a/3)^{1/2}\cos\Phi/3]/\partial t;$$

$$-\sin\Phi\dot{\Phi} = \partial[(b/2)/(-a^3/27)^{1/2}]/\partial t; \ldots$$

$$27\dot{b} = 6p^2\dot{p} - 9\dot{p}q - 9p\dot{q} + 27\dot{r}; \qquad \dot{a} = \dot{q} - (2/3)p\dot{p}, \ldots$$

$$-\dot{p} = \dot{D}_1 + \dot{D}_2 + \dot{D}_3;$$

$$\dot{q} = \dot{D}_2D_3 + \dot{D}_3D_2 + \dot{D}_3D_1 + \dot{D}_1D_3 + \dot{D}_1D_2 + \dot{D}_2D_1$$

$$-2\Sigma_4^6 D_n\dot{D}_n; \ldots$$

The Euler's angles of the frame $(M, \mathbf{d}_n)$ can be obtained by the integration of the usual forms involving the components Ω_δ^a ($\dot{\theta}_\delta = \Omega_\delta^1\cos\psi_\delta + \Omega_\delta^2\sin\psi_\delta$; $\phi_\delta\sin\theta_\delta$; $\phi_\delta\sin\theta_\delta = \Omega_\delta^1\sin\psi_\delta - \Omega_\delta^2\cos\psi_\delta$; ...).

2.2. The "power inertia" tensor I

2.2.1. In order to follow the clue given above (Sec. 1.3.5, point 3a,b), it is necessary:

i. To define **I** giving the inertia-like frame $(M, \mathbf{i}_n(M,t))$ and $\Omega_\phi(M,t)$;

ii. To define the scalar function (or functional) f involved in the splitting giving the spin of the PRF. The second issue is studied below (Sec. 3). Here the attention is focused on the definition of **I**.

2.2.2. As soon as a rather general approach is needed, the relevant method of definition of $\mathbf{I}_\phi(M,t)$ must be, in principle, introduced working "on the chart of the convected co-ordinates x^k, in the field of the DARF, $(M, \mathbf{g}_i)$". The two main steps of the approach are, first, to define the relevant field of power (say Φ) and, second, to define the inertia-like tensor of the material point in the four relevant cases, namely: a) the Φ – homogeneous and isotropic case; b) the

Φ – homogeneous and anisotropic case; c) the Φ – heterogeneous and isotropic case; d) the Φ – heterogeneous and anisotropic case. In this preliminary study it is reasonable to deal only with the isotropic cases a) and c). Let us consider, in the Φ – homogeneous isotropic case, the pseudo-scalar field $\Phi(t)$ of intrinsic dissipation. The problem under consideration being kinematically homogeneous, the co-ordinates: $x^k = \text{ident} = Z^k$; $k = 1, 2, 3$ are rectilinear at the initial time $t = 0$, and remain rectilinear during the deformation. At the current time:

$$\mathbf{I}(M,t) = I^{ij}\mathbf{g}_i \otimes \mathbf{g}_j \tag{2.2}$$

$$\overset{\text{def}}{=} \left[\int\int\int x^i(M)x^j(M)\phi(t)\rho(g)^{1/2}dx^i dx^j dx^k\right]\mathbf{g}_i \otimes \mathbf{g}_i$$

$$\overset{\text{ident}}{=} \left[\int\int\int x^i(M)x^j(M)\hat{\Phi}(t)dx^i dx^j dx^k\right]\mathbf{g}_i \otimes \mathbf{g}_j.$$

Performing the integration from $-1/2$ to $1/2$ one obtains

$$[12/\Phi(t)]\mathbf{I}(t) = \mathbf{g}_1 \otimes \mathbf{g}_1 + \mathbf{g}_2 \otimes \mathbf{g}_2 + \mathbf{g}_3 \otimes \mathbf{g}_3.$$

The frame $(M, \mathbf{i}_n)$ is therefore defined by the principal directions of $\mathbf{I} = \delta^{ij}\mathbf{g}_i \otimes \mathbf{g}_j$. Instead, making use of the covariant form I_{ij} and of the associated determinant equation $\det[(I - d)g_{ii} - I_{ij}] = 0$, $I = g_{ij}I^{ij}$, it is relevant, in a theoretical study of "homogeneous problems", to express the tensor $\mathbf{I}$ in the fixed frame $(0, \mathbf{e}_a)$:

$$\mathbf{I} = (J_1\mathbf{e}_1 + 2\gamma_1\mathbf{e}_3) \otimes (J_1\mathbf{e}_1 + 2\gamma_1\mathbf{e}_3) + (2\gamma_2\mathbf{e}_1 + J_2\mathbf{e}_2)$$

$$\otimes (2\gamma_2\mathbf{e}_1 + J_2\mathbf{e}_2) + (2\gamma_3\mathbf{e}_2 + J_3\mathbf{e}_3) \otimes (2\gamma_3\mathbf{e}_2 + J_3\mathbf{e}_3)$$

$$= [(J_1)^2 + (2\gamma_2)^2]\mathbf{e}_1 \otimes \mathbf{e}_1 + [(J_2)^2 + (2\gamma_3)^2]\mathbf{e}_2 \otimes \mathbf{e}_2$$

$$+[(J_3)^2 + (2\gamma_1)^2]\mathbf{e}_3 \otimes \mathbf{e}_3 + [J_3 2\gamma_3](\mathbf{e}_2 \otimes \mathbf{e}_3 + \mathbf{e}_3 \otimes \mathbf{e}_2)$$

$$+[J_1 2\gamma_1](\mathbf{e}_3 \otimes \mathbf{e}_1 + \mathbf{e}_1 \otimes \mathbf{e}_3) + [J_2 2\gamma_2](\mathbf{e}_1 \otimes \mathbf{e}_2 + \mathbf{e}_2 \otimes \mathbf{e}_1).$$

It is worth noting firstly, that in the heuristic one-shear case, one obtains immediately not only the usual results: $\operatorname{tg} 2\theta_\phi = 0/0$ or $\operatorname{tg} 2\theta_\phi = 0$ and $J_3/2\gamma_3$ for the cube, the rectangle and the rhombus, but also the previously introduced expression (1.10) of $\operatorname{tg} 2\theta_\phi$; secondly, that the initial orientation of the PRF $(M, \mathbf{H}_k)$ may be chosen arbitrarily (0/0 form). From the above expression of $\mathbf{I}$, one obtains the frame $(M, \mathbf{i}_n)$ using the previous forms (cf. Sec. 2.1). The only difference with the treatment concerning $\mathbf{D}$ comes from the fact that the time derivative of the components in $(0, \mathbf{e}_i)$ of $\mathbf{I}$ does not involve the second derivatives $\ddot{J}_n$ and $\ddot{\gamma}_n$ of the stretches.

2.2.3. Let us now consider, in the heterogeneous isotropic case, a material point endowed with a characteristic sub-structure at a physically relevant mesoscale of Néel-Krumhansl type. For example, the field of power (intrinsic dissipation Φ or elastic power $\dot{E}_r$) is so strongly heterogeneous that it is almost homogeneously located near the faces of the material cube. Owing to the definition of $\mathbf{I}$, two basic types of mesostructural processes must be distinguished, according to the existence or absence of a perfect dragging along of the power field. In the first case the principal directions $\mathbf{i}_n$ are insensitive with respect to the mesostructure. On the contrary, if the microprocesses taking place in the walls involve a typical invariant micro-length e_0 and an associated typical meso-length J_0 (and if the process is sufficiently slow to allow the homogeneity of the power in the walls), then the vectors $\mathbf{i}_n$ are dependent on the nondimensional parameter: $e = e_0/J_0$. For example, in the two-dimensional case, one obtains the $\mathbf{i}_n$ from:

$$\begin{aligned}\mathbf{I}^* = \mathbf{I} - \mathbf{I}(\text{core}) = [(J_2)^2 + (2\Gamma_3)^2]\mathbf{e}_2 \otimes \mathbf{e}_2 + [(J_3)^2]\mathbf{e}_3 \otimes \mathbf{e}_3 \\ +[J_3 2\Gamma_3](\mathbf{e}_2 \otimes \mathbf{e}_3 + \mathbf{e}_3 \otimes \mathbf{e}_2) - [(J_2)^2 + (2\gamma_3)^2]\mathbf{e}_2 \otimes \mathbf{e}_2 \\ -[(J_3)^2]\mathbf{e}_3 \otimes \mathbf{e}_3 - [J_3 2\gamma_3](\mathbf{e}_2 \otimes \mathbf{e}_3 + \mathbf{e}_3 \otimes \mathbf{e}_2).\end{aligned}$$

In spite of the fact that sophisticated mesoscopic modelling [11, 12] are not currently included in the theory, it is worth noting that the definition of the Pattern of Rate Form in PRF may, in principle, be mesoscale-dependent, through the first order effects (for example those of anisotropy) as well as through the second order effects, as suggested above: the theory is not "incomplete" in the sense supported by Bunge.

2.3. The definitions of the thermomechanical spins through spin-spin isotropic constitutive relationships

2.3.1. Pure hysteresis ($\mathbf{S} = \mathbf{S}_a$) and Φ - homogeneity. Let us consider the current amplitude of rotation and the current amplitude by branch:

$$\Delta_0^t R_\phi = \int_0^t (\mathrm{tr}\boldsymbol{\Omega}_\phi^2)^{1/2} d\tau, \qquad \Delta_R^t R_\phi = \int_R^t (\mathrm{tr}\boldsymbol{\Omega}_\phi^2)^{1/2} d\tau \tag{2.3}$$

given by the integration in $(0, \mathbf{e}_i)$ of the history of the spin $\boldsymbol{\Omega}_\phi$. The thermomechanical spin $\boldsymbol{\Omega}_\mu$ is defined as equal to $\boldsymbol{\Omega}_\phi$ up to a scalar functional f_i of R_ϕ:

$$\boldsymbol{\Omega}_\mu = f\boldsymbol{\Omega}_\phi \tag{2.4}$$

where f is defined by taking as previously (Sec. 1.5.5, point 3c) the derivative

$$f_a(R_\phi/\omega) = \partial F_a[R_\phi/\omega]/\partial R_\phi \tag{2.5}$$

with respect to R_ϕ of the constitutive scalar functional of pure hysteresis type:

$$F_a(\Delta_R^t R_\phi) = -a_0[1 - \exp -(\Delta_R^t R_\phi / R_0)^2]\mathrm{th}(\Delta_R^t R_\phi / \omega R_0);$$

(2.6)

$$0 < a_0 \ll 1; \qquad 0 < R_0 \ll 1; \qquad \omega = 1 \text{ or } 2,$$

The resulting global spin components Ω^k in $(0, \mathbf{e}_a)$ of the PRF are such as

$$\Omega^k = \Omega_\delta^k(J_n, \gamma_n; \dot{J}_n, \dot{\gamma}_n; \ddot{J}_n, \ddot{\gamma}_n) + f[\Delta_R^t R_\phi]\Omega_\phi^k(J_n, \gamma_n; \dot{J}_n, \dot{\gamma}_n).$$

2.3.2. Reversibility ($\mathbf{S} = \mathbf{S}_r$) and homogeneity with respect to the reversible power. The approach is similar, but now f is defined as a function:

$$f_r(R_\phi) = \partial F_r(R_\phi)/\partial R_\phi, \tag{2.7}$$

$$F_r(R_\phi) = -a_0[1 - \exp -(R_\phi/R_0)^2]\mathrm{th}(R_\phi/R_0); \tag{2.8}$$

$$0 < a_0 \ll 1; \qquad 0 < R_0 \ll 1.$$

2.3.3. The coupled cases $\mathbf{S} = \mathbf{S}_r + \mathbf{S}_a$, or $\mathbf{S} = \mathbf{S}_v + \mathbf{S}_r$, or $\mathbf{S} = \mathbf{S}_v + \mathbf{S}_a$, or $\mathbf{S} = \mathbf{S}_v + \mathbf{S}_r + \mathbf{S}_a$, with associated "homogeneity" with respect to the inertia of the powers. In the first case the approach is similar ($F_a = F_r$) to that suggested in the Introduction (Sec. 1.3.5). But in the three cases including $\mathbf{S}_v$, the theory cannot provide reasonable physical arguments to choose between the two following types of definitions: firstly, a partial spin splitting up obtained through the amalgamation of $\mathbf{h}_r$ and $\mathbf{h}_v$ leading to the unique PRF of base vectors $\mathbf{h}_{rv}$; secondly, a perfect splitting leading to separate definitions of $\mathbf{h}_v$, $\mathbf{h}_r$ and $\mathbf{h}_a$. The partial splitting associated with the first definition may be defined as above. On the contrary, the total splitting associated with the second definition imply that the base vectors $\mathbf{h}_v$ are defined by a viscous pattern.

2.4. From the differential-difference equations and/or differential equations of the PRF to the constitutive equations in the fixed frame

i. The base vectors $\mathbf{h}_n$ of the PRF (in fact each type, $\mathbf{h}(a)_n$ and $\mathbf{h}(r\nu)_n$, of base vectors of the PRF(a) and of the PRF($r\nu$)) are obtained by the integration of the differential-difference system (cf. Eq. (2.7)) defined above (cf. Sec. 2.1.3).

ii. In $(0, \mathbf{e}_m)$:

$$\dot{\mathbf{h}}_n = \dot{H}_n^m \mathbf{e}_m = \Omega \wedge \mathbf{h}_n = \Omega \wedge (H_n^m \mathbf{e}_m) = [\Omega]_n^m \mathbf{e}_m \tag{2.9}$$

$$[\Omega]_n^l = H_n^3 \Omega^2 - H_n^2 \Omega^3; \ldots; \quad H_1^1 = \cos\phi\cos\psi - \sin\psi\cos\theta\sin\phi; \ldots; \quad F_3^3 = \cos\theta.$$

The generalization of (1.11) results in intricate forms of the complementary deviatoric tensor $[\Sigma]$. It is indeed linear with respect to the components Σ^{kl} and Ω^i:

$$[\Sigma]^{11} = 2(\Omega^2\Sigma^{13} - \Omega^3\Sigma^{12}); ...; [\Sigma]^{23} = \Omega^1(\Sigma^{22} - \Sigma^{33}) - \Omega^2\Sigma^{12} + \Omega^3\Sigma^{13}; ...,$$

but Ω^i are given by (2.7).

2.5. Remark concerning the comparison between the PRF spin term and the usual spin terms

Instead of the constitutive definition such as:

$$[\partial S^{ij}/\partial t]\mathbf{h}_i \otimes \mathbf{h}_j \overset{\text{def}}{=} B^{ij}\mathbf{hr}_i \otimes \mathbf{hr}_j = \mathbf{B}$$

given in the relevant PRF, let us consider similar usual definitions of Oldroyd type, of Rivlin type and of Jaumann type:

$$(L\nu^{\cdot\cdot}S)_0 \overset{\text{def}}{=} [\partial S^{ij}/\partial t]\mathbf{g}_i \otimes \mathbf{g}_j \overset{\text{def}}{=} B^{ij}\mathbf{gr}_i \otimes \mathbf{gr}_j = \mathbf{B},$$

$$(L\nu_{\cdot\cdot}S)_r \overset{\text{def}}{=} [\partial S_{ij}/\partial t]\mathbf{g}^i \otimes \mathbf{g}^j \overset{\text{def}}{=} B_{ij}\mathbf{gr}^i \otimes \mathbf{gr}^j = \mathbf{B},$$

$$(L\nu^{\cdot\cdot}S)_j \overset{\text{def}}{=} (1/2)[(\partial S^{ij}/\partial t)\mathbf{g}_i \otimes \mathbf{g}_j + (\partial S_{ij}/\partial t)\mathbf{g}^i \otimes \mathbf{g}^j] \overset{\text{def}}{=} B^{ij}\mathbf{gr}_i \otimes \mathbf{gr}_j = \mathbf{B}.$$

In $(0, \mathbf{e}_i)$ the constitutive definition involves the complementary terms of Oldroyd, Rivlin and Jaumann types:

$$\begin{aligned}
[\Sigma]_o &= S^{ij}(\Sigma^{kl}_{re})(\dot{\mathbf{g}}_i \otimes \mathbf{g}_j + \mathbf{g}_i \otimes \dot{\mathbf{g}}_j),\\
[\Sigma]_r &= S_{ij}(\Sigma^{kl}_{re})(\dot{\mathbf{g}}^i \otimes \mathbf{g}^j + \mathbf{g}^i \otimes \dot{\mathbf{g}}^j),\\
[\Sigma]_j &= (1/2)([\Sigma]_o + [\Sigma]_r),
\end{aligned}$$

respectively, instead of

$$[\Sigma]_{\text{PRF}} = S^{ij}(\Sigma^{kl})(\dot{\mathbf{h}}_i \otimes \mathbf{h}_j + \mathbf{h}_i \otimes \dot{\mathbf{h}}_j).$$

The linearity with respect to the stress components Σ^{kl}_r in $(0, \mathbf{e}_i)$ is a feature the four constitutive definitions have in common. But the main difference between the PRF definition and the usual ones lies in the fact that the PRF definition is not directly linked to the kinematics. A constitutive ingredient may be involved

through the definition of a *vectorial* function or functional of the power-inertia spin Ω_ϕ. Moreover, *it is even possible to make use of a scalar* function or functional, if one addmits, *like in this paper*, that the orientation of Ω_ϕ needs not to be modified. The point deserves thinking about with the aid of a formally simple illustration. In the special case of the one-shear kinematics, for example, the explicit forms of the $[\Sigma\,]$ tensors are:

$$[\Sigma]_o = (2\Sigma_1 D_1)(\mathbf{e}_1 \otimes \mathbf{e}_1) + (2\Sigma_2 D_2 + 4\Sigma_4 D_4)(\mathbf{e}_2 \otimes \mathbf{e}_2)$$
$$+(2\Sigma_3 D_3)(\mathbf{e}_3 \otimes \mathbf{e}_3) + [2\Sigma_3 D_4 + \Sigma_3(D_2 + D_3)](\mathbf{e}_2 \otimes \mathbf{e}_3 + \mathbf{e}_3 \otimes \mathbf{e}_2),$$

$$[\Sigma]_r = (-2\Sigma_1 D_1)(\mathbf{e}_1 \otimes \mathbf{e}_1) + (-2\Sigma_2 D_2)(\mathbf{e}_2 \otimes \mathbf{e}_2)$$
$$+(-2\Sigma_3 D_3 - 4\Sigma_4 D_4)(\mathbf{e}_3 \otimes \mathbf{e}_3) + [-2\Sigma_2 D_4$$
$$-\Sigma_3(D_2 + D_3)](\mathbf{e}_2 \otimes \mathbf{e}_3 + \mathbf{e}_3 \otimes \mathbf{e}_2),$$

$$[\Sigma]_{\mathrm{PRF}} = (\Sigma_4 \dot{\alpha})(\mathbf{e}_2 \otimes \mathbf{e}_2) + (-\Sigma_4 \dot{\alpha})(\mathbf{e}_3 \otimes \mathbf{e}_3)$$
$$+((\Sigma_3 - \Sigma_2)\dot{\alpha}(\mathbf{e}_2 \otimes \mathbf{e}_3 + \mathbf{e}_3 \otimes \mathbf{e}_2).$$

If $D_4 = (\dot{\gamma}_3 + \dot{\gamma}_3)D_2/J_3$ may be reduced to $\dot{\gamma}_3$, the components of $[\Sigma]_j$ are factorised by $\dot{\gamma}_3$, but that of $[\Sigma]_{\mathrm{PRF}}$ are factorised by a function or functional, as it has been stressed in Sec. 1.3.5.

3. Remarks on the definitions of the three basic sets of thermomechanical rates, of viscous type, of reversible type and of elastoplastic type, respectively

3.1. The viscous and reversible stress contributions

i. An Oldroyd-like viscous stress contribution is defined through the usual covariant pattern:

$$\mathbf{S}_\nu = \mathbf{S}_1 + \mathbf{S}_2; \qquad \mathbf{S}_2 = (\theta_2 \lambda_2) I_D \boldsymbol{\delta} + 2(\theta_2 \mu_2)\mathbf{D} = \eta_{02} I_D \boldsymbol{\delta} + 2\eta_{\delta 2}\mathbf{D}$$

associated with the unusual rate form:

$$[\partial S_1^{ij}/\partial t]\mathbf{hv}_i \otimes \mathbf{hv}_j = (1/\theta_\nu)[-S_1^{ij} + \eta_{01} I_D \delta^{ij} + 2\eta_{\delta 1} D^{ij}]\mathbf{hv}_i \otimes \mathbf{hv}_j$$

defined in the relevant PRF. Eliminating S_1 and S_2 one obtains the global form:

$$[\partial S_\nu^{ij}/\partial t] - \partial(\eta_{02} I_D \delta^{ij} + 2\eta_{\delta 2} D^{ij})/\partial t]\mathbf{hv}_i \otimes \mathbf{hv}_j$$
$$= (1/\theta_\nu)] - S_\nu^{ij} + (\eta_{01} + \eta_{02})D^{ij}]\mathbf{hv}_i \otimes \mathbf{hv}_j$$

and the associated splitting into isotropic and deviatoric forms:

$$\theta_\nu \dot{I}_\nu + I_\nu = [3(\eta_{01} + \eta_{02}) + 2(\eta_{\delta 1} + \eta_{\delta 2})I_D + \theta_\nu(3\eta_{02} + 2\eta_{\delta 2})\dot{I}_D,$$

$$\left[\theta_\nu \overset{\cdot}{\overline{S}}{}^{ij}_{\nu} + \overline{S}^{ij}_{\nu}\right] \mathbf{hv}_i \otimes \mathbf{hv}_j = \left[2(\eta_{\delta 1} + \eta_{\delta 2})\overline{D}^{ij} + \theta_\nu 2\eta_{\delta 2}\overset{\cdot}{\overline{D}}{}^{ij}\right] \mathbf{hv}_i \otimes \mathbf{hv}_j.$$

The thermomechanical rates have been already given (Sec. 1.2). Owing to the fact that the definition of the PRF $(M(x^k), \mathbf{hv}_i(M(x^k,t))$ is obtained through integration of an angular velocity with respect to the *fixed frame* $(0, \mathbf{e}_i)$, the only possible interesting invariance of the above constitutive pattern is that under *constant* rotation of the co-ordinates system z^k referred to the *fixed material reference frame* associated with $(0, \mathbf{e}_i)$.

Moreover, the boundary conditions are specified in the fixed frame $(0, \mathbf{e}_i)$ of the experimental machinery, whatever may be the underlying clue of the strategy of the loading. This specified program, actually "defined" in $(0, \mathbf{e}_i)$, is endowed with the above invariance.

The set [constitutive equations ; boundary conditions] is then endowed with the invariance introduced by W.A. FOCK [13].

ii. The simplest differential definition of the generalized Hooke law is:

$$\overset{\cdot}{S}{}^{ij}_{r}\mathbf{hr}_i \otimes \mathbf{hr}_j = (\lambda_r I_D \delta^{ij} + 2\mu_r D^{ij})\mathbf{hr}_i \otimes \mathbf{hr}_j; \qquad \dot{I}_r = (3\lambda_r + 2\mu_r) I_D;$$

$$\overset{\cdot}{\overline{S}}_r \mathbf{hr}_i \otimes \mathbf{hr}_j = 2\mu_r \overline{\mathbf{D}}$$

In order to obtain a diversity of qualitative simulations, it may be supplemented with:

$$\overset{\cdot}{S}{}^{ij}_{r}\mathbf{hr}_i \otimes \mathbf{hr}_j = [[\lambda_r + (2\mu_r/3)(1 - (Q/Q_0)^n)] I_D \delta^{ij}$$

$$+2\mu_r (Q/Q_0)^n D^{ij}]\mathbf{hr}_i \otimes \mathbf{hr}_j,$$

$$\dot{I}_r = (3\lambda_r + 2\mu_r) I_D; \qquad \overset{\cdot}{\overline{S}}{}^{ij}_{r}\mathbf{hr}_i \otimes \mathbf{hr}_j = 2\mu_r (Q/Q_0)^n \overline{\mathbf{D}},$$

$$Q^2 = \mathrm{tr}[(\overline{\Delta}^t_R \overline{\varepsilon})^2]; \qquad \overline{\Delta}^t_R \overline{\varepsilon} = \Delta^t_R \varepsilon - (1/3)\mathbf{G}\mathrm{tr}(\Delta^t_R \varepsilon);$$

$$2\Delta^t_R \varepsilon = \mathbf{G} - {}^t_R\,\mathbf{G},$$

for example, or with

$$\overset{\cdot}{S}{}^{ij}_{r}\mathbf{hr}_i \otimes \mathbf{hr}_j = \left(\lambda_r I_D \delta^{ij} + 2\mu_r D^{ij} + \overline{\beta}_r \overline{P}_r \overline{S}^{ij}_{R}\right) \mathbf{hr}_i \otimes \mathbf{hr}_j$$

$$\Rightarrow \dot{I}_r = (3\lambda_r + 2\mu_r) I_D;$$

$$\overset{\cdot}{\overline{S}}{}^{ij}_{r}\mathbf{hr}_i \otimes \mathbf{hr}_j = 2\mu_r \dot{\mathbf{D}} + \overline{\beta}_r \overline{P}_r \overline{\mathbf{S}}_r; \qquad \overline{P}_r = \mathrm{tr}(\overline{\mathbf{S}}_r \overline{\mathbf{D}});$$

$$\overline{\beta}_r = 2\mu_r / Q_0^2.$$

in the case where bounded stress states have to be simulated. The last form may be easily modified in order to obtain a classical "three stages" behaviour along the first loading paths. The thermomechanical rates have been already

given (Sec. 1.3.1). Concerning the question of invariance, the useful remarks are similar to those given above.

3.2. The pure hysteresis stress contribution

Some rather detailed analysis of the formal features of the tensorial pattern have been introduced recurrently (cf. particularly [5, 6] and [7]).

The basic features which are to be considered here are the following:

i. The definition is *built* in the Iliushin space, making use of the components in the PRF of the relevant tensors.

ii. For each stress (or strain) path it gives the corresponding strain (or stress) path.

iii. To a fixed rotation of the co-ordinate system referred to the testing machinery, is associated a rotation in the Iliushin space. Consequently, the question of invariance arises as stated above.

3.3. Remark concerning the boundary conditions specified in the fixed frame in order to study a pattern defined in the PRF

Regarding the complexity of the loading processes it is worth noting that the constitutive patterns defined in PRF do not result in more intricate problems than those following classical approaches. Let us consider an example of one-shear test, namely that performed in order to obtain, in the stress space, a deviatoric path along the circle: $I_s = Q_s - Q_0 = 0$. The path definition involving an invariant, one can make use of the components in the PRF or of the components in the fixed frame: the representations are identical. The complexity of the control stems from the classical geometrical non-linearity associated with finite strains: the rotation of the PRF is not involved.

Let us now consider a much more intricate case, namely the case of a path defined not only by relations which are invariant in the ordinary sense (such as $I_s = 0$, for example) but also by non-invariant relations between components in the PRF. In such a case, the rotation of the PRF is explicitly involved in order to obtain the relations of the above components with the components in the fixed frame and finally, with the forces on the facets of the material point. The complexity of the problem is of a standard level: well-founded approximations of the spin forms are useful. The last issue is all the more important that the strains are large because the classical geometrical nonlinearity is able to hide the genuine constitutive features. In the one-shear case, for example, the forces on the faces $n (n = 1, 2, 3)$ of the "cube" of dimensions $0 \leqslant x^k \leqslant 1$, $k = 1, 2, 3$,

$$\mathbf{F}^{(n)} = \mathbf{g}^i S_i^j \sqrt{g} \nu_j^{(n)} = \mathbf{g}^i S_i^j \sqrt{g} \delta_j^n,$$

the associated forces per unit area $\mathbf{f}^{(n)}$, and the normal and tangential components $p^{(n)}$ and $t^{(n)}$associated with the forces $\mathbf{f}^{(n)}$are indeed connected with the mixed stress components S_i^j in $(M, \mathbf{g}^i, \mathbf{g}_j)$, and with the stress components Σ_{kl} in $(0, \mathbf{e}_k)$ through the following equations:

$$\mathbf{f}^{(1)} = \mathbf{F}^{(1)}/J_2J_3 = \mathbf{g}^1 S_1^1 J_1; \qquad p^{(1)} = S_1^1 = \Sigma_{11}; \qquad t^{(1)} = 0,$$

$$\mathbf{f}^{(3)} = \mathbf{F}^{(3)}/J_1J_2 = \mathbf{g}^2 S_2^3 J_3 + \mathbf{g}^3 S_3^3 J_3;$$

$$p^{(3)} = S_3^3 - (2\gamma/J_2)S_2^3 = \Sigma_{33}; \qquad t^{(3)} = S_2^3 J_3/J_2 = \Sigma_{23},$$

$$\mathbf{f}^{(2)} = \mathbf{F}^{(2)}/J_1\sqrt{J_3^2 + 4\gamma^2} = (\mathbf{g}^2 S_2^2 + \mathbf{g}^3 S_3^2)(J_2J_3/\sqrt{J_3^2 + 4\gamma^2}),$$

$$p^{(2)} = S_2^2 - [(2\gamma J_2)/(J_3^2 + 4\gamma^2)]S_3^2; \qquad t^{(2)} = S_3^2[J_3J_2/(J_3^2 + 4\gamma^2)],$$

$$S_2^2 = \Sigma_{22} - \Sigma_{23}(2\gamma/J_3); \qquad S_3^3 = \Sigma_{33} + \Sigma_{23}(2\gamma/J_3); \qquad S_2^3 = \Sigma_{23}J_2/J_3,$$

$$S_3^2 = (\Sigma_{22} - \Sigma_{33})((2\gamma/J_3) + \Sigma_{23}[(J_3^2 - 4\gamma^2)/J_2J_3].$$

The geometry is involved (with $2\gamma/J_3$) in the relationships between $\Sigma_{22}, \Sigma_{33}, \Sigma_{23}, p^{(2)}$ and $t^{(2)}$, resulting in a noticeable experimental difficulty if one tries to perform accurately a path selected in the stress space of Iliushin associated with the stress definition in PRF. For the facets $n = 2$, intricate rate-form equation are involved.

4. Concluding remarks

A number of numerical simulations has been performed. It may be useful to give a brief account of the features of this study and of the results from now on available.

4.1. Features of a short span numerical study of homogeneous problems

i. The numerical study has been restricted as follows.

In order to suppress the effect of hardening one considers the pure hysteresis case such as $\mathbf{S} = \mathbf{S}_a$. Moreover, the global form of the pattern is strongly simplified, firstly because only its deviatoric part is of pure hysteresis form (its isotropic part being reversible), secondly because the plastic limit is as simple as possible, namely of Huber – von Mises type. The physical parameters are always $\lambda = 2\mu = 150$ GPa, $S_0 = 200$ MPa for the first order pattern, and $\alpha_0 = S_0/2\mu$, $R_0 = 4S_0/\mu$ concerning the definition of the PRF. Regarding the kinematics, only the one-shear case is implemented. Generally, the loading programmes are either such as $J_1 = J_2 = J_3 = 1$ or such as $S_1 = S_2 = 0$.

ii. All the loading programmes have been two-fold:

a) firstly, a preliminary irrotational loading is specified through $\gamma_3 = 0$ and Σ_3 increasing from zero towards a small fraction of S_0 : $\Sigma_3 = \pm S_0/n$ (in fact, $n = 2$, or 10, or 20, or 1000, or 10000);

b) secondly, a cyclic loading is performed (under the constant axial stress $\Sigma_3 = \pm S_0/n$ previously reached) through a cyclic shear $\gamma_3(\tau)$ on constant intervals, "symmetrical" or "not symmetrical" with respect to the origin of the shear axis.

iii. In order to compare the *thermomechanical* definition of the thermomechanical spin Ω_ϕ with an intuitive definition, each simulation has been performed two times, making use first of (1.11) and then of (1.16).

iv. The numerical study being not devoted to the identification of a well-specified actual material, a last simplification has been implemented trough the assumption $\dot{\alpha}_\delta = 0$, an assumption which is exactly verified only in the case $J_1 = J_2 = J_3 = 1$.

v. The case of loading involving "nonsymmetrical" cycles has been studied also under the stress control, namely under the conditions $S_1 = S_2 = 0$, and for the small traction $S_3 = S_0/10000$. Simulations have been performed for several values of the axial stress S_3 (for a unique set of cycles). The result is as follows: for large axial traction $S_3(S_0/2, S_0/10$, for example), the two definitions of the spin give the same ratchet, but for small $S_3(10^{-3}S_0$ or $10^{-4}S_0$, for example) the intuitive definition of the spin results in irrelevant effects.

vi. The same conclusion has been obtained in the case of a special stress control, of tri-traction type, which may be a priori able to reduce a ratchet effect existing under small axial traction (and even under small axial compression, of the order of $-10^{-4}S_0$). The stress control $S_1 = S_2 = S_0/100$, $S_3 = 10^{-4}S_0$ has been studied only in the case of a unique set of "symmetrical" cycles. The intuitive definition of the spin results in a "ratchet" effect of the first order magnitude, which is irrelevant to experimental evidence.

4.2. Provisional results

i. With the aid of the proposed pattern, the ratchet effect is hardening-independent and existing under zero axial load, or even under a small compression, in accordance with experimental evidence [14, 15].

ii. Saturation of the ratchet effect may be obtained after a suitable number of cycles (50 cycles; $\Sigma_3 = S_0/10$, cf. Fig. 6).

iii. In order to define the thermomechanical spin Ω_ϕ, a *thermomechanical* approach has proved to be effective up to now. Moreover, it allows to avoid the implementation of intricate approaches extracted from a general tensorial formalism, or the implementation of non-effective approaches based on some intuitive sketches.

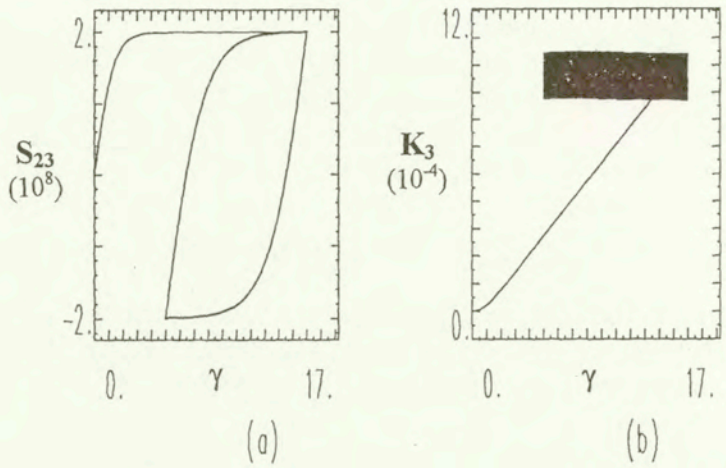

FIG. 6. Saturation of the ratchet after 50 cycles (initial traction $S_3 = S_0/10$).

4.3. Remark

One of the main gaps in the study is that concerning the features of the ratchet effect during demagnetization-like processes [7]. Some hints are already obtained, but this interesting issue has not been studied as yet (following, for example, the method proposed in [7]).

References

1. P. GUELIN, *Remarques sur l'hysteresis mécanique*, J. Mec. Th. et Appl., **19**, 2, 217–247, 1980.
2. P. GUELIN, W.K. NOWACKI and P. PEGON, *Etude des schémas thermomécaniques á mémoire discréte*, Arch. Mech. 37, 343–363, 1985.
3. P. PEGON and P. GUELIN, *On thermomechanical Zaremba schemes of hysteresis*, Res. Mech. Letters, 21–34, 1987.
4. D. FAVIER, P. GUELIN, A. TOURABI, B. WACK and P. PEGON, *Ecrouissages-Schémas thermomécaniques et á variables internes*, Arch. Mech., **40**, 5-6, 611–640, 1988.
5. P. PEGON, P. GUELIN and D. FAVIER, B. WACK and W.K. NOWACKI, *Constitutive scheme of discrete memory form for granular materials*, Arch. Mech., **43**, 1, 3–27, 1991.
6. A. TOURABI, P. GUELIN and D. FAVIER, *Towards the modelling of deformable ferromagnetics and ferroelectrics*, Arch. Mech., **47**, 3, 437–483, 1995.
7. A. TOURABI, P. GUELIN, D. FAVIER and W.K. NOWACKI, *From material discrete memory patterns to the study of demagnetization-like processes*, Arch. Mech., **49**, 4, 737–766, 1997.
8. A. TOURABI, P. GUELIN, B. WACK, P. PEGON, D. FAVIER and W.K. NOWACKI, *Useful scalar parameters for multiaxial fatigue deformations studies*, Fatigue Fract. Engng. Mater. Struct., 19-10, 1181–1195, 1996.

9. E. MADELUNG, *Über Magnetisierung durch Schnellverlaufende Ströme und die Wirkungweise des Rutherford-Marconischen Magnetdetektors*, Annalen der Physik, **17**, 861–890, 1905.

10. M. KLEIBER, *On errors inherent in commonly accepted rate forms of elastic constitutive law*, Arch. Mech., **38**, 271–279, 1986.

11. D. JEULIN, *Random models for the morphological analysis of powders*, Journal of Microscopy, **172**, 1, 13–21, 1993.

12. J. SERRA, *Image analysis and mathematical morphology*, Academic Press, London 1982.

13. W.A. FOCK, *Les principes physiques de la théorie de la gravitation d'Einstein*, Annales de l'Institut Henri Poincaré, **5**, 3, 205–215, 1966.

14. G. BLES, S.P. GADAJ, P. GUELIN, W.K. NOWACKI and A. TOURABI, *Thermomechanics of viscoplastic large strains and isotropic patterns of solid polymers*, submitted to Arch. Mech., Warsaw 1999.

15. A.S. LODGE, *Body tensor fields in continuum mechanics with applications to polymer rheology*, Academic Press, 1974.

16. P. PEGON and P. GUELIN, *Etude des schémas thermomécaniques á mémoire discréte: problémes aux limites en grandes déformations elastoplastiques*, Arch. Mech. **37**, 4-5, 465–483, 1985.

17. P. PEGON and P. GUELIN, *Finite strain plasticity in dragged along frames*, Int. J. Numer. Meth. in Eng., **39**, 245–285, 1983.

18. P. PEGON and P. GUELIN, *Implicit finite strain analysis in dragged along frames*, 5th Int. Symp. on Numerical Methods in Engineering, Lausanne 1989.

19. P. PEGON, W.K. NOWACKI, P. GUELIN, D. FAVIER and B. WACK, *From the modelling of granular media to the numerical study of the modes of bifurcations*, 2nd Int. Workshop on Num. Meth. for localization and bifurcation of granular bodies, 141–159, Eds. Dembicki, Gudehus, Sikora, Gdańsk 1989.

20. G. RIO, P.Y. MANACH and D. FAVIER, *Finite element simulation of shell and 3D mechanical behaviour of NiTi shape memory alloys*, Arch. Mech., **47**, 3, 537–556, 1995.

21. P.Y. MANACH, D. FAVIER and G. RIO, *Finite element simulations of internal stresses generated during the pseudoelastic deformation of NiTi bodies*, J. de Physique, **C1**, 6, 253–244, 1996.

22. T. INOUE, *Benchmark project on inelastic deformation and life prediction of 21/4 Cr-1 mo steel under multiaxial stresses*, Trans. 10th Int. Conf. on S.M.i.R.T., 141–152, 1989.

23. N. OHNO and J.-D. WANG, *Kinematic hardening rules with critical state of dynamic recovery, Parts* I *an* II. Int. J. of Plasticity, **9**, 375–403, 1993.

24. N. OHNO, *Current state of the art in constitutive modeling for ratchetting*, Trans. 14th Int. Conf. on S.M.i.R.T., LW/1, 201–212, 1997.

25. Z. XIA and F. ELLYIN, *A constitutive model with capability to simulate complex multiaxial ratchetting behaviour of materials*, Int. J. of Plasticity, **13**, 14/2, 127–142, 1997.

26. L. BRILLOUIN, *Qu'entend-on par systéme de référence en mécanique?* Mémoires de la Section des Sciences, Publications du Comité des Travaux Historiques et Scientifiques, Bibliothéque Nationale, Paris 1968.

27. W. ŚLEBODZIŃSKI, *Sur les Equations de Hamilton*, Bull. Acad. Roy. De Belg., **17**, 864–870, 1931.

28. M. ARIB and J.L. ILLE, *Toward an energetic model of ferromagnetic hysteresis*, Int. J. of Applied Electromagnetics and Mechanics, **8**(3), 273–284, 1997.

29. M. ARIB and J.L. ILLE, *Magnetoelastic couplings in ferromagnetic solids*, Int. J. of Applied Electromagnetics and Mechanics, **8**(4), 329–341, 1997.

30. M. ARIB, *Contribution á l'étude des interactions magnéto-mécaniques dans les ferromagnétiques solides*, Ph D., Univ. of Compiégne 1998.

31. I.D. MAYERGOYZ, *Mathematical models of hysteresis*, Springer, 1991.

32. I.D. MAYERGOYZ and G. FRIEDMAN, *Generalized preisach model of hysteresis*, I.E.E.E. Trans. Magn. 24, 212–217, 1988.

33. A. VISINTIN, *Differential Models of Hysteresis*, Springer, 1994.

34. M. BROKATE, K. DRESSLER and P. KREJCI, *The Mroz model: a hysteresis operator for rate-independent plasticity*, Proc. of World Congress of Nonlinear Analysis, Tampa 1992.

35. M. BROKATE, N. KENMOCHI, I. MULLER, J.F. RODRIGUEZ and C. VERDI, Phase transitions and hysteresis, Springer-Verlag, 1994.

Received October 29, 1998; new version February 26, 1999.

Arch. Mech., **51**, 3–4, pp. 391–397, Warszawa 1999

Foundations of mechanics of corroding materials

T.J. HOFFMANN and B. NIECHCIAŁKOWSKA

Poznań University of Technology
Institute of Applied Mechanics, Poznań, Poland

IN THIS PAPER the basic principles of mechanics concernning the balance laws of the corrosion process models are presented. The corrosion process has been described by a linear law of creation of the oxide layer using a single corrosive rate constant. The mass defect is neglected in the balance law of mass. In the balance of momentum, the corrosion processes are treated as a source of the additional compressive stresses. The kinematic magnitudes are treated independently of the corrosion processes. This approach is based on the infinitesimal strains and linear constitutive equations. Two linear versions of the theory, which are from the formal point of view certain variants of the Coupled Fields Theory, have been proposed. The first of them includes the corrosive term in the displacement equation of motion and has no mechanical term in the equation of corrosion. The second of them contains the coupling terms, both in the equation of motion and in the equation of corrosion.

1. Introduction

PROCESS OF CORROSION plays a negative role in technology and it is a source of economical losses. The costs which people have to pay for protection against corrosion are high and they are not justifiable from the economical viewpoint. The economical aspect of the mentioned problem is not only limited to the loss of the materials, but it is mainly connected with the necessity of permanent replacement of the corroded elements of the constructions. The corrosion processes lead to degradation of the materials and reduce their capability of transferring the loads.

Fast development of the modern technology creates the increasing requirements concerning the metallic constructions which are assumed to work in various oxidation environments. In the modern chemical industry, where the elements of construction are exposed to the action of the gases and vapours, the gaseous corrosion of the metals has particularly drastic forms. The car, aircraft and space industry as well as nuclear technologies require the use of materials of the appropriate mechanical properties.

Speaking in short words, we can say that the corrosion processes increase forces and tensions which are transferred through the parts of machines and the elements of structures. When we take into consideration the basic chemical

reactions, it is possible to model the influence of the corrosion process on the loss of the mass of the materials which transfer the loads.

In this paper, the basic principles of mechanics in the concept of the balance laws [1, 2] are presented taking into consideration the model of the corrosion process. The corrosion process has been described by a linear law of the oxidised layer creation using a single corrosive rate constant [3, 4, 5]. The mass loss is neglected in the balance law of mass. In the balance of momentum, the corrosion processes are treated as a source of the additional compressive stresses. From the formal point of view, the compression stresses are introduced as the additional, external field forces. In the presented model of the corrosion processes, the classical symmetry of the stress tensor follows from the balance of moment of momentum. It is worth to remember that the theoretical and experimental results confirm the influence of the mechanical stresses on the corrosive rate constants. It means that the corrosion and mechanical processes can be treated as coupled fields in the formal description.

2. Basic equations

From the point of view of mechanics of materials it seems convenient to create the theory using the laws of the balance of mass, of momentum and of moment of momentum.

Let us consider the body B which occupies space $\tau(B)$. The surface $S(B)$ is the fringe of the space τ. We will take advantage of the general equation of the balance formulated by KOSIŃSKI [2]:

$$\frac{d}{dt}\Psi = -W(\Psi) + P(\Psi) + R(\Psi). \tag{2.1}$$

In Eq. (2.1) the symbols have the following meaning: $W(\Psi)$ – is the outflow of the quantity Ψ through the fringe of the space τ, $P(\Psi)$ – is the creation of the quantity Ψ inside the space τ, $R(\Psi)$ – is the inflow of the quantity Ψ to the space τ from the surroundings.

The quantity R is very often assumed to be equal to zero, thus in this paper we will make the same assumption.

The law of the balance has to be fulfilled for the body B and for each subsystem. The physical quantities in Eq. (2.1) are generally described by means of the proper constitutive equation.

The balance of mass is assumed to be expressed by the equation of the conservation law [1]:

$$\frac{d}{dt}\int_{\tau} \rho d\tau = 0, \tag{2.2}$$

where ρ is mass density.

The balance of momentum can be expressed as follows:

$$\frac{d}{dt}\int_{\tau}\rho v_k d\tau = \oint_{S} t_{kl} dS_1 + \int_{\tau}\rho f_k d\tau, \tag{2.3}$$

where v_k is the velocity, t_{kl} is the stress and f_k is the body force.
The balance of the moment of momentum leads to the conclusion that the stress tensor is the symmetric tensor [1]:

$$t_{kl} = t_{lk}. \tag{2.4}$$

We will neglect the balance of energy since we do not consider the thermodynamic aspects of the investigated processes.

3. Model of the mass defect

In the studies of the corrosion of materials [4, 5], the laws of the growth of the layer thickness of the corrosive product are formulated and they can be interpreted as the constitutive law for the quantity $P(\Psi)$ in the Eq. (2.1) with Ψ as mass. Generally speaking, in such a study the polynomial laws can be expressed in the form

$$P(m) = \sum_{i=1}^{u} k_i (m)^i, \tag{3.1}$$

m being the mass. For simplicity we will assume the linear law as follows:

$$P(m) = -\nu I m = -\alpha m, \tag{3.2}$$

where symbols denote: ν – the stechiometric coefficient, I – reaction rate constant, $\alpha = \nu I$, and they correspond to the linear chemical reaction [3].
In such a case the balance of mass is expressed by the integral formula:

$$\frac{d}{dt}\int_{\tau}\rho d\tau = -\alpha\int_{\tau}\rho d\tau, \tag{3.3}$$

and the corresponding differential formula has the following form:

$$d_t\rho + \rho\partial_k v_k = -\alpha\rho, \tag{3.4}$$

where d_t is the material derivative and ∂_k is the space derivative. The application of the balance of mass (3.3) and (3.4) to the balance of momentum (2.3) enables us to obtain the local balance of momentum in the form:

$$\rho d_t v_k = \partial_l t_{kl} + \alpha\rho v_k + \rho f_k. \tag{3.5}$$

Moreover, it is found that the balance of the moment of momentum has not changed and has the form of Eq. (2.4). The balance of momentum (Eq. (3.5)) is the classical differential equation of motion, however the term on the right-hand side with the coefficient α is due to the mass defect (Eqs. (2.3) and (2.4)).

Let us assume now that we consider the isotropic, elastic material which is described by the Hooke's law:

$$t_{kl} = 2\mu\varepsilon_{kl} + \lambda\delta_{kl}\varepsilon_{rr}, \tag{3.6}$$

where: λ, μ, are the Lamé elastic constants, δ_{kl} is the Kronecker delta, $2\varepsilon_{kl} = \partial_k k u_l + \partial_l u_k$ is the infinitesimal strain tensor and u_k is the displacement vector.

By substitution of Eq. (3.6) to Eq. (3.5) we will obtain the Lamé displacement equations:

$$c_T^2 \partial_s \partial_s u_r + (c_L^2 - c_T^2)\partial_r \partial_s u_S + \alpha_t \partial_t u_r = \partial_t \partial_t u_r, \tag{3.7}$$

where $c_T^2 = \mu/\rho$, $c_L^2 = (\lambda + 2\mu)/\rho$ and it is assumed that $f_k = 0$.

Symbols c_T and c_L denote the transverse and longitudinal wave phase velocity, respectively. Let us assume that perturbation depends only on the one space co-ordinate and time:

$$u_r = u_r(x_1, t), \qquad r = 1, 2, 3...$$

Then Eq. (3.7) has a form:

$$\begin{aligned} c_L^2 \partial_1^2 u_1 + \alpha \partial_t u_1 &= \partial_t^2 u_1, \\ c_T^2 \partial_1^2 u_2 + \alpha \partial_t u_2 &= \partial_t^2 u_2, \\ c_T^2 \partial_1^2 u_3 + \alpha \partial_1 u_3 &= \partial_1^2 u_3. \end{aligned} \tag{3.8}$$

On the basis of Eq. (3.8) we can draw the conclusion that both the longitudinal and transverse perturbations undergo the modification which is connected with the mass defect. In the asymptotic case when α approaches zero, one obtains the classical equation of perturbation. Taking into account the general character of this paper, we will not explore this problem any further.

4. Model of additional stresses

Now we will present another model of the chemical reaction which describes the corrosion processes. Let us suppose that the mass defect is sufficiently small and can be neglected in the balance equation of mass, and that the corrosion processes create the particular centres on the surface of the body which contribute to the balance of momentum. The corrosion process can be described as the

chemical reaction by the progress variable. Time derivative describes the reaction rate. We assume that the progress variable and the reaction rate are the time-space fields. The progress variable can be expressed as

$$z = z(x_i, t),$$

and the rate of reaction as

$$I(x_i, t) = \partial_t z(x_i, t).$$

The contribution of the corrosive processes in the balance of momentum is described by the scalar function of the progress variable which can be expressed as a surface source in the form:

$$\frac{d}{dt}\int_\tau \rho v_k d\tau = \oint_S P(z)\delta_{kl} dS_l + \oint t_{kl} dS_l + \int_\tau \rho f_k d\tau. \tag{4.1}$$

Using the standard approach, the local balance of momentum can be expressed in the following differential form:

$$\rho d_t v_k = \partial(t_{kl} + P(z)\delta_{kl}) + \rho f_k. \tag{4.2}$$

From Eq. (4.2) it is easily seen that the extended stress tensor:

$$T_{kl} = t_{kl} + P(z)\delta_{kl}, \tag{4.3}$$

can be used in our theoretical approach. On the basis of the balance of moment of momentum we can show that the extended stress tensor is a symmetric tensor:

$$T_{pk} = T_{kp}. \tag{4.4}$$

We will postulate the evolution equation of the corrosive rate in the simple form [1]:

$$\partial_t z = \frac{1}{\tau_r} z + r(I_1, I_2, I_3), \tag{4.5}$$

where τ_r is the relaxation time of the corrosion process and r is the function of invariants of strain, I_1, I_2, I_3. Introduction of the r function means that one takes into account the influence of the strain on the corrosion processes.

In order to formulate this problem as a linear problem, we will make the following assumptions:

1. The corrosion process is stable; it means that the relaxation time approaches infinity.

2. The corrosive rate is the linear function of the first invariant of strain, i.e. it is the linear function of the relative volume change.

3. The corrosion source of momentum is linearly dependent on the progress variable.

The above assumptions can be formulated as: relaxation time $\tau_r \to \infty$, the evolution equation of the corrosive rate

$$\partial_t z = AI_l = |A\frac{\Delta\tau}{\tau} = A\varepsilon_{kk} = A\partial_k u_k, \tag{4.6}$$

where A is constant.

The corrosion source of momentum can be expressed by

$$P(z) = \gamma z, \tag{4.7}$$

where γ is constant.

On the basis of the above equation and Eq. (4.3), we obtain the extended stress tensor in the form

$$\tau_{kl} = 2\mu\varepsilon_{kl} + (\lambda\varepsilon_{rr} + \gamma z)\delta_{kl}. \tag{4.8}$$

It leads to the displacement equations:

$$c_T^2\partial_s\partial_s u_r + (c_L^2 - c_T^2)\partial_r\partial_s u_s + g\partial_r z = \partial_t\partial_t u_r, \tag{4.9}$$

where $g = \gamma/\rho$.

The evolution equation of the corrosive rate (4.6) and displacement Eqs. (4.9) form the set of equations which describe the coupled fields of displacement and progress variable.

In the one-dimensional particular case:

$$u_r = u_r(x_1, t), \qquad z = z(x_1, t), \tag{4.10}$$

we obtain

$$c_L^2\partial_1\partial_1 u_1 + g\partial_1 z = \partial_t\partial_t u_1, \tag{4.11}$$

$$\partial_t z = A\partial_1 u_1, \tag{4.12}$$

$$c_T^2\partial_1\partial_1 u_2 = \partial_t\partial_t u_2, \tag{4.13}$$

$$c_T^2\partial_1\partial_1 u_3 = \partial_t\partial_t u_3. \tag{4.14}$$

It is easily noticed that the coupled problem concerns only the voluminal strains (Eqs. (4.11) and (4.12)). In other words, in the assumed model, perturbation of the displacement u_1 is coupled with the corrosion effects. The transverse perturbations u_2 and u_3 are independent of these effects. It is the result of the previous Assumption 2 that the corrosive rate depends on the relative change

of the volume only. On the basis of the assumptions made it is not possible to obtain addditional coupled effects.

5. Concluding remarks

The presented models of the corrosion, the model of the mass defect and the model of the additional stresses, are qualitatively different. They differ from each other in the character of coupling between the field of displacement and the corrosion effects. To stress the character of the two models, one-dimensional problems are formulated. In Eqs. (3.8) of the model of the mass defect, the α parameter which describes the corrosion process is present in all equations, both in the longitudinal perturbation and in the transverse perturbation.

In the model of the additional stresses, the coupling between the voluminal strain and the progress variable is shown (Eqs. (4.11) and (4.12)). Eqs. (4.13) and (4.14) do not show such a coupling. The obtained results open the field for the further investigations.

It seems that the model of the additional stresses creates more possibilities by introducing fewer simple assumptions. It is obvious that it is possible to complete the evolution Eqs. (4.6) by further invariants of the strain tensor and with the relaxation time.

Acknowledgements

The paper was supported by the Poznań University of Technology TB 21 – 880/99 DS.

References

1. C. RYMARZ, *Mechanics of continuous media* (in Polish), PWN, Warszawa 1993.
2. W. KOSIŃSKI, *Introduction to singularities field theory and analysis of waves* (in Polish), PWN, Warszawa–Poznań 1981.
3. B. BARANOWSKI, *Non-equilibrium thermodynamics in physical chemistry* (in Polish), PWN, Warszawa 1974.
4. S. MROWEC and T. WEBER, *Gaseous corrosion of metals* (in Polish), Wydawnictwo Śląsk Katowice 1976.
5. H. SCHMALZRIED, *Solid state reactions* (in Polish), PWN Warszawa 1976.

Received December 16, 1998; revised version August 4, 1999.

Arch. Mech., **51**, 3–4, pp. 399–418, Warszawa 1999

Stochastic finite element analysis of transient heat transfer in composite materials with interface defects

M. KAMIŃSKI[1] and T.D. HIEN[2]

[1] *Division of Mechanics of Materials, Faculty of Civil Engrng., Arch. and Env. Engrng. Technical University of Łódź, Al. Politechniki 6, 93–590 Łódź, POLAND*

[2] *Institute of Ocean and Ship Technology, Technical University of Szczecin, Al. Piastów 41, 71–065 Szczecin, POLAND*

THE PAPER PRESENTED is devoted to the application of the probabilistic computational analysis based on the stochastic finite element methods in the transient heat transfer problems; the field of application of the method introduced is the mechanics of composite materials.The composite materials considered have randomly defined thermal characteristics and, moreover, the interface discontinuities appearing between constituents have a probabilistic character. The influence of all these parameters on the first two probabilistic moments of temperature are verified on the example of a two-component layered composite with an interphase between the constituents.

1. Introduction

IT HAS BEEN PROVED by the numerous theoretical considerations and computational experiments that randomness of the material properties as well as geometrical parameters of the structural defects play a crucial role in the overall behaviour of solids. It is especially visible in the field of composite materials where the quality of bonds between the constituents in the context of some micro- or even macro-defects [13] may be decisive for the whole composite structure as it was proved for stochastic elastostatics of fiber-reinforced composite problems [6].

The paper is devoted to the probabilistic computational analysis of composite materials. The field of interest is the transient heat transfer phenomena, expected values of temperature as well as spatial and time cross-covariances. The mathematical model of the interface is based on the "bubble" model introduced in [6 – 8] where the defects have the form of semicircles lying with their diameters on the interface boundary. This strictly theoretical interface is replaced, taking into account the needs of numerical analysis, with the interphase containing all such defects. The interphase has the boundaries parallel to the original

interface and thermal properties inserted together with structural defects into its region. The variational statement of the problem is formulated on the basis of the second order perturbation, second central probabilistic moment version of the classical transient formulation of the virtual temperatures principle. Starting from such variational equations of the zeroth, first and second order, the respective stochastic finite element equations containing the probabilistic characteristics of component materials thermal characteristics as well as interphase parameters are derived. The numerical procedure built up starting from such a model enables us to perform computational experiments with the transient heat transfer in stochastically defected composite materials. It is important to stress that all the considerations provided within the paper are valid for the stochastic linear potential field problems in electrostatic, magnetic as well as hydraulic fields [1, 15]. The approach proposed is illustrated by the example of two-component stratified composite including the interphase located between the constituents.

Finally, it should be mentioned that further computational studies on these phenomena are to be performed. Especially recommended are the stochastic sensitivity studies of the problem to verify the influence of material parameters and interface defects on overall thermal behaviour of different composite structures (stratified, fiber-reinforced or structures with periodic as well as nonperiodic geometry [6]).

2. Mathematical model

2.1. Transient heat transfer equation in composite materials

Generally, transient heat transfer problem consists in determining the temperature field T governed by the following differential equation [2]:

$$\rho c\dot{T} - (\lambda_{ij}T_{,j})_{,i} - g = 0; \qquad x_i \in \Omega; \qquad \tau \in [0, \infty), \tag{2.1}$$

where $c = c(T)$ is the heat capacity characterizing the region Ω and being a temperature-dependent variable of the problem. Further, $\rho = \rho(T)$ is the density of the material contained in Ω, $\lambda_{ij} = \lambda_{ij}(T)$ is the thermal conductivity tensor while $g = g(T)$ is the rate of heat generated per unit volume; τ denotes time. This equation should fulfill the boundary conditions on $\partial\Omega$ being a continuous and sufficiently smooth contour bounding the Ω region. The boundary conditions discussed for (2.1) are as follows:

1) temperature (essential) boundary conditions

$$T = \hat{T}; \qquad x \in \partial\Omega_T, \tag{2.2}$$

and for $\partial\Omega_q$ part of the total $\partial\Omega$:

2) heat flux (natural) boundary conditions

$$\frac{\partial T}{\partial n} = \hat{q}; \qquad x \in \partial\Omega_q, \tag{2.3}$$

where $\partial\Omega_T \cup \partial\Omega_q = \partial\Omega$ and $\partial\Omega_T \cap \partial\Omega_q = \{\oslash\}$.

3) Initial conditions have the following form:

$$T^0 = T(x_i; 0); \qquad x_i \in \Omega, \quad \tau = 0. \tag{2.4}$$

Further, let Ω contains n coherent and disjoint subregions Ω_a for $a = 1, ..., n$ fulfilling the following conditions

$$\Omega = \bigcup_{a=1}^{n} \Omega_a; \quad \Omega_a \cap \Omega_b = \oslash; \quad a \neq b; \quad 1 \leqslant a, b \leqslant n. \tag{2.5}$$

Thus, all material parameters, denoted by f in the equation presented below, characterizing the composite structure considered (variables ρ, c, g, λ), can be described as

$$f = \chi_a f^{(a)}; \quad 1 \leqslant a \leqslant n, \tag{2.6}$$

where χ_a is a characteristic function given as follows:

$$\chi^{(a)} = \begin{cases} 1; & x \in \Omega_a, \\ 0; & x \notin \Omega_a. \end{cases} \tag{2.7}$$

Including Eqs. (2.6) and (2.7) in the formulation given by the formula (2.1) it is obtained that

$$\chi_a \rho^{(a)} \chi_a c^{(a)} T - \left(\chi_a \lambda_{ij}^{(a)} T_{,j}\right)_{,i} - \chi_a g^{(a)} = 0; \tag{2.8}$$

$$x_i \in \Omega; \quad \tau \in [0, \infty).$$

Considering the fact that

$$\chi_a \chi_a = \chi_a^2 = \chi_a, \tag{2.9}$$

we obtain finally that

$$\chi_a \left(\rho^{(a)} c^{(a)} T - \left(\lambda_{ij}^{(a)} T_{,j}\right)_{,i} - g^{(a)}\right) = 0; \qquad x_i \in \Omega; \quad \tau \in [0, \infty). \tag{2.10}$$

The example of the composite structure considered is shown below in Fig. 1.

Let us suppose that all material parameters of the composite considered are uncorrelated, bounded random variables defined uniquely by their first two probabilistic moments as follows:

$$0 < \rho < \infty, \tag{2.11}$$

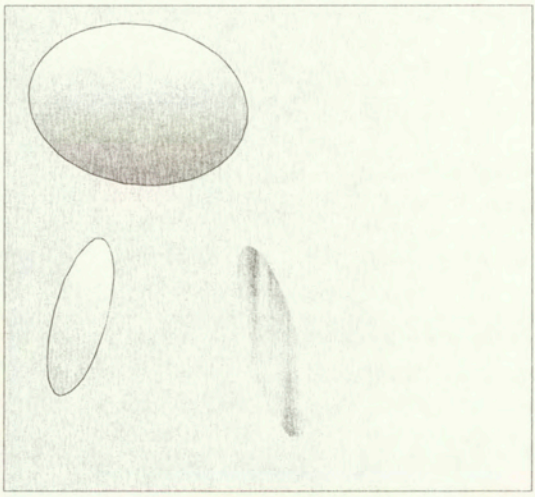

FIG. 1. The n-component composite structure.

$$E[\rho] = \chi_a E[\rho^{(a)}]; \qquad 1 \leqslant a \leqslant n, \tag{2.12}$$

$$\mathrm{Var}(\rho) = \chi_a \mathrm{Var}(\rho^{(a)}); \qquad 1 \leqslant a \leqslant n, \tag{2.13}$$

where $E[\rho]$ and $\mathrm{Var}(\rho)$ are the expected value and the variance of material density, respectively, which can be calculated by means of the following definitions given in Eqs. (2.14) and (2.15):

$$E\left[\rho^{(a)}(x_i)\right] = \int_{-\infty}^{+\infty} \rho^{(a)}(x_i) p(\rho^{(a)}) d\rho, \tag{2.14}$$

$$\mathrm{Var}\left(\rho^{(a)}(x_i)\right) = \int_{-\infty}^{+\infty} \left(\rho^{(a)}(x_i) - E\left[\rho^{(a)}(x_i)\right]\right)^2 p(\rho^{(a)}) d\rho. \tag{2.15}$$

Analogically, we obtain for the random variable of the heat capacity

$$0 < c < \infty, \tag{2.16}$$

$$E[c] = \chi_a E\left[c^{(a)}\right]; \qquad 1 \leqslant a \leqslant n, \tag{2.17}$$

$$\mathrm{Var}(c) = \chi_a \mathrm{Var}\left(c^{(a)}\right); \qquad 1 \leqslant a \leqslant n, \tag{2.18}$$

and the random conductivity tensor components

$$0 < \lambda_{ij} < \infty; \qquad i, j = 1, 2, 3, \tag{2.19}$$

$$E[\lambda_{ij}] = \chi_a E\left[\lambda_{ij}^{(a)}\right]; \qquad 1 \leqslant a \leqslant n, \tag{2.20}$$

$$\mathrm{Var}\,(\lambda_{ij}) = \chi_a \mathrm{Var}\left(\lambda_{ij}^{(a)}\right); \qquad 1 \leqslant a \leqslant n, \tag{2.21}$$

what completes the stochastic description of physical properties of the composite constituents. The mathematical proof that the solution of Eq. (2.10) exists and is unique may be done on the basis of the considerations provided in [3].

2.2. An idea of the stochastic interface defects

Let the material with indices a contains the stochastic structural interface defects. These defects are be modeled further as semicircles placed with their diameters on the boundary between the composite constituents. Moreover, we assume that the total number of these defects as well as their diameter are Gaussian random variables defined uniquely by their expected values and variances. Spatial averaging or computation of effective characteristics for materials containing voids of some specific shapes may be done in general in different ways [5], however we use the spatial averaging method. Due to that method, we can derive the effective thermal property of the region containing defects as follows [6]:

$$\lambda^{\mathrm{eff}} = \frac{\Omega_d}{\Omega_i}\lambda_d + \frac{\Omega_i - \Omega_d}{\Omega_i}\lambda_i, \tag{2.22}$$

where Ω_i is a region considered for which the effective parameter λ^{eff} is computed, Ω_d denotes the total area of the defects lying in the interior of the region Ω_i, while λ_d and λ_i denote the conductivity coefficients of the regions Ω_d and Ω_i, respectively. The geometrical idealization of the stochastic interface defects for the fiber-reinforced composites is presented in Figs. 2 and 3, while for the laminated structure in Figs. 4 and 5.

Next, let us assume that r and n are random variables of the radii and the total number of the defects considered, thus Ω_d and, at the same time λ^{eff}, can be evaluated as follows:

$$\Omega_d = \frac{1}{2}\Pi n r^2, \tag{2.23}$$

and

$$\lambda^{\mathrm{eff}} = \frac{\Pi}{2\Omega_i} n r^2 \lambda_d + \frac{\Omega_i - \frac{1}{2}\Pi n r^2}{\Omega_i}\lambda_i = \frac{\Pi}{2\Omega_i} n r^2 \lambda_d + \left(1 - \frac{\frac{1}{2}\Pi n r^2}{\Omega_i}\right)\lambda_i. \tag{2.24}$$

Starting from the formula (2.24), the partial derivatives of the first and the second order of the effective conductivity coefficient can be evaluated with respect to the variables r and n. Thus we have

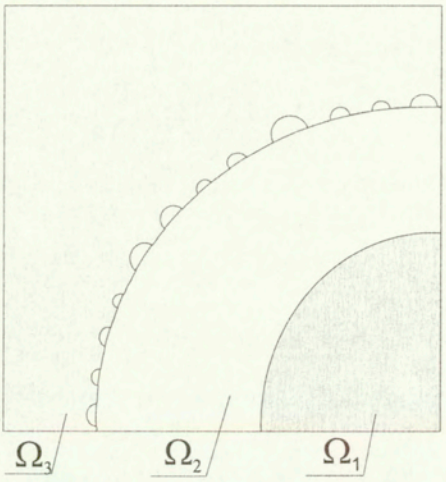

FIG. 2. Interface micro-geometry of fiber-reinforced composite.

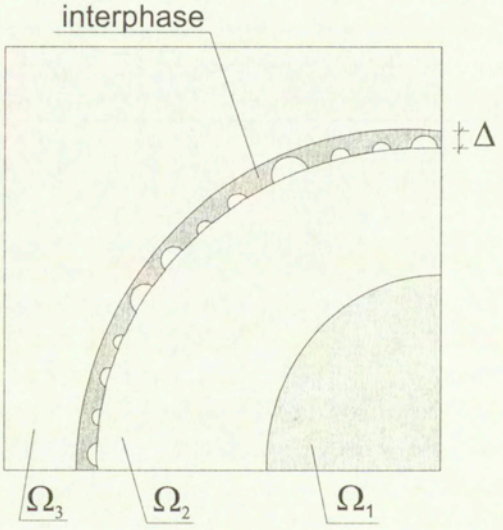

FIG. 3. Interface defects in fiber-reinforced composite.

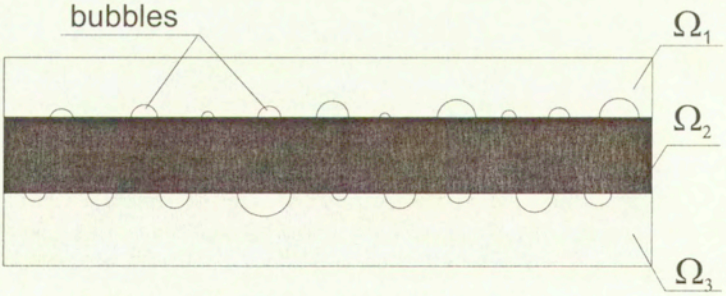

FIG. 4. Outline of the interface for stratified composite.

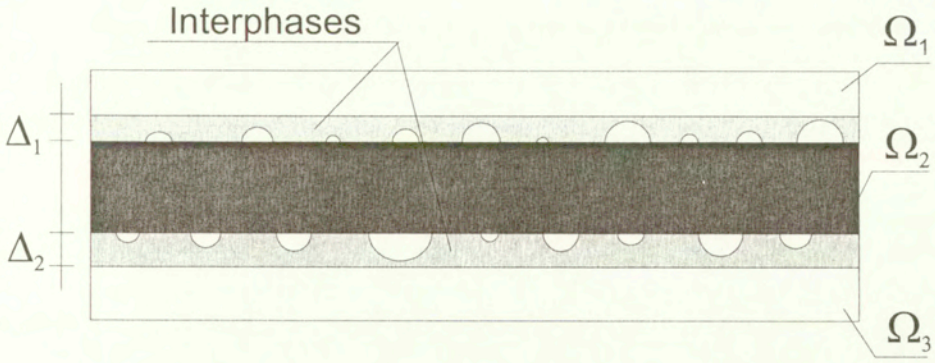

FIG. 5. Interface micro-geometry of stratified composite.

$$\frac{\partial \lambda^{\text{eff}}}{\partial \lambda_d} = \frac{\Pi}{2\Omega_i} n r^2, \tag{2.25}$$

$$\frac{\partial^2 \lambda^{\text{eff}}}{\partial \lambda_d^2} = 0, \tag{2.26}$$

$$\frac{\partial \lambda^{\text{eff}}}{\partial \lambda_i} = 1 - \frac{\Pi n r^2}{2\Omega_i}, \tag{2.27}$$

$$\frac{\partial^2 \lambda^{\text{eff}}}{\partial \lambda_i^2} = 0, \tag{2.28}$$

$$\frac{\partial \lambda^{\text{eff}}}{\partial n} = \frac{\Pi r^2}{2\Omega_i}(\lambda_d - \lambda_i), \tag{2.29}$$

$$\frac{\partial^2 \lambda^{\text{eff}}}{\partial n^2} = 0, \tag{2.30}$$

$$\frac{\partial \lambda^{\text{eff}}}{\partial r} = \frac{\Pi n r}{\Omega_i}(\lambda_d - \lambda_i), \tag{2.31}$$

$$\frac{\partial^2 \lambda^{\text{eff}}}{\partial r^2} = \frac{\Pi n}{\Omega_i}(\lambda_d - \lambda_i). \tag{2.32}$$

By analogous way we derive the effective values of heat capacity as well as material density for the composite components. The derivatives calculated above will be used next in the canonical formulation of the Stochastic Finite Element Method approach to the problem presented below.

2.3. Variational formulation of the problem

Let us consider any continuous temperature variations $\delta T(x_i)$ defined in the interior of the region Ω and vanishing on $\partial\Omega_T$. Multiplying Eq. (2.10) by the test function specified and integrating over Ω, we obtain

$$\int_{\Omega} \chi_a \left(\rho^{(a)} c^{(a)} T - \left(\lambda_{ij}^{(a)} T_{,j} \right)_{,i} - g^{(a)} \right) \delta T d\Omega = 0; \quad 1 \leqslant a \leqslant n; \tag{2.33}$$

$$x_i \in \Omega; \qquad \tau \in [0, \infty).$$

Taking into account that the derivative defined on the temperature variation is in fact a variation of the respective temperature derivative

$$\frac{\partial(\delta T)}{\partial x_i} = \delta \left(\frac{\partial T}{\partial x_i} \right) \equiv \delta T_{,i} \, , \tag{2.34}$$

we can arrive at

$$\int_{\Omega} \chi_a \left(\rho^{(a)} c^{(a)} T \delta T - \left(\lambda_{ij}^{(a)} T_{,j} \delta T \right)_{,i} - \left(\lambda_{ij}^{(a)} T_{,j} \right) \delta T_{,i} - g^{(a)} \delta T \right) d\Omega = 0; \tag{2.35}$$

$$1 \leqslant a \leqslant n; \qquad x_i \in \Omega; \qquad \tau \in [0, \infty), \, .$$

Introducing the respective heat transfer boundary conditions

$$\int_{\Omega} \left(\lambda_{ij} T_{,j} \delta T \right)_{,i} d\Omega = \int_{\partial\Omega} \lambda_{ij} T_{,j} n_{,i} \delta T d(\delta\Omega) = \int_{\partial\Omega_q} \hat{q} \delta T d(\partial\Omega) \tag{2.36}$$

and integrating by parts, we obtain

$$\int_{\Omega} \chi_a \left(\rho^{(a)} c^{(a)} \dot{T} \delta T + \lambda_{ij}^{(a)} T_{,j} \delta T_{,i} - g^{(a)} \delta T \right) d\Omega \tag{2.37}$$

$$- \int_{\partial\Omega_q} \hat{q} \delta T d(\partial\Omega) = 0; \qquad 1 \leqslant a \leqslant n; \qquad x_i \in \Omega; \tau \in [0, \infty).$$

The equation stated above is the transient formulation of the principle of virtual temperatures. This principle is discretized in the next section by the use of the finite element approach.

2.4. Stochastic perturbation technique

The stochastic variational principle for linear transient heat transfer problems is formulated on the basis of Eq. (2.37) and is employed by the combination of

the second-order perturbation technique and second-moment stochastic analysis [4, 6, 9].

To provide the formulation let us denote the random variable vector of the problem by $\{b^r(x;\omega)\}$ and the probability densities of its components by $g(b^r)$ and $g(b^r, b^s)$, respectively. Indices r, s are running from 1 to R, where R denotes the total number of random vector components. The expected value of the vector $\{b^r(x;\omega)\}$ can be thus expressed by

$$E[b^r] = \int_{-\infty}^{+\infty} b^r g(b^r) db^r, \tag{2.38}$$

while the covariance is equal to

$$\mathrm{Cov}(b^r, b^s) = \int_{-\infty}^{+\infty}\int_{-\infty}^{+\infty} (b^r - E[b^r])(b^s - E[b^s]) g(b^r, b^s) db^r db^s. \tag{2.39}$$

The coefficient of variation of the random vector components is derived in the form

$$\alpha[b(x;\omega)] = \sqrt{\frac{\mathrm{Var}[b(x;\omega)]}{E^2[b(x;\omega)]}}. \tag{2.40}$$

Next, let us expand all the random variables into the Taylor series. According to the method, all functions of the problem (heat conductivity, heat capacity, temperature and its gradient as well as the material density) are expressed in the form similar fo the following expansion of function F:

$$F(x) = F^0(x) + \theta F^{,r}(x)\Delta b^r + \frac{1}{2}\theta^2 F^{,rs}(x)\Delta b^r \Delta b^s, \tag{2.41}$$

where θ is a given small perturbation, $\theta\Delta b^r$ denotes the first order variation of b_r from its expected value

$$\theta\Delta b^r = \delta b_r = \theta\left(b_r - b_r^0\right), \tag{2.42}$$

while the second variation is given as follows:

$$\theta^2\Delta b^r \Delta b^s = \delta b_r \delta b_s = \theta^2\left(b_r - b_r^0\right)\left(b_s - b_s^0\right). \tag{2.43}$$

Moreover, symbols $(.)^0, (.)^{,r}$ and $(.)^{,rs}$ represent the expected value, the first and the second partial derivatives with respect to the random variables evaluated at the expected values of input random parameters.

According to the second-order perturbation technique [4, 9], the expansion (2.41) is now substituted in the formulation (2.37). As the result, we obtain the three sets of algebraic equations of 0th, 1st and 2nd order. Hence we have:

- one zeroth-order partial differential equation

$$\int_{\Omega} \chi_a \left(\rho^{(a)0} c^{(a)0} T^0 \delta T + \lambda_{ij}^{(a)0} T_{,j}^0 \delta T_{,i} \right) d\Omega = \int_{\partial\Omega_q} \hat{q}^0 \delta T d(\partial\Omega) + \int_{\Omega} \chi_a g^{(a)0} \delta T d\Omega, \tag{2.44}$$

- R first-order partial differential equations, $r = 1, 2, ..., R$:

$$\int_{\Omega} \chi_a \left(\rho^{(a)0} c^{(a)0} T^{,r} \delta T + \lambda_{ij}^{(a)0} T_{,j}^{,r} \delta T_{,i} \right) d\Omega = \int_{\partial\Omega_q} \hat{q}^{,r} \delta T d(\partial\Omega) + \int_{\Omega} \chi_a g^{(a),r} \delta T d\Omega - \int_{\Omega} \chi_a \left(\left(\rho^{(a),r} c^{(a)0} + \rho^{(a)0} c^{(a),r} \right) T^0 \delta T + \lambda_{ij}^{(a),r} T_{,j}^0 \delta T_{,i} \right) d\Omega, \tag{2.45}$$

- one second-order partial differential equation:

$$\int_{\Omega} \chi_a \left(\rho^{(a)0} c^{(a)0} T^{(2)} \delta T + \lambda_{ij}^{(a)0} T_{,j}^{(2)} \delta T_{,i} \right) d\Omega = \int_{\partial\Omega_q} \hat{q}^{(2)} \delta T d(\partial\Omega) + \int_{\Omega} \chi_a g^{(a)(2)} \delta T d\Omega - \int_{\Omega} \chi_a \left(\left(\rho^{(a),rs} c^{(a)0} + 2\rho^{(a),r} c^{(a),rs} \right) T^0 + \left(\rho^{(a),r} c^{(a)0} + \rho^{(a)0} c^{(a),r} \right) T^{,s} \right) S^{rs} \delta T d\Omega - \int_{\Omega} \left(\lambda_{ij}^{(a),rs} T_{,j}^0 + 2\lambda_{ij}^{(a),r} T_{,j}^{,s} \right) S^{rs} \delta T_{,j} d\Omega, \tag{2.46}$$

where the symbol $(.)^{(2)}$ denotes the double sum $(.)^{,rs} S^{rs}$, $r, s = 1, 2, ..., R$. Having solved these Eqs. (2.44), (2.45) and (2.46) for T^0, $T^{,r}$ and $T^{,rs}$, respectively, we derive the expressions for the expected values and covariances of the temperature field. We obtain [4]:

- the expcted values

$$E\left[T(x_i, \tau)\right] = T^0(x_i, \tau) + \frac{1}{2} T^{(2)}(x_i, \tau); \tag{2.47}$$

- the covariances

$$\mathrm{Cov}\left(T\left(x_i^{(1)}; t_1\right), T\left(x_i^{(2)}; t_2\right) \right) = T^{,r}\left(x_i^{(1)}; t_1\right) T^{,s}\left(x_i^{(2)}; t_2\right) S^{rs}. \tag{2.48}$$

Symbol S_b^{rs} denotes the matrix of the input random variables of the problem which can be expressed as follows:

$$S_b^{rs} = \mathrm{Cov} \begin{pmatrix} \mathrm{Var}\,\lambda_d & 0 & 0 & 0 \\ & \mathrm{Var}\,\lambda_i & 0 & 0 \\ & & \mathrm{Var}\,n & 0 \\ \text{symm.} & & & \mathrm{Var}\,r \end{pmatrix}, \tag{2.49}$$

where the respective variances are submatrices with different diagonal terms for different components of the composite or different interfaces. Moreover, it should be stressed that the formulation proposed deals with the input random variables which are not stochastic processes, i.e. they are not random in space and in time at the same time.

3. Computational implementation

3.1. Classical finite element technique

Let us assume that the region Ω is discretized by the use of the set of finite elements and that the scalar temperature field T is described by the nodal temperatures vector θ_α

$$T(x_i) = H_\alpha(x_i)\theta_\alpha; \qquad i = 1,2; \qquad \alpha = 1,2,..,N, \tag{3.1}$$

where N is the total number of degrees of freedom introduced. The temperature derivatives can be written in the form

$$T_{,i} = H_{\alpha,i}\theta_\alpha. \tag{3.2}$$

Moreover, let us introduce the capacity matrix $\mathbf{C}_{\alpha\beta}$, the heat conductivity matrix $\mathbf{K}_{\alpha\beta}$ and the vector $\mathbf{P}_\alpha$ as follows [14]:

$$\mathbf{C}_{\alpha\beta} = \int_\Omega \chi_a \rho^{(a)} c^{(a)} H_\alpha H_\beta d\Omega; \qquad 1 \leqslant a \leqslant n, \tag{3.3}$$

$$\mathbf{K}_{\alpha\beta} = \int_\Omega \chi_a \lambda_{ij}^{(a)} H_{\alpha,i} H_{\beta,j} d\Omega; \qquad 1 \leqslant a \leqslant n, \tag{3.4}$$

and

$$\mathbf{P}_\alpha = \int_\Omega g H_\alpha d\Omega + \int_{\partial\Omega} \hat{q} H_\alpha d\Omega. \tag{3.5}$$

Next, let us introduce these matrixes into the variational formulation (2.37). Hence we must solve the following algebraic equations system [10 – 12]:

$$\mathbf{C}_{\alpha\beta}\dot{\theta}_\beta + \mathbf{K}_{\alpha\beta}\theta_\beta = \mathbf{P}_\alpha. \tag{3.6}$$

Finally, to obtain the solution of the transient heat problem the following algorithm has been applied, cf. Fig. 6.

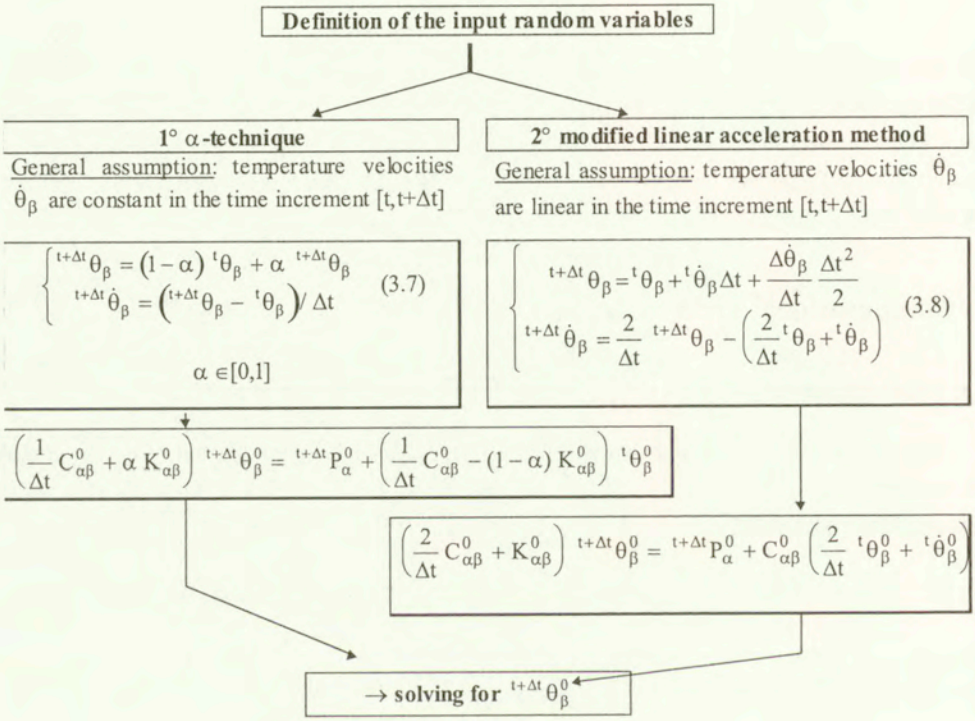

FIG. 6. Transient heat flow solution algorithm.

It should be mentioned that the equations of the 1st and the 2nd order derived by means of the Eqs. (2.45) and (2.46) can be solved by the use of α technique represented by Eq. (3.7), or the modified acceleration method – by Eq. (3.8).

3.2. Stochastic finite element formulation of the problem

Analogically to the previous considerations, we can obtain the following system of algebraic equations describing the second-order stochastic formulation of the transient heat transfer problem [4]:

- zeroth-order, one system of N ordinary differential equations

$$C^0_{\alpha\beta}\dot{\theta}^0_\beta + K^0_{\alpha\beta}\theta^0_\beta = P^0_\alpha; \tag{3.7}$$

- first-order, R systems of N ordinary differential equations

$$C^0_{\alpha\beta}\dot{\theta}^{,r}_{\beta} + K^0_{\alpha\beta}\theta^{,r}_{\beta} = P^{,r}_{\alpha} - \left(C^{,r}_{\alpha\beta}\dot{\theta}^0_{\beta} + K^{,r}_{\alpha\beta}\theta^0_{\beta}\right); \tag{3.8}$$

- second-order, one system of N ordinary differential equations

$$C^0_{\alpha\beta}\dot{\theta}^{(2)}_{\beta} + K^0_{\alpha\beta}\theta^{(2)}_{\beta} = \left[P^{,rs}_{\alpha} - 2\left(C^{,r}_{\alpha\beta}\dot{\theta}^{,s}_{\beta} + K^{,r}_{\alpha\beta}\theta^{,s}_{\beta}\right) - \left(C^{,rs}_{\alpha\beta}\dot{\theta}^0_{\beta} + K^{,rs}_{\alpha\beta}\theta^0_{\beta}\right)\right] S^{rs}_b. \tag{3.9}$$

In the equations stated above we have introduced the following matrix notation:

- the heat capacity matrix and their derivatives

$$C^0_{\alpha\beta} = \int_{\Omega} \rho^0 c^0 H_\alpha H_\beta d\Omega, \tag{3.10}$$

$$C^{,r}_{\alpha\beta} = \int_{\Omega} \left(\rho^{,r} c^0 + \rho^0 c^{,r}\right) H_\alpha H_\beta d\Omega, \tag{3.11}$$

$$C^{,rs}_{\alpha\beta} = \int_{\Omega} \left(\rho^{,rs} c^0 + 2\rho^{,r} c^{,s} + \rho^0 c^{,rs}\right) H_\alpha H_\beta d\Omega; \tag{3.12}$$

- the heat conductivity matrix and their derivatives

$$K^0_{\alpha\beta} = \int_{\Omega} \lambda^0_{ij} H_{\alpha,i} H_{\beta,j} d\Omega, \tag{3.13}$$

$$K^{,r}_{\alpha\beta} = \int_{\Omega} \lambda^{,r}_{ij} H_{\alpha,i} H_{\beta,j} d\Omega, \tag{3.14}$$

$$K^{,rs}_{\alpha\beta} = \int_{\Omega} \lambda^{,rs}_{ij} H_{\alpha,i} H_{\beta,j} d\Omega; \tag{3.15}$$

- the Right-Hand Side (RHS) vector and their derivatives

$$P^0_{\alpha} = \int_{\Omega} g^0 H_\alpha d\Omega + \int_{\partial\Omega_q} \hat{q}^0 H_\alpha d\Omega, \tag{3.16}$$

$$P^{,r}_{\alpha} = \int_{\Omega} g^{,r} H_\alpha d\Omega + \int_{\partial\Omega_q} \hat{q}^{,r} H_\alpha d\Omega, \tag{3.17}$$

$$P^{,rs}_{\alpha} = \int_{\Omega} g^{,rs} H_\alpha d\Omega + \int_{\partial\Omega_q} \hat{q}^{,rs} H_\alpha d\Omega, \tag{3.18}$$

where all expressions are evaluated at the expectated values of the input random variables vector components.

4. Computational experiments

The example deals with the computational modeling of the two-component layered composite with randomly defined heat conductivity coefficient (test 1) and heat capacity (test 2) and stochastic interface defects. The finite element discretization as well as boundary conditions of the problem are shown in Fig. 7.

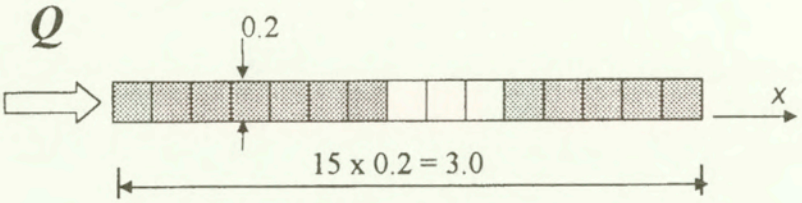

FIG. 7. Semi-infinite composite subjected to surface heat flux.

Heat conductivity has been taken as $E[\lambda] = \{1.2; 0.3; 0.5\}$ and $\mathrm{Cov}\,(\lambda^r, \lambda^s) = \alpha \exp[-\mathrm{abs}(x^r - x^s)]$, while the heat capacity as $E[c] = 1.0$ and its covariance matrix has the same form. The coefficient of variation α has been taken as 0.14 for all tests. The results of the computational experiments in the sense of SFEM analysis, are presented in Figs. 8–13.

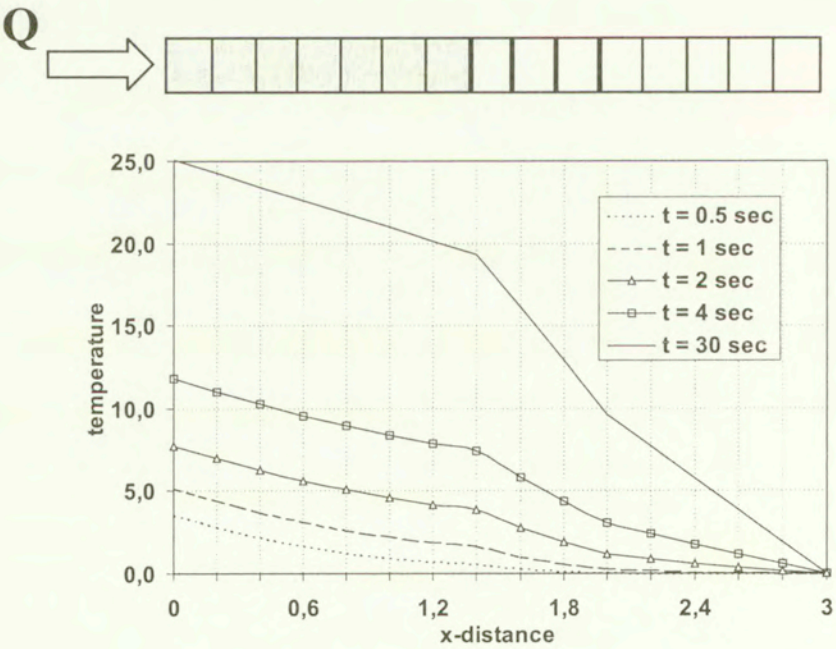

FIG. 8. Spatial expected values for test 1.

Figure 8 shows spatial expectations of the temperature field in the function of the composite thickness. It is visible that the expected values of temperature decrease quasi-linearly from the left boundary to the right one for the composite structure. Next, we observe that temperature expectations are not smooth at the interfaces of the composite being modeled and, moreover, that the expected values of temperature generally increase with time, what agrees with engineering intuition very well.

Figure 9 illustrates the cross-covariances of temperature field in function of the composite thickness. We observe that these cross-covariances increase together with time and non-smoothness appears at the composite interfaces analogically to the case of expected values. Moreover, it can be seen that decrease of cross-covariances together with the increase of the distance x has a quasi-linear character. Finally, it should be underlined that some negative values of probabilistic characteristics computed are obtained near the initial state of the structure (caused by the SFEM procedure instabilities only).

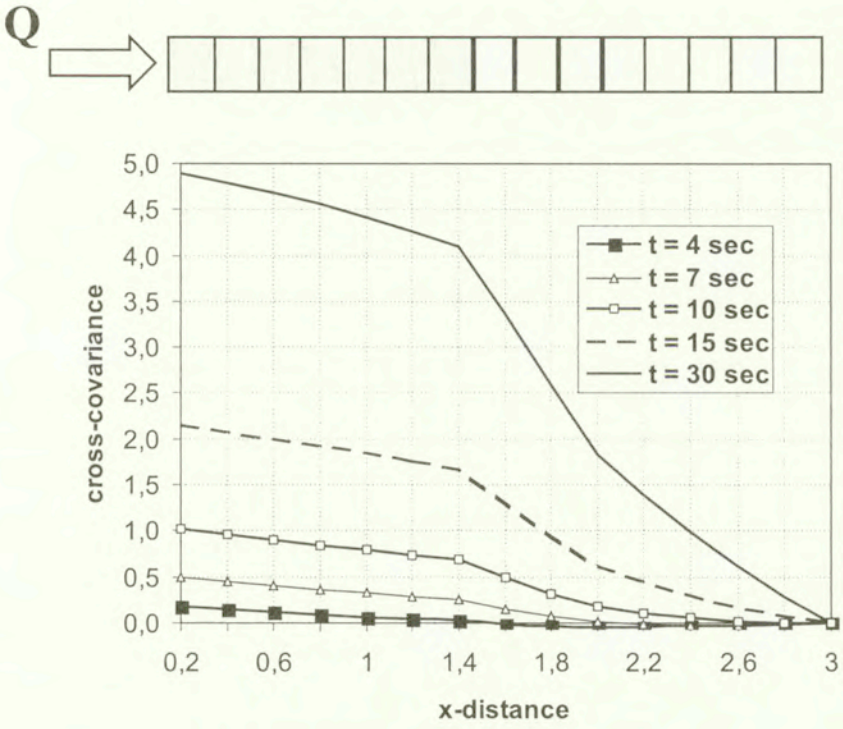

FIG. 9. Spatial cross-covariances for test 1.

Next figure (Fig. 10) shows us the expected values of temperature histories in the composite considered. It can be seen that temperature expectations increase together with time and that the greatest temperatures appear at the left-hand

boundary of the composite while the smallest – at the right-hand one. Contrary to the previous figures, these expectations change very smoothly at all interfaces.

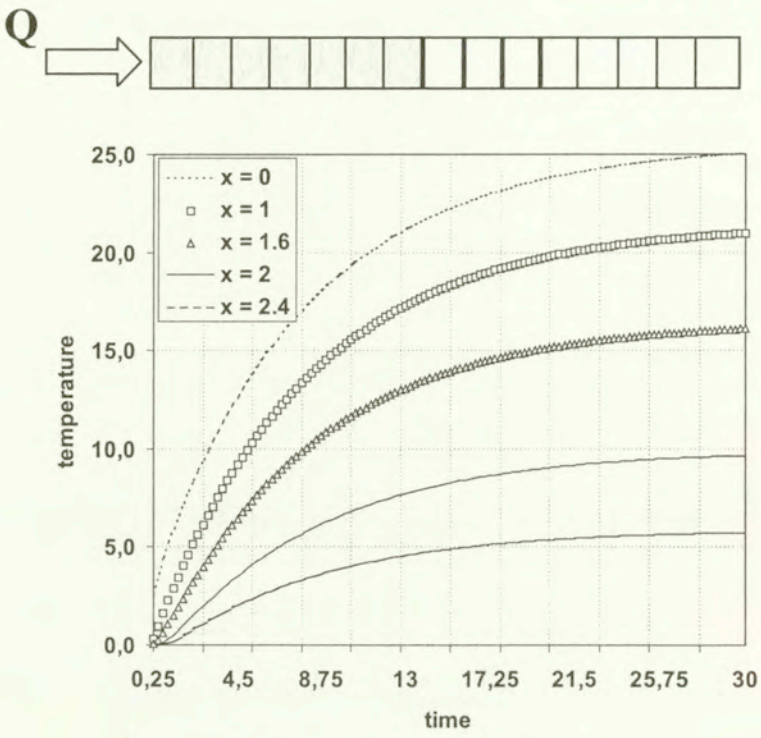

FIG. 10. Time expected values for test 1.

The cross-covariances of nodal temperatures are presented in Fig. 11 – these covariances increase together with time. Analogically to the cross-covariances in the function of composite thickness, we observe some negative values at the beginning of the heat transfer process. The greatest values are observed at the left-hand surface while the smallest – near the right-hand one.

Figures 12 and 13 illustrate the spatial and time cross-covariances for the test 2. It should be mentioned that the expected values in the function of time and composite thickness for random specific heat capacity have the same character as previously. Analogically to the case 1, cross-covariances are greater near the left-hand boundary of the structure where the heat flux is applied and seem to be smaller at the other boundary. Moreover, we can see that cross-covariances tend to 0 when the solution tends to a stationary state. Finally, it can be observed that there is some characteristic time when the cross-covariances reach their maximum (8 seconds for the example being analyzed). Analogically to the previous figure, the time cross-covariances for nodal temperatures have smooth and strongly nonlinear character.

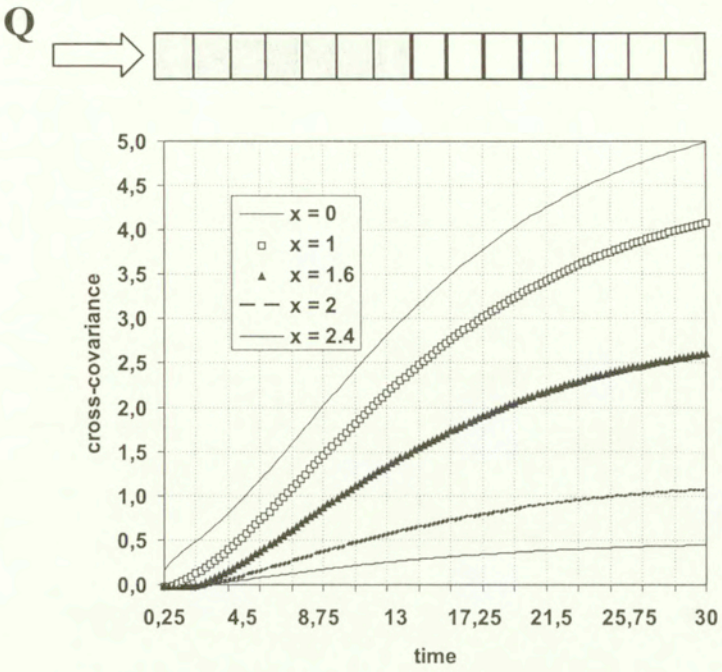

FIG. 11. Time cross-covariances for test 1.

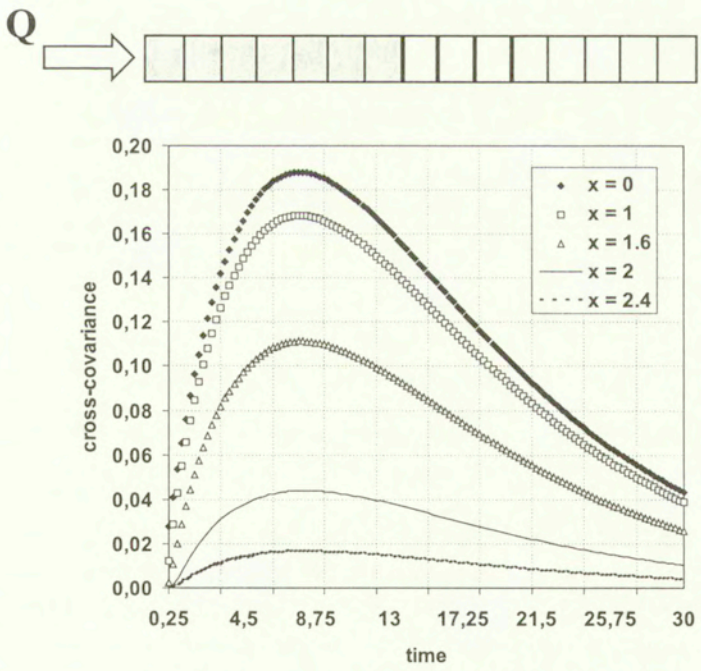

FIG. 12. Time cross-covariances for test 2.

The relation between the cross-covariances and composite thickness is presented in Fig. 13. We may observe that the covariance changes are of a quasi-linear character and non-smoothness appears at the composite interfaces. Moreover, it is visible that for time equal to some characteristic value, the cross-covariances reach the extremum values. These values are equal to 0 near the right-hand surface of the composite structure and, for time equal to approximately 30 seconds we obtain a quasi-stationary state. Analogically to the cross-covariances in case 1, the second probabilistic moments change quasi-linearly and show non-smoothness at interfaces between the constituents.

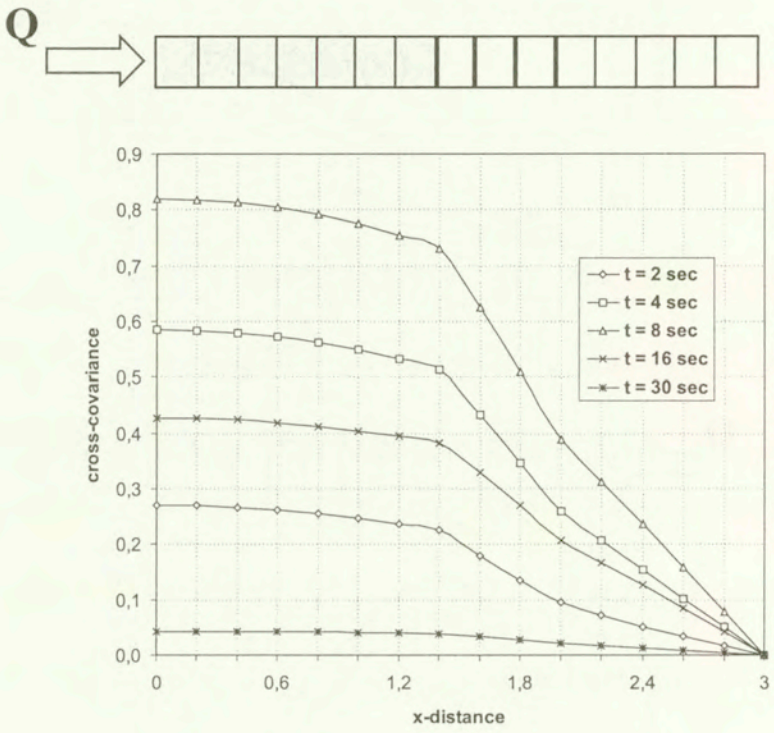

FIG. 13. Spatial cross-covariances for test 2.

5. Conclusions

1. Numerical analysis carried out in the paper proved that transient heat transfer problems in layered composites with spatially random parameters and stochastic interface defects can be efficiently modeled by the use of the stochastic finite element methodology based on the second order perturbation, stochastic second central moment analysis. Moreover, the methodology improved can be applied to stochastic modeling of general composites as well as to simulation

of the composite materials with stochastic interface defects due to the model presented in [6].

2. Computational experiments provided in the paper show that the heat transfer in composite materials is very sensitive to random changes of material parameters of their constituents. The procedure involved may be applied for seepage, torsion, irrotational and incompressible flow, film lubrication, acoustic vibration as well as for electric conduction, electrostatic field, electromagnetic waves and all field problems with stochastically defined physical or geometrical characteristics [1, 15].

3. Further computational studies on the phenomena are recommended in the context of the stochastic sensitivity of the problem. The influence of material parameters and interface defects on overall thermal behavior of different composite structures (stratified, fiber-reinforced or structures with periodic as well as non-periodic geometry) should be numerically approximated to find out the crucial parameters for the composite structure thermal behavior.

Acknowledgements

The paper has been financially supported by the State Committee for the Scientific Research (KBN) under Grant No 8T11F 008 12 PO2.

References

1. K.J. Bathe, *Finite element procedures.* Prentice Hall, Englewood Cliffs, New York 1996.
2. H.S. Carslaw and J.C Jeager, *Conduction of heat in solids.* Oxford Univ. Press, London 1959.
3. L. Collatz, *The numerical treatment of differential equations.* 3rd Edition, Springer-Verlag, 1966.
4. T.D. Hien and M. Kleiber, *Stochastic finite element modelling in linear transient heat transfer.* Comput. Methods Appl. Mech. Engrg., **144**, 111–124, 1997.
5. I. Jasiuk, J. Chen and M.F. Thorpe, *Elastic moduli of two-dimensional materials with polygonal and elliptical holes*, Appl. Mech. Rev. ASME, **47**(1), 18–28, 1994.
6. M. Kamiński, *Stochastic problem of the fiber-reinforced composite with interface defects* (in Polish). Ph.D. Thesis, Łódź 1997.
7. M. Kamiński and M. Kleiber, *Stochastic finite element method in random non-homogeneous media.* [In:] J.A. Desideri *et al.*, *Numerical methods in engineering'96*, 35–41, Wiley 1996.
8. M. Kamiński and M. Kleiber, *Stochastic structural interface defects in composite materials.* Int. J. Sol. Struct., **33**(20-22): 3035–3056, 1996.
9. M. Kleiber and T.D. Hien, *The stochastic finite element method. Basic perturbation technique and computer implementation.* Wiley 1992.
10. M. Kleiber and Cz. Woźniak, *Nonlinear mechanics of structures.* PWN/Kluwer 1991.

11. C.S. KRISHNAMOORTHY, *Finite element analysis*, 2nd Edition, McGraw-Hill, 1994.

12. J.T. ODEN, *Finite elements of nonlinear continua*. McGraw-Hill, 1972.

13. T. MURA, *Micromechanics of defects in solids*. Sijthoff and Noordhoff, 1982.

14. D.W. PEPPER and J.C. HEINRICH, *The finite element method. Series in computational and physical processes in mechanics and thermal sciences*. Hemisphere 1992.

15. O.C. ZIENKIEWICZ and Y.K. CHEUNG, *Finite elements in the solution of field problems*, The Engineer, **220**, 507–510, 1965.

Received December 2, 1998; revised version April 15, 1999.

Arch. Mech., **51**, 3–4, pp. 419–446, Warszawa 1999

Stiffness degradation in gradient-dependent coupled damage-plasticity

J. PAMIN[1)] and R. de BORST

Koiter Institute Delft, Faculty of Aerospace Engineering,
Delft University of Technology,
P.O. Box 5058, 2600 GB Delft, the Netherlands,
e-mail R.deBorst@lr.TUDelft.nl

TWO GRADIENT-DEPENDENT COMBINATIONS of isotropic plasticity and scalar damage are proposed. The gradient enhancements of either the plasticity or the damage component of the theory are performed by introducing the Laplacian of a strain measure and an internal length parameter. This makes the constitutive models applicable to localization analyses. The models are used for finite element simulations of localization in a one-dimensional tensile bar problem. The coupling of hardening/softening plasticity with damage governed by different damage evolution functions is discussed. Then, attention is focused on the response of the models in unloading from localized deformation states. The model of gradient damage combined with hardening plasticity is used to predict progressive damage of concrete in a beam subjected to four-point bending. The simulated stiffness degradation is compared with experimental results.

Keywords: gradient-dependent continuum, plasticity, damage, strain localization, finite elements

1. Introduction

IN A PHENOMENOLOGICAL CONSTITUTIVE description, a combination of plasticity and damage theories is physically appealing since a host of materials exhibit an interaction of inelastic mechanisms of microcrack or microvoid growth with plastic flow. The coupled models make it possible to reproduce a realistic elastic stiffness degradation, which is crucial for cyclic loading and extensive stress redistributions.

The research on the incorporation of elastic stiffness degradation within the theory of plasticity goes back to the works [1, 2, 3, 4, 5]. Confining interest to

[1)] on leave from Faculty of Civil Engineering, Cracow University of Technology, Cracow, Poland

small strain theories, plasticity and damage combinations have been considered amongst others in [6, 7, 8, 9, 10, 11], although they all restricted themselves to a local continuum form.

In quasi-brittle materials the inelastic behaviour is accompanied by localization of deformation and progressive fracture. The problem of localization, driven by material instabilities like strain softening, has recently been thoroughly investigated, see for instance [12] and references therein. Within a classical, local continuum formulation this phenomenon is associated with the loss of well-posedness of the governing partial differential equations, and therefore discretization methods used to solve them may give mesh-sensitive results. To overcome this problem, some form of nonlocal or rate-dependent enhancement of the constitutive model must be adopted [13, 14, 15]. In other words, a continuum formulation should be equipped with an internal length parameter.

This paper investigates the damage evolution and the resulting elastic stiffness degradation using gradient-enhanced plastic-damage theories. The coupling of plasticity and damage is based on the effective stress concept and strain equivalence [7, 8]. However, a gradient enhancement of either plasticity or damage has been adopted [16, 17]. The gradient-dependent plasticity enhancement is based on [18, 19, 20]. The gradient damage model follows [21, 22]. A gradient-regularized hardening plasticity theory has so far been coupled to damage in [23].

The numerical response of the gradient-dependent coupled plasticity-damage models in localization problems involving load reversals is examined. Although the models are general, consideration is focused on the tensile regime. Section 2 summarizes the adopted plasticity-damage theory. In Sections 3 and 4 the two gradient-enhanced constitutive models are presented [17]. In Section 5 the employed equivalent strain measures and damage evolution laws are discussed. Section 6 presents the results of one-dimensional numerical studies. Section 7 contains some simulations of damage and stiffness degradation in a notched concrete beam subjected to four-point bending. Final remarks are gathered in Section 8.

2. Coupling of local damage and plasticity theories

In the following we assume that configurations are loaded quasi-statically and exhibit small strains, which is usually realistic for quasi-brittle materials. Hence, the equilibrium and kinematic equations have the form:

$$\mathbf{L}^{\mathrm{T}}\boldsymbol{\sigma} + \mathbf{b} = \mathbf{0}, \tag{2.1}$$

$$\boldsymbol{\epsilon} = \mathbf{L}\mathbf{u}, \tag{2.2}$$

where $\mathbf{L}$ is a differential operator matrix, $\boldsymbol{\sigma}$ is the stress tensor in a vector form, $\mathbf{b}$ is the body force vector, $\boldsymbol{\epsilon}$ is the strain tensor in a vector form, $\mathbf{u}$ is the

displacement vector and the superscript T is the transpose symbol. The stresses and displacements satisfy the relevant natural and essential boundary conditions, respectively.

We start the discussion of constitutive relations by selecting a form of coupling between plasticity and damage theories. We combine a plasticity theory formulated in stress space and a damage theory formulated in strain space. The theories have a simple, isotropic format (intrinsic and induced anisotropy is neglected). However, as will be shown in the next sections, one of the two theories is made gradient-dependent [17] in order to assure that numerical simulations of strain localization give meaningful results.

Considering the damage evolution, we distinguish the actual body with strains $\boldsymbol{\epsilon}$ and stresses $\boldsymbol{\sigma}$ and its fictitious undamaged counterpart with stresses $\hat{\boldsymbol{\sigma}}$ and strains $\hat{\boldsymbol{\epsilon}}$. The fictitious counterpart represents the undamaged "skeleton" of the body, and the stresses $\hat{\boldsymbol{\sigma}}$ acting on it are called effective. We adopt the postulate that the strains observed in the actual body and in its undamaged representation are equal [7, 8]:

$$\boldsymbol{\epsilon} = \hat{\boldsymbol{\epsilon}}, \tag{2.3}$$

and that the stresses are related by means of a scalar damage measure ω

$$\boldsymbol{\sigma} = (1 - \omega)\hat{\boldsymbol{\sigma}}. \tag{2.4}$$

The damage ω is a function of a damage history parameter κ^{d} that will be specified below:

$$\omega = \omega(\kappa^{\mathrm{d}}). \tag{2.5}$$

It grows from zero to one as κ^{d} grows from a damage threshold κ_0 to an ultimate value κ_{u}.

Next, we define a damage function which limits the elastic (or elasto-plastic) behaviour of the material in the strain space:

$$f^{\mathrm{d}} = \tilde{\epsilon} - \kappa^{\mathrm{d}} = 0, \tag{2.6}$$

where $\tilde{\epsilon}$ is an equivalent strain measure. During the damage evolution the history parameter κ^{d} is equal to the largest value of $\tilde{\epsilon}$ reached in the loading history. Suitable loading/unloading conditions complete the formulation of the scalar damage model:

$$\dot{\kappa}^{\mathrm{d}} \geqslant 0\,, \quad f^{\mathrm{d}} \leqslant 0\,, \qquad \dot{\kappa}^{\mathrm{d}} f^{\mathrm{d}} = 0, \tag{2.7}$$

where the superposed dot denotes the rate of a quantity.

Although damage and plastic processes can be coupled, plastic flow occurs in the undamaged skeleton of the body, so we can write the elastic constitutive relation between the effective stresses and elastic strains as follows:

$$\hat{\boldsymbol{\sigma}} = \mathbf{D}^{\mathrm{e}}\boldsymbol{\epsilon}^{\mathrm{e}}, \tag{2.8}$$

where $\mathbf{D}^{\mathrm{e}}$ is the elastic stiffness operator. Combining Eqs. (2.4) and (2.8) we obtain the relation:

$$\boldsymbol{\sigma} = (1-\omega)\mathbf{D}^{\mathrm{e}}\boldsymbol{\epsilon}^{\mathrm{e}}, \tag{2.9}$$

in which the damage measure ω accounts for the degradation of the elastic stiffness. Damage does not grow during unloading, so that for a pure damage model the constant (secant) stiffness $(1-\omega)\mathbf{D}^{\mathrm{e}}$ results in unloading to the origin, i.e. no residual strains remain after unloading, which means that microcracks and microvoids are assumed to close completely. The motivation for coupling the model with plasticity is thus to incorporate irreversible strains.

The plastic component of the coupled model is formulated in the effective stress space. The yield condition is as follows

$$f^{\mathrm{p}} = \tilde{\sigma}(\hat{\boldsymbol{\sigma}}) - \sigma_{\mathrm{y}}(\kappa^{\mathrm{p}}) = 0, \tag{2.10}$$

where $\tilde{\sigma}$ is an equivalent stress function, σ_{y} is the yield strength and isotropic hardening is assumed. The yield function satisfies the Kuhn-Tucker conditions:

$$\dot{\lambda} \geqslant 0\,,\ f^{\mathrm{p}} \leqslant 0\,, \qquad \dot{\lambda} f^{\mathrm{p}} = 0, \tag{2.11}$$

in which λ is the plastic multiplier. For simplicity, the equivalence of the plastic multiplier λ and the plastic strain measure κ^{p} is adopted, but extension of the theory to cases where λ and κ^{p} are not equal is straightforward.

The plastic multiplier determines the magnitude of plastic strains according to the classical flow rule, which may be non-associated. Assuming the standard additive decomposition of strain rates into an elastic and a plastic part, the elastic strain rate can be written as:

$$\dot{\boldsymbol{\epsilon}}^{\mathrm{e}} = \dot{\boldsymbol{\epsilon}} - \dot{\lambda}\mathbf{m}(\hat{\boldsymbol{\sigma}}), \tag{2.12}$$

where $\mathbf{m}$ is the plastic flow direction vector in the effective stress space.

Next, we invoke the local plastic consistency condition $\dot{f}^{\mathrm{p}} = 0$ in order to compute $\dot{\lambda}$ and substitute it into Eq. (2.12) to obtain:

$$\dot{\boldsymbol{\epsilon}}^{\mathrm{e}} = \dot{\boldsymbol{\epsilon}} - \frac{1}{h}\mathbf{m}\mathbf{n}^{\mathrm{T}}\dot{\hat{\boldsymbol{\sigma}}}, \tag{2.13}$$

where the classical definitions of the gradient $\mathbf{n}$ normal to the yield function and the softening modulus h are used:

$$\mathbf{n}^{T}(\hat{\boldsymbol{\sigma}}) = \frac{\partial\tilde{\sigma}}{\partial\hat{\boldsymbol{\sigma}}}\,, \qquad h = \frac{\mathrm{d}\sigma_{\mathrm{y}}}{\mathrm{d}\kappa^{\mathrm{p}}}. \tag{2.14}$$

After some rearrangements and with the help of Sherman-Morrison formula, we obtain the tangential relation:

$$\dot{\hat{\boldsymbol{\sigma}}} = \mathbf{D}^{\mathrm{ep}}\dot{\boldsymbol{\epsilon}}, \tag{2.15}$$

with the classical elasto-plastic matrix

$$\mathbf{D}^{\mathrm{ep}} = \mathbf{D}^{\mathrm{e}} - \frac{\mathbf{D}^{\mathrm{e}}\mathbf{m}\mathbf{n}^{\mathrm{T}}\mathbf{D}^{\mathrm{e}}}{h + \mathbf{n}^{\mathrm{T}}\mathbf{D}^{\mathrm{e}}\mathbf{m}}. \tag{2.16}$$

This tangent operator is valid during loading, and the unloading process for the pure plasticity model is completely elastic.

The effective stress rate during the evolution of damage and plasticity can also be obtained by differentiating Eq. (2.8):

$$\dot{\hat{\boldsymbol{\sigma}}} = \mathbf{D}^{\mathrm{e}}\dot{\boldsymbol{\epsilon}}^{\mathrm{e}}, \tag{2.17}$$

and the stress rate can be computed by differentiating Eq. (2.9):

$$\dot{\boldsymbol{\sigma}} = (1-\omega)\,\mathbf{D}^{\mathrm{e}}\dot{\boldsymbol{\epsilon}}^{\mathrm{e}} - \dot{\omega}\,\hat{\boldsymbol{\sigma}}, \tag{2.18}$$

where $\dot{\boldsymbol{\epsilon}}^{\mathrm{e}}$ follows from Eq. (2.12) and the rate of damage during evolution ($\kappa^{\mathrm{d}} = \tilde{\epsilon}$) is computed as:

$$\dot{\omega} = \frac{\partial\omega}{\partial\kappa^{\mathrm{d}}}\frac{\partial\tilde{\epsilon}}{\partial\boldsymbol{\epsilon}}\,\dot{\boldsymbol{\epsilon}}. \tag{2.19}$$

During unloading we have $\dot{\omega} = 0$. Comparing Eq. (2.17) and Eq. (2.15) and using the following definitions:

$$H = \frac{\mathrm{d}\omega}{\mathrm{d}\kappa^{\mathrm{d}}}, \qquad \mathbf{s}^{\mathrm{T}} = \frac{\partial\tilde{\epsilon}}{\partial\boldsymbol{\epsilon}}, \tag{2.20}$$

we obtain the linearized constitutive relation for the coupled model:

$$\dot{\boldsymbol{\sigma}} = [(1-\omega)\,\mathbf{D}^{\mathrm{ep}} - H\hat{\boldsymbol{\sigma}}\,\mathbf{s}^{\mathrm{T}}]\,\dot{\boldsymbol{\epsilon}}. \tag{2.21}$$

3. Gradient plasticity coupled to damage

Now, we revisit the gradient plasticity formulation [18, 19] and write the yield function, which depends on the Laplacian of an equivalent plastic strain measure κ^{p}, in the effective stress space:

$$f^{\mathrm{p}} = \tilde{\sigma}(\hat{\boldsymbol{\sigma}}) - \sigma_{\mathrm{y}}(\kappa^{\mathrm{p}}) + g\nabla^2\kappa^{\mathrm{p}} = 0, \tag{3.1}$$

where $\tilde{\sigma}$ is a classical (e.g. Huber-von Mises or Rankine) yield function and g is a positive gradient influence factor. The yield function satisfies the Kuhn-Tucker

conditions (2.11), but it is now a partial differential equation which must be solved simultaneously with the equilibrium equations.

The enhancement of the classical theory was made in order to preserve well-posedness of the governing equations for materials which do not comply with the material stability requirement [24], e.g. when a softening relation between stresses and strains is assumed ($h < 0$). For a softening medium the factor g can be associated with an internal length parameter l, e.g. in a one-dimensional analytical solution we have $g = -hl^2 > 0$ [19]. However, also for a hardening material the Laplacian term with $g > 0$ regularizes the solution [20] in the sense that a higher-order continuity of the strain field is obtained.

The finite element implementation is based on the following two weak-form equations governing the static equilibrium and the plastic consistency, respectively:

$$\int_V (\mathbf{L}\mathbf{v})^{\mathrm{T}}\boldsymbol{\sigma}\,\mathrm{d}V = \int_V \mathbf{v}^{\mathrm{T}}\mathbf{b}\,\mathrm{d}V + \int_S \mathbf{v}^{\mathrm{T}}\mathbf{t}\,\mathrm{d}S,$$

(3.2)

$$\int_V w\, f^{\mathrm{p}}(\hat{\boldsymbol{\sigma}}, \lambda, \nabla^2\lambda)\mathrm{d}V = 0\,,$$

where $\mathbf{v}$ and w are suitable weighted functions, $\mathbf{t}$ is the traction vector. Equation $(3.2)_2$, which requires the discretization of the λ field, refers to the effective stress space and therefore does not change in presence of damage.

Equations (3.2) are written for iteration $i+1$ of the incremental-iterative algorithm and the following decomposition is used:

$$\boldsymbol{\sigma}^{(i+1)} = \boldsymbol{\sigma}^{(i)} + \mathrm{d}\boldsymbol{\sigma}\,, \quad \lambda^{(i+1)} = \lambda^{(i)} + \mathrm{d}\lambda, \tag{3.3}$$

so that the yield function can be developed in a truncated Taylor series around $(\hat{\boldsymbol{\sigma}}^{(i)}, \lambda^{(i)})$. We obtain the following incremental equations:

$$\int_V (\mathbf{L}\mathbf{v})^{\mathrm{T}}\mathrm{d}\boldsymbol{\sigma}\,\mathrm{d}V = f_{\mathrm{ext}} - f_{\mathrm{int}},$$

(3.4)

$$\int_V w\,[\mathbf{n}^{\mathrm{T}}\mathrm{d}\hat{\boldsymbol{\sigma}} - h\,\mathrm{d}\lambda + g\nabla^2(\mathrm{d}\lambda)]\,\mathrm{d}V = -\int_V w\, f^{\mathrm{p}}(\hat{\boldsymbol{\sigma}}^{(i)}, \kappa^{\mathrm{p}(i)}, \nabla^2\kappa^{\mathrm{p}(i)})\,\mathrm{d}V,$$

with

$$f_{\mathrm{ext}} = \int_S \mathbf{v}^{\mathrm{T}}\mathbf{t}\,\mathrm{d}S + \int_V \mathbf{v}^{\mathrm{T}}\mathbf{b}\,\mathrm{d}V,$$

(3.5)

$$f_{\mathrm{int}} = \int_V (\mathbf{L}\mathbf{v})^{\mathrm{T}}\boldsymbol{\sigma}^{(i)}\,\mathrm{d}V.$$

It is important to notice that, if the yield condition (3.1) is used in the classical return mapping algorithm to distinguish between elastic and plastic states, a C^1-continuous interpolation of λ is unavoidable, otherwise $\nabla^2\lambda$ loses its meaning [20]. Therefore, the Laplacian term is not removed from the left-hand side of Eq. $(3.4)_2$, although this can be done using Green's formula if a homogeneous non-standard boundary condition $(\nabla \mathrm{d}\lambda)^{\mathrm{T}}\boldsymbol{\nu} = 0$ is assumed ($\boldsymbol{\nu}$ is a vector normal to the surface of the plastic part of the body).

Next, we substitute Eq. (2.12) into Eqs. (2.18) and (2.17) and substitute their incremental forms into Eqs. $(3.4)_1$ and $(3.4)_2$, respectively:

$$\begin{aligned}
&\int_V (\mathbf{L}\mathbf{v})^{\mathrm{T}}[(1-\omega^{(i)})\mathbf{D}^{\mathrm{e}}\mathrm{d}\boldsymbol{\epsilon} - \hat{\boldsymbol{\sigma}}^{(i)}\mathrm{d}\omega]\,\mathrm{d}V \\
&\qquad - \int_V (\mathbf{L}\mathbf{v})^{\mathrm{T}}[(1-\omega^{(i)})\mathbf{D}^{\mathrm{e}}\mathbf{m}^{(i)}\,\mathrm{d}\lambda]\,\mathrm{d}V = f_{\mathrm{ext}} - f_{\mathrm{int}}, \\
&\int_V w\,\mathbf{n}^{\mathrm{T}(i)}\mathbf{D}^{\mathrm{e}}\mathrm{d}\boldsymbol{\epsilon}\,\mathrm{d}V - \int_V w\,[(h^{(i)} + \mathbf{n}^{\mathrm{T}(i)}\mathbf{D}^{\mathrm{e}}\mathbf{m}^{(i)})\mathrm{d}\lambda + g\nabla^2(\mathrm{d}\lambda)]\,\mathrm{d}V \\
&\qquad = -\int_V w\,f^{\mathrm{p}}(\hat{\boldsymbol{\sigma}}^{(i)}, \kappa^{\mathrm{p}(i)}, \nabla^2\kappa^{\mathrm{p}(i)})\,\mathrm{d}V.
\end{aligned} \tag{3.6}$$

The increment of damage $\mathrm{d}\omega$ is non-zero only when damage grows, i.e. when Eq. (2.6) is satisfied. With the definitions in Eq. (2.20) it can be related to the strain increment:

$$\mathrm{d}\omega = H\,\mathbf{s}^{\mathrm{T}}\mathrm{d}\boldsymbol{\epsilon}. \tag{3.7}$$

Substituting Eq. (3.7) into Eq. $(3.6)_1$ and defining the elastic-damage tangent operator as:

$$\mathbf{D}^{\mathrm{ed}} = (1-\omega^{(i)})\mathbf{D}^{\mathrm{e}} - H^{(i)}\,\hat{\boldsymbol{\sigma}}^{(i)}\mathbf{s}^{\mathrm{T}(i)} \tag{3.8}$$

we obtain the following final form of Eqs. (3.6):

$$\begin{aligned}
&\int_V (\mathbf{L}\mathbf{v})^{\mathrm{T}}\mathbf{D}^{\mathrm{ed}}\mathrm{d}\boldsymbol{\epsilon}\,\mathrm{d}V - \int_V (\mathbf{L}\mathbf{v})^{\mathrm{T}}[(1-\omega^{(i)})\mathbf{D}^{\mathrm{e}}\mathbf{m}^{(i)}\,\mathrm{d}\lambda]\,\mathrm{d}V = f_{\mathrm{ext}} - f_{\mathrm{int}}, \\
&\int_V w\,\mathbf{n}^{\mathrm{T}(i)}\mathbf{D}^{\mathrm{e}}\mathrm{d}\boldsymbol{\epsilon}\,\mathrm{d}V - \int_V w\,[(h^{(i)} + \mathbf{n}^{\mathrm{T}(i)}\mathbf{D}^{\mathrm{e}}\mathbf{m}^{(i)})\mathrm{d}\lambda + g\nabla^2(\mathrm{d}\lambda)]\,\mathrm{d}V \\
&\qquad = -\int_V w\,f^{\mathrm{p}}(\hat{\boldsymbol{\sigma}}^{(i)}, \kappa^{\mathrm{p}(i)}, \nabla^2\kappa^{\mathrm{p}(i)})\,\mathrm{d}V.
\end{aligned} \tag{3.9}$$

Details of the finite element implementation can be found in [17].

4. Gradient damage coupled to isotropic plasticity

In the second formulation the plasticity theory remains standard and the damage theory is made nonlocal. It is emphasized that in this combination, the unstable material behaviour is caused by damage, and the plasticity model (for instance Huber-von Mises or Drucker-Prager plasticity) is hardening.

Following [21], the damage evolution is now governed by the following damage loading function:

$$f^{\mathrm{d}} = \bar{\epsilon} - \kappa^{\mathrm{d}} = 0, \tag{4.1}$$

where the averaged (nonlocal) strain measure $\bar{\epsilon}$ satisfies the Helmholtz equation:

$$\bar{\epsilon} - c\nabla^2\bar{\epsilon} = \tilde{\epsilon}. \tag{4.2}$$

The loading/unloading conditions (2.7) still apply. The parameter $c > 0$ has a unit of length squared and is hence related to an internal length scale. It is assumed here to be constant, although, with some modifications in the formulation, it can be made a function of $\tilde{\epsilon}$ or $\bar{\epsilon}$ [22].

The finite element implementation is based on the equilibrium Eq. $(3.2)_1$ and a weak form of Eq. (4.2) obtained using Green's formula and the non-standard boundary condition $(\nabla\bar{\epsilon})^{\mathrm{T}}\mathbf{\nu} = 0$:

$$\int_V [w\bar{\epsilon} + c(\nabla w)^{\mathrm{T}}\nabla\bar{\epsilon}]\mathrm{d}V = \int_V w\,\tilde{\epsilon}\mathrm{d}V. \tag{4.3}$$

In the ensuing two-field formulation the average strain measure must be discretized in addition to the displacements, but C^0-continuity now suffices for all shape functions. The coupling to plasticity influences only the equilibrium Eq. $(3.2)_1$, while Eq. (4.3) is exactly the same as for pure gradient damage.

We write Eqs. $(3.2)_1$ and (4.3) for iteration $i+1$ of the incremental-iterative algorithm and decompose the stress vector, the strain measure and its averaged version as

$$\boldsymbol{\sigma}^{(i+1)} = \boldsymbol{\sigma}^{(i)} + \mathrm{d}\boldsymbol{\sigma}\,, \qquad \tilde{\epsilon}^{(i+1)} = \tilde{\epsilon}^{(i)} + \mathrm{d}\tilde{\epsilon}\,, \qquad \bar{\epsilon}^{(i+1)} = \bar{\epsilon}^{(i)} + \mathrm{d}\bar{\epsilon} \tag{4.4}$$

to obtain:

$$\begin{aligned} \int_V (\mathbf{L}\mathbf{v})^{\mathrm{T}}\mathrm{d}\boldsymbol{\sigma}\,\mathrm{d}V &= f_{\mathrm{ext}} - f_{\mathrm{int}} \\ &\quad - \int_V w\,\mathrm{d}\tilde{\epsilon}\,\mathrm{d}V + \int_V [w\,\mathrm{d}\bar{\epsilon} + c(\nabla w)^{\mathrm{T}}\nabla(\mathrm{d}\bar{\epsilon})]\,\mathrm{d}V \\ &= \int_V w\,\tilde{\epsilon}^{(i)}\,\mathrm{d}V - \int_V [w\bar{\epsilon}^{(i)} + c(\nabla w)^{\mathrm{T}}\nabla\bar{\epsilon}^{(i)}]\,\mathrm{d}V. \end{aligned} \tag{4.5}$$

Equation (2.21) is now invoked in an incremental form:

$$\mathrm{d}\boldsymbol{\sigma} = (1-\omega)\mathbf{D}^{\mathrm{ep}}\mathrm{d}\boldsymbol{\epsilon} - \mathrm{d}\omega\hat{\boldsymbol{\sigma}}, \tag{4.6}$$

and, when Eq. (4.1) holds, the damage increment $\mathrm{d}\omega$ can be computed as

$$\mathrm{d}\omega = H\mathrm{d}\bar{\epsilon}, \tag{4.7}$$

with H defined in Eq. $(2.20)_1$. The increment of strain measure $\mathrm{d}\tilde{\epsilon}$ is computed as:

$$\mathrm{d}\tilde{\epsilon} = \mathbf{s}^{\mathrm{T}}\mathrm{d}\boldsymbol{\epsilon}, \tag{4.8}$$

with $\mathbf{s}^{\mathrm{T}}$ defined in Eq. $(2.20)_2$. Equation (4.7) is substituted into Eq. (4.6) and next Eqs. (4.6) and (4.8) are substituted into Eqs. $(4.5)_1$ and $(4.5)_2$, respectively, to obtain:

$$\begin{aligned} &\int_V (\mathbf{Lv})^{\mathrm{T}}(1-\omega^{(i)})\mathbf{D}^{\mathrm{ep}}\mathrm{d}\boldsymbol{\epsilon}\,\mathrm{d}V - \int_V (\mathbf{Lv})^{\mathrm{T}}H^{(i)}\hat{\boldsymbol{\sigma}}^{(i)}\mathrm{d}\bar{\epsilon}\,\mathrm{d}V = f_{\mathrm{ext}} - f_{\mathrm{int}} \\ &- \int_V w\,\mathbf{s}^{\mathrm{T}(i)}\mathrm{d}\boldsymbol{\epsilon}\,\mathrm{d}V + \int_V [w\,\mathrm{d}\bar{\epsilon} + c(\nabla w)^{\mathrm{T}}\nabla(\mathrm{d}\bar{\epsilon})]\,\mathrm{d}V \\ &\qquad = \int_V w\,\bar{\epsilon}^{(i)}\,\mathrm{d}V - \int_V [w\,\bar{\epsilon}^{(i)} + c(\nabla w)^{\mathrm{T}}\nabla\bar{\epsilon}^{(i)}]\,\mathrm{d}V. \end{aligned} \tag{4.9}$$

In fact, a similar matrix form of incremental equations is obtained upon discretization for both combinations of the local and gradient-dependent theories, leading to two-field mixed finite elements. Further details of the numerical implementation, consistent linearization and other algorithmic aspects can be found in [17].

5. Equivalent strain measures and damage laws

So far, the equivalent strain measure $\tilde{\epsilon}$ has been left unspecified. It can be defined as the damage energy release rate, cf. [8], or a modified form thereof which satisfies the condition that for a uniaxial strain $\tilde{\epsilon} = |\epsilon|$:

$$\tilde{\epsilon} = \sqrt{\frac{1}{E}\boldsymbol{\epsilon}^{\mathrm{T}}\mathbf{D}^{\mathrm{e}}\boldsymbol{\epsilon}}, \tag{5.1}$$

where E is Young's modulus. For quasi-brittle materials a more suitable form, taking into account the difference between the tensile and compressive strength,

can be adopted [25, 26], e.g. the modified von Mises definition of the equivalent strain measure [26], which has been used here:

$$\tilde{\epsilon} = \frac{k-1}{2k(1-2\nu)} I_1 + \frac{1}{2k}\sqrt{\left(\frac{k-1}{1-2\nu} I_1\right)^2 + \frac{12k}{(1+\nu)^2} J_2}, \tag{5.2}$$

where k is a ratio of uniaxial compressive and tensile strength, ν is Poisson's ratio, I_1 is the first invariant of the strain tensor and J_2 is the second invariant of the strain deviator. In Fig. 1 this strain measure is compared with the definition in Eq. (5.1). The figure has been plotted for plane-stress conditions, $\tilde{\epsilon} = 0.001$, $k = 10$ and $\nu = 0.2$.

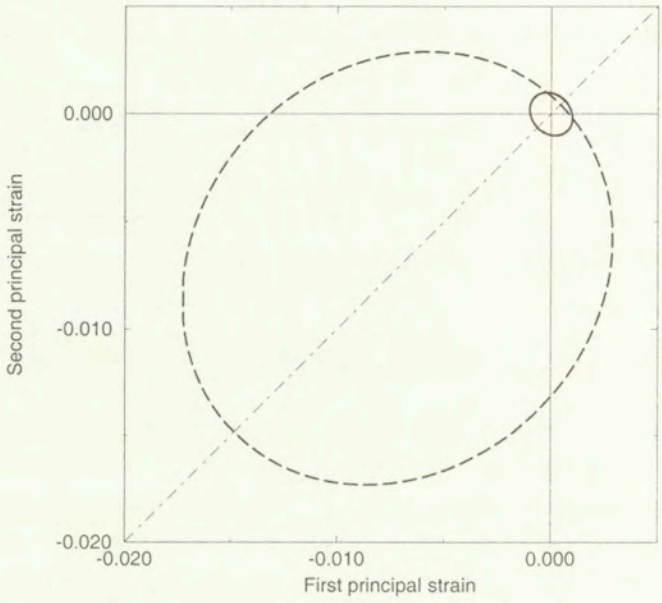

FIG. 1. Comparison of equivalent strain measure definitions: Eq. (5.1) – solid versus Eq. (5.2) – dashed.

Another issue is whether $\tilde{\epsilon}$ should be a measure of total strains, their elastic part or some other function of elastic and plastic strains [8]. If it is assumed that the equivalent strain measure is a function of elastic strains only, $\tilde{\epsilon}(\boldsymbol{\epsilon}^{\mathrm{e}})$, which means that the damage growth is driven by the effective stresses, see Eq. (2.8), the two theories become weakly coupled. If a full coupling exists, for instance for plastically induced damage in metals, plastic strains should also contribute to $\tilde{\epsilon}$.

In this paper, for gradient plasticity combined with damage, $\tilde{\epsilon}$ has been assumed to be an equivalent measure of the total strains $\tilde{\epsilon}(\boldsymbol{\epsilon})$. A measure of elastic strains only obviously loses sense in the case of softening plasticity and, for the

gradient regularization to be active within the considered model, the damage growth should depend on the nonlocal plastic strains. For gradient damage combined with plasticity we consider two possibilities: $\tilde{\epsilon}(\boldsymbol{\epsilon})$ and $\tilde{\epsilon}(\boldsymbol{\epsilon}^{\mathrm{e}})$. In the latter case the computation of $\mathbf{s}^{\mathrm{T}}$ in Eq. (2.20) becomes slightly more intricate, since it then equals:

$$\mathbf{s}^{\mathrm{T}} = \frac{\mathrm{d}\tilde{\epsilon}}{\mathrm{d}\boldsymbol{\epsilon}^{\mathrm{e}}} \frac{\mathrm{d}\boldsymbol{\epsilon}^{\mathrm{e}}}{\mathrm{d}\boldsymbol{\epsilon}} = \frac{\mathrm{d}\tilde{\epsilon}}{\mathrm{d}\boldsymbol{\epsilon}^{\mathrm{e}}} (\mathbf{D}^{\mathrm{e}})^{-1} \mathbf{D}^{\mathrm{ep}}. \tag{5.3}$$

The damage growth function (2.5), which governs the stress evolution and elastic stiffness degradation, represents a uniaxial stress-strain relationship. It can be validated by experimental measurements. In this paper we use three different damage growth functions. A linear dependence of ω on κ^{d}:

$$\omega(\kappa^{\mathrm{d}}) = \frac{\kappa^{\mathrm{d}} - \kappa_{\mathrm{o}}}{\kappa_{\mathrm{u}} - \kappa_{\mathrm{o}}} \tag{5.4}$$

means that, although eventually the stress drops to zero, there is a hardening stage in the stress-strain relationship. Secondly, the function can represent a linear softening stress-strain diagram:

$$\omega(\kappa^{\mathrm{d}}) = \frac{\kappa_{\mathrm{u}}}{\kappa^{\mathrm{d}}} \frac{\kappa^{\mathrm{d}} - \kappa_{\mathrm{o}}}{\kappa_{\mathrm{u}} - \kappa_{\mathrm{o}}}. \tag{5.5}$$

Case (5.4) will further be called "linear damage", while case (5.5) will just be called "damage". Finally, we will use an exponential damage function which represents exponential softening:

$$\omega(\kappa^{\mathrm{d}}) = 1 - \frac{\kappa_{\mathrm{o}}}{\kappa^{\mathrm{d}}} \left(1 - \alpha + \alpha e^{-\eta(\kappa^{\mathrm{d}} - \kappa_{\mathrm{o}})}\right), \tag{5.6}$$

where α and η are additional parameters. This function is suitable for reproducing the experimental tensile fracture in concrete, since the experimental uniaxial softening relation is exponential [27]. Since it approaches the complete loss of coherence ($\omega = 1$) asymptotically, singularities caused by a complete loss of strength are also avoided.

6. One-dimensional numerical studies

Firstly, implications of the three damage laws are illustrated using a uniaxial problem shown in Fig. 2 and a pure gradient-damage theory. We analyze a bar with a unit cross-section and a geometrical imperfection, subjected to tension. In order to initiate strain localization, a 10% smaller cross-section is adopted in the central zone $d = 10$ mm. Symmetry of deformation is imposed. The length of the bar is $L = 100$ mm, Young's modulus is $E = 20000$ N/mm^2. Eighty

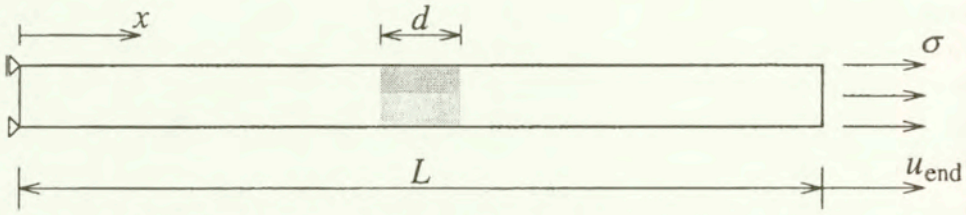

FIG. 2. Tensile bar with imperfection for localization studies.

C^0-continuous three-noded gradient damage elements are used with two-point Gaussian integration [21]. The elements have a quadratic and linear interpolation of the displacement and averaged strain, respectively. A gradient constant $c = 4$ mm^2 is adopted.

In a one-dimensional problems the equivalent strain measure $\tilde{\epsilon}$ is equal to the absolute value of the axial strain ϵ. For all damage laws the same damage threshold $\kappa_0 = 0.0001$ is used. For linear damage, Eq. (5.4), we adopt $\kappa_u = 0.0005$ and for the damage growth function representing linear softening, Eq. (5.5), $\kappa_u = 0.0125$. The exponential damage parameters, Eq. (5.6), are: $\alpha = 1.00$, $\eta = 200$.

Figures 3–4 demonstrate that the response of the model is quite different although the gradient influence factor is the same for all cases. The load-displacement diagrams in Fig. 3 show the computed relations between the stress at the right-hand end of the bar σ and the elongation of the bar u_{end}. For linear damage we first observe a hardening stage and then a severe snap-back behaviour while the originally distributed damage profile in Fig. 3b strongly localizes and damage finally grows only in the smallest possible volume (two integration points).

For the second case (Fig. 4a) the damage zone first broadens and then the points at its boundary gradually enter unloading, which is also accompanied by snap-back behaviour in Fig. 3a. In the final stage the deformation also localizes in the two central integration points. This is because the strain and damage finally localize in a crack at midspan of the bar. Up to this moment, localization is limited during the whole deformation history.

For the exponential law the damage zone in Fig. 4b is narrower, since softening is more pronounced in the first stage of the damage process. However, for this case the bar extension does not exhibit a snap-back and $\omega = 1$ is approached simultaneously in a larger set of central points. The interpretation of a continuous damage evolution into a crack is lost in this case.

The gradient-enhanced coupled theories will now be applied in the uniaxial localization problem from Fig. 2 in order to illustrate the basic properties of the models in loading and unloading. It is noted that mesh sensitivity studies have been presented in [17] and will not be repeated here.

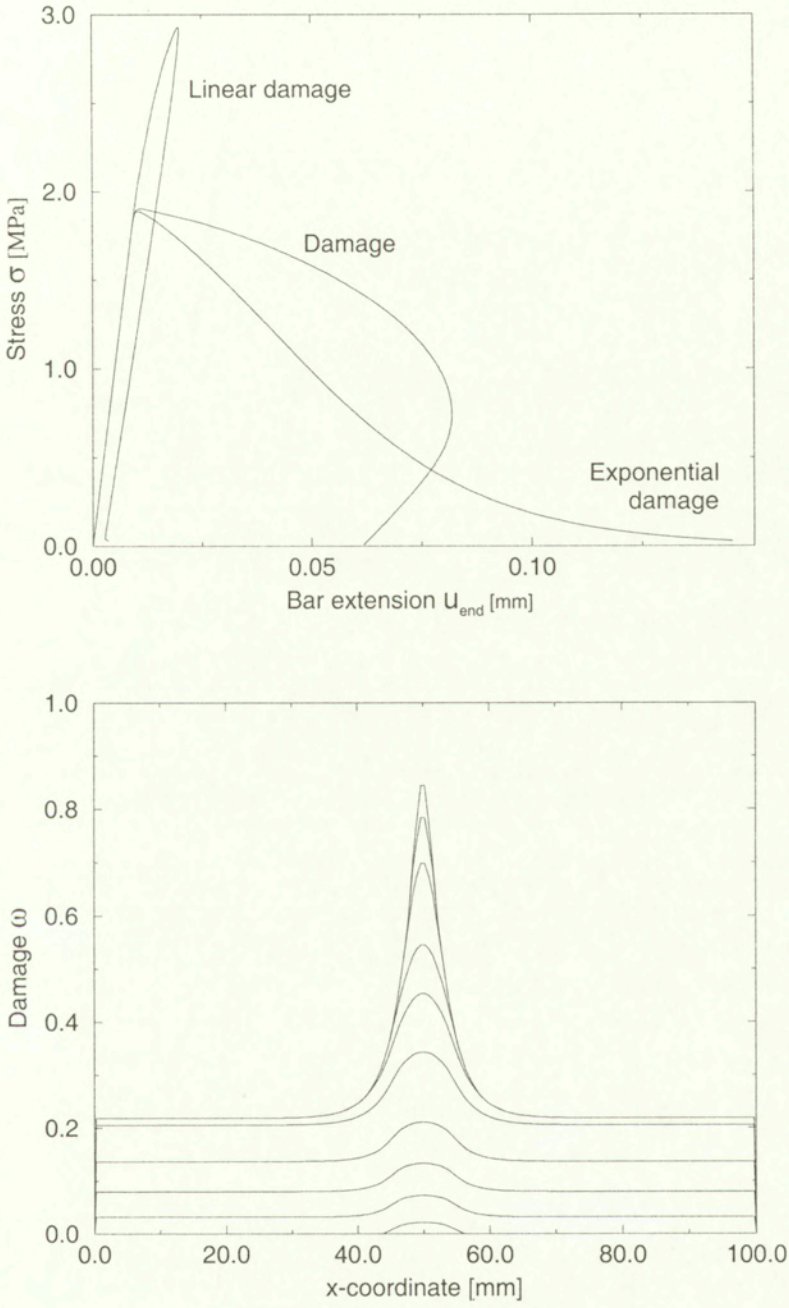

FIG. 3. Comparison of results for different damage growth functions and $c = 4$ mm^2: (a) load-displacement diagrams, (b) damage evolution for linear damage.

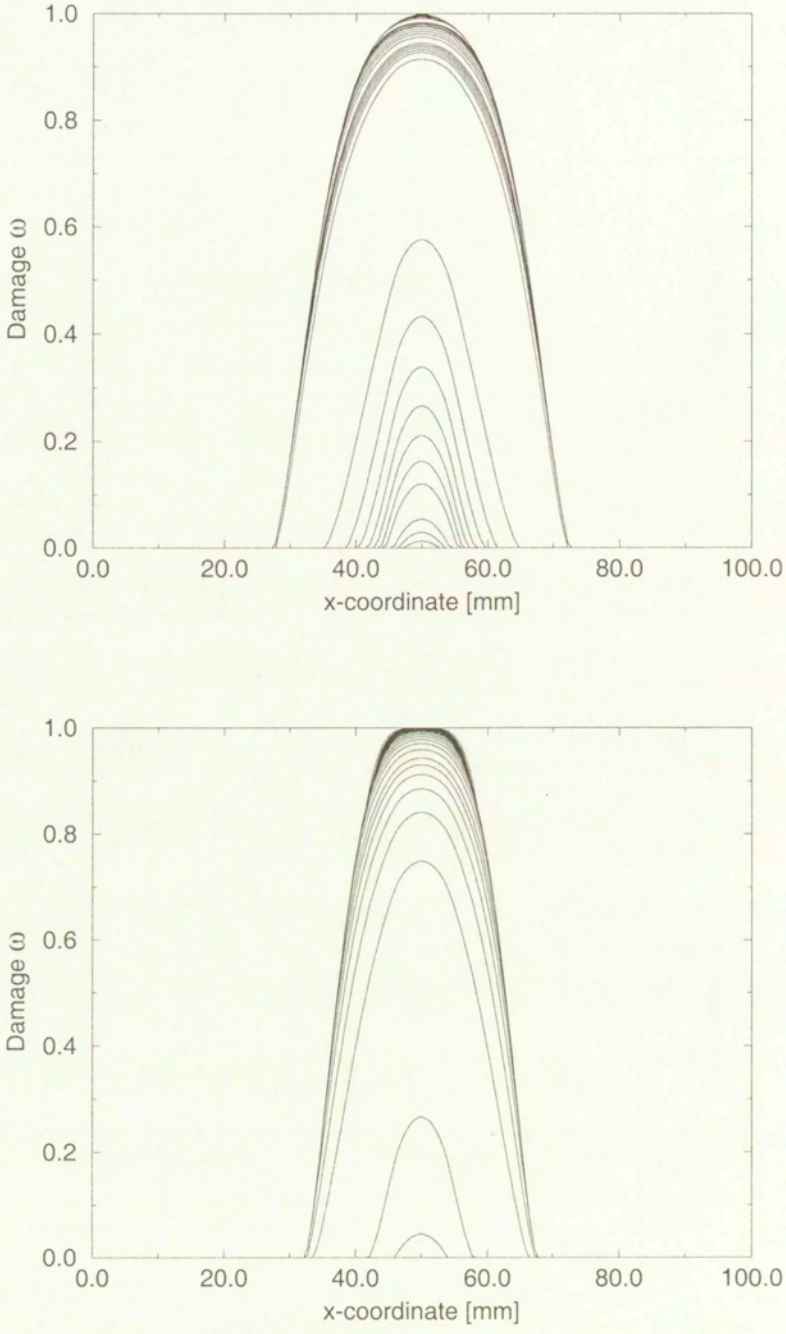

FIG. 4. Damage evolution for $c = 4$ mm^2 and: (a) damage growth function representing linear softening, (b) exponential damage growth function.

6.1. Gradient plasticity coupled to scalar damage

In the uniaxial case the Huber-von Mises or Rankine yield functions give $\tilde{\sigma} = |\sigma|$. The tensile strength is $\sigma_y = 2$ N/mm^2. We employ a discretization with eighty C^1-continuous three-noded gradient plasticity elements [20]. The derivative of the plastic multiplier is set to zero at both ends of the bar to allow for reduced integration.

First, softening gradient plasticity is coupled to damage. Linear softening with $h = -500$ N/mm^2 and the gradient constant $g = 12500$ N are adopted, so that the width of the localization zone predicted by gradient plasticity is $w = 2\pi l = 31.4$ mm [19]. In Fig. 5a the solution obtained for pure gradient plasticity is compared with the coupled model, in which $\bar{\epsilon}$ is the total strain. The damage evolution is activated later than the plastic flow by adopting the damage threshold $\kappa_o = 0.001$. The linear damage with $\kappa_u = 0.01$ and the damage law from Eq. (5.5) with $\kappa_u = 0.1$ are used. For the linear relation $\omega(\kappa^d)$ the damage growth is initially much slower, but the ultimate value $\kappa_u = 0.01$ associated with $\omega = 1$ and $\sigma = 0$ is reached for smaller extension of the bar.

It is observed that the localization zone first expands from the imperfect elements, then its width remains almost constant and, finally, the plastic zone starts to grow again while the load-displacement diagram bends upwards, since in the central points the softening diagram is exited. For pure gradient plasticity the width of the localization zone is equal to the expected value during the linear softening stage. For the coupled model the plastic strains are more localized due to interaction with damage, but a spurious tendency to localize in the smallest possible volume is not observed [17]. Apparently, the gradient regularization is active in spite of adding the second destabilizing component to the constitutive description.

In Fig. 5a unloading branches at some extension levels are also shown. For pure gradient plasticity the unloading is elastic, but, quite surprisingly, also for the coupling to damage the unloading stiffness reduction is very small. The plasticity model dominates.

Secondly, for hardening gradient plasticity, we preserve the gradient constant $g = 12500$ N and we adopt a linear hardening with $h = 500$ N/mm^2. For the linear damage model $\kappa_o = 0.0005$ and $\kappa_u = 0.01$. For the damage growth function representing linear softening $\kappa_u = 0.1$ and two damage thresholds are considered: $\kappa_o = 0.0001$ and $\kappa_o = 0.0005$. For the former case the damage and plastic processes are activated simultaneously, i.e. κ_o is reached for the same load as σ_y. Figure 5b presents the obtained load-displacement diagrams and Fig. 6 gives the damage evolution in the bar.

For the case of pure gradient plasticity or when the onset of the damage process is delayed until after the initiation of plasticity we first observe yielding

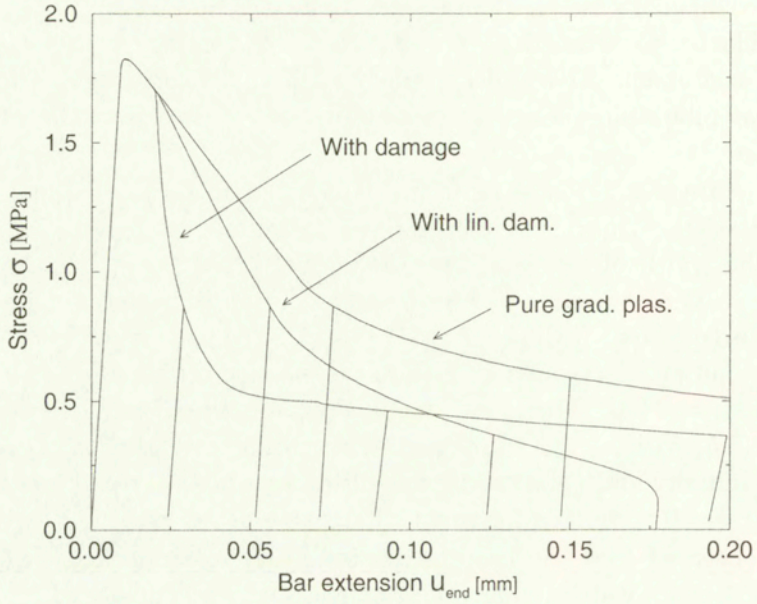

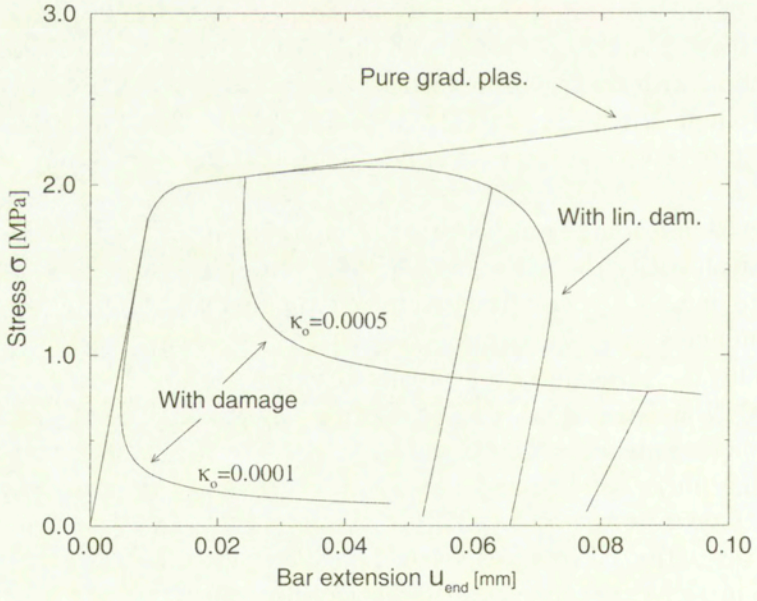

FIG. 5. (a) Load-displacement diagrams for gradient plasticity with damage: (a) softening plasticity, (b) hardening plasticity.

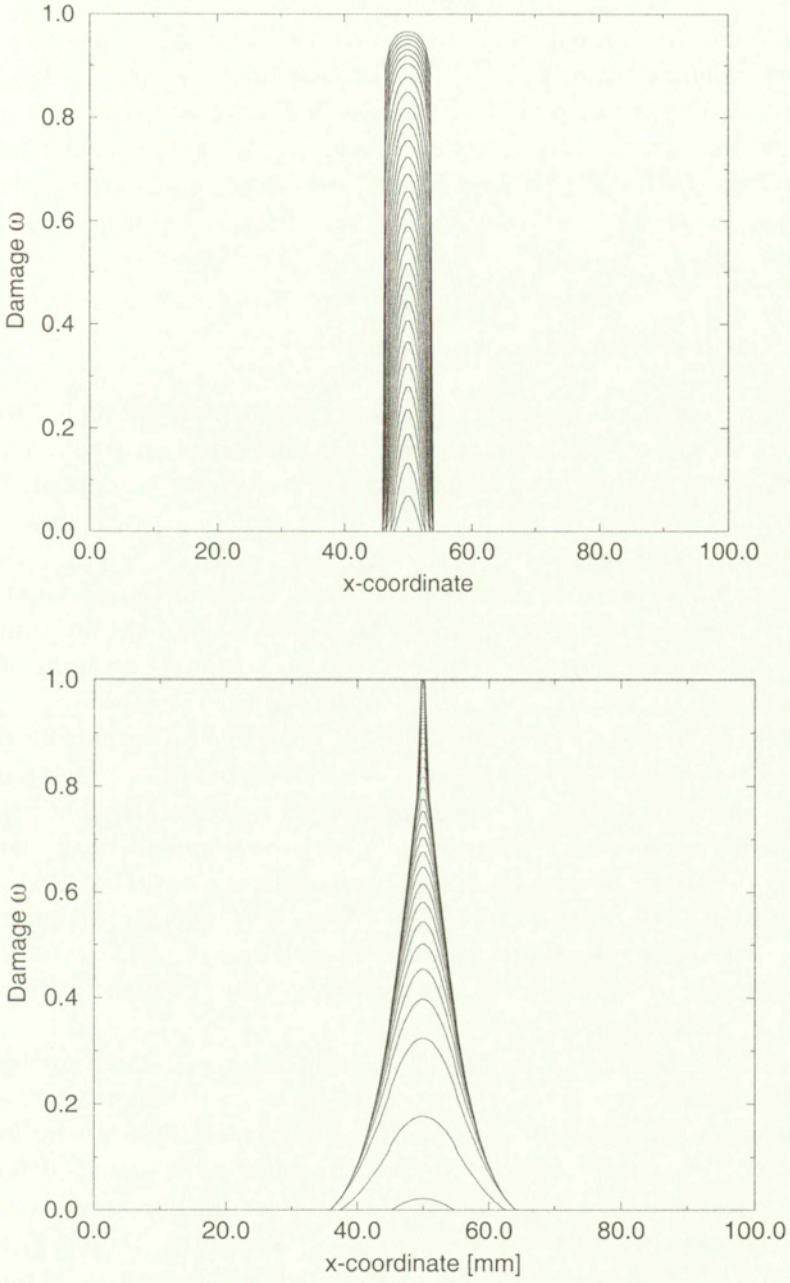

FIG. 6. Damage evolution for hardening gradient plasticity coupled to (a) damage with the damage law representing linear softening, and (b) linear damage. The damage threshold $\kappa_o = 0.0001$.

in the imperfect part of the bar and then, due to hardening, a plastic state is reached in the whole bar. However, once damage starts, softening is observed and localization of both damage and plastic processes takes place in a zone whose size and evolution depend on the damage law and threshold as shown in Fig. 6. For $\kappa_o = 0.0001$ a fast growth of damage is first observed in two central finite elements and then the damage zone gradually expands. The regularization related to plasticity seems to be active for the softening caused by damage, see also [23]. However, the predicted stiffness degradation is again unrealistically small (Fig. 5b).

6.2. Gradient damage coupled to hardening plasticity

We now consider the case of gradient damage theory coupled to hardening plasticity. The length of the bar, the size of the imperfection and Young's modulus are the same as before. The gradient constant $c = 1$ mm^2 is adopted. The damage growth function representing linear softening, Eq. (5.5), with $\kappa_o = 0.0001$ and $\kappa_u = 0.0125$ is employed.

The strain measure is either the total strain $\tilde{\epsilon} = \epsilon$ or the elastic strain $\tilde{\epsilon} = \epsilon^e$. In Figs. 7–8 the solutions obtained for pure gradient damage are compared with the two combinations with hardening plasticity. Now, the beginning of the plastic process is slightly delayed with respect to the damage threshold ($\sigma_y = 5$ N/mm^2).

Figure 7a shows a comparison of load-displacement diagrams for different values of the hardening modulus h. For $\tilde{\epsilon} = \epsilon$ the coupled model gives a more brittle response and for $\tilde{\epsilon} = \epsilon^e$ the results show an increased ductility. The value adopted in this test for the hardening modulus h may seem unrealistically large, but we note that plasticity now represents the behaviour of the material "skeleton" (the fictitious body, see Section 2) and the evolution of microcracks and microvoids which causes the strength and stiffness degradation of the material is modelled by the damage component. For an increasing value of h the solution for pure damage is approached.

Figure 7b compares the unloading branches for $h = E$. Both combined models result in irreversible strains. If the strain measure is based on elastic strains, damage evolution is governed by the effective stress. This is why for this case and for pure damage, the same stiffness degradation is observed for the same stress level. However, a large irreversible strain is now present.

The damage evolution for the two damage measures and $h = E$ is shown in Fig. 8. For $\tilde{\epsilon} = \epsilon^e$ the obtained damage evolution is the same as for pure gradient damage. This is because plasticity and damage contribute to the response without mutual interaction. For $\tilde{\epsilon} = \epsilon$ no further expansion of the damage zone is observed after the plastic process has started, so the solution is more localized.

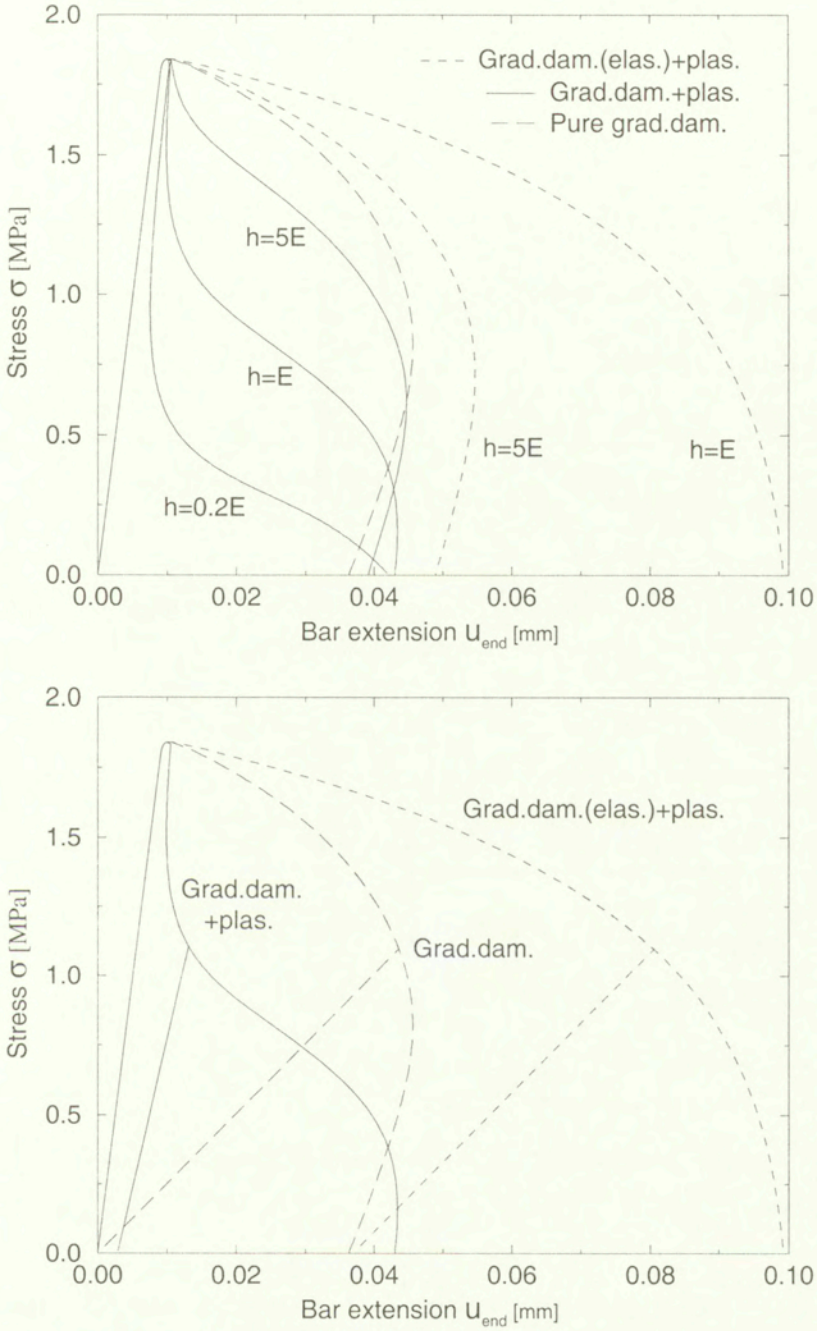

FIG. 7. Gradient damage combined with plasticity ($c = 1$ mm^2): (a) sensitivity of load-displacement diagrams to hardening modulus h, (b) unloading stiffness for damage measure based on total and elastic strains.

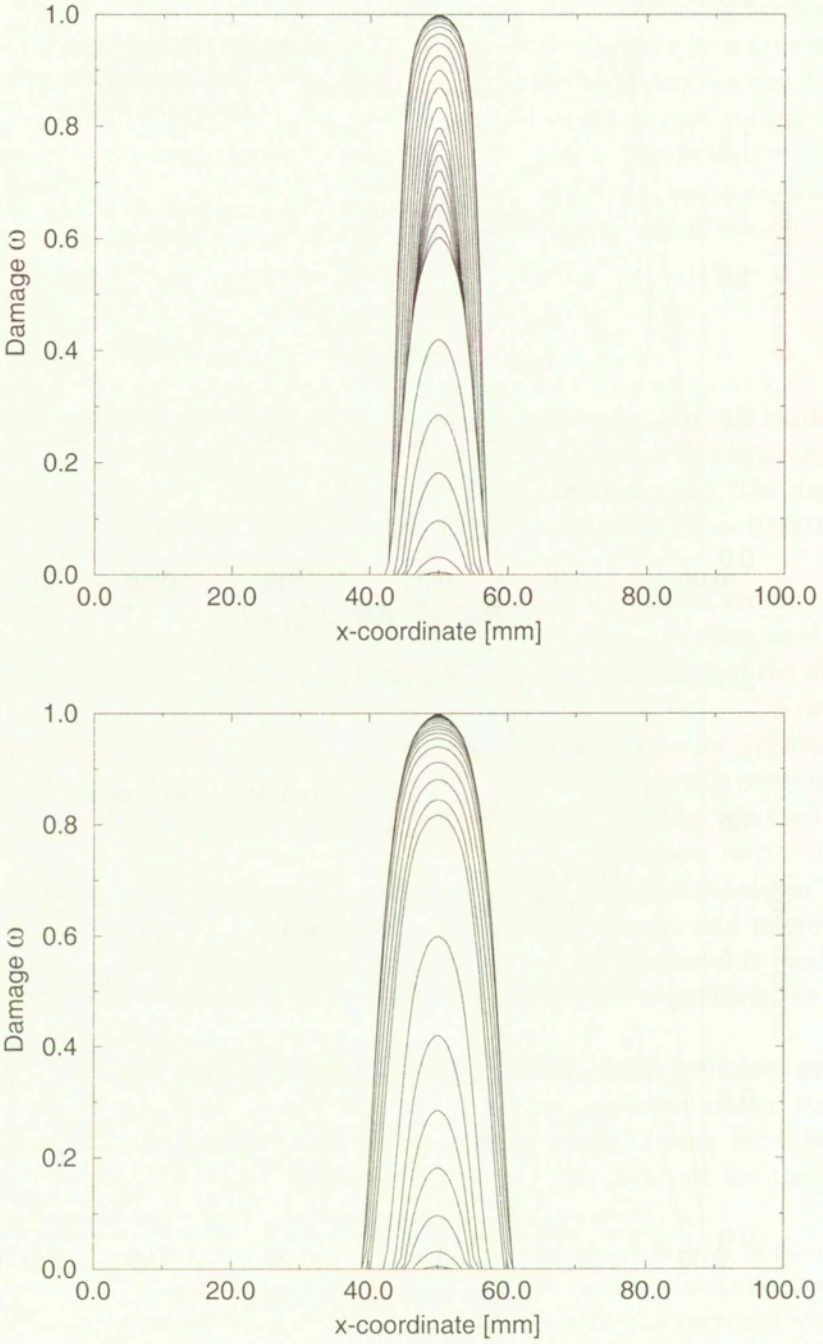

FIG. 8. Damage evolution for (a) gradient damage with total strain measure $\tilde{\epsilon} = \epsilon$ and (b) gradient damage with elastic strain measure $\tilde{\epsilon} = \epsilon^{\mathrm{e}}$. Gradient factor $c = 1$ mm^2.

The only unstable part of the constitutive model, i.e. the damage growth, is regularized by the gradient enhancement, so the results do not exhibit spurious mesh sensitivity [17].

7. Four-point bending test

The four-point bending test is a plane-stress simply-supported beam configuration which has been used in standard experiments of concrete fracture under monotonic and reversed loading in [27]. A symmetric half of the original specimen is shown in Fig. 9 together with the finite element mesh employed in the present computations. The thickness of the beam is 50 mm. The vertical force is exerted under deformation control.

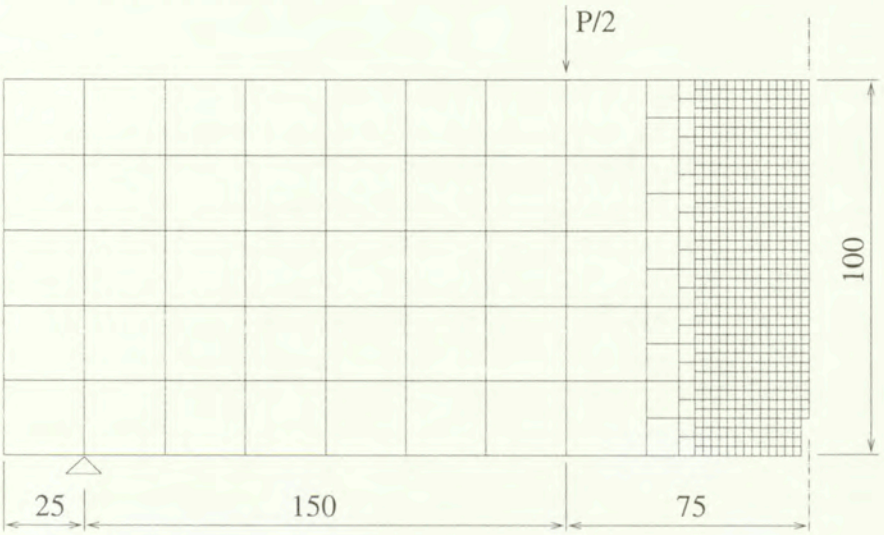

FIG. 9. Four-point bending test – discretized configuration (dimensions in mm).

Four cases have been analyzed: pure gradient damage, gradient damage coupled to plasticity by the equivalent strain measure based on total strains $\tilde{\epsilon}(\boldsymbol{\epsilon})$, the gradient damage-plasticity with damage driven by elastic strains $\tilde{\epsilon}(\boldsymbol{\epsilon}^{\mathrm{e}})$ and, finally, pure gradient plasticity. Although the softening gradient plasticity with the Rankine failure function, i.e. when $\tilde{\sigma}$ in Eq. (3.1) is the maximum principal stress, is capable of reproducing to some extent the decohesive material failure which usually underlies damage [20, 28], the lack of elastic stiffness degradation makes the model unacceptable for cyclic loading. However, coupling of this theory to damage pursued in Sec. 6.1 suffers from three drawbacks: the predicted stiffness degradation is too small, the results are excessively sensitive to the damage threshold [17], and, more importantly, it is difficult to find physical grounds for

a combination of two softening mechanisms even if the regularization of only the plastic component of the model leads to mesh-insensitive results. Therefore, this coupled model will not be used here.

For gradient damage coupled to plasticity the Huber-von Mises criterion has served as the yield function. However, the Drucker-Prager plasticity theory can also be used in the combined model if the difference between the uniaxial and biaxial compressive strength and the possible non-normality of plastic flow become important. The modified von Mises definition of the equivalent strain measure from Eq. (5.2) with $k = 10$ and the exponential damage law from Eq. (5.6) have been used, cf. [29].

The following model parameters have been adopted: Young's modulus $E = 40000$ N/mm^2, Poisson's ratio $\nu = 0.20$, damage threshold $\kappa_o = 0.000075$, damage growth function parameters $\alpha = 0.92$, $\eta = 300$, yield strength $\sigma_y = 4.5$ N/mm^2, hardening modulus $h = E/2$, gradient influence factor $c = 4$ mm^2. The value of σ_y is chosen such that the damage and plastic processes commence almost simultaneously. Gradient damage elements with quadratic interpolation of displacements, linear interpolation of the averaged strain measure, and 2×2 Gauss integration have been employed [21].

For pure gradient plasticity the Rankine failure function has been used with the exponential softening law $\sigma_y(\kappa^p)$ of CORNELISSEN, HORDIJK and REINHARDT [27]. The following model parameters have been adopted: Young's modulus as above, Poisson's ratio $\nu = 0$, uniaxial tensile strength $f_t = 3.0$ N/mm^2, fracture energy $G_f = 0.125$ Nmm/mm^2. The gradient influence factor g is assumed to decrease with the increase of the equivalent inelastic strain measure $g = -l^2\sigma_y'(\kappa^p)$, cf. [20], and an internal length scale $l = 3$ mm is adopted. Gradient plasticity elements with quadratic interpolation of displacements, Hermitean interpolation of the plastic multiplier and reduced Gauss integration (2×2) have been employed [20].

In Fig. 10 the computed load-displacement diagrams are compared. The deflection v is measured at midspan at the bottom of the beam. It is first observed that, with the adopted parameters, the diagrams for Rankine gradient plasticity and pure gradient damage coincide rather closely. However, the response in unloading is far from reality. In loading, a more brittle response is observed for gradient damage coupled to damage through $\tilde{\epsilon}(\boldsymbol{\epsilon})$, while for $\tilde{\epsilon}(\boldsymbol{\epsilon}^e)$ a larger ductility is obtained, since damage is then a function of elastic strains which grow much slower during the plastic process.

Figure 11 shows the incremental deformation pattern obtained for the pure gradient plasticity and gradient damage models at the final points on the curves in Fig. 10. It is observed that in both cases localization appears in a zone broader than one row of elements. It is also noticed that while for the gradient-damage model a quadratic convergence of the incremental-iterative algorithm is

observed, for gradient plasticity the convergence is slow due to problems with the satisfaction of the weak form of the yield condition $(3.2)_2$ at the notch.

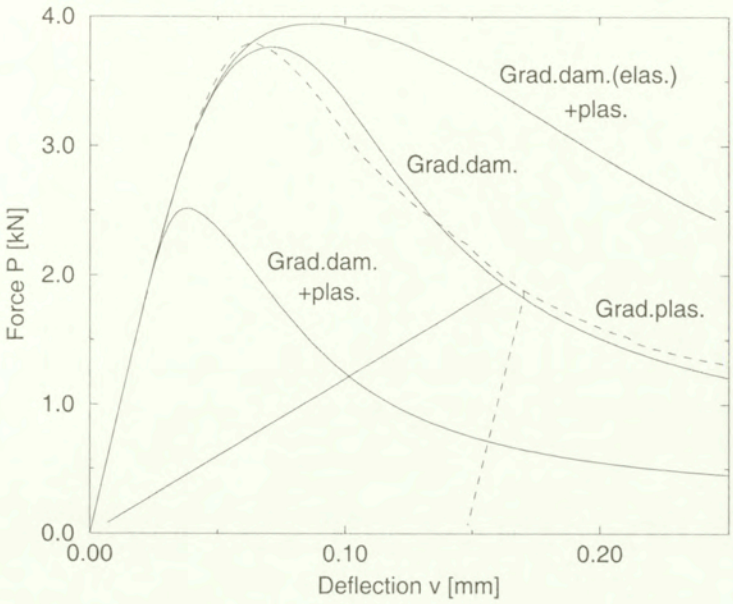

FIG. 10. Load-displacement diagrams for four-point bending test (gradient plasticity diagram dashed).

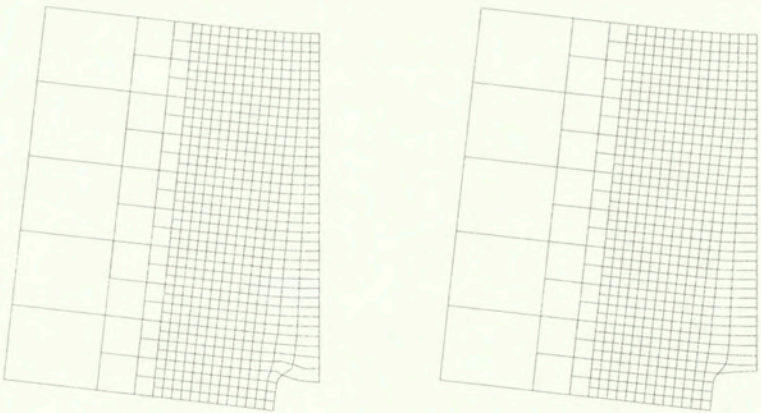

FIG. 11. Four-point bending: final displacement pattern in the central zone for (a) gradient plasticity and (b) for pure gradient damage.

As shown in Figs. 12–13 the two gradient damage-plasticity models can easily be tuned to fit the experimental results of [27]. The crucial point is that for both damage-plasticity combinations, the load reversals exhibit a proper gradual in-

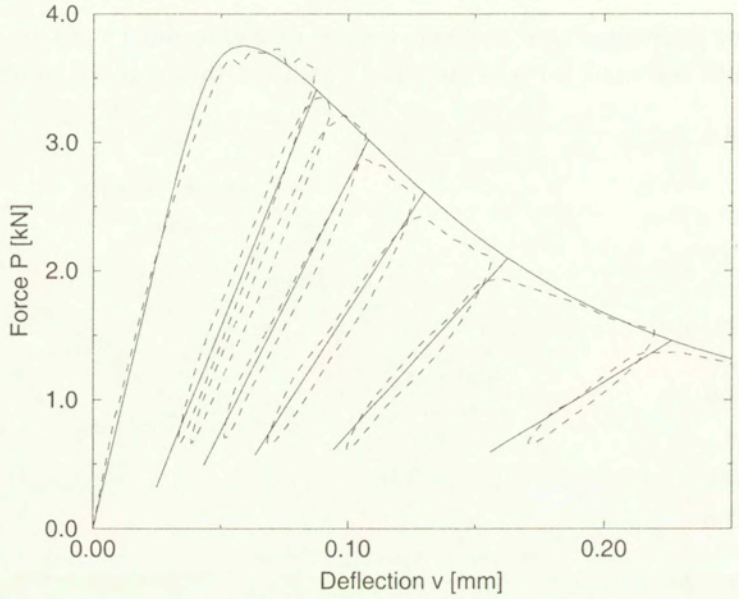

FIG. 12. Experimental and simulated load-displacement diagrams – gradient damage coupled to plasticity $\tilde{\epsilon}(\epsilon)$. Model parameters: $c = 4$ mm^2, $\sigma_y = 6.5$ N/mm^2, $h = E/2$, $\kappa_o = 0.00011$, $\alpha = 0.90$, $\eta = 160$.

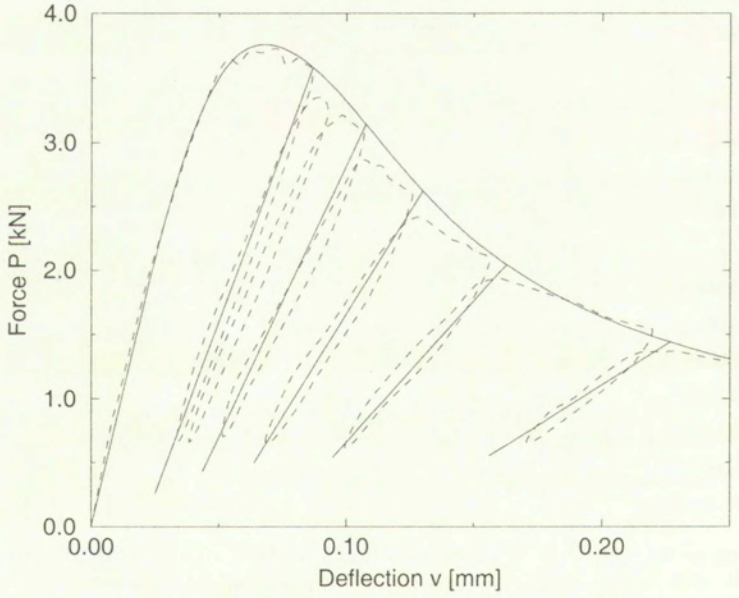

FIG. 13. Experimental and simulated load-displacement diagrams – gradient damage with plasticity $\tilde{\epsilon}(\epsilon^e)$. Model parameters: $c = 4$ mm^2, $\sigma_y = 4.5$ N/mm^2, $h = E/2$, $\kappa_o = 0.00008$, $\alpha = 0.92$, $\eta = 600$.

crease of elastic stiffness degradation. However, the hysteretic loops observed in the experiment can not be reproduced with the present model. To achieve this, the plasticity model must be augmented by a kinematic hardening and the damage description must be split into parts related to positive and negative strains, see for instance [6, 8]. This would also allow for a simulation of crack closure effects. Another solution may be to enhance a generalized plasticity model like that shown in [30] with a localization limiter.

Finally, Fig. 14 presents the damage zone, the averaged strain distribution and the equivalent plastic strains distribution for gradient damage coupled to plasticity. The results are plotted for the final point on the computed load-displacement diagram in Fig. 12. We observe that the averaged and, especially, plastic strains are much more localized than the damage distribution.

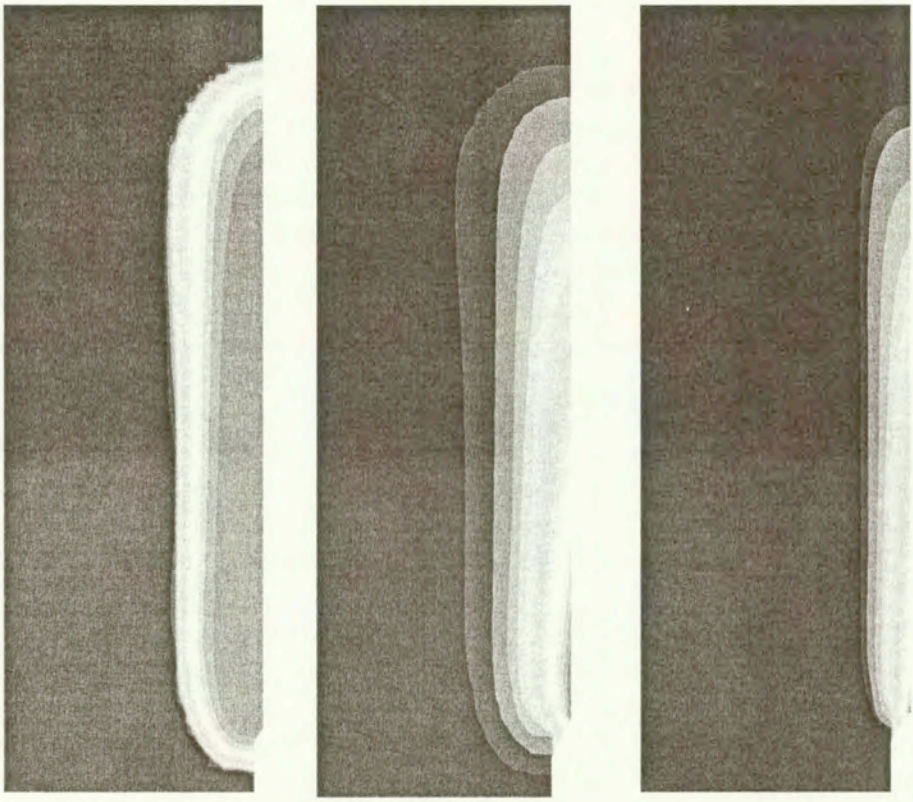

FIG. 14. Fracture zone of four-point bending test: (a) final damage distribution, (b) averaged strain and (c) equivalent plastic strain distribution for gradient damage based on total strains.

As has been noticed in [22], the damage predictions of the model with a constant gradient influence factor c and the exponential damage evolution law may be unrealistic for two-dimensional configurations, since the damage zone tends to broaden instead of evolving into a crack when failure is approached. The coupling to plasticity does not solve this problem. If a localized final damage pattern is to be simulated, the gradient-damage model must be improved, for instance by making the gradient influence factor variable and adopting a different damage law, see [22].

8. Final remarks

Plasticity and damage theories are both capable of reproducing the experimental load-displacement diagrams obtained for quasi-brittle materials under monotonic loading. However, since strain softening and localization are involved, the models must be regularized. To reproduce a realistic stiffness degradation and get closer to a proper modelling of damaging or fracture processes, a combination of the two theories is proposed. It seems that a compromise must be made between a sophisticated modelling of constitutive properties like anisotropic damage and a proper treatment of ill-posedness problems. In this paper a higher weight has been attributed to the latter issue while the constitutive description retains a rather simple, isotropic format. This obviously limits its applicability, although the use of concepts as the modified von Mises equivalent strain measure allows to incorporate the difference of the response to tensile and compressive forces. As also shown in [29], this leads to quite realistic fracture simulations in concrete.

Two types of gradient-dependent couplings of plasticity and damage have been summarized. They are formulated is such a way that the coupling influences only the equilibrium equations, while the second differential equation, which serves the purpose of regularization, preserves the original format of gradient plasticity [19] and gradient damage [21], respectively. For both couplings, consistently linearized two-field finite element formulations have been used [17].

The combination of softening gradient plasticity with damage, in spite of being considered in the numerical experiments, does not seem to have a good physical motivation. The combination of hardening gradient plasticity with damage, considered here and also in a slightly different form in [23], has the weakness that the attachment of the regularization procedure to a hardening plasticity model raises doubts. As shown in [17], these models also seem to suffer from an excessive sensitivity to the damage threshold.

On the other hand, the combination of gradient damage with hardening plasticity gives promising results: the physical interpretation of the model components is convincing, there are few model parameters to be determined, the elastic stiffness degradation is properly reproduced and spurious mesh sensitivity of re-

sults is avoided [17]. Although the fully coupled model with a strain measure based on total strains has a better physical background, no clear evidence has been found that the coupling based on an elastic strain measure should be discarded.

Acknowledgments

Valuable discussions on gradient damage with Dr M.G.D. GEERS from the Eindhoven University of Technology/Royal Military Academy, Brussels are gratefully acknowledged. Financial support of the von Humboldt Foundation and the Max-Planck Society through the Max-Planck Research Award 1996 to the second author and of the Polish Committee for Scientific Research (grant PB 7 T07A 03612) to the first author are gratefully acknowledged.

References

1. J.W. DOUGILL, *Some remarks on path independence in the small in plasticity*, Qt. Appl. Math., **32**, 233–243, 1975.
2. Y.F. DAFALIAS, *Elasto-plastic coupling within a thermodynamic strain space formulation of plasticity*, Int. J. Non-Linear Mechanics, **12**, 327–337, 1977.
3. G. MAIER and T. HUECKEL, *Nonassociated and coupled flow rules of elastoplasticity for rock-like materials*, Int. J. Rock Mech. Min. Sci. & Geomech. Abstr., **16**, 77–92, 1979.
4. Z.P. BAŽANT and S.S. KIM, *Plastic-fracturing theory for concrete*, ASCE J. Eng. Mech., **105**(3), 407–421, 1979.
5. A. DRAGON and Z. MRÓZ, *A continuum theory for plastic-brittle behaviour of rock and concrete*, Int. J. Engng Sci., **17**(2), 121–137, 1979.
6. M. ORTIZ, *A constitutive theory for the inelastic behaviour of concrete*, Mechanics of Materials, **4**, 67–93, 1985.
7. J.C. SIMO and J.W. JU, *Strain- and stress-based continuum damage models – I. Formulation, II. Computational aspects*, Int. J. Sol. Struct., **23**(7), 821–869, 1987.
8. J.W. JU, *On energy-based coupled elastoplastic damage theories: constitutive modeling and computational aspects*, Int. J. Sol. Struct., **25**(7), 803–833, 1989.
9. N.R. HANSEN and H.L. SCHREYER, *A thermodynamically consistent framework for theories of elastoplasticity coupled with damage*, Int. J. Sol. Struct., **31**(3), 359–389, 1994.
10. I. DOGHRI, *Numerical implementation and analysis of a class of metal plasticity models coupled with ductile damage*, Int. J. Num. Meth. Eng., **38**, 3403–3431, 1995.
11. F. MAROTTI de SCIARRA, *General theory of damage elastoplastic models*, ASCE J. Eng. Mech., **123**(10), 10003–1011, 1997.
12. R. DE BORST and E. VAN DER GIESSEN, *Material instabilities in solids*, IUTAM, John Wiley & Sons, Chichester 1998.
13. Z.P. BAŽANT and G. PIJAUDIER-CABOT, *Nonlocal continuum damage, localization instability and convergence*, ASME J. Appl. Mech., **55**, 287–293, 1988.

14. L.J. SLUYS, *Wave propagation, localization and dispersion in softening solids*, Ph. D. disseration, Delft University of Technology, Delft 1992.

15. R. DE BORST, L.J. SLUYS, H.-B. MÜHLHAUS, and J. PAMIN, *Fundamental issues in finite element analyses of localization of deformation*, Eng. Comput., **10**, 99–121, 1993.

16. R. DE BORST, J. PAMIN, R.H.J. PEERLINGS, and L.J. SLUYS, *On gradient-enhanced damage and plasticity models for failure in quasi-brittle and frictional materials*, Computational Mechanics, **17**, 130–141, 1995.

17. R. DE BORST, J. PAMIN, and M.G.D. GEERS, *On coupled gradient-dependent plasticity and damage theories with a view to localization analysis*, Eur. J. Mech.: A/Solids, 1999. Accepted for publication.

18. H.-B. MÜHLHAUS and E.C. AIFANTIS, *A variational principle for gradient plasticity*, Int. J. Sol. Struct., **28**, 845–857, 1991.

19. R. DE BORST and H.-B. MÜHLHAUS, *Gradient-dependent plasticity: Formulation and algorithmic aspects*, Int. J. Num. Meth. Eng., **35**, 521–539, 1992.

20. J. PAMIN, *Gradient-dependent plasticity in numerical simulation of localization phenomena*, Ph. D. dissertation, Delft University of Techology, Delft 1994.

21. R.H.J. PEERLINGS, R. DE BORST, W.A.M. BREKELMANS, and J.H.P. DE VREE, *Gradient-enhanced damage for quasi-brittle materials*, Int. J. Num. Meth. Eng., **39**, 3391–3403, 1996.

22. M.G.D. GEERS, *Experimental analysis and computational modelling of damage and fracture*, Ph. D. dissertation, Eindhoven University of Technology, Eindhoven 1997.

23. T. SVEDBERG and K. RUNESSON, *A thermodynamically consistent theory of gradient-regularized plasticity coupled to damage*, Int. J. Plasticity, **13**(6-7), 669–696, 1997.

24. R. HILL, *A general theory of uniqueness and stability in elastic-plastic solids*, J. Mech. Phys. Solids, **6**, 236–249, 1958.

25. J. MAZARS and G. PIJAUDIER-CABOT, *Continuum damage theory – application to concrete*, ASCE J. Eng. Mech., **115**, 345–365, 1989.

26. J.H.P. DE VREE, W.A.M. BREKELMANS, and M.A.J. VAN GILS, *Comparison of nonlocal approaches in continuum damage mechanics*, Comp. & Struct., **55**(4):581–588, 1995.

27. D.A. HORDIJK, *Local approach to fatigue of concrete*, Ph. D. dissertation, Delf University of Technology, Delft 1991.

28. R. DE BORST and J. PAMIN, *Gradient plasticity in numerical simulation of concrete cracking*, Eur. J. Mech.: A/Solids, **15**:295–320, 1996.

29. R.H.J. PEERLINGS, R. DE BORST, W.A.M. BREKELMANS, and M.G.D. GEERS, *Gradient-enhanced damage modelling of concrete fracture*, Mech. Cohes.-frict. Mater., **3**:323–342, 1998.

30. A. WINNICKI and CZ. CICHOŃ, *Plastic model for concrete in plane stress state.* I: *Theory*, II: *Numerical validation*, ASCE J. Eng. Mech., **124**(6), 591–602, 603–613, 1998.

Received December 23, 1999; new version May 5, 1999.

Arch. Mech., **51**, 3–4, pp. 447–467, Warszawa 1999

On the description of anisotropy and evolutionary phenomena in bone

S. PIETRUSZCZAK

McMaster University, Hamilton, Ont., Canada

A MATHEMATICAL FORMULATION is outlined for describing the mechanical properties of bone, including the process of age-related degradation as well as functional adaptation. Bone is considered as an anisotropic material, with the microstructure described in terms of distribution of void space. Both the elastic and elastoplastic formulations are provided, relevant to cortical and highly porous cancellous bone, respectively. The description of aging process invokes the concept of a physiological time, whose evolution depends, among other factors, on the level of activity of a living bone. Short term remodelling due to hyperphysiological stress is described within a framework which is conceptually similar to that of age-related degradation, with bone being considered as a hypoelastic/plastic material.

1. Introduction

OVER THE LAST FEW DECADES, there has been a considerable research effort devoted to description of living bone as a material. The research was prompted by various clinical problems, such as age-related bone fractures, prostheses loosening, etc. In macroscopic terms, both cortical (compact) and cancellous (trabecular) bone represent a heterogeneous, anisotropic material. In a typical bone structure (femur, tibia, etc.), the material properties strongly depend on the anatomical location of the specimen. This is due to the fact that the distribution of porosity as well as the principal directions of anisotropy vary throughout the whole bone. The mechanical characteristics also change according to the biological variations (age, sex, etc.) and possible state of pathological degradation. The existing constitutive theories, commonly adopted for computational/analytical analyses, describe the bone tissue as an orthotropic linearly elastic continuum (e.g. [1, 2]). As an alternative, micromechanically based formulations are used incorporating the homogenization technique (e.g. [3]).

Living bone is a material which undergoes a continuous evolution with time. One form of such an evolution is known as functional adaptation. The idea is partly derived from Wolff's law, which states that there is a direct correlation between the stress field in the bone and its overall architecture. In other words,

bone is an optimal structure relative to its mechanical environment and it has the ability to maintain an optimal configuration by adopting its external form and internal microstructure to changes in the load environment. The phenomenon of short-term adaptation is commonly described within the framework of adaptive elasticity [4]. A variety of mechanical stimuli have been considered, which include strain [4], strain rate [5], stress [6], strain energy [7], etc.

In parallel with studies on functional adaptation, a considerable research has been undertaken on age-related changes in the structure and composition of bone tissue. These changes influence the mechanical properties of bone and are largely responsible for the increased incidence of fractures in elderly. The problem is becoming increasingly important as people continue to live longer. Although several experimental studies have examined the degradation of mechanical properties of bone associated with aging process (e.g. [8 – 11]), the existing information is still too fragmentary to draw any quantitative conclusions from this research. Moreover, there is no comprehensive mathematical framework available addressing the issue of bone aging process.

The main objective of this paper is to outline a general mathematical formulation for the description of mechanical properties of bone. The bone tissue is considered as an anisotropic material, with the microstructure described in terms of a fabric tensor. The definition of the fabric tensor is derived from a scalar-valued function characterizing the spatial distribution of voids within the bone. The cortical and cancellous bone are considered as the same tissue with different porosity characteristics. The age-related degradation is attributed to mechanical as well as hormonal influences. The former are assumed to be closely related to the level of activity of a living bone, whereas the bone itself is considered as a material which possesses a limited memory of mechanical events. Finally, the formulation for functional adaptation of a living bone is discussed as a special case of that corresponding to aging process. The differences in the mathematical treatment of these two evolutionary phenomena are pointed out.

One of the primary reasons for studying the bone degradation process is to assess the risk of bone fracture in individuals subjected to a prolonged period of reduced physical activity or immobilization. Typical example relevant to the latter case involves patients with spinal cord injuries, who can develop osteoporosis already in the first year after the injury. In these cases, fractures are caused by relatively minor trauma; most occur due to transfers or during turning in bed. Also, long bone fractures (typically within proximal tibia or distal femur) have a high incidence of non-union and delayed union. The other class of problems where the evolutionary phenomena are of importance, are those associated with the long-term performance of bone implants. In this case, the analysis requires the prediction of shape changes in whole bones as well as adaptation of spongy bone tissue architecture to the insertion of an implant. A rapid progress has be-

en made toward this goal, particularly in the context of computational analyses based on finite element algorithms (cf. [12]).

2. Description of mechanical properties of trabecular/cortical bone

The existing experimental evidence indicates that both cortical and trabecular bone represent an inhomogeneous anisotropic material. The anisotropy effects are primarily due to geometric arrangement of the porous microstructure, while the matrix material itself may be considered as isotropic. In order to describe the mechanical properties of such a "structured medium", it is convenient to implement the notion of a fabric tensor ([1, 13]). Over the last few decades, several different internal structure measures have been proposed, including mean intercept length, volume orientation, star length distribution, etc. A comprehensive review may be found, for example, in ref. [14]. The emphasis in this work is not specifically on quantification of bone architecture but rather on incorporation of one of its measures in the formulation of the problem. The particular measure employed here is analogous to that proposed in refs. [15, 16] and it attributes the anisotropy of bone fabric to the bias in the spatial distribution of lineal/areal porosity.

In order to define the distribution of lineal porosity, isolate in the neighbourhood of a material point a sphere (S) of a unit radius, which encloses a representative volume of the material. Consider now a test line of length $\overline{L}$, emanating from the centroid, with the orientation ν_i with respect to the fixed Cartesian coordinate system. Denoting by $l(\nu_i)$ the total length of interceptions of this line with the void space, one can write

$$L(\nu_i) = l(\nu_i)/\overline{L}; \qquad L_{a\nu} = \frac{1}{4\pi} \int_S L(\nu_i) g(\nu_i) dS, \tag{2.1}$$

where $L(\nu_i)$ represents the fraction of $\overline{L}$ occupied by voids, and $g(\nu_i)$ is a scalar-valued function describing the spatial distribution of test lines. It can be shown that the mean value of $L(\nu_i)$ is the measure of the average porosity of the material, n, whereas the lineal fraction occupied by pores is an unbiased estimator of the volume fraction of voids in the direction ν_i, i.e.

$$n = L_{\mathrm{av}}; \qquad \overline{n}(\nu_i) \equiv L(\nu_i). \tag{2.2}$$

Note that the distribution of void fraction may also be described in terms of *areal* porosity. In this case the function $L(\nu_i)$ will be defined as the areal fraction of voids on a plane with unit normal ν_i, i.e.

$$L(\nu_i) = \frac{1}{4\pi} \int_{C(\nu_i)} l(\mu_i) g(\mu_i) dC, \tag{2.3}$$

where $C(\nu_i)$ is a unit circle rounding the centroid of the sphere and μ_i, which is orthogonal to ν_i , specifies the orientation of the test line.

The scalar-valued function $\overline{n}(\nu_i)$, as defined in Eq. (2.2), can be represented by the generalized double Fourier series. The desired best fit approximation can be established by the "least square" method leading to representation in terms of symmetric traceless tensors Ω_{ij}, Ω_{ijkl}, ... (cf. [17])

$$\overline{n}(\nu_i) = n(1 + \Omega_{ij}\nu_i\nu_j + \Omega_{ijkl}\nu_i\nu_j\nu_k\nu_l + ...). \tag{2.4}$$

The higher rank tensors Ω_{ijkl}... relate to the higher order fluctuations in void space distribution. Thus, in order to describe a smooth orthogonal anisotropy it is sufficient to employ an approximation based on the first two terms of the expansion (2.4). In such a case, the function $\overline{n}(\nu_i)$ may be defined as

$$\overline{n}(\nu_i) = 3nA_{ij}\nu_i\nu_j; \qquad A_{ij} = \frac{1}{3}(\delta_{ij} + \Omega_{ij}) \Rightarrow A_{ii} = 1, \tag{2.5}$$

where A_{ij}, referred to as fabric tensor, is a non-singular measure of the spatial distribution of voids.

With the notion of fabric tensor, as defined above, the mechanical properties of bone should be considered as an explicit function of its architecture. Thus in the elastic range, the constitutive relation will assume the form

$$\sigma_{ij} = D_{ijkl}\varepsilon_{kl}; \qquad D_{ijkl} = D_{ijkl}(A_{pq}, n) \tag{2.6}$$

in which the components of D_{ijkl} are a function of the fabric tensor and the average porosity.

In the above formulation, viz. Eq. (2.6), no explicit distinction has been made between the cortical and cancellous bone. Thus, both are considered here as the same material (in phenomenological sense); the only discriminating factor being $\overline{n}(\nu_i)$, Eq. (2.4). Cortical bone, which occurs for example on the cortex of central sections of femur, is compact (average porosity $3\% - 5\%$), contains no marrow (other than in the central medula) and its blood vessels are microscopically small. For a broad range of external loads, it may be considered as an elastic material. Cancellous bone, which is predominant in the neighbourhood of the joints, is much softer; it consists of a network of trabeculae interspersed with marrow and a large number of small blood vessels. Given the fact that the porosity of the cancellous bone may be as high as 90%, it is reasonable to expect that this material, *under certain loading conditions*, will exhibit some irreversible (plastic) deformations. It is recognized that in an intact bone subjected to typical physiological loads, the response of the trabecular network will still be predominantly elastic. However, for problems involving a surgical intervention, e.g. bone/prosthesis interaction, the irreversible deformations are likely to occur

in the region adjacent to bone-implant interface. This may be an important factor contributing to loosening of the implant and it should be properly taken into account.

The properties in the elastoplastic range should also be considered as fabric-dependent. In general, the yield function can be expressed as an isotropic function of stress and fabric tensors as well as the average porosity n. This leads to a rather complex form which employs ten independent invariants of both tensors and a set of material functions which depend on n. A simpler formulation may be established by following the framework similar to that recently proposed by the author in ref. [16]. In this case, the expression for the yield function incorporates directly the void space distribution $\overline{n}$, i.e.

$$f = f(\sigma_{ij}, \kappa, \overline{n}(l_i)) = 0; \qquad \kappa = \kappa(\varepsilon^p_{ij}), \tag{2.7}$$

where $\overline{n}$ is evaluated in the so-called "loading direction" $l_i = l_i(\sigma_{kl})$. According to Eq. (2.7), the consistency condition reads

$$\dot{f} = \left(\frac{\partial f}{\partial \sigma_{ij}} + \frac{\partial f}{\partial l_k} \frac{\partial l_k}{\partial \sigma_{ij}} \right) \dot{\sigma}_{ij} + \frac{\partial f}{\partial \varepsilon^p_{ij}} \dot{\varepsilon}^p_{ij} = \dot{h} + \frac{\partial f}{\partial \varepsilon^p_{ij}} \dot{\varepsilon}^p_{ij} = 0. \tag{2.8}$$

In order to specify the irreversible (plastic) deformations, assume that the flow rule takes the form

$$\dot{\varepsilon}^p_{ij} = \dot{h} G_{ij}; \qquad G_{ij} = \hat{G}_{ij} \left(\psi_{ij}, \omega_{ij} \right) \tag{2.9}$$

where

$$\psi_{ij} = \frac{\partial \Psi}{\partial \sigma_{ij}} \Big/ \left\| \frac{\partial \Psi}{\partial \sigma_{kl}} \right\|; \quad \omega_{ij} = \Omega_{ij} / \|\Omega_{kl}\|; \quad \Psi(\sigma_{ij}, \overline{n}(l_i)) = \text{const} \tag{2.10}$$

and $\Psi = \text{const}$ is a parametric equation defining the plastic potential. Apparently $\dot{h} \to 0 \Rightarrow \dot{\varepsilon}^p_{ij} \to 0$, so that the plastic deformation vanishes for all neutral loading histories. In Eq. (2.9), G_{ij} is an isotropic tensor-valued function. Assuming that G_{ij} is linear ψ_{ij}, leads to the general representation, which incorporates six functions of ten independent invariants of both tensors defined in (2.10). A particular form of this representation, as discussed in ref. [16], is given by

$$\dot{\varepsilon}^p_{ij} = \dot{\lambda} \left(\psi_{ij} + (b_1 \psi_{kk} + b_2 \omega_{kl} \psi_{kl}) \omega_{ij} \right) \tag{2.11}$$

where b_1 and b_2 are constants. Equation (2.11) represents a simple generalization of the flow rule, which incorporates the effect of material fabric. It is noted that the functional form (2.11) has, to some extent, similar numerical repercussions to those of incorporating a rotation of the plastic potential surface. In general, the deviation from isotropy results in a progressive deviation of the direction of plastic

flow from that specified by the gradient of the potential function. Apparently, for an isotropic material, $\omega_{ij} = 0$, so that the classical formulation is recovered.

3. Modelling of the evolution of bone architecture

(i) Aging of bone

Consider now the question of degradation of mechanical properties of bone with age. Apparently, the existing experimental evidence is insufficient to provide a complete formulation of the problem. Therefore, the main objective here is to introduce a set of hypotheses which lead to a general mathematical framework. These hypotheses in themselves, may serve to define appropriate experimental procedures, which are required in order to quantify the problem.

In general, the aging process will result in an increase in average porosity, n, of the bone material. At the same time, the bias in the spatial distribution of voids may also be altered. The question of age-related changes in the trabecular bone architecture was addressed by a number of researchers (cf. [10, 11, 18]). In a typical plate-like structure, the process of bone loss involves a progressive perforation of plates combined with the thinning and subsequent disappearance of the supporting horizontal rods [19]. A similar mechanism occurs in rod-like structures, where the age-related changes invoke primarily the thinning and disappearance of the horizontal struts leading, in extreme cases, to an advanced breakdown of the continuous trabecular network [10]. In both these cases, the bone resorption leads to an increase in the bone porosity as well as to the change in the bone architecture.

In order to address the problem, it may be convenient to introduce the notion of *physiological* time (t'), as opposed to the linear *chronological* time (t). The physiological time may be defined through an incremental relation

$$(3.1)_1 \qquad dt' = g_1(w, \dot{w}) g_2(x_\alpha) dt; \qquad x_\alpha = x_1, x_2, ..., x_n,$$

where

$$(3.1)_2 \qquad w = \frac{1}{\Delta \bar{t}} \int_{\Delta \bar{t}} W dt; \qquad W = \int \sigma_{ij} d\varepsilon_{ij}.$$

In general, both functions g_1 and g_2 are scalar-valued functions defined within the range between 0 and 1. The function g_1 defines the mechanical influences, while g_2 is introduced to account for complex hormonal, nutritional and genetic ($x_\alpha, \alpha = 1, ..., n$) influences. Recognizing the apparent difficulty in quantifying g_2, the discussion here is focused primarily on the mechanical aspects. In the first approximation, g_1 may be defined as a scalar-valued function of w alone,

i.e. $g_1 = g_1(w)$. The function w, Eq. $(3.1)_2$, represents the average strain energy density input due to loading over a fixed time interval $\Delta\bar{t}$. Thus, the main assumption embedded here is that, in the absence of any degenerative bone disease and at a given hormonal/nutritional level ($g_2 = \text{const}$), the degradation process is an implicit function of the level of physical activity of a living bone which, in turn, is measured by w. The bone is said to possess the memory of mechanical events which extends over a time interval $\Delta\bar{t} = \text{const}$. As time elapses, the events occurring before $t - \Delta\bar{t}$ are continually erased from the memory. In general, the bone tends to degrade with time towards a pathological state; this process however can be slowed down, and even partially reversed, depending on the degree of physical activity. The dependence of g_1 on w alone, implies that a systematic activity involving moderate strain energy inputs is, in general, more efficient than a sporadic intensive exercise. If this assumption is at variance with experimental observation, then a more general form $(3.1)_1$, incorporating $\dot{w}$ should be employed.

Apparently, the incremental relation $(3.1)_1$ is not, in general, integrable, implying that it cannot be reduced to a unique relation between t and t'. Also, Eqs. $(3.1)_1$ and $(3.1)_2$ are formulated in *local* sense, so that for a particular boundary value problem the physiological time will not be uniform in space. A somewhat simpler, though more restrictive formulation may be obtained by postulating that Eq. $(3.1)_2$ may be defined in the context of a specific structural bone as a whole (e.g. femur, tibia, etc.). In this case,

$$(3.1)_3 \qquad w = \frac{1}{\Delta\bar{t}} \int_{\Delta\bar{t}} \overline{w} dt; \qquad \overline{w} = \frac{1}{V} \int_{V} W dV,$$

where w represents the strain energy per unit volume (V) of the entire structural system. The hypotheses $(3.1)_1$ and $(3.1)_3$ imply that the physiological clock runs uniformly throughout the entire bone as a structural element, leading to a homogeneous degradation process.

The specification of the functions g_1 as well as $n = n(t')$, i.e. the evolution of average porosity, requires a comprehensive experimental programme. As an example, the following simple representations may be suggested

$$(3.2) \qquad g_1(w) = \frac{< w_{\text{opt}} - w >}{w_{\text{opt}}}; \qquad n = n_p + (n_i - n_p)(1 - t'/t'_p)^{\xi}.$$

Here, w_{opt} represents a certain optimum strain energy input over $\Delta\bar{t}$ and the expression within the angular bracket is defined as $< x >= x$ for $x > 0$, otherwise $x = 0$. Thus, for a very active person (in terms of physical exercise), $w \to w_{\text{opt}}$ implying $dt' \to 0$, so that the aging process can be substantially slowed down. (Note that an activity resulting in $w > w_{\text{opt}}$ has the same effect as that corresponding to $w \to w_{\text{opt}}$). On the other hand, for an immobilized individual $w \to 0$

so that $dt' \to dt$, which results in a progressively increasing rate of degradation. This case corresponds to, for example, persons with spinal cord injury which develop osteoporosis, a metabolic disorder of bone leading to increased risk of fracture, already in the first year after the injury. In the second equation of (3.2), $\zeta = \text{const}, 0 \leqslant t' \leqslant t'_p, n_i$ is the initial average porosity and n_p corresponds to the maximum pathologically admissible value of n. Thus, $n = n_i$ at $t' = 0$, whereas for $t' \to t'_p$ there is $n \to n_p$.

Given the definitions (3.1), the constitutive relation in the elastic range can be derived by differentiation of Eq. (2.5) with respect to time

$$\dot{\sigma}_{ij} = \dot{D}_{ijkl}\varepsilon_{kl} + D_{ijkl}\dot{\varepsilon}_{kl}. \tag{3.3}$$

The specification of the first term in Eq. (3.3) requires an evolution law for the components of the fabric tensor A_{ij}. According to the experimental evidence, mentioned earlier in this section, the age-related changes in the microstructure invoke primarily the thinning and disappearance of the supporting rods with no significant reorientation of the vertical trabeculae. Such a mechanism is not likely to promote any significant changes in the principal directions of anisotropy, thus rendering $\dot{A}_{ij}$ to be coaxial with A_{ij}, and thus Ω_{ij}. In this case,

$$\dot{A}_{ij} = g_1 g_2 (c_1 \delta_{ij} + c_2 \Omega_{ij} + c_3 \Omega_{ip}\Omega_{pj}) \tag{3.4}$$

where c_1, c_2, c_3 are functions of t' and the basic invariants of Ω_{ij}. Restricting the formulation to an approximation which retains terms of the order two in Ω_{ij} yields the evolution law in the form

$$\dot{A}_{ij} = g_1 g_2 \left(d_1 \Omega_{ij} + d_2 (\Omega_{ip}\Omega_{pj} - \frac{2}{3}\text{II}_\Omega \delta_{ij}) \right), \tag{3.5}$$

where II_Ω is the second invariant of Ω_{ij} and d_1, d_2 are function of t' alone.

In general, at this preliminary stage of considerations, a simplified approach may be advocated in which the degradation of properties is attributed to the changes in the average porosity alone, so that

$$\dot{D}_{ijkl} \approx g_1 g_2 \frac{\partial n}{\partial t'} \frac{\partial}{\partial n} D_{ijkl}. \tag{3.6}$$

Equations (3.3) and (3.6) represent a set of differential equations describing the aging process under the assumption that the bone is an anisotropic elastic material. Apparently, the elastic regime is defined in terms of

$$f < 0 \rightrightarrows \dot{\sigma}_{ij} = \dot{D}_{ijkl}\varepsilon_{kl} + D_{ijkl}\dot{\varepsilon}_{kl} \tag{3.7}$$

whereas $f = 0$ implies the onset of irreversible deformations. The behaviour in the elastoplastic range can be defined by invoking the consistency condition, which according to Eqs. (2.8) and (2.12) takes the form

$$\dot{f} = \left(\frac{\partial f}{\partial \sigma_{ij}} + \frac{\partial f}{\partial l_k} \frac{\partial l_k}{\partial \sigma_{ij}} \right) \dot{\sigma}_{ij} + \frac{\partial f}{\partial \kappa} \frac{\partial \kappa}{\partial \varepsilon^p_{ij}} \dot{\lambda} (\psi_{ij} + b\omega_{ij}) + g_1 g_2 \frac{\partial f}{\partial \overline{n}} \frac{\partial \overline{n}}{\partial t'} = 0, \tag{3.8}$$

where $b = b_1 \psi_{kk} + b_2 \omega_{kl} \psi_{kl}$ and

$$\frac{\partial \overline{n}}{\partial t'} = 3 \left(\frac{\partial n}{\partial t'} A_{ij} + n d_1 \Omega_{ij} + n d_2 (\Omega_{ip} \Omega_{pj} - \frac{2}{3} \mathrm{II}_\Omega \delta_{ij}) \right) \nu_i \nu_j. \tag{3.9}$$

Assuming the additivity of elastic and plastic strain rates

$$\dot{\sigma}_{ij} = \dot{D}_{ijkl} \varepsilon^e_{kl} + D_{ijkl} (\dot{\varepsilon}_{kl} - \dot{\varepsilon}^p_{kl}) \tag{3.10}$$

and substituting Eq. (3.10) in Eq. (3.8), the following constitutive relation may be established after some algebraic operations

$$\dot{\sigma} = D^{ep}_{ijkl} \dot{\varepsilon}_{kl} - \left[\frac{1}{H} D_{ijrs} \left(\frac{\partial f}{\partial \sigma_{pq}} + \frac{\partial f}{\partial l_t} \frac{\partial l_t}{\partial \sigma_{pq}} \right) (\psi_{rs} + b\omega_{rs}) \right. \tag{3.11}_1$$

$$\left. - \delta_{ip} \delta_{jq} \right] \dot{D}_{pqkl} C_{klmn} \sigma_{mn} - \frac{1}{H} D_{ijkl} (\Psi_{kl} + b\omega_{kl}) \frac{\partial f}{\partial \overline{n}} \frac{\partial \overline{n}}{\partial t'} g_1 g_2;$$

$$D^{ep}_{ijkl} = D_{ijkl} - \frac{1}{H} D_{ijrs} \left(\frac{\partial f}{\partial \sigma_{pq}} + \frac{\partial f}{\partial l_t} \frac{\partial l_t}{\partial \sigma_{pq}} \right) (\psi_{rs} + b\omega_{rs}) D_{pqkl}$$

where

$$H = \left(\frac{\partial f}{\partial \sigma_{ij}} + \frac{\partial f}{\partial l_m} \frac{\partial l_m}{\partial \sigma_{ij}} \right) D_{ijkl} (\psi_{kl} + b\omega_{kl}) - \frac{\partial f}{\partial \kappa} \frac{\partial \kappa}{\partial \varepsilon^p_{ij}} (\psi_{ij} + b\omega_{ij}); \tag{3.11}_2$$

$$C_{ijkl} = D^{-1}_{ijkl}.$$

Equation (3.11) describes bone as an anisotropic elastoplastic material with degrading properties. Once again, the formulation may be simplified by neglecting the terms involving the evolution of fabric in Eq. (3.9). It should be emphasized, that for problems restricted to an intact bone subjected to normal physiological loads, there will be, in general, $f < 0$, in which case Eq. (3.11) will simplify to representation (3.7).

(ii) Bone as a regenerating material; internal adaptation process

The time scale associated with age-related degradation of bone may extend to several decades in humans. However, over a shorter time interval (of the order of months) the living bone may undergo yet another type of internal remodelling

process. The latter is related to functional adaptation to changes in the load environment, which are prompted by an increase in physical activity, i.e. taking up jogging or other form of athletic exercise. In this case, the mechanical stimuli trigger biological processes which occur at a cellular and microstructural level and manifest themselves in a progressive increase in density, which is again coupled with the reorganization of the trabecular architecture.

The phenomenon of short-term remodelling due to hyperphysiological stress may be described within a framework which is conceptually similar to that outlined in the previous section. In order to specify the required modifications, consider first the rate of energy dissipation due to the evolution of elastic properties under $\sigma_{ij} = \text{const}$. Inverting Eq. (2.5) and differentiating it with respect to time (under $\sigma_{ij} = \text{const}$), leads to

$$\varepsilon_{ij} = C_{ijkl}\sigma_{kl} \rightrightarrows \sigma_{ij}\dot{\varepsilon}_{ij} = \sigma_{ij}\dot{C}_{ijkl}\sigma_{kl} \geqslant 0 \rightrightarrows \det[C_{ijkl}] \geqslant 0. \tag{3.12}$$

In general, the above inequality is satisfied for a degrading material only, implying that the representation (2.6) is not suitable for our purpose here. Thus, the elastic properties of a regenerating material should be described by invoking *hypoelastic* relation

$$\dot{\sigma}_{ij} = D_{ijkl}\dot{\varepsilon}_{kl}; \qquad D_{ijkl} = D_{ijkl}(A_{pq}, n) \tag{3.13}$$

which ensures that, under a sustained load, $\sigma_{ij}\dot{\varepsilon}_{ij} = 0$.

Equation (3.13) must be supplemented by an appropriate evolution law for the components of D_{ijkl}. Since the functional adaptation involves relatively short time intervals, the notion of a physiological time may now be abandoned. The formulation of the problem requires, among other factors, the specification of the evolution of n. In general, for a normal level of activity $n = \text{const}$, whereas hyperactivity will result in reduction of n to a finite, physiologically possible value. The level of activity can again be measured in terms of average strain energy density, Eqs. $(3.1)_2$ or $(3.1)_3$, with an understanding that the time interval associated with memory of mechanical events is now much shorter than that corresponding to age-related degradation. A possible form of evolution law, which may be adopted here, is

$$\dot{n} = h_1(w, \dot{w})\dot{h}_2(t); \qquad 0 \leqslant h_1 \leqslant 1, \tag{3.14}$$

where h_1 reflects the level of physical activity, whereas $h_2(t)$ describes the maximum, physiologically admissible variation of n under $h_1 \to 1$. Apparently, for standard levels of activity $h_1 = 0$, which corresponds to remodelling equilibrium.

The response in the elastoplastic range can be obtained by following the same procedure as that outlined in the previous section, Eqs. (3.8) – (3.11). Invoking the consistency condition

$$\dot{f} = \left(\frac{\partial f}{\partial \sigma_{ij}} + \frac{\partial f}{\partial l_k} \frac{\partial l_k}{\partial \sigma_{ij}} \right) \dot{\sigma}_{ij} + \frac{\partial f}{\partial \kappa} \frac{\partial \kappa}{\partial \varepsilon^p_{ij}} \dot{\varepsilon}^p_{ij} + \frac{\partial f}{\partial \overline{n}} \dot{\overline{n}} = 0 \tag{3.15}$$

and the assumption of additivity of elastic and plastic strain rates, the following constitutive relation may be established

$$\dot{\sigma}_{ij} = D^{ep}_{ijkl} \dot{\varepsilon}_{kl} - \frac{1}{H} D_{ijkl} (\psi_{kl} + b\omega_{kl}) \frac{\partial f}{\partial \overline{n}} \dot{\overline{n}}, \tag{3.16}$$

where D^{ep}_{ijkl} and H are defined in Eq. (3.11). It should be noted that in a regenerating material, under $\sigma_{ij} = \text{const}$, there is $(\partial f / \partial \overline{n}) \dot{\overline{n}} < 0$ leading to $\dot{\lambda} < 0 \Rightarrow \sigma_{ij} \dot{\varepsilon}_{ij} = 0$. On the other hand, in a degrading material, Eqs. (3.11), $\dot{\lambda} > 0$ and $\sigma_{ij} \dot{\varepsilon}_{ij} > 0$, so that the evolution of microstructure under a sustained load leads to dissipation of energy. The above constraints are consistent with the second law of thermodynamics.

Equation (3.16), supplemented by the evolution law (3.14), defines a simple framework for modelling of the bone tissue undergoing an internal adaptation process. Apparently, if the irreversible deformations are negligible, i.e. $H \to \infty$, then Eq. (3.16) reduces to the hypoelastic relation (3.13). The formulation may again be enriched by incorporating the effect of the changes in the trabecular architecture, which requires an appropriate evolution law for the fabric tensor A_{ij}. The latter issue was addressed, for example, in ref. [20], or more recently in ref. [21], where the evolution law employed the notion of optimally effective bone remodelling.

(iii) An example

In order to illustrate the mathematical framework outlined in this section, a simple numerical example is provided here. The objective is to demonstrate the effect of the age-related degradation of elastic properties on the mechanical characteristics of trabecular bone.

Consider the behaviour of the material under uniaxial compression ($\sigma_1 = \sigma_2 = 0, \sigma_3 < 0$) in the direction of principal material axes. Choose the properties which may be considered as representative of a trabecular bone from the human proximal tibia [22]. Assume that $\overline{n}(\nu_i)$ is defined in terms of, say, lineal porosity, i.e. Eq. (2.1), and let $\mathbf{\Omega}_1 = 0.15$, $\mathbf{\Omega}_2 = 0.1$, $\mathbf{\Omega}_3 = -0.25$, $n_i = 0.53$, which corresponds to $\overline{n}(e_1) = 0.61$, $\overline{n}(e_2) = 0.58$, $\overline{n}(e_3) = 0.40$. Following ref. [23], assume that the orthotropic Young's and shear moduli are defined as

$$E_i = E_0 [\rho_s (1 - n)]^2 A_i^{-2}; \qquad G_{ij} = G_0 [\rho_s (1 - n)]^2 A_i^{-1} A_j^{-1}.$$

In the above equations $i, j = 1, 2, 3 (i \neq j)$, A_i are the eigenvalues of the fabric tensor, ρ_s and n represent the density of the tissue and the average porosity, respectively, and E_0, G_0 are material constants. Take $\eta_{12} = \eta_{23} = 0.25$ (Poisson's

ratios) and $E_0 = 230$ (MPa cm^3/g^2), $\rho_s = 1.93$ g/cm^3, so that $E_1 = 1.29$ GPa, $E_2 = 1.40$ GPa, $E_3 = 3.00$ GPa. The degradation of properties is described in terms of evolution laws (3.2) and (3.5). Assume that $\xi = 0.5$ and $t' \to 10$ ph.y (*physiological years*) results in an increase in the average porosity to its pathological value of $n_p = 0.85$. Moreover, take $a_1 = 0.01$/ph.y and $a_2 = 0$ in the evolution law for the fabric tensor, Eq. (3.5).

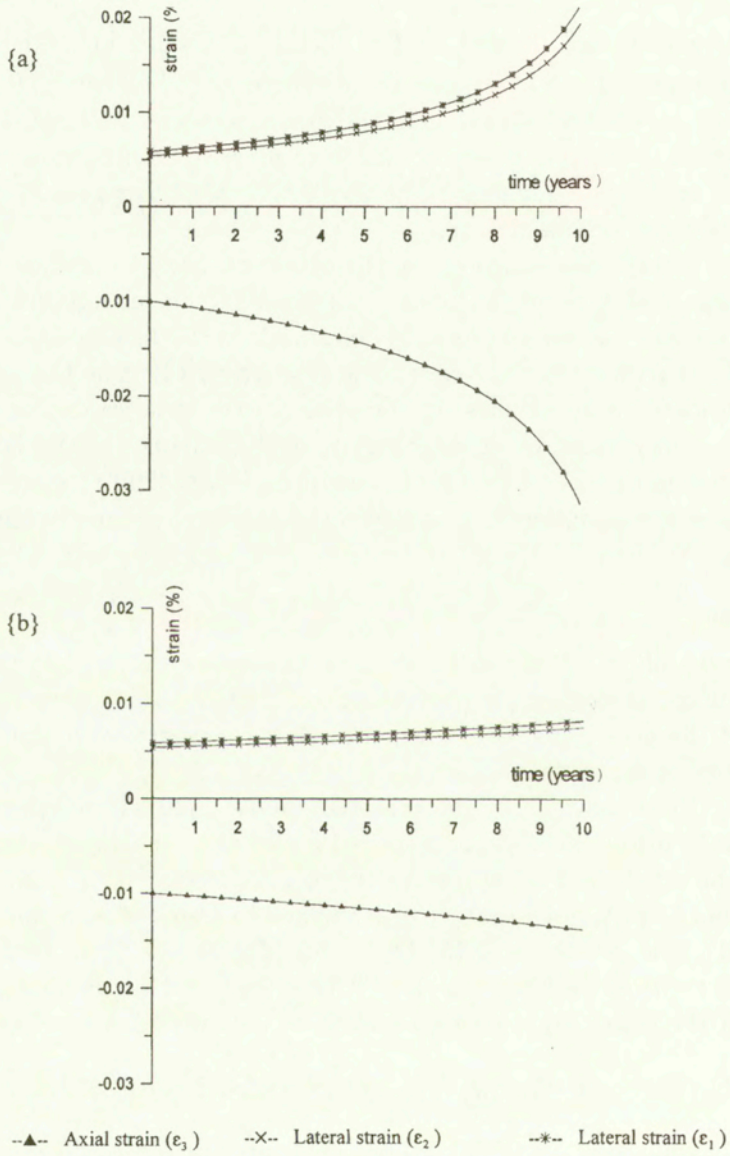

FIG. 1. Evolution of normal strain under a constant load of $\sigma_3 = 0.3$ MPa; solution for: (a) $w/w_{\text{opt}} = 0.1$, (b) $w/w_{\text{opt}} = 0.6$.

The results of numerical simulations are presented in Figures 1 and 2. The figures show the mechanical characteristics and the evolution of microstructure for the bone material subjected to a sustained axial load of $\sigma_3 = -0.3$ MPa.

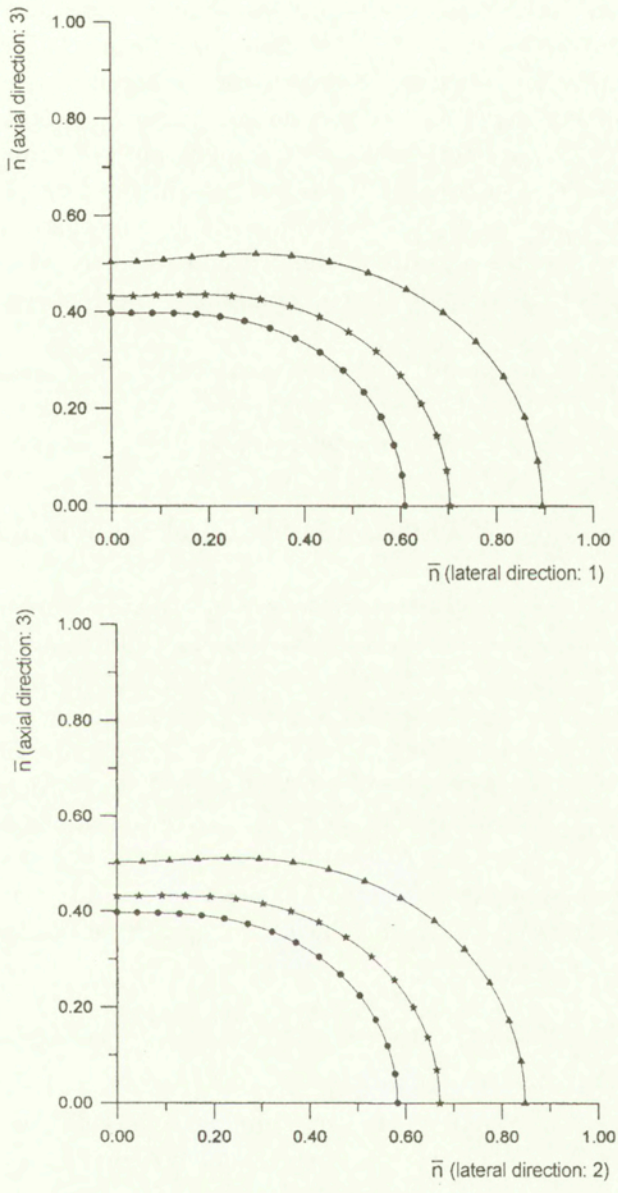

FIG. 2. Spatial distribution of $\overline{n}(\nu_i)$ at $t = 10$ years.

Figure 1 provides the time history of normal strain for $w/w_{\text{opt}} = 0.1$ and 0.6, respectively. In the former case, a continuous development of deformation takes place and the strain rates progressively increase with time. When the *chronological* time approaches 10 years, the deformation gradients become very high, which is triggered by a significant degradation in material microstructure. On the other hand, the response for $w/w_{\text{opt}} = 0.6$ is characterized by a relatively slow progress in degradation, resulting in constant deformation gradients.

Figure 2 presents the evolution of bone architecture for both of these scenarios. The initial distribution of void fraction displays an orthotropic characteristic. For the case of $w/w_{\text{opt}} = 0.1$, the lineal porosity in the lateral direction increases to nearly 0.9, prompting a severe degradation of mechanical properties. At $w/w_{\text{opt}} = 0.6$, the average porosity as well as the bias in the directional distribution of voids are only marginally altered, implying a much slower progress of the degradation.

Finally, it should be pointed out that a similar loading history imposed on a regenerating material, Sec. 3(ii), would trigger a progressive decrease in the average porosity accompanied by no deformation.

4. Specification of material functions; numerical analysis of bones

The identification of bone architecture requires the use of modern 3D imaging techniques such as high resolution magnetic resonance imaging, micro-computed tomography, etc. Apparently, the microstructure and thus the mechanical properties of bone depend on several factors including the anatomic location, age, sex, etc. In general, given an image of a fixed volume of bone material, in the form of 3D binary data, one can determine a set of $\overline{n}_\alpha (\alpha = 1, 2...N)$ defining, according to Eq. (2.1) or (2.3), the values of $\overline{n}(\nu_i)$ for discrete orientations ν_i. The obtained distribution can be approximated by the first two terms of the representation (2.4) using the least squares approach. The error involved is the sum of squares of the differences between the given values of $\overline{n}_\alpha$ and those due to approximation (2.4), i.e.

$$E = \sum_\alpha \left[\overline{n}_\alpha - n(1 - \boldsymbol{\Omega}^T \mathbf{N}_\alpha)\right]^2 \tag{4.1}$$

where $\boldsymbol{\Omega}^T = \{\Omega_{11}, \Omega_{22}, \Omega_{12}, \Omega_{13}, \Omega_{23}\}$; $\mathbf{N}^T = \{(\nu_1^2 - \nu_3^2), (\nu_2^2 - \nu_3^2), -2\nu_1\nu_2, -2\nu_1\nu_3, -2\nu_2\nu_3)\}$. The constants $\boldsymbol{\Omega}$ should minimize the total least squares error, i.e. $\partial E/\partial \boldsymbol{\Omega} = \mathbf{0}$, which leads to a set of simultaneous equations

$$\left(\sum_\alpha \mathbf{N}_\alpha \mathbf{N}_\alpha^T\right) \boldsymbol{\Omega} = \sum_\alpha \mathbf{N}_\alpha - n^{-1} \sum_\alpha \overline{n}_\alpha \mathbf{N}_\alpha \tag{4.2}$$

which can be solved for individual components of $\boldsymbol{\Omega}$.

The properties in the elastic range are defined by Eq. (2.6). The general representation of the elasticity tensor D_{ijkl} in terms of the fabric tensor, has been derived by COWIN [1]. The representation employs nine scalar functions of the three basic invariants of the fabric tensor. In the same reference Cowin has also developed an approximation based on retaining the terms of order two in A_{ij} and expanding the scalar functions in powers of A_{ij}. The result of this approximation is

$$d_\alpha = B_{\alpha\beta} k_\beta(n) \tag{4.3}$$

where d_α denotes the individual non-zero components of D_{ijkl}, k_β are functions of n only and $B_{\alpha\beta}$ depends on the basic invariants of the fabric tensor.

Taking d_α as $\mathbf{d}^T = \{D_{11}, D_{22}, D_{33}, D_{44}, D_{55}, D_{66}, D_{12}, D_{13}, D_{23}\}$ one has

(4.4)

$$[\mathbf{B}] = \begin{bmatrix}
1 & \text{II} & 2A_{11} & 2A_{11}^2 & A_{11}^2 & 2 & 2\text{II} & 4A_{11} & 4A_{11}^2 \\
1 & \text{II} & 2A_{22} & 2A_{22}^2 & A_{22}^2 & 2 & 2\text{II} & 4A_{22} & 4A_{22}^2 \\
1 & \text{II} & 2A_{33} & 2A_{33}^2 & A_{33}^2 & 2 & 2\text{II} & 4A_{33} & 4A_{22}^2 \\
0 & 0 & 0 & 0 & 0 & 1 & \text{II} & (A_{22}+A_{33}) & (A_{22}^2+A_{33}^2) \\
0 & 0 & 0 & 0 & 0 & 1 & \text{II} & (A_{11}+A_{33}) & (A_{11}^2+A_{33}^2) \\
0 & 0 & 0 & 0 & 0 & 1 & \text{II} & (A_{11}+A_{22}) & (A_{11}^2+A_{22}^2) \\
1 & \text{II} & (A_{11}+A_{22}) & (A_{11}^2+A_{22}^2) & A_{11}A_{22} & 0 & 0 & 0 & 0 \\
1 & \text{II} & (A_{11}+A_{33}) & (A_{11}^2+A_{33}^2) & A_{11}A_{33} & 0 & 0 & 0 & 0 \\
1 & \text{II} & (A_{22}+A_{33}) & (A_{22}^2+A_{33}^2) & A_{22}A_{33} & 0 & 0 & 0 & 0
\end{bmatrix}$$

where

$$\text{II} = A_{11}A_{22} + A_{11}A_{33} + A_{22}A_{33}; \qquad A_{11} + A_{22} + A_{33} = 1.$$

The question of the specification of $k_\beta(n)$ has been addressed in ref. [22]. In that study, k_β were approximated as power functions of normalized density and fitted (using the least squares analysis) to an extensive set of experimental data. The representation (4.3), although attractive, has a serious limitation. Namely, the matrix $[B]$, Eq. (4.4), is singular implying that there is no unique set of k's describing the given material properties. Over the recent years, other approximations have been developed (e.g., [20, 24]). However, most of them are restrictive, as they neglect certain terms in the general representation, which may be of significance. The formulation adopted here is based on the approximation developed in ref. [23], quoted earlier in this paper. The estimates of elastic properties are derived from general representation theorems which incorporate an assumption of homogeneity of the constitutive relation with respect to the measures of the material fabric. Following this work, the orthotropic elastic moduli are defined as

$$E_i = E_0 A_i^{-2}; \qquad G_{ij} = G_0 A_j^{-1}; \qquad \eta_{ij} = \eta_0 \frac{A_i}{A_j} \tag{4.5}$$

subject to the constraint $\eta_0 = E_0/(2G_0) - 1$. In the above expressions, E and G are the Young's and shear moduli, respectively, and η is the Poisson's ratio. Moreover, $i, j = 1, 2, 3 (i < j)$, A's are the eigenvalues of the fabric tensor, whereas E_0, G_0, η_0 are considered to be material functions which depend on structural density. A specific form of (4.5) has been employed in the example given in Sec. 3(ii).

A simple fracture criterion for bone, consistent with general representation (2.7), has been recently proposed by the author and his coworkers [25]. This criterion is expressed in the functional form

$$F = \overline{\sigma} - g(\theta)\overline{\sigma}_c = 0; \qquad \overline{\sigma}_c = \frac{-a_1 + \sqrt{(a_1^2 + 4a_2(a_3 + I/f_c))}}{2a_2} f_c, \tag{4.6}$$

where $I = -\sigma_{ii}, \overline{\sigma} = (1/2 s_{ij} s_{ij})^{1/2}, \theta = -1/3 \sin^{-1} \{(\sqrt{3} s_{ij} s_{jk} s_{ki})/2\overline{\sigma}^3\}$ and s_{ij} denotes the stress deviator. In Eq. (4.6), a_1, a_2, a_3 represent dimensionless material constants and the function $g(\theta)$ satisfies $g(\pi/6) = 1$, $g(-\pi/6) = K$, where $K \leqslant 1$ is a constant. Moreover, f_c which represents the uniaxial compressive strength of bone tissue, is assumed to be an explicit function of the void space distribution, i.e.

$$f_c(l_i) = f_{c0} \left(\frac{\rho}{\rho_0} \right)^{\gamma} = f_{c0} \left(\frac{1 - \overline{n}(l_i)}{1 - n_0} \right)^{\gamma} \tag{4.7}$$

where n_0 and γ are constants and γ is typically within the range $1 \leqslant \gamma \leqslant 2$ (cf. [26]). The function $\overline{n}$ is evaluated in the "loading direction" l_i which has been defined as the direction of the average stress vector t_i at a point,

$$l_i = \frac{t_i}{\|t_i\|}; \qquad t_i = \sigma_{ij}(e_j^{(1)} + e_j^{(2)} + e_j^{(3)}) = \sqrt{3}\sigma_{ij} m_j, \tag{4.8}$$

where e_i are the base vectors associated with the principal material axes and $m_i = \{1, 1, 1\}/\sqrt{3}$ is a unit vector along the space diagonal.

In order to provide an illustration to the notions brought up above, the results of numerical simulations pertaining to evaluation of the risk of fracture in a proximal femur are reviewed here (after ref. [25]). A 3D model of the proximal two thirds of an adult human right femur has been created based on external surface contours extracted from CT scans. A set of elastic constants was assigned to each element to model a heterogeneous distribution of orthotropic material properties. In particular, representation (4.5) has been employed with average porosity values obtained from CT data. At this preliminary stage, the bias in the distribution of void fraction was assumed to be constant, with the principal magnitudes of the tensor Ω_{ij} taken as $\Omega_1 = -0.15$, $\Omega_2 = 0.04$, $\Omega_3 = 0.11$. The latter

choice gives $E_1/E_3 = 1.7$, $E_1/E_2 = 1.5$ and $G_{12}/G_{23} = 1.3$, $G_{12}/G_{13} = 1.07$, which is consistent with typical experimental data for human femoral bone [27] over a broad range of average porosities. The numerical analysis has been carried out in two stages. First, a supplementary finite element simulations were conducted in order to estimate the distribution of the principal material directions. The problem was solved by performing a linear elastic analysis of the femur subjected to loading conditions corresponding the one-legged stance phase of gait under the constraint that the matrix multiplication of the stress and fabric tensors is commutative. The latter follows directly from Wolff's hypothesis, which postulates that the principal stress axes coincide with the principal trabecular directions at remodelling equilibrium. The second phase of the analysis involved the numerical simulations of a fall from standing height to the lateral aspect of the greater trochanter.

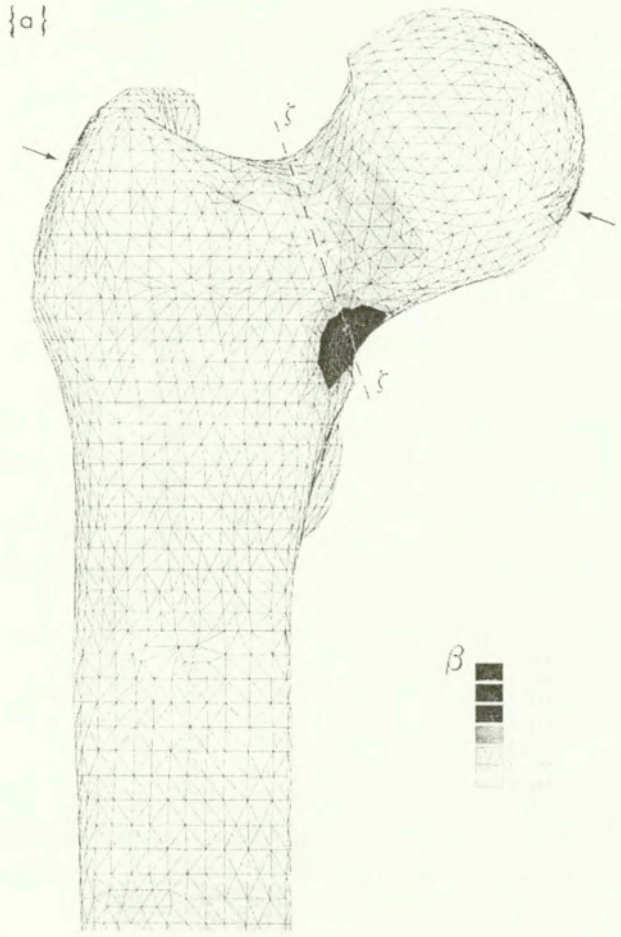

[FIG. 3.]

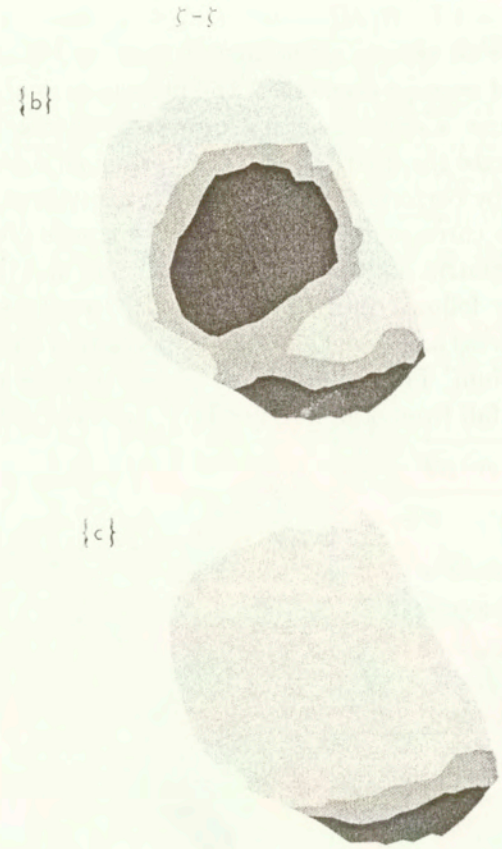

FIG. 2. Predicted contours of damage factor β in an osteoporotic bone; (a) anterior view of the proximal femur; (b) transcervical cross-section (orthotropic formulation); (c) transcervical cross-section (isotropic formulation).

The main results of the simulations are presented in Fig. 3. Figure 3a shows the anterior view of the proximal femur together with superimposed surface distribution of the *damage factor* β. The latter has been defined, based on the proposed fracture criterion (4.6), as

$$\beta = \frac{\overline{\sigma}}{g(\theta)\overline{\sigma}_c}. \tag{4.9}$$

It should be noted that, according to Eq. (4.6), $F \leqslant 0$ requires $0 \leqslant \beta \leqslant 1$. The case of $\beta \to 1$ results in $F \to 0$ and signifies the local failure of the bone material associated with formation of macro/micro cracks (e.g. fracture of individual trabeculae). Clearly, $\beta > 1$ is physically inadmissible as the stress state corresponds to $F > 0$. The distribution shown in Fig. 3 corresponds to an osteoporotic bone. It is evident that in the inferior region of the femoral neck, the stress field vio-

lates the fracture criterion, implying that a lateral fall to the hip will trigger a transcervical fracture. The fracture zone will initiate at the outer cortical shell and propagate through the trabecular network in the femoral neck. In general, given the fact that the porosity in the region of trabecular bone is relatively high, the propagation of the fracture zone will require little mechanical effort. In this context the elastic analysis alone, incorporating the criterion (4.6), may be sufficiently accurate for estimating the potential for fracture risk. Finally, Figs. 3b and 3c present the distribution of damage in the transcervical cross-section. The distribution shown in Fig. 3c corresponds to the case of isotropic formulation ($\Omega_{ij} = 0$). Comparing both results it is evident that the isotropic representation will, in general, overestimate the fracture potential.

5. Final remarks

An appropriate representation of the effects of aging on the mechanical properties of bone is essential for numerical evaluation of the risks of fractures and the design of prosthetic implants in elderly. With this objective in mind, a set of hypotheses has been put forward in order to form a general mathematical framework for the description of age-related degradation of bone structure. In general, the degradation phenomenon manifests itself in a progressive increase in the average porosity of the material coupled with the reorganization of the microstructure. The latter usually involves a thinning of vertical and horizontal trabeculae. This would indicate a possible simplification in the evolution law of the fabric, whereby the primary effect is that of the change in the eigenvalues of the fabric tensor. The formulation presented here distinguishes between the mechanical and hormonal/nutritional influences. The discussion is essentially restricted to mechanical effects, which is particularly relevant to studies on the degradation of bone due to prolonged periods of reduced physical activity.

Apparently, the most important clinical problems in orthopaedics today involve the regions which are dominated by the cancellous bone. Therefore, an adequate description of its mechanical properties is important. In general, the mechanical competence of the entire bone, as a structure, is enforced by the presence of cortical bone, which constrains the deformation. In this context, under typical physiological loads, the system may be considered as elastic. This is not the case however, when considering for example the bone-implant interaction. In order to predict the relative micromotions at the bone-prosthesis interface, it is important to recognize that the trabecular tissue has a high average porosity and it will experience some irreversible deformations (c.f. [24]). The formulation given in this paper is still in its preliminary stage and falls short of quantifying some of the material functions involved. It is believed that this and similar approaches are useful in directing the experimentation towards more specifically defined objecti-

ves. Clearly, the identification of properties in the elastoplastic range will require a series of uniaxial compression tests on trabecular bone specimens, performed at different values of confining pressures (within a range typically experienced in the region adjacent to bone-stem interface). Such tests should be performed in the principal material direction, which could be identified through measurements of material fabric involving high resolution imaging.

Various evolutionary phenomena in bones may be described within a similar conceptual framework. It has been demonstrated that the formulation for functional adaptation of the bone may be derived from that corresponding to aging process, by imposing different evolution laws for the material fabric. It is important to emphasize that the approach adopted for description of a regenerating material requires the framework of *hypoelasticity*, Eq. (3.13), rather than the conventional elasticity. This fact has been generally ignored in the existing formulations of the problem. Finally, it is apparent that much work needs still to be done on the development of quantitative theories, their verification and finally, the numerical simulations of specific clinical problems.

References

1. S.C. COWIN, *The relationship between the elasticity tensor and the fabric tensor*, Mech. Mater., **4**, 137–147, 1985.
2. S.C. COWIN and M.M. MEHRABADI, *Identification of the elastic symmetry of bone and other materials*, J. Biomech., **22**, 503–515, 1989.
3. S.J. HOLLISTER, D.P. FYHRIE, K.J. JEPSEN and S.A. GOLDSTEIN, *Application of homogenization theory to the study of trabecular bone mechanics*, J. Biomech., **24**, 825–839, 1991.
4. S.C. COWIN and D.H. HEGEDUS, *Bone remodelling I: theory of adaptive elasticity*, J. Elasticity, **6**, 313–326, 1976.
5. G. LUO, C.S. COWIN, A.M. SADEGH and Y.P. ARRAMON, *Implementation of strain rate as a bone remodeling stimulus*, J. Biomech. Engng., **117**, 329–338, 1995.
6. D.R. CARTER and W.C. HAYES, *The behaviour of bone as a two-phase porous structure*, J. Bone Jt. Surg., **59**, 954–962, 1977.
7. R. HUISKES, H. WEINANS, H.J. GROOTENBOER, M. DALSTRA, B. FUDALA and T.J. SLOOFF, *Adaptive bone-remodeling theory applied to prosthetic-design analysis*, J. Biomech., **20**, 1135–1150, 1987.
8. F.G. EVANS, *Mechanical properties and histology of cortical bone from younger and older man*, Anat. Rec., **185**, 1–11, 1976.
9. A.H. BURSTEIN, D.T. REILLY and M. MARTENS, *Aging of bone tissue: mechanical properties*, J. Bone Jt. Surg., **21**, 939–945, 1976.
10. M. MOSEKILDE, *Age-related changes in verbal trabecular bone architecture – assessed by new method*, Bone., **9**, 247–250, 1988.
11. A.M. PARFITT, *Implications of architecture for the pathogenesis and prevention of vertebral fracture*, Bone., **13**, S41–S47, 1992.

12. R. HUISKES and S.J. HOLLISTER, *From structure to process, from organ to cell: recent developments of FE-analysis in orthopaedic biomechanics*, J. Biomech. Engng., **115**, 520–526, 1993.

13. S. JEMIOŁO and J.J. TELEGA, *Fabric tensors in bone mechanics*, Eng.Trans., **46**, 3–26, 1998.

14. A. ODGAARD, *Three-dimensional methods for quantification of cancellous bone architecture*, Bone, **20**, 315–328, 1997.

15. S. PIETRUSZCZAK and S. KRUCIŃSKI, *Description of anisotropic response of clays using a tensorial measure of structural disorder*, Mech. Mater., **8**, 327–249, 1989.

16. S. PIETRUSZCZAK, *On inelastic behaviour of anisotropic frictional materials*, Mech.Cohes.-Frict.Mater., **4**, 281–293, 1999.

17. Ken-Ichi. KANATANI, *Distribution of directional data and fabric tensor*, Int. J. Eng. Sci., **22**, 149–161, 1984.

18. R.W. GOULET, S.A. GOLDSTEIN, M.J. CIARELLI, J.L. KUHN, M.B. BROWN and L.A. FELDKAMP, *The relationship between the structural and orthogonal compressive properties of trabecular bone*, J. Biomech., **27**, 375–389, 1993.

19. R. MUELLER and P. RUEGSEGGER, *Analysis of mechanical properties of cancellous bone under conditions of simulated bone atrophy*, J. Biomech., **29**, 1053–1060, 1996.

20. S.C. COWIN, A.M. SADEGH and G.M. LUO, *An evolutionary Wolff's law for trabecular architecture*, J. Biomech. Engng., **114**, 129–136, 1991.

21. C.R. JACOBS, J.C. SIMO, G.S. BEAPURE and D.R. CARTER, *Adaptive bone remodeling incorporating simultaneous density and anisotropy considerations*, J. Biomech., **30**, 603–614, 1997.

22. C.H. TURNER, S.C. COWIN, J.Y. RHO, R.b. ASHMAN and J.C. RICE, *The fabric dependence of the orthotropic elastic constants of cancellous bone*, J. Biomech., **23**, 549–561, 1990.

23. P.K. ZYSSET and A. CURNIER, *A 3D damage model for trabecular bone based on fabric tensors*, J. Biomech., **29**, 1549–1558, 1996.

24. P.J. RUBIN, R.L. RAKOTOMANANA, P.F. LEYVRAZ, P.K. ZYSSET, A. CURNIER and J.H. HEEGAARD, *Frictional interface micromotions and anisotropic stress distribution in a femoral total hip component*, J. Biomech.,**26**, 725–739, 1993.

25. S. PIETRUSZCZAK, D. INGLIS and G.N. PANDE, *Fabric-dependent fracture criterion for corticla/trabecular bone*, J. Biomech., 1999 (in print).

26. T.S. KELLER, *Predicting the compressive mechanical behavior of bone*, J. Biomech., **27**, 1159–1168, 1994.

27. C.H. TURNER and S.C. COWIN, *Errors induced by off-axis measurements of the elastic properties of bone*, J. Biomech. Engng., **110**, 213–215, 1988.

Received September 28, 1998; new version April 26, 1999.

Arch. Mech., **51**, 3–4, pp. 469–486, Warszawa 1999

Homogenization of compressible fluid flow in porous media with interfacial flow barrier

P. ROYER and J.-L. AURIAULT

Laboratoire "Sols, Solides, Structures",
Université Joseph Fourier, Institut National Polytechnique de Grenoble,
Centre National pour la Recherche Scientifique (UMR 5521),
Domaine Universitaire, BP 53X, 38041 Grenoble cedex 9, France.

THIS WORK IS CONCERNED with modelling compressible fluid flow in a composite porous medium with interfacial flow barrier. The macroscopic behaviour and the effective permeability are obtained by homogenization, i.e. by upscaling the description at the heterogeneity scale. Five distinct macroscopic models are derived that relate to five relative orders of magnitude of the interfacial conductance with respect to the permeabilities of the constituents.

1. Introduction

THIS WORK IS AIMED towards deriving the macroscopic governing equations of the flow of a compressible fluid in a porous medium with interfacial flow barrier. Such a medium is locally characterised by a representative elementary volume (REV) whose size is $O(l)$ and that consists of two porous solids (Ω_1 and Ω_2) whose common boundary (Γ) is a thin layer of very low porosity which constitutes a flow barrier (Fig. 1). This situation occurs for example in sedimentary structures that contain shales.

At the local scale, (i.e. at the REV scale), the flow of a compressible fluid in such a medium is governed by the following equations:

$$\nabla \cdot (k_1 p_1 \nabla p_1) = \phi_1 \frac{\partial p_1}{\partial t} \qquad \text{in } \Omega_1, \tag{1.1}$$

$$\nabla \cdot (k_2 p_2 \nabla p_2) = \phi_2 \frac{\partial p_2}{\partial t} \qquad \text{in } \Omega_2, \tag{1.2}$$

$$(k_1 p_1 \nabla p_1) \cdot \mathbf{n} = (k_2 p_2 \nabla p_2) \cdot \mathbf{n} \qquad \text{on } \Gamma, \tag{1.3}$$

$$(k_1 p_1 \nabla p_1) \cdot \mathbf{n}_1 = -\frac{h}{2}(p_1^2 - p_2^2) \qquad \text{on } \Gamma. \tag{1.4}$$

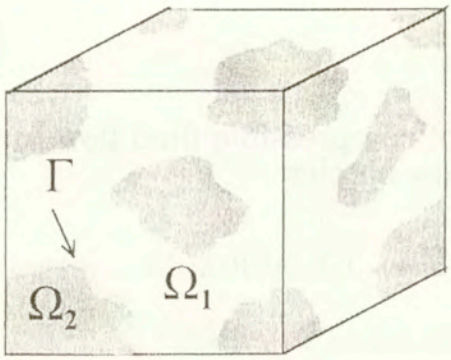

FIG. 1. Periodic cell of the two-constituent porous medium with interfacial flow barrier.

In these equations, p_1 and p_2 are the fluid pressures in Ω_1 and Ω_2, respectively; fluid densities, ρ_1 and ρ_2 are assumed to be such that $\rho_1 = Ap_1$, $\rho_2 = Ap_2$, where A is constant. Equations (1.1) – (1.2) describe the flow of the compressible fluid in Ω_1 and Ω_2, respectively [1]. k_1 and k_2 are the permeabilities of Ω_1 and Ω_2, respectively, and are positive functions of the space variable. For simplicity, they are assumed to be isotropic. ϕ_1 and ϕ_2 are the porosities of Ω_1 and Ω_2, respectively, and are assumed to be constant. Equation (1.3) expresses continuity of fluxes on the interface Γ. The interface flow barrier gives rise to boundary condition (1.4), where h is the interfacial conductance and is a positive function of the space variable. Equation (1.4) is the non-linear counterpart of Eq. (1.8) below.

In the present study, both domains, Ω_1 and Ω_2 are assumed to be connected.

Due to the high compressibility of the fluid, this problem is strongly non-linear. Investigations of similar but linear problems have been carried out via homogenization in the context of heat conduction in composites with heat barrier [2, 3] and of pollutant transfer in a medium with interfacial diffusion barrier [4]. In these studies, the local description is of the following type:

$$\nabla \cdot (\alpha_1 \nabla u_1) = \beta_1 \frac{\partial u_1}{\partial t} \qquad \text{in } \Omega_1, \tag{1.5}$$

$$\nabla \cdot (\alpha_2 \nabla u_2) = \beta_2 \frac{\partial u_2}{\partial t} \qquad \text{in } \Omega_2, \tag{1.6}$$

$$(\alpha_1 \nabla u_1) \cdot \mathbf{n} = (\alpha_2 \nabla u_2) \cdot \mathbf{n} \qquad \text{on } \Gamma, \tag{1.7}$$

$$(\alpha_1 \nabla u_1) \cdot \mathbf{n}_1 = -h(u_1 - u_2) \qquad \text{on } \Gamma. \tag{1.8}$$

The non-dimensional number arising from equation (1.8)

$$b = \frac{|h(u_1 - u_2)|}{|\alpha_1 \nabla u_1|} = \frac{hl}{\alpha_1}, \tag{1.9}$$

is the Biot number and characterises the interfacial barrier.

The flow of an incompressible fluid in a medium with interfacial flow barrier is also locally described by the linear set of equations (1.5) – (1.8). Therefore, the originality of the present work relies upon the non-linearities due to the strong compressibility of the fluid.

Whereas equation (1.8) is well admitted and currently used, to our knowledge, equation (1.4) that describes the effect of an interfacial flow barrier on a non-linear process, has never been proposed yet. However we see that equation (1.4) is physically consistent as it is obtained by replacing u_1 and u_2 by u_1^2 and u_2^2, respectively, in (1.8). The validity of both equations (1.4) and (1.8) can be demonstrated via homogenization. The rigorous derivation of (1.4) by homogenization will be the purpose of a further paper.

The essence of homogenization method is to determine an equivalent macroscopic behaviour by upscaling the local description. The purpose of the present study is to homogenize the local description (1.1) – (1.4), in order to determine the influence of the interfacial barrier on the effective permeability and on the structure of the macroscopic seepage equations.

The fundamental assumption behind homogenization theory is that the scales are separated:

$$l << L, \tag{1.10}$$

where l and L are the characteristic lengths at the heterogeneity scale and at the macroscopic scale, respectively. As this definition conjures up a geometrical separation of scales, we shall draw attention to the fact that this fundamental condition must also be checked regarding the phenomenon. For example, in the case of a wave propagation, the microscopic characteristic length, l, must also be small compared to the wavelength.

In this study, we use the method of homogenization for periodic structures – also called method of multiple scales – introduced by [5] and [6]. The key parameter of the method is the small parameter

$$\varepsilon = \frac{l}{L} << 1, \tag{1.11}$$

in which L is the macroscopic characteristic length and, depending on the problem under consideration, is either geometrical (i.e. the sample size) or related to the excitation (e.g. wavelength).

We also assume the medium to be periodic. This assumption is actually not a restriction: it allows determination of the macroscopic behaviour without any prerequisite on the form of the macroscopic equations. In the context of a periodic medium, the REV is simply the period.

In this study, we use the approach suggested in [7], by which the problem is tackled in a physical rather than mathematical manner. Indeed, it offers the

additional benefit that the conditions under which homogenization does apply are expressly stated. This formulation of the method is the basis of definition and estimation of the non-dimensional numbers arising from the local description under consideration. This fundamental step is called normalisation and is aimed at specifying all cases that can be homogenized.

In the present work, we show that fluid flow in a porous medium with interfacial flow barrier is not, a priori, described by a single model. The normalisation of the local description (1.1) – (1.4) is presented in Sec. 2. It highlights five distinct physical situations to be homogenized that relate to five distinct relative values of the interfacial conductance with respect to the permeabilities. Section 3 sets out to examine the mathematical formulation of the method as a result of the separation of scales. Finally, in Sec. 4 details are given of the derivation of the five corresponding macroscopic models. Three models are single-pressure field models and the two others are two-pressure field models. We show that besides its link to the relative value of the interfacial conductance with respect to the permeabilities, the choice of the model is also related to the excitation.

2. Normalisation

The purpose of this section is to define the set of non-dimensional numbers that characterise the local description (1.1) – (1.4) and then to estimate them with respect to the small parameter ε.
From equation (1.1) we can define

$$T_1 = \frac{|\nabla \cdot (k_1 p_1 \nabla p_1)|}{\left|\phi_1 \dfrac{\partial p_1}{\partial t}\right|}. \tag{2.1}$$

Similarly, equation (1.2) introduces

$$T_2 = \frac{|\nabla \cdot (k_2 p_2 \nabla p_2)|}{\left|\phi_2 \dfrac{\partial p_2}{\partial t}\right|} = O(T_1) \times O\left(\frac{k_2}{k_1}\right) \times O\left(\frac{p_2}{p_1}\right) \times O\left(\frac{\phi_1}{\phi_2}\right). \tag{2.2}$$

Now, from Eq. (1.3) arises

$$A = \frac{|(k_1 p_1 \nabla p_1) \cdot \mathbf{n}|}{|(k_2 p_2 \nabla p_2) \cdot \mathbf{n}|} = O\left(\frac{k_1}{k_2}\right) \times O\left(\frac{(p_1)^2}{(p_2)^2}\right). \tag{2.3}$$

Finally, from Eq. (1.4) we get the following non-dimensional number:

$$B = \frac{\left|\dfrac{h}{2}\left(p_1^2 - p_2^2\right)\right|}{|(k_1 p_1 \nabla p_1) \cdot \mathbf{n}_1|}, \tag{2.4}$$

which is similar to the Biot number defined in (1.9) and which characterises the relative value of the interfacial conductance with respect to the permeabilities of the constituents.

For estimating these non-dimensional numbers, let us consider l as the reference characteristic length. This arbitrary choice does not affect the final result. When using l as the reference length, the estimations of T_1, T_2, A and B are denoted by T_{1_l}, T_{2_l}, A_l and B_l . By assuming for simplicity that:

$$\left|\frac{k_1}{k_2}\right|_l = O(1); \qquad \left|\frac{p_1}{p_2}\right|_l = O(1); \qquad \left|\frac{\phi_1}{\phi_2}\right|_l = O(1), \tag{2.5}$$

it turns out that

$$T_{1_l} = O(T_{2_l}), \tag{2.6}$$

$$A_l = O(1), \tag{2.7}$$

and

$$B_l = O\left(\frac{hl}{2k_1}\right). \tag{2.8}$$

Since we want to describe a transient flow at the macroscopic scale, we may consider that:

$$|\nabla \cdot (k_1 p_1 \nabla p_1)|_L = O\left(\left|\phi_1 \frac{\partial p_1}{\partial t}\right|_L\right), \tag{2.9}$$

$$|\nabla \cdot (k_2 p_2 \nabla p_2)|_L = O\left(\left|\phi_2 \frac{\partial p_2}{\partial t}\right|_L\right), \tag{2.10}$$

which means

$$T_{1_L} = O(T_{2_L}) = O(1). \tag{2.11}$$

Thus, when using l for estimating T_1 and T_2, we get

$$T_{1_l} = O(T_{2_l}) = O(\varepsilon^{-2}). \tag{2.12}$$

The orders of magnitude (2.12) are actually related to the previously mentioned condition of separation of scales regarding the excitation. In effect, they express the fact that the characteristic time of the flow must be sufficiently large to ensure a good separation of scales. Estimations (2.12) are required for applying homogenization as there would not exist any equivalent macroscopic continuous description for $T_{1_l} = O(T_{2_l}) < O(\varepsilon^{-2})$, whereas orders of magnitude (2.5) are pure assumptions.

Once the orders of magnitude of T_{1_l}, T_{2_l} and A_l have been fixed, the local description remains only conditioned by the order of magnitude of B_l, which

is actually a measure of the influence of the interfacial conductance. The non-dimensional description is the following, in which all quantities are now non-dimensional quantities:

$$\nabla \cdot (k_1 p_1 \nabla p_1) = \varepsilon^2 \phi_1 \frac{\partial p_1}{\partial t} \qquad \text{in } \Omega_1, \tag{2.13}$$

$$\nabla \cdot (k_2 p_2 \nabla p_2) = \varepsilon^2 \phi_2 \frac{\partial p_2}{\partial t} \qquad \text{in } \Omega_2, \tag{2.14}$$

$$(k_1 p_1 \nabla p_1) \cdot \mathbf{n} = (k_2 p_2 \nabla p_2) \cdot \mathbf{n} \qquad \text{on } \Gamma, \tag{2.15}$$

$$(k_1 p_1 \nabla p_1) \cdot \mathbf{n}_1 = -O(B_l) \frac{h}{2} (p_1^2 - p_2^2) \qquad \text{on } \Gamma. \tag{2.16}$$

We shall now apply the homogenization procedure to this local description.

3. Mathematical formulation of the method

As a result of the separation of scales, two non-dimensional space variables may be defined:

$$\mathbf{y} = \frac{\mathbf{X}}{l}, \qquad \mathbf{x} = \frac{\mathbf{X}}{L},$$

where $\mathbf{X}$ is the physical space variable.

If the condition of separation of scales is verified, then $\mathbf{y}$ and $\mathbf{x}$ appear as two independent space variables: $\mathbf{y}$ is the microscopic variable and describes the heterogeneity scale whereas $\mathbf{x}$ is the macroscopic variable.

As a consequence, the physical variables of the problem, p_1 and p_2, are *a priori* functions of $\mathbf{y}$ and $\mathbf{x}$:

$$p_1 = p_1(\mathbf{y}, \mathbf{x}, t),$$

$$p_2 = p_2(\mathbf{y}, \mathbf{x}, t).$$

Moreover, the partial derivative with respect to the physical space variable $\mathbf{X}$ can be written as:

$$\frac{\partial}{\partial X_i} = \frac{1}{l} \frac{\partial}{\partial y_i} + \frac{1}{L} \frac{\partial}{\partial x_i}. \tag{3.1}$$

Since l is the reference characteristic length, the non-dimensional gradient operator is therefore given by

$$\nabla_y + \varepsilon \nabla_x, \tag{3.2}$$

where ∇_y and ∇_x are the gradient operators with respect to variables $\mathbf{y}$ and $\mathbf{x}$, respectively. The homogenization method of multiple scales is based on the

fundamental statement that if the scales are well separated, then all physical variables can be looked for in the form of asymptotic expansions in powers of ε:

$$p_1 = p_1^0(\mathbf{y}, \mathbf{x}, t) + \varepsilon p_1^1(\mathbf{y}, \mathbf{x}, t) + ..., \tag{3.3}$$

$$p_2 = p_2^0(\mathbf{y}, \mathbf{x}, t) + \varepsilon p_2^1(\mathbf{y}, \mathbf{x}, t) + ..., \tag{3.4}$$

in which the functions p_1^i and p_2^i are $\mathbf{y}$-periodic.

The method consists in incorporating expansions (3.3) and (3.4) in the non-dimensional local description (2.13) – (2.16). Solving the boundary-value problems arising at the successive orders of ε leads to the macroscopic description. It turns out that five distinct macroscopic descriptions can be derived from the local description (2.13) – (2.16), that correspond to five distinct orders of magnitude for B_l:

$$B_l = O(\varepsilon^p), \qquad p = -1, 0, 1, 2, 3. \tag{3.5}$$

The derivation of these macroscopic models via homogenization is the purpose of the next section.

4. Derivation of the macroscopic models

4.1. Model I: $B_l = O(\varepsilon^{-1})$

First-order problem (Eqs. (2.13), (2.14) and (2.16) at the order of ε^0 and Eq. (2.16) at the order of ε^{-1}):

$$\nabla_y \cdot \left(k_1 p_1^0 \nabla_y p_1^0\right) = 0 \qquad \text{in } \Omega_1, \tag{4.1}$$

$$\nabla_y \cdot \left(k_2 p_2^0 \nabla_y p_2^0\right) = 0 \qquad \text{in } \Omega_2, \tag{4.2}$$

$$\left(k_1 p_1^0 \nabla_y p_1^0\right) \cdot \mathbf{n} = \left(k_2 p_2^0 \nabla_y p_2^0\right) \cdot \mathbf{n} \qquad \text{on } \Gamma, \tag{4.3}$$

$$p_1^0 = p_2^0 \qquad \text{on } \Gamma, \tag{4.4}$$

(p_1^0 and p_2^0 are $\mathbf{y}$-periodic).

Let $\mathcal{V}(\Omega)$ be the Hilbert space of functions θ defined and continuous over Ω, that are $\mathbf{y}$-periodic and that satisfy the condition

$$\int_{\Omega} \theta \, d\Omega = 0. \tag{4.5}$$

$\mathcal{V}(\Omega)$ is equipped with the following inner product:

$$(\alpha, \beta)_{\mathcal{V}(\Omega)} = \int_{\Omega} \nabla_y \alpha \; k \; \nabla_y \beta \; d\Omega. \tag{4.6}$$

The equivalent variational formulation of (4.1) – (4.4) is given by

$$\forall \theta \in \mathcal{V}(\Omega) : (\theta, (p^0)^2)_{\mathcal{V}(\Omega)} = 0. \tag{4.7}$$

Existence and uniqueness of the solution to (4.7) are proved by Lax-Milgram Lemma. Equation (4.7) gives

$$(p^0)^2 = (p^0)^2(\mathbf{x}, t). \tag{4.8}$$

Therefore, we get

$$p_1^0 = p_2^0 = p^0(\mathbf{x}, t). \tag{4.9}$$

Second-order problem (Eqs. (2.13), (2.14) and (2.15) at the order of ε^1 and Eq. (2.16) at the order of ε^0).

Since $p^0 = p^0(\mathbf{x}, t)$, the system reduces to the following linear boundary value problem:

$$\nabla_y \cdot \left[k_1 \left(\nabla_y p_1^1 + \nabla_x p^0 \right) \right] = 0 \qquad \text{in } \Omega_1, \tag{4.10}$$

$$\nabla_y \cdot \left[k_2 \left(\nabla_y p_2^1 + \nabla_x p^0 \right) \right] = 0 \qquad \text{in } \Omega_2, \tag{4.11}$$

$$\left[k_1 \left(\nabla_y p_1^1 + \nabla_x p^0 \right) \right] \cdot \mathbf{n} = \left[k_2 \left(\nabla_y p_2^1 + \nabla_x p^0 \right) \right] \cdot \mathbf{n} \qquad \text{on } \Gamma, \tag{4.12}$$

$$p_1^1 = p_2^1 \qquad \text{on } \Gamma. \tag{4.13}$$

(p_1^1 and p_2^1 are $\mathbf{y}$-periodic).

The equivalent variational formulation of this system is:

$$\forall \theta \in \mathcal{V}(\Omega) : \left(\theta, p^1 \right)_{\mathcal{V}(\Omega)} = - \int_{\Omega} \nabla_y \theta \; k \; \nabla_x p^0 \; d\Omega. \tag{4.14}$$

Hence, by the Lax-Milgram Lemma, there is a unique solution to (4.14). As a result, there is a solution modulo a constant to the system (4.10) – (4.14). Let τ_i^{I} be the particular solution of (4.14) for $\dfrac{\partial p^0}{\partial x_j} = \delta_{ij}$. Thus, p^1 is written as:

$$p^1 = \boldsymbol{\tau}^{\mathrm{I}} \cdot \nabla_x p^0 + \bar{p}^1(\mathbf{x}, t), \tag{4.15}$$

where p^1 stands for p_1^1 in Ω_1 and for p_2^1 in Ω_2 and where $p^1(\mathbf{x}, t)$ is an arbitrary function. $\boldsymbol{\tau}^{\mathrm{I}}$ is $\mathbf{y}$-periodic, its mean value is zero,

$$< \boldsymbol{\tau}^{\mathrm{I}} >_{\Omega} = \frac{1}{|\Omega|} \int_{\Omega} \boldsymbol{\tau}^{\mathrm{I}} d\Omega = \mathbf{0}, \tag{4.16}$$

and $\boldsymbol{\tau}^{\mathrm{I}}$ is the solution of the following boundary-value problem:

$$\frac{\partial}{\partial y_i}\left(\frac{\partial \tau_k^I}{\partial y_i}+\delta_{ik}\right)=0 \qquad \text{in } \Omega, \tag{4.17}$$

$$k_1\left(\frac{\partial \tau_k^I}{\partial y_i}+\delta_{ik}\right)n_i = k_2\left(\frac{\partial \tau_k^I}{\partial y_i}+\delta_{ik}\right)n_i \qquad \text{on } \Gamma, \tag{4.18}$$

in which k stands for k_1 in Ω_1 and for k_2 in Ω_2.

Third-order problem (Eqs. (2.13), (2.14) and (2.15) at the order of ε^2):

$$\nabla_y\cdot\left[k_1\left(p^0\left(\nabla_y p_1^2+\nabla_x p_1^1\right)+p_1^1\left(\nabla_y p_1^1+\nabla_x p^0\right)\right)\right] \tag{4.19}$$

$$+\nabla_x.\left[k_1\left(p^0\left(\nabla_y p_1^1+\nabla_x p^0\right)\right)\right]=\phi_1\frac{\partial p^0}{\partial t} \qquad \text{in } \Omega_1,$$

$$\nabla_y\cdot\left[k_2\left(p^0\left(\nabla_y p_2^2+\nabla_x p_2^1\right)+p_2^1\left(\nabla_y p_2^1+\nabla_x p^0\right)\right)\right] \tag{4.20}$$

$$+\nabla_x\cdot\left[k_2\left(p^0\left(\nabla_y p_2^1+\nabla_x p^0\right)\right)\right]=\phi_2\frac{\partial p^0}{\partial t} \qquad \text{in } \Omega_2,$$

$$\left[k_1\left(p^0\left(\nabla_y p_1^2+\nabla_x p_1^1\right)+p_1^1\left(\nabla_y p_1^1+\nabla_x p^0\right)\right)\right]\cdot\mathbf{n} \tag{4.21}$$

$$=\left[k_2\left(p^0\left(\nabla_y p_2^2+\nabla_x p_2^1\right)+p_2^1\left(\nabla_y p_2^1+\nabla_x p^0\right)\right)\right]\cdot\mathbf{n} \qquad \text{on } \Gamma.$$

(p_1^2 and p_2^2 are $\mathbf{y}$-periodic).

Integrating (4.19) over Ω_1 and (4.20) over Ω_2 and then using the divergence theorem, the condition of periodicity and boundary condition (4.21) leads to

$$\nabla_x.\left(p^0<k(\nabla_y p^1+\nabla_x p^0>_\Omega\right)=<\phi>\frac{\partial p^0}{\partial t}, \tag{4.22}$$

where

$$<\phi>=n_1\phi_1+n_2\phi_2; \qquad n_i=\frac{|\Omega_i|}{\Omega}. \tag{4.23}$$

Equation (4.22) can also be written as:

$$\nabla_x.\left(\tilde{K}^I p^0\nabla_x p^0\right)=<\phi>\frac{\partial p^0}{\partial t}, \tag{4.24}$$

in which $\tilde{K}^I$ is componentwise defined by:

$$K_{ij}^I=\frac{1}{|\Omega|}\int_\Omega k\left(\frac{\partial \tau_i^I}{\partial y_j}+\delta_{ij}\right)d\Omega. \tag{4.25}$$

It can be shown that $\tilde{K}$ is positive definite. When $B_l = O(\varepsilon^p), p < -1$, the macroscopic behaviour is also described by Model I.

4.2. Model II: $B_l = O(\varepsilon^0)$

First-order problem (Eqs. (2.13), (2.14), (2.15) and (2.16) at the order of ε^0):

$$\nabla_y \cdot \left(k_1 p_1^0 \nabla_y p_1^0\right) = 0 \qquad \text{in } \Omega_1, \tag{4.26}$$

$$\nabla_y \cdot \left(k_2 p_2^0 \nabla_y p_2^0\right) = 0 \qquad \text{in } \Omega_2, \tag{4.27}$$

$$\left(k_1 p_1^0 \nabla_y p_1^0\right) \cdot \mathbf{n} = \left(k_2 p_2^0 \nabla_y p_2^0\right) \cdot \mathbf{n} \qquad \text{on } \Gamma, \tag{4.28}$$

$$\left(k_1 p_1^0 \nabla_y p_1^0\right) \cdot \mathbf{n}_1 = -\frac{h}{2}\left[(p_1^0)^2 - (p_2^0)^2\right] \qquad \text{on } \Gamma. \tag{4.29}$$

(p_1^0 and p_2^0 are **y**-periodic).
Let $\mathcal{W}(\Omega)$ be the Hilbert space of functions θ that are **y**-periodic, continuous over Ω_1 and Ω_2 and possibly discontinuous over Γ and such that

$$\int_{\Omega} \theta \, \Omega = 0. \tag{4.30}$$

$\mathcal{W}(\Omega)$ is equipped with the following inner product:

$$(\alpha, \beta)_{\mathcal{W}(\Omega)} = \int_{\Omega} \nabla_y \alpha \; k \; \nabla_y \beta \; d\Omega + \int_{\Gamma} h(\alpha_1 - \alpha_2)(\beta_1 - \beta_2) \; dS. \tag{4.31}$$

The equivalent formulation of (4.26) – (4.29) is

$$\forall \theta \in \mathcal{W}(\Omega) : \left(\theta, (p^0)^2\right)_{\mathcal{W}(\Omega)} = 0, \tag{4.32}$$

from which we get

$$(p^0)^2 = (p^0)^2(\mathbf{x}, t). \tag{4.33}$$

Thus, the solution is

$$p_1^0 = p_2^0 = p^0(\mathbf{x}, t). \tag{4.34}$$

Second-order problem (Eqs. (2.13), (2.14), (2.15) and (2.16) at the order of ε^1).
This system reduces to the following linear boundary value problem:

$$\nabla_y \cdot \left[k_1 \left(\nabla_y p_1^1 + \nabla_x p^0\right)\right] = 0 \qquad \text{in } \Omega_1, \tag{4.35}$$

$$\nabla_y \cdot \left[k_2 \left(\nabla_y p_2^1 + \nabla_x p^0\right)\right] = 0 \qquad \text{in } \Omega_2, \tag{4.36}$$

$$\left[k_1 \left(\nabla_y p_1^1 + \nabla_x p^0\right)\right] \cdot \mathbf{n} = \left[k_2 \left(\nabla_y p_2^1 + \nabla_x p^0\right)\right] \cdot \mathbf{n} \qquad \text{on } \Gamma, \tag{4.37}$$

$$\left[k_1 \left(\nabla_y p_1^1 + \nabla_x p^0\right)\right] \cdot \mathbf{n}_1 = -h(p_1^1 - p_2^1) \qquad \text{on } \Gamma. \tag{4.38}$$

(p_1^1 and p_2^1 are $\mathbf{y}$-periodic).

The equivalent variational formulation of (4.35) – (4.38) is the following:

$$\forall \theta \in \mathcal{W}(\Omega) : \left(\theta, p^1\right)_{\mathcal{W}(\Omega)} = -\int_\Omega \nabla_y \theta \; k \; \nabla_x p^0 \; d\Omega. \tag{4.39}$$

Let $\boldsymbol{\tau}_{1i}^{\mathrm{II}}$ and $\boldsymbol{\tau}_{2i}^{\mathrm{II}}$ be the particular solutions in Ω_1 and Ω_2 for $\dfrac{\partial p^0}{\partial x_j} = \delta_{ij}$. Then, p_1^1 and p_2^1 are given by:

$$p_1^1 = \boldsymbol{\tau}_1^{\mathrm{II}} . \nabla_x p^0 + \bar{p}_1^1(\mathbf{x}, t), \tag{4.40}$$

$$p_2^1 = \boldsymbol{\tau}_2^{\mathrm{II}} . \nabla_x p^0 + \bar{p}_2^1(\mathbf{x}, t). \tag{4.41}$$

$\boldsymbol{\tau}_1^{\mathrm{II}}$ and $\boldsymbol{\tau}_2^{\mathrm{II}}$ are $\mathbf{y}$-periodic and are the solutions of the following system:

$$\frac{\partial}{\partial y_i}\left[k_1 \left(\frac{\partial \tau_{1k}^{\mathrm{II}}}{\partial y_i} + \delta_{ik}\right)\right] = 0 \qquad \text{in } \Omega_1, \tag{4.42}$$

$$\frac{\partial}{\partial y_i}\left[k_2 \left(\frac{\partial \tau_{2k}^{\mathrm{II}}}{\partial y_i} + \delta_{ik}\right)\right] = 0 \qquad \text{in } \Omega_2, \tag{4.43}$$

$$k_1 \left(\frac{\partial \tau_{1k}^{\mathrm{II}}}{\partial y_i} + \delta_{ik}\right) n_i = k_2 \left(\frac{\partial \tau_{2k}^{\mathrm{II}}}{\partial y_i} + \delta_{ik}\right) n_i \qquad \text{on } \Gamma, \tag{4.44}$$

$$k_1 \left(\frac{\partial \tau_{1k}^{\mathrm{II}}}{\partial y_i} + \delta_{ik}\right) n_{1i} = -h\left(\tau_{1k}^{\mathrm{II}} - \tau_{2k}^{\mathrm{II}}\right) \qquad \text{on } \Gamma. \tag{4.45}$$

$\boldsymbol{\tau}_1^{\mathrm{II}}$ and $\boldsymbol{\tau}_2^{\mathrm{II}}$ also verify

$$\int_{\Omega_1} \boldsymbol{\tau}_1^{\mathrm{II}} \, d\Omega = 0 + \int_{\Omega_2} \boldsymbol{\tau}_2^{\mathrm{II}} \, d\Omega = 0. \tag{4.46}$$

It turns out that $\boldsymbol{\tau}_1^{\mathrm{II}}$ and $\boldsymbol{\tau}_2^{\mathrm{II}}$, and therefore p_1^1 and p_2^1 are h-dependent.

Third-order problem (Eqs. (2.13), (2.14) and (2.15) at the order of ε^2):
This problem is similar to the third-order problem in Sec. 4.1. Using identical

reasoning to that outlined in Sec. 4.1, we arrive at the following macroscopic description:

$$\nabla_x \cdot \left(\tilde{K}^{\mathrm{II}} p^0 \nabla_x p^0 \right) = < \phi > \frac{\partial p^0}{\partial t}, \tag{4.47}$$

in which

$$K_{ij}^{\mathrm{II}} = \frac{1}{|\Omega|} \int_{\Omega} k \left(\frac{\partial \tau_i^{\mathrm{II}}}{\partial y_j} + \delta_{ij} \right) d\Omega. \tag{4.48}$$

$\tilde{K}^{\mathrm{II}}$ is h-dependent.

4.3. Model III: $B_l = O(\varepsilon^1)$

First-order problem (Eqs. (2.13), (2.14), (2.15) and (2.16) at the order of ε^0). It consists of two non-coupled boundary value problems:

$$\nabla_y \cdot \left(k_1 p_1^0 \nabla_y p_1^0 \right) = 0 \qquad \text{in } \Omega_1, \tag{4.49}$$

$$\left(k_1 p_1^0 \nabla_y p_1^0 \right) \cdot \mathbf{n} = 0 \qquad \text{on } \Gamma, \tag{4.50}$$

$$\nabla_y \cdot \left(k_2 p_2^0 \nabla_y p_2^0 \right) = 0 \qquad \text{in } \Omega_2, \tag{4.51}$$

$$\left(k_2 p_2^0 \nabla_y p_2^0 \right) \cdot \mathbf{n} = 0 \qquad \text{on } \Gamma. \tag{4.52}$$

(p_1^0 and p_2^0 are $\mathbf{y}$-periodic).
The equivalent variational formulations are

$$\forall \theta_1 \in \mathcal{V}(\Omega_1) : \left(\theta_1, (p_1^0)^2 \right)_{\mathcal{V}} (\Omega_1) = 0, \tag{4.53}$$

$$\forall \theta_2 \in \mathcal{V}(\Omega_2) : \left(\theta_2, (p_2^0)^2 \right)_{\mathcal{V}} (\Omega_2) = 0. \tag{4.54}$$

($\mathcal{V}(\Omega)$ and $(.,.)_{\mathcal{V}(\Omega)}$ are defined in Subsec. 4.1). Therefore, the solutions are

$$p_1^0 = p_1^0(\mathbf{x}, t), \tag{4.55}$$

$$p_2^0 = p_2^0(\mathbf{x}, t). \tag{4.56}$$

Second-order problem (Eqs. (2.13), (2.14), (2.15) and (2.16) at the order of ε^1):

$$\nabla_y \cdot \left[k_1 p_1^0 \left(\nabla_y p_1^1 + \nabla_x p_1^0 \right) \right] = 0 \qquad \text{in } \Omega_1, \tag{4.57}$$

$$\nabla_y \cdot \left[k_2 p_2^0 \left(\nabla_y p_2^1 + \nabla_x p_2^0 \right) \right] = 0 \qquad \text{in } \Omega_2, \tag{4.58}$$

$$\left[k_1 p_1^0 \left(\nabla_y p_1^1 + \nabla_x p_1^0 \right) \right] \cdot \mathbf{n} = \left[k_2 p_2^0 \left(\nabla_y p_2^1 + \nabla_x p_2^0 \right) \right] \cdot \mathbf{n} \qquad \text{on } \Gamma, \tag{4.59}$$

$$\left[k_1 p_1^0 \left(\nabla_y p_1^1 + \nabla_x p_1^0 \right) \right] \cdot \mathbf{n}_1 = -\frac{h}{2} \left[(p_1^0)^2 - (p_2^0)^2 \right] \qquad \text{on } \Gamma. \tag{4.60}$$

(p_1^1 and p_2^1 are $\mathbf{y}$-periodic).

Integrating (4.57) over Ω_1 and using the divergence theorem, the periodicity and (4.60) leads to

$$\frac{1}{|\Omega|}\int_{\Gamma} hdS\ \left[\left(p_1^0 - p_2^0\right)\right] = 0, \tag{4.61}$$

from which we deduce

$$p_1^0 = p_2^0 = p^0(\mathbf{x}, t). \tag{4.62}$$

As a consequence, the set (4.57) – (4.60) reduces to the two following linear non-coupled boundary value problems:

$$\nabla_y \cdot \left[k_1 \left(\nabla_y p_1^1 + \nabla_x p^0\right)\right] = 0 \qquad \text{in } \Omega_1, \tag{4.63}$$

$$\left[k_1 \left(\nabla_y p_1^1 + \nabla_x p^0\right)\right] \cdot \mathbf{n} = 0 \qquad \text{on } \Gamma, \tag{4.64}$$

$$\nabla_y \cdot \left[k_2 \left(\nabla_y p_2^1 + \nabla_x p^0\right)\right] = 0 \qquad \text{in } \Omega_2, \tag{4.65}$$

$$\left[k_2 \left(\nabla_y p_2^1 + \nabla_x p^0\right)\right] \cdot \mathbf{n} = 0 \qquad \text{on } \Gamma. \tag{4.66}$$

The equivalent variational formulations are

$$\forall \theta_1 \in \mathcal{V}(\Omega_1) : (\theta_1, p_1^1)_{\mathcal{V}(\Omega_1)} = -\int_{\Omega_1} \nabla_y \theta_1\ k_1\ \nabla_x p^0\ d\Omega, \tag{4.67}$$

$$\forall \theta_2 \in \mathcal{V}(\Omega_2) : (\theta_2, p_2^1)_{\mathcal{V}(\Omega_2)} = -\int_{\Omega_2} \nabla_y \theta_2\ k_2\ \nabla_x p^0\ d\Omega. \tag{4.68}$$

Let $\boldsymbol{\tau}_{1i}^{\mathrm{III}}$ and $\boldsymbol{\tau}_{2i}^{\mathrm{III}}$ be the particular solutions for $\dfrac{\partial p^0}{\partial x_j} = \delta_{ij}$. The solutions are:

$$p_1^1 = \boldsymbol{\tau}_1^{\mathrm{III}} \cdot \nabla_x p^0 + \bar{p}_1^1(\mathbf{x}, t), \tag{4.69}$$

$$p_2^1 = \boldsymbol{\tau}_2^{\mathrm{III}} \cdot \nabla_x p^0 + \bar{p}_2^1(\mathbf{x}, t), \tag{4.70}$$

where $\boldsymbol{\tau}_1^{\mathrm{III}}$ and $\boldsymbol{\tau}_2^{\mathrm{III}}$ are $\mathbf{y}$-periodic, and they satisfy

$$\int_{\Omega_1} \boldsymbol{\tau}_1^{\mathrm{III}}\ d\Omega = \mathbf{0}, \qquad \int_{\Omega_2} \boldsymbol{\tau}_2^{\mathrm{III}}\ d\Omega = \mathbf{0}, \tag{4.71}$$

and are the solutions of:

$$\frac{\partial}{\partial y_i}\left(\frac{\partial \tau_{1k}^{\mathrm{III}}}{\partial y_i} + \delta_{ik}\right) = 0 \qquad \text{in } \Omega_1, \tag{4.72}$$

$$\left(\frac{\partial \tau_{1k}^{\mathrm{III}}}{\partial y_i} + \delta_{ik}\right) n_i = 0 \qquad \text{on } \Gamma, \tag{4.73}$$

$$\frac{\partial}{\partial y_i}\left(\frac{\partial \tau_{2k}^{\mathrm{III}}}{\partial y_i} + \delta_{ik}\right) = 0, \qquad \text{in } \Omega_2, \tag{4.74}$$

$$\left(\frac{\partial \tau_{2k}^{\mathrm{III}}}{\partial y_i} + \delta_{ik}\right) n_i = 0 \qquad \text{on } \Gamma. \tag{4.75}$$

The macroscopic behaviour is derived from the third-order problem as in Subsecs. 4.1 and 4.2 and is given by:

$$\nabla_x . \left(\tilde{K}^{\mathrm{III}} p^0 \nabla_x p^0\right) = < \phi > \frac{\partial p^0}{\partial t}, \tag{4.76}$$

in which

$$\tilde{K}^{\mathrm{III}} = \tilde{K}_1^{\mathrm{III}} + \tilde{K}_2^{\mathrm{III}}, \tag{4.77}$$

where $\tilde{K}_1^{\mathrm{III}}$ and $\tilde{K}_2^{\mathrm{III}}$ are the effective permeabilities of both constituents:

$$K_{1ij}^{\mathrm{III}} = \frac{1}{|\Omega|} \int_{\Omega_1} k_1 \left(\frac{\partial \tau_{1i}^{\mathrm{III}}}{\partial y_j} + \delta_{ij}\right) d\Omega, \tag{4.78}$$

$$K_{2ij}^{\mathrm{III}} = \frac{1}{|\Omega|} \int_{\Omega_2} k_2 \left(\frac{\partial \tau_{2i}^{\mathrm{III}}}{\partial y_j} + \delta_{ij}\right) d\Omega. \tag{4.79}$$

$\tilde{K}^{\mathrm{III}}$ is independent of h.

4.4. Model IV: $B_l = O(\varepsilon^2)$

First-order problem (Eqs. (2.13), (2.14), (2.15) and (2.16) at the order of ε^0). This system is identical to the first-order problem in 4.3 and therefore leads to

$$p_1^0 = p_1^0(\mathbf{x}, t), \tag{4.80}$$

$$p_2^0 = p_2^0(\mathbf{x}, t). \tag{4.81}$$

Second-order problem (Eqs. (2.13), (2.14), (2.15) and (2.16) at the order of ε^1). This problem reduces to two non-coupled linear boundary value problems that are identical to (4.63) – (4.66). The solutions are

$$p_1^1 = \boldsymbol{\tau}_1^{\mathrm{IV}} \cdot \nabla_x p_1^0 + \bar{p}_1^1(\mathbf{x}, t), \tag{4.82}$$

$$p_2^1 = \boldsymbol{\tau}_2^{\mathrm{IV}} \cdot \nabla_x p_2^0 + \bar{p}_2^1(\mathbf{x}, t), \tag{4.83}$$

where $\boldsymbol{\tau}_1^{\mathrm{IV}} = \boldsymbol{\tau}_1^{\mathrm{III}}$ and $\boldsymbol{\tau}_2^{\mathrm{IV}} = \boldsymbol{\tau}_2^{\mathrm{III}}$.

Third-order problem (Eqs. (2.13), (2.14), (2.15) and (2.16) at the order of ε^2). This problem can be expressed as follows:

$$\nabla_y \cdot \left[k_1 \left(p_1^0 \left(\nabla_y p_1^2 + \nabla_x p_1^1\right) + p_1^1 \left(\nabla_y p_1^1 + \nabla_x p^0\right)\right)\right] + \nabla_x \cdot \left[k_1 \left(p_1^0 \left(\nabla_y p_1^1 + \nabla_x p_1^0\right)\right)\right] = \phi_1 \frac{\partial p_1^0}{\partial t} \quad \text{in } \Omega_1, \tag{4.84}$$

$$\left[k_1 \left(p_1^0 \left(\nabla_y p_1^2 + \nabla_x p_1^1\right) + p_1^1 \left(\nabla_y p_1^1 + \nabla_x p_1^0\right)\right)\right] \cdot \mathbf{n} = -\frac{h}{2}\left[\left(p_1^0\right)^2 - \left(p_2^0\right)^2\right] \quad \text{on } \Gamma, \tag{4.85}$$

$$\nabla_y \cdot \left[k_2 \left(p_2^0 \left(\nabla_y p_2^2 + \nabla_x p_2^1\right) + p_2^1 \left(\nabla_y p_2^1 + \nabla_x p_2^0\right)\right)\right] + \nabla_x \cdot \left[k_2 \left(p_2^0 \left(\nabla_y p_2^1 + \nabla_x p_2^0\right)\right)\right] = \phi_2 \frac{\partial p_2^0}{\partial t} \quad \text{in } \Omega_2, \tag{4.86}$$

$$\left[k_2 \left(p_2^0 \left(\nabla_y p_2^2 + \nabla_x p_2^1\right) + p_2^1 \left(\nabla_y p_2^1 + \nabla_x p_2^0\right)\right)\right] \cdot \mathbf{n} = +\frac{h}{2}\left[\left(p_1^0\right)^2 - \left(p_2^0\right)^2\right] \quad \text{on } \Gamma. \tag{4.87}$$

(p_1^2 and p_2^2 are $\mathbf{y}$-periodic).

Integrating (4.84) and (4.86) over Ω_1 and Ω_2, respectively, applying the divergence theorem and using the condition of periodicity and boundary conditions (4.85) and (4.87) yields:

$$\nabla_x \cdot \left(\tilde{K}_1^{\mathrm{IV}} p_1^0 \nabla_x p_1^0\right) - \frac{H}{2}\left[\left(p_1^0\right)^2 - \left(p_2^0\right)^2\right] = n_1 \phi_1 \frac{\partial p_1^0}{\partial t}, \tag{4.88}$$

$$\nabla_x \cdot \left(\tilde{K}_2^{\mathrm{IV}} p_2^0 \nabla_x p_2^0\right) + \frac{H}{2}\left[\left(p_1^0\right)^2 - \left(p_2^0\right)^2\right] = n_2 \phi_2 \frac{\partial p^0}{\partial t}, \tag{4.89}$$

in which

$$H = \frac{1}{|\Omega|} \int_\Gamma h \, dS, \tag{4.90}$$

and where

$$\tilde{K}_1^{\mathrm{IV}} = \tilde{K}_1^{\mathrm{III}}, \tag{4.91}$$

$$\tilde{K}_2^{\mathrm{IV}} = \tilde{K}_2^{\mathrm{III}}. \tag{4.92}$$

4.5. Model V: $B_l = O(\varepsilon^3)$

The derivation of model V is similar to that of model IV, but with the difference that there is no source term. As a result, the macroscopic behaviour is described by:

$$\nabla_x \cdot \left(\tilde{K}_1^{\mathrm{V}} p_1^0 \nabla_x p_1^0 \right) = n_1 \phi_1 \frac{\partial p_1^0}{\partial t}, \tag{4.93}$$

$$\nabla_x \cdot \left(\tilde{K}_2^{\mathrm{V}} p_2^0 \nabla_x p_2^0 \right) = n_2 \phi_2 \frac{\partial p^0}{\partial t}, \tag{4.94}$$

in which

$$\tilde{K}_1^{\mathrm{V}} = \tilde{K}_1^{\mathrm{IV}} = \tilde{K}_1^{\mathrm{III}}, \tag{4.95}$$

$$\tilde{K}_2^{\mathrm{V}} = \tilde{K}_2^{\mathrm{IV}} = \tilde{K}_2^{\mathrm{III}}. \tag{4.96}$$

When $B_l = O(\varepsilon^p), p > 3$, the macroscopic behaviour is also described by model V.

5. Conclusions

We have homogenized the problem of compressible fluid flow in a porous medium with interfacial flow barrier. An important conclusion drawn from this study is that the macroscopic description strongly depends upon the relative value of the interfacial conductance with respect to the permeabilities of the constituents. Thus, we have derived five distinct macroscopic models whose domains of validity are related to the value of B (Fig. 2).

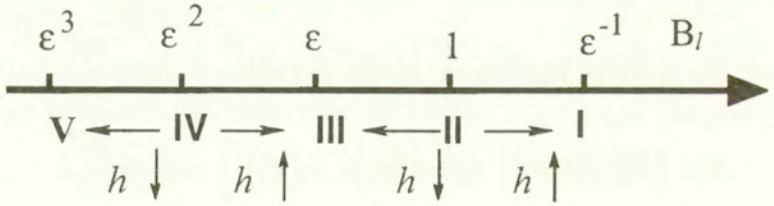

FIG. 2. The five macroscopic models and the corres-ponding orders of magnitude of B_l.

Models I, II and III are written in the form:

$$\nabla \cdot \left(\tilde{K}^{\alpha} p \nabla p \right) = < \phi > \frac{\partial p}{\partial t}, \qquad \alpha = \mathrm{I}, \mathrm{II}, \mathrm{III}. \tag{5.1}$$

They are single-pressure fields models, which means that the pressure field is constant over the REV. As a consequence, these models describe a state of local equilibrium. $\tilde{K}^{\mathrm{I}}$, $\tilde{K}^{\mathrm{II}}$ and $\tilde{K}^{\mathrm{III}}$ are three distinct effective permeabilities. $\tilde{K}^{\mathrm{I}}$ is

the effective permeability in the absence of interfacial barrier ($h = \infty$). $\tilde{K}^{\mathrm{II}}$ is h-dependent. $\tilde{K}^{\mathrm{III}}$ is different from $\tilde{K}^{\mathrm{I}}$ and $\tilde{K}^{\mathrm{II}}$, is independent of h and is such that $\tilde{K}^{\mathrm{III}} = \tilde{K}_1 + \tilde{K}_2$, where $\tilde{K}_1$ and $\tilde{K}_2$ are the effective permeabilities of both constituents.
Models IV and V are two- pressure field models, and as a consequence they describe a state of local non-equilibrium. Model IV is written as:

$$\nabla \cdot \left(\tilde{K}_1 p_1 \nabla p_1 \right) = \phi_1 \frac{\partial p_1}{\partial t} - \frac{H}{2} \left((p_1)^2 - ((p_2)^2 \right), \tag{5.2}$$

$$\nabla \cdot \left(\tilde{K}_2 p_2 \nabla p_2 \right) = \phi_2 \frac{\partial p_2}{\partial t} + \frac{H}{2} \left((p_1)^2 - ((p_2)^2 \right), \tag{5.3}$$

where H is the average of the interfacial barrier.
Model V is derived from model IV by taking $H = 0$.

Although these models are strongly non-linear, the effective permeabilities are the same as in the linear seepage problem. The fact that all boundary value problems reduce to linear boundary value problems is a remarkable feature. A few continuous passages between the models are possible (Fig. 2): by either increasing or decreasing h, Models I and III can be derived from Model II and Models III and V can be derived from Model IV.

An important issue to be addressed is the estimation of B_l with respect to ε. Since it is related to the knowledge of the microstructure, the value of B is well defined, whilst ε, as a measure of the separation of scales, depends in particular on the macroscopic characteristic length, which is either the sample size or related to the pressure gradient. As a consequence, if the macroscopic length is modified (e.g. by changing the pressure gradient), then the value of B_l remains the same but its measure in powers of ε may be changed. In the latter case, the macroscopic model itself is also modified. Therefore, the choice of the macroscopic model is conditioned by both the size of the sample and the pressure gradient.

Acknowledgements

J.L. AURIAULT wishes to thank Mobil Oil Technology Company for financial support via a research gift.

References

1. J.L AURIAULT, T. STRZELECKI, J. BAUER, S. HE, *Porous deformable media saturated by a very compressible fluid: Quasi-Statics*, Eur. J. Mech. A/Solids, **9**, (4), 373–392, 1990.
2. J.L. AURIAULT, H.I. ENE, *Macroscopic modelling of heat transfer in composites with interfacial thermal barrier*, Int. J. Heat Mass Transfer, **37** (18), 2885–2892, 1994.

3. J.N. PERNIN, *Homogénéisation en milieux composites*, Thèse de Doctorat d'Etat de l'Université de Franche-Comté, 1995.

4. J.L. AURIAULT, J. LEWANDOWSKA, *Modelling of pollutant migration in porous media with interfacial transfer: Local equilibrium /Non-Equilibrium*, Mechanics of Cohesive-Frictional Materials, **2**, 205–221, 1997.

5. A. BENSOUSSAN, J.l. LIONS, G. PAPANICOLAOU, *Asymptotic analysis for periodic structures*, North-Holland, Amsterdam 1978.

6. E. SANCHEZ-PALENCIA, *Non-homogeneous media and vibration theory*, Springer-Verlag, Lecture Notes in Physics 127, Berlin 1980.

7. J.L. AURIAULT, *Heterogeneous medium: Is an equivalent description possible?* Int. J. Engng. Sci., **29**, 785–795, 1981.

Received November 30, 1998; new version March 22, 1999.

Arch. Mech., **51**, 3–4, pp. 487–507, Warszawa 1999

Probability density equivalent linearization and non-linearization techniques

L. SOCHA

Institute of Transport, Silesian Technical University,
ul. Krasińskiego 8, 40–019 Katowice, POLAND

THE CONCEPT of equivalent linearization and non-linearization for dynamic systems under Gaussian excitations with criteria in probability density space is considered in this paper. The term non-linearization used in the literature means the procedure of finding an equivalent nonlinear system for stochastically excited Hamiltonian system. New criteria of linearization and non-linearization and two approximate approaches are proposed. In the first one, the direct minimization of a criterion is applied and the approximation of the probability density function by the truncated Gram-Charlier expansion is used. In the second approach, equivalent linearization or non-linearization is made for the Fokker-Planck equations corresponding to the original nonlinear and linearized or non-linearized dynamic systems, respectively. Two examples are given to illustrate the results obtained.

1. Introduction

EQUIVALENT LINEARIZATION was first proposed by CAUGHEY [3] who considered the replacement of a nonlinear oscillator by a linear one for which coefficients of linearization can be found from the mean square criterion. These coefficients depend on the first and second order moments of the response. Equivalent linearization has been developed in the field of control, mechanical and structural engineering, and has been generalized by many authors. Numerous studies have been performed in the context of this method, and they are summarized in the monograph by ROBERTS and SPANOS [11] and the review article by SOCHA and SOONG [12]. In almost all studies of different versions of stochastic linearization, the difference between variances of nonlinear and linearized systems has been taken as a measure of the accuracy of the considered version. The most important reason for considering only this measure is the fact that stochastic linearization is treated as one of the numerous approximate methods used in studies of vibration systems, where the well known and simple covariance analysis can be used. From theoretical point of view, the best linearization technique in the sense of previously discussed measure should be the "true linearization" proposed by KOZIN [7],

where the variances of the outputs of nonlinear and linearized systems are the same. In fact, this true linearization is not true with respect to other criteria, for instance, higher order moments, correlation functions or spectral densities of responses of nonlinear and linearized systems. The difference between the correlation functions and the spectral densities of responses of nonlinear and linearized systems as a measure of accuracy was considered, for instance, by KAZAKOV and DOSTUPOV [6] and by APETAUR and OPICKA [1], IYENGAR [5], respectively. The idea of equivalent linearization has been developed to the case when the original nonlinear system is replaced by another equivalent nonlinear system for which the exact probability density function of the stationary solution is known. Numerous studies have been performed in the context of this method, see, for instance, [4, 8, 14, 16], where mainly the mean-square criteria were used.

Since the complete information about random variable is contained in probability density function, it would be reasonable to consider a criterion depending on the difference between probability densities of responses of nonlinear and linearized or non-linearized systems. Therefore in this paper a new philosophy for stochastic equivalent linearization and non-linearization is proposed. We introduce new criteria of linearization and non-linearization and we discuss two approximate approaches. In the first one, the direct minimization of a criterion is applied and the approximation of the probability density function by the Gram-Charlier expansion is used. In the second approach, the linearization or non-linearization is made for the Fokker-Planck equations corresponding to the original nonlinear and linearized or non-linearized dynamic systems, respectively. The proposed approach is a generalization of the considerations given in [13]. The detailed analysis for two-dimensional systems is given to illustrate the results obtained. To compare characteristics of the responses obtained by the proposed methods and other equivalent linearization or non-linearization techniques, the examples with exactly known stationary probability density functions have been chosen.

2. Equivalent linearization

We consider a nonlinear stochastic model of dynamic system described by the Ito vector differential equation

$$d\mathbf{x}(t) = \mathbf{\Phi}(x,t)dt + \sum_{k=1}^{M} \mathbf{G}_k(t)d\xi_k(t), \tag{2.1}$$

where $\mathbf{x} = [x_1, \ldots, x_n]^T$ is vector state, $\mathbf{\Phi} = [\Phi_1, \ldots, \Phi_n]^T$ is a vector nonlinear function, $\mathbf{G}_k = [G_{k1}, \ldots, G_{kn}]^T$ are deterministic vectors, ξ_k are independent standard Wiener processes.

We assume that the unique solution of Eq. (2.1) exists and an equivalent linear system has the form

$$dx(t) = [\mathbf{A}(t)x(t) + \mathbf{C}(t)]dt + \sum_{k=1}^{M} \mathbf{G}_k(t)d\xi_k(t), \tag{2.2}$$

where $\mathbf{A} = [\mathbf{a}_{ij}]$ is a matrix and $\mathbf{C} = [C_1, \ldots, C_n]^T$ is a vector of linearization coefficients.

The objective of the probability density equivalent linearization is to find the elements a_{ij} and C_i which minimize the criterion

$$I_1 = \int_{-\infty}^{+\infty} w(\mathbf{x})\Psi(g_N(\mathbf{x}) - g_L(\mathbf{x}))d\mathbf{x}, \tag{2.3}$$

where Ψ is a convex function, $w(\mathbf{x})$ is a weight function, $g_N(\mathbf{x})$ and $g_L(\mathbf{x})$ are probability density functions of stationary solutions of nonlinear system (2.1) and linearized system (2.2), respectively. It means that the discussed equivalent linearization method is made for criteria in the space of probability densities. In the case of linearized system, the probability density of the solution of system (2.2) is known and can be expressed as follows:

$$g_L(x) = [(2\pi)^n |\mathbf{K}_L|]^{-1/2} \exp\left\{-\frac{1}{2}(\mathbf{x} - \mathbf{m})^T \mathbf{K}_L^{-1}(\mathbf{x} - \mathbf{m})\right\}, \tag{2.4}$$

where $\mathbf{m} = \mathbf{m}(t) = E[\mathbf{x}(t)]$ and $\mathbf{K}_L = \mathbf{K}_L(t) = E[\mathbf{x}(t)\mathbf{x}(t)^T] - \mathbf{m}(t)\mathbf{m}(t)^T$ are the mean value and the covariance matrix of the solution $\mathbf{x} = \mathbf{x}(t)$ of system (2.2), respectively, $|\mathbf{K}_L|$ denotes the determinant of the matrix $\mathbf{K}_L$. The vector $\mathbf{m}$ and matrix $\mathbf{K}_L$ satisfy the following equations:

$$\frac{d\mathbf{m}}{dt} = A(t)m + C(t), \tag{2.5}$$

$$\frac{d\mathbf{K}_L}{dt} = \mathbf{K}_L\mathbf{A}^T(t) + \mathbf{A}(t)\mathbf{K}_L + \sum_{k=1}^{M} \mathbf{G}_k(t)\mathbf{G}_k^T(t). \tag{2.6}$$

To apply the proposed criterion (2.3) we have to find the probability density $g_N(\mathbf{x})$. Unfortunately, except for some special cases, it is impossible to find the function $g_N(\mathbf{x})$ in analytical form. However, it can be done by approximation methods or by simulations.

To obtain approximate the probability density function of the stationary solution of a nonlinear dynamic system one can use for instance, the Gram-Charlier

expansion. For n-dimensional system the one-dimensional density has the following truncated form [10]

$$g_N(\mathbf{x}) = g_{GC}(\mathbf{x}) = g_G(\mathbf{x}) \left[1 + \sum_{k=3}^{N} \sum_{\sigma(\nu)=k} \frac{c_\nu H_\nu(\mathbf{x}-\mathbf{m})}{\nu_1!...\nu_n!} \right], \tag{2.7}$$

where $g_G(\mathbf{x})$ is the probability density of a vector Gaussian random variable $\mathbf{x} \in R^n$,

$$g_G(\mathbf{x}) = [(2\pi)^n |\mathbf{K}_G|]^{-1/2} \exp\left\{ -\frac{1}{2}(\mathbf{x}-\mathbf{m})^T \mathbf{K}_G^{-1}(\mathbf{x}-\mathbf{m}) \right\}, \tag{2.8}$$

$\mathbf{m}$ and $\mathbf{K}_G$ are the mean value and covariance matrix of vector variable $\mathbf{x}$, ν is the multi-index $\nu = [\nu_1, ..., \nu_n]^T$, $\sigma(\nu) = \sum_{i=1}^{n} \nu_i$, N is a number of elements in truncation series, $c_\nu = E[G_\nu(\mathbf{x}-\mathbf{m})]\nu_i$ are quasimoments. H_ν and G_ν are Hermite's polynomials defined by

$$H_m(x) = (-1)^{\sigma(m)} \exp\left\{ \frac{1}{2}\mathbf{x}^T \mathbf{K}^{-1}\mathbf{x} \right\} \frac{\partial^{\sigma(m)}}{\partial x_1^{m_1} \dots \partial x_N^{m_n}} \exp\left\{ -\frac{1}{2}\mathbf{x}^T \mathbf{K}^{-1}\mathbf{x} \right\}, \tag{2.9}$$

$$G_m(x) = (-1)^{\sigma(m)} \exp\left\{ \frac{1}{2}\mathbf{x}^T \mathbf{K}^{-1}\mathbf{x} \right\} \left[\frac{\partial^{\sigma(m)}}{\partial y_1^{m_1} \dots \partial y_N^{m_n}} \exp\left\{ -\frac{1}{2}\mathbf{y}^T \mathbf{K}^{-1}\mathbf{y} \right\} \right]_{\mathbf{y}=\mathbf{K}^{-1}\mathbf{x}} \tag{2.10}$$

where $\mathbf{K}$ is a real positive definite matrix.

To obtain quasimoments c_ν, first we must derive the moment equations for the system (2.1) which can be closed, for instance, by the cumulant closure technique, and next we use the algebraic relationships between quasimoments and moments.

3. Direct optimization method

Since the probability density of the linearized system $g_L(x)$ is a function of coefficients of linearization a_{ij} and C_i, therefore in the case when the function $\Psi(x)$ is differentiable, the necessary conditions of minimization one can find, for instance, from conditions

$$\frac{\partial I_1}{\partial a_{ij}} = 2 \int_{-\infty}^{+\infty} w(x) \frac{\partial \Psi(g_N, g_L)}{\partial g_L} \frac{\partial g_L(x)}{\partial a_{ij}} dx = 0, \tag{3.1}$$

$$\frac{\partial I_1}{\partial C_i} = 2 \int_{-\infty}^{+\infty} w(x) \frac{\partial \Psi(g_N, g_L)}{\partial g_L} \frac{\partial g_L(x)}{\partial C_i} dx = 0. \tag{3.2}$$

In this paper we consider both differentiable and non-differentiable functions, for instance if $w(x) = 1$ and $\Psi(x) = x^2$ then we have

$$I_2 = \int_{-\infty}^{+\infty} (g_N(\mathbf{x}) - g_L(\mathbf{x}))^2 d\mathbf{x}. \tag{3.3}$$

Another criterion with non-differentiable function we propose is

$$I_3 = \int_{-\infty}^{+\infty} |x|^{2l} |g_N(\mathbf{x}) - g_L(\mathbf{x})| d\mathbf{x}, \qquad l = 1, 2 \ldots \tag{3.4}$$

Since the criteria I_2 and I_3 are known in the mathematical literature of probabilistic metrics, as square metric and pseudo-moment metric, respectively [15], we propose to call the corresponding linearization techniques by square metric equivalent linearization and $2l$-order pseudo-moment equivalent linearization, respectively. The necessary conditions (3.1) and (3.2) for criterion (3.3) will be shown in details in Sec. 5 and 6.

4. The Fokker – Planck equation approach

When the probability density function of nonlinear system is unknown and for some reason the direct optimization technique can not be applied, we propose instead of the state equations (2.1) and (2.2) to consider the corresponding reduced Fokker-Planck equations

$$\frac{\partial g_N}{\partial t} = -\sum_{i=1}^{n} \frac{\partial}{\partial x_i} [\Phi_i(\mathbf{x}, t) g_N] + \frac{1}{2} \sum_{i=1}^{n} \sum_{j=1}^{n} \frac{\partial^2}{\partial x_i \partial x_j} [b_{ij} g_N] = 0 \tag{4.1}$$

and

$$\frac{\partial g_L}{\partial t} = -\sum_{i=1}^{n} \frac{\partial}{\partial x_i} \left[\left(A_i^T \mathbf{x} + C_i \right) g_L \right] + \frac{1}{2} \sum_{i=1}^{n} \sum_{j=1}^{n} \frac{\partial^2}{\partial x_i \partial x_j} [b_{ij} g_L] = 0, \tag{4.2}$$

where A_i^T is i-th row of matrix $\mathbf{A}$, $\mathbf{B} = [b_{ij}]$ is the diffusion matrix

$$b_{ij} = \sum_{k=1}^{M} G_{ki} G_{kj}. \tag{4.3}$$

If we denote $p_1 = g_N$, $p_{2i} = \dfrac{\partial g_N}{\partial x_i}$ and $q_1 = g_L$, $q_{2i} = \dfrac{\partial g_L}{\partial x_i}$ then the Eqs. (4.1) and (4.2) can be transformed to the following two-dimensional vector systems:

$$\frac{\partial p_1}{\partial x_i} = p_{2i}$$

$$\sum_{i=1}^{n}\left[\frac{\partial \mathbf{\Phi}}{\partial x_i}p_1 + \Phi_i p_{2i}\right] - \frac{1}{2}\sum_{i=1}^{n}\sum_{j=1}^{n}\left[\frac{\partial^2 b_{ij}}{\partial x_i \partial x_j}p_1 + \frac{\partial b_{ij}}{\partial x_j}p_{2i} + \frac{\partial b_{ij}}{\partial x_i}p_{2j} + b_{ij}\frac{\partial p_{2j}}{\partial x_i}\right] = 0, \tag{4.4}$$

$$\frac{\partial q_1}{\partial x_i} = q_{2i},$$

$$\sum_{i=1}^{n}\left[a_{ii}q_1 + A_i^T x q_{2i}\right] - \frac{1}{2}\sum_{i=1}^{n}\sum_{j=1}^{n}\left[\frac{\partial^2 b_{ij}}{\partial x_i \partial x_j}q_1 + \frac{\partial b_{ij}}{\partial x_j}q_{2i} + \frac{\partial b_{ij}}{\partial x_i}q_{2j} + b_{ij}\frac{\partial q_{2j}}{\partial x_i}\right] = 0. \tag{4.5}$$

Comparing the system Eqs. (4.4) with (4.5) we find that g_N and $\dfrac{\partial g_N}{\partial x_i}$ will be approximated by g_L and $\dfrac{\partial g_L}{\partial x_i}$ respectively, when the error ε defined by

$$\varepsilon = \sum_{i=1}^{n}\frac{\partial}{\partial x_i}\left[(\Phi_i - \mathbf{A}_i^T\mathbf{x} - C_i)g_L\right] \tag{4.6}$$

will be minimal "in some sense" for all x. We note that $g_L(x)$ is the probability density of linearized system and depends on the parameters of linearized system i.e. on a_{ij} and C_i. Since $\varepsilon = \varepsilon(x)$ is a function of x, the criterion I_4 and the necessary conditions of minimum can be proposed, for instance, as follows:

$$I_4 = \int_{-\infty}^{+\infty}\varepsilon^2(\mathbf{x})d\mathbf{x}, \tag{4.7}$$

$$\frac{\partial I_4}{\partial a_{ij}} = 0, \qquad \frac{\partial I_4}{\partial C_i} = 0. \tag{4.8}$$

5. Application to a nonlinear oscillator

Consider a nonlinear oscillator described by

$$\begin{aligned} dx_1 &= x_2 dt, \\ dx_2 &= [-2hx_2 - f(x_1)]dt + gd\xi, \end{aligned} \tag{5.1}$$

where h and q are constant parameters, $f(x_1)$ is a nonlinear function such that $f(0) = 0$, ξ is a standard Wiener process, and an equivalent linearized oscillator

$$\begin{aligned} dx_1 &= x_2 dt, \\ dx_2 &= [-2hx_2 - k_1 x_1]dt + qd\xi, \end{aligned} \tag{5.2}$$

where k_1 is a linearization coefficient.

First we show the application of criterion I_2. In that case the probability densities of stationary solutions of nonlinear and linearized oscillators are known and have the form

$$g_N(x) = \frac{1}{C_N} \exp\left\{ -\frac{4h}{q^2} \left(\int_0^{x_1} f(s)ds + \frac{x_2^2}{2} \right) \right\}, \tag{5.3}$$

$$g_L(x_1, x_2, k_1) = \frac{1}{C_L} \frac{4h\sqrt{k_1}}{q^2} \exp\left\{ -\frac{2h}{q^2} \left(k_1 x_1^2 + x_2^2 \right) \right\}, \tag{5.4}$$

where C_N and C_L are normalized constants.

Since in this case $E[x_1] = E[x_2] = 0$, the application of the Gram-Charlier expansion leads to the following formula of approximate probability density function:

$$g_N(x) = g_{GC}(x) = g_G(x) \left[1 + \sum_{k=3}^{N} \sum_{\sigma(\nu)=k} \frac{c_{\nu_1\nu_2} H_{\nu_1\nu_2}(x)}{\nu_1!\nu_2!} \right] \tag{5.5}$$

where

$$g_G(x) = \frac{1}{2\pi\sqrt{k_{11}k_{22} - k_{12}^2}} \exp\left\{ -\frac{k_{11}(x_2)^2 - 2k_{12}x_1x_2 + k_{22}(x_1)^2}{2(k_{11}k_{22} - k_{12}^2)} \right\}, \tag{5.6}$$

$c_{\nu_1\nu_2} = E[G_{\nu_1\nu_2}(\mathbf{x})]$ are quasimoments, $\nu_1, \nu_2 = 0, 1, ..., N$, $\nu_1 + \nu_2 = 3, 4, \ldots, N$, $H_{\nu_1\nu_2}(x)$ and $G_{\nu_1\nu_2}(x)$ are Hermite's polynomials defined by

$$H_{pr}(x_1,x_2)=(-1)^{p+r}\exp\left\{\frac{1}{2}\left(q_{11}x_1^2+2q_{12}x_1x_2+q_{22}x_2^2\right)\right\} \tag{5.7}$$

$$\times\frac{\partial^{p+r}}{\partial x_1^p\partial x_2^r}\exp\left\{-\frac{1}{2}\left(q_{11}x_1^2+2q_{12}x_1x_2+q_{22}x_2^2\right)\right\},$$

$$G_{pr}(x_1,x_2)=(-1)^{p+r}\exp\left\{\frac{1}{2}\left(q_{11}x_1^2+2q_{12}x_1x_2+q_{22}x_2^2\right)\right\} \tag{5.8}$$

$$\times\left[\frac{\partial^{p+r}}{\partial y_1^p\partial y_2^r}\exp\left\{-\frac{1}{2}\left(k_{11}y_1^2+2k_{12}y_1y_2+k_{22}y_2^2\right)\right\}\right]_{y=Qx},$$

where

$$\mathbf{K}=\begin{bmatrix}k_{11} & k_{12}\\ k_{21} & k_{22}\end{bmatrix},\qquad \mathbf{K}^{-1}=Q=\begin{bmatrix}q_{11} & q_{12}\\ q_{21} & q_{22}\end{bmatrix}, \tag{5.9}$$

$$k_{ij}=E[x_ix_j],\qquad i,j=1,2.$$

In the case of stationary probability density function the corresponding moments are as follows:

$$k_{12}=0,\qquad k_{22}=\frac{1}{q_{22}},\qquad q_{12}=0,\qquad k_{11}=\frac{1}{q_{11}}. \tag{5.10}$$

The second moment k_{11}, the quasimoments $c_{\nu_1\nu_2}$ and two-dimensional Hermite's polynomials $H_{\nu_1\nu_2}(x_1,x_2)$ and $G_{\nu_1\nu_2}(x_1,x_2)$ are presented in the Appendix. The moment k_{11} has to be found from moment equations. The necessary condition of minimum of I_2 defined by (3.3) takes the form

$$\frac{\partial I_2}{\partial k_1}=2\int\limits_{-\infty}^{+\infty}\int\limits_{-\infty}^{+\infty}(g_N(x)-g_L(x))\left(\frac{1}{2k_1}-2h\frac{x_1^2}{q^2}\right)g_L(x)dx_1dx_2=0. \tag{5.11}$$

In the case of pseudo-moment equivalent linearization, the linearization coefficient we find by minimization of the following criterion:

$$I_3=\int\limits_{-\infty}^{+\infty}\int\limits_{-\infty}^{+\infty}x_1^{2l}|g_N(x_1,x_2)-g_L(x_1,x_2,k_1)|dx_1dx_2,\qquad l=1,3. \tag{5.12}$$

The linearization coefficient k_1 can be calculated numerically in two considered cases from equality (3.3) and directly from (3.4).

Next we consider the application of the Fokker-Planck equation approach to the system (5.1) – (5.2). In that case the transformed Fokker-Planck Eqs. (4.4)

– (4.5) are as follows: for nonlinear system

$$\begin{aligned} \frac{\partial p_1}{\partial x_2} &= p_2, \\ \frac{\partial p_2}{\partial x_2} &= -\frac{2}{q^2}\frac{\partial}{\partial x_2}\left[(2hx_2 + f(x_1))p_1\right] + \frac{2x_2}{q^2}\frac{\partial p_1}{\partial x_1}; \end{aligned} \tag{5.13}$$

for linearized system

$$\begin{aligned} \frac{\partial q_1}{\partial x_2} &= q_2, \\ \frac{\partial q_2}{\partial x_2} &= -\frac{2}{q^2}\frac{\partial}{\partial x_2}\left[(2hx_2 + k_1x_1)q_1\right] + \frac{2x_2}{q^2}\frac{\partial q_1}{\partial x_1}. \end{aligned} \tag{5.14}$$

Then the following criterion is proposed

$$I_4 = \int_{-\infty}^{+\infty}\int_{-\infty}^{+\infty}\left\{\frac{\partial}{\partial x_2}\left[(f(x_1) - k_1x_1)g_L(x_1, x_2, k_1)\right]\right\}^2 dx_1dx_2, \tag{5.15}$$

where g_L is defined by (5.4).

The necessary condition of minimum of criterion (5.15) is the following:

$$\begin{aligned} \frac{\partial I_4}{\partial k_1} = 2\int_{-\infty}^{+\infty}\Bigg\{&\frac{\partial}{\partial x_2}\left[(f(x_1) - k_1x_1)g_L(x_1, x_2, k_1)\right] \\ &\left[f(x_1)\frac{\partial}{\partial k_1}\left(\frac{\partial}{\partial x_2}g_L(x_1, x_2, k_1)\right) - x_1\frac{\partial}{\partial x_2}g_L(x_1, x_2, k_1)\right. \\ &\left.-kx_1\frac{\partial}{\partial k_1}\left(\frac{\partial}{\partial x_2}g_L(x_1, x_2, k_1\right)\right]\Bigg\}dx_1dx_2 = 0 \end{aligned} \tag{5.16}$$

where

$$\begin{aligned} \frac{\partial g_L}{\partial x_2} &= -\frac{4hx_2}{q^2}g_L(x_1, x_2, k_1), \\ \frac{\partial}{\partial k_1}\left(\frac{\partial g_L}{\partial x_2}\right) &= \left[-\frac{1}{2k_1} + \frac{2hx_1^2}{q^2}\right]\frac{4hx_2}{q^2}g_L(x_1, x_2, k_1). \end{aligned} \tag{5.17}$$

EXAMPLE 1.

Consider a nonlinear Duffing oscillator excited by a stationary white noise described by Eq. (5.1) for

$$f(x_1) = \omega_0^2 x_1 + \varepsilon x_1^3, \tag{5.18}$$

where ω_0^2 and ε are constant parameters.

The probability density of stationary solution of the system (5.1) with conditions (5.18) has the form

$$g_N(x) = \frac{1}{C_N} \exp\left\{-\frac{2h}{q^2}\left(\omega_0^2 x_1^2 + \varepsilon\frac{x_1^4}{2} + x_2^2\right)\right\}, \tag{5.19}$$

where C_N is a normalized constant.

To apply the approximate probability density function we use formula (5.5) for $N = 6$ and $m = 0$. The second moment k_{11}, the quasimoments $c_{\nu_1\nu_2}$ and two-dimensional Hermite's polynomials $H_{\nu_1\nu_2}(x_1, x_2)$ and $G_{\nu_1\nu_2}(x_1, x_2)$ are presented in the Appendix.

The application of criterion I_2 leads to equality (5.11) with $g_N(x)$ and $g_L(x)$ given by (5.19) and (5.4), respectively, i.e.

$$\begin{aligned}\frac{\partial I_2}{\partial k_1} = 2\int_{-\infty}^{+\infty}\Bigg[&\frac{1}{C_N}\exp\left\{-\frac{2h}{q^2}\left(\omega_0^2 x_1^2 + \varepsilon\frac{x_1^4}{2} + x_2^2\right)\right\} \\ &- \frac{1}{C_L}\frac{4h\sqrt{k_1}}{q^2}\exp\left\{-\frac{2h}{q^2}\left(k_1 x_1^2 + x_2^2\right)\right\}\Bigg] \\ &\times\left(\frac{1}{2k_1} - \frac{2hx_1^2}{q^2}\right)\frac{1}{C_L}\frac{4h\sqrt{k_1}}{q^2}\exp\left\{-\frac{2h}{q^2}\left(k_1 x_1^2 + x_2^2\right)\right\} dx_1 dx_2 = 0.\end{aligned} \tag{5.20}$$

In the case of pseudo-moment equivalent linearization, we find the linearization coefficient by minimization of the following criterion:

$$I_3 = \int_{-\infty}^{+\infty} (x_1)^{2l} |g_N(x_1, x_2) - g_L(x_1, x_2, k_1)| dx_1 dx_2, \qquad l = 1, 3. \tag{5.21}$$

The linearization coefficient k_1 can be calculated numerically in two considered cases from equality (5.20) and directly from (5.21). The application of criterion I_4 leads to equality (5.16) with conditions (5.17) and with $f(x)$ given by (5.18), i.e.

$$(5.22)\qquad \int_{-\infty}^{+\infty} \left[(\omega_0^2 - k_1)x_1 + \varepsilon x_1^3\right]^2 \left(\frac{1}{2k_1} - \frac{2hx_1^2}{q^2}\right) x_2^2 g_L^2(x_1, x_2, k_1)\,dx_1\,dx_2$$

$$- \int_{-\infty}^{+\infty}\int_{-\infty}^{+\infty} \left[(\omega_0^2 - k_1)x_1 + \varepsilon x_1^3\right] x_2^2 x_1 g_L^2(x_1, x_2, k_1)\,dx_1\,dx_2 = 0.$$

Using the properties of Gaussian process we calculate from Eq. (5.22) the integrals and we show (see Appendix) that the linearization coefficient k_1 satisfies the following algebraic equation:

$$(5.23)\qquad 192h^2k_1^4 - 128\omega_0^2h^2k_1^3 - 64\omega_0^2h^2k_1^2 + 48\varepsilon hq^2k_1$$

$$-144\varepsilon hq^2\omega_0^2k_1 - 75\varepsilon^2q^4 = 0.$$

To illustrate all the methods discussed we compare stationary mean-square displacements of linearized systems (for different linearization coefficients) obtained by applying the exact and the approximate (by the Gram-Charlier expansion) probability density functions of the Duffing oscillator, and by applying the Fokker-Planck equation approach. The numerical results for parameters $\omega_0^2 = 1.85$, $\varepsilon = 1.85 \times i$, $i = 1, \ldots, 10$, $q^2 = 0.2$, $h = 0.05$ are presented in Fig. 1.

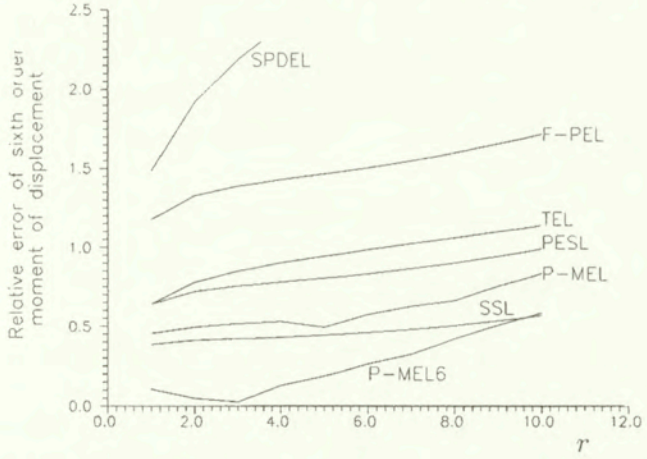

FIG. 1. a) Comparison of the relative errors of the displacement variance $E[x_1^2]$ versus the ratio of parameters $r = \varepsilon/\omega_0^2$ for $\omega_0^2 = 1.85$, $\varepsilon = 1.85 \times i$, $i = 1, \ldots, 10$ and $q^2 = 0.2$, $h = 0.05$ with notations: standard statistical linearization (SSL), potential energy statistical linearization (PESL), Fokker-Planck equation linearization (F-PEL), second order pseudo-moment equivalent linearization (P-MEL2), sixth order pseudo-moment equivalent linearization (P-MEL6), square metric probability density equivalent linearization (SPDEL).

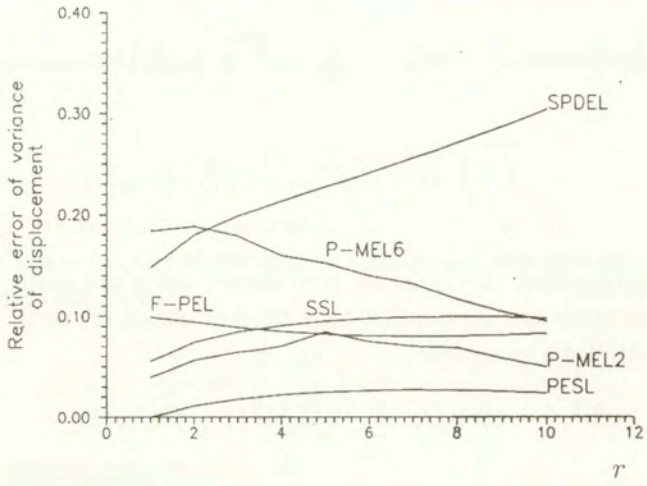

FIG. 1. b) Comparison of the relative errors of the sixth order moments of the displacement $E[x_1^6]$ versus the ratio of parameters $r = \varepsilon/\omega_0^2$ for $\omega_0^2 = 1.85$, $\varepsilon = 1.85 \times i$, $i = 1, \ldots, 10$ and $q^2 = 0.2$, $h = 0.05$ with notations: standard statistical linearization (SSL), potential energy statistical linearization (PESL), true equivalent linearization (TEL), Fokker-Planck equation linearization (F-PEL), second order pseudo-moment equivalent linearization (P-MEL2), sixth order pseudo-moment equivalent linearization (P-MEL6), square metric probability density equivalent linearization (SPDEL).

Figures 1a and 1b show that for the second order moments of the displacement, the relative error obtained by (TEL) is equal to zero and the errors obtained by (PESL) and (P-MEL2) are almost zero while the errors obtained by the other methods are significantly greater. The opposite situation is observed for sixth order moments of the displacement.

6. Equivalent non-linearization

As it was mentioned in the Introduction, the idea of finding an equivalent model for a nonlinear system has not been limited to a linear model. It has been extended to the case when the original nonlinear system is replaced by another equivalent nonlinear system for which the probability density of the exact stationary solution is known (see, for instance, [4, 8, 9, 14, 16]), and mainly the mean-square criterion was used. In all these approaches the most important role is played by the moments of response. In this paper a new philosophy for equivalent non-linearization is proposed. Instead of moment equations of responses of original nonlinear and non-linearized systems, the corresponding probability density functions are considered. The detailed discussion is given for a nonlinear oscillator described by the Ito vector differential equation

$$
\begin{aligned}
dx_1 &= x_2 dt, \\
dx_2 &= [-f(x_1, x_2) - g(x_1]dt + q d\xi(t),
\end{aligned}
\tag{6.1}
$$

where $f(.,.)$ and $g(.)$ are known nonlinear functions, $\xi(t)$ is a standard Wiener process, q is a parameter intensity of noise. An equivalent nonlinear system is proposed in the form

$$
\begin{aligned}
dx_1 &= x_2 dt, \\
dx_2 &= [-f_E(H)x_2 - g(x_1)]dt + q dw(t),
\end{aligned}
\tag{6.2}
$$

where H is the Hamiltonian

$$
H = \frac{1}{2}x_2^2 + \int_0^{x_1} g(s)ds, \tag{6.3}
$$

f_E is a nonlinear function.

For further consideration we assume that the integral $\int_0^H f_E(s)ds$ has the polynomial form, i.e.

$$
\int_0^H f_E(s)ds = \sum_{i=0}^{N_2} \alpha_i H^i \tag{6.4}
$$

where α_i are non-linearization coefficients. They have to be determined from a proposed criterion, for instance

$$
I = \int_{-\infty}^{+\infty}\int_{-\infty}^{+\infty} \left[f(x_1, x_2) - \left(\sum_{i=1}^{N_2} \alpha_i H^i \right) x_2 \right] \rho(x_1, x_2) dx_1 dx_2 \tag{6.5}
$$

where $\rho(x_1, x_2)$ is a weight function. Taking this function in a particular form we obtain the earlier literature results. For instance, in one of the best approximations obtained by POLIDORI and BECK [9], the weight function is given by

$$
\rho(x_1, x_2) = g_{\text{Lin}}(x_1, x_2) = \frac{1}{2\pi\sigma_{x_1}\sigma_{x_2}} \exp\left\{ -\frac{x_1^2}{2\sigma_{x_1}^2} - \frac{x_2^2}{2\sigma_{x_2}^2} \right\}, \tag{6.6}
$$

where $\sigma_{x_1}^2$ and $\sigma_{x_2}^2$ are constant parameters. As for the case of equivalent linearization, new criteria of non-linearization and two approximate approaches are proposed. In the first one the direct minimization of a criterion is applied and the approximation of the probability density function of the stationary solution of Eq. (6.1) by the Gram-Charlier expansion is proposed.

The probability density of a stationary solution of Eq. (6.2) is known exactly and has the form

$$g_{EN}(x) = \frac{1}{C_N} \exp\left\{ -\frac{2}{q^2} \int_0^H f_E(s)ds \right\}. \tag{6.7}$$

where C_N is a normalized constant.

As in the case of equivalent linearization, we consider two particular cases of modified criterion (2.3) for both differentiable and non-differentiable functions $\Psi(x)$ and $w(x)$, namely

$$I_2 = \int_{-\infty}^{+\infty} (g_N(x) - g_{EN}(x))^2 dx, \tag{6.8}$$

$$I_3 = = \int_{-\infty}^{+\infty} |x|^{2l} |g_N(x) - g_{EN}(x)| dx, \quad l = 1, 2 \ldots \tag{6.9}$$

Also, when for some reason the direct optimization technique can not be applied we propose, instead of state Eqs. (6.1) and (6.2), to consider the corresponding reduced Fokker-Planck equations in vector form

$$\begin{aligned} \frac{\partial p_1}{\partial x_2} &= p_2, \\ \frac{\partial p_2}{\partial x_2} &= -\frac{2}{q^2} \frac{\partial}{\partial x_2} [(-f(x_1, x_2) - g(x_1))p_1] + \frac{2x_2}{q^2} \frac{\partial p_1}{\partial x_1}, \end{aligned} \tag{6.10}$$

$$\begin{aligned} \frac{\partial q_1}{\partial x_2} &= q_2, \\ \frac{\partial q_2}{\partial x_2} &= -\frac{2}{q^2} \frac{\partial}{\partial x_2} [(-f_E(H)x_2 - g(x_1)q_1] + \frac{2x_2}{q^2} \frac{\partial q_1}{\partial x_1}, \end{aligned} \tag{6.11}$$

where $p_1 = p_1(x_1, x_2) = g_N(x_1, x_2)$, $q_1 = q_1(x_1, x_2) = g_{EN}(x_1, x_2)$.

Comparing the system Eqs. (6.10) with (6.11) we find that g_N and $\partial g_N / \partial x_i$ will be approximated by g_{EN} and $\partial g_{EN} / \partial x_i$ respectively, when the error ε defined by

$$\varepsilon = \frac{\partial}{\partial x_2} [(-f(x_1, x_2) + f_E(H)x_2)g_{EN}] \tag{6.12}$$

will be minimal " in some sense" for all x. We note that $g_{EN}(x)$ is the probability density of non-linearized system and depends on parameters of non-linearized

system i.e. on α_i. Since $\varepsilon = \varepsilon(x)$ is a function of x, the criterium I_{FP} and the necessary conditions of minimum can be proposed, for instance, as follows:

$$I_{FP} = \int_{-\infty}^{+\infty} \varepsilon^2(x)dx, \tag{6.13}$$

$$\frac{\partial I_{FP}}{\partial \alpha_i} = 0, \qquad i = 1, 2, \ldots, N_2. \tag{6.14}$$

EXAMPLE 2.

We consider a nonlinearly damped Duffing oscillator excited by the white noise previously studied in the literature

$$\begin{aligned} dx_1 &= x_2 dt, \\ dx_2 &= \left[-\beta x_2 - \alpha x_2^2 - \gamma x_1 - \varepsilon x_1^3\right] dt + q d\xi(t). \end{aligned} \tag{6.15}$$

The equivalent nonlinear system is proposed in the form

$$\begin{aligned} dx_1 &= x_2 dt, \\ dx_2 &= \left[-f_E(H) x_2 - \gamma x_1 - \varepsilon x_1^3\right] dt + q d\xi(t). \end{aligned} \tag{6.16}$$

where H is the Hamiltonian

$$H = \frac{1}{2}x_2^2 + \gamma\frac{x_1^2}{2} + \varepsilon\frac{x_1^4}{4}. \tag{6.17}$$

The exact probability density of stationary solution of Eq. (6.16) is given by

$$g_{EN}(x) = \frac{1}{C_N} \exp\left\{-\frac{2}{q^2}\int_0^H f_E(s)ds\right\}. \tag{6.18}$$

However, the function f_E is unknown. We seek an approximation of the form

$$f_E(H) = b_0 + b_1 H. \tag{6.19}$$

Then the approximate probability density function is given by

$$g_{EN}(x) = \frac{1}{C_N} \exp\left\{-\frac{2}{q^2}\left(b_0 H + \frac{b_1}{2}H^2\right)\right\}, \tag{6.20}$$

In the case of the Fokker-Planck approach, the following criterion is proposed:

$$I_{FP} = \int_{-\infty}^{+\infty}\int_{-\infty}^{+\infty} \Big[\frac{\partial}{\partial x_2}\big[(-\beta x_2 - \alpha x_2^3 + b_0 x_2 + b_1 H x_2) g_{EN}(x_1, x_2, h_0, h_1)\big]\Big]^2 dx_1 dx_2. \tag{6.21}$$

To illustrate all the methods discussed we compare stationary mean-square displacements of non-linearized systems versus parameters ε and α, using the approximation of probability density function in the form of the Gram-Charlier expansion (for $N = 6$) and also by applying the Fokker-Planck equation approach. Since in this case exact response characteristics does not exist, the comparison is given for simulations. The numerical results for parameters $\alpha = 0.5$, $\beta = 0.1$, $\gamma = 1$, $q^2 = 2\pi$ are presented in Fig. 2.

Figures 2a and 2b show that for the second order moments of the displacement there are no significant differences between the methods proposed in this paper and the best techniques known from the literature.

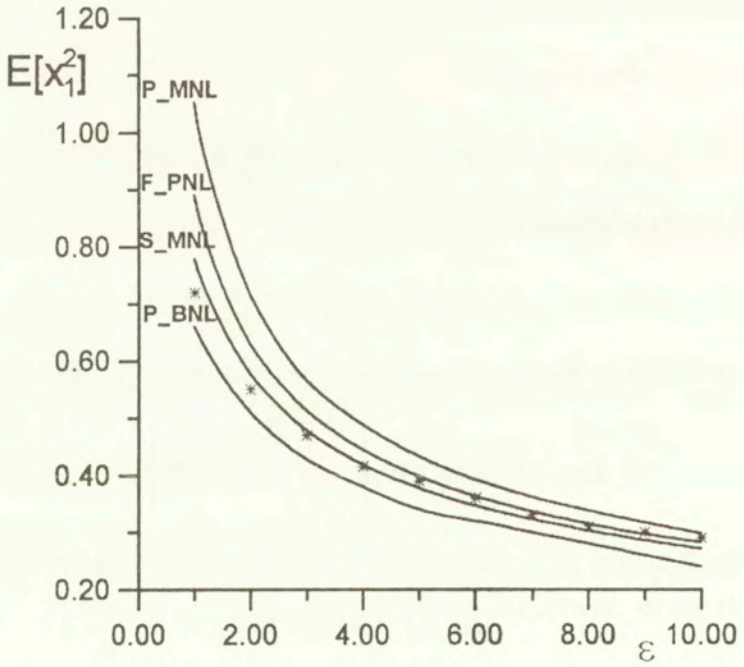

FIG. 2. a) Mean-square displacement variance $E[x_1^2]$ versus parameter ε for $\alpha = 0.5$, $q^2 = 2\pi$, $\beta = 0.1$, $\gamma = 1$ with notations: Polidori-Beck non-linearization (P-BNL), Fokker-Planck equation non-linearization (F-PNL), pseudo-moment metric equivalent non-linearization (P-MNL), square metric equivalent non-linearization (S-MNL), simulations (stars).

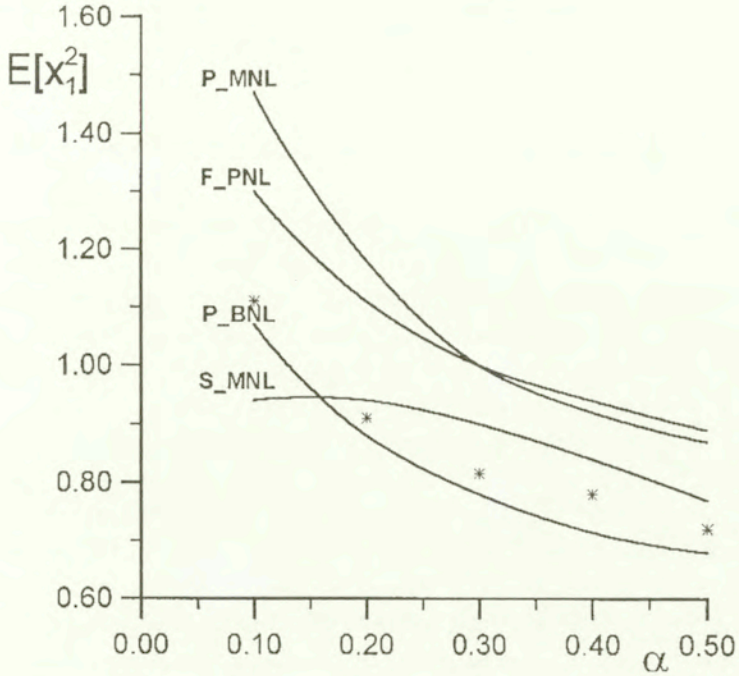

FIG. 2b) Mean-square displacement variance $E[x_1^2]$ versus parameter α for $\varepsilon = 1$, $q^2 = 2\pi$, $\beta = 0.1$, $\gamma = 1$ with notations: Polidori-Beck non-linearization (P-BNL), Fokker-Planck equation non-linearization (F-PNL), pseudo-moment metric equivalent non-linearization (P-MNL), square metric equivalent non-linearization (S-MNL), simulations (stars).

7. Conclusions and generalizations

The probability density equivalent linearization and non-linearization techniques applied to dynamic systems subjected to external Gaussian excitations have been considered. Two different approaches: direct optimization method and Fokker-Planck equation method have been examined on two examples of nonlinear oscillators. It has been shown in Example 1, that although some stochastic linearization techniques such as (PESL), (TEL) and (P-MEL2) approximate very well the mean-square error of the response, they fail in the case of higher order moments. In contrast to them, (F-PEL) and (P-MEL6) methods are more accurate for higher order moments than for the second order. It means that some of the proposed probability density equivalent linearization techniques are more accurate for second order moments of the response while the other – for higher order moments. Here it should be stressed that the standard statistical linearization technique which was criticized by many authors because it did not approximate well the second order moment of the response, is in fact "not so bad". In both

comparisons (second and sixth order moments of the response) the results are "in the middle". It means that the (SSL) method can be treated as a kind of compromise between methods which approximate very well the second order and higher order moments. In contrast to the SSL method, the relative error obtained by the SPDL method was significantly greater for second and higher order moments of the response.

In the case of equivalent non-linearization, from numerical results it follows that for the second order moments of the displacement there are no significant differences between the methods proposed in this paper and the best techniques known from the literature. However, it should be stressed that the comparison was given for the second order moments while the criteria proposed in this paper were given in the space of probability density functions.

We note that, similarly to the generalization obtained for standard equivalent linearization and non-linearization techniques, several new approaches of probability density equivalent linearization and non-linearization methods can be considered. It includes the cases of criteria depending on the probability density of energy of the response and linearization of stochastic dynamic systems under parametric excitations. Also other probabilistic measures (metrics) discussed in mathematical literature [15] can be analyzed. Another generalization can be done with application of the idea of equivalent systems derived by CAI and LIN [2].

Acknowledgments

This study is supported in part by State Committee of Scientific Research in Poland under Grant No 7 TO7A 074 08. Computer programming assistance given by M.Sc. M.Pawleta is gratefully acknowledged.

Appendix

1. The second moment k_{11}, the quasimoments $c_{\nu_1\nu_2}$ and two-dimensional Hermite's polynomials $H_{\nu_1\nu_2}(x_1, x_2)$:

$$\text{(A.1)} \qquad k_{11} = E[x_1^2], \quad c_{\nu_1\nu_2} = 0 \quad \text{for} \quad \nu_1 + \nu_2 = 3, 5,$$

$$c_{40} = E[x_1^4] - 3k_{11}^2, \quad c_{31} = E[x_1^3 x_2] = 0, \quad c_{22} = E[x_1^2 x_2^2] - k_{22}k_{11},$$

$$c_{13} = E[x_1 x_2^3], \quad c_{04} = E[x_2^4] - 3k_{22}^2,$$

$$c_{60} = E[x_1^6] - 15k_{11}E[x_1^4] + 30k_{11}^3,$$

$$c_{51} = E[x_1^5 x_2] = 0,$$

$$c_{42} = E[x_1^4 x_2^2] - k_{22}E[x_1^4] + 6k_{11}^2 k_{22} - 6k_{11}E[x_1^2 x_2^2],$$

$$c_{33} = E[x_1^3 x_2^3] - 3k_{11}E[x_1 x_2^3],$$

$$c_{24} = E[x_1^2 x_2^4] - k_{11}E[x_2^4] - 6k_{22}E[x_1^2 x_2^2] + 6k_{11}k_{22}^2,$$

$$c_{15} = E[x_1 x_2^5] - 10k_{22}E[x_1 x_2^3], \quad c_{06} = E[x_2^6] - 15k_{22}E[x_2^4] + 30k_{22}^3,$$

(A.2)
$$H_{40}(x_1, x_2) = q_{11}^4 x_1^4 - 6q_{11}^3 x_1^2 + 3q_{11}^2,$$

$$H_{31}(x_1, x_2) = q_{11}^3 q_{22} x_1^3 x_2 - 3q_{11}^2 q_{22} x_1 x_2,$$

$$H_{22}(x_1, x_2) = q_{11}^2 q_{22}^2 x_1^2 x_2^2 - q_{11}^2 q_{22} x_1^2 - q_{11} q_{22}^2 x_2^2 + q_{11} q_{22},$$

$$H_{13}(x_1, x_2) = q_{11} q_{22}^3 x_1 x_2^3 - 3q_{22}^2 q_{11} x_1 x_2^2,$$

$$H_{04}(x_1, x_2) = q_{22}^4 x_2^4 - 6q_{22}^3 x_2^2 + 3q_{22}^2,$$

$$H_{60}(x_1, x_2) = q_{11}^6 x_1^6 - 15q_{11}^5 x_1^4 + 45q_{11}^4 x_1^2 - 15q_{11}^3,$$

$$H_{51}(x_1, x_2) = q_{11}^5 q_{22} x_1^5 x_2 - 10q_{11}^4 q_{22} x_1^3 x_2 + 15q_{11}^3 q_{22} x_1 x_2,$$

$$H_{42}(x_1, x_2) = q_{11}^4 q_{22} x_1^4 (q_{22} x_2^2 - 1) + 6q_{11}^3 q_{22} x_1^2 (1 - q_{22} x_2^2) + 3q_{11}^2 q_{22}(q_{22} x_2^2 - 1),$$

$$H_{33}(x_1, x_2) = q_{11}^3 q_{22}^3 x_1^3 x_2^3 + 9q_{11}^2 q_{22}^2 x_1 x_2 - 3q_{11}^2 q_{22}^2 x_1^3 x_2 - 3q_{11}^2 q_{22}^3 x_1 x_2^3,$$

$$H_{24}(x_1, x_2) = q_{11} q_{22}^4 x_2^4 (q_{11} x_1^2 - 1) + 6q_{11} q_{22}^3 x_2^2 (1 - q_{11} x_1^2) + 3q_{11} q_{22}^2 (q_{11} x_1^2 - 1),$$

$$H_{15}(x_1, x_2) = q_{11} q_{22}^5 x_1 x_2^5 - 10q_{11} q_{22}^4 x_1 x_2^3 + 15q_{11} q_{22}^3 x_1 x_2,$$

$$H_{06}(x_1, x_2) = q_{22}^6 x_2^6 - 15q_{22}^5 x_2^4 + 45q_{22}^4 x_2^2 - 15q_{22}^3.$$

2. Derivation of Eq. (5.23)

We introduce the notation

$$\alpha_2 = \frac{4hk}{q^2}, \qquad c_{L_2} = \frac{16h^2}{c_L^2 q^4}, \qquad g_L^2(x_1, x_2, k) = c_{L_2} k_1 \exp(-\alpha_2 x^2),$$

(A.3)
$$I_{L_2} = \sqrt{\frac{\pi}{\alpha_2}} \int_{-\infty}^{+\infty} c_{L_2} x_2^2 \exp\left\{-\frac{4h}{q^2} x_2^2\right\} dx_2.$$

Using the properties

$$\int_{-\infty}^{+\infty} x^{2p} \exp(-\alpha x^2) dx = \sqrt{\frac{\pi}{\alpha}} \frac{(2p-1)!!}{(2\alpha)^p}, \tag{A.4}$$

we calculate the integrals appearing in Eq. (5.22)

$$\int_{-\infty}^{+\infty}\int_{-\infty}^{+\infty} \left[(\omega_0^2 - k_1)x_1 + \varepsilon x_1^3\right]^2 \left(\frac{1}{2k_1} - \frac{2hx_1^2}{q^2}\right) x_2^2 g_L^2(x_1, x_2, k_1) dx_1 dx_2 \tag{A.5}$$

$$= I_{L_2}\left[-\frac{2hk_1\varepsilon^2}{q^2}\frac{105}{16\alpha_2^4} + \left(\frac{\varepsilon^2}{2} - \frac{4hk_1\varepsilon(\omega_0^2 - k_1)}{q^2}\right)\frac{15}{8\alpha_2^3}\right.$$

$$\left. + \left(\varepsilon(\omega_0^2 - k_1) - \frac{2hk_1(\omega_0^2 - k_1)^2}{q^2}\right)\frac{3}{4\alpha_2^2} + \frac{(\omega_0^2 - k_1)^2}{4\alpha_2}\right],$$

$$\int_{-\infty}^{+\infty} \left[(\omega_0^2 - k_1)x_1 + \varepsilon x_1^3\right] x_2^2 x_1 g_L^2(x_1, x_2, k_1) dx_1 dx_2 \tag{A.6}$$

$$= I_{L_2} k_1 \left[\varepsilon\frac{3}{4\alpha_2^2} + \frac{(\omega_0^2 - k_1)}{2\alpha_2}\right].$$

References

1. M. APETAUR and F. OPICKA, *Linearization of nonlinear stochastically excited dynamic system*, J.Sound and Vibr., **86**, 563–585,1983.
2. G.Q. CAI and Y.K. LIN, *On exact stationary solutions of equivalent nonlinear stochastic systems*, Int.J. Non-linear Mechanics, **23**, 315–325,1988.
3. T.K. CAUGHEY, *Response of a nonlinear string to random loading*, Trans. ASME J.Appl.Mech., **81**, 345–348, 1959.
4. T.K. CAUGHEY, *On the response of a nonlinear oscillators to stochastic excitations*, Prob. Engrg. Mech., **1**, 2–4, 1986.
5. R.N. IYENGAR, *Higher order linearization in nonlinear random vibration*, Int. J. Nonlinear Mechanics, **23**, 385–391, 1988.
6. I.E. KAZAKOV and B.F.DOSTUPOV, *Statistical dynamics of nonlinear automatic systems*, (Moscow: Fizmatgiz) 1962 (in Russian)
7. F. KOZIN, *The method of statistical linearization for nonlinear stochastic vibration* [in:] Nonlinear Stochastic Dynamic Engineering Systems, F.Ziegler and G.I. Schueller [Eds.] (Berlin: Springer), 45–56, 1989.

8. L.D. LUTES, *Approximate technique for treating random vibration of hysteretic systems*, J.Acoust.Soc.Americ., **48**, 299–306, 1970.

9. D.C. POLIDORI and J.L. BECK, *Approximate solutions for non-linear random vibration problems*, Prob.Engrg.Mech., **11**, 179–185, 1996.

10. V.S. PUGACEV and I.N. SINICYN, *Stochastic differential systems*, (Chichester: Willey), 1987.

11. J.B. ROBERTS and P.D. SPANOS, *Random vibration and statistical linearization*, (Chichester: Willey), 1990.

12. L. SOCHA and T.T. SOONG, *Linearization in analysis of nonlinear stochastic systems*, Appl. Mech. Rev., **44**, 399–422, 1991.

13. L. SOCHA, *Application of probability metrics to the linearization and sensitivity analysis of stochastic dynamic systems* [in:] Proc. International Conference on Nonlinear Stochastic Dynamics, Hanoi, Vietnam, Dec. 7-10, 1995, 193–202.

14. R. WANG, S. KUSUMOTO and Z. ZHANG, *A new equivalent non-linearization technique*, Prob. Engrg. Mech., **11**, 129–137, 1996.

15. M.W. ZOLOTAREV, *Modern theory of summation of independent random quantities* [in Russian], (Moscow: Nauka), 1986.

16. W.Q. ZHU, T.T. SOONG and Y. LEI, *Equivalent nonlinear system method for stochastically excited Hamiltonian system*, Trans. ASME Appl. Mech., **61**, 618–623, 1994.

Received December 12, 1998.

Arch. Mech., **51**, 3–4, pp. 509–528, Warszawa 1999

Some models of chaotic motion of particles and their application to cryptography*

J. SZCZEPAŃSKI [1], K. GÓRSKI [2], Z. KOTULSKI [1], A. PASZKIEWICZ [2] and A. ZUGAJ [2]

[1] *Institute of Fundamental Technological Research, Polish Academy of Sciences*

[2] *Warsaw University of Technology, Institute of Telecommunication*

IN THE PAPER reflection law models describing the motion of a free particle in a bounded domain are considered. Properties of such dynamical systems are strongly related to the boundary conditions, expressed by a map called a reflection law. We discuss recent results concerning the problem of transferring important properties like chaos, ergodicity and mixing from the reflection law to the motion of the particle. Then we present in a consistent way a method of construction of block cryptosystems, using chaotic reflection law models with appropriate properties. We also propose an application of the mechanical particle model (possessing the transferring property) for constructing pseudo-random numbers generator which can be applied in stream ciphers. The security of the cryptosystem based on particle's motion is due to the property of statistical independence of the actual location of the particle, after a number of reflections, of its initial location.

1. Introduction

DURING THE PROGRESS of civilisation many branches of science of very particular specialisations appeared, so experts in one field do not know what is being done in another. However, it often happens that tools and methods developed in one branch of science can be applied in others, apparently very far away. Let us remember, for example, the use of genetic algorithms in engineering tasks of structural optimisation. In this paper we give another example: the application of non-classical reflection law models, originating from the kinetic theory of dilute gases, for constructing cryptographic algorithms applied in secure communication and information systems.

*The paper has been prepared with the financial support of the Committee of Scientific Research (KBN) under grant no. 8T11D01112

In classical mechanics, the problem of elastic reflection of a moving body from a rigid wall is governed by the fundamental conservation laws, which determine the behaviour of the velocity of the body after the reflection. This gives the following reflection law: the reflection angle is equal to the incidence angle of the body. However, in kinetic theory, where the scale of the reflected bodies (particles) is smaller, the structure of the boundary must be taken into account. Up to now there are only hypotheses as to what happens when the particle reaches the boundary, more or less confirmed by experiment. This results in the necessity of assuming some more complicated boundary conditions for the description of the behaviour of gas particles in a container. The concept of non-classical reflection law models is an attempt at a description of such complicated conditions by some global method.

The theory of non-classical reflection laws found its place in the literature [3, 30, 32, 35, 36, 37]. Reflection law models are an intermediate case between the deterministic systems first considered by SCHNUTE and SHINBROT [32], and the systems with random reflection laws [9]. Namely, we admit a system with strictly deterministic reflection laws that are not one-to-one maps. Thus, in this case it can happen that two different initial configurations in the phase space lead to the same final configuration which is impossible in the Schnute and Shinbrot model. There are a number of maps which can play the role of the reflection law. These and other authors investigated the properties of reflection laws finding that they can lead to non-slip reflection on the boundary, non-increasing entropy, chaos, ergodicity and mixing property of systems describing the behaviour of the particle. These phenomena are examples of a more general effect of transferring chaos (ergodicity, mixing) from some subsystem to an extended system [8, 12, 25, 29, 35, 36, 37].

Non-classical reflection laws found their place in modelling real physical phenomena. A certain interesting physical process governed by a non-classical reflection law was observed and investigated by ANDREYEV [2]. He studied the motion of an electron in the neighbourhood of the boundary separating normal and superconducting phases. It was found that the electron, reflected from the superconducting phase, changes the sign of all three components of the velocity (the "anti-reflection" law), what is essentially different from the classical reflection, where only the sign of the orthogonal component is changed. An interesting step in description of the mesoscopic scale physical systems in solids [1], where the theory of the Andreyev reflection law is developed (approaching practical construction of such systems), is the recent paper of NAZAROV [24] devoted to the novel circuit theory of superconductivity.

Problems of transferring some imposed properties from a dynamical system to its extension appear in various situations and seem to be interesting both from the theoretical and practical point of view. They naturally arise from many pro-

blems of engineering dynamics or physics. In general, by an extended dynamical system we understand a system with state space of dimension greater than the original one and functionally dependent on it (e.g. vibrations of a vehicle excited by a working engine). Such a system can be a simple extension of the given dynamical system obtained by adding more co-ordinates without changing the form of the primary ones, or it can be some higher-dimensional dynamical system driven by the lower-dimensional one. Many practical engineering applications dealt with this problem, posed as, for example, the stabilisation of systems by small perturbations (noise or chaos). In this paper we consider the transfer problems in the case of a free particle motion inside a bounded plane domain. We assume the reflection law as a primary dynamical system and the motion of the reflecting particle as an extended system. For our cryptographic applications, the transferring property of "irregularities" in the model used is the basis for constructing a secure algorithm.

Cryptography is a permanent field of interest [31]. At present, the secret communication plays an increasing role in many fields of common life. The basic idea of encryption is to modify the message in such a way that its contents can be reconstructed only by a legal recipient. The message should be represented by a sequence of symbols from a finite alphabet. In practice, the message written e.g. in Latin alphabet, must be transformed, by some known, standard algorithm, to a certain sequence of numbers M (in decimal or binary representation). This procedure is called message encoding. The process of encryption $e(M)$ can be regarded as a function or algorithm producing the ciphertext $C = e(M, k)$. By k we denote a parameter (number), called the secret key chosen at random from a large set. The function inverse to e is the decryption function d, which from the ciphertext C and the secret key k produces the plaintext: $M = d(C, k)$. The security of the algorithm is based on the fact that the decryption is possible only for people who know the secret key k.

One of the fundamental properties of cryptosystems required for their security is statistical independence of plaintexts and the corresponding ciphertexts, strongly connected with the concepts of ergodicity, mixing and chaos [7, 22]. The idea of ergodicity and sensitive dependence on initial conditions (chaos) has its source in the theory of gases (e.g. n-particle models, Lorentz gas, Brownian motion). In the theory, two properties play a fundamental role: ergodicity, that is the convergence of the average value over trajectory to the ensemble mean value, and mixing, which guarantees the convergence from local non-equilibrium to equilibrium state. Analysing the behaviour of individual particles, assuming ergodicity or mixing, we go from any initial conditions of the particles to some macroscopic equilibrium state, where the particles are practically non-discriminable. Therefore, using the reflecting system for encryption, we expect that the position of our particle, describing at its initial state the message being encrypted, after

several reflections will take some non-predictable position and will not be statistically distinguishable from any other possible position, making the algorithm cryptographically secure.

In this paper we present in a consistent way (pointing out the mechanical aspects of the models used) the application of two-dimensional discrete dynamical systems describing the motion of particles, so-called reflection law models, for constructing secure cryptosystems. In the block cryptosystem we take the initial condition of the first coordinate of the system (which describes the position of the particle on the boundary at the moment of reflection) as the plaintext, and the initial condition of the second coordinate (representing the angle of reflection) as the secret key. Both coordinates are iterated; the second, independently of the first, in a chaotic way; the first with some dependence on the second coordinate at each step. For the chaotic dynamical system, taking two initial conditions, we observe an exponential divergence of their trajectories, depending on the distance between the initial conditions of both trajectories. The required statistical properties (ergodicity, mixing) and chaos are obtained in the dynamical system describing the motion of the particle by a transfer from the reflection law.

Except for the results concerning the block ciphers, we suggest an idea of application of the particle motion models for construction of pseudo-random number generators used in the stream cipher. In the models, the required property of the system could be obtained by the transferring process. The basic idea of bit generation is that the actual location of the particle (in a phase space) indicates which bit we choose: "0" or "1". We hope that such a theoretical construction (usually simulated in the computers) can be further developed to some physical realisation, slightly increasing the speed of generation of bits and avoiding the computer calculations errors.

2. Reflection law models

To establish a reflection law model, one must select a domain with a certain shape of the boundary and define the reflection law. Usually, the boundary is assumed to be a closed, sufficiently regular surface. The reflection laws describe in a macroscopic way the behaviour of the velocity of a freely moving particle during its contact with the boundary of the domain. From this point of view, non-classical reflection laws need not satisfy such a fundamental physical law as the conservation of linear momentum. However, one can find some situations where such laws can describe realistic physical phenomena. Consider for example a container, the wall of which has some microstructure (Fig. 1). We assume that the mass of the reflected particle is negligible in comparison to the mass of the container. Then the reflection process, observed as non-classical, can in fact be the effect of several classical elastic reflections where, for every micro-

reflection, the conservation of linear momentum is satisfied. In this model, due to the small scale of the microreflection, we identify the outgoing position with the incoming position. The reflection law is usually quite general and it can be written symbolically as:

$$\nu_{\text{ref}} := T_x(\nu_{\text{inc}}), \tag{2.1}$$

where ν_{inc} is the incoming velocity of the particle at the boundary point x, and ν_{ref} is the velocity of the particle after the reflection.

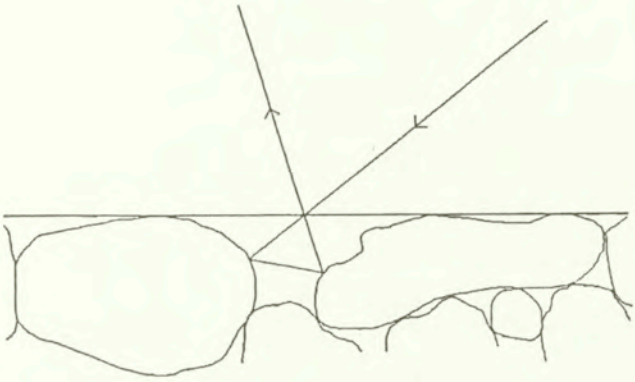

FIG. 1. Effect of the boundary microstructure on the reflection law.

In our considerations we assume that the particle moves with a constant velocity, changing only the direction at the moment of reflection. In the particular case of the reflection law conserving the angle of incidence (the angle of incidence is equal to the angle of reflection), one obtains the class of dynamical systems called billiards. This conservative reflection law (as a map) is neither ergodic nor chaotic [35]. (However, it is well known that in appropriate domains it can lead to ergodic or chaotic motion of a particle.) Thus, to obtain ergodic [7] and chaotic properties [29] of a reflection law, one must assume another map relating the incident and outgoing angles. In this paper we consider the reflection law models in two dimensions, where we can observe the qualitative results we are interested in, especially the transferring property. We approximate the boundary of the plane domain of particle's motion by some closed, sufficiently smooth curve. Extensions of the results in two dimensions to more-dimensional spaces lead to some technical problems, which can be also observed in the case of the widely studied classical billiards theory. However, the results in $\mathbb{R}^2$ can give some suggestions concerning the behaviour of more-dimensional systems.

In order to get the simplest form of equations of particle motion, we use the following co-ordinate system introduced by BIRKHOFF [5]: (x_n, ν_n), where x_n denotes the position of the particle on the boundary at the moment of the n-th reflection, and ν_n is the angle between the velocity of the particle after the

reflection and the tangent to the boundary at x_n (see Fig. 2) [7, 36, 37]. In the case of a fixed plane domain we obtain a two-dimensional discrete dynamical system $F_T(.,.)$ whose properties are dependent functionally on the reflection law $T_x(.)$ (under some assumptions, a dynamical system itself). Thus, $F_T(.,.)$ acts from the product of two intervals onto the same product:

$$F_T : [0, L) \times (0, \pi) \to [0, L) \times (0, \pi) \tag{2.2}$$

and can be written in the following form:

$$(x_{n+1}, \nu_{n+1}) = F_T(x_n, \nu_n). \tag{2.3}$$

The symbol L in Eq. (2.2) denotes the length of the boundary of the domain.

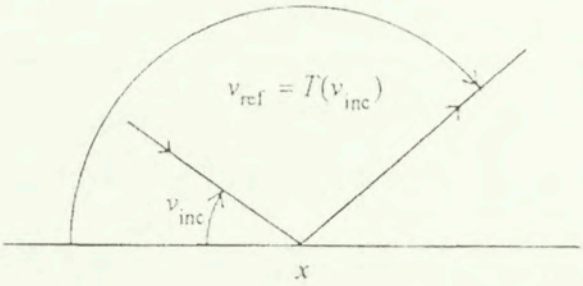

FIG. 2. The reflection law in local coordinates.

In our further considerations the reflection law $T_x(.)$ is assumed to be independent of x (which means that the properties of the walls of the container are identical at every point x),

$$T_x(.) \equiv T(.). \tag{2.4}$$

Then the reflection law $T(.)$ is a one-dimensional dynamical system itself and it is used for construction of the two-dimensional dynamical system $F_T(.,.)$. It is interesting to know, how properties of the smaller system $T(.)$ affect the larger one – $F_T(.,.)$, which describes the motion of a particle in the container.

3. Transferring problems

In the previous section we considered reflection laws as dynamical systems with certain properties. If the reflection law extracted from the extended dynamical system describing the motion of a freely moving particle is independently considered, one can ask the following questions: what are the properties of the extended system if we use a non-classical reflection law? What is the effect of the specific properties of the reflection law (like chaos or ergodicity) on the behaviour of the particle? Is the particle motion chaotic or ergodic? In our model

the shape of the boundary also affects the properties of motion and it leads to a new question: what is the influence of the shape of the container on the motion of the particle? In this section we present some interesting results concerning the above problems.

To give some insight into transferring properties we study this phenomenon in two typically used containers: a circle and a square. In the case of a circle, after simple geometrical considerations, making use of the rotational symmetry, we obtain the following system of evolution equations:

$$\begin{aligned} \nu_{n+1} &= T(\nu_n), \\ x_{n+1} &= x_n - 2\nu_{n+1} (\mathrm{mod}\ 2\pi), \end{aligned} \tag{3.1}$$

where $x_n \in [0, 2\pi)$, $\nu_n \in (0, \pi)$. The first equation constitutes a reflection law and the second one is inherently connected with systems of such type. It turned out [36] that in this model, ergodicity (and also chaotic behaviour) of a reflection law implies ergodicity (chaos) of the trajectories of a particle. Moreover, if the reflection law has an attracting periodic orbit then the trajectories of moving particles are asymptotically periodic.

Related questions were studied in the context of Brownian motions and also as a purely mathematical problem. In [4] a class of non-linear dynamical systems describing the motion of a particle in a viscous liquid under the influence of a kick force was investigated. In this case the time evolution of velocity of the particle is governed by the system of equations:

$$\begin{aligned} x_{n+1} &= T(x_n), \\ y_{n+1} &= \lambda y_n + f(x_n). \end{aligned} \tag{3.2}$$

It was proven [4] that under appropriate conditions on the map $T(.)$, the force $f(.)$ and the constant λ ($|\lambda| < 1$ depends on the viscosity of the liquid) periodicity, ergodicity and the mixing property (see Sec. 5 for definitions) of $T(.)$ imply the same properties of the extended dynamical system (3.2). The variable y_n in Eq. (3.2) corresponds to the velocity of the kicked particle and the ergodic (periodic, mixing) property is supported by the vicinity consisting of other particles (whose evolution is governed by $T(.)$ through the force $f(.)$). In our model (3.1), ergodicity (periodicity, chaos) is transmitted to the velocity of the particle from the boundary of the container by means of the reflection law.

The equation (3.1) has another interesting physical interpretation. It turned out that this evolution equation is topologically conjugated [37] to the well-known "standard maps" (see [23, 34] and the literature therein), for the first time introduced by the physicists B.V. Chirikov and J.B. Taylor. The standard maps appear

in many situations; they are obtained as a Poincaré map describing the motion of an electron rotating in the plane perpendicular to a uniform magnetic field in circular accelerators [13, 14].

Considering our second model of the container, that is the square, we come to quite different results concerning the transferring property. We show that if we assume $T(.)$ to be a unimodal map, for example:

$$\nu_{n+1} = T(\nu_n) = \frac{4}{\pi}\nu_n(\pi - \nu_n), \tag{3.3}$$

then in the square the transferring problem reduces to the study of dynamical systems given by the following one-dimensional map:

$$G = T \circ h : [0, \pi] \to [0, \pi], \tag{3.4}$$

where h is some involution, i.e.

$$h^2(\nu) = \nu \quad \text{for every} \quad \nu \in [0, \pi]. \tag{3.5}$$

We proved that in the square containers, ergodic and chaotic reflection laws $T(.)$ can even lead to some periodic motion of the particle [37]. This result can be generalised to containers with convex polygon boundaries.

The interesting question is if for a given container, equivalent reflection laws (topologically conjugated) lead to the same qualitative properties of the motion of the particle. We found [35] two topologically equivalent reflection laws, both ergodic and chaotic which in the square domain transfer to the extended system in completely different ways. For the first law, the motion of the particle is asymptotically periodic, that is the particle tends to some fixed periodic orbit. In contrast, for the second reflection law and almost all initial points (x_0, ν_0), the set of velocities $\{\nu_n, n = 1, 2, ...\}$ corresponding to each initial point is dense in a set of Lebesgue measure of at least $\pi/2$.

In Sec. 5 we give an example of a reflection law satisfying the transferring property in the square, which is useful for our cryptographic purposes. It is interesting to find some general assumptions on the reflection law that assure the transferring property for a large class of containers. It seems that these types of reflection laws could be interesting from a physical point of view.

4. Elements of cryptology

Before we start the presentation of a cryptographic algorithm taking its source from some mechanical phenomena or, more precisely, from the theory of rarefied gases, we introduce the definitions of fundamental terms needed for understanding the procedures. The first procedure, preceding the encryption, is a coding algorithm. It is the method of translation of the natural message (spoken

or written) into a sequence of numbers. This can be for example the representation of letters and numbers by the ASCII code in digital computers, or transfer of human voice to a sequence of binary pulses in telephone communication. When the message is coded, i.e. represented in the form of a sequence of numbers (decimal or binary), it can undergo some additional transformation, which makes it non-understandable for everyone except the intended recipient. This is the field of interest of cryptology.

Cryptology is the branch of science [31] dealing with the design of encryption algorithms and the investigation of their strength (by studying methods of breaking them). Cryptology has been of some interest at all times. Mostly it has been used in connection with military or diplomatic affairs and for instance, in its early stages it was almost exclusively concerned with secretly written information. With the development of an ever refined communication technology, nowadays secret communication plays also an increasing role in commercial, industrial and banking sectors. It is due to the actually increasing importance of cryptology in economics that the research activities in the field and the search for new cryptographic methods still continues.

Cryptography is the process of transforming information (plaintext) into unintelligible form (ciphertext) so that it may be sent over insecure channels or it may be stored in insecure files. Cryptographic procedures can also be used for personal identification, digital signatures, access control etc.

A cryptosystem is a cryptographic algorithm, which is usually known, and which depends on some parameter called the key. With encryption we can transform the plaintext to a form which an outsider cannot interpret unless he knows the method and the key used in the process. Decryption is the inverse process in which encrypted data are translated to clear data. Thus, a cryptosystem is a two-way procedure: encryption – decryption. Let us also remark, that the coding procedure must be also two-way. If we precede the encryption algorithm with some encoding procedure, then we must follow the decryption with some decoding, inverse to the encoding process.

There are two types of encryption algorithms: stream ciphers and block ciphers [31]. A stream cipher is a method in which we have some secret key generator which produces a bit stream (the key stream) which enciphers the plaintext bit stream by simple modulo 2 addition. The stream cipher system thus hides the plaintext by changing the bits of it in a random-like way. An interceptor, who does not know the key, will not know which bits have been changed (corresponding to the occurrence of "1" in the key stream), and which ones remain unchanged ("0" in the key stream). Unlike stream ciphers, where only one bit at a time is encrypted, in block ciphers whole blocks of bits are treated simultaneously. In this case the plaintext information is hidden by the fact that, depending on the key, a ciphertext block can be deciphered to any combination of plaintext bits

or to as many combinations as there are keys. If the keys are chosen with equal probability, then to the interceptor observing a ciphertext block, all the possible plaintext blocks are equally likely to have occurred.

5. Chaotic dynamical systems - new tool for cryptology

In recent years a new approach to constructing cryptosystems based on application of the theory of both continuous and discrete chaotic dynamical systems has been developed. Within the continuous theory, methods of synchronisation of chaotic systems [15, 16, 27, 28] and the idea of controlling chaos [11, 15, 26] are applied. In the discrete systems approach, the constructions of cryptosystems based on iterations and inverse iterations of chaotic maps (with possible methods for introducing keys) are developed.

The earliest applications of chaotic systems in cryptography were proposed by PECORA and CAROLL in 1990 [28] as a possible application of the synchronisation of chaotic dynamical systems. This idea has been developed by KOCAREV *et al.* [16] and PARLITZ *et al.* [27], where an experimental test system based on chaotic electronic circuits was presented. The first paper employed analogue signals while the second one used binary signals. An overview of the methods connected with encrypting messages with the modulation of trajectories of continuous dynamical systems can be found in [15].

Application of discrete chaotic dynamical systems to cryptography was first analysed by HABUTSU *et al.* [10] and then developed by KOTULSKI and SZCZEPAŃSKI [19, 20]. Before we present the algorithm of encryption and decryption, we introduce all the required properties and definitions.

Chaos is the property of sensitive dependence of trajectories of the dynamical system on the initial conditions [22, 34]. More precisely, a non-linear system is chaotic if it has positive Lyapunov exponents in a certain domain. Consider for example a one-dimensional dynamical system (I, φ), where φ is a C^1 -class map transforming the interval I into itself. If at some point $x \in I$, the Lyapunov exponent $\lambda_x > 0$, then

$$(5.1) \qquad \forall \varepsilon > 0 \exists n_1, n_2 \exists U_{n_1,n_2} \ni x, \forall n_1 \leqslant n \leqslant n_2, \forall z_1, z_2 \in U_{n_1,n_2}$$

$$\exp\{(\lambda_x - \varepsilon)\, n\}\, |z_1 - z_2| < |\varphi^n(z_1) - \varphi^n(z_2)| < \exp\{(\lambda_x + \varepsilon)\, n\}\, |z_1 - z_2|,$$

where U_{n_1,n_2} is some neighbourhood of $x \in I$. The above expression means that the initial distance $|z_1 - z_2|$ between two arbitrary points z_1, z_2 (which are elements of the neighbourhood U_{n_1,n_2} of point x) after n iterations will increase at least $\exp\{(\lambda_x - \varepsilon)\, n\}$ times.

Let us illustrate the idea of including the secret key into the initial condition by some elementary one-dimensional example [19]. Let γ be a one-dimensional

chaotic map with positive Lyapunov exponent λ:

$$\gamma : [0,1] \to [0,1], \tag{5.2}$$

and $P \in (0,1)$ be the message to encrypt. Fix a natural number n (number of iterations) and choose the secret key $k \in (0,1)$. Let $\overline{C}$ be some selected pre-image of P under the map γ^n:

$$\overline{C} = \gamma^{-n}(P); \tag{5.3}$$

$$\gamma^n(\overline{C}) = \gamma^n\left(\gamma^{-n}(P)\right) = P. \tag{5.4}$$

Then, we calculate C, the ciphertext of P as

$$C = \overline{C} + k (\mathrm{mod}\, 1). \tag{5.5}$$

Decryption is the inverse operation, that is

$$P = \gamma^n(C - k). \tag{5.6}$$

An outsider tries to approximate the key k assuming some value of the secret key, say k_1 such that $|k - k_1| < 10^{-20}$. Then he calculates the value of plaintext $P_1 = \gamma^n(C - k_1)$. For $n = 30$, $\lambda - \varepsilon \approx 1.558$ (which is a reasonable value for many dynamical systems), due to chaos we have:

$$|P - P_1| = |\gamma^n(C - k) - \gamma^n(C - k_1)| \geqslant e^{n(\lambda-\varepsilon)}\,|k - k_1| \approx 0.5. \tag{5.7}$$

Formula (5.1) and the above example suggest how to choose a chaotic map with suitable Lyapunov exponent to construct DDC cryptosystem. First we select an admissible class of maps (with respect to possibility of practical implementations), e.g. of parabolic type, and establish the number of iterations n to guarantee the required speed and accuracy of calculations. Then we fix the map with the Lyapunov exponent such that the obtained speed of divergence (governed by formula (5.1)) makes ciphertexts corresponding to close plaintexts completely different. For example, for $n = 30$, the accuracy equal to 10^{-20}, the estimation (5.7) shows that the map with the Lyapunov exponent $\lambda \approx 1.6$ could be used.

The formula (5.7) demonstrates how the chaos property protects the system against a brute force attack (where the algorithm is tested with all possible secret keys). However, cryptoanalysts use some more sophisticated attacks to break cryptosystems. To make the cryptosystem based on the chaos property more robust against statistical cryptoanalytical attacks, we postulate some other important properties of the applied dynamical system, like ergodicity and mixing property. For cryptographic purposes we shall use dynamical systems with invariant measure equivalent to the Lebesgue measure.

We say that the measure μ is invariant, if and only if it satisfies

$$\forall A \in \sigma(X), \qquad \mu(A) = \mu(\varphi^{-1}(A)). \tag{5.8}$$

We postulate that μ is equivalent to the Lebesgue measure, i.e.:

$$\forall A \in \sigma(X), \qquad \mu(A) = \int_A g(x)dx, \tag{5.9}$$

with its density function $g(.)$ satisfying for all x the following condition:

$$0 < g_1 \leqslant g(x) \leqslant g_2, \tag{5.10}$$

where g_1 is close to g_2.

We say that (X, φ) is ergodic if and only if it has only trivial invariant sets, i.e., if $\varphi(B) \subset B$ then $\mu(B) = 0$ or $\mu(B) = \mu(X)$. The ergodicity implies that the state space cannot be nontrivially divided into several parts. Therefore if some trajectory starts from any point x, it never localises in a small region. It means that the plaintext space which can correspond to a given ciphertext cannot be restricted to a "smaller" subspace (smaller than X). Thus, for the ciphertext C the corresponding plaintext P (during brute attack) must be searched for over all the state space X. We can also postulate a stronger condition, assuring better probabilistic properties of the set of possible ciphertexts. The system is mixing if the following condition is satisfied (we assume that $\mu(X) = 1$) for any sets A and B:

$$\lim_{n\to\infty} \frac{\mu(\varphi^{-n}(A) \cap B)}{\mu(B)} = \frac{\mu(A)}{\mu(X)}. \tag{5.11}$$

This property means that the part of B which after n iterations of φ will be contained in A, is asymptotically proportional to the ratio of A in X with respect to the measure μ. Thus for any ciphertext C, all the possible plaintexts P (during brute attack) are μ-equiprobable.

6. A new type of block ciphers – the DCC algorithm

In this section we outline the application of our encryption algorithm using the reflection law model. The first step is the coding procedure, where the message expressed in natural language (a sequence of symbols from a finite alphabet) is transformed to a binary sequence by some public method. Then the sequence is divided into finite blocks of bits of the same length. Now we can identify the usual elements of a block cryptosystem. We assume, that every plaintext is some number $P \in (0, 1)$, the secret key is the parameter k – a number from some interval (usually also a representation of some finite binary sequence). The ciphertext is also a number, $C \in (0, 1)$.

In the general formulation of the DCC cryptosystem we use some chaotic map $\varphi_k(.)$, depending on the parameter k,

$$\varphi_k : (0,1) \to (0,1). \tag{6.1}$$

The encryption is the n-fold iteration of the inverse map φ_k^{-1} with the initial value P according to some (secret, determined by k) rule of choices of the successive pre-images of φ_k^{-1}. The ciphertext C is obtained as:

$$C = \varphi_k^{-n}(P) = \varphi_k^{-1}(\varphi_k^{-1}(...\varphi_k^{-1}(P))). \tag{6.2}$$

The sender encrypts all the blocks of the coded message, say P_i, $i = 1, 2, ..., m$, using the secret key k and obtains the sequence of ciphertexts C_i, $i = 1, 2, ..., m$. The ciphertexts are sent by an open channel to the recipient. The legal recipient (person, who knows the secret key k), to obtain the plaintext performs the following decryption algorithm using the n-th iteration of the map φ_k:

$$P = \varphi_k^n(C) = \varphi_k(\varphi_k(...\varphi_k(C))) \tag{6.3}$$

He does this for all C_i, $i = 1, 2, ..., m$ and obtains the plaintext which is the coded message. The final step is the application of the decoding procedure, inverse to the initial coding step. It is obvious that the above construction of DCC block cryptosystems can be generalised to more dimensions (more dimensional spaces of plaintexts and ciphertexts).

There are two possibilities of introducing the secret key k into the algorithm. First, k can be an internal parameter of the map φ [10], second, k can be included into the initial condition [19, 20].

The map $\varphi(.)$ applied in (6.2) – (6.3) is quite general. However, to assure sufficient security of the cryptosystem we should apply maps that are chaotic, ergodic and even mixing. Maps describing particle's motion governed by appropriate reflection laws have the required properties and after some adaptation they can be applied for constructing secure cryptosystems.

To construct a concrete reflection law model useful for cryptographic purposes, we must take into account not only security but also the computational aspects – in this case the accuracy of numerical calculations and computational complexity. Therefore we propose the square as a domain and a piece-wise parabolic reflection law to construct the reflection law model. In the system the state variable is the pair (x, ν), where $x \in [0, L)$ represents the message evolving (during encryption) iterations from the plaintext P to the ciphertext C (we identify x with the distance of the particle's reflection point from some fixed point of the square measured along the sides of the square), and $\nu \in (0, \pi)$ is the reflection

angle. We take the reflection law T_D of the following form:

$$T_D(\nu) = \begin{cases} \dfrac{\nu^2}{\pi} + \dfrac{3\nu}{2} & \text{for } \nu \in \left(0, \dfrac{\pi}{2}\right), \\ \dfrac{\left(\nu - \dfrac{\pi}{2}\right)^2}{\pi} + \dfrac{3\left(\nu - \dfrac{\pi}{2}\right)}{2} & \text{for } \nu \in \left[\dfrac{\pi}{2}, \pi\right). \end{cases} \tag{6.4}$$

This map is chaotic, ergodic and even mixing [18]. For $T_D(.)$ these properties transfer to the larger system describing the motion of a particle as required.

Thus, a general form of the two-dimensional dynamical systems, describing the motion of a particle that we use for construction of the cryptosystems, is $F_{T_D}(x, \nu) = (S(x, \nu), T_D(\nu))$. The inverse iterations of this system are the steps of encryption. During encryption, the first co-ordinate describes the evolution of the message and the second one – the evolution of the secret key. Decryption involves forward iterations transforming the position representing the ciphertext to the one corresponding to the plaintext. As before, the second co-ordinate describes the evolution of the secret key. The details of the algorithm together with the results of numerical experiments can be found in [21].

7. DCC as a pseudo-random number generator

The chaotic dynamical systems with good properties can be used for constructing pseudo-random sequences of bits [17], being, among other applications, the foundation for construction of stream cryptosystems. As we mentioned, such sequences (called the secret key streams) hide the content of the original binary message by changing the value of a bit to the opposite, if the corresponding bit of the key stream is 1 and leaves it unchanged if the corresponding bit of the key stream is 0. An ideal stream cipher would use some physical system (true random number generator) as a key stream generator. However, since its output cannot be reproduced, decryption (the operation which in the case of a stream cipher is the repetition of the same algorithm as in encryption with the same key stream) would be impossible unless the whole key stream would be transported to the legitimate recipient via a secure channel. This procedure is often impractical, therefore mostly so-called pseudo-random number generators with special properties, controlled by a relatively short key (called the seed), have to be used as key stream generators (instead of physical generators commonly used).

The most important property of the binary sequences used as the key streams, guaranteeing the security of the cryptosystems, is impossibility of reconstruction or prediction of unknown bits on the basis of a known sequence of bits. In other words, the key stream must have properties analogous to a white noise process, that is independence of its states for different instants of time. As is known,

the concept of white noise is strongly connected with a description of a particle's motion called the Brownian motion. This fact indicates a possibility of application of the reflection law models. To assure good statistical properties of the generated sequences we propose to make use of the physical systems with transferring phenomena, where the required properties (e.g. mixing, chaotic behaviour) of a smaller system affects the extended one, describing globally the physical process.

Consider the motion of a particle in the square with the reflection law given by (6.4). In this case the state space is the Cartesian product of two intervals:

$$S = [0, L) \times (0, \pi). \tag{7.1}$$

The basic idea of the method is the following. We divide (in some appropriate way) the state space S of the reflection law model into two parts S_0, S_1 ($S_0 \cup S_1 = S$). We start observation of the evolution of the particle starting from an initial state (x_0, ν_0), playing the role of the seed. We generate a sequence of bits by taking the n-th bit equal to "0" if the state of the particle is at the moment of the n-th iteration in the set S_0, that is $(x_n, \nu_n) \in S_0$, and "1" otherwise.

The most important decision in this construction is the choice of the sets S_0, S_1. Observing histograms of the moving particle we identify the invariant measure μ of this dynamical system. In further considerations we normalise this measure to 1. It is known that such a measure is close to the Lebesgue measure on S, but is not exactly equal to it. To have the opportunity to use ergodic theory we choose the sets S_0, S_1 in such a way that

$$\mu(S_0) = \mu(S_1) = \frac{1}{2}. \tag{7.2}$$

(In our investigations we assumed $S_0 = \left\{(x, \nu) \in S, |x| < \frac{L}{2}\right\}$). Then, by condition (7.2) we obtain that the expected number of "0" in the generated sequence is equal to the expected number of "1". To be more precise, we can use the Birkhoff - Khinchin Ergodic Theorem [7], which for our reflection law model can be written as:

$$\lim_{n\to\infty} \frac{1}{n} \sum_{i=0}^{n-1} p\left(F_{T_D}^i(x_0, \nu_0)\right) = \int_S p d\mu, \tag{7.3}$$

(for almost all $(x_0, \nu_0) \in S$ with respect to μ), where p is an arbitrary μ – integrable function. Taking as the function p the indicator function of the set S_1, that is

$$p(.) = \chi_{S_1}(.), \tag{7.4}$$

we obtain that in the pseudo-random sequence determined by the seed

$(x_0, \nu_0) \in S$, the average number of "1" is:

$$\frac{1}{n}\sum_{i=0}^{n-1} \chi_{S_1}\left(F_{T_D}^i(x_0,\nu_0)\right) \xrightarrow[n\to\infty]{} \int_S \chi_{S_1} d\mu = \mu(S_1) = \frac{1}{2}, \tag{7.5}$$

due to (7.2). This condition guarantees that both values in the sequence of bits, that is "1" and "0" are equiprobable and any illegal recipient has no *a priori* indication concerning the sequence. Now we should show that bits of the generated sequence are statistically independent, which practically assures the impossibility of determining some bit on the basis of some others. To show this we use the mixing property.

Define the random variable B_n, responsible for the generation of the n-th bit, in the following way:

$$B_n(x_0,\nu_0) = \chi_{S_1}(F_{T_D}^n(x_0,\nu_0)), \tag{7.6}$$

where the set S is the space of elementary events and the normalised invariant measure μ is the probability distribution describing our binary random variable B_n:

$$B_n : S \to \{0,1\}. \tag{7.7}$$

For every n, the probabilities that the random variables B_n are equal to "1" and "0" are:

$$P(B_n = 1) = \mu\left(F_{T_D}^{-n}(S_1)\right), \qquad P(B_n = 0) = \mu\left(F_{T_D}^{-n}(S_0)\right) \tag{7.8}$$

respectively. Applying the mixing property (5.11) we can show asymptotic independence of random variables B_n and B_{n+m} for m sufficiently large. Then, taking the modified dynamical system $G_{T_D}(.,.)$:

$$G_{T_D}(x_0,\nu_0) := F_{T_D}^m(x_0,\nu_0) \tag{7.9}$$

in definition (7.6) instead of F_{T_D}, we obtain the sequence of statistically independent random bits.

Generating bits according to the proposed algorithm we require the complete repeatability of the obtained sequences (what is the necessary condition of correct decryption in the stream cipher methods). In practical implementations the numbers used in calculations are expressed with some accuracy. Therefore, if our moving particle is close to the boundary of separation of the sets S_0 and S_1, then the numerical error can make that "0" generated in one computer becomes "1" in another (or *vice versa*). The idea of how to prevent this inconvenience was presented in [6]. The authors suggest to introduce a forbidden gap of small size at the partition $S_0 - S_1$ boundary an then to neglect all the trajectories which

go through this gap. For some chaotic maps describing the dynamical systems it is possible to characterize the forbidden trajectories imposed by the dynamics itself. They give also arguments (computing the topological entropy and analysing successive approximations of the grammar of the symbolic dynamics by means of a sequence of transition matrices) that for sufficiently small gap, the loss of the trajectories generating the sequences is only incremental and, what it follows, such a procedure does not deteriorate the statistical properties of the sequences.

We presented the construction of a single pseudo-random sequence described by the seed $(x_0, \nu_0) \in S$ (which is the elementary event in our model). We showed that statistical properties of such a sequence are sufficiently good for cryptographic purposes. In practice users of a stream cryptosystem need a large number of sequences. We can generate them by changing the initial conditions (seeds). Using the mixing property (provided by transferring phenomenon) of the reflection law models we can show that two sequences (corresponding to two different seeds) are different; moreover, by the chaos we obtain, that they cannot overlap over long sub-sequences of bits. Thus we have presented a method of generating bits which can be quite useful in practical applications.

8. Conclusions

Reflection law models arise in a natural way in the theory of rarefied gases (Knudsen gases) [3, 36], in description of particle's motion in accelerators [13, 14, 23] and in mesoscopic models of superconductive media [2, 24]. In the first case the model takes into account the behaviour of the gas particles at the boundary and the shape of the container (which is important, because we neglect the mutual interactions of the particles). Investigating the accelerators one finds that the corresponding Poincaré maps (being the standard maps) are topologically conjugated to some reflection law models. The theory of standard maps [23, 34] is extensively investigated in the literature. Authors studied the coexistence problem [34], that is the possibility of simultaneous existence of chaotic and regular trajectories in the same system. Another important problem is the transferring of certain properties of a smaller system to the larger one. In our paper this phenomenon was studied in the context of the effect of boundary conditions (represented by the reflection law) on the motion of the particle described by the reflection law model. We studied the possibility of transfer of chaotic, ergodic and mixing behaviour of the dynamical system modelling the reflection law to the dynamical system describing particle's motion (the reflection law model). We found that, under some additional assumptions concerning the reflection law and the shape of the container, the reflection law model governed by some chaotic, ergodic and mixing reflection law can have the same properties. However, we also observed an unexpected effect where the chaotic reflection law leads to regular

(even periodic) motion of the particle [37]. It is the interesting problem to construct chaotic and mixing reflection laws which guarantee the transfer of these properties to dynamical systems describing the motion of a particle in a large class of containers.

In the second part of our paper we gave a practical application of the observed effects. Among recent uses of chaos one can find also secure communicatons [15]. In [19, 20] we proposed a method of extending discrete dynamical sysems for constructing secure cryptosystems. The algorithms presented in this paper are examples of a realisation of the general scheme with application of the reflection law model [21]. The applied unified approach using the theory of abstract dynamical systems made it possible to prove the security of the proposed cryptosystems. Mathematical tools used for this purpose are quite general and hey are extensively studied in the literature. This new approach allowed us to obtain rigorous mathematical results concerning the cryptosystems (especially theirstatistical properties) but on the other hand, it opens a new area of investigaions in the theory of dynamical systems in the context of secure communications.

The presented DCC algorithm is an idealised model. In practice, developing software implementations, one should take into account the usual computational restrictions [31, 33]. Since numbers in digital computations have a finite representation, one must assume the lengths of computed values (key, plainext, ciphertext) such that both the forward iterations and inverse iterations can be performed uniquely and in such a manner that one can obtain the required number of significant bits of plaintext in the decryption process. In other words one must fix the information rate R

$$R = \frac{\text{plaintext size}}{\text{ciphertext size}}$$

specific for the algorithm applied and the computer accuracy. Therefore, devlopment of programs implementing our algorithms and useful in advanced pracical applications need some additional investigations taking into account this aspect of the problem. From the other side, it could be promising to consider a posibility of construction of physical systems realising our cryptographical algoritms. In spite of the fact that, in this case, we avoid the problem of computation erors, we face another one – the accuracy of measurements.

References

1. B.L. ALTSHULER, P.A. LEE and R.A. WEBB, *Mesoscopic Phenomena in Solids, series Modern Problems in Condensed Matter Sciences*, vol. **30**, North-Holland, Amsterdam 191.

2. A.F. ANDREYEV, *Thermal conductivity of the intermediate state of superconductors*, Zh.Exp.Theor.Fis., **46**, 1823–1828, 1964.

3. H. BABOVSKY, *Initial and boundary value problems in kinetic theory. I. The Knudsen gas, II. The Boltzmann equation*, Transp.Theor.Stat.Phys., **13**, Part I-455–474, Part II-475–498, 1984.

4. C. BECK, *Ergodic properties of a kicked damped particle*, Comm.Math.Phys., **130**, 51–60, 1990.

5. G.D. BIRKHOFF, *Dynamical Systems*, New York 1927.

6. E. BOLLT, Y-CH. LAI and C. GREBOGI, *Coding, channel capacity and noise resistance in communicating with chaos*, Phys. Rev. Lett., **79**, 19, 3787–3790, 1997.

7. I.P. CORNFELD, S.V. FOMIN and YA.G. SINAI, *Ergodic theory*, Springer-Verlag, Berlin 1982.

8. M.S. EL NASCHIE, *Complex dynamic in a 4D Peano-Hilbert space*, Il Nuovo Cimento, **107B**, 5, 583–594, 1992.

9. S. GOLDSTEIN and C. KIPNIS, N. IANIRO, *Stationary states for a mechanical systems with stochastic boundary conditions*, J. Stat. Phys. **41**, 915, 1985.

10. T. HABUTSU, Y. NISHIO, I. SASASE and S. MORI, *A secret key cryptosystem by iterating a chaotic map*, EUROCRYPT'91, 127–140.

11. S. HAYES, C. GREBOGI and E. OTT, *Communicating with chaos*, Physical Review Letters, **70**, 20, 3031–3034, 1993.

12. K. HIKAMI, P.P. KULISH and M. WADATI, *Integrable spin systems with long range interactions*, Chaos, Solitons & Fractals, **2**, 5, 543–550, 1992.

13. J.M. HOWETT, M. MONTH and S. TURNER, *Nonlinear dynamics, aspects of particle accelerators*, Proceedings, Sardinia, Lecture Notes in Physics, Springer, Berlin 1985.

14. Y.H. ICHIKAVA, T. KAMIMURA, T. HATORI and S.Y. KIM, *Stochasticity and symmetry of the standard map*, Prog.Theor.Phys., Supplement, **98**, 1–18, 1989.

15. T. KAPITANIAK, *Controlling chaos, Theoretical and practical methods in non-linear dynamics.*, Academic Press, London 1996.

16. LJ. KOCAREV, K.S. HALLE, K. ECKERT, L.O. CHUA and U. PARLITZ, *Experimental demonstration of secure communications via chaotic synchronisation*, Int.J.Bifurc. & Chaos, **2**, 709–713, 1992.

17. T. KOHDA and A. TSUNEDA, *Statistics of chaotic binary sequences*, IEEE Transactions on Information Theory, **43**, 1, 104, 1997.

18. A.A. KOSJAKIN, E.A. SANDLER, *Ergodic properties of some class of piecewise smooth maps on the interval*, Matiematika, **3**, 32–40, 1972.

19. Z. KOTULSKI and J. SZCZEPAŃSKI, *Discrete chaotic cryptography*, Annalen der Physik, **6**, 5, 381-394, 1997.

20. Z. KOTULSKI and J. SZCZEPAŃSKI, *Discrete chaotic cryptography (DCC). New method for secure communication*, Proc.Non-linear Evolution Eequations and Dynamical Systems '97, Crete, Grece, http://www.roma1.infn.it/ ragnisco/proc97.htm, 1997.

21. Z. KOTULSKI, J. SZCZEPAŃSKI, K. GÓRSKI, A. PASZKIEWICZ and A. ZUGAJ, *Application of discrete chaotic dynamical systems in cryptography – DCC method*, International Journal of Bifurcation and Chaos, **9**, 6, 1121–1195, 1999.

22. H.B. LIN, *Chaos*, World Sc. Publ. Corp., Hong-Kong 1984.

23. R.S. MACKAY, *Transition to chaos for area preserving maps*, in: Nonlinear Dynamics Aspects of Particle Acceleretors, J.M. JOWETT, M. MONTYH and S. TURNER (Eds.), Lecture Notes in Physics, 247, 390–454, Springer, Berlin 1986.

24. Y.V. NAZAROV, *Novel circuit of Andreev reflection*, Preprint cond-mat 9811155, Los Alamos 1998.

25. G. NICOLIS and I. PRIGOGINE, *Die Erforschung des Komplexen*, Piper, Munich 1987.

26. E. OTT, C. GREBOGI and J.A. YORKE, *Controlling chaos*, Physical Review Letters, **64**, 11, 1196–1199, 1990.

27. U. PARLITZ, L.O. CHUA, LJ. KOCAREV, K.S. HALLE and A. SHANG, *Transmission of digital signals by chaotic synchronization*, Int.J.Bifurc. & Chaos, **2**, 973–977, 1992.

28. L.M. PECORA, T.L. CAROLL, *Synchronization in chaotic systems*, Phys. Rev.Lett. **64**, 8, 821–824, 1990.

29. Y. POMEAU, *Intermittancy: a simple mechanism of continuous transition from order to chaos*, [In:] Bifurcation Phenomena in Mathematical Physics and Related Topics, 155, Reidel, 1980.

30. M. SHINBROT, *Entropy change and no-slip condition*, Arch.Rat.Mech.Anal., **67**, 351–363, 1978.

31. B. SCHNEIER, *Applied Cryptography. Practical Algorithms and Source Codes in C*, John Wiley, New York 1996.

32. J. SCHNUTE and M. SHINBROT, *Kinetic theory and boundary conditions for fluids*, Can. J. Math.,. **25**, 1183, 1973.

33. I. SHIMADA and T. NAGASHIMA, *A numerical approach to ergodic problem of dissipative dynamical systems*, Progress Theor. Phys., **61**, 1605–1616, 1979.

34. J-M. STRELCYN, *The "coexistence problem" for conservative dynamical systems: A review*, Colloqium Mathematicum, **62**, 2, 331–345, 1991.

35. J. SZCZEPAŃSKI and Z. KOTULSKI, *On topologically equivalent ergodic and chaotic reflection laws leading to different types of particle's motion*, Arch.Mech, **50**, 5, 865–875, 1998.

36. J. SZCZEPAŃSKI and E. WAJNRYB, *Long-time behaviour of the one-particle distribution function for the Knudsen gas in a convex domain*, Physical Review A, **44**, 6, 3615–3621, 1991.

37. J. SZCZEPAŃSKI and E. WAJNRYB, *Do ergodic or chaotic properties of the reflection law imply ergodicity or chaotic behaviour of a particle's motion?*, Chaos, Solitons & Fractals, **5**, 1, 77–89, 1995.

Received December 30 1998; revised version March 18, 1999.

DIRECTIONS FOR THE AUTHORS

The journal *ARCHIVES OF MECHANICS (ARCHIWUM MECHANIKI STOSOWANEJ)* deals with the printing of original papers which should not appear in other periodicals.

As a rule, the volume of a paper should not exceed 40 000 typographic signs, that is about 20 type-written pages, format: 210×297 mm, leaded. The papers should be submitted in two copies. They must be set in accordance with the norms established by the Editorial Office. Special importance is attached to the following directions:

1. The title of the paper should be as short as possible.

2. The text should be preceded by a brief introduction; it is also desirable that a list of notations used in the paper should be given.

3. The formula number consists of two figures: the first represents the section number and the other the formula number in that section. Thus the division into subsections does not influence the numbering of formulae. Only such formulae should be numbered to which the author refers throughout the paper, and also the resulting formulae. The formula number should be written on the left-hand side of the formula; round brackets are necessary to avoid any misunderstanding. For instance, if the author refers to the third formula of the set (2.1), a subscript should be added to denote the formula, viz. $(2.1)_3$.

4. All the notations should be written very distinctly. Special care must be taken to write small and capital letters as precisely as possible. Semi-bold type should be underlined in black pencil. Explanations should be given on the margin of the manuscript in case of special type face.

5. It has been established to denote vectors by semi-bold type. Trigonometric functions are denoted by sin, cos, tg and ctg, inverse functions – by arc sin, arc cos, arc tg and arc ctg; hyperbolic functions are denoted by sh, ch, th and cth, inverse functions – by Arsh, Arch, Arth and Arcth.

6. Figures in square brackets denote reference titles. Items appearing in the reference list should include the initials of the first name of the author and his surname, also the full title of the paper (in the language of the original paper); moreover;

a) In the case of books, the publisher's name, the place and year of publication should be given, e.g.,

5. S. Ziemba, *Vibration analysis*, PWN, Warszawa 1970;

b) In the case of a periodical, the full title of the periodical, consecutive volume number, current issue number, pp. from ... to ..., year of publication should be mentioned; the annual volume number must be marked in black pencil so as to distinguish it from the current issue number, e.g.,

6. M. Sokołowski, *A thermoelastic problem for a strip with discontinuous boundary conditions*, Arch. Mech., **13**, 3, 337–354, 1961.

7. The authors should enclose a summary of the paper. The volume of the summary is to be about 100 words.

8. The authors are kindly requested to enclose the figures prepared on diskettes (format PCX, BitMap or PostScript).

Upon receipt of the paper, the Editorial Office forwards it to the reviewer. His opinion is the basis for the Editorial Committee to determine whether the paper can be accepted for publication or not.

The printing of the paper completed, the author receives 25 copies of reprints free of charge. The authors wishing to get more copies should advise the Editorial Office accordingly, not later than the date of obtaining the galley proofs.

The papers submitted for publication in the journal should be written in English. No royalty is paid to the authors.

Please send us, in addition to the typescript, the same text prepared on a diskette (flopy disk) 3 1/2″ as an ASCII file, preferably in the TEX or LATEX format in Dos or Unix format.

EDITORIAL COMMITTEE
ARCHIVES OF MECHANICS
(ARCHIWUM MECHANIKI STOSOWANEJ)

Archives of Mechanics

Contents of issue 3–4 vol. 51

Arch. Mech., T. **51**, nr 3–4, str. 225–528, Warszawa 1999